



**BRITISH
COLUMBIA**

**Ministry of Employment and Investment
Energy and Minerals Division
Geological Survey Branch**

GEOLOGICAL FIELDWORK 1997

**A Summary of Field Activities
and Current Research**

PAPER 1998-1



**BRITISH
COLUMBIA**

**Ministry of Employment and Investment
Energy and Minerals Division
Geological Survey Branch**

GEOLOGICAL FIELDWORK 1997

**A Summary of Field Activities
and Current Research**

PAPER 1998-1

Energy and Minerals Division

Geological Survey Branch

Parts of this publication may be quoted or reproduced if credit is given. The following is the recommended format for referencing individual works contained in this publication:

MacIntyre, D.G. and Struik, L.C. (1998): Nechako NATMAP Project, 1997 Overview, in Geological Fieldwork 1997, *British Columbia Ministry of Employment and Investment*, Paper 1998-1, pages 1-1 to 1-8.

British Columbia Cataloguing in Publication Data

Main entry under title:

Geological fieldwork: - 1974 -

Annual.

Issuing body varies

Vols. For 1978-1996 issued in series: Paper / British Columbia. Ministry of Energy, Mines and Petroleum Resources; vols for 1997- , Paper / British Columbia. Ministry of Employment and Investment.

Includes Bibliographical references.

ISSN 0381-243X = Geological fieldwork

1. Geology - British Columbia - Periodicals. 2. Mines and mineral resources - British Columbia - Periodicals. 3. Geology, Economic - British Columbia - Periodicals. 4. British Columbia. Geological Survey Branch - Periodicals. I. British Columbia. Geological Division. II. British Columbia. Geological Branch. III. British Columbia. Geological Survey Branch. IV. British Columbia. Department of Mines and Petroleum Resources. V. British Columbia. Ministry of Energy, Mines and Petroleum Resources. VI. British Columbia. Ministry of Employment and Investment. VII. Series: Paper (British Columbia. Ministry of Energy, Mines and Petroleum Resources). VIII. Series: Paper (British Columbia. Ministry of Employment and Investment).

QE187.G46

553'.09711

C76-083084-3 (Rev.)



VICTORIA
BRITISH COLUMBIA
CANADA

JANUARY 1998

FOREWORD

Geological Fieldwork: A Summary of Fieldwork and Current Research, 1997 is the twenty-third edition of this annual publication. It contains reports of Geological Survey Branch activities and projects during 1997. The base budget of the Branch for the 1997-98 fiscal year was \$4.6 million, down from \$6.6 million the previous year. The Branch also received \$135 000 from the Corporate Resource Inventory Initiative to maintain the Mineral Potential database of the province and for mineral potential studies of the Cassiar-Iskut-Stikine planning area. In addition, a new Geoscience Partnership Program with external clients was initiated in 1997. Results of the Moyie Partnership are reported on in this volume.

The contents of this year's volume reflect the emphasis of Branch programs. Highlights were:

- Continuation of the Nechako Plateau NATMAP project, which is a collaborative effort with the Geological Survey of Canada and various universities. The focus of GSB work is the Babine porphyry belt with its important mineral potential;
- Regional geochemical sampling of the Mesilinka River Map Sheet (94C) in east central British Columbia;
- Year 2 of the multidisciplinary Eagle Bay Project which is utilizing surficial geology and geochemistry to look for clues for buried mineral deposits in the Adams Plateau area;
- The Moyie industrial partnership project which will result in new 1:50 000 scale compilation maps for areas underlain by the Aldridge Formation;
- The Devonian-Mississippian VMS project which continued to test potential extensions of strata that host the Kudze Kayah and Wolverine deposits in northern British Columbia; and
- The McConnell Range regional mapping project which extended existing coverage of the Toodoggone volcanic belt southward from the area of the Kemess deposit.

A variety of mineral deposits and deposit types are profiled in this year's volume, including a stratabound zinc deposit in the Caribou terrane, an epithermal gold deposit in northern-most British Columbia, nickel mineralization in the Turnagain Alaskan ultramafic complex, sediment-hosted gold mineralization near Watson Bar and mineral occurrences near Bella Coola. There is also a report on Tertiary mineralization in the Queen Charlotte Islands and results of a study of the Slocan camp, as well as three reports on mineral deposit studies and age dating from MDRU at the University of British Columbia.

The Mineral Potential project completed coverage of the Queen Charlotte Islands, hence the province is now completely covered at 1:250 000 scale. Much information from the project is posted on the Ministry Internet site (address: <http://ei.gov.bc.ca/geology>). The intent is to have geology, mineral potential estimates, MINFILE, mineral titles information and other data available on the Internet. Through the Map Guide viewer (downloadable at the site) data posted may be viewed and manipulated. The geology and some associated datasets may also be downloaded in Arc Export (E00) format from the site.

The Branch is now employing print-on-demand technology for its geoscience publications. Material will also be posted on the Ministry Internet site for viewing or downloading. Production of Geological Fieldwork to the camera-ready stage has been done in Microsoft WORD by the authors using a template prepared by Brian Grant and updated by Dave Lefebure and Bill McMillan. Thanks are due to Dave Lefebure and Bill McMillan for editing and guiding the process, and Dorthe Jakobsen for administrative backup to ensure completion of this report on schedule.

W.R. Smyth
Chief Geologist
Geological Survey Branch



NECHAKO NATMAP PROJECT, CENTRAL BRITISH COLUMBIA 1998 OVERVIEW

D.G. MacIntyre and L.C. Struik (Cordilleran Section, GSC Vancouver, British Columbia)

KEYWORDS: Nechako plateau, Eocene, extension, Natmap, Babine porphyry belt, Sitlika Assemblage, Nechako map, Fort Fraser map, Endako, plutonism, multidisciplinary, bedrock mapping, surficial mapping, biogeochemistry, till geochemistry, geochronology, conodonts, radiolarian, geophysics.

INTRODUCTION

The Nechako NATMAP project (Figure 1) is a joint mapping venture between the Geological Survey of Canada (GSC) and the British Columbia Geological Survey Branch (BCGSB) (McMillan and Struik, 1996; Struik and McMillan, 1996; Struik and MacIntyre, 1997; MacIntyre and Struik, 1997; Struik and MacIntyre, 1998). This was the fourth and final year of field work for the project which has encompassed more than 30 000 km² in central British Columbia (Figures 1 and 2). Its main focus is to improve the quality and detail of bedrock and surficial maps to help resolve several geological problems. In particular it addresses the following questions: 1) the extent and nature of Tertiary crustal extension, 2) Mesozoic compression and the manner of accretion of exotic terranes, 3) the geological and geophysical definition of the terranes, 4) the sequence of changing Pleistocene glacial ice flow directions, and 5) the character and dispersion of glacial deposits.

In this fourth field season of the Nechako NATMAP project, staff geologists from the GSC and BCGSB, with the assistance of students and researchers from Simon Fraser University (SFU), University of Alberta (UA), University of Bristol, England (UB), University of British Columbia (UBC), University of Guelph (UG), University of New Brunswick (UNB), University of Ottawa (UO), University of Victoria (UVic), University of Waterloo

(UW), and University of Wisconsin-Eau Claire, USA (UWis), completed bedrock mapping in 14 and surficial mapping in 6 1:50,000 scale map areas (Figures 2 and 3). In addition, researchers sampled till, silt, lodgepole pine, and rocks in various geochemical studies. Others measured magnetic signatures; studied biostratigraphy; sampled for isotopic-age dating; and conducted detailed sedimentological and stratigraphic studies. Stratigraphic studies concentrated on sections within the Hazelton Group south of Burns Lake and mainly volcanic sequences of the Ootsa Lake Group. Digital Geographic Information System (GIS) projects included construction and addition to the digital field mapping databases, cartography of geological maps, internet GIS data sharing, surficial geology GIS data sets, analysis of RADARSAT and LandSat imagery, generation of Digital Elevation Models and creation of a general interest geological map of the Fort Fraser map area (Hastings *et al.*, 1998). New geoscience contributions include: 1) extending southeastward the distribution of the Sitlika Group sediments and volcanics through the Fort Fraser map area (NTS 93K), 2) redefining large tracts of western Cache Creek Group as Stikine and Sitlika assemblages, 3) recognition of Jura-Cretaceous contraction structures which may be correlative with Skeena Fold Belt structures to the north, 4) better definition of the nature, distribution and tectonic setting of the Miocene and Eocene basalt, andesite and felsic volcanic and associated intrusive suites, 5) characterizing the geophysical and geochemical signature of the Endako Batholith and adjacent suites, and 6) establishing an area of high background mercury in till and lodgepole pine bark in the area north of Ootsa Lake in NTS map area 93F.

This paper outlines research that is in many cases preliminary. References are given to more in depth summaries in this volume and Current

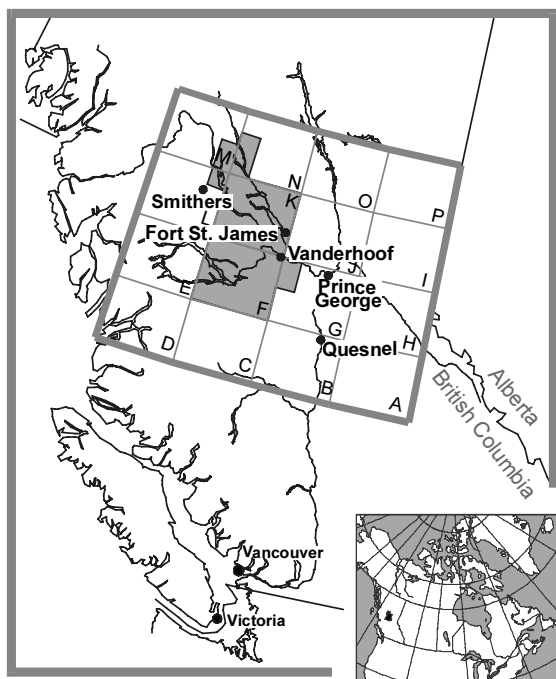


Figure 1. Location of the Nechako NATMAP project area within British Columbia. The Parsnip River (NTS 93) 1:1 000 000 scale map area and its 1:250 000 scale component map areas are shown for reference.

Research 1999 of the Geological Survey of Canada. For others the continuing research will lead to more comprehensive government and journal reports and maps. Analytical data is not reported in this paper.

OVERVIEW OF 1998 NECHAKO PROJECT RESULTS

Babine Porphyry Belt and Sitlika Studies

In the 1998 field season, the B.C. Geological Survey Branch focused on bedrock mapping in the Babine-Takla lakes area. Don MacIntyre and Paul Schiarizza were co-leaders of the bedrock mapping crew, which included geology students Angelique Justason (2nd year Camosun), Sheldon Modeland (4th year UVic), Stephen Munzar (4th year UBC) and Deanne Tackaberry (4th year UVic).

Accomplishments

From early June until the end of August, the bedrock geology of NTS map sheets 93K/11, 12, 14 and 93N/3 (Figures 2 and 3) were mapped at 1:100 000 scale. In addition, fill-in mapping was done in areas mapped in previous summers

including map sheets 93K/13, 93N/4 and 5. In the Babine Porphyry belt bedrock mapping was extended into adjoining map sheets 93L/9, 93M/2 and 93M/7. This work built on previous mapping in the Babine Porphyry belt (MacIntyre *et al.*, 1996; MacIntyre *et al.*, 1997; MacIntyre, 1998) and in the Sitlika belt east of Takla Lake (Schiarizza and Payie, 1997; Schiarizza *et al.*, 1998; MacIntyre *et al.*, 1998).

The following are the main highlights of work completed in 1998.

- ♦ significant revisions and refinements were made to the existing bedrock geology maps for the northwest quadrant of the Fort Fraser map sheet (93K/11,12,13 and 14), most of which were based on Armstrong's mapping and compilation (Armstrong, 1949).
- ♦ an area of limestone, metavolcanic and metasedimentary rocks intruded by pyroxenite and amphibole gabbro was mapped in the northwest corner of the 93K/12 map sheet. These rocks, previously mapped as Jurassic Hazelton Group, are tentatively correlated with the Permian Asitka Group. They appear to stratigraphically underlie pyroxene porphyry flows of the Takla Group that are exposed further to the east.
- ♦ additional mapping in the western parts of 93N/4 and 93N/5 has revealed that the Takla Range, previously mapped as Upper Triassic Takla Group, also includes Jurassic strata of the Hazelton and Bowser Lake groups.
- ♦ mapping in the vicinity of the Fort prospect suggests mineralization formed as a result of relatively low temperature open space filling in a dilational breccia zone along the fault contact between a pyroxenite-gabbro-diorite-tonalite intrusive complex and Takla volcanics. The pyroxenite intrusive complex intrudes chlorite schists and pyroxene-phyric metabasalts that may correlate with the Takla Group and/or the Asitka or Sitlika assemblages.
- ♦ the Sitlika eastern clastic unit was traced southeastwards from 93K/13, into the 93K/14, 93K/11 and 93K/12 map sheets, where it was previously mapped as Cache Creek Group. Felsic and mafic metavolcanic rocks that form a narrow belt directly west of the eastern clastic unit are correlated with

the Sitlika volcanic unit; a U-Pb geochronology sample was collected from one of the felsic volcanic members to test this correlation.

- ♦ new mapping in the southern part of 93N/4, together with visits to previously mapped outcrops in 93N/4 and 5, has resulted in an improved understanding of the Sitlika western clastic unit. Most of the unit is now interpreted as a structural repetition of the eastern clastic unit within a west-vergent fold-fault system. Chert pebble conglomerate that dominates the unit where it was originally defined in 93N/12 is interpreted as a fault-bounded panel derived from the Stikine terrane (Bowser basin), which forms the foot-wall of this west-vergent thrust system.
- ♦ the ultramafic unit that marks the boundary between the Sitlika assemblage and Cache Creek Group in 93N continues southward along the contact through 93K/13 and 14 and into 93K/11. This unit includes serpentinite melange, as well as coherent sections of tectonized harzburgite with dunite pods, gabbro-diorite intrusive complexes and mafic volcanic rocks. A sheeted diabase dike complex was discovered along the eastern margin of the unit in 93K/11, consistent with an ophiolitic origin for the ultramafic unit. Tonalite, which occurs locally as a late stage differentiate within some of the gabbro-diorite intrusive complexes was sampled for U-Pb dating in an effort to determine the age of the ophiolite complex.
- ♦ from Stuart Lake to Tsitsutl Mountain, the Cache Creek Group directly east of the ultramafic unit is represented by a belt of mafic metavolcanic rocks and associated chert, phyllite and minor limestone, that is intruded by numerous mafic (locally ultramafic) sills and dikes. The dikes and sills are similar to intrusive rocks found within the adjacent ultramafic unit, suggesting that these rocks may represent the upper part of the ophiolite succession. The volcanic-sedimentary succession is, at least in part, Late Triassic in age, and displays evidence of syn-sedimentary intrusion and faulting. It represents the remnants of an active (back arc?) basin that may have potential for VMS deposits of the Windy Craggy type.

Cache Creek Group tectonostratigraphic studies

Studies this season in the Cache Creek Group of Fort Fraser and Manson River map areas consisted of improving fossil collections. This work was conducted by Hilary Taylor (GSC) with assistance of Mike Hruday (UA), Kelly Franz (UBC), and Paul Schiarizza (BCGSB). Primary access was by forest service roads branching from Fort St. James, and the extensive lake system.

Accomplishments

This sampling is meant to confirm and increase the size of unique conodont fossil collections made in previous years in the Cache Creek Group, Sitlika Formation and Stikine Terrane. These collections contain Permian and Early Triassic faunal assemblages rare or previously unknown in western North America and in particular to these rock assemblages (Orchard *et al.*, 1999).

Endako Plutonism and Tectonics

Bedrock was mapped in detail within the Tchesinkut (93K/4), Burns Lake (93K/5), and Tintagel Lake (93K/6) map areas (1:50 000 scale, Figures 2, 3). This mapping built on previous mapping by the British Columbia Geological Survey, the Geological Survey of Canada and the Endako Mines group (Kimura *et al.*, 1980; G. Johnson, pers. comm., 1997). Joe Whalen (GSC) and Bert Struik (GSC) were ably assisted by Karen Fallas (UA), Mike Hruday (UA), Marianne Quat (GSC), Crystal Huscroft (UBC), Selena Billesberger (UBC), Kelly Franz (UBC) and Matthew Clapham (UBC). Carmel Lowe (GSC) augmented investigations of the magnetic signature of the Endako molybdenum camp through detailed magnetic measurements within the Endako Mine. The area was accessed through forest roads and highways.

Accomplishments

Detailed bedrock maps of southwestern Fort Fraser map area (93K/4, 5 and 6) were completed. Stratigraphic sequences in the Ootsa Lake and Endako groups were constrained within the limits of the poor exposure. Nancy Grainger (UA, M.Sc.) and Mike Villeneuve (GSC) sam-

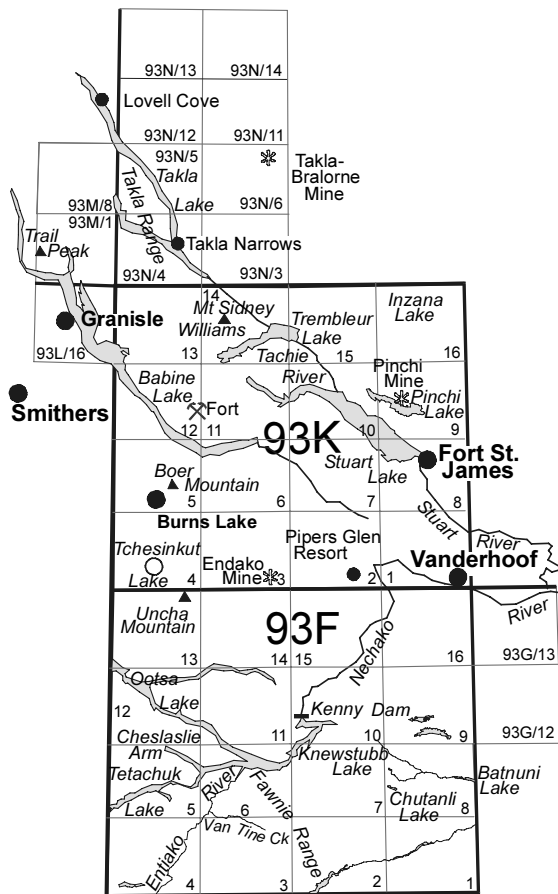


Figure 2. Reference map of geographic and NTS map locations mentioned in the text. See Figure 1 for the location of the Nechako NATMAP project area within central British Columbia.

pled igneous suites for U-Pb and Ar-Ar isotopic dating in key areas concentrating on the Tertiary volcanic units to constrain their stratigraphy and the tectonic events that generated them. Representative samples of each of the Tertiary volcanic units and the Jura-Cretaceous plutonic phases were taken for detailed litho geochemistry to constrain interpretations of the genetic history of those rocks. Samples were taken from within the Endako Mine and from Tertiary dikes and flows of the surrounding area for magnetic measurements to quantitatively constrain detailed aeromagnetic interpretations.

The following are the main highlights of the Endako study of 1998:

- ♦ Endako Group basalt occurs in small areas mainly in the southern and western parts of southwestern Fort Fraser map area. At one locality Endako Group basalt is cut by rhyo-

lite typical of the Ootsa Lake Group; previously considered to be entirely older than the Endako

- ♦ The Eocene age Ootsa Lake Group in southwestern Fort Fraser map area contains rhyolite, rhyodacite and dacite flows, crystal tuffs, agglomerates, breccias and conglomerates. Andesite and some dacite previously interpreted to be within the Ootsa Lake Group (Whalen *et al.* 1998) are now considered older; probably Cretaceous. Rhyolite of the Ootsa Lake Group around Tchesinkut Lake commonly shows textures associated with deposition in shallow water environments.
- ♦ The Boer pluton at Boer Mountain was determined to be gabbro to diorite that is different from the various plutons mapped as Boer phase to the east and northeast.
- ♦ The Tintagel phase of the Endako Batholith occupies a much smaller area than previously mapped; much of the Tintagel phase appears to be a more foliated variation of the McKnab or Shass Mountain phases.
- ♦ Sitlika assemblage andesite and sedimentary rocks mapped to the north (Schiarizza *et al.*, 1998; Schiarizza and MacIntyre, 1999) continue southeastward through the Tintagel map area (NTS 93K/6; Hrudey *et al.*, 1999). They were previously mapped as Cache Creek Group in the Fraser Lake area (Struik, 1997).
- ♦ Amphibolite, marble, quartzite and various foliated diorites of the Babine Lake area appear to be part of Stikine Terrane and are of higher metamorphic grade than to the northwest or southeast (Hrudey *et al.*, 1999). No clearly defined structures bound these medium grade metamorphic rocks.

Nechako River Map Area Bedrock Mapping

Bob Anderson, Bert Struik (GSC) and crews continued bedrock mapping in the Nechako River (NTS 93F) map area at 1:100 000 and 1:50 000 scales. Carmel Lowe and Judith Baker recorded additional geophysical data to augment profiles previously initiated across the various shear zones surrounding the Vanderhoof Metamorphic Complex. Mapping concentrated

on the Knapp Lake (NTS 93F/14; Anderson *et al.*, 1999a), Takysie Lake (NTS 93F/13), Marilla (NTS 93F/12), Cheslatta Lake (NTS 93F/11) and Tetachuck Lake (NTS 93F/05) map areas. Contributions were made to improve the detail of the bedrock mapping in the Euchiniko River (NTS 93F/08), Qualcho Lake (NTS 93F/4) and Suscha Creek (NTS 93F/01) map areas (Struik *et al.*, 1999). Bob Anderson's core crew of senior mappers, Lori Snyder (UWis), Nancy Grainger (UA), and Jonah Resnick (UBC) was augmented by volunteers Elspeth Barnes (University of Glasgow), Tina Pint (UWis), Stephen Sellwood (UWis), Amber McCoy, Daniella Jost and Nancy Anderson. Assisting Bert were the Endako crew and Steve Williams (GSC) and volunteers, Ruth Paterson (University of Melbourne) and Christina Struik.

Accomplishments

In addition to completion of bedrock mapping in most of Nechako River map area (Anderson *et al.*, 1999a, 1999b; Struik *et al.*, 1999), several theses and directed study projects were undertaken, and additional magnetic and gravity readings were taken along profiles crossing the Nulki Shear zone (Wetherup, 1997) in northeastern Nechako River map area. Profiles were extended to the west and south and the density of the measurements increased in the vicinity of the suspected positions of buried shear zones. The university theses and directed studies include the petrogenesis of Miocene basalts (Resnick *et al.*, 1999), geochronology and genesis of the Ootsa Lake Group felsic volcanic and related plutonic rocks (Grainger and Anderson, 1999), structural and stratigraphic mapping of the Jurassic and Tertiary volcanogenic and plutonic suites of Uncha Mountain in the northwest (Barnes and Anderson, 1999), structural studies of deformed Hazelton Group rocks, plutonic studies (Sellwood *et al.*, 1999; S. Billesberger, UBC) and sedimentological and stratigraphic studies of the Hazelton Group to the southwest (M. Quat, GSC). Detailed laboratory studies included investigation of the development of saprolitic horizons beneath Miocene basalt by Resnick and mineralogical identifications by Barnes of the large variety of zeolite and other minerals that fill vesicles of basalt flows in the Ootsa Lake and Endako groups and less commonly in Miocene basalt.

Highlights of the Nechako River bedrock mapping for 1998 include:

- ♦ Recognition of important and widespread Cretaceous volcanic units in eastern Knapp Lake map area. They include felsic feldspar phenocryst-rich units and andesitic hornblende-plagioclase porphyry flows that strongly resemble the Upper Cretaceous Holy Cross porphyry andesite (Lane, 1995; Lane and Schroeter, 1997)
- ♦ A regional-scale reverse fault in the southern Takaysie (NTS 93F/13) and northern Marilla (NTS 93F/12) map areas juxtaposes Lower and Middle Jurassic Hazelton Group and Bowser Lake Group units, and is cross-cut by a Cretaceous? porphyritic pluton (Anderson *et al.*, 1999a). Up to 4 generations of ductile and or brittle minor structures were recognized by Tina Pint (UWis) in the Hazelton Group hangingwall rocks; equivalent Hazelton Group rocks elsewhere are comparatively undeformed. Interpreted thrust faulting in the Euchiniko River map area imbricated Lower and Middle Jurassic Hazelton Group volcanic and sedimentary rocks (Struik *et al.*, 1999)
- ♦ Miocene basalt intrusive centres and associated lava flows are clearly distinguished from Eocene Endako Group basaltic andesite based on texture, the presence of olivine phenocrysts, megacryst and xenocryst content, and the common association of mantle and crustal xenoliths in the Miocene rocks (Resnick *et al.*, 1999). Many centres occur along extensions of older fault systems, and locally, are themselves deformed, suggesting reactivation of Eocene faults and a Miocene extensional tectonic setting during emplacement.
- ♦ Ootsa Lake Group volcanic stratigraphy in northwestern Nechako River map area has been refined to include a generalized stratigraphy of amethyst-bearing amygdaloidal andesite and flow-layered rhyolite and rhyolitic tuff as well as a variety of flow-layered, aphanitic to porphyritic high level intrusions related to the volcanism (Grainger *et al.*, 1999). Mafic rocks are rare but significant in the upper part of the Ootsa Lake Group because they may provide the strati-

graphic and petrological linkage to the Newman Volcanics recognized by D. MacIntyre of BCGSB.

- ♦ The distribution, composition, textures and intrusive relationships of high level, miarolitic leucogranite and associated porphyry phases in the Hallett Lake and Knapp Lake areas indicate that these intrusions are the closest plutonic analogues of the Ootsa Lake Group volcanic units (Sellwood *et al.*, 1999).
- ♦ Similar plutonic rocks, as well as aphanitic and porphyritic felsic intrusions at Uncha Mountain, were shown to be clearly co-spatial and synkinematic with north-northeast-trending brittle faults and associated development of fracture cleavage (Barnes and Anderson, 1999). The orientations of the Tertiary faults and intrusions on Uncha Mountain suggests a rotation of the uniaxial extensional stress directions from NW-SE in the Hallett Lake area in the east to E-W at Uncha Mountain in the west.

Nechako River Map Area Quaternary Geological Mapping

Surficial mapping concentrated on the southwest and southeast quadrants of Nechako River map area and 93F/12. The mapping verified aerial photographic interpretations, catalogued Quaternary stratigraphy, studied landslide hazards and included collection of till samples for geochemistry. That work was done by Alain Plouffe (GSC) and student assistant Jean Bjornson (UO), and by Vic Levson (BCGSB), David Mate (Uvic, M.Sc.), Don McClenagan (Uvic, Ph.D.) and Andrew Stuart (University of Waterloo, M.Sc.) and involved staff of the British Columbia Ministry of Forests.

Accomplishments

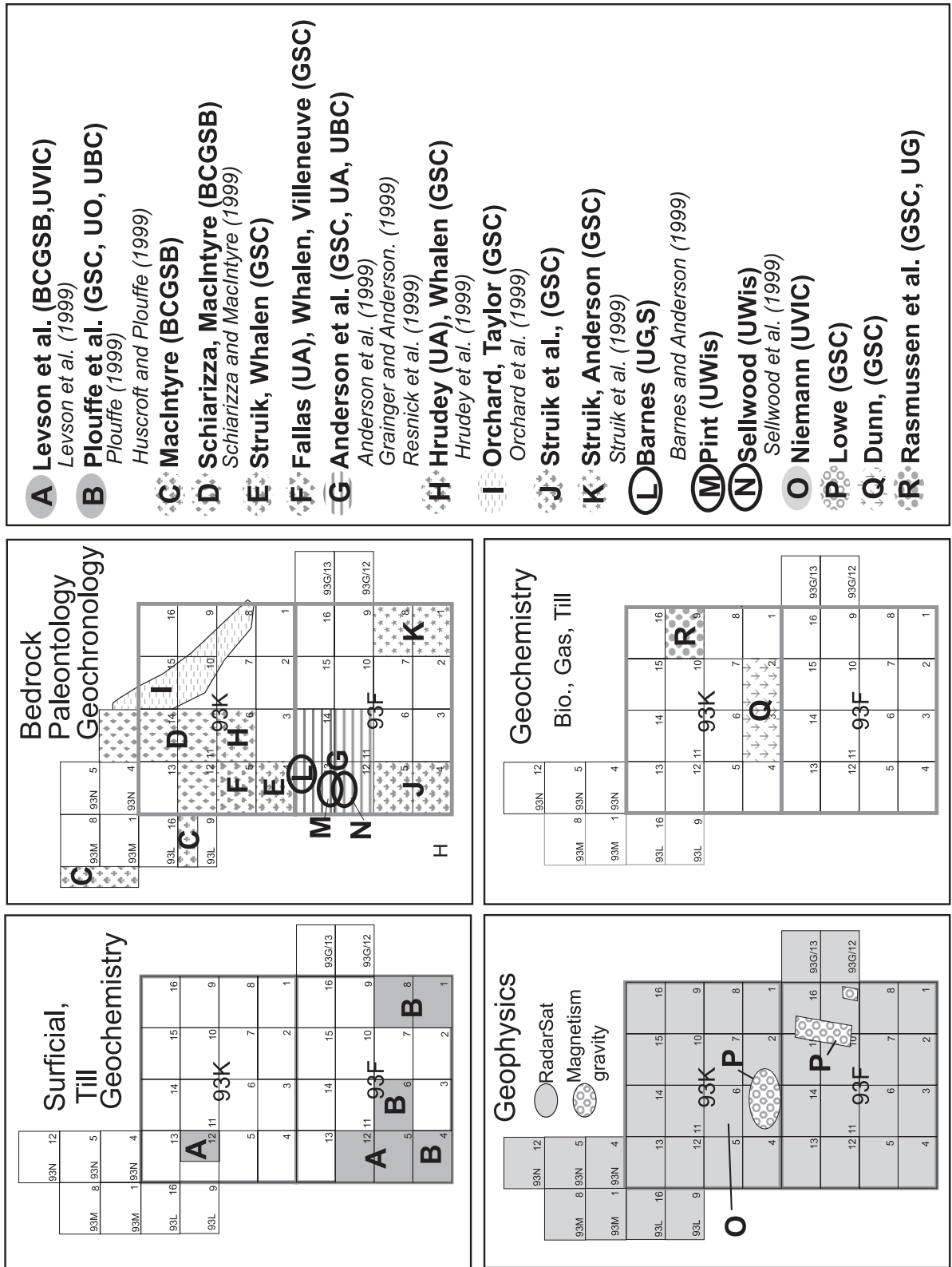
Alain Plouffe and Jean Bjornson mapped surficial geology and sampled till at a regional scale (ca. one sample per 25 square kilometers) in the eastern and central part of Nechako River map sheet. They collected a total of 131 till samples for geochemical analyses that will be completed on the clay-sized (< 0.002 mm) and silt plus clay-sized (<0.063 mm) fractions. The

samples were collected on the following 1:50 000 scale NTS map sheets: 93F/1, F/6, F/8, and F/9. Results of the 1996 and 1997 regional till sampling programs will be published as two sets of colored geochemical maps along with digital geochemical data (Plouffe, 1998a; Plouffe, in press).

One new surficial geology map was published in 1998 (Plouffe, 1998b) and a second one is in press (Plouffe, 1998c). With the combined effort of the British Columbia Geological Survey and the Geological Survey of Canada, by the end of the Nechako NATMAP project, four new surficial geology maps at a scale of 1:100 000 will be available for the entire Nechako River map sheet.

Glacial striations were measured on a total of 53 bedrock outcrops which included several sites that revealed more than one ice movement; for some of these, age relationships were established. Information on Quaternary stratigraphy was recorded at a limited number of sites located in the Batnuni Lake, Van Tine Creek, and Entiako River valleys. A site located on the shore of Cheslalie Arm of Ootsa Lake was revisited by A. Plouffe and V. Levson to sample nonglacial sediments that predate the last glaciation. The site was first described by Levson *et al.* (1998) who reported a single radiocarbon date of $27\ 790 \pm 200$ BP (Beta-101017) on the fine organic detritus of the nonglacial sediments.

Field work for two Bachelor's theses on Quaternary geology topics was completed during the 1998 field season. Crystal Huscroft (Huscroft and Plouffe, in press) studied the Pleistocene lake sediments deposited in the area of Knewstubb Lake. She investigated the sedimentology of the glacial lake sediments and took a series of elevation measurements of the glacial lake outlets and sediments to reconstruct the deglaciation history. Her work will contribute to the regional study of the glaciolacustrine deposits of central British Columbia (Plouffe, 1997). Her thesis will be completed at the University of British Columbia under the supervision of Dr. M. Church. Jean Bjornson completed a detailed investigation of ice-flow indicators (glacial striations, till fabrics, rat tail, flutes, drumlins, and crag and tail) for a 50 square kilometers area located along the western margin of 93 F/11 NTS map sheet. He will compare ice-flow data obtained from micro- and macro-landforms and will reconstruct the ice-



- A** Levson et al. (BCGSB,UVIC)
Levson et al. (1999)
- B** Plouffe et al. (GSC, UO, UBC)
Plouffe (1999)
Huscroft and Plouffe (1999)
- C** MacIntyre (BCGSB)
- D** Schiarizza, MacIntyre (BCGSB)
Schiarizza and MacIntyre (1999)
- E** Struik, Whalen (GSC)
- F** Fallas (UA), Whalen, Villeneuve (GSC)
- G** Anderson et al. (GSC, UA, UBC)
Anderson et al. (1999)
Grainger and Anderson. (1999)
Resnick et al. (1999)
- H** Hrudey (UA), Whalen (GSC)
Hrudey et al. (1999)
- I** Orchard, Taylor (GSC)
Orchard et al. (1999)
- J** Struik et al., (GSC)
- K** Struik, Anderson (GSC)
Struik et al. (1999)
- L** Barnes (UG,S)
Barnes and Anderson (1999)
- M** Pint (UWIS)
- N** Sellwood (UWIS)
Sellwood et al. (1999)
- O** Niemann (UVIC)
- P** Lowe (GSC)
- Q** Dunn, (GSC)
- R** Rasmussen et al. (GSC, UG)

Figure 3. Location of various Nechako subprojects active in 1998.

flow history of that region. His research will be conducted at the University of Ottawa, under the supervision of Dr. B. Lauriol.

Surficial geological mapping conducted by the BCGSB concentrated on the Tetachuck Lake (93F/5) and Marilla (93F/12) 1:50,000 NTS mapsheets (Levson *et al.*, 1999). Surficial geology studies in this area are a continuation of work started in 1997 (Levson *et al.*, 1998).

Highlights of the Nechako River surficial geological mapping for 1998 include:

- ♦ Stratigraphic sections at Batnuni Lake, Van Tine Creek, and Entiako River valleys provide new information about the advance-phase paleogeography of the last glaciation.
- ♦ Preliminary results from ice flow indicators show an east-northeast ice flow, followed by an eastward movement. Glacial striations, roches moutonnées, and erratics found in the Fawnie Range all indicate a general eastward ice movement. This new information suggests that the ice divide identified by Levson *et al.* (1998) which extended from the Babine Lake to the Ootsa Lake valleys during the last glacial maximum, did not migrate as far easterly as the Fawnie Range.
- ♦ Anomalous westward ice flow during the Late Wisconsinan glaciation, recently described by Levson and Stumpf (1998), Levson *et al.* (1998), and Stumpf *et al.* (in prep) for the Babine Range and Hazelton mountains area, was also found this field season on the west side of the Marilla map sheet (93F/12). This indicates that a Late Wisconsinan ice divide was located east of the Tweedsmuir area, subjecting that region to westerly ice flow and consequent west-directed glacial dispersal. Westerly flow was independent of large topographic barriers such as the Tweedsmuir, Babine and Hazelton mountains and occurred when ice centers over the Hazelton and Coast mountains migrated eastward into the Interior Plateau. Evidence for westerly flow is most readily found in the western part of the map region and is absent in the east. Consequently, the effects of westward flow on geochemical dispersal are expected to diminish rapidly eastward.

- ♦ Westerly ice-flow locally continued to the end of the last glaciation as indicated by preservation of paleoflow indicators at unprotected, low elevation sites. These observations confirm that the maximum buildup of interior ice extended late into the last glaciation and that a topographically controlled, late-glacial, ice-flow phase was short-lived in this part of the Interior Plateau (Levson *et al.*, 1998).

Geophysical Studies

In order to better constrain the geometry of Nulki Shear zone at depth Carmel Lowe and Judith Baker (GSC) extended gravity and magnetic traverses previously conducted across the structure (Lowe *et al.*, 1998a). In addition they undertook detailed measurements of the magnetic field and the magnetic susceptibility of exposed rocks within the Endako Mine to augment existing airborne magnetic (Lowe *et al.*, 1998a, b) and detailed paleomagnetic studies (Enkin *et al.*, 1997, Lowe and Enkin, 1998). The magnetic data will be integrated with geochemical data to further explore the observed correlation between increasing molybdenum concentrations and decreasing magnetic susceptibilities (L'Heureux and Anderson, 1997). As a contribution to this work, magnetic susceptibility and density was measured for samples from a large part of the project area.

Geochemical Studies

Biogeochemical surveys

Colin Dunn (GSC), Rob Scagel (Pacific Phytometric Consultants, Surrey, BC) and a volunteer, Daniella Jost conducted a reconnaissance level, lodgepole pine sampling program surrounding the Endako Molybdenum camp (NTS 93K/02, 93K/03). The sampling extends 1996 and 1997 coverage throughout the northern half of the Nechako River map area. Samples were the outer bark of lodgepole pine. The bark was collected from sites at 2 km intervals along all driveable roads and trails.

Till samples collected in 1997 in the north-western quadrant of Nechako River map area had high background concentrations of mercury.

To supplement that information all the lodgepole pine bark samples collected in that region (also in 1997) were analyzed for mercury. The analyses show that the pine trees are taking up high background levels of mercury and corroborate the till data (Plouffe, 1998a, 1999; Dunn, 1998).

Metals in the environment (MITE)

Pat Rasmussen, Colin Dunn, and Alain Plouffe (GSC) and Grant Edwards with 4 students: Jeff Kemp (Ph.D.), Laurie Halfpenny, Sophie Wong and Edwina Wong (University of Guelph) are working near the former Pinchi and Bralorne Takla mercury mines and at additional sites along the Pinchi fault zone. This work is part of the GSC Metals in the Environment (MITE) initiative. Objectives of this project are to determine if an anthropogenic signature is detectable around the mercury mine sites, to establish criteria that could be used to distinguish between natural and anthropogenic metal enrichments, and to identify the forms and phases in which metals are bound. Epiphytic moss and B horizon soil samples were collected in 1996 and 1997 at these locations and in 1998 Alain Plouffe continued this work collecting samples of humus, B-horizon, till, and glacial lake sediments along two transects near the Pinchi Mine. In addition, these orientation surveys found suitable sites for the in situ monitoring of mercury fluxes to the atmosphere, which was conducted in the summer of 1998.

Information on the natural air-surface exchange of mercury is relevant to risk assessors, in particular for apportioning exposure amongst natural and anthropogenic sources, and to provide a perspective for understanding releases from anthropogenic sources in the context of natural background variations.

The Pinchi mercury flux study is part of a larger survey of natural mercury emissions from representative geological settings across Canada (Rasmussen *et al.*, 1998), a collaborative project between Geological Survey of Canada, University of Guelph, and Atmospheric Environment Service (Environment Canada). Two methods for determining fluxes are used: the micrometeorological gradient method and the dynamic flux chamber method. Both methods are coupled with Tekran Model 2537A cold vapour atomic fluorescence detectors. Time series measurements include wind speed and

direction, net radiation, humidity, barometric pressure, air and soil temperature, and soil moisture. The focus of the current study is to develop methods to obtain reliable measurements of air-surface exchange of mercury representative of natural and perturbed surfaces in the vicinity of the Pinchi fault zone, and to understand factors causing temporal and spatial variations. In future, more portable methods are required to obtain spatially representative natural emissions data in remote areas.

Lake Sediment Geochemistry

Three regional lake water geochemical surveys are in the process of being written up. These studies were undertaken in conjunction with earlier lake sediment surveys in the southern Nechako, Pinchi Lake and Babine Porphyry Belt areas. This data (Cook *et al.*, 1999), the first Geological Survey Branch release of regional multi-element lake water geochemical data in British Columbia, will be available at the 1999 Cordilleran Roundup. Several other geochemical studies are also in advanced stages of completion. These include studies of molybdenum distribution in lake sediments adjacent to porphyry molybdenum deposits of the Endako region, and studies of contamination of organic lake sediments during sample preparation. Interior Plateau lake sediment case study results from areas such as Hill-Tout and Chutanli lakes are also nearing completion, as are regional geochemical compilations of stream sediment, lake sediment and till geochemical data from the Babine Porphyry Belt and the Pinchi Fault Zone areas.

Industrial Minerals Investigations

Dani Hora and George Simandl (BCGSB) continued follow up on industrial mineral and precious stone sites previously known and newly reported during mapping of the Nechako project. Dimension stone, decomposed lapilli tuffs (for clays), ornamental and landscaping rock (basalts mainly), perlite, opal, and agate were investigated. In addition the hypothesis connecting diamonds to subduction generated and mantle derived high pressure rock types was explored.

Highlights of the 1998 mapping include:

- ♦ A fairly large area north of Mount Sidney Williams is underlain by soapstone altered ultramafic rocks. The stone is massive, with joints in rectangular systems allowing blocks of 1 cubic foot or more, macroscopically the stone is free of pyrite in most of the outcrops. The polished stone colour is mottled light green and grey. This is a very good potential source of carving material.
- ♦ The area of soapstone near Mount Sidney Williams also has outcrops of siliceous listwanite, locally very rich in bright green mica. The listwanite could provide an attractive facing stone. The area is very accessible.
- ♦ Scoracious rhyolitic volcanic rock south of Burns Lake may have pozzolanic properties. It resembles material quarried in Nisconlith Creek area south of Quesnel, which was successfully used by a local ready-mix operator some 20 years ago.

Geographic Information System Development

Stephen Williams and Nikki Hastings (GSC) continued development of the Nechako Project digital point, line and areal database and query system. This work produces and releases digital geological map and point data sets. In addition it contributes to the computer production of standard and thematic geological maps and reports.

Accomplishments

Work focused on the digitization and cartography of geological maps, the addition of GIS data to an intranet GIS data sharing system, generating a non-geoscientist readable geological map (GEOSCAPE) for the Fort Fraser map area (Hastings, 1999), production of a CD-ROM of all digital surficial geology data of the Fort Fraser and Manson River map areas, and production of internet readable Current Research Reports for the Project. Carmel Lowe generated Digital Elevation Models for the project area from British Columbia 1:20 000 scale TRIM data. Olaf Niemann (UVic) has continued work on the integration of the Digital Elevation Modeling (DEM) and RADARSAT thematic data for the Nechako project area. In turn this work is being integrated with surficial and bedrock geological mapping in the Nechako

River map area.

Highlights from this year's GIS work include:

- ♦ Several new geological maps published as coloured 1:100 000 and 1:50 000 scale open file bedrock and surficial maps, and geochemical data sets.
- ♦ The MapGuide intranet GIS data sharing system is now operational for project participants. We continue to aspire to have this same information available to the public.
- ♦ Several Current Research reports previously published for the Nechako project are now available for use on the WEB at the Nechako Project WEB site (em.gov.bc.ca/natmap).
- ♦ The GeoScape map for the Fort Fraser map area is complete.
- ♦ Digital Elevation Models integrated with the geology and geophysics of the eastern Fort Fraser map area are completed and available (Lowe *et al.*, 1999).
- ♦ The complete digital data set for the surficial geology of the Fort Fraser and Manson River map areas is ready to transfer to CD-ROM for publication this spring (Plouffe and Williams, 1999)

For monthly updates of Nechako NATMAP Project developments, see the Nechako Newsletters posted on the Nechako Project website (em.gov.bc.ca/natmap) during the life of the project.

ACKNOWLEDGMENTS

All project participants contributed to the success of this year's research and to this overview. Project funding comes directly through continuing GSC and BCGSB programs and the GSC NATMAP program. In addition, in-kind funding comes from the many universities and companies listed throughout the text.

REFERENCES

- Anderson, R.G., Snyder, L.D., Grainger, N., Resnick, J., and Barnes, E.M., (1999b): Bedrock geology of the Takysie Lake and Marilla map areas, central British Columbia; *in* Current Research 1999-A, *Geological Survey of Canada*.

- Anderson, R.G., Snyder, L.D., Resnick, J., Grainger, N., and Barnes, E.M. (1999a): Bedrock geology of the Knapp Lake map area, central British Columbia; *in* Current Research 1999-A, *Geological Survey of Canada*.
- Armstrong, J.E. (1949): Fort St. James map-area, Cassiar and Coast Districts, British Columbia; *Geological Survey of Canada*, Memoir 252, 210 pages.
- Barnes, E., and Anderson, R.G. (1999): Bedrock geology of the Uncha Mountain area, northwestern Nechako River map area, central British Columbia; *in* Current Research 1999-A, *Geological Survey of Canada*.
- Cook, S.J., Jackaman, W., Lett, R.E.W., McCurdy, M.W. and Day, S.J. (1999): Regional Lake Water Geochemistry of parts of the Nechako Plateau, Central British Columbia (93F/2, 3, 93K/9, 10, 15, 16; 93L/9, 16; 93M/1, 2, 7, 8); *B.C. Ministry of Energy and Mines*, Open File 1999-5.
- Dunn, C.E., (1998): Reconnaissance biogeochemical survey in the Nechako area, central British Columbia (NTS 93F/15 and 16); *Geological Survey of Canada*, Open File 3594.
- Enkin, R., Baker, J., Struik, L.C., Wetherup, S., and Selby, D. (1997): Paleomagnetic determination of post-Eocene tilts in the Nechako region; *in* Abstract Volume 22, *Geological Association of Canada/Mineralogical Association of Canada*, Annual Meeting 1997, p.A-46.
- Grainger, N.C., and Anderson, R.G. (1999): Geology of the Eocene Ootsa Lake Group in northern Nechako River and southern Fort Fraser map areas, central British Columbia; *in* Current Research 1999-A, *Geological Survey of Canada*.
- Hastings, N.L., Plouffe, A., Struik, L.C., Turner, R.J.W., Williams, S.P., Anderson, R.G., Clague, Kung, R., and Taccogna, G. (1998): Development of a geoenvironmental map for the non-geoscientist, Nechako plateau, British Columbia; *Geological Society of America*, Abstracts of the Annual Meeting, Toronto, Canada.
- Hrudey, M.G., Struik, L.C. and Whalen, J.B. (1999): Geology of the Tintagel map area, central British Columbia; *in* Current Research 1999-A, *Geological Survey of Canada*.
- Huscroft, C.A., and Plouffe, A. (1999): Field investigations of a late glacial lake of the Fraser Glaciation, central British Columbia; *in* Current Research 1999-A, *Geological Survey of Canada*.
- Kimura, E.T., Bysouth, G.D., Cyr, J., Buckley, P., Peters, J., Boyce, R., and Nilsson, J. (1980): Geology of parts of southeast Fort Fraser and northern Nechako River map areas, central British Columbia; *Placer Dome Incorporated*, Internal Report and Maps, Vancouver, British Columbia.
- Lane, B. (1995): Preliminary bedrock geology, Holy Cross Mt. to Bentzi Lake, central British Columbia (NTS 93F/14E and 15W); *B.C. Ministry of Energy, Mines and Petroleum Resources*, Open file 1995-22.
- Lane, R.A. and Schroeter, T.G. (1997): A review of metallic mineralization in the Interior Plateau, central British Columbia (Parts of 93B, C and F); *in* Interior Plateau Geoscience Project: Summary of Geological, Geochemical and Geophysical Studies, L.J. Diakow and J.M. Newell, Editors, *B.C. Ministry of Employment and Investment*, Paper 1997-2, pages 237-256.
- Levson, V., Stumpf, A., and Stuart, A. (1998): Quaternary geology studies in the Smithers and Hazelton map areas (93L and M): Implications for exploration; *in* Geological Fieldwork 1997, *B.C. Ministry of Employment and Investment*, Paper 1998-1.
- Levson, V.M. and Stumpf, A.J. (1998): Quaternary geology and ice-flow studies in the Smithers and Hazelton map areas (93 L and M): implications for exploration; *in* Geological Fieldwork 1997, *B.C. Ministry of Employment and Investment*, Paper 1998-1, p. 5-1 - 5-8.
- Levson, V.M., Mate, D. and Stuart, A.J. (1999): Quaternary geology and drift prospecting studies in the north central nechako plateau (93F and K); *in* Geological Fieldwork 1998, *B.C. Ministry of Energy and Mines*, Paper 1999-1, this volume.
- L'Heureux and Anderson, R.G., (1997): Early Cretaceous plutonic rocks and molybdenite showings in the Nithi Mountain area, central British Columbia; *in* Current Research 1997-A, *Geological Survey of Canada*, p. 117-124.

- Lowe, C. and Enkin, R.J. (1998): New constraints on bedrock geology and mineral exploration in central British Columbia: Analyses of aeromagnetic, paleomagnetic and gravity data; *in* Short Course on New geological constraints on Mesozoic to Tertiary metallogenesis and on mineral exploration in central British Columbia: Nechako NATMAP project, Extended Abstracts, Cordilleran Section, *Geological Association of Canada*, p. 110-117.
- Lowe, C., Enkin, R.J., and Dubois, J. (1998a): Magnetic and paleomagnetic constraints on Tertiary deformation in the Endako region, central British Columbia; *in* Current Research 1998-A; *Geological Survey of Canada*, p.125-134.
- Lowe, C., R.J. Enkin, J. Dubois, L. Struik, J. Baker, and R. Anderson (1998b): Magnetic constraints on Tertiary deformation in central British Columbia; Lithoprobe SNORCLE and Cordilleran Tectonics Workshop, Vancouver, pp. 274-275.
- Lowe, C., Struik, L.C., Kung, R. (in prep): DEM and bedrock geology of eastern Fort Fraser map area, central British Columbia; *Geological Survey of Canada*, Open File.
- MacIntyre, D.G. and Struik, L.C. (1998): Nechako NATMAP Project: 1997 Overview; *in* Geological Fieldwork 1997, *B.C. Ministry of Employment and Investment*, Paper 1998-1.
- MacIntyre, D.G., Schiarizza, P. and Struik L.C. (1998): Preliminary bedrock geology of the Tochcha Lake map sheet (93K/13), British Columbia; *in* Geological Fieldwork 1997, *B.C. Ministry of Employment and Investment*, Paper 1998-1.
- MacIntyre, D.G., Webster, I.C.L. and Villeneuve, M. (1997): Babine Porphyry Belt Project: Bedrock Geology of the Old Fort Mountain Area (93M/1), British Columbia; *in* Geological Fieldwork 1996, *B.C. Ministry of Employment and Investment*, Paper 1997-1.
- MacIntyre, D.G., Webster, I.C.L., and Bellefontaine, K., (1996): Babine Porphyry Belt project, Bedrock Geology of the Fulton Lake map area (NTS 93L16); *in* Geological Fieldwork 1995, *B.C. Ministry of Energy, Mines and Petroleum Resources*, Paper 1996-1.
- MacIntyre, D.G. (1998): Babine Porphyry Belt Project: Bedrock geology of the Nakinilerak Lake map sheet (93M/8), British Columbia; *in* Geological Fieldwork 1997, *B.C. Ministry of Employment and Investment*, Paper 1998-1.
- Orchard, M.J., Struik, L.C., and Taylor, H. (1999): More new conodont data from the Cache Creek Group, central British Columbia; *in* Current Research 1999-A, *Geological Survey of Canada*.
- Plouffe, A. (1998a): Regional till geochemistry of the northern sector of Nechako River map sheet (NTS 93F); *Geological Survey of Canada*, Open File, 2 sheets and one diskette.
- Plouffe, A. (1998b): Surficial geology, Tahultzu Lake, British Columbia (93 F/NE); *Geological Survey of Canada*, Open File 3620, scale 1:100,000.
- Plouffe, A. (1998c): Surficial geology, Binta Lake, British Columbia (93 F/11, 13, and 14); *Geological Survey of Canada*, Open File 3640, scale 1:100,000.
- Plouffe, A. and Williams, S.P. (in press): Digital surficial geology data set for the Manson River and Fort Fraser map area; *Geological Survey of Canada*, Open File, 1 CD-ROM.
- Plouffe, A. (1997): Ice flow and late glacial lakes of the Fraser Glaciation, central British Columbia; *in* Current Research 1997-A, *Geological Survey of Canada*, p. 133-144.
- Plouffe, A. (1999): New data on till geochemistry in the northern sector of the Nechako River map sheet (NTS 93 F), British Columbia; *in* Current Research 1999-A, *Geological Survey of Canada*.
- Plouffe, A. (1999): New data on till geochemistry in the northern sector of the Nechako River map sheet (NTS 93 F), British Columbia; *in* Current Research 1999-A, *Geological Survey of Canada*.
- Rasmussen, P.E., Edwards, G.C., Kemp, J., Hubble-Fitzgerald, C., and Schroeder, W.H. (1998): Towards an improved natural sources inventory for mercury; *in* Proceedings of Metals and the Environment: An International Symposium, J. Skeaff, Editor, *Metallurgical Society of the Canadian Institute of Mining, Metallurgy and Petroleum* (CIM), Montreal, May 5-6, 1998, p. 73-83.
- Resnick, J., Anderson, R.G., Russell, J.K., Edwards, B.R., and Grainger, N. (1999): Chilcotin Group basalt and related intrusions, northern Nechako River map area, central British Columbia; *in* Current Research 1999-A, *Geological Survey of Canada*.

- Schiarizza, P. and Payie, G. (1997): Geology of the Sitlika Assemblage in the Kenny Creek - Mount Olsen Area (93N/12, 13); *in Geological Fieldwork 1996, B.C. Ministry of Employment and Investment, Paper 1997-1.*
- Schiarizza, P. and MacIntyre, D.G. (1999): Geology of the Sitlika, Stikine and Cache Creek assemblages in northwestern Fort Fraser and southwestern Manson River map areas (93K/11, 12,14, 93N/3); *in Geological Fieldwork 1998, B.C. Ministry of Energy and Mines, Paper 1999-1, this volume.*
- Schiarizza, P., Massey, N.W.D., and MacIntyre, D.G. (1998): Geology of the Sitlika assemblage in the Takla Lake area (93N/3,4,5,6,12); *in Geological Fieldwork 1997, B.C. Ministry of Employment and Investment, Paper 1998-1.*
- Sellwood, S.M., Snyder, L.D., and Anderson, R.G. (1999): Geology of two high-level Tertiary granite plutons, northern Nechako River map area, central British Columbia; *in Current Research 1999-A, Geological Survey of Canada.*
- Struik, L.C. and MacIntyre, D.G. (1999): Overview of the Nechako NATMAP Project, central British Columbia, year four: Part 2; *in Current Research 1999-A, Geological Survey of Canada.*
- Struik, L.C. and MacIntyre, D.G. (1999): Overview of the Nechako NATMAP Project, central British Columbia, year four: Part 1; *in Current Research 1999-A, Geological Survey of Canada.*
- Struik, L.C. and McMillan, W.J. (1996): Nechako Project Overview, central British Columbia; *in Current Research 1996-A, Geological Survey of Canada, p. 57-62.*
- Struik, L.C. and McMillan, W.J. (1996): Nechako Project Overview, central British Columbia; *in Current Research 1996-A, Geological Survey of Canada, p. 57-62.*
- Struik, L.C., Anderson, R.G. and Plouffe, A. (1999): Geology of the Euginiko map area, central British Columbia; *in Current Research 1999-A, Geological Survey of Canada.*
- Struik, L.C. (1997): Bedrock geology, Fraser Lake, central British Columbia; *Geological Survey of Canada, Open File 3559.*
- Whalen, J.B., Struik, L.C., and Hrudehy, M.G. (1998): Bedrock geology of the Endako map area, central British Columbia; *in Current Research 1998-A, Geological Survey of Canada.*
- Wetherup, S. (1997): Geology of the Nulki Hills and surrounding area (NTS 93F/9, 16), central British Columbia; *in Current Research 1997-A, Geological Survey of Canada, p. 125-132.*

QUATERNARY GEOLOGY AND DRIFT PROSPECTING STUDIES IN THE NORTH CENTRAL NECHAKO PLATEAU (93 F AND K)

By Victor M. Levson (B.C. Geological Survey), David Mate (University of Victoria) and Andrew J. Stuart (University of Waterloo)

(British Columbia Geological Survey Branch contribution to the Nechako NATMAP Project)

KEYWORDS: Applied geochemistry, ice-flow history, glaciation, mineral exploration, surficial geology, Quaternary stratigraphy

INTRODUCTION

This paper provides an overview of Quaternary geology and drift prospecting studies conducted in the Nechako River and Fort Fraser 1:250 000 map areas (NTS 93 F and K, respectively) by the British Columbia Geological Survey in 1998. Research efforts were concentrated in the Tetachuck Lake (93 F/5), Marilla (93 F/12) and Pendleton Bay (93 K/12E) 1:50 000 NTS map areas (Figure 1). This work included surficial geology mapping, Quaternary stratigraphy and landslide hazard studies in the Tetachuck Lake and Marilla map areas, and till geochemistry and ice flow studies on all three map sheets. These investigations are part of the Nechako National Mapping Project, coordinated by the Geological Survey of Canada and the British Columbia Geological Survey (MacIntyre and Struik, 1999). Summaries of results of associated Quaternary geology and regional till geochemistry surveys previously conducted in parts of the Nechako Plateau were provided by Levson and Giles (1997) and Levson *et al.* (1997a,b, 1998). A more detailed description of surficial geology mapping and Quaternary studies in the Marilla map area is provided by Mate and Levson (1999).

The main objectives of the Quaternary geology component of this work are to understand and map the distribution of surficial deposits, decipher the glacial history and ice-flow patterns, locate areas most suitable for conducting drift exploration programs, and provide data to aid in interpreting till geochemical results. Procedures used include compilation of existing surficial geology data, interpretation of air photographs, field checking, till sampling, and stratigraphic and sedimentologic investigations

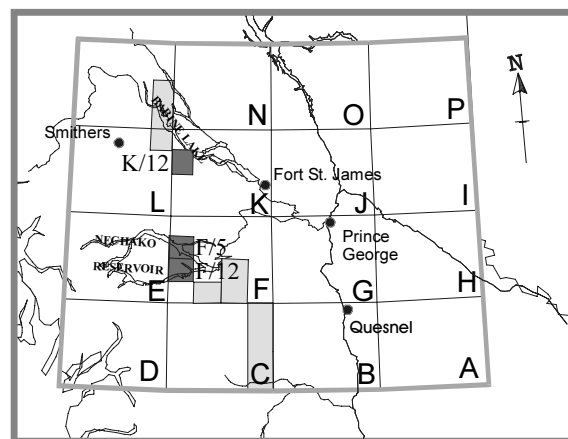


Figure 1. Location map of the study region. Dark shading shows area of Quaternary geology studies conducted in 1998 (93 F/5, F/12, K/12); lightly shaded blocks are areas previously mapped at 1:50 000 scale.

of Quaternary exposures. Ice-flow history was largely deciphered from measurement of the orientation of crag-and-tail features, flutings, drumlins and striae.

The main objectives of the drift prospecting component of this study are to collect regional till geochemical samples, conduct case study investigations around known mineral occurrences, evaluate geochemical dispersal processes and locate mineralized erratics in surficial materials. Procedures used for this work including field methods, types of data collected, laboratory analyses and quality control procedures, are described in detail by Levson and Giles (1997).

PREVIOUS WORK

Reconnaissance (1:250 000-scale) mapping of glacial features in the Nechako River map area was originally conducted by Tipper (1963). This mapping shows dominant landforms such as drumlins, eskers and meltwater channels. Terrain mapping of the southern part of the Nechako Plateau area, showing surficial materi-

als and landforms, was completed by Howes (1977). More recently, Plouffe (1996a,b, in press) conducted 1:100 000-scale surficial geology mapping in the Burns Lake (93 K/SW), Cunningham Lake (93 K/NW) and Binta Lake (93 F/11, 13, 14) regions. The ice flow history and Quaternary geology of the study area and surrounding regions are described by Levson *et al.* (1997a, 1998). The implications of these studies for mineral exploration, in terms of geochemical transport distance and direction, are discussed by Levson and Stumpf (1998) and Stumpf *et al.* (in prep.). Levson and Giles (1997) and Levson *et al.* (1997b) provided descriptions of till geochemistry programs previously conducted on the Nechako Plateau.

PHYSIOGRAPHY AND GEOLOGY

The Nechako Plateau is an area of low relief with surface elevations generally ranging from about 850 to 1500 metres above sea level. The Tetachuck Lake and Marilla map areas occur near the centre of the Nechako Reservoir system where the land rises to only about 500 m above lake level (Figures 1 and 2). Relief generally increases from east to west with the highest elevations (about 1370 m) in the Windfall Hills area (Figure 2). Tetachuck Lake, Chelaslie Arm and Ootsa Lake are all part of the Nechako Reservoir and are joined via Euchu Reach just east of the map sheets. These map areas are dominated by volcanic and sedimentary rocks of the Jurassic Hazelton Group as well as by mainly volcanic rocks of the Tertiary Ootsa Lake and Endako Groups. The bedrock geology of the Nechako River map area was described by Tipper (1963). The Pendleton Bay map area straddles the southern end of Babine Lake. Northeast of the lake, the map sheet is dominated by a low relief plateau area with elevations up to about 900 m asl (Figure 3). An area of relatively high relief occurs in the southeast corner of the map area where the highest peak is about 1400 m asl. The geology of the Pendleton Bay map area is discussed by Schiarizza and MacIntyre (1999).

Glacial drift is extensive in the Nechako Plateau and well developed flutings and drumlinoid ridges are dominant landform features. Although these landforms obscure the bedrock in many areas, small bedrock exposures can often be found at the up-ice end of crag-and-tail

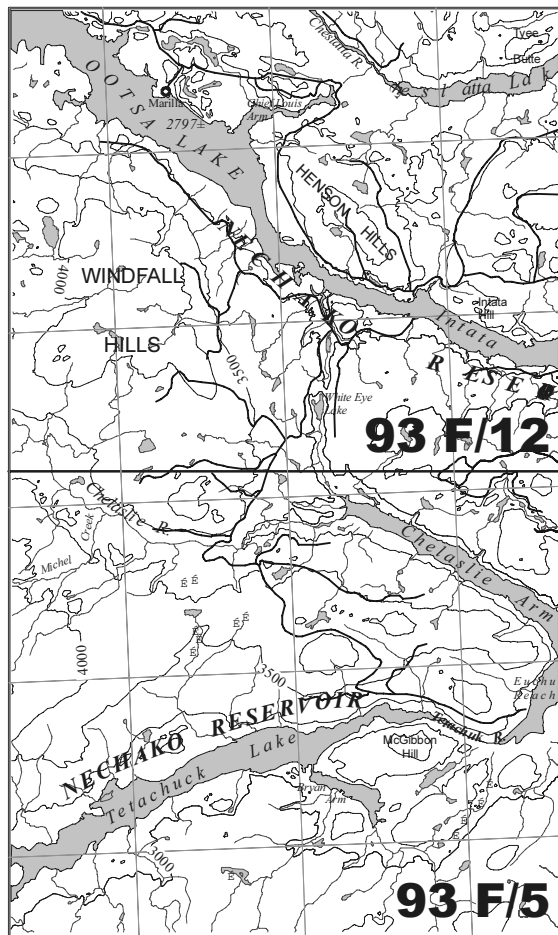


Figure 2. Physiography and access in the Tetachuck Lake (93 F/5) and Marilla (93 F/12) map areas. Road access south of Ootsa Lake is via private barge only. Note low relief; highest elevations are in the Windfall Hills (~1370 m) about 500 m above lake level. Contour interval 150 m (500 ft).

features. These landforms are locally well developed and their identification and application in mapping and exploration programs is probably under utilized. Other glacial features commonly present in the study area include stagnant ice topography, large esker complexes, glaciofluvial deposits and meltwater channels that developed during deglaciation. Recognition of these features is locally important for the identification of aggregate resources for road building and other construction purposes.

1998 TILL GEOCHEMISTRY SURVEYS

Regional till geochemical sampling in 1998 was completed in the, Tetachuck Lake, Marilla and east half of the Pendleton Bay map sheets (Figure 1). The primary objectives of till geo-

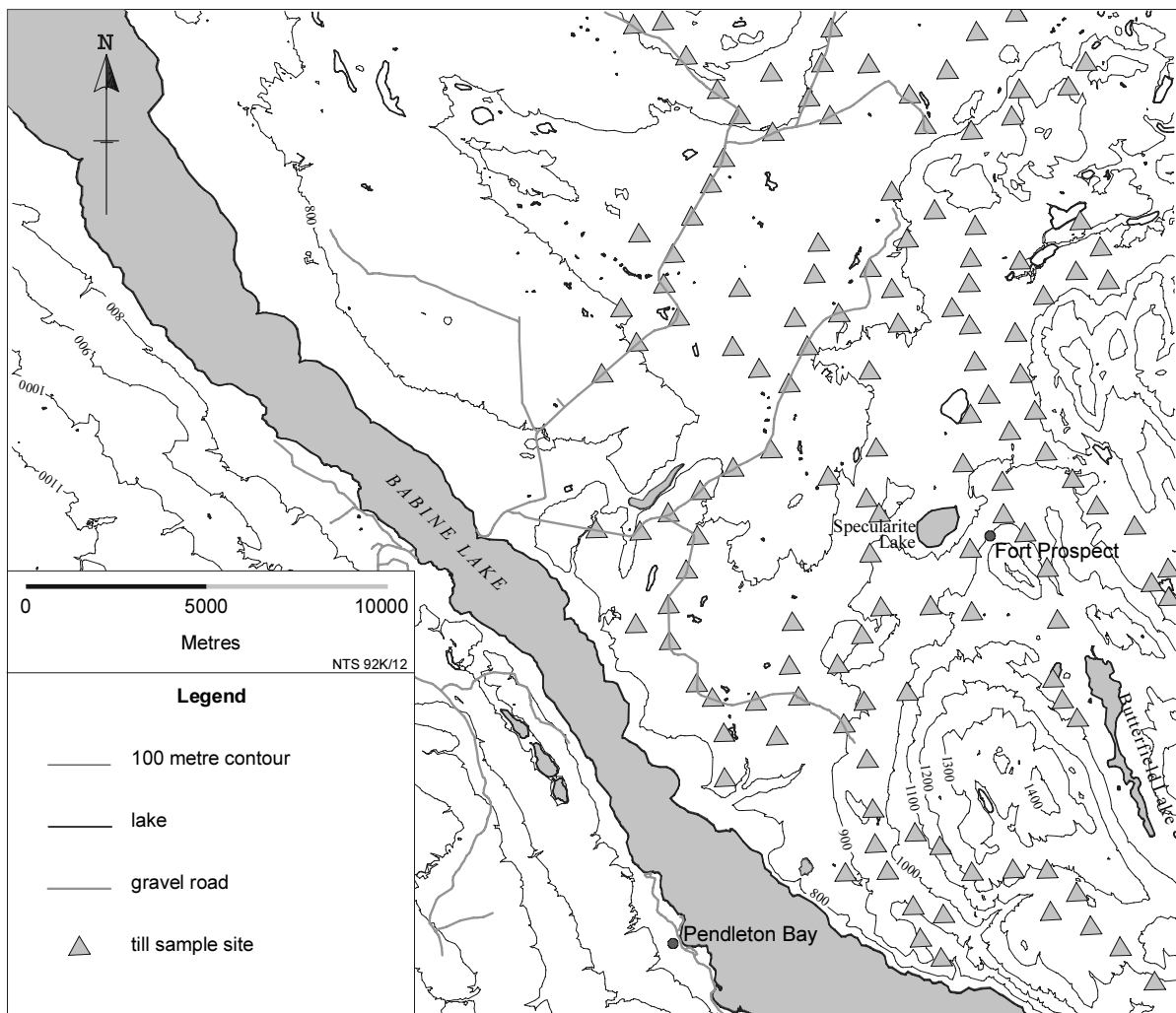


Figure 3. Regional till geochemical sites in the Pendleton Bay map area (93 K/12E). Case study till geochemical sample sites in the vicinity of the Fort mineral prospect are not shown.

chemical studies conducted in the region were to identify geochemically anomalous sites that might reflect areas of buried mineralization and to investigate patterns of glacial dispersal. Regional till geochemistry surveys previously conducted elsewhere in the Nechako Plateau for this purpose have been described by Levson and Giles (1997) and Levson *et al.* (1997b, 1998). The effects of glaciation on till geochemical dispersal patterns in west central British Columbia were discussed by Levson (1998) and Levson and Stumpf (1998).

Approximately 450 regional till geochemical samples were collected in the Tetachuck Lake, Marilla and east half of the Pendleton Bay map sheets. The distribution of samples in the Pendleton Bay map area is shown in Figure 3. In addition to samples taken in 1998, over 100 samples were collected in the Tetachuck Lake

and Marilla map areas in 1997. Till dispersal studies were also carried out in the vicinity of known gold and copper prospects including the Uduk Lake (93F/12) and Wolf (93K/12) prospects. Till and profile sampling were conducted at these sites to document glacial dispersal and mineral concentrations in various soil horizons. Sulphide-rich mineralized erratics were found at a number of sites that are not explained by known mineral showings and, in one region, define an dispersal train several kilometres in length.

QUATERNARY STRATIGRAPHY AND SIGNIFICANCE FOR EXPLORATION

The Quaternary stratigraphy of the study area was first described from exposures along the shores of Nechako Reservoir by Levson and

Giles (1997) and Levson *et al.* (1998). These sections provide a relatively rare record of pre-Late Wisconsinan events in the region. The only sub-till radiocarbon date reported from this area ($27,790 \pm 200$ BP; Beta-101017), was obtained on wood recovered from interstadial lacustrine deposits underlying till along Chelaslie Arm on Euchu Lake (Levson *et al.*, 1998). These deposits were mapped in detail in 1998 and were found to be much more extensive than previously thought. The interstadial unit consists of organic silts and clays, interpreted as lacustrine deposits, that are overlain by a thick glaciolacustrine, glaciofluvial and till sequence. Interstadial deposits are rare in central British Columbia.

The widespread presence of sub-till sediments in the Nechako Reservoir basin has important implications for interpretation of geochemical data in the region. For example, tills overlying older lacustrine and glaciolacustrine deposits will be enriched in clay-rich sediments that probably were not derived locally. Element concentrations within these tills, normally useful for locating buried mineral deposits, will therefore be diluted by the more regionally derived clays and will not be directly comparable with geochemical results from tills derived from more local sources. Sub-till clays are also significant because they may be an important controlling factor in the distribution of large landslides in the region. The clay rich sediments are relatively impermeable and highly plastic. They have been observed at the base of numerous large slumps in the study region, as well as in surrounding areas such as the Bulkley and Morice River valleys. They are commonly sheared with abundant slickensided surfaces. These observations suggest that the clays act as slip surfaces for these large slides. The spatial association of the clays with areas of active slumping suggests that detailed mapping of their distribution may aid in the identification of high slide hazard areas.

A section representative of the interstadial stratigraphy is provided in Figure 4. The lowest exposed unit (Unit 1, Figure 4) is a horizontally laminated silt with minor clay and sand. The unit generally coarsens upwards and shows increasing internal deformation towards the top, in the form of folded laminae and small scale, normal faulting. Abundant, finely disseminated, organ-

ics are present throughout much of the unit resulting in a dark grey to black color. These strata are interpreted as interstadial lacustrine sediments correlative with the radiocarbon dated unit described by Levson *et al.* (1998). An increase in rhythmic bedding towards the top of the unit may reflect more pronounced seasonal effects due to climate change associated with the onset of glaciation. Unit 2 (Figure 4) is a complex unit of fine sands and silts with horizontal to wavy bedding that is commonly folded and faulted. The general coarsening-upward trend in Unit 2 probably is due to the increase of more proximal (coarser) sedimentation associated with the advance of glaciers into the lake drainage area. Abundant deformation in the unit probably reflects lake bed instability caused by one or more of several glacially-induced processes such as ice-damming, increased glaciofluvial activity, fluctuating lake levels, rapid sedimentation, slope oversteepening and the advance of ice into the lake basin.

Unit 3 (Figure 4) consists of a remarkably widespread mud breccia that is intermittently exposed across a distance of about 10 kilometres. The breccia generally has a clay-rich matrix with silt and clay clasts that vary in shape from

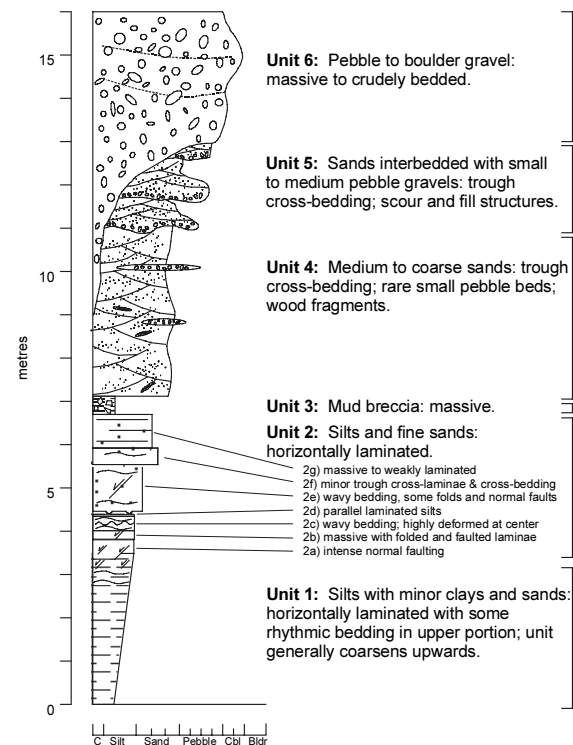


Figure 4. Stratigraphic section of interstadial site on Chelaslie Arm of Tetachuck Lake.

angular to rounded. Some of the clasts are rhythmically laminated. The breccia is interpreted as a mud flow deposit derived from a subaqueous failure of glaciolacustrine sediments. Clast angularity and size generally increase to the southeast, suggesting a source from that direction. The mud flow is sharply overlain by relatively coarse, trough cross-bedded sands and gravels (Units 4 to 6, Figure 4) of inferred fluvial and glaciofluvial origin. The mud breccia stratigraphically separates subaqueous and subaerial deposits and the catastrophic event that resulted in its deposition may have also been responsible for the change in depositional environment.

A widespread, massive, matrix-supported, dense, silty diamicton unit, interpreted as a till, stratigraphically overlies the stratified sands and gravels. Loose, massive to crudely bedded, sandy diamictons of inferred debris-flow origin are commonly interbedded in the gravels and sands that both underlie and overlie the till. The diamictons often have loaded or gradational contacts with the interbedded sediments. These deposits indicate that debris-flow deposition occurred during both the advance and retreat phases of the last glaciation.

Due to the widespread presence of these debris flow deposits in the study region, care must be taken to sample only basal tills while conducting till geochemistry programs. Fortunately, the extent of other surficial sediment types such as glaciolacustrine and glaciofluvial deposits in the study area is not great and tends to be concentrated in specific areas.

ICE-FLOW HISTORY AND EFFECTS ON DISPERSAL

Pendleton Bay map area

The ice flow history of the Babine Lake valley, west and northwest of the Pendleton Bay map area was described by Levson *et al.* (1997a). Glaciers flowing southeast along the Babine Lake valley were deflected to the east at the south end of the lake by east-flowing ice in the Bulkley River valley. In the Pendleton Bay map area, Plouffe (1996a) identified a few easterly-trending crag-and-tail forms on the northern periphery of the map sheet as well as a large number of glacial flutings, mainly in the north-

ern half of the map area, that generally show a southeast to east-northeast paleoflow direction (Figure 5). Although the down-ice flow direction can not be determined from the flutings alone, their association with the crag-and-tails suggests a paleoflow direction towards the southeast along Babine Lake in the northwest corner of the map area, gradually shifting towards easterly flow, and locally east-northeasterly flow, in the north central and northwest parts of the map area (Figure 5). Late Wisconsinan ice flow indicators described in this study generally conform to this pattern with the exceptions described below.

In the southeast corner of the map area, a number of southeast trending topographic ridges rise up to several hundred metres above the surrounding valleys. No glacial flow indicators were mapped by Plouffe (1996a) in this region. Topographic control on ice flow in this area is illustrated by a number of sites with well developed, valley parallel (110° to 155°) striae. With the development of a relatively thick regional ice sheet as glaciation progressed, the influence of topography on ice flow direction decreased. The eventual dominance of an ice centre to the west of the map area is reflected by easterly to north-easterly ice flow indicators including both large scale forms (i.e. crag-and-tails, drumlins and flutings) and small scale forms (striae, rat-tails and roches-moutonnées) throughout the region (Figure 5). At a few sites, valley-parallel striae are cross-cut by younger striae sets reflecting this regional flow. For example, at site 2 (Figure 5), southeast-trending flutes and roches-moutonnées are cross-cut by younger, east to east-northeast trending striae and roches-moutonnées.

Evidence for a gradual eastward migration of this ice centre is seen in the striae record at a number of sites. In the northeast corner of the map area, the oldest and most dominant striae sets invariably show east to east-northeast flow (Figure 5). Cross-cutting striae in this region indicate later flows to the northeast, southeast and south-southwest. These complicated patterns may reflect variable flow directions in the ice divide area. The best evidence for migration of an ice centre to at least the east side of the map area, comes from site 3, located along a valley side in the southeast corner of the map sheet at about 1050 m asl. A glacially molded and heavily striated outcrop at this site clearly indicates a westerly ice-flow direction. On a bedrock ridge

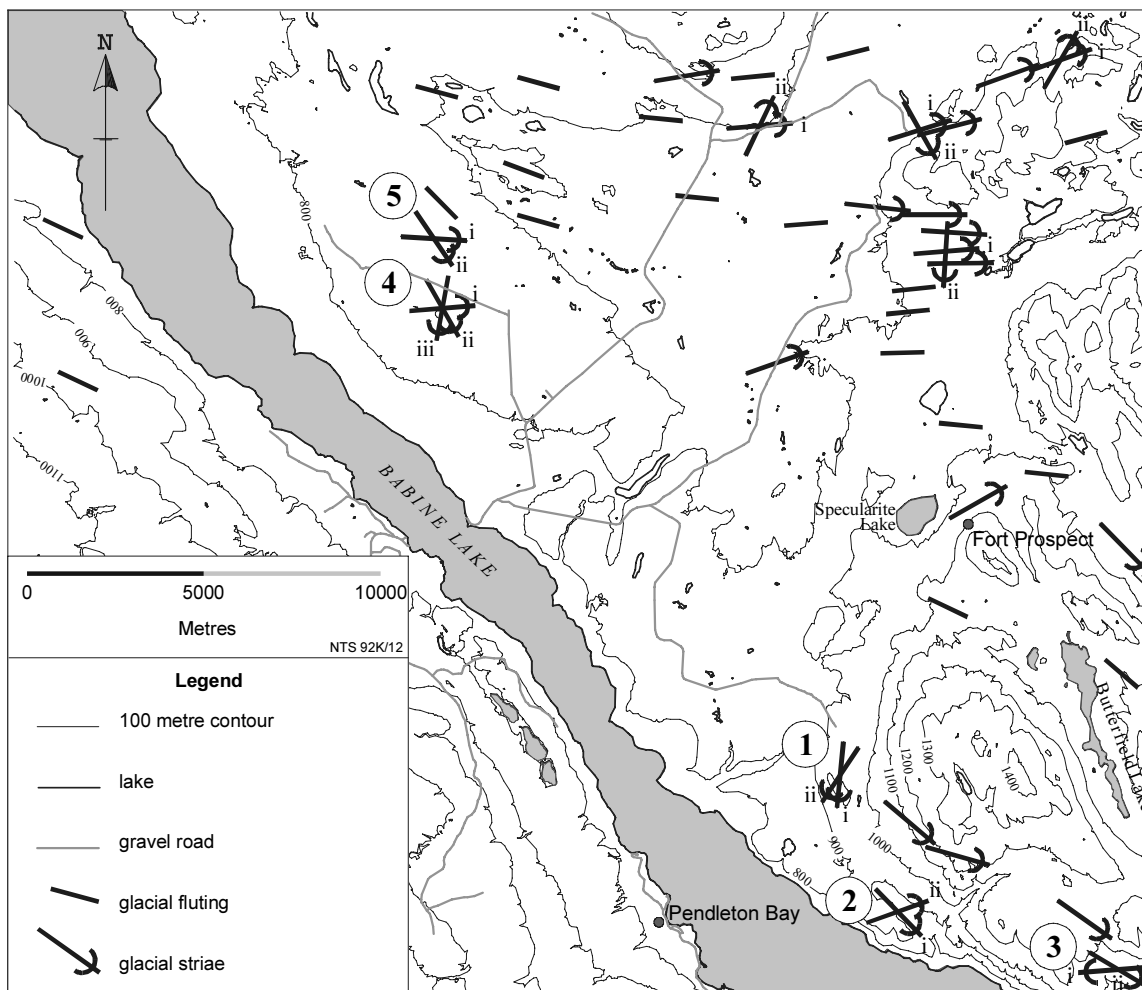


Figure 5. Inferred ice flow directions in the Pendleton Bay map sheet. At multiple striae sites, striae are shown in relative temporal sequence (i - oldest, ii - younger, etc.) at each site, but no time equivalence is suggested between sites. Striae data are from this study; fluting orientations are generalized from Plouffe (1996a). Contour intervals are in metres above sea level.

crest at about 975 m asl (site 1, Figure 5) striae record a strong south-southeast (190°) flow followed by a relatively weak southwesterly (218°) flow. Finally, at sites 4 and 5 in a low relief area in the north central part of the map sheet, ice flow indicators show a progressive shift from easterly (090° - 119°) to southeasterly (145° - 155°), to south-southwesterly (180° - 195°) flow. Although the latest westerly and southwesterly paleoflow at these four sites may locally be explained by late-stage, topographically controlled flow into the Babine Lake valley, it is unlikely that the same pattern would be observed across much of the map area in a variety of topographic settings. Instead, an ice divide located east of the Babine Lake valley is suggested as the cause of the westerly flow in this area. Regardless, evidence for this event in the Pendleton Bay map sheet is rare

and confined mainly to small scale features and, as a consequence, its effects on glacial dispersal in the area are probably not extensive.

Marilla and Tetachuck Lake map areas

The dominant regional ice flow direction in the Marilla and Tetachuck map sheets was northeasterly. This is clearly indicated by well developed northeast trending crag-and-tail ridges, drumlinoids, flutings, roches-moutonnées and striae throughout the map areas. An average paleoflow direction of about 065° is consistent with that reported by Tipper (1963) and Plouffe (in press) in the surrounding map sheets. The extent of well developed streamlined landforms associated with this northeasterly flow strongly

suggests that glacial dispersal in these map sheets was controlled mainly by this event. This is also supported by till geochemical studies in the Uduk Lake area and at two other sites in the Nechako River map area (O'Brien *et al.*, 1997).

Anomalous westward ice flow during the Late Wisconsinan glaciation, recently described by Levson and Stumpf (1998), Levson *et al.* (1997a, 1998), and Stumpf *et al.* (in prep) from the region east of the study area, was also found this field season at a few sites near the west side of the Marilla map sheet as well as in the Pendleton Bay map area (see above). This indicates that a Late Wisconsinan ice divide was located east of the Tweedsmuir area, subjecting that region to westerly ice flow and consequent west-directed glacial dispersal. Westerly flow was independent of large topographic barriers such as the Tweedsmuir, Babine and Hazelton mountains and occurred when ice centres over the Hazelton and Coast mountains migrated eastward into the Interior Plateau. Evidence for westerly flow was only found in the westernmost part of the map region and is absent in the east. Consequently, the effects of westward flow on geochemical dispersal are expected to rapidly diminish eastward. Westerly ice-flow locally extended to the end of the last glaciation as indicated by preservation of paleoflow indicators at unprotected low elevation sites. These observations confirm that the maximum buildup of interior ice extended late into the last glaciation and that a topographically controlled, late-glacial, ice-flow phase was short-lived in this part of the Interior Plateau (Levson *et al.*, 1998).

CONCLUSIONS AND RECOMMENDATIONS

Stratigraphic studies indicate that clay-rich, interstadial lacustrine, and glaciolacustrine sediments are widespread in the Nechako Reservoir basin. These sub-till clay-rich sediments are a probable cause of slope instability in the region and their presence has important implications for interpretation of geochemical data. Element concentrations in overlying tills probably are diluted by these regionally derived clays and therefore may not be directly comparable with other regional till geochemical results. Surficial mapping in the study area indicates the widespread presence of basal till but debris flow deposits,

glaciolacustrine sediments and glaciofluvial deposits overlie till in a number of areas. As a consequence, till geochemical programs should be effective in the map areas but care must be taken to sample only basal tills. In some areas till sampling will be hindered by glaciolacustrine or glaciofluvial surficial sediments.

Results of ice-flow studies indicate that for most areas the dominant flow-direction was easterly. Glacial dispersal patterns appear to be dominated by this regional ice-flow direction. However, in the westernmost parts of the study area, a regionally anomalous, westerly ice-flow event occurred. Westerly ice flow appears to have occurred when ice centres over the Hazelton and Coast mountains migrated eastward into the Interior Plateau. Evidence for west flow is most readily found west of the study areas and diminishes eastward suggesting that the study areas were near the eastward limit of the divide or that ice-centre migration east of those areas was not long-lived. Consequently, westward flow apparently did not influence glacial dispersal to any great extent in valleys such as the Babine Lake valley but it did have a significant effect further west. Since evidence for westward flow is preserved in valleys at unprotected, low elevation sites, the erosional effects of the later, topographically-controlled flows must have been minimal. These observations suggest that the maximum buildup of interior ice extended late into the last glaciation and that a topographically controlled, late-glacial, ice-flow phase was short-lived in this part of the Nechako Plateau.

Implications of shifting ice divides for exploration are significant because 180° changes in ice flow direction and complex glacial dispersal patterns are possible. Explorationists working in these regions should base paleoflow interpretations on directional features such as roches-moutonnées, drumlinoids and rat-tails. Some locations show both eastward and westward flow directions, even on outcrops that occur in close proximity, and therefore a clear understanding of the temporal relationships of multiple flow events is required. We recommend that inferences regarding glacial dispersal directions in this area be based on regional data and that sampling strategies initially be designed to evaluate the dominant dispersal direction before intensive 'up-ice' surveys are conducted.

ACKNOWLEDGMENTS

Quaternary stratigraphy and ice-flow studies in the area were conducted in collaboration with Alain Plouffe from the Geological Survey of Canada. Field investigations were conducted in collaboration with Don McClenagan of the University of Victoria. The cooperation of Bert Struik and Don MacIntyre through the NATMAP program is much appreciated. Analytical assistance and quality control on all laboratory analyses were provided by Ray Lett. Helicopter support was provided by Norm Rafuse of Westland Helicopters Inc. Sample preparation was completed by Rossbacher Laboratory Limited. Figures 3, 4 and 5 were drafted by Isaac Ferbey.

REFERENCES

- Howes, D.E. (1977): Terrain inventory and Late Pleistocene history of the southern part of the Nechako Plateau; *B.C. Ministry of Environment*, RAB Bulletin 1, 29 pages and 1:100,000 scale map.
- Levson, V.M. (1998): Glaciation and its effects on the dispersal and burial of mineral deposits in west-central British Columbia; *in* New Geological Constraints on Mesozoic to Tertiary Metallogenesis and on Mineral Exploration in Central British Columbia: Nechako NATMAP Project Short Course Extended Abstracts, L.C. Struik, and D.G. MacIntyre, Editors, *Geological Association of Canada*, Cordilleran Section, 8 pages.
- Levson, V.M. and Giles, T.R. (1997): Quaternary geology and till geochemistry studies in the Nechako and Fraser Plateaus, central British Columbia; *in* Interior Plateau Geoscience Project: Summary of Geological, Geochemical and Geophysical Studies, L.J. Diakow, and J.M. Newell, Editors, *Geological Survey of Canada*, Open File 3448 and *B. C. Ministry of Employment and Investment*, Paper 1997-2, pages 121-145.
- Levson, V.M., Stumpf, A.J., Meldrum, D.G., O'Brien, E.K., and Broster, B.E. (1997a): Quaternary geology and ice flow history of the Babine Lake region: (NTS 93 L/NE, M/SE); *in* Geological Fieldwork 1996, D. V. Lefebure, W. J. McMillan, and J. G. McArthur, Editors, *B. C. Ministry of Employment and Investment*, Paper 1997-1, pages 427-438.
- Levson, V.M., Meldrum, D.G., Cook, S.J., Stumpf, A.J., O'Brien, E.K., Churchill, C., Coneys, A.M. and Broster, B.E. (1997b): Till geochemical studies in the Babine porphyry belt: regional surveys and deposit-scale studies (NTS 93 L/16, M/1, M/2, M/7, M/8); *in* Geological Fieldwork 1996, D.V. Lefebure, W. J. McMillan, and J.G. McArthur, Editors, *B. C. Ministry of Employment and Investment*, Paper 1997-1, pages 457-466.
- Levson, V.M. and Stumpf, A.J. (1998): Glacial controls on geochemical transport distance and direction in north-central Stikinia: implications for exploration; *in* Cordillera Revisited: Recent Developments in Cordilleran Geology, Tectonics and Mineral Deposits Short Course Notes, P. Mustard, and S. Gareau, Editors, *Geological Association of Canada*, Cordilleran Section, pages 68-75.
- Levson, V.M., Stumpf, A.J., and Stuart, A.J. (1998): Quaternary geology and ice flow studies in the Smithers and Hazelton map areas (93 L and M): implications for exploration; *in* Geological Fieldwork 1997, *B.C. Ministry of Employment and Investment*, Paper 1998-1, pages 5-1 to 5-8.
- Mate D. and Levson, V.M. (1999): Quaternary geology of the Marilla map area (93F/12), British Columbia; *in* Geological Fieldwork 1998, *B.C. Ministry of Energy and Mines*, Paper 1999-1, this volume.
- MacIntyre, D.G. and Struik, L.C. (1999): Nechako NATMAP Project Overview, central British Columbia, year four; *in* Geological Fieldwork 1998, *B.C. Ministry of Energy and Mines*, Paper 1999-1, this volume.
- O'Brien, E.K., Levson, V.M. and Broster, B.E. (1997): Till geochemical dispersal in central British Columbia, *B.C. Ministry of Employment and Investment*, Open File 1997-12.
- Plouffe, A. (1996a): Surficial geology, Cunningham Lake (93K/NW); *Geological Survey of Canada*, Open File 3183 (1:100 000 scale map).
- Plouffe, A. (1996b): Surficial geology, Burns Lake (93K/SW); *Geological Survey of Canada*, Open File 3184 (1:100 000 scale map).
- Plouffe, A. (in press): Surficial geology, Binta Lake, British Columbia (93 F/11, 13, and 14), *Geological Survey of Canada*, Open file 3640, (1:100 000 scale map).
- Schiarizza, P. and MacIntyre, D.G. (1999): Geology of the Babine Lake - Takla Lake area, central British Columbia (93K/11, 12, 13, 14; 93N/3, 4, 5, 6); *in* Geological Fieldwork 1998, *B. C. Ministry of Employment and Investment*, Paper 1999-1, this volume.

Stumpf, A.J., Broster, B.E. and Levson, V.M. (in prep.): Shifts in Late Wisconsinan ice sheet centres, west-central British Columbia, Canada; to be submitted to the Canadian Journal of Earth Sciences.

Tipper, H.W. (1963): Nechako River map-area, British Columbia; *Geological Survey of Canada*, Memoir 324, 59 pages.

QUATERNARY GEOLOGY OF THE MARILLA MAP SHEET (NTS 93 F/12)

By David J. Mate (University of Victoria) and Victor M. Levson (B.C. Geological Survey)

KEYWORDS: geomorphology, ice-flow, landslides, Nechako Plateau, Quaternary stratigraphy, surficial geology

INTRODUCTION

This paper summarizes surficial geology, Quaternary stratigraphy and ice flow history studies conducted in the Marilla map area (NTS 93 F/12) in central British Columbia as part of the Nechako National Mapping Project (NATMAP) (Figure 1). Regional scale (1:50 000) till sampling was also undertaken and is summarized by Levson *et al.* (1999). This work expands preliminary surficial geology mapping and till sampling from the previous summer (Levson *et al.*, 1998).

Mapping objectives were to produce a

for future drift prospecting work and help aid in the interpretation of till geochemical data.

RELATED STUDIES

Mapping of Quaternary deposits in the Interior Plateau was pioneered by Tipper (1971). Terrain mapping at a scale of 1:50 000 was completed by Howes (1977) for several NTS map sheets, south and east of the Marilla area. More recent surficial mapping within the Interior Plateau is a component of the Nechako NATMAP project. Several 1:100 000 surficial geology maps produced by Plouffe (1994, 1996) cover central parts of the Nechako Plateau. A summary of 1:50 000 scale Quaternary geology mapping projects in the Nechako Plateau is provided by Levson and Giles (1997). In conjunction with this fieldwork, NTS map sheet 93 F/5 was mapped by Levson *et al.* (1999).

FIELD PROCEDURES

Air photo interpretation, field checking and stratigraphic and sedimentologic investigations were used to complete surficial geology mapping. Over 180 field check stations were compiled for the map sheet. At each field station the mappable surficial material was recorded and described (sediment texture, areal extent of map unit, and surface topography). Mapping followed guidelines of the Terrain Classification System for British Columbia (Howes and Kenk, 1997). Stratigraphic and sedimentologic studies were carried out on large Quaternary exposures within the area. The regional ice-flow history was determined from the study of striae, crag-and-tail features, and flutings.

Road access within the map area is quite extensive, consisting mostly of logging roads and some well maintained secondary roads. A forest company barge was needed to access

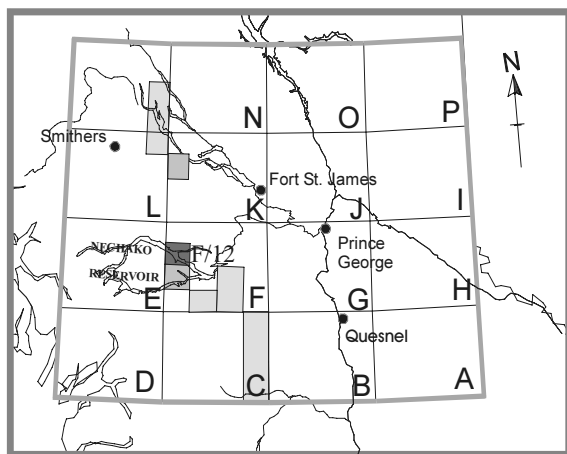


Figure 1. Location of study area in central British Columbia. Area straddles the Ootsa Lake reach of the Nechako Reservoir.

1:50 000 scale surficial geology map and understand the distribution of Quaternary deposits and ice flow patterns for the Marilla area. Objectives of stratigraphic and sedimentologic studies were to interpret the glacial history of the area. Data from these studies will help locate suitable areas



Photo 1. Aerial view of Cheslatta Lake showing general landscape characteristics of the study area. Cheslatta River can be seen entering Cheslatta Lake from the left of the picture.

roads south of Ootsa Lake. Places that could not be reached by truck were accessed using an all terrain vehicle and motor boat.

PHYSIOGRAPHY AND LANDFORMS

The Marilla map area occurs within the Nechako Plateau physiographic region (Holland, 1976). A general physiographic description of the study area is provided by Levson *et al.* (1999; see their Figure 2). Low relief and large surfaces of flat or gently rolling topography are diagnostic features of the plateau, which has elevations up to about 1500 m (Photo 1). The plateau is flanked by the Hazelton and Coast mountains to the west and the Skeena and Omineca ranges to the north. The Quanchus Range (Mt. Wells, Tweedsmuir Peak and Michel Peak) lie immediately west of the map area in Tweedsmuir park, while the Fawnie and Nechako ranges are to the southeast. The majority of the ground surface is covered by glacial drift with very little exposed bedrock.

The dominant landforms within the map area are flutings and drumlinoid ridges. Up-ice (stoss ends) of these features are commonly bedrock knobs, while down-ice (lee) portions

appear as ridges of glacial diamicton. Well defined depressions with flat bottoms are consistently seen at the stoss ends and around the sides of these streamlined landforms. These depressions are commonly bog filled. Occasionally crescent-shaped lakes occur at the stoss end of drumlins and flutes (Photo 2). These depressions resemble crescentic scours and lateral furrows as described by Shaw and Sharpe (1987). Therefore, it is quite likely that drumlins and flutes within the map area are remnant ridges formed by subglacial meltwater erosion. Esker complexes, glaciofluvial deposits and meltwater channels can also be found within the map area and rare glaciolacustrine deposits are found at elevations below 950 m.

QUATERNARY STRATIGRAPHY

Stratigraphic information was collected from large, well exposed Quaternary sections along Ootsa Lake on the Nechako Reservoir and Cheslatta River. Some sections on the Cheslatta River occur in the southern part of the Takysie Lake map sheet (NTS 93 F/13). A summary of the Quaternary stratigraphy from these areas is provided below. Stratigraphy from other parts of



Photo 2. Crescentic-shaped lake at the stoss (up-ice) end of a bedrock ridge. Ice-flow direction is from right to left. Ootsa Lake is in the background and Marilla is located at the end of the road on the far right.

the reservoir have been described by Levson and Giles (1997) and Levson *et al.* (1998).

Surficial sediments encountered within the map sheet are mainly a product of the last or Late Wisconsinan glaciation (Tipper, 1971; Levson *et al.*, 1998). Pre-Late Wisconsinan sites are rare on the Nechako Plateau but a few sites have been described by Harington *et al.* (1974), Levson and Giles (1997), Plouffe and Jetté (1997) and Levson *et al.* (1998). The closest of these sites to the study area can be found off Euchu Reach on Chelaslie Arm. Radiocarbon dates from organics in sediments under till at these sites, generally range from about 27,000 to >45,000 years BP and correspond to the Olympia Nonglacial interval. Hence, these dates support a Late Wisconsinan age (Fraser Glaciation) for the glacial drift overlying these older organic-rich deposits.

The most common stratigraphic unit in the map area is a massive diamicton unit. This unit is poorly sorted, and well jointed, with striated and faceted clasts, strong fissility and high density. It has clear to sharp lower contacts. This diamiction is consistently found in stratigraphic sections throughout the map area and is inter-

preted as till. Till is defined as a poorly sorted sediment deposited directly from glacier ice with little or no reworking by water or gravity (Dreimanis, 1989). The till is stratigraphically underlain by well to crudely stratified sands and gravels interpreted as advance-phase glaciofluvial deposits. Commonly these sediments are moderately well to well sorted, pebble and cobble gravels and sands. Clasts are typically rounded to well rounded. These sediments also have a moderate to high density and often contain faults and soft sediment deformation features. Locally, similar sands and gravels overlie till and are interpreted as being glaciofluvial and fluvial in origin. Overall, the density of these glaciofluvial and fluvial deposits is low. Local veneers of poorly sorted sand and gravel, formed from washing of the till surface are present within the map area. Surprisingly, glaciofluvial sand and gravel deposits useful for road building purposes are rare in much of the area.

Other sediments commonly found in Quaternary sections in the region are diamictons that originated as glacigenic debris flows. These diamictons possess a low to moderate density and are commonly interbedded with and contain



Photo 3. Interstadial site on Ootsa Lake. The basal unit is till which is overlain by organic-bearing, blue-grey, fine sands (at the level of the sledge hammer), advance-phase glaciofluvial sediments, and till. Crystal Huscroft for scale.

lenses of silt, sand and gravel. Texturally, debris flow diamictons are usually more sandy than basally derived diamictons and have clear to sharp lower contacts. Debris flow units occur in both advance and retreat phase glacial events. They can also be deposited subaerially in glaciofluvial environments or as subaqueous flows in glaciolacustrine environments.

The most complete stratigraphic section in the map area occurs at a newly discovered interstadial site found during this summer's fieldwork along the Nechako Reservoir (Photo 3). The basal unit of this section is a massive, dense, diamicton, containing striated clasts and interpreted as till. Directly overlying it is a blue-grey, very fine sand with silt and clay laminations. Thin lenses and small fragments of organic detritus are present within this unit. This package is interpreted as being lacustrine and is overlain by advance-phase glaciofluvial sediments. A massive, dense, matrix-supported diamicton (interpreted as till) sharply overlies the entire sequence. Rare sand lenses were present near the top of the unit.

LANDSLIDE STUDIES

A number of rotational landslides present along the Cheslatta River were investigated during stratigraphic studies in the region. These slides probably result in increased siltation in the river and locally may pose a safety hazard. Rotational landslides form along concave slip surfaces with displaced material experiencing little internal deformation (Cruden and Varnes, 1996). Understanding the processes that trigger slides along the river has been aided by stratigraphic work.

Longitudinal profiles, determining the surface topography, and detailed field observations were made at two landslides along the river. Evidence of back-tilted slump blocks (trees on slump blocks leaning back towards the main scarp) and sag ponds helped classify these slides. Both slides have an amphitheatre shape with steep, curved head scarps, and mudflows at their bases. The largest slide was approximately 230 m wide with a 3 m high head scarp and had three separate slump blocks. This slide was found on the south side of Cheslatta River close to where it enters Cheslatta Lake (Photo 4). The

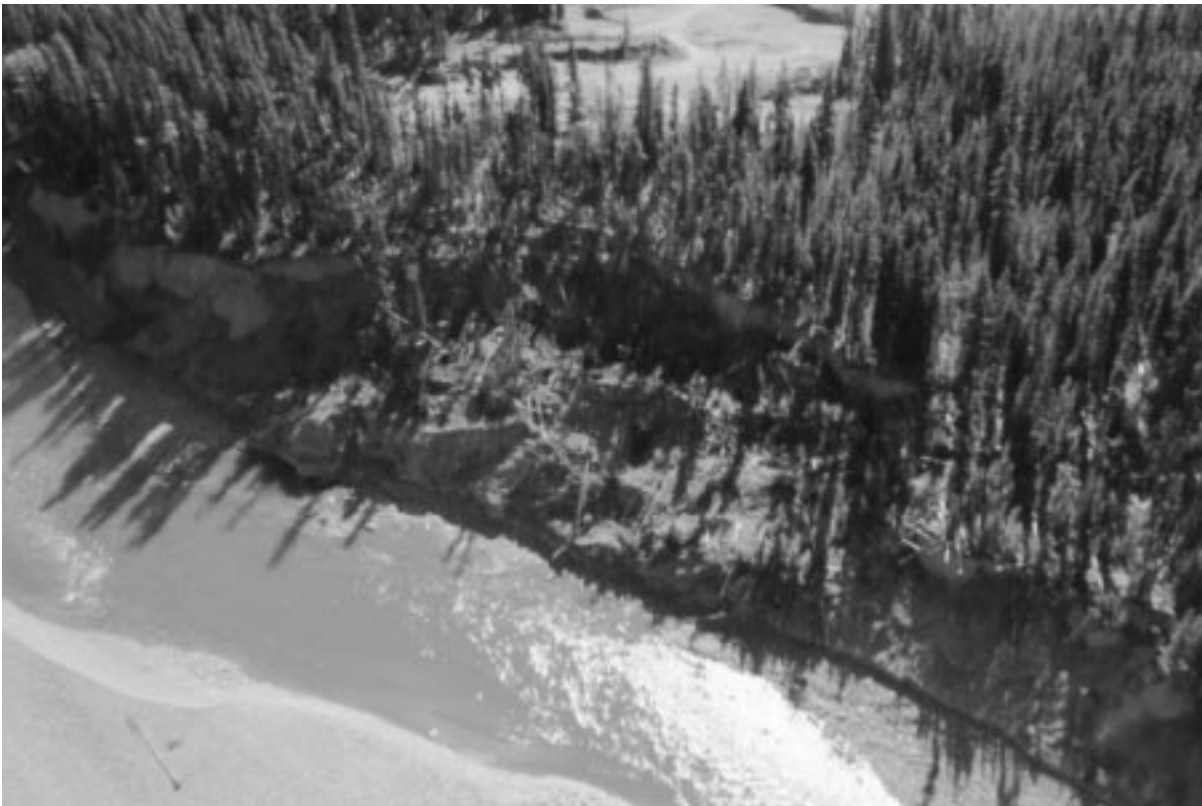


Photo 4. Rotational landslide on the south side of Cheslatta River close to Cheslatta Lake. Note presence of numerous uprooted trees and erosive, turbulent river water flowing along toe of slide.

second slide, was 34 m wide with a 6 m high head scarp and had one slump block. It was found close to the head waters of Cheslatta River. The two factors thought to be responsible for triggering both landslides were the presence of a deep, basal, interbedded very fine sand, silt and clay unit and the removal of material from the toe of each slide by river undercutting.

The presence of basal, interbedded very fine sands, silts and clays is significant because they provide a potential slip surface for the slide to initiate along. At both sites this unit was semi-continuous, highly sheared and brecciated. Bedding plane and slickenside measurements within this unit locally dip toward the main body of the slide (Photo 5). Erosion at high water level (Photo 6) within the Cheslatta River was responsible for undercutting at the toe of each slide (Photo 7). When material was eroded from the toe of each slide, slopes steepened, became unstable, and failed. Eroded material is replaced by material from above, perpetuating the landslide processes.

ICE-FLOW HISTORY

Glacial ice flowing off the Coast Mountains moved in an east and northeast direction onto the Nechako Plateau (Tipper, 1971). Ice flow direction within the map area is dominantly northeast and is reflected by the orientation of large scale landforms (crag-and-tail features, drumlins and glacial flutings) and by striae measurements from exposed bedrock. These data show a dominant regional ice-flow direction between 68° and 75° . Some striae measurements at low elevations along Ootsa Lake provided evidence of valley-parallel (topographically controlled) ice-flow. Measured striae at these sites ranged from 125° to 150° . A roche-moutonnée showing signs of anomalous westerly ice-flow was found at one site in the northwest corner of the map sheet. Striae oriented at 300° were found on east facing surfaces of this form. Westerly ice flow, interpreted as a late glacial event has been observed in surrounding areas but evidence for this event is not widespread in this map sheet (Levson *et al.*, 1999).



Photo 5. Brecciated and sheared, interbedded very fine sands, silts and clays at base of a landslide along Cheslatta River. Beds dip into the slope at 37° to 54° . 20 cm knife for scale.



Photo 6. Evidence of high water level along Cheslatta River (dark line close to base of section) roughly 3 meters above river level. Stephen Mate for scale.



Photo 7. Evidence of undercutting along banks of the Cheslatta River. This deep scour occurs at maximum water level just above the till-bedrock interface. Stephen Mate for scale.

SUMMARY

Quaternary geology studies within the Marilla map area reveal extensive areas of rolling ground moraine with a thick till cover. This material was deposited during the Late Wisconsinan. Numerous bog and swamp deposits are present throughout the area. They commonly form in crescent-shaped erosional depressions that wrap around fluted landforms and are interpreted as large subglacial meltwater erosion features

The regional ice flow direction in the map area is approximately 68° to 75° . Mineral dispersal is expected to reflect this trend. However, mineral dispersal patterns in the northwest corner of the map sheet, where evidence of westerly ice-flow indicators are found, may be more complicated. More detailed work will be needed in this part of the map area to gain a better understanding of the ice-flow history and effects on dispersal.

ACKNOWLEDGEMENTS

Special thanks is extended to Andrew Stuart who collaborated in field work throughout this project. Quaternary stratigraphy and ice-flow studies were also conducted in collaboration with Alain Plouffe from the Geological Survey of Canada. Bert Struik and Alain Plouffe, through the Nechako NATMAP project, provided much appreciated support. Volunteer field assistance was provided by Stephen Mate. Crystal Huscroft and Steve Williams also provided temporary assistance. Special thanks to Fiore Milinazzo and Kevin Partington from the Burns Lake Ministry of Forests office for providing a float plane flight over the map area.

REFERENCES

- Cruden, D.M. and Varnes, D.J. (1996): Landslide types and processes; *in* Landslides: Investigation and Mitigation, A.K. Turner, and R.L. Schuster, Editors, *National Academy Press*, Washington D.C., pages 36-75.

- Dreimanis, A. (1989): Tills: Their genetic terminology and classification; *in* Genetic Classification of Glacigenic Deposits, R.P. Goldthwait, and C.L. Matsch, Editors, *A.A. Balkema*, Rotterdam, pages 17-83.
- Harington, C.R., Tipper, H.W. and Mott, R.J. (1974): Mammoth from Babine Lake British Columbia; *Canadian Journal of Earth Sciences*, Volume 11, pages 285 – 303.
- Holland, S.S. (1976): Landforms of British Columbia, a physiographic outline; *B.C. Ministry of Energy, Mines and Petroleum Resources*, Bulletin 48, 138 pages.
- Howes, D.E. (1977): Terrain inventory and Late Pleistocene history of the southern part of the Nechako Plateau; *B.C. Ministry of Lands and Parks*, RAB Bulletin 1, 29 pages.
- Howes, D.E., and Kenk, E. (Editors)(1997): Terrain classification system for British Columbia Ministry of Environment, *British Columbia Ministry of Environment*, Manual 10, version 2, 102 pages.
- Levson, V.M. and Giles, T.R. (1997): Quaternary geology and till geochemistry studies in the Nechako and Fraser Plateaus, central British Columbia; *in* Interior Plateau Geoscience Project: Summary of Geological, Geochemical and Geophysical Studies, L.J. Diakow and J.M. Newell, Editors, *Geological Survey of Canada* Open File 3448 and *B.C. Ministry of Employment and Investment*, Paper 1997-2, pages 121-145.
- Levson, V.M., Stumpf, A.J., and Stuart, A.J. (1998): Quaternary geology and ice-flow studies in the Smithers and Hazelton map areas (93 L and M): Implications for Exploration; *in* Geological Fieldwork 1997, *B.C. Ministry of Employment and Investment*, Paper 1998-1, pages 5-1 to 5-8.
- Levson, V.M., Mate, D.J., and Stuart, A.J. (1999): Quaternary geology and drift prospecting studies in the north central Nechako Plateau (93 F and K): *in* Geological Fieldwork 1998, *B.C. Ministry of Energy and Mines*, Paper 1999-1, this volume.
- Plouffe, A. (1994): Surficial geology, Chuchi Lake (93N/SE) and Tezzeron Lake (93K/NE), British Columbia; *Geological Survey of Canada*, Open Files 2842 and 2846 (1:100 000 maps).
- Plouffe, A. (1996): Surficial geology, Tsayta Lake (93N/SW), Fraser Lake (93K/SE), Cunningham Lake (93K/NW), Burns Lake (93K/SW), Manson Creek (93N/NE) and Old Hogem (93N/NW); *Geological Survey of Canada*, Open Files 3071, 3182, 3183, 3184, 3312, and 3313 (1:100 000 maps).
- Plouffe, A. and Jetté, H. (1997): Middle Wisconsinan sediments and paleoecology of central British Columbia: sites at Necoslie and Nautley Rivers; *Canadian Journal of Earth Sciences*, Volume 34, pages 200-208.
- Shaw, J., and Sharpe, D.R. (1987): Drumlin formation by subglacial meltwater erosion; *Canadian Journal of Earth Sciences*, Volume 28, pages 2316-2322.
- Tipper, H.W. (1971): Glacial geomorphology and Pleistocene history of central British Columbia; *Geological Survey of Canada*, Bulletin 196, 89 pages.

GEOLOGY OF THE BABINE LAKE - TAKLA LAKE AREA, CENTRAL BRITISH COLUMBIA (93K/11, 12, 13, 14; 93N/3, 4, 5, 6)

By Paul Schiarizza and Don MacIntyre

(British Columbia Geological Survey Branch contribution to the Nechako NATMAP Project)

KEYWORDS: Bedrock mapping, Nechako Natmap, Stikine Terrane, Asitka Group, Takla Group, Hazelton Group, Cache Creek Complex, Sitlika assemblage, Trembleur ultramafic unit, North Arm succession, ophiolite, sheeted dikes, Fort showing.

INTRODUCTION

This paper summarizes the results of bedrock mapping in the area between Babine Lake and Takla Lake in central British Columbia (Figure 1). This work was done as part of the Nechako Natmap project (see MacIntyre and Struik, 1999, this volume). The 1998 bedrock mapping crew was comprised of Don MacIntyre and Paul Schiarizza as co-leaders and geology students Angelique Justason (Camosun College), Sheldon Modeland (University of Victoria), Stephen Munzar (University of British Columbia) and Deanne Tackaberry (University of Victoria). The primary objective in 1998 was to complete mapping in the northwest quadrant of the Fort Fraser (93K) map sheet. This work was started in 1997 with preliminary mapping of the Tochcha Lake (93K/13) map sheet (MacIntyre *et al.*, 1998). It also builds on mapping by Ash and Macdonald (1993) and Ash *et al.* (1993) around Stuart Lake, and incorporates data gathered by the GSC Natmap crew in the vicinity of Trembleur Lake (Hrudey and Struik, 1998). Within most of the area, however, the only previous regional mapping dates back to Armstrong (1949).

From early June until the end of August, the bedrock geology of NTS map sheets 93K/11, 12, 14 and 93N/3 (Figure 1) were mapped at 1:100 000 scale. In addition, fill-in mapping was done in map sheets 93K/13, 93N/4 and 93N/5, which had been largely completed in 1997 (MacIntyre *et al.*, 1998; Schiarizza *et al.*, 1998). This work provides continuity between Natmap programs concentrated on the Sitlika assemblage in west-

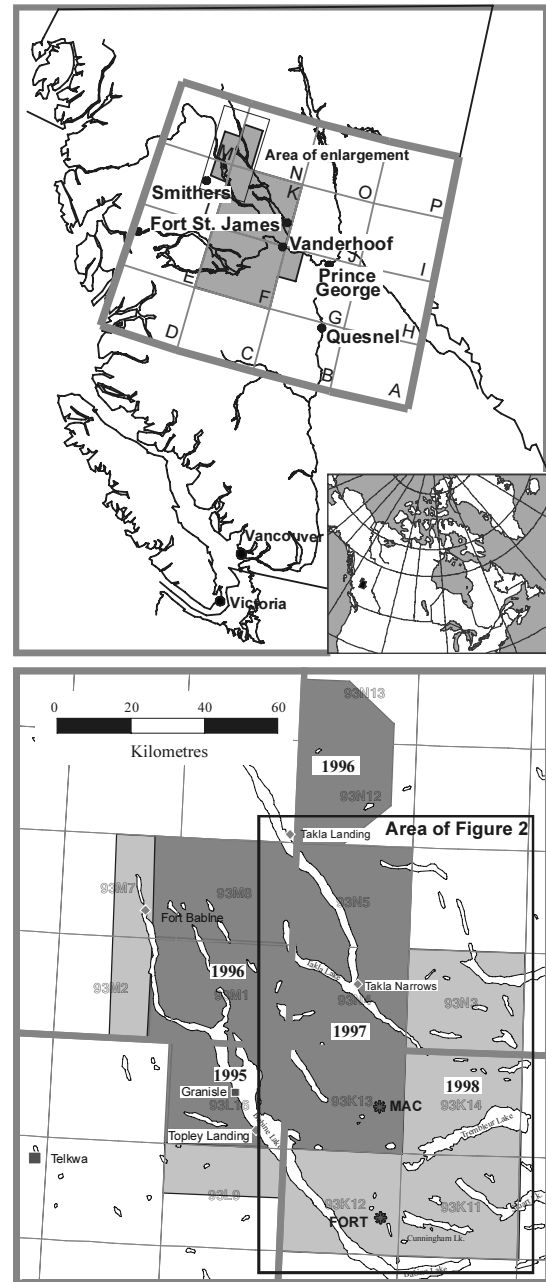


Figure 1. Location of bedrock mapping completed in 1998. Inset shows location relative to the Nechako Natmap Project (light grey shading), central British Columbia. Also shown is the area covered by Figure 2.

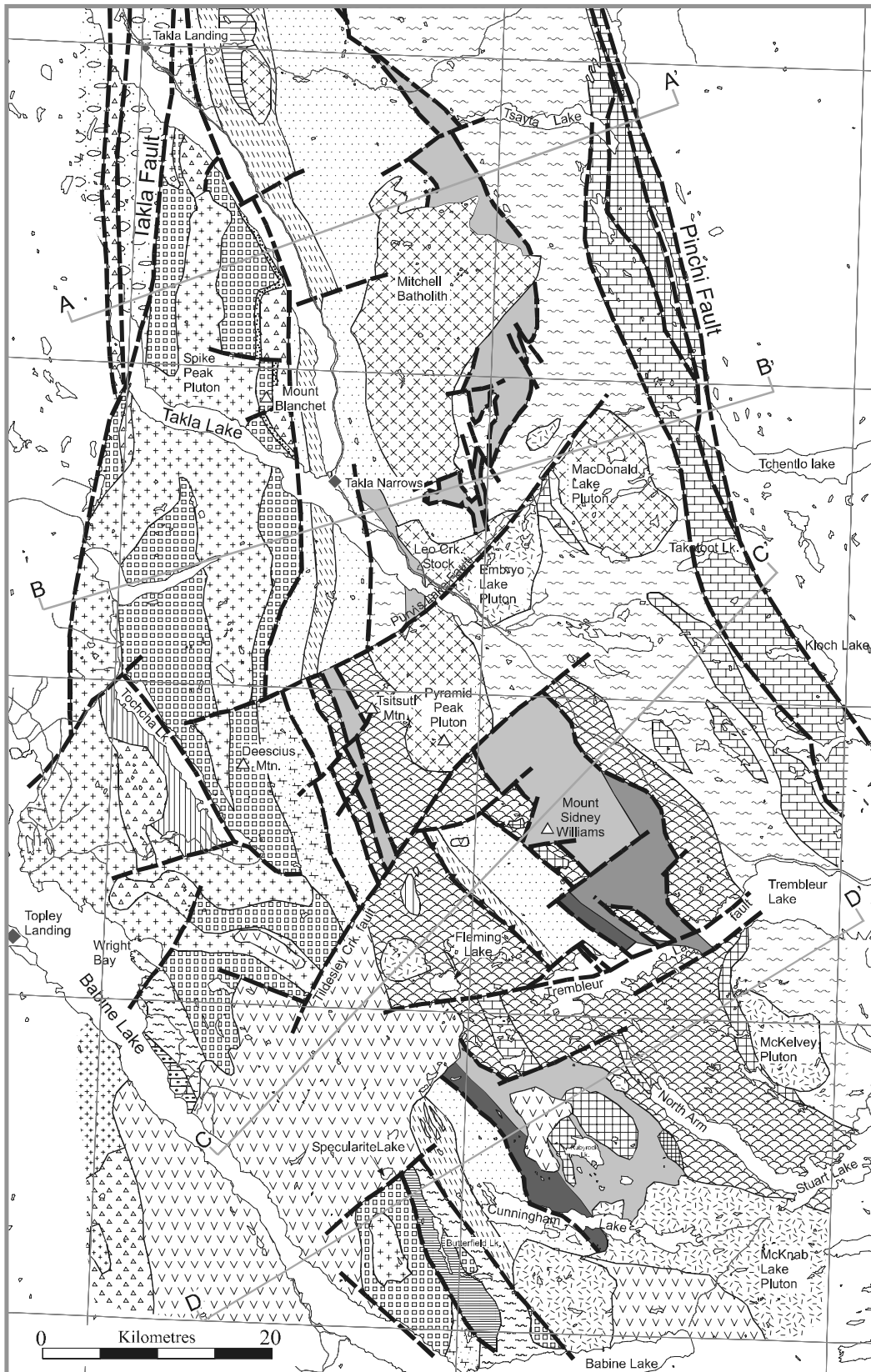


Figure 2a. General geology of the Babine-Takla lake area. See Figure 2b for legend.

OVERLAP ASSEMBLAGES

Eocene

- basalt, andesite, ash flow, minor debris flow, conglomerate, mudstone
- K-feldspar-biotite porphyry, biotite-hornblende-feldspar porphyry

Upper Cretaceous

Sustut Group

- chert pebble conglomerate, minor sandstone, shale

Early Cretaceous

- Mitchell Range intrusions: medium to coarse-grained granite and granodiorite; locally includes diorite and quartz diorite.

Late Jurassic to Early Cretaceous

- Francois Lake suite: granite, quartz monzonite, biotite granodiorite, quartz porphyry

Middle Jurassic

- McKnab Lake intrusive suite: quartz diorite, tonalite, diorite

STIKINE TERRANE

Middle Jurassic

- Spike Peak intrusive suite: red to pink monzonite, quartz monzonite, hornblende diorite; locally porphyritic (176-167 Ma.)

Late Triassic to Early Jurassic

- Topley intrusive suite: pink to grey, K-feldspar megacrystic granite, quartz monzonite; monzonite; varies from fine-grained equigranular to porphyritic (230-195 Ma.)

Lower to Middle Jurassic

Hazelton Group

- subaerial andesite to dacite flows and associated pyroclastic rocks, feldspathic fossiliferous siltstone and sandstone; volcanic conglomerate; typically feldspar or feldspar-pyroxene phyrlic; locally foliated.

Upper Triassic to Lower Jurassic

- quartzose-feldspathic turbidites; wacke, argillite, chert and limestone clast polymictic conglomerate

Upper Triassic

Takla Group

- submarine to subaerial basalt and basaltic andesite flows and associated pyroclastic and epiclastic rocks; minor mudstone and siltstone interbeds; typically pyroxene to pyroxene-feldspar phyrlic; some coarse-grained bladed feldspar phyrlic andesite; locally deformed to chlorite schist; may be equivalent to the Savage Mountain and/or Moosevale formations.
- Marine siltstone, mudstone, cherty argillite; minor limestone, chert and chert-limestone clast conglomerate; locally strongly deformed; may be equivalent to the Dewar Peak formation.

Late Triassic

- Tochcha Lake stock: foliated hornblende diorite (219 Ma.)

Paleozoic and/or Triassic

- Butterfield Lake intrusive complex: pyroxenite, hornblende gabbro, diorite, chlorite schist
- Taltapin metamorphic complex: chlorite-feldspar-amphibole schist, amphibolite, greenstone

Upper Pennsylvanian to Lower Permian

Asitka Group

- massive grey limestone; argillaceous limestone, chlorite schist; minor felsic tuff or flows, metasiltstone, metachert.

CACHE CREEK TERRANE

SITLIKA ASSEMBLAGE

Upper Triassic to Lower Jurassic

- Clastic unit: medium to dark grey slate, phyllite; banded siltstone, sandstone and conglomerate; minor limestone and green chloritic phyllite; locally contains felsic volcanic and plutonic clasts; distal to proximal turbidite succession.

Early Triassic

- Light grey, medium to coarse-grained tonalite

Late Permian or Early Triassic

- Medium grained epidote-chlorite-feldspar schist to semischist; sericite-chlorite-feldspar schist; weakly foliated chloritized hornblende diorite

Permian to Lower Triassic

- Volcanic unit: medium to dark green chlorite schist, fragmental chlorite schist and pillowed metabasalt; chlorite-sericite schist containing felsic metavolcanic fragments; lesser amounts of quartz-sericite schist, quartz-feldspar porphyry, flow banded metadacite, metasandstone and metachert.

CACHE CREEK COMPLEX

Permian to Triassic?

North Arm succession

- massive to pillowed basalt flows with interbeds of pillow breccia, chlorite schist, chert, limestone and graphitic phyllite; includes greenstone dikes and sills; minor metagabbro, amphibolite, serpentinite and listwanite.
- sheeted diabase dike complex.
- gabbro, diorite, diabase; locally includes clinopyroxenite, amphibolite, tonalite.

Trembleur Ultramafic Unit

- variably serpentinized harzburgite and dunite; serpentinite, serpentine-magnesite-talc schist; locally includes clinopyroxenite, gabbro, greenstone, diabase, amphibolite, chert, limestone, listwanite, nephrite
- mainly carbonate-talc altered ultramafic rocks; minor listwanite.
- foliated serpentinite, commonly with lozenges of massive serpentinized ultramafite.

Permian to Jurassic

- Phyllite-chert unit: light to medium grey quartz phyllite, platy quartzite and metachert; lesser amounts of recrystallized limestone, dark grey phyllite, massive to pillowed greenstone, fragmental greenstone and chlorite schist; minor amounts of meta sandstone.

Pennsylvanian to Permian

- massive limestone, minor basalt

Figure 2b. Legend to accompany Figure 2a (facing page).

ern 93N map sheet (Schiarizza and Payie, 1997; Schiarizza *et al.*, 1998), the Babine porphyry belt of Stikine Terrane in eastern 93L and 93M map sheets (MacIntyre *et al.*, 1996, 1997; MacIntyre, 1998), and the Cache Creek Terrane in the eastern 93K map sheet (Struik and Orchard, 1998, and references therein).

The information contained in this report is preliminary; the results from samples submitted for radiometric dating and microfossil extraction have not yet been received. This forthcoming data may change or refine some of the interpretations presented here.

REGIONAL GEOLOGIC SETTING

The northwest quadrant of the Fort Fraser map sheet (93K) and southwest quadrant of the Manson River map sheet (93N) straddle the boundary between Stikine and Cache Creek terranes. The oldest rocks exposed along the eastern margin of the Stikine Terrane are upper Paleozoic carbonates and island-arc volcanic and volcanoclastic rocks of the Asitka Group. Overlying the Asitka Group are basaltic calc-alkaline to alkaline island arc volcanic and sedimentary rocks of the Middle to Upper Triassic Takla Group and mafic to intermediate calc-alkaline volcanic and sedimentary rocks of the Lower to Middle Jurassic Hazelton Group. These arc successions are overlain by predominantly marine clastic sedimentary rocks of the upper Middle Jurassic to Lower Cretaceous Bowser Lake and Skeena groups, which in turn are overlapped by Upper Cretaceous to Paleocene nonmarine clastic sedimentary rocks of the Sustut Group or Upper Cretaceous continental arc volcanic rocks of the Kasalka Group. Younger rocks, which overlie both the Stikine Terrane and adjacent Cache Creek Terrane, include Eocene volcanic rocks of the Ootsa Lake and Endako groups, as well as Miocene-Pliocene plateau basalts of the Chilcotin Group.

The Cache Creek Terrane includes the Sitlika assemblage in the west and the Cache Creek Complex to the east. The Sitlika assemblage consists of Permo-Triassic bimodal volcanic rocks overlain by Upper Triassic to Lower Jurassic clastic sedimentary rocks. This assemblage is structurally overlain by a poorly dated, but partially age-equivalent ophiolitic sequence that forms the western part of the Cache Creek

Complex. Eastern elements of the Cache Creek Complex include a Permian to Lower Jurassic succession of predominantly pelagic metasedimentary rocks and thick Pennsylvanian - Permian carbonate sequences associated with ocean island basalts. Structural imbrication of Cache Creek Terrane, across predominantly west-directed thrust faults, occurred in Early to Middle Jurassic time, and was approximately coincident with its amalgamation with the adjacent Stikine Terrane.

Intrusive rocks are common in the region and belong to several distinct suites. In the current study area Late Triassic-Early Jurassic and Middle Jurassic plutons assigned to the Topley and Spike Peak intrusive suites cut rocks of the Stikine Terrane; whereas the adjacent Cache Creek Terrane is host to at least three distinct plutonic suites of late Middle Jurassic, Late Jurassic-Early Cretaceous and Early Cretaceous age.

LITHOLOGIC UNITS

Stikine Terrane

In the current study area the Stikine Terrane is represented by the upper Paleozoic Asitka Group, Middle to Upper Triassic Takla Group and Lower Jurassic Hazelton Group.

Asitka Group

The Asitka Group, as defined by Lord (1948), includes aphanitic basalts, rhyolites, breccia, feldspar porphyry, chert, limestone and argillites of mid-Pennsylvanian to Early Permian age. The type area is located between the Asitka and Niven rivers in the northeast McConnell Creek map area. Diakow and Rogers (1998) describe a two fold subdivision in the McConnell Range. There, the Asitka Group is comprised of a lower volcanic unit of mainly aphanitic basalt and basaltic andesite with minor interbeds of fragmental and felsic volcanic rocks and marine sediments. The upper part of the Asitka Group is sedimentary and is characterized by a lower member of massive grey limestone overlain by thinly bedded chert, tuffaceous siltstone and sandstone, siliceous mudstone and carbonaceous chert. The contact with overlying Takla sediments is believed to be

a disconformity with a depositional hiatus ranging from Early Permian to Late Triassic. However, west of the current study area at the Fulton river dam site, a bedded chert that overlies Early Permian limestone of the Asitka Group contains Middle Triassic radiolarians (Fabrice Cordey, personal communication, 1996). This suggests that some of the sedimentary rocks included in the upper sedimentary unit of the Asitka Group may actually be Triassic in age and should, therefore, be included with the Takla Group.

Within the current study area, rocks assigned to the Pennsylvanian to Permian Asitka Group underlie the northwest corner of the 93K/12 map sheet, southeast of Wright Bay on Babine Lake (Figure 2). Here, a belt of greenschist facies metasedimentary and metavolcanic rocks crop out as a series of northwest trending ridges with the best exposures occurring in areas that have been logged and burned. This belt of



Photo 1. Paul Schiarizza collecting a U-Pb geochronology sample from a flow banded phylolite lense within chlorite schists of the Asitka Group, northwest corner, 93K/12 map sheet.

metamorphic rocks, which dips moderately to the northeast, is bounded to the west by an area underlain by massive grey limestone and to the east by pyroxene phyric flows of the Takla Group. The limestone is lithologically identical to one in the Fulton Lake area west of Babine Lake that contains Early Permian (Sakmarian and Artinskian) conodonts (Orchard, 1996; MacIntyre *et al.*, 1996). A similar age is implied for the limestone in the northwest corner of the 93K/12 map sheet. These limestone members are assigned to the Pennsylvanian-Permian Asitka Group which typically has limestone beds near its upper contact with the Upper Triassic Takla Group (Diakow and Rogers, 1998).

The metavolcanic rocks east of the limestone in the 93K/12 map sheet are predominantly chlorite schists and phyllites which locally have layers containing flattened felsic clasts. A sample for U-Pb isotopic dating was collected from a lens of feldspar phyric, banded rhyolite within the chlorite schist succession (Photo 1). The protoliths for these metamorphic rocks are interpreted to be aphanitic mafic volcanics with lesser associated felsic pyroclastic rocks, a lithological mix that is typical of the lower part of the Asitka succession in the McConnell Creek map area (Diakow and Rogers, 1998). If these correlations are correct it implies the presence of a northeast dipping, overturned antiform cored by metavolcanic rocks of the Asitka Group. The western overturned limb of this antiform is mainly massive limestone; the eastern upright limb near the contact with Takla Group rocks is medium to thin bedded, metachert and metasiltstone (Photo 2). These metasedimentary rocks may comprise an upper member of the Asitka Group; alternatively they are a lower deformed sedimentary member of the Takla Group, possibly the Dewar Peak Formation. These metasediments are similar to those overlying the Early Permian limestone at the Fulton River dam site in the Fulton Lake map sheet (MacIntyre *et al.*, 1996). There, cherts have yielded Middle Triassic radiolarians and are included with the Takla Group.

The metavolcanic rocks assigned to the Asitka Group are intruded by numerous dikes and sills of pyroxenite, coarse grained hornblende gabbro and diorite. These intrusions are believed to be comagmatic with overlying pyroxene phyric flows of the Takla Group.



Photo 2. Well bedded metachert and metasiltstone, northwest corner, 93K/12 map sheet. These rocks apparently underlie pyroxene phyric flows of the Takla Group.

Taltapin Metamorphic Complex and Butterfield Lake Pluton

Metamorphic rocks that crop out along the east end of Babine Lake were examined by Struik and Erdmer (1990), who noted that they were at higher metamorphic grade than is typical for this part of the Intermontane Belt. These medium grade metamorphic rocks, consisting of amphibolite, marble, quartzite and foliated diorite, were traced southeastward into the Tintagel (93K/6) map sheet by Hruday *et al.* (1999), who assign them to the Taltapin metamorphic complex. They extend northwestward into the present map area as a narrow belt that encompasses Butterfield Lake (Figure 2). This belt is juxtaposed against the Sitlika assemblage to the east, across an inferred fault that in part follows Gullwing Creek. It is bounded by Eocene basalt to the north, and by exposures of Takla Group to the west. Variably foliated augite-phyric metabasalts assigned to the Takla Group also occur as two separate outliers in the eastern part of the belt. This suggests that the Taltapin metamorphic complex, which had been included in the Cache Creek Group by Armstrong (1949) and Struik and Erdmer (1990), actually comprises part of the Stikine Terrane.

Much of the Taltapin belt within the present map area consists of ultramafic to mafic intrusive rocks assigned to the Butterfield Lake pluton (Figure 2). The pluton consists mainly of weakly to strongly foliated gabbro and diorite, but pyroxenite, locally cut by dikes of gabbro and diorite, predominates in the west. Dikes and pods of fractured to foliated tonalite locally cut the ultramafic

to mafic rocks and may be the youngest phase of the pluton; alternatively, they may represent a separate intrusive event. The Butterfield Lake pluton is undated, but is suspected to be of Late Triassic age, possibly correlative with the Tochcha Lake pluton (described in a following section).

The western margin of the Butterfield Lake pluton consists of foliated serpentinite that is inferred to mark a fault contact with adjacent volcanic rocks of the Takla Group. Along the southern boundary of the map area, however, the pluton truncates a west-dipping contact that juxtaposes the Takla volcanics above an assemblage that includes marbles, amphibolites, quartz-chlorite schists and local metachert units. Although rocks on both sides of the contact are strongly foliated and locally sheared, this may be a stratigraphic contact between the Takla Group and underlying Asitka Group. Eastern exposures of the Taltapin metamorphic belt are dominated by fine-grained amphibolites, chlorite schists, and chlorite-amphibole-feldspar schists that appear to have been derived from a complex assemblage of dioritic plutonic rocks and metavolcanic or metasedimentary rocks. The two outliers of augite-phyric metabasalts within this part of the belt suggest that these rocks are stratigraphically or structurally beneath the Takla Group. It is suspected, therefore, that the Taltapin metamorphic complex consists mainly of metasedimentary and metavolcanic rocks derived from the Asitka Group, together with plutonic rocks that correlate with the Butterfield Lake pluton.



Photo 3. Volcanic breccia with moderately flattened, subrounded clasts of pyroxene phyric basalt, typical of the lower part of the Takla Group volcanic succession, northwest corner, 93K/12 map sheet.

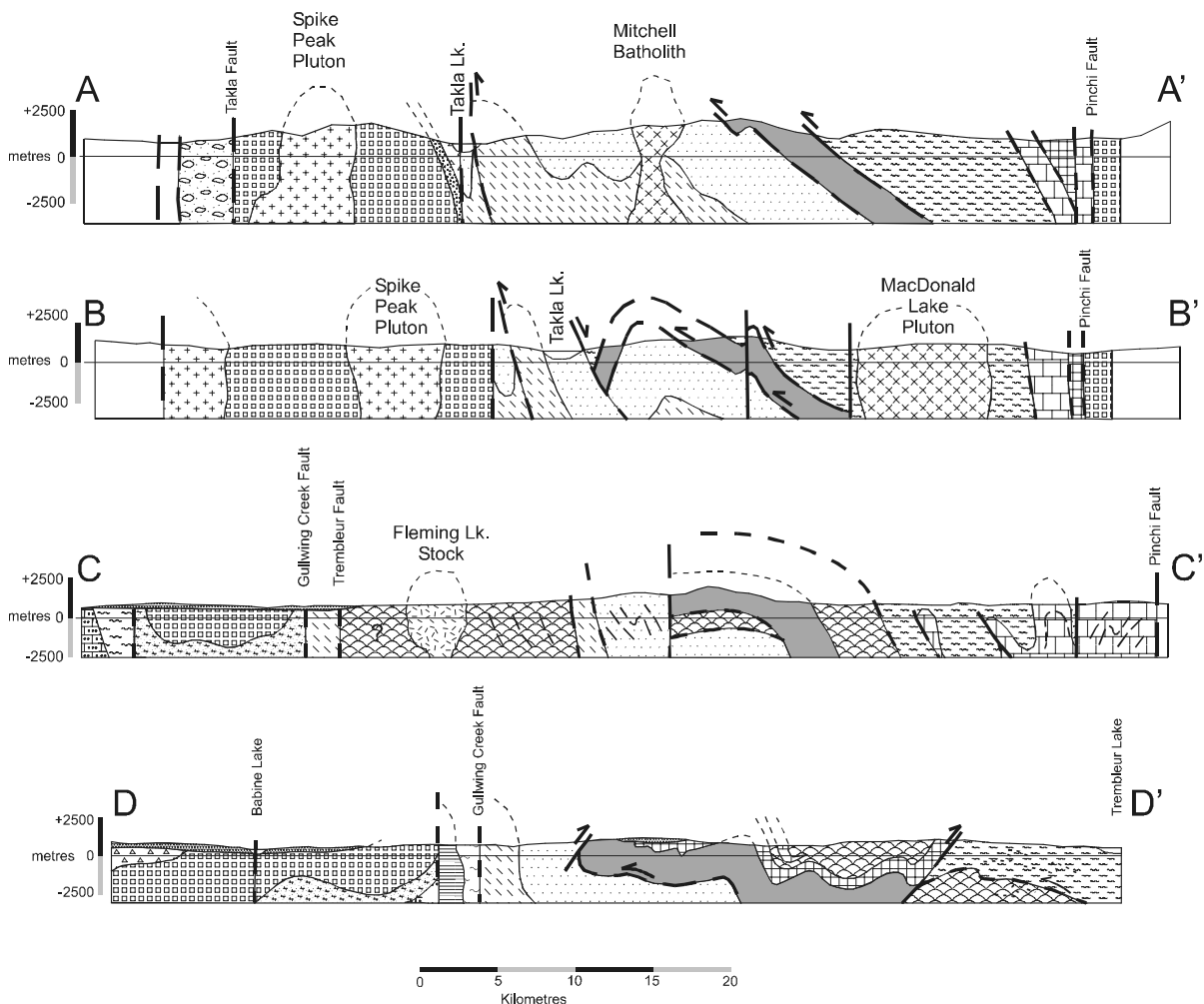


Figure 3. Interpretive structural cross sections, Babine-Takla lakes area. See Figure 2a for location of sections and Figure 2b for legend.

Takla Group

The Takla Group was first defined by Armstrong (1946, 1949) in the Fort St. James map-area. The type area is located west of Takla Lake in the 93N/4 and 93N/5 map sheets (Armstrong, 1949). As originally defined, the Takla Group included upper and lower divisions of arc related volcanic and sedimentary rocks ranging in age from Late Triassic to Late Jurassic, a subdivision also used by Lord (1948) in the McConnell Creek map area. Monger (1976) and Monger and Church (1977) redefined the Takla Group to include only sedimentary and basaltic volcanic rocks of Late Triassic age; the Jurassic part of the Takla Group was assigned to the

Hazleton Group. Monger and Church further subdivided the Takla Group into the Dewar, Savage Mountain and Moosevale Formations. The Dewar Formation, which occurs at the base, is the most widespread, and includes thin to medium-bedded dark grey or greenish grey, brown weathering volcanic sandstone or bedded tuff, siltstone and interbedded argillite. It is a marine turbiditic succession up to 300 metres thick, and, near its base, consists mainly of graphitic and pyritic argillite with silty and sandy laminae and interbeds of argillaceous limestone and cherty argillite. Fossils collected from the Dewar Formation are upper Carnian in age (Monger and Church, 1977).

The Dewar Formation is overlain by and in part interbedded with the Savage Mountain Formation.



Photo 4. Outcrop of lapilli tuff with clasts of pink, flow-banded rhyolite, feldspar phyric andesite and fine-grained monzonite in a greenish grey crystal-ash matrix exposed at Wright Bay on Babine Lake. This lithology is typical of much of the Wright Bay succession.

This succession is up to 3000 metres thick and includes massive submarine volcanic breccias, aphanitic and augite-feldspar phyric pillowed and massive basalt flows and minor interbedded volcanoclastic sedimentary rocks and tuffs. The volcanic rocks are characterized by the presence of augite phenocrysts, which occasionally reach 1 centimetre in diameter. Coarse, bladed feldspar phyric basalt flows, with feldspar phenocrysts up to 3 centimetres, are also locally present.

The Savage Mountain Formation, which in places becomes subaerial near its upper contact, is overlain by the Moosevale Formation. The contact varies from gradational to sharp. Fossils from the Moosevale Formation, which is up to 1800 metres thick, are Late Triassic (Norian). Overall, the formation is more intermediate in composition than the underlying Savage Mountain Formation, and includes varying amounts of massive, red, green and maroon volcanic breccia, graded red and grey sandstone, argillite, fossiliferous mudstone, red volcanic conglomerate and lahar. Clasts in the fragmental volcanic rocks and conglomerates are typical of the underlying Savage Mountain Formation. The Moosevale Formation is mainly marine near its base, becoming non-marine up section.

Augite phyric dark green to grey basaltic flows, volcanic breccias, tuffs and minor interbedded volcanoclastic sedimentary rocks crop out along the western half of the Tochcha Lake map sheet and are correlated with the Savage Mountain Formation of the Takla Group.

These rocks are at the southern end of a 65 kilometre long belt that can be traced northward into the 93N/4 and 93N/5 map sheets, terminating at Takla Landing on Takla Lake (Figure 2). Within this belt the Takla Group succession can be divided into four mappable subdivisions. The base of the succession, which is not well-exposed, is comprised of graphitic cherty argillite, argillaceous limestone, calcareous siltstone, mudstone and minor pebble conglomerate that are probably correlative with the Dewar Formation. Similar sedimentary beds also interfinger with overlying, predominantly volcanic units. In general these marine sedimentary rocks are overlain by a thick volcanic succession. The base of this succession is predominantly dark green, pyroxene rich basaltic flows and related breccias. These grade upward into a middle unit of interbedded volcanic breccia, agglomerate, volcanic conglomerate and lapilli tuff, all of which contain abundant pyroxene-phyric basalt clasts. The upper part of the volcanic succession is mainly brown to buff weathering, greenish grey to purplish pyroxene-feldspar to hornblende-pyroxene-feldspar phyric andesite flows, volcanic breccias and lapilli tuffs. The andesitic flows locally have a trachytic texture comprised of 35 to 40 percent, 4 to 6 millimetre feldspar laths. Mike Villeneuve of the Geological Survey of Canada, Ottawa, reports that hornblende from a hornblende-pyroxene-feldspar phyric andesite flow in the Fulton Lake area gave a 208 ± 2 Ma Ar-Ar isotopic age (MacIntyre *et al.*, 1996). This suggests the top of the Takla succession is close to the Triassic-Jurassic boundary.

The best exposures of the upper part of the Takla Group are on the west slope of Deescius Mountain (Figure 2), where several hundred metres of massive pyroxene-feldspar phyric andesite flows and breccias are exposed. Thin sedimentary interbeds between flows indicate the succession dips moderately to the northeast. These volcanic rocks are underlain to the southwest by a poorly exposed interval of mudstone, siltstone and conglomerate. These sediments overlie aphanitic basalt and pyroxene phyric flows typical of the lower part of the Takla Group volcanic succession. Near the top of this sedimentary interval is a foliated pebble conglomerate that contains flattened clasts of limestone and chert. A sample of limestone clasts extracted from the conglomerate yielded Norian conodonts (M.J. Orchard, written communication, 1998)

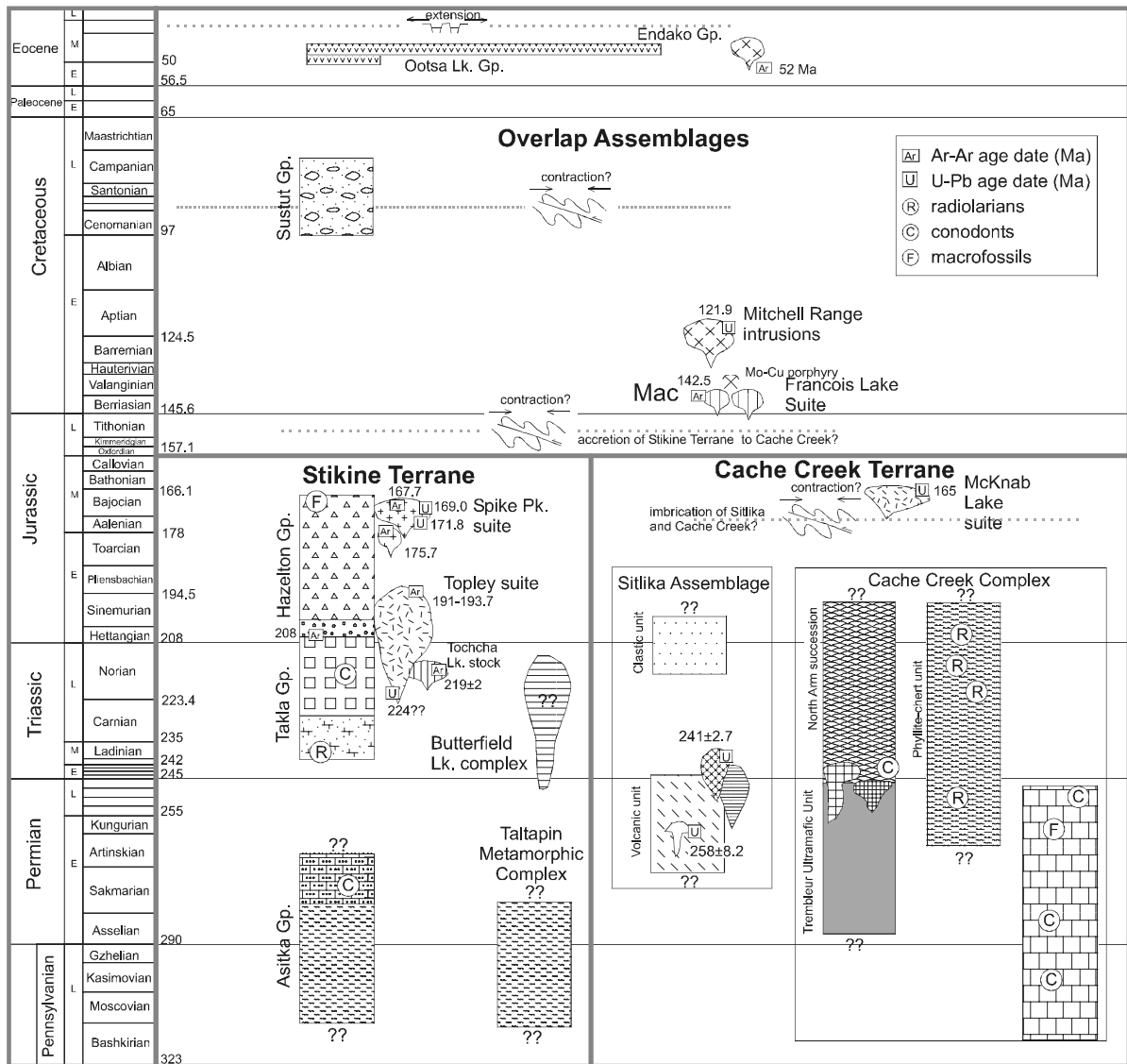


Figure 4. Schematic illustration of the generalized stratigraphy, plutonic and structural events of the Babine Lake - Takla Lake area. See figure 2b for the legend.

suggesting that the clasts are locally derived from limestone beds within the Takla Group.

East of Deescius Mountain is a belt of folded, well bedded siltstone, argillaceous limestone and cherty argillite. These rocks, which are only exposed along logging roads southeast of Deescius Mountain, are in fault contact with the upper part of the Takla Group. East of the valley of Gloyazikut Creek they are in apparent fault contact with the clastic unit of the Sitlika assemblage. These sedimentary rocks are tentatively included with the Takla Group.

Peroxene phyric mafic volcanic rocks, typical of the Upper Triassic Takla Group, crop out in the northwest and southeast corners of the 93K/12 map sheet. In the southeast corner of

93K/12, a good section through part of the Takla Group succession is exposed along a new logging road located between Butterfield and Babine lakes. There, the Takla Group consists predominantly of green weathering, chloritic basalt flows, breccias and tuffs with 60 to 70 percent, 2 to 4 millimetre pyroxene crystals. Locally the flows and tuffs are strongly deformed to a chlorite schist with stretched pyroxene phenocrysts. Foliation and bedding trends suggest the Takla succession is dipping moderately to steeply southwestward. To the east, the contact with the Butterfield Lake pyroxenite-gabbro-diorite pluton, which is exposed in road cuts at the Fort prospect, is interpreted to be a high angle fault. Along the

shores of Babine Lake, a southwest dipping section of pyroxene rich schists and phyllites interpreted to be deformed Takla Group is underlain by interbedded graphitic phyllites, argillaceous limestone and marble. The latter are well exposed at Boling Point and are tentatively mapped as the lower sedimentary unit of the Takla Group (Figure 2); alternatively they may be an upper member of the Asitka Group.

The Takla Group rocks that crop out in the northwest corner of the 93K/12 map sheet overlie metavolcanic rocks of the Asitka Group. Here, the succession dips moderately to the northeast. The stratigraphic succession in this area is the same as that observed further north in the Tochcha Lake area. The lowest volcanic members are dark green, relatively coarse grained, pyroxene phyric flows and related volcanic breccias (Photo 3). These grade up section into finer-grained, brown weathering feldspar-pyroxene phyric flows, volcanic breccias and lapilli tuffs that are probably andesitic in composition. Locally, these rocks have a trachytic texture comprised of 2 to 4 millimetre feldspar laths in a finer-grained, pyroxene-bearing groundmass. These intermediate volcanic rocks may correlate with the Moosevale Formation of the Takla Group; alternatively they may be a lower member of the Jurassic Hazelton Group.

The Takla Group is well exposed on Mount Blanchet in the 93N/4 map sheet. There, the Takla succession, which dips moderately to the east, is largely intact and less deformed than exposures in the southern Babine Lake area. Exposures on the west slope of the mountain comprise more than 500 metres of massive, lenticular feldspar-pyroxene phyric basalt to andesite flows with minor thin-bedded tuffaceous sedimentary intervals. The base of the succession is not exposed and to the west it is intruded by Middle Jurassic hornblende diorite. Near the top of Mount Blanchet and down its eastern slope, the massive flows are overlain by thin bedded, finer-grained pyroxene-bearing tuffs and tuffaceous clastic sediments.

Quartzose-feldspathic turbidites

A distinctive succession, up to 100 metres thick, of medium to thick bedded quartzose-feldspathic turbidites crops out on the east slope of Mount Blanchet and along the western shores of the main arm of Takla Lake. These turbidites,

which apparently occupy a stratigraphic position between the Upper Triassic Takla Group and Lower Jurassic Hazelton Group, are comprised of beds of siliceous fine-grained siltstone, quartz wacke and chert clast-bearing pebble conglomerate separated by thin intervals of mudstone and siltstone. The finer-grained siltstone members are locally cross laminated. The composition of clasts in the pebble and granule conglomerates varies from predominantly chert to a mixture of chert and limestone with lesser feldspar phyric andesite clasts. The clasts may have been derived from the Asitka or Takla groups of Stikine Terrane, or from the adjacent Cache Creek Terrane. Limestone clasts collected from a conglomerate bed along Takla Lake are being processed for conodont extraction in an attempt to constrain their age.

Tochcha Lake Pluton

Medium-grained, equigranular hornblende-biotite diorite underlies the hills along the west side of Tochcha lake. The diorite has a pronounced mineral lineation that is defined by the alignment of hornblende and biotite. Xenoliths of biotite microdiorite, up to 10 centimetres in diameter, have indistinct (resorbed?) margins and are abundant in the intrusive. Fine-grained, pink aplitic dikes cut the diorite. Mike Villeneuve of the Geological Survey of Canada, Ottawa, reports an Ar-Ar isotopic age of 219 ± 2 Ma for hornblende from the diorite (MacIntyre *et al.*, 1996). If this age is representative it indicates that the Tochcha Lake diorite is approximately the same age as the Takla volcanic rocks that it intrudes and may be comagmatic with the volcanic rocks. Additional dating is required to verify this correlation. The 219 Ma Ar-Ar isotopic age is similar to dates determined for diorites of the Boer Lake intrusive suite in the Endako area (Mike Villeneuve, personal communication, 1997).

Hazelton Group

The Hazelton Group (Leach, 1910) is a calcalkaline island-arc assemblage that evolved in Early to Middle Jurassic time. In the current study area, and the McConnell Creek map area to the north (94D), it rests unconformably to disconformably on volcanic and sedimentary strata of the Upper Triassic Takla Group (MacIntyre *et al.*, 1996).

Tipper and Richards (1976) divided the

Hazelton Group into the Telkwa, Nilkitkwa and Smithers formations based on lithology, fossil assemblages and stratigraphic position. Of these only the Telkwa Formation has been mapped in the current study area. Here, as elsewhere, the Telkwa Formation is comprised of subaerial to submarine, predominantly calcalkaline volcanic rocks.

Wright Bay succession

A distinctive succession of subaerial volcanic rocks is exposed on the shores of Wright Bay and in several localities between Wright Bay and Tochcha Lake. This succession, which at Wright Bay dips moderately to the west, is comprised of a lower member of flow banded rhyolite that may in part be intrusive, a middle member of feldspar phyric lapilli tuff, volcanic breccia, lahar, and volcanic conglomerate and an upper member of massive feldspar phyric andesite to dacite flows. In places the lapilli tuffs are welded and may be ash flows. The succession is believed to overlie feldspar-pyroxene phyric andesite flows of the Upper Triassic Takla Group. It is uncertain whether the Wright Bay volcanics are an upper member of the Takla Group and therefore equivalent to the Moosevale Formation or a lower member of the Hazelton Group and correlative with the Telkwa Formation. A sample was collected from a massive feldspar phyric flow at Wright Bay for U-Pb isotopic dating.

A feature that distinguishes the Wright Bay succession from possible age equivalent rocks of the Telkwa Formation is the presence of 1 to 5 centimetre, subrounded to angular clasts of aphanitic pink and white weathering monzonite and flow-banded rhyolite clasts in a greenish grey crystal-ash matrix (Photo 4). The clasts are similar to phases of the Topley intrusions suggesting a comagmatic association. In one locality a pink-weathering, aphanitic Topley-like dike cuts flows of the upper member suggesting at least some Topley magmatism continued after the main phase of volcanic eruption. In places the pyroclastic rocks resemble the Nose Bay intrusive breccia which is located east of Wright Bay. This breccia, which was described in a previous report (MacIntyre *et al.*, 1996), may have been a feeder vent for the Wright Bay volcanic rocks. Similar breccias containing Topley clasts crop out south of Tachek Creek on the west side of Babine Lake, and these too may be related to the Wright Bay

volcanic rocks. The latter were mapped as the Tachek Group by Armstrong (1949) and were thought to be Jurassic or younger. In a previous report it was suggested the Wright Bay volcanics might be as young as Eocene (MacIntyre *et al.*, 1998); additional mapping in 1998 suggests this is not the case. Although the Wright Bay succession is here included with the Hazelton Group, additional isotopic age dating may show that these rocks are older and more appropriately correlated with the upper part of the Takla Group.

Topley Intrusive Suite

The Topley intrusions, as defined by Carter (1981), include quartz diorite to quartz monzonite of Late Triassic to Early Jurassic age. Earlier studies (Carr, 1965; Kimura *et al.*, 1976) used the term Topley intrusions for granite, quartz monzonite, granodiorite, quartz diorite, diorite and gabbro intrusions of probable Jurassic age that intrude Triassic volcanic rocks from Babine Lake to Quesnel. Included in this Topley suite were high-potassium intrusions associated with the Endako porphyry molybdenum deposit. However, subsequent K-Ar isotopic dating showed most of these high-K intrusions were Late Jurassic to Early Cretaceous in age. Consequently, the intrusions around Endako were renamed the Francois Lake intrusions to distinguish them from the older Topley suite.

Potassium-argon isotopic dates for the Topley intrusions, as defined by Carter (1981), would include ages as young as 176 Ma and as old as 210 Ma (MacIntyre *et al.*, 1996). Initial dating of the Topley suite is from large plutons in the Topley area and southwest of Babine Lake. These plutons gave ages in the 190 to 210 Ma range using the K-Ar dating method. In the current study, the Topley intrusions are restricted to this Late Triassic to Early Jurassic suite which is characterized by typically pink, potassium feldspar rich granite, quartz monzonite and monzonite. A lithologically similar suite of predominantly Middle Jurassic (179-169 Ma) plutons occurs in the northwest Fort Fraser map area. These plutons are mapped as the Spike Peak intrusive suite. The Topley suite is restricted to older plutons in the type area near Topley Landing on Babine Lake. Within the current map area, it is represented only by poorly exposed granite to monzonite that crops out along the western edge of the area south of Babine Lake (Figure 2).

Spike Peak Intrusive Suite

The Spike Peak intrusive suite comprises Middle Jurassic plutons that include pink to red weathering granites and quartz monzonites that are lithologically identical to rocks that characterize the older Topley intrusive suite. The Middle Jurassic isotopic ages determined for the suite are similar to those determined for hornblende diorite of the Stag Lake-Twenty-six Mile Lake plutonic suite in the Hallet Lake area (Anderson *et al.*, 1997). Within the Takla Lake - Babine Lake area, the Spike Peak suite is represented by a continuous belt of plutonic rocks that extends from the Takla Range, near Takla Landing, southward to Wright Bay on Babine Lake (Figure 2). These plutonic rocks intrude mainly the Takla Group, but locally cut the Hazelton Group or the Late Triassic Tochcha Lake pluton. The northern part of this composite pluton, which includes quartz monzonite, granite, hornblende diorite and biotite-hornblende granodiorite, was referred to as the Northwest Arm pluton by Schiarizza *et al.* (1998). Subsequent to that report, Mike Villeneuve of the Geological Survey of Canada has determined two U-Pb isotopic ages on zircons extracted from samples taken from this part of the pluton. These ages are 169.0 ± 0.6 Ma for a hornblende diorite on the west flank of Mt. Blanchet, and 171.8 ± 0.6 Ma for quartz monzonite that underlies Spike Peak, 4 km to the west. These ages are virtually identical to the $169.1 +1.0/-4.8$ U-Pb zircon date reported by Schiarizza *et al.* (1998) for monzogranite of the smaller Takla Landing pluton, which crops out on either side of Takla Lake a short distance to the north. Farther south, just east of Tochcha Lake, hornblende from a hornblende diorite phase of the main pluton gave a 167.7 ± 1.7 Ma Ar-Ar isotopic age. All of these ages are slightly younger than two other isotopic dates determined as part of the Babine project. Hornblende from a small hornblende feldspar porphyritic monzonite stock exposed in a clearcut west of Tochcha Lake gave an Ar-Ar isotopic age of 175.7 ± 1.7 Ma. (MacIntyre *et al.*, 1996), and zircon extracted from a biotite granite phase east of Babine Lake gave a U-Pb isotopic age of 178.7 ± 0.5 Ma. West of Babine Lake, at the Tachek Creek porphyry copper prospect, biotite from a biotite-quartz-feldspar porphyry dike was dated at 176 ± 7 Ma (178 Ma revised) by the K-Ar method (Carter, 1981).

Sitlika Assemblage

The Sitlika assemblage comprises upper Paleozoic to lower Mesozoic metavolcanic and metasedimentary rocks that crop out in the western part of Cache Creek Terrane in central British Columbia. These rocks were first described by Paterson (1974) who mapped them on the east side of Takla Lake, where they had previously been included in the Cache Creek and Takla groups by Armstrong (1949). Monger *et al.* (1978) correlated the Sitlika assemblage with the Kutcho Formation, host to the Kutcho Creek volcanogenic massive sulphide deposit, which occurs in the eastern part of the King Salmon allochthon in northern British Columbia. They suggested that the Kutcho and Sitlika assemblages might have been contiguous prior to dispersion along Late Cretaceous or early Tertiary dextral strike-slip faults.

Schiarizza and Payie (1997) confirmed that the Sitlika assemblage resembles the Kutcho Formation and overlying metasedimentary rocks (Sinwa and Inklin formations) in general lithology and stratigraphy, while Childe and Schiarizza (1997) documented that volcanic rocks of the two assemblages are similar in age, geochemistry and Nd isotopic signature. Furthermore, Childe *et al.* (1997, 1998) and Schiarizza and Payie (1997) correlated the Kutcho-Sitlika succession with rocks in southern British Columbia, suggesting that the Sitlika assemblage is part of an extensive tract within or adjacent to Cache Creek Terrane that occurs over most of the length of the Canadian Cordillera.

Paterson (1974) divided the Sitlika assemblage into three subdivisions. A similar scheme was adopted by Schiarizza and Payie (1997), who referred to the subdivisions as the volcanic unit (equivalent to Paterson's volcanic division), the eastern clastic unit (equivalent to Paterson's greywacke division) and the western clastic unit (equivalent to Paterson's argillite division). Schiarizza and Payie established that the eastern clastic unit rests stratigraphically above the Permo-Triassic volcanic unit, but did not establish the age or stratigraphic relationships of the western clastic unit. Subsequent work by Schiarizza *et al.* (1998) traced the three units of the Sitlika assemblage to the south side of Takla Lake, but likewise did not resolve the stratigraphic affinity of the western clastic unit.

During the 1998 field season the Sitlika assemblage was traced southward to Babine

Lake, although continuity of the belt is broken by major transverse faults along Purvis Lake, Tildesley Creek and Trembleur Lake (Figure 2). As was the case to the north, it comprises rocks that had been included in the Cache Creek Group by Armstrong (1949). In addition, new mapping south of Takla Lake, together with visits to previously mapped outcrops to the north, has resulted in an improved understanding of the western clastic unit. Most of the unit is now interpreted as a structural repetition of the eastern clastic unit. Chert pebble conglomerate that dominates the western part of the unit where it was originally defined north of Takla Landing is interpreted as a fault-bounded panel derived from the Stikine Terrane (upper part of the Takla Group). Consequently, the Sitlika assemblage is now defined in terms of two components: a Permo-Triassic volcanic unit, and an overlying Upper Triassic - Lower Jurassic clastic sedimentary unit.

Volcanic Unit

The volcanic unit of the Sitlika assemblage is best exposed in a continuous belt that extends from Mount Olson southward to Takla Lake (Schiarizza and Payie, 1997; Schiarizza *et al.*, 1998). It comprises greenschist facies mafic to felsic flow and fragmental rocks, comagmatic mafic to felsic intrusions, and subordinate sedimentary rocks that include sandstone, slate and chert. The age of the volcanic unit is in part constrained by Late Permian U-Pb dates on zircons from two separate weakly foliated quartz-plagioclase-phyric rhyolite units that crop out north of the area shown in Figure 2. One, north of Mount Bodine, is dated at $258 \pm 10/-1$ Ma (Childe and Schiarizza, 1997), and the other, northeast of Diver Lake, yielded a date of 248.4 ± 0.3 Ma (Mike Villeneuve, personal communication, 1998). These dates are corroborated by Permian radiolarians (*Latentibifistula* sp.) extracted from a narrow chert interval intercalated with the volcanic rocks south of Mount Olson (Fabrice Cordey, written communication, 1997). Magmatism within the Sitlika assemblage continued into the Early Triassic, as indicated by U-Pb zircon dates from two separate tonalite stocks within the volcanic unit. One, the Diver Lake pluton, yielded a date of 241 ± 1 Ma (Childe and Schiarizza, 1997), while tonalite from the composite Maclaing Creek pluton (Schiarizza *et al.*,

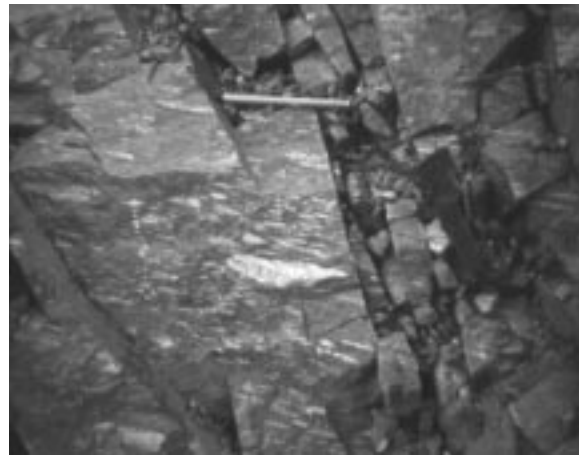


Photo 5. Outcrop of dark grey, feldspar phyric metadacite or meta-andesite of the Sitlika volcanic unit exposed in road cuts south of Cunningham Lake, 93K/11 map sheet. Note flattened and stretched felsic clasts.

1998; Figure 2) is dated at 243 ± 3 Ma (Mike Villeneuve, personal communication, 1998).

The Sitlika volcanic unit continues southward from Takla Lake as a narrow belt of chlorite schist that was traced to the Purvis Lake fault. It was not recognized within the offset continuation of the Sitlika belt south of the fault, but might be present under the belt of Quaternary cover along Gloyazikut Creek that separates exposures of the Sitlika clastic unit from Stikine Terrane to the west (MacIntyre *et al.*, 1998). South of the Tildesley Creek fault, pillowed metabasalts and chlorite schists that crop out directly west of the Sitlika clastic unit might represent the volcanic unit, but alternatively might be part of the North Arm succession of the Cache Creek Complex, which is widely exposed still farther west. More definitive exposures of the volcanic unit occur west of Cunningham Lake, in the offset extension of the Sitlika belt south of the Trembleur Lake fault system. These rocks define a belt that separates the Sitlika clastic unit from exposures of Stikine Terrane to the west.

The western part of the Cunningham Lake belt is dominated by felsic metavolcanic rocks, including weakly to moderately foliated feldspar-phyric metadacite with relict flow-banding, variably schistose quartz-feldspar-phyric metarhyolite, and chlorite-sericite schist containing flattened felsic clasts and quartz and feldspar grains (Photo 5). These rocks are locally cut by pre-metamorphic intrusive units that

include granitoid gneiss, metadiorite and narrow dikes of chlorite-feldspar-amphibole schist. The eastern part of the unit consists mainly of epidote-chlorite schist and semischist, commonly with relict feldspar and pyroxene phenocrysts.

The metavolcanic rocks west of Cunningham Lake are readily assigned to the Sitlika volcanic unit on the basis of a characteristic suite of lithologies derived from felsic and mafic volcanic rocks, as well as felsic and mafic intrusive phases. The correlation is consistent with the position of the belt directly west of the Sitlika clastic unit, although the contact was not observed so it is not known if it is structural or stratigraphic. A felsic metavolcanic member of the succession was collected for U-Pb dating of zircons in an attempt to confirm the correlation.

Clastic Sedimentary Unit

The Sitlika clastic sedimentary unit consists of slate, siltstone, and sandstone, with local intercalations of conglomerate and limestone. It is locally well exposed within a continuous belt almost 100 km long that crops out east of the volcanic unit from Mount Olson southward to the Purvis Lake fault. The base of the unit is exposed at several places within this belt, where it is in abrupt, disconformable(?) stratigraphic contact with the underlying volcanic unit (Schiarizza and Payie, 1997; Schiarizza *et al.*, 1998). The clastic sedimentary unit also crops out to the west of the volcanic unit over this distance, where it is interpreted as a structural repetition localized along the fault contact with Stikine Terrane. The clastic unit is dated at a single locality, 3 km west of Tsayta Lake, where Late(?) Norian conodonts were extracted from a schistose calcarenite bed (M.J. Orchard, written communication 1998). Its age is suspected to extend from the Late Triassic into the Early Jurassic based on correlation with Lower Jurassic clastic sedimentary units that overlie Sitlika-correlative volcanic rocks in both northern and southern British Columbia (Schiarizza, 1998).

The clastic sedimentary unit crops out in three separate areas south of the Purvis Lake fault; these are inferred to be parts of a once-continuous belt offset by the Tildesley Creek and Trembleur Lake fault systems. This belt correlates with the eastern belt north of the Purvis Lake fault, based on its structural position directly west of the Cache

Creek ultramafic unit and, at least locally, directly east of metavolcanic rocks correlated with the Sitlika volcanic unit (Figure 2). The contact with the volcanic unit was nowhere observed south of the Purvis Lake fault, but facing directions within the well-exposed northeast-dipping succession of clastic metasedimentary rocks west of Mount Sidney Williams are consistently to the east, as predicted by this interpretation.

Exposures of the Sitlika clastic unit between Takla and Babine lakes are dominated by a rather monotonous succession of thin-bedded, medium to dark grey slates, slaty siltstones and siltstones. Thin to thick beds of fine to coarse-grained sandstone are fairly common, and include schistose feldspar-lithic wackes as well as massive well-indurated quartz-rich arenites. Foliated pebble conglomerate was observed rarely in western exposures of the unit near Cunningham Lake; some conglomerate units contain mainly felsic volcanic clasts whereas others are dominated by flattened chert clasts. Foliated limestone is an important component of the succession between the Purvis Lake and Tildesley Creek faults (MacIntyre *et al.*, 1998), and also occurs locally in the western part of the succession north of Cunningham Lake. Thin to medium beds of grey chert were noted over a narrow stratigraphic interval at a single locality within the central part of the unit southwest of Mount Sidney Williams.

Most of the above lithologies are characteristic of the Sitlika clastic unit in its main exposure belt north of the Purvis Lake fault. The exception is the chert-clast conglomerates near Cunningham Lake which have not been observed elsewhere. Samples of chert and limestone collected from the 1998 field area have been submitted for microfossil extraction in an attempt to further constrain the age of the Sitlika clastic unit.

Cache Creek Complex

The Cache Creek Complex is an imbricated assemblage of upper Paleozoic and lower Mesozoic oceanic rocks. Within the Babine Lake - Takla Lake area it is subdivided into 4 major lithotectonic units. The western part of the complex includes the Trembleur ultramafic unit and the overlying North Arm succession, which are interpreted as mantle and crustal portions, respectively, of an ophiolite sequence. This ophiolite succession is in thrust contact above the clastic unit of the

Sitlika assemblage to the west. Faulted against the ophiolitic rocks to the east is a succession of pelagic metasedimentary rocks referred to as the phyllite-chert unit of the Cache Creek Complex. These rocks are in stratigraphic and/or fault contact with several thick limestone units that occur mainly along the eastern margin of the Cache Creek belt and comprise the fourth mappable unit within it.

Trembleur Ultramafic Unit

Ultramafic rocks within the Cache Creek belt were referred to as the Trembleur intrusions by Armstrong (1949), who interpreted them to be intrusive bodies cutting the Cache Creek sedimentary and volcanic rocks. Paterson (1974) recognized that the ultramafic rocks east of Mount Bodine comprised a major fault zone that separated the Cache Creek Group from the Sitlika assemblage. This faulted belt was traced by Schiarizza *et al.* (1998) into the southern Mitchell Range, where Armstrong's Trembleur intrusions had been interpreted by Elliot (1975) and Whittaker (1983) to be structurally emplaced alpine-type peridotites. Mapping to the south during the 1998 field season has documented that the apparently isolated ultramafic massifs at Mount Sidney Williams and Rubyrock Lake occupy the same structural position, thrust above the Sitlika clastic unit, as the ultramafic belt to the north (Figure 3). They are therefore inferred to be part of the same, once continuous belt, offset along the Tildesley Creek and Trembleur Lake fault systems. Furthermore, the identification of a sheeted dike complex as a component of the overlying North Arm succession corroborates earlier interpretations (Whittaker, 1983; Ash and Macdonald, 1993) that the ultramafic rocks comprise part of an ophiolite succession.

The Trembleur ultramafic unit consists of variably serpentinized harzburgite, dunite and orthopyroxenite, together with zones of serpentinite, serpentinite melange, variably foliated carbonate-talc rocks and listwanite. The ultramafic rocks are intruded by dikes and pods of diabase, clinopyroxenite and gabbro, and locally contain fault slivers and tectonic inclusions of metavolcanic and metasedimentary rock.

Relatively unaltered ultramafic rocks were observed in parts of the northern and southern Mitchell Range, on Tsitsutl Mountain, on the

Mount Sidney Williams ridge system and to the east and southeast of Rubyrock Lake. The dominant rock type is rusty-brown to grey-brown weathering harzburgite characterized by a warty texture resulting from resistant orthopyroxene grains standing in relief against a background of mainly serpentinized olivine. Layering is observed locally and is defined by bands of orthopyroxenite, 1 to 3 cm wide, separated by wider layers of typical harzburgite. Many harzburgite exposures exhibit a penetrative, locally mylonitic foliation that is inferred to be a mantle transport fabric. The foliation typically has a platy to ribbonous aspect, and is defined by mm-scale bands dominated by flattened orthopyroxene grains interleaved with less resistant fine-grained olivine-rich bands. Although not mapped in detail, this ductile foliation is commonly at a high angle to the external contacts of the ultramafic unit, and in places is clearly cut by foliations defined mainly by talc or serpentine minerals that are parallel to the external contacts and are presumably related to the thrust imbrication of the ultramafic rocks with adjacent units.

Dunite, distinguished by its tan-weathering colour and smooth-textured surface, is commonly associated with the harzburgite as a volumetrically subordinate phase. It consists of serpentinized olivine accompanied by up to a few per cent chromite and, locally, rare grains of orthopyroxene. Dunite most commonly occurs as irregular pods and lenses within harzburgite that are typically several metres to tens of metres in size. Whittaker (1983) describes these in some detail, and also describes zones of interlayered dunite and harzburgite, as well as tabular dikes of dunite that emanate from large dunite pods and crosscut the tectonite fabric in the host harzburgite. He interprets these, and other features of the ultramafic rocks, as reflecting an origin in depleted mantle beneath an oceanic spreading centre, and suggests that the ultramafic rocks exposed in the Mitchell Range represent a deeper level than those at Mount Sidney Williams.

Large parts of the Trembleur ultramafic unit are altered to the extent that protolith compositions are not recognizable. Foliated serpentinite, locally passing into serpentine-magnesite-talc schist, commonly forms a zone several hundred metres wide along the structural base of the unit. Relatively narrow zones of similar rock occur throughout the unit, perhaps reflecting local

shear zones. Listwanite likewise occurs as narrow, fault or fracture-controlled zones of alteration that are relatively widespread but generally do not comprise a major proportion of the unit. The largest alteration zone within the area consists of variably foliated carbonate-talc rocks that cover more than 50 square km to the east and southeast of Mount Sidney Williams (Figure 2). These rocks typically weather to an orange-rust colour, presumably reflecting an ankeritic component to the carbonate. Zones of more resistant listwanite occur locally within the unit, and a lens of pure talc was observed at one locality, covered by the Dial claim, about 7.5 km east-southeast of Mount Sidney Williams.

Diabase and microgabbro, in many places partially altered to rodingite, are relatively common as tabular to boudinaged dike-like bodies that intrude harzburgite and associated rocks of the ultramafic unit. Larger bodies of clinopyroxenite, gabbro and amphibolite also occur, but adjacent ultramafic rocks are typically sheared and/or serpentized such that original relationships are not clear. These mafic intrusive rocks are typical of the North Arm succession and constitute part of the link connecting the mantle and crustal portions of the Cache Creek ophiolite sequence.

North Arm Succession

The North Arm succession, named for exposures along the North Arm of Stuart Lake, is characterized by diabasic to gabbroic intrusive rocks, but also includes significant proportions of mafic metavolcanic rock and metasedimentary rocks. This unit is widespread in the western part of the Cache Creek belt south of the Purvis Lake fault. It typically occurs structurally above the Trembleur ultramafic unit, where it is inferred to have originated as the upper part of an ophiolite sequence. Fault panels of the North Arm succession also occur to the west of and structurally beneath the ultramafic unit, where they are inferred to comprise structural repetitions resulting from both west directed imbrication of Cache Creek Terrane and later faulting (Figure 3).

The base of the North Arm succession comprises an igneous complex dominated by gabbroic to dioritic rocks. These rocks occur directly above the ultramafic unit at Rubyrock Lake, and are repeated along the structural base of the unit



Photo 6. Foliated gabbro and amphibolite from intrusive complex within the North Arm succession, south of Mt. Sidney Williams.

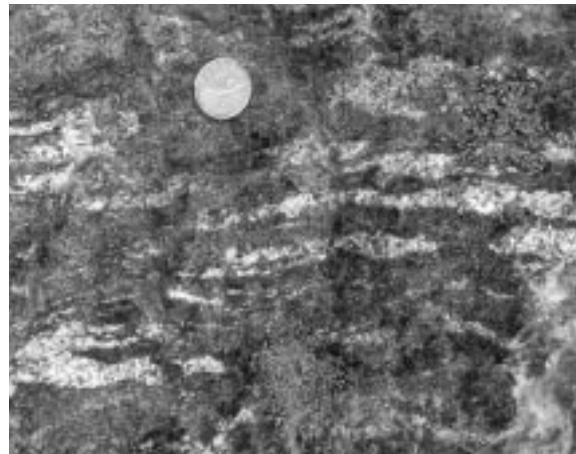


Photo 7. Tonalite lenses within gabbro/diorite intrusive complex of the North Arm succession, west of Mt. Sidney Williams.



Photo 8. Sheeted dike complex, east of Rubyrock Lake.

between Trembleur and McKelvey lakes, where they rest structurally above the phyllite-chert unit across a west-dipping fault (Figure 3, Section D). Similar rocks are also exposed south and west of Mount Sidney Williams, within the imbricate fault sliver structurally beneath the ultramafic unit (Figure 2). This igneous complex is dominated by isotropic to weakly foliated gabbro and diorite, but locally includes strongly foliated diorite and amphibolite localized along high strain zones of variable orientation (Photo 6). The complex also includes diabase and hornblende-feldspar porphyry dikes, as well as local dikes and pods of tonalite. Tonalite is most common in exposures west of Mount Sidney Williams (Photo 7). A sample collected from this area is being processed for zircon extraction, in an attempt to date the crystallization of the unit by the U-Pb method.

The basal part of the North Arm succession also includes a sequence of sheeted diabase dikes that are well exposed on a prominent ridge 6 km east of Rubyrock Lake. Individual dikes vary from a few cm to about 1 m in thickness and display uniform, steep northeast dips. Most dikes are chilled against an older dike to the east, and are intruded by a younger dike to the west (Photo 8). The opposite relationship occurs locally, however, and some dikes display chilled margins along both contacts. Elsewhere dike contacts are obscure or sheared across intervals of several metres. The average width and uniform dip of individual dikes, combined with the across-strike exposure width of the ridge, indicates that the complex includes many hundreds to thousands of individual dikes. They resemble diabase dikes and dike-boudins that cut the underlying Trembleur ultramafic unit, as well as dikes that occur at higher structural levels within the North Arm succession. They provide a link between the Trembleur ultramafic unit and the overlying North Arm succession, and provide compelling evidence for postulating an ophiolitic origin for the sequence.

The main part of the North Arm succession, which appears to reside structurally above the plutonic and dike complexes described above (Figure 3, Section D) consists of submarine mafic metavolcanic and metasedimentary rocks cut by numerous dikes and sills of greenstone, diabase and microdiorite. These rocks are well exposed on the shores of Trembleur Lake and on the alpine ridges east of Tsitsutl Mountain.

The rocks exposed along the shores of

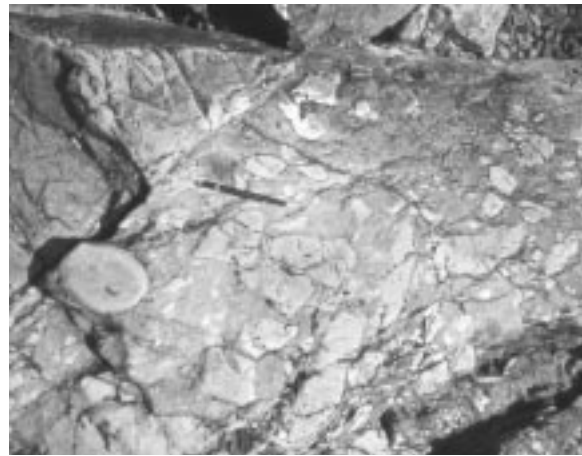


Photo 9 Chert-clast conglomerate interbedded with massive greenstone and pillowed flows, north shore Trembleur Lake. Disruption of chert beds may be related to emplacement of dikes into unlithified sediments during periods of active volcanism.

Trembleur Lake are predominantly mafic pillowed flows, pillow breccia and chlorite schist. In general pillowed flows are found in the central and eastern parts of the belt while chlorite schists predominate to the west. Although the chlorite is in part the result of regional greenschist facies metamorphism, some chloritization may have resulted from submarine hydrothermal activity. Evidence for the latter are zones of quartz-carbonate veining and disseminated pyrite associated with strong chlorite and epidote alteration. Marine sedimentary rocks comprise approximately 10 percent of the succession and are present as 10 to 50 metre-thick intervals of well bedded chert, cherty argillite, graphitic phyllite, argillaceous limestone and, in places, conglomerates or debris flows comprised of angular, rip-up clasts of chert and siltstone (Photo 9). Lithologically, these sediments resemble those of the phyllite-chert unit to the east. The volcanic and sedimentary rocks are intruded by numerous aphanitic greenstone dikes and sills which comprise 25 to 30 percent of the outcrop on the south shore of Trembleur Lake. These intrusions, which are compositionally similar to pillowed flows in the section, are massive, blocky weathering and form prominent headlands. Sediments near the contacts of these intrusions display chaotic fold patterns with many individual beds attenuated and dismembered. This implies that the dikes and sills, which are most likely feeders to flows higher up in the succession, cut through and deformed rel-

atively unconsolidated marine sediments.

Other belts assigned to the North Arm succession are generally similar to the Trembleur Lake section, and are distinct from the phyllite-chert unit in the predominance of mafic volcanic and intrusive rocks over associated sedimentary intervals. In places, such as to the east of Fleming Lake and south of the west end of Trembleur Lake, massive greenstone, locally grading to fine-grained diabase or microdiorite is the predominant rock type over many square km, and associated metasedimentary rocks are restricted to narrow screens and xenoliths. Serpentinized ultramafic rocks are locally an important component of western exposures of the unit, where it is inferred to be imbricated along the base of the Trembleur ultramafic unit. These serpentinite lenses may actually be fault slivers derived from the overlying unit that are structurally interleaved with the North Arm succession.

The age of the North Arm succession is not well known. The only definitive fossil locality is on the east flank of Tsitsutl Mountain where a limestone bed interbedded with chlorite schists and greenstones has yielded Early(?) Triassic conodonts (M.J. Orchard, written communication, 1998). Two narrow limestone beds within the succession, one near the west end of Trembleur Lake and the other north of Fleming Lake, contain crinoid debris and fusulinids, suggesting that part of the succession is Late Paleozoic. Samples from these and other limestone units within the succession are currently being processed for conodonts in an attempt to better constrain its age.

The North Arm succession is interpreted as the upper part of an ophiolite sequence, generated in an oceanic spreading centre. The available age data, although sparse, suggest that sedimentary intervals intercalated with and intruded by the mafic volcanic and intrusive rocks related to this spreading event are Late Paleozoic and Early Triassic. This same age range is represented by volcanic and intrusive rocks of the Sitlika assemblage, which may represent an intraoceanic volcanic arc. This apparent coincidence of ages, coupled with their present spatial juxtaposition, suggests that the Trembleur ultramafic unit and overlying North Arm succession may have formed in a back-arc spreading centre behind the Sitlika arc. This interpretation predicts that the pending U-Pb zircon date from tonalite of the North Arm succession will be Late Permian or Early Triassic.

Another implication of the inferred geologic environment of the North Arm succession (regardless of its age or relationship to the Sitlika assemblage) is that it presents an exploration target for volcanogenic massive sulphide deposits of the Besshi and Cyprus subtypes.

Phyllite-Chert Unit

Quartz phyllite, chert and associated metasedimentary rocks that crop out directly east of the Cache Creek ophiolitic sequence are assigned the phyllite-chert unit. These rocks are equivalent to the Cache Creek sedimentary unit of Schiarizza *et al.* (1998), and are at least in part equivalent to the Sowchea succession of Struik and Orchard (1998).

The phyllite-chert unit consists mainly of light to dark grey platy quartz phyllites that consist of plates and lenses of fine-grained recrystallized granular quartz, typically a centimetre or less thick, separated by phyllitic mica-rich partings. Associated with the phyllites are intervals of less recrystallized, light to medium grey or green chert that occurs as beds and lenses, from 1 to 5 centimetres thick, separated by phyllitic partings. Locally the platy phyllites and cherts are intercalated with less siliceous and more homogeneous medium to dark grey phyllites or slates.

Light to dark grey recrystallized limestone is locally intercalated or structurally interleaved with the siliceous metasedimentary rocks, and occurs as units ranging from a few metres to more than 100 metres thick. Some of these are sufficiently large to be mapped as separate units on Figure 2. Mafic metavolcanic rocks, including chlorite schist, pillowed greenstone and fragmental greenstone, occur rarely. They form lenses, ranging from a few metres to tens of metres thick, parallel to the synmetamorphic foliation and transposed compositional layering in surrounding metasedimentary intervals. Locally they are associated with weakly foliated, fine-grained chlorite-feldspar semischists that were probably derived from mafic dikes or sills.

The phyllite-chert unit rests structurally above the Trembleur ultramafic unit north of the Purvis Lake fault (Figure 3, Sections A and B). The contact was not observed in this area, but is inferred to be an east-directed thrust fault based on observations made along the same contact farther north (Schiarizza and Payie, 1997). A

similar relationship is suspected for the contact between the phyllite-chert unit and structurally underlying North Arm succession between the Purvis Lake and Trembleur Lake faults, but the contact is obscured by the Pyramid Peak pluton in the north, and by Quaternary alluvium along the Middle River valley in the south. South of Trembleur Lake, the phyllite-chert unit rests structurally beneath the North Arm succession across an inferred west-dipping thrust fault (Figure 3, Section D). A similar relationship is documented farther south, near Shass Mountain, where Struik and Orchard (1998) show ultramafic and mafic rocks thrust above the Sowchea succession across a west-dipping thrust fault.

Samples from a limestone breccia within the phyllite-chert unit north of the present map area contained both Early and Middle Triassic conodonts (M.J. Orchard, written communication, 1997), whereas a limestone lens northeast of Purvis Lake yielded conodonts of Pennsylvanian or Permian age (M.J. Orchard, written communication, 1998). Other age constraints come from south of the present map area, where correlative rocks of the Sowchea succession have yielded Late Permian and Middle and Late Triassic radiolaria and conodonts (Struik and Orchard, 1998). Radiolarians of possible Early Jurassic age occur within the succession southwest of Stuart Lake, and a collection of radiolaria that has been assigned a definite Early Jurassic (Pliensbachian) age was extracted from a potentially correlative chert succession in the Prince George map area (Cordey and Struik, 1996).

Limestone

Massive to well-bedded, light grey-weathered limestone forms several mappable units within and east of the phyllite-chert unit north of Trembleur Lake. The most extensive belt, best represented by exposures around Kazchek and Kloch mountains near the eastern boundary of the map area, is up to 5 km wide and has been traced northward and southeastward from the present map area for a total strike length of about 100 km (Armstrong, 1949). Near Takatoot and Kloch lakes this limestone unit is juxtaposed directly against Quesnel Terrane across the Pinchi fault. To the north, however, it is separated from Quesnel Terrane by panels of serpentine-gabbro-greenstone and limestone that are

inferred to be slivers of Cache Creek rocks caught up in the Pinchi fault zone (Figure 2; Bellefontaine *et al.*, 1995). To the southeast of the present map area it is likewise separated from Quesnel Terrane by a northward-tapering fault panel of Upper Triassic - Lower Jurassic greywacke and basalt tuff that Struik and Orchard (1998) assign to the Tezzeron succession of the Cache Creek Group.

The Kazchek Mountain limestone unit dips mainly to the west or southwest, although local dip reversals provide evidence for some internal folding. The limestone belt includes rare exposures of chert, phyllite and fine-grained intrusive or extrusive mafic rock, but it is not clear if these rocks form part of the unit or are fault slivers derived from the adjacent phyllite-chert unit. Despite the possibility of internal structural repetitions, local well-exposed homoclinal sections indicate a minimum stratigraphic thickness of almost 1000 m. A sample from the central part of the Kazchek Mountain limestone unit, collected 3 km north of the west end of Tchentlo Lake in 1997, yielded Bashkirian - Moscovian (Late Carboniferous) conodonts (M.J. Orchard, written communication, 1998). Conodonts and macrofossils of the same age are reported from the eastern part of the unit both north and south of Kloch Lake (Orchard *et al.*, 1998, Samples N3-3 and K14-3). Samples collected from the western part of the unit farther to the south and southeast also yielded conodonts of the same, Late Carboniferous age (Orchard *et al.*, 1998, Samples K14-1, K15-3, K15-4, K15-5). These age data, together with its thickness and location near the eastern edge of the Cache Creek belt, indicate correlation of the Kazchek Mountain limestone unit with the Mount Pope limestone unit of the Fort St. James area (Sano and Struik, 1997; Orchard *et al.*, 1998), which is, at least in part, in thrust contact with metasedimentary rocks that may correlate with the phyllite-chert unit of the present study area (Struik and Orchard, 1998). Within the present map area, the western contact of the Kazchek Mountain limestone unit is not well exposed, but appears to dip steeply. It is suspected to be a steep fault, possibly related to the Pinchi fault system.

Other mappable limestone units within the eastern part of the Cache Creek belt are, at least in map view, enclosed within the phyllite-chert unit. The most extensive of these units is well

exposed on Mount Copley, north of eastern Trembleur Lake. It has been traced for 25 km to the northwest (Figure 2) and continues south-eastward beyond the map area for a total strike length of about 35 km (Armstrong, 1949). Exposures on the north flank of Mount Copley, as well as those near the northern end of the belt west of Kloch Lake, suggest that the Mount Copley limestone unit occupies the core of an anticline (Figure 3, Section C). Conodonts from within the unit west of Kloch Lake are Late Permian (Orchard *et al.*, 1998, Sample N3-1), whereas a suite of samples from the gradational contact with the overlying phyllite-chert unit to the east yield Late Permian and Early Triassic conodonts (Orchard *et al.*, 1998, Samples N3-2). These dates are within the range of ages established for the phyllite-chert unit regionally, suggesting that the Mount Copley unit represents a carbonate facies within it. Other mappable limestone bodies within the phyllite-chert unit to the west and northwest might be fold or fault repetitions of the Mount Copley unit (e.g. Figure 3, Section C), or might be separate carbonate lenses. Samples collected during the 1998 field season are currently being processed for conodonts in an attempt to establish their ages.

Late Middle Jurassic to Early Cretaceous Intrusions

Middle Jurassic granitoid plutons within Stikine Terrane were described in a previous section. A number of other map-scale plutons occur within the area, where they intrude the Cache Creek Complex and Sitlika assemblage. Most are undated, but at least three temporally distinct magmatic events are represented by the plutons with known ages. These include the late Middle Jurassic McKnab Lake pluton, Late Jurassic to Early Cretaceous stocks at the Mac porphyry molybdenum prospect, and the Early Cretaceous Mitchell batholith. The McKnab Lake pluton is coeval with or slightly younger than Middle Jurassic plutons within the adjacent Stikine Terrane, and the composite Endako batholith, within Stikine Terrane to the south-southeast, includes Middle Jurassic to mid-Cretaceous plutonic suites that apparently correlate with the plutons described here. These plutons are therefore inferred to comprise part of a Middle Jurassic and younger magmatic belt that overlaps the contact between the previously amal-

gamated Stikine and Cache Creek terranes.

In the summary that follows undated plutons are described immediately following the dated pluton to which they bear the closest lithological resemblance.

Middle Jurassic McKnab Lake Pluton

Tonalite, quartz diorite and diorite in the southeastern part of the map area comprise the west end of the McKnab Lake pluton, a large east to southeast-trending plutonic body that extends for an additional 40 km beyond the southeastern boundary of the study area (Struik, 1998). It was referred to as the Shass Mountain pluton by Ash and Macdonald (1993), but Letwin and Struik (1997) introduced the new name because detailed mapping had shown that, contrary to the map of Armstrong (1949), Shass Mountain itself was underlain by imbricated rocks of the Cache Creek Group.

Within the present study area, the McKnab Lake pluton is predominantly medium to coarse-grained hornblende-biotite quartz diorite and tonalite. Diorite occurs locally along the northern margin of the pluton, and also occurs as xenoliths within the quartz-bearing phases. The predominant quartz-bearing phases range from isotropic to moderately foliated. Foliation is commonly parallel to the pluton contact and is accentuated by flattened xenoliths of foliated diorite and amphibolite.

The McKnab Lake pluton is assigned a late Middle Jurassic age based on a U-Pb zircon date of 165 \pm 2/-1 Ma reported by Ash *et al.* (1993) from west of southern Stuart Lake, almost 35 km east-southeast of the southeastern corner of the present map area. A sample collected in 1998 from near the western margin of the pluton, south of Cunningham Lake, has been submitted for U-Pb dating to test for uniformity of age in this large plutonic body. This date will help constrain the age of the fault contact between the Trembleur ultramafic unit and the Sitlika clastic unit, which is truncated by the pluton at Cunningham Lake (Figure 2).

McKelvey Lake Pluton

The McKelvey Lake pluton intrudes the North Arm succession and phyllite-chert unit of the Cache Creek Complex between Stuart and

Trembleur lakes. It was examined by Ash and Macdonald (1993) and Hrudehy and Struik (1998), who describe it as biotite quartz diorite, diorite and tonalite, and suggest that it correlates with the McKnab Lake pluton.

Fleming Lake Stock

Relatively resistant exposures of hornblende diorite, locally cut by tonalite or granodiorite phases, define a stock measuring about 4 by 5 km to the west-northwest of Fleming Lake. On its eastern margin the stock intrudes, and locally contains xenoliths of, metachert, greenstone and actinolite-epidote-feldspar semischist assigned to the North Arm succession of the Cache Creek Complex. The country rock adjacent to the eastern part of the stock is not exposed. The Fleming Lake stock is not dated, but is suspected to be Middle Jurassic in age.

Embryo Lake Pluton and Purvis Lake Stock

The Embryo Lake pluton consists of medium-grained, isotropic to weakly foliated \pm biotite-hornblende quartz diorite, tonalite and diorite. It forms prominent exposures northeast of the southern tip of Takla Lake, where it intrudes the phyllite-chert unit of the Cache Creek Complex. The northwestern contact of the pluton is inferred to be the Purvis Lake fault, across which it is juxtaposed against granodiorite of the Leo Creek stock (Figure 2). The Embryo Lake pluton is distinguished from the Early Cretaceous(?) Leo Creek stock, as well as from the adjacent Pyramid Peak and MacDonald Lake plutons by the general absence of potassium feldspar and the presence of hornblende as the predominant mafic phase. It is lithologically very similar to the Middle Jurassic McKnab Lake pluton, with which it is tentatively correlated.

The Purvis Lake stock, which intrudes the Cache Creek phyllite-chert unit on the northwest side of the Purvis Lake fault, 5 km northeast of the Embryo Lake pluton, is likewise inferred to be Middle Jurassic in age. It consists mainly of medium-grained, equigranular hornblende diorite to quartz diorite, but also includes clinopyroxenite and gabbro, which are locally common as xenoliths and screens within the diorite (Schiarizza *et al.*, 1998).

Late Jurassic - Early Cretaceous Francois Lake Plutonic Suite

At the Mac property near Tildesley Creek, small granitoid stocks and dikes, some with associated molybdenum mineralization, intrude mafic metavolcanic rocks and serpentinite assigned to the North Arm succession of the Cache Creek Complex. The largest plutonic body is an unmineralized stock of medium-grained biotite granodiorite that crops out west and southwest of the main mineralized zones. Biotite from this stock has been dated at 141 ± 5 Ma by the K-Ar method (Godwin and Cann, 1985). Godwin and Cann also report a K-Ar date of 136 ± 5 Ma on biotite from altered leucocratic granite of the mineralized Camp zone stock (Cope and Spence, 1995). More recently, an Ar-Ar date of 142.5 ± 1.4 Ma was obtained on biotite from a sample of drill core from the same stock (MacIntyre *et al.*, 1997, Table 1). These dates are slightly younger than new 145-148 Ma Ar-Ar isotopic ages determined for the younger subsuite of the Francois Lake plutonic suite, which hosts molybdenum mineralization in the Endako batholith (Anderson *et al.*, 1998).

Early Cretaceous Mitchell Batholith

The Mitchell batholith occupies the core of the Mitchell Range, where it intrudes the sedimentary unit of the Sitlika assemblage, as well as the ultramafic and phyllite-chert units of the Cache Creek Complex (Schiarizza *et al.*, 1998). The northern part of the batholith is dominated by K-feldspar megacrystic, \pm hornblende-biotite monzogranite, locally accompanied by an older border phase of mafic-rich biotite-hornblende quartz diorite to diorite along its east-central and northwestern margins. The southern part of the batholith is mainly medium to coarse-grained \pm muscovite-biotite granodiorite, locally intruded by thick dikes of quartz-feldspar porphyry.

Zircons extracted from K-feldspar megacrystic monzogranite of the Mitchell batholith, sampled 2 km south of Sawtooth Mountain, yielded a U-Pb date of 121.9 ± 0.1 Ma (Mike Villeneuve, personal communication, 1998). This is apparently a unique crystallization age for major plutons in the region, although it is not a great deal older than the 90 to 115 Ma Fraser Lake plutonic suite that is represented by stocks of biotite monzogranite and granodiorite

that occur locally along the margins of the composite Endako batholith (Anderson *et al.*, 1998). This date from the Mitchell batholith places some constraints on the age of the east-dipping thrust fault that places the Trembleur ultramafic unit above the Sitlika clastic unit, as this fault is truncated by the batholith (Figure 2).

Leo Creek Stock

The Leo Creek stock consists of medium to coarse-grained \pm muscovite-biotite granodiorite that is exposed along the lower reaches of Leo Creek, on the northeast side of southern Takla Lake. It intrudes various units of the Cache Creek Complex and Sitlika assemblage to the north and west, and is inferred to be truncated by the Purvis Lake fault to the southeast. The Leo Creek stock resembles granodiorite that comprises the southern part of the Mitchell batholith, just 3 km to the north, and is presumed to be the same age.

Pyramid Peak Pluton

The Pyramid Peak pluton, named and described by MacIntyre *et al.* (1998), comprises biotite granodiorite that underlies the prominent peaks and ridges southwest of the southern end of Takla Lake (Figure 2). The pluton intrudes the North Arm succession of the Cache Creek Complex on the west, and the phyllite-chert unit to the east. It is truncated by the Purvis Lake fault to the north, and its southern margin is apparently defined by the Tildesley Creek fault. The age of the Pyramid Peak pluton is presently unknown, but samples have been submitted for U-Pb and Ar-Ar radiometric dating. It is here provisionally correlated with the Early Cretaceous Mitchell batholith and Leo Creek stock. In fact, it moves to a position directly opposite the Leo Creek stock when 7 to 8 km of dextral offset are restored on the Purvis Lake fault, suggesting that these two bodies represent offset portions of a single pluton.

Small plugs and dikes of white to pink weathering quartz-feldspar porphyry intrude the Cache Creek Complex on the ridge southeast of Tsitsutl Mountain, 2 to 3 km west of the Pyramid Peak pluton. The stocks are enclosed by a zone of disseminated pyrite within hornfelsed metavolcanic and metasedimentary country

rocks of the Cache Creek Complex. These porphyry bodies may correlate with the thick dikes of quartz-feldspar porphyry that intrude granodiorite of the southern Mitchell batholith.

MacDonald Lake Pluton

The MacDonald Lake pluton intrudes the phyllite-chert unit of the Cache Creek Complex to the east and southeast of Purvis Lake. It and the adjacent Embryo Lake pluton were mapped as a single body by Armstrong (1949), but more detailed mapping shows that they are separated by 3 to 4 km of Cache Creek metasedimentary rocks. Furthermore, the MacDonald Lake pluton consists mainly of medium to coarse-grained, isotropic, biotite tonalite and granodiorite, in contrast to the hornblende-rich, locally foliated quartz diorite of the Embryo Lake pluton. Based on these lithologic attributes, the MacDonald Lake pluton is provisionally correlated with the Early Cretaceous Mitchell batholith.

Cretaceous Sedimentary Rocks

Sustut Group

The Sustut Group (Lord, 1948; Eisbacher, 1974) includes Cretaceous and Tertiary non-marine clastic rocks that overlap rocks of the Stikine Terrane and the Bowser Lake Group. The areal distribution of these rocks defines the northwest trending Sustut Basin which extends from the Stikine River in the northwest to Takla Lake in the southeast. The Sustut Group is restricted to the northwest corner of the present map area, where it is represented by exposures of conglomerate, sandstone and shale of the Tango Creek Formation. These rocks, which crop out west of the Takla fault, were mapped in 1997 and are described by MacIntyre (1998) and Schiarizza *et al.* (1998). They were not revisited during the 1998 field season.

Tertiary Volcanic Rocks

A gently southeast dipping section of Tertiary volcanic rocks is preserved in a down-dropped fault block that underlies a low-lying region in the central part of the 93K/12 map sheet. The western limit of these volcanics is an

angular unconformity with Takla and Asitka Group rocks. The succession thickens eastward until it is truncated by a northeast-trending high angle fault that bounds an uplifted fault block. Outliers of Tertiary volcanics cap uplifted areas south of Tochcha Lake and north of Rubyrock Lake (Figure 2). Where exposed, the basal members of the succession are brown to dark grey vesicular and amygdaloidal basalt flows with local beds of basalt clast pebble conglomerate. The vesicles range from 1 to 10 millimetres in diameter and comprise 20 to 35 percent of the rock. Vesicles and amygdules are often flattened parallel to the flow direction. Individual flows are 5 to 15 metres thick and are separated by thin beds of volcaniclastic material. Coarse debris flows or lahars comprised of vesicular and aphanitic basalt or andesite clasts up to 2 metres in diameter are locally interbedded with the flows. These rocks, which crop out sporadically through the central part of the 93K/12 map sheet and along the shores of Babine Lake (Figure 2), form a relatively thick unit. The best exposures are opposite Pendleton Bay where beautifully columnar jointed basalt flows are overlain by a thick debris flow unit containing clasts up to 4 metres in diameter.

Grey to pinkish grey weathering, hornblende-biotite-feldspar phyric to aphyric rhyodacitic ash flows, with lesser, thin, andesite and brown weathering basalt flows crop out as a series of knolls along the southern edge of the Tochcha Lake map sheet. The ash flows locally contain 5-10 percent hornblende and biotite phenocrysts that are up to one centimetre in diameter. Granitic inclusions are also common in some cooling units. Outcrops to the south and at lower elevation are aphanitic, dark grey basalt, feldspar phyric andesite and vesicular basalt. These rocks are interpreted to lie below the ash flow succession; alternatively they are separated by a high angle fault. Above the ash flow succession is a dark grey, aphanitic basalt flow that has a subconchoidal fracture. A sample of ash flow with fresh hornblende and biotite was collected for Ar-Ar isotopic dating in 1997; additional samples were collected by Nancy Grainger of the GSC in 1998.

Dark grey and red mudstones crop out near the eastern limit of Tertiary volcanic cover. Because the Tertiary succession is interpreted to thicken eastward as a wedge, these sediments are believed



Photo 10. Flat-lying, Tertiary debris flow overlying ultramafic rocks north of Rubyrock Lake, 93K/11 map sheet. The debris flow contains feldspar phyric andesite boulders up to 2 metres in diameter.

to be relatively high in the volcanic stratigraphy.

The ridge north of Rubyrock Lake, in the 93K/11 map sheet, is also capped by Tertiary volcanic rocks. Here, hornblende-feldspar phyric dacite flows overlie serpentized ultramafic rocks. The highest member in the Tertiary succession is a flat lying debris flow containing feldspar phyric andesite clasts up to 2 metres in diameter (Photo 10).

The age of the Tertiary volcanic cover in the southwest corner of the study area is unknown but presumed to be Eocene based on the ages of similar rocks elsewhere in central B.C. Hornblende-biotite phyric rhyolite to rhyodacite flows that crop out south of Tochcha Lake and north of Rubyrock lake are tentatively correlated with the Ootsa Lake Group, as are vesicular basalts, feldspar phyric andesites and aphanitic basalts that apparently underlie these rocks. Basaltic flows that overlie rhyodacite are correlated with the Endako Group based on lithology and stratigraphic position.

Eocene Intrusions

A distinctive suite of potassium feldspar megacrystic quartz monzonite or granite dikes cut Sitlika volcanic rocks along the crest of the ridge northwest of Cunningham Lake in the 93K/12 and 11 map sheets. These dikes, which are up to 100 metres thick, are characterized by a megacrystic texture defined by the presence of 25 to 30 percent, 1 to 2 centimetre, equant potassium feldspar phenocrysts. In addition these

rocks contain 5 to 10 percent, 1 to 2 millimetre hornblende and/or biotite and 5 to 10 percent, 2 to 4 millimetre quartz phenocrysts, all in a pinkish grey quartz-feldspar groundmass. Biotite extracted from one of these dikes on the Ascot Resources Fort property gave an Ar-Ar isotopic age of 52 Ma, suggesting this suite of intrusions is Eocene in age. This age is similar to those determined for the Babine Intrusions in the Babine Porphyry Belt (Villeneuve and MacIntyre, 1997) located west of the project area. On the northern part of the Fort property, emplacement of the dikes produced a broad zone of biotite hornfels that typically contains 1 to 5 percent disseminated pyrite.

Finer-grained, crowded biotite-hornblende-feldspar and biotite-quartz-feldspar porphyritic granodiorite dikes that are lithologically similar to the Eocene Babine Intrusions also occur in the Cunningham Lake area. These dikes intrude the pyroxenite-gabbro-diorite complex at the Fort prospect. A similar suite of dikes intrudes serpentinite along the crest of the ridge north of Rubyrock Creek in the 93K/11 map sheet and one of these has porphyry copper style sulphide mineralization associated with it.

STRUCTURE

The Babine Lake - Takla Lake area is comprised of two main structural domains. The eastern domain includes penetratively deformed, greenschist facies rocks of the Cache Creek Complex and Sitlika assemblage, arranged as a series of linear, north to northwest trending fault panels that apparently originated as east-dipping thrust slices in Middle Jurassic time. The western domain is underlain by the various stratigraphic and plutonic components of Stikine Terrane. Only some of these rocks display penetrative fabrics, and east-dipping thrust faults are only locally preserved. Regional relationships suggest, however, that Stikine Terrane formed the footwall to the west-directed thrust system within adjacent Cache Creek Terrane.

Younger structures within the map area include steep, north to northwest-striking faults, many of which formed during a period of orogen-parallel dextral strike-slip in Late Cretaceous - Early Tertiary time. Other prominent structures are northeast-striking faults, most with apparent dextral displacements, that locally

offset the northerly trending fault panels. The most significant of these structures are the Purvis Lake, Tildesley Creek and Trembleur Lake fault systems. The northeast-striking faults may be coeval with, or younger than, the northwest-striking dextral strike-slip faults.

Sitlika - Cache Creek Belt

Mesoscopic Fabrics

Both units of the Sitlika assemblage are characterized by a single penetrative cleavage or schistosity defined by the preferred orientation of greenschist facies metamorphic minerals and variably flattened clastic grains or volcanic fragments. The cleavage dips steeply to the east or east-northeast through most parts of the Sitlika belt, although steep westerly dips prevail locally. It is axial planar to upright folds of bedding, most commonly observed in well-bedded metasedimentary rocks of the Triassic-Jurassic clastic unit, with axes that plunge north-northwest or south-southeast. Younger folds and crenulations with similarly oriented axes deform the cleavage locally, as do rare east or west plunging kink folds and crenulations.

Most of the Cache Creek Complex comprises greenschist facies rocks that are of comparable metamorphic grade to the Sitlika assemblage, but contrast markedly in structural style (Paterson, 1974; Wright, 1997; Schiarizza *et al.*, 1998). Mesoscopic structures are best displayed in the phyllite-chert unit and metasedimentary intervals of the North Arm succession, where compositional layering has been transposed into parallelism with a prominent metamorphic foliation. This foliation dips at moderate to steep angles to the east or northeast throughout most of the area, but dips are mainly to the west or southwest south of the Trembleur Lake fault system. The foliation is axial planar to fold hinges defined by thin chert beds, but these were observed only locally and are quite variable in orientation. The primary foliation and transposed bedding within the Cache Creek metasedimentary intervals are commonly deformed by younger structures, represented mainly by a set of east-verging folds with moderately west-dipping axial surfaces, generally marked by a crenulation or fracture cleavage. The axes of

these folds, along with associated crenulation lineations, typically plunge to the northwest or south. Metamorphic minerals that define the first generation schistosity are, at least in part, bent and kinked by these younger structures, indicating that these folds postdated most of the metamorphism.

Mesoscopic fabrics that apparently predate those described above occur locally within specific units of the Trembleur ultramafic unit and North Arm succession. These include the ductile, locally mylonitic foliations within harzburgite that are inferred to be mantle transport fabrics, as well as variably oriented zones of plastic deformation that were observed within gabbrodiorite plutonic complexes of the North Arm succession. The latter fabrics may have been localized along high strain zones associated with plutonism during construction of oceanic crust in a spreading centre environment.

Macroscopic Structure

The Cache Creek and Sitlika assemblages comprise a regular arrangement of fault-bounded panels that has been traced from Ogden Mountain southward to Cunningham Lake, a distance of 150 km (Schiarizza and Payie, 1997; Schiarizza *et al.*, 1998; Figure 2). The easterly dips that prevail in most of the belt are presumed to reflect the primary assembly of the sheets by way of west-directed thrusting. The east-dipping thrust sequence comprises 3 main levels which are, in ascending order, the Sitlika assemblage, ophiolitic rocks of the Cache Creek Complex, and sedimentary rocks of the Cache Creek Complex (Figure 3, Sections A, B and C). It is suspected that this stacking was broadly coeval with greenschist facies metamorphism and the development of penetrative fabrics within both the Sitlika assemblage and the Cache Creek Complex. South of the Trembleur Lake fault system, however, dips are mainly to the west and the apparent stacking order is, at least locally, reversed. This is presumed to reflect the influence of second generation east-directed folds and thrust faults, which are prominent mesoscopic features of the Cache Creek rocks in this part of the belt (Figure 3, Section D). Alternatively, or in addition, there may be a component of down-to-the-east tilting of this panel, perhaps related to movement along the

Trembleur Lake fault system.

The Sitlika assemblage comprises, for the most part, an east-dipping and facing succession in which the volcanic unit lies to the west of the overlying clastic sedimentary unit. North of the Purvis Lake fault, however, the clastic sedimentary unit also occurs as a narrow panel to the west of the volcanic unit. This repetition may be the result of west-directed thrust-imbrication, coeval with synmetamorphic folding within the Sitlika succession and stacking of Cache Creek Complex above the Sitlika rocks. Rocks of Stikine Terrane directly to the west may have formed the footwall to this thrust system. Alternatively, however, the Sitlika/Stikine contact might be part of a younger dextral strike-slip system, and the western panel of Sitlika clastic rocks might have been localized by this faulting rather than by earlier thrust imbrication.

The thrust contact between the Trembleur ultramafic unit and underlying Sitlika assemblage was observed on the north margin of the Mitchell batholith (Figure 3, Section A; Schiarizza *et al.*, 1998), whereas the contact between the ultramafic unit and the overlying phyllite-chert unit was observed at two localities north of the area shown in Figure 2 (Schiarizza and Payie, 1997). Both exposures display kinematic evidence for east-directed thrusting. The relationships between the three main levels of the thrust system are also apparent from exposures near Takla Narrows, where folds along the southern margin of the Mitchell batholith and a repetition due to a young east-side-down normal fault demonstrate the stacking order and the sheet-like nature of the Trembleur ultramafic unit (Figure 3, Section B).

The North Arm succession, comprising the upper, crustal portion of the Cache Creek ophiolite sequence, is widespread south of the Purvis Lake fault, but does not occur to the north. This is consistent with the interpretation of Whittaker (1983), who suggested that the ultramafic rocks in the Mitchell Range were derived from lower depleted mantle whereas those at Mount Sidney Williams represent upper depleted mantle. It suggests that the thrust faults bounding the ultramafic unit have ramped upward from north to south across the area presently occupied by the Purvis Lake fault. The North Arm succession occurs mainly above the ultramafic unit, across a contact that is at least in part faulted but is interpreted as representing the transition from mantle to crustal

levels within the ophiolite sequence (Figure 3, Section D). Between Mount Sidney Williams and Tsitsutl Mountain, however, the North Arm succession also occurs structurally beneath the ultramafic unit, where it is inferred to comprise an imbricate fault slice along the footwall of the ophiolitic allochthon. A wide panel of the North Arm succession also occurs to the west of the Sitlika assemblage in the area between the Tildesley Creek and Trembleur Lake faults. It comprises a separate fault panel that must have been downdropped relative to the adjacent Sitlika rocks, either by normal faulting or an out-of-sequence east-dipping reverse fault. Displacement along this fault may not have been large if the Mount Sidney Williams area is broadly antiformal in nature, as suggested by the apparent envelopment of the ultramafic unit by the North Arm succession along the south shore of Trembleur Lake (Figure 2; Figure 3, Section C).

The east-dipping thrust fault that juxtaposes the Trembleur ultramafic unit above the Sitlika assemblage south of Tsayta Lake is truncated by the Early Cretaceous Mitchell batholith (Figure 2). Tighter constraints are placed on the age of imbricate thrusting within the Cache Creek Complex near Shass Mountain, where structures are cut by the 165 Ma McKnab Lake and older(?) Boer suite plutons (Struik, 1998; Struik and Orchard, 1998). The western end of the McKnab Lake pluton also cuts the fault contact between the Sitlika assemblage and Trembleur ultramafic unit near Cunningham Lake. These relationships indicate that imbrication of the Cache Creek Complex and Sitlika assemblage occurred in Early to Middle Jurassic time.

Stikine Belt

Volcanic flows and breccias of the Takla and Hazelton groups do not generally display the penetrative tectonic foliation that is typical of adjacent Sitlika and Cache Creek rocks, although sedimentary rocks within the Takla Group commonly show a moderately to strongly developed slaty cleavage, and clasts within conglomeratic intervals may be flattened in the plane of this cleavage. In contrast, both metavolcanic and metasedimentary rocks of the Asitka Group tend to be foliated, although it is not clear whether this is related to a pre-Takla deformational event or simply to relative depth in the stratigraphic sequence.

The thrust faults that form the major structural boundaries between the main lithotectonic units of Cache Creek Terrane are likewise not well represented in the Stikine Terrane, although an east-dipping thrust(?) fault that places the Takla Group above the Hazelton Group south-southeast of Takla Landing is of appropriate orientation and age (post Hazelton Group and pre 170 Ma Spike Peak pluton) to be correlative (Figure 2). Elsewhere, however, changes in stratigraphic level typically occur across apparently steeply-dipping northwest or northeast striking faults, giving rise to a pattern that suggests block faulting rather than thrusting.

The contact between rocks of Stikine Terrane and the adjacent Sitlika assemblage was not observed, but is fairly well constrained north of the Purvis Lake fault, as well as in the southern part of the map area, between Babine and Specularite lakes. In the northern part of the area the contact is apparently a steep fault that juxtaposes a narrow panel of Sitlika clastic rocks against various units of Stikine Terrane that are progressively truncated along the fault (Figure 2). Some of these truncated units, such as the thin sedimentary interval between the Takla and Hazelton groups, and the Takla Landing pluton, occur as narrow slivers along the fault zone north of the present map area (Schiarizza and Payie, 1997), suggesting that there has been significant dextral strike-slip along the fault. A southeast plunging asymmetric fold outlined by the Takla/Hazelton contact about 15 km north of Takla Narrows may have formed during dextral translation along the fault.

North of Babine Lake, the eastern boundary of Stikine Terrane appears to be a steep fault that juxtaposes the Taltapin metamorphic belt against the Sitlika volcanic unit. In contrast to other parts of the area, volcanic rocks of the Takla Group are commonly strongly foliated within and adjacent to this belt, as are the underlying Taltapin/Asitka rocks and the associated Butterfield Lake pluton. It is not clear, however, if movement along the bounding fault was linked to the deformation and metamorphism within the Taltapin belt, or if the bounding fault is only linked to the exhumation of these more deformed and higher grade rocks.

MINERAL OCCURRENCES

Mineral occurrences in the northern part of

the Babine Lake - Takla Lake area (93N map sheet) were described by Schiarizza *et al.*, (1998). Here we discuss only those occurrences in the northwest quadrant of the Fort Fraser (93K) map sheet (Table 1; Figure 5).

Occurrences Within Stikine Terrane

BABS (MINFILE 93L 325)

The BABS property straddles the boundary between the 93K/13 and 93L/16 map sheets. This property was described in MacIntyre *et al.* (1996). Showings on the property include altered rhyolitic tuffs with low grade, disseminated chalcopryrite and a boulder train of well-mineralized biotite-feldspar porphyry typical of the Babine porphyry camp. The source of these boulders has not yet been located.

BL (MINFILE 93K 054)

The BL showing occurs in a region underlain dominantly by metasedimentary and metavolcanic rocks of the Takla Group and by pyroxenite, hornblende gabbro, diorite and chlorite schist of the Butterfield Lake pluton (Figure 5). Mineralization comprises disseminated chalcopryrite in pyroxenite and coarse-grained gabbro. Chalcopryrite and malachite also occur in andesite adjacent to a pyritic tuff unit. In 1987, a grab sample from an outcrop of pyroxenite containing chalcopryrite and malachite on the Butter claim assayed 0.053 percent copper (Shaede, 1998).

Mary Ann (MINFILE 93K 075)

The Mary Ann showing is located at the end of Wright Bay on Babine Lake (Figure 5). The showing comprises chalcopryrite and malachite in strongly deformed limestone interbedded with mafic volcanic rocks of the Pennsylvanian-Permian Asitka Group. The showing is near a northeast trending fault that juxtaposes Lower Jurassic Wright Bay succession of the Hazelton Group against metavolcanic and metasedimentary rocks of the Asitka Group. The showing may be related to hydrothermal activity along this fault.

Fort (MINFILE 93K 093)

Richard Haslinger staked the Fort property in late 1997 after Elden Nyberg discovered significant sulphide mineralization in rocks exposed along a new logging road in the 93K/12 map sheet. The property was subsequently optioned by Eastfield Resources who staked some 632 claim units in the vicinity of the new showing. The main target on the property is a breccia zone that is healed with calcite, quartz and locally high grade sulphide mineralization. The breccia is exposed sporadically over an area 700 metres long and up to 400 metres wide. Eight grab samples averaged 0.34 percent copper, 0.017 percent molybdenum and 72.3 grams per tonne silver. Three of the samples returned values ranging from 0.36 to 1.01 percent zinc and 0.33 to 0.48 percent lead. Gold values are generally low with the highest being 98 parts per billion (Eastfield Resources web site). Encouraged by these initial results, Eastfield entered into a joint venture agreement with Ascot Resources Ltd. to explore the property. In the summer of 1998, the joint venture did line-cutting, soil geochemistry, prospecting and an induced polarization survey. This work defined a 300 by 800 metre copper soil anomaly and coincident 1600 metre long IP chargeability high along the western margin of the Butterfield Lake pyroxenite intrusive complex (Ascot Resources web site). Although this work defined a number of potential exploration targets, Ascot Resources Ltd. decided to terminate its option agreement with Eastfield in the fall of 1998.

The Fort breccia zone is located approximately 700 metres due east of Specularite Lake (Figure 5) where it is exposed along a new logging road. This road is located at the base of a northwest trending ridge that is cored by the Butterfield Lake pyroxenite-hornblende gabbro intrusive complex. Contacts observed in road cuts suggest this complex dips moderately to the northeast and that its upper contact is intrusive into chlorite schists and metasedimentary rocks that are probably correlative with the Pennsylvanian-Permian Asitka Group. The pyroxenite is cut by potassic altered porphyritic monzonite to granodiorite dikes. The southwest contact of the intrusive complex is interpreted to be a fault with weak to moderately deformed pyroxene phyric flows and breccias of the Upper Triassic Takla Group forming the struc-

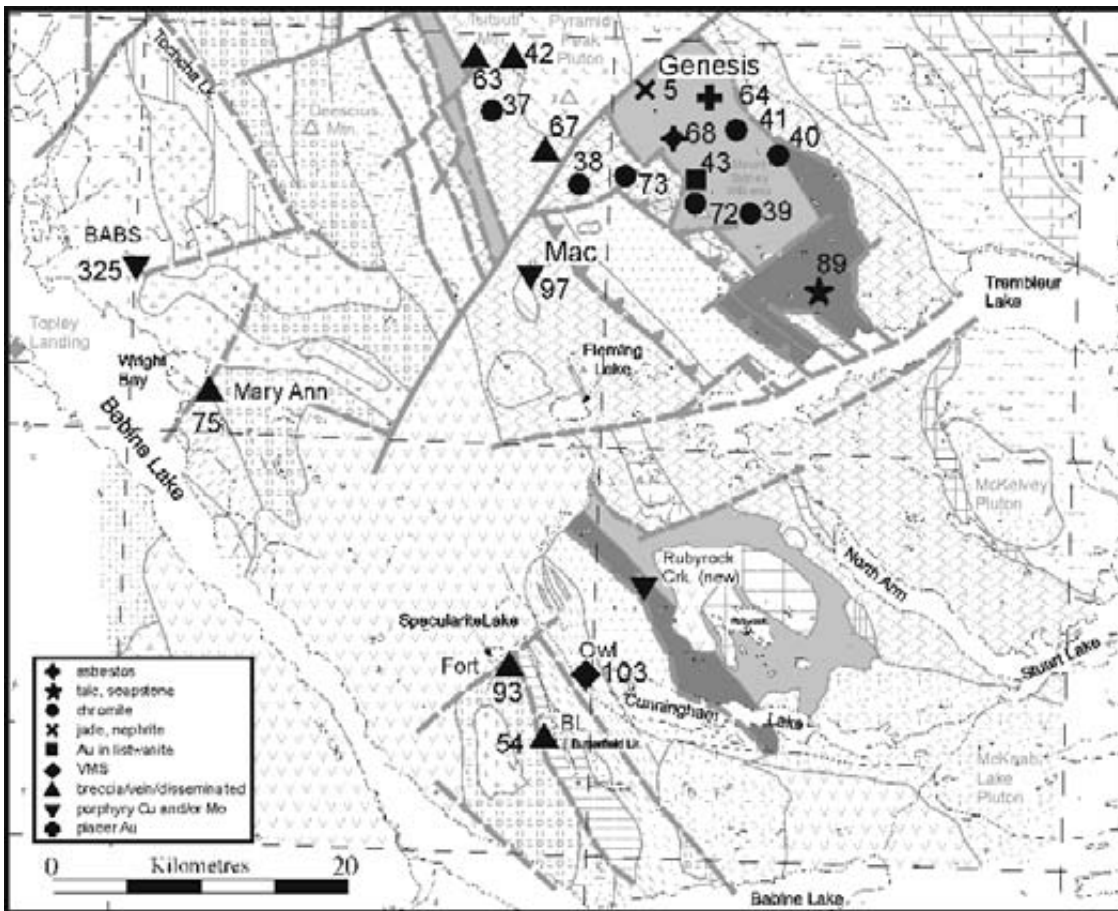


Figure 5. Generalized geology and location of mineral occurrences, northwest Fort Fraser (93K) map sheet. See Table 1 for list of occurrences and Figure 2b for legend.

tural footwall. The Fort breccia occurs at or near this structural contact and is interpreted to be a dilational zone related to faulting. The breccia is well exposed in a road cut where it is at least 200 metres wide. Several small outcrops of breccia occur up slope from the road cut and indicate that the breccia extends at least 400 metres to the southeast.

The Fort breccia is comprised of angular to subrounded, 2 to 20 centimetre clasts of pyroxenite, chlorite schist and fine grained foliated diorite to monzonite healed by coarse grained rhombs of calcite and well formed quartz crystals that have grown in open cavities. In places the breccia matrix, which locally has remnant vuggy cavities, also contains abundant chlorite and biotite. The breccia varies from clast to matrix supported. Sulphide mineralization is interstitial to breccia clasts although clasts may also have some disseminated pyrite and chalcopyrite. Interstitial sulphides are intergrown with calcite and quartz and are typically coarse grained and in places massive. Pyrite is the most abundant sulphide mineral but chalcopyrite is

locally abundant as high grade intergrowths with pyrite. Other, less common sulphide minerals include molybdenite, sphalerite and galena. Alteration associated with the breccia is mainly potassium feldspar, green biotite and silica.

Minerals in-filling the Fort breccia are coarsely crystalline and have clearly formed slowly from relatively low temperature fluids circulating through open spaces in the breccia. The matrix minerals are undeformed and this suggests healing of the breccia post dates tectonic activity. The predominance of metamorphic and foliated intrusive clasts in the breccia suggests the Butterfield Lake intrusive was the primary protolith to the breccia. The breccia does not appear to cut younger diorite, quartz latite and hornblende-biotite-feldspar porphyry dikes that intrude the complex to the east and up slope from the breccia. However, hydrothermal activity may have been related to heat flow generated by emplacement of these dikes. Similar dikes occur on ridges in the northern part of the property and have produced zones of disseminated pyrite along their margins. Biotite from one of these dikes

Table 1. Mineral occurrences in the northwest Fort Fraser map sheet

Minfile No.	Names	Status	Commodity	Map Sheet	Type
093K 005	GENESIS, GREEN, JADE QUEEN, O'NE-ELL CREEK, TEZZERON NEPHRITE	Past Producer	Nephrite, tremolite	093K14W	Jade
093K 037	TSITSUTL MOUNTAIN CHROMIUM	Show ing	Cr	093K13E	Podiform chromite
093K 038	TILDESLEY CREEK	Show ing	Cr	093K13E	Podiform chromite.
093K 039	MT. SIDNEY WILLIAMS, CR, VAN 1, P.G.4, PG-3,	Show ing	Cr	093K14W	Podiform chromite
093K 040	PAULINE, MIDDLE RIVER RIDGE, PG, P.G.	Show ing	Cr	093K14W	Podiform chromite
093K 041	VAN DECAR CREEK, PG,	Show ing	Cr	093K14W	Podiform chromite
093K 042	TSITSUTL MOUNTAIN TIN	Show ing	Sn, Mn, V, Co, Zn, Rhodonite	093K13E	Veins
093K 043	MT. SIDNEY WILLIAMS, VAN, KLONE	Show ing	Au, Ag, Cr, Asbestos	093K14W	listw anite-hosted Au
093K 054	BL, SMJ, BUTTER	Show ing	Cu	093K12E	Vein, disseminated
093K 063	TSITSUTL MOUNTAIN	Show ing	Cu	093K13E	Disseminated
093K 064	VAN DECAR CREEK PLACER	Show ing	Au	093K14W	Surficial placer
093K 067	DIANE, BORNITE	Show ing	Cu, Au, Zn	093K13E	Vein, disseminated
093K 068	VAN DECAR ASBESTOS	Show ing	Asbestos	093K14W	Ultramafic-hosted asbestos
093K 072	SIDNEY	Show ing	Cr	093K14W	Podiform chromite
093K 073	O'NE-ELL CREEK	Show ing	Cr	093K14W	Podiform chromite
093K 075	MARY ANN, DAVE	Show ing	Cu	093K13W	Vein, disseminated
093K 089	BAPTISTE, MOUNT SIDNEY WILLIAMS	Show ing	Talc, Soapstone	093K14W	Ultramafic-hosted talc-magnesite
093K 093	FORT, SPECULARITE LAKE, ELDEN	Show ing	Cu, Ag, Mo, Pb, Zn	093K12E	Breccia, vein
093K 097	MAC, CAMP, PAULA CREEK, PEAK, POND	Developed Prospect	Mo, Cu	093K13E	Porphyry Mo (Low F-type)
093K 103	OWL, FORT, BUT 4	Show ing	Cu, Ag, Au, Zn, Pb	093K12E 093K11W	Volcanogenic massive sulphide; quartz veins
093L 325	BABS	Prospect	Cu, Au	093L16E, 093K13W	Porphyry Cu \pm Mo \pm Au
	RUBYROCK CREEK	Show ing	Cu	093K11W	Porphyry Cu

gave a 52 Ma Ar-Ar isotopic age and a similar age is implied for mineralization at the Fort. A sample of hydrothermal biotite has been submitted for Ar-Ar isotopic dating.

Pyroxenite, hornblende gabbro and diorite with narrow panels of chlorite schist are exposed in road cuts northeast of the breccia. These rocks, which are interpreted to be in the structural hangingwall of the breccia, contain disseminated pyrite and minor chalcopyrite and are cut by numerous small breccia lenses and quartz-carbonate veins with potassic alteration selvages. The veins and breccia lenses strike southeast, dip moderately to the northeast and appear to parallel the trend of the main breccia body. In contrast, Takla volcanic rocks, which presumably lie structurally below the breccia, lack significant

sulphide mineralization or veining. This suggests that hydrothermal fluids circulating through the breccia moved upward into a shattered hanging-wall but did not penetrate downward into a more massive and impermeable footwall.

The northwest extension of the Fort breccia is probably truncated by a northeast trending high angle fault that is coincident with a topographic linear. Eocene volcanic rocks crop out in the low-lying region west of the fault and are interpreted to be in a downdropped block. The same fault terminates the aeromagnetic anomaly associated with the Butterfield lake pyroxenite body northeast of the breccia zone. This fault may also have been a conduit for hydrothermal activity in Eocene or younger time and could potentially be a drill target.

If the breccia at the Fort property is tectonic in origin and related to development of a dilational zone along the western margin of the Butterfield Lake pyroxenite intrusive complex then this contact may have potential for additional discoveries elsewhere along its length.

Occurrences Within the Sitlika Assemblage

Owl (MINFILE 93K 103)

The Owl claims were staked in 1989 and 1990 to cover mineralized outcrops exposed along and adjacent to the Cunningham Lake Forest Service road, about 2 km west of the west end of Cunningham Lake. The claims were explored in 1990 through 1992, but were subsequently allowed to lapse. The showing is presently included in ground staked after discovery of the Fort occurrence, 5 km to the west-northwest.

Mineralization at the Owl showing is within a succession of predominantly rhyolitic to dacitic metavolcanic rocks that are here assigned to the Sitlika volcanic unit. It is developed sporadically over a strike length of 2 km, and includes disseminated chalcopyrite-pyrite within the metavolcanics, as well as quartz and quartz-carbonate veins and stringers that locally contain significant amounts of copper, gold and silver (Halleran and Halleran, 1990; Halleran, 1991). In addition, several massive sulphide boulders were discovered in the vicinity of the mineralized outcrops. These, combined with the predominance of felsic metavolcanic rocks in this part of the Kutcho-correlative Sitlika volcanic unit, suggest that this area may warrant further exploration for volcanogenic massive sulphide mineralization.

Occurrences Within the Cache Creek Belt

Chromite

MINFILE lists six chromite occurrences within the Cache Creek ultramafic unit in the Mount Sidney Williams area (93K 038, 039, 040, 041, 072, 073), and another within the same unit south of Tsitsutl Mountain (93K 037) (Figure 5). All of these showings were mapped

by Armstrong (1949), who provided brief descriptions of the 5 most important occurrences. Subsequent work included prospecting and rock sampling programs over the Pauline showing in 1974 (MINFILE 93K 040; Stelling, 1975), and the Van Decar Creek showing in 1979 (MINFILE 93K 041; Guinet, 1980). In 1982 Northgane Minerals Ltd. commissioned an airborne VLF-EM and Magnetometer survey over the 4 occurrences east and northeast of Mount Sidney Williams (Pezzot and Vincent, 1982), but no follow-up work was recorded. The Mount Sidney Williams area was also examined by Whittaker (1983) as part of a broader study of chromite occurrences associated with alpine-type peridotites in southern and central British Columbia.

The chromite occurrences in the Mount Sidney Williams - Tsitsutl Mountain area, none of which were examined during the present study, comprise massive pods and disseminations within dunite. Armstrong (1949) reported that the best occurrence, Van Decar Creek, includes a lens measuring about 1.5 m by 8 m in surface area containing at least 50% chromite, as well as an adjacent zone of disseminated chromite. This lens was hand trenched and sampled by Guinet (1980), who reports Cr values ranging from 17.7 percent to 38.9 percent.

Mt. Sidney Williams Au (MINFILE 93K 043)

The Mt. Sidney Williams area, underlain by the Trembleur ultramafic unit and associated North Arm succession, was investigated as a possible platinum/gold prospect in 1987 (Mowat, 1988a). Geochemical sampling at this time yielded only a single sample with a slightly elevated Pt/Pd value, but significant gold values were obtained from silt and listwanite-altered rock samples. Subsequent exploration from 1988 through 1994 focused on these and other auriferous listwanite zones, although mention was also made of chromium and asbestos occurrences. Early work during this exploration phase consisted mainly of prospecting and mapping together with soil, silt and rock geochemical surveys (Mowat, 1988b). Subsequent work included trenching, geophysical surveys and diamond drilling (Mowat, 1990, 1991, 1994). More recent work, while continuing to address gold mineralization, has also been concerned with the nickel-

cobalt potential of the area (Mowat, 1997).

The Mt. Sidney Williams gold prospect was not examined during the present study. Elevated gold values occur mainly in listwanite alteration zones and are specifically associated with arsenopyrite that is erratically distributed along fault zones and in areas of intense silicification (Mowat, 1990). Mowat (1990, 1994) reports that the auriferous listwanites show a spatial relationship to norite intrusions. C. Ash collected a sample from one of the Mt. Sidney Williams listwanites in 1992, and submitted it to P.H. Reynolds of Dalhousie University for Ar-Ar dating of marioisite. The age spectrum (provided to the authors by C. Ash) shows prominent plateaus at about 170 and 180 Ma, but these dates must be considered preliminary as we do not, at this time, have a report on the quality or error limits associated with the data. Nevertheless, the suggested Middle Jurassic age for the listwanite alteration and associated gold mineralization is intriguing, as it coincides with the inferred age of thrust-imbrication of the Cache Creek assemblage. This, together with the setting of the occurrence near the structural base of the Mt. Sidney Williams ultramafic allochthon (Figure 3, Section C) suggests that the alteration and mineralization may, at least in part, be controlled by structures associated with this thrust-imbrication.

Diane (MINFILE 93K 067)

The Diane claim group was staked on the west side of upper Tildesley Creek in 1969, to cover an area of anomalous copper values identified in a reconnaissance silt sampling program. Soil sampling, electromagnetic and magnetic surveys were conducted over the claims later that year (Dodson, 1970), but no follow-up work was recorded and the Diane claims were allowed to lapse. The area was subsequently re-staked as the western part of the Bornite claim group, which was subjected to a soil sampling, chip sampling and diamond drilling program in 1995 (Mowat, 1996).

The area of the original Diane claims, on the west side of Tildesley Creek, is underlain by the North Arm succession of the Cache Creek Complex, comprising variably foliated mafic metavolcanic and meta-intrusive rocks along with local metasedimentary intervals. Three holes from 2 setups were drilled into this succession in 1995 to test copper-in-soils anom-

alies. The holes all encountered sub-economic chalcopyrite mineralization within a succession of predominantly chlorite-epidote-actinolite-calcite-altered mafic volcanic rocks. Slightly anomalous gold concentrations were associated with the highest copper concentrations (up to 500 ppm Cu) in all three holes (Mowat, 1996).

The eastern part of the Diane claim group, on the east side of Tildesley Creek, is underlain by fault-imbricated slivers of ultramafic rock, slate and siltstone, and greenstone. These rocks are inferred to represent either the North Arm succession or the Sitlika assemblage imbricated with the ultramafic unit in the footwall of the Mount Sidney Williams ultramafic allochthon (*e.g.* Figure 3, Section C). Mowat (1996) reports that the metasedimentary rocks, which are highly anomalous in Zn, Ag and Ba, host bedding-parallel sulphide mineralization consisting of pyrrhotite with minor chalcopyrite intergrowths.

Tsitsutl Mountain Tin (MINFILE 93K 042)

The Tsitsutl Mountain tin occurrence comprises a vein of rhodonite that contains minor amounts of tin, zinc, manganese, vanadium and cobalt. It occurs on the ridge south of Tsitsutl Mountain, within metasedimentary rocks of the North Arm succession near the contact of a small quartz porphyry stock. The vein was discovered in 1942 and explored in 1943 (Armstrong, 1949, page 194), but has not apparently received any recent attention. The northwest striking vein consists of about 70 percent rhodonite, with 2 to 3 percent arsenopyrite and variable amounts of calcite, garnet and ilmenite. It was uncovered at two places, a little more than 7 m apart, where it is 46 and 61 cm wide, respectively. Armstrong reports that an assay of vein material yielded 0.37 percent zinc and 0.09 percent tin, whereas specimens of wall-rock contained 0.65 percent vanadium oxide.

Mac (MINFILE 93K 097)

The Mac porphyry molybdenum prospect has been described in a previous report (MacIntyre *et al.*, 1998). No significant work was done on the property in 1998.

The Mac property is underlain by metavolcanic, metasedimentary and serpentinitized ultramafic rocks that are here included in the North Arm succession of the Cache Creek Complex. These

rocks are intruded by stocks of biotite granodiorite to porphyritic quartz monzonite that are part of the latest Jurassic to earliest Cretaceous Francois Lake intrusive suite. These intrusions also host the Endako porphyry molybdenum deposit in the Fraser Lake area, approximately 90 kilometres south-southeast of the Mac. As at Endako, molybdenum mineralization at Mac is associated with these intrusions and occurs in three areas - the Peak, Camp and Pond zones. Drilling to date has mainly focused on the Camp zone. There, a 300 by 500 metre, northerly elongate stock of porphyritic quartz monzonite intrudes the Cache Creek Complex. The southern end of the stock is truncated and possibly offset southeastward by a north-west trending, high angle, sinistral strike-slip fault. The intrusion is medium-grained, leucocratic, and porphyritic to equigranular with 15 percent 1-3 millimetre feldspar, 25 percent 1-2 millimetre quartz, 35-45 percent 1-4 millimetre K-feldspar, and up to 5 percent biotite, muscovite and hornblende (Cope and Spence, 1995).

Molybdenum mineralization at Mac occurs as molybdenite on fractures, as disseminations and in quartz veinlet stockworks peripheral to and within the porphyritic quartz monzonite or granite stock. Where the quartz monzonite stock is exposed on surface it is leached and has only minor ferri-molybdenite staining on fractures. Disseminated chalcopyrite also occurs in the mineralized zones at Mac. Drill results indicate that the best molybdenum grades occur in a 50 metre wide zone of biotite-bearing, hornfelsed rocks along the east, north and west contacts of the stock. One of the best drill intersections from this zone was 90 metres grading 0.308 percent MoS₂ and 0.256 percent Cu. A pyritic halo also encloses the stock and is roughly coincident with the biotite hornfels zone. Limited drilling in the Peak and Pond zones has intersected similar styles of mineralization. These zones are still relatively untested.

Rubyrock Creek (new)

Mapping within the Trembleur ultramafic unit along the crest of the ridge northeast of Rubyrock Creek in the 93K/11 map sheet resulted in the discovery of several small outcrops of crowded biotite-feldspar porphyritic granodiorite with up to 15 percent disseminated and fracture controlled pyrite. These outcrops occur in a small saddle and define an area of sulphide min-

eralization that is at least 300 metres long and 200 metres wide. The extent of mineralization, which is centered at UTM coordinates 341970E, 6062210N (NAD83), is constrained to the west by the occurrence of unmineralized serpentinite but is open in all other directions. A single sample collected from this locality contained 183 ppm Cu. The discovery is considered significant because the style of sulphide mineralization and the nature of the porphyritic host rocks suggest the presence of a porphyry copper style hydrothermal system of probable Eocene age. Although no significant copper mineralization was located within the zone of disseminated and fracture controlled pyrite, followup work may locate a copper rich zone associated with the porphyritic intrusions.

Genesis Jade Deposit (MINFILE 93K 005)

The Genesis deposit is located on O'Ne-ell Creek, a little more than 5 km upstream from its confluence with the Middle River. It was discovered in 1968 by Ms. W. Robertson, who found jade boulders along the creek and traced them upstream to the in situ nephrite outcrop. Limited production, from boulders and bedrock, took place from 1968 through 1970 (B.C. Minister of Mines and Petroleum Resources Annual Report, 1968, p. 309; Geology, Exploration and Mining in British Columbia, 1969, p. 389; 1970, p. 498). The deposit was re-staked as the Green 1-4 claims in 1993, and Global Metals Ltd. tested the nephrite with 29 shallow diamond drill holes in 1995 (McIntyre and McIntyre, 1995). No subsequent development has been reported.

The Genesis deposit is within the Trembleur ultramafic unit, about 2 km southeast of the inferred trace of the Tildesley Creek fault. It comprises lenses of nephrite, massive tremolite, and foliated tremolite-talc-chlorite rock within a structurally complex contact zone between serpentinite and an overlying assemblage of metasedimentary and metavolcanic rocks that includes chert, quartzite, greenstone, slate and sandstone (Fraser, 1972; McIntyre and McIntyre, 1995). The metasedimentary and metavolcanic rocks are inferred to be a tectonic inclusion within the ultramafic unit, although it is possible that they represent part of the structurally overlying North Arm succession. McIntyre and McIntyre (1995) estimate that

about 2 800 000 kg of marketable stone are present on the property, including both nephrite and hard, polishable milky grey tremolite.

Talc and Soapstone

As described in a previous section, massive to weakly foliated carbonate-talc rocks dominate the Trembleur ultramafic unit over a broad area east and southeast of Mt. Sidney Williams. The Baptiste MINFILE occurrence (93K 089) is located in this area, apparently on the basis of Armstrong's (1949, page 89) report that "talc-carbonate rocks predominate in the southern half of the Mount Sydney Williams peridotitic batholith, underlying most of the area between Baptiste Creek and Trembleur Lake." Although there are no assessment reports related to talc exploration on file, sawn blocks noted at two localities during the course of this year's fieldwork attest to some recent interest in this commodity. Of particular interest is a lens of almost pure talc exposed over several square metres within more typical marble-textured carbonate-talc rock. This locality, 7.5 km east-southeast of Mount Sidney Williams, is covered by the Dial claim, owned by A.D. Halleran of Fort St. James.

Asbestos

Armstrong (1949, page 197) describes a deposit of chrysotile asbestos on the north slope of Mount Sidney Williams, and a separate occurrence of tremolite asbestos about 3 km to the northwest. The former is in the area of the Mount Sidney Williams Au prospect (MINFILE 93K 043), and the latter is referred to as the Van Decar asbestos occurrence (MINFILE 93K 068). Armstrong considered the asbestos in both areas to be of poor commercial quality, but noted that this did not preclude there being better quality material elsewhere within the Trembleur ultramafic unit. However, there is no record of subsequent exploration directed toward this commodity.

Placer Gold

Van Decar Creek, which flows northeastward from Mount Sidney Williams to the Middle River, yielded a minor amount of placer gold in the 1930s, from workings about 3 km above its mouth (Armstrong, 1949, page 152; MINFILE 93K 064).

The Van Decar Creek drainage basin is entirely within the Trembleur ultramafic unit, and includes the gold-bearing listwanites of the Mount Sidney Williams prospect (MINFILE 93K 043).

ACKNOWLEDGMENTS

We thank Angelique Justason, Sheldon Modeland, Stephen Munzar, and Deanne Tackaberry for their cheerful and capable contributions to our field program. We also thank Bert Struik and Mike Hrudey, of the Geological Survey of Canada, and Dan Hora and Bill McMillan of the Geological Survey Branch, for informative discussions, field trips and joint fieldwork. We are grateful to Grant and West Luck of Interior Helicopters Ltd. for providing safe and reliable helicopter transportation, and thank Carol, Dieter and Mary Ann Berg for their hospitality during our stay at Takla Rainbow Lodge. Bill McMillan reviewed an earlier version of the manuscript and suggested improvements.

REFERENCES

- Anderson, R., L'Heureux, R., Wetherup, S. and Letwin, J.M. (1997): Geology of the Hallet Lake map area, central British Columbia: Triassic, Jurassic, Cretaceous, and Eocene? plutonic rocks; in *Current Research 1997-A, Geological Survey of Canada*, pages 107-116.
- Anderson, R.G., Whalen, J.B. and Villeneuve, M.E. (1998): Triassic to Eocene composite intrusions and molybdenum metallogeny: The Endako batholith redefined; in *New geological constraints on Mesozoic to Tertiary metallogenesis and on mineral exploration in central British Columbia: Nechako NATMAP Project, Geological Association of Canada, Cordilleran Section*, March 27, 1998, Short Course Notes.
- Armstrong, J.E. (1946): Takla, Cassiar District, British Columbia; *Geological Survey of Canada*, Map 844A.
- Armstrong, J.E. (1949): Fort St. James map-area, Cassiar and Coast districts, British Columbia; *Geological Survey of Canada*, Memoir 252, 210 pages.
- Ash, C.H. and Macdonald, R.W.J. (1993): Geology, mineralization and lithochemistry of the Stuart Lake area, central British Columbia (parts of 93K/7, 8, 10 and 11); in *Geological Fieldwork 1992, B.C. Ministry of Energy, Mines and Petroleum Resources*, Paper 1993-1, pages 69-86.

- Ash, C.H., Macdonald, R.W.J. and Paterson, I.A. (1993): Geology of the Stuart - Pinchi lakes area, central British Columbia (parts of 93K/7, 8, 9, 10 and 11); *B.C. Ministry of Energy, Mines and Petroleum Resources*, Open File 1993-9.
- Bellefontaine, K.A., Legun, A., Massey, N.W.D. and Desjardins, P. (1995): Digital geological compilation of northeast B.C. - southern half; *B.C. Ministry of Energy, Mines and Petroleum Resources*, Open File 1995-24.
- Carr, J.M. (1965): The Geology of the Endako Area; in Lode Metals in British Columbia 1965; *B.C. Ministry of Energy, Mines and Petroleum Resources*, pages 114-135.
- Carter, N.C. (1981): Porphyry Copper and Molybdenum Deposits West Central British Columbia; *B.C. Ministry of Energy, Mines and Petroleum Resources*, Bulletin 64.
- Childe, F.C. and Schiarizza, P. (1997): U-Pb geochronology, geochemistry and Nd isotopic systematics of the Sitlika assemblage, central British Columbia; in *Geological Fieldwork 1996*, *B.C. Ministry of Employment and Investment*, Paper 1997-1, pages 69-77.
- Childe, F.C., Friedman, R.M., Mortensen, J.K. and Thompson, J.F.H. (1997): Evidence for Early Triassic felsic magmatism in the Ashcroft (92I) map area, British Columbia; in *Geological Fieldwork 1996*, *B.C. Ministry of Employment and Investment*, Paper 1997-1, pages 117-123.
- Childe, F.C., Thompson, J.F.H., Mortensen, J.K., Friedman, R.M., Schiarizza, P., Bellefontaine, K. and Marr, J.M. (1998): Primitive Permo-Triassic volcanism in the Canadian Cordillera: Tectonic and metallogenic implications; *Economic Geology*, Volume 93, pages 224-231.
- Cope, G.R. and Spence, C.D. (1995): Mac porphyry molybdenum prospect, north-central British Columbia; in *Porphyry Deposits of the Northwestern Cordillera of North America*, T.G. Schroeter, Editor, *Canadian Institute of Mining, Metallurgy and Petroleum*, Special Volume 46, pages 757-763.
- Cordey, F. and Struik, L.C. (1995): Radiolarian biostratigraphy and implications, Cache Creek Group of Fort Fraser and Prince George map areas, central British Columbia; in *Current Research 1996-E*, *Geological Survey of Canada*, pages 7-18.
- Diakow, L. and Rogers, C., (1998): Toodoggone-McConnell Project: Geology of the McConnell range - Serrated Peak to Jensen Creek, parts of NTS 94E/2 and 94D/15; in *Geological Fieldwork*, *B.C. Ministry of Employment and Investment*, Paper 1998-1, pages 8a-1 to 8a-14.
- Dodson, E.D. (1970): Report on a geochemical and geophysical survey on the Diane 1-16 mineral claims, Tsitsutl Mountain area, Omineca Mining Division; *B.C. Ministry of Energy, Mines and Petroleum Resources*, Assessment Report 2414.
- Eisbacher, G.H. (1974): Sedimentary history and tectonic evolution of the Sustut and Sifton basins, north-central British Columbia; *Geological Survey of Canada*, Paper 73-31, 57 pages.
- Elliot, A. J. M. (1975): Geology and metamorphism of the Mitchell Mountains ultramafite, Fort St. James map area, British Columbia; unpublished M.Sc. thesis, *University of British Columbia*, 144 pages.
- Fraser, J.R. (1972): Nephrite in British Columbia; unpublished M.Sc. thesis, *The University of British Columbia*, 144 pages.
- Godwin, C.I. and Cann, R. (1985): The Mac molybdenite property, central British Columbia (93K/13E); in *Geological Fieldwork 1984*, *B.C. Ministry of Energy, Mines and Petroleum Resources*, Paper 1985-1, pages 443-449.
- Guinet, V. (1980): Prospecting report on the C R claims, Omineca Mining Division; *B.C. Ministry of Energy, Mines and Petroleum Resources*, Assessment Report 8135.
- Halleran, A.A.D. (1991): Trenching and mapping report on the Owl property, NTS 93K/12E and 11W, Omineca Mining Division; *B.C. Ministry of Energy, Mines and Petroleum Resources*, Assessment Report 21 640.
- Halleran, W. and Halleran, A.A.D. (1990): Geochemical and geological report on the Owl property, NTS 93K/12E and 11W, Omineca Mining Division; *B.C. Ministry of Energy, Mines and Petroleum Resources*, Assessment Report 20 377.
- Hrudey, M.G. and Struik, L.C. (1998): Field observations of the Tachie Pluton near Fort St. James, central British Columbia; in *Current Research 1998-A*, *Geological Survey of Canada*, pages 107-111.
- Hrudey, M.G., Struik, L.C. and Whalen, J.B. (in press): Geology of the Tintagel map area, central British Columbia; in *Current Research 1999-A*, *Geological Survey of Canada*.

- Kimura, E.T., Bysouth, G.D. and Drummond, A.D. (1976): Endako; in *Porphyry Deposits of the Canadian Cordillera*, A. Sutherland Brown, Editor, *Canadian Institute of Mining and Metallurgy*, Special Volume 15, pages 444-454.
- Leach, W.W. (1910): The Skeena River District; *Geological Survey of Canada*, Summary Report 1909.
- Letwin, J.M. and Struik, L.C. (1997): Geology of Shass Mountain, central British Columbia; in *Current Research 1997-A*, *Geological Survey of Canada*, pages 103-106.
- Lord, C.S. (1948): McConnell Creek map-area, Cassiar District, British Columbia; *Geological Survey of Canada*, Memoir 251, 72 pages.
- MacIntyre, D.G. (1998): Babine porphyry belt: Bedrock geology of the Nakinilerak Lake map sheet (93M/8), British Columbia; in *Geological Fieldwork 1997*, *B.C. Ministry of Employment and Investment*, Paper 1998-1, pages 2-1 to 2-18.
- MacIntyre, D.G., Webster, I.C.L. and Bellefontaine, K.A. (1996): Babine porphyry belt project: Bedrock geology of the Fulton Lake map area (93L/16), British Columbia; in *Geological Fieldwork 1995*, B. Grant, and J.M. Newell, Editors, *B.C. Ministry of Energy, Mines and Petroleum Resources*, Paper 1996-1, pages 11-35.
- MacIntyre, D.G., Webster, I.C.L. and Villeneuve, M. (1997): Babine porphyry belt project: Bedrock geology of the Old Fort Mountain area (93M/1), British Columbia; in *Geological Fieldwork 1996*, *B.C. Ministry of Employment and Investment*, Paper 1997-1, pages 47-68.
- MacIntyre, D.G., Schiarizza, P. and Struik, L.C. (1998): Preliminary bedrock geology of the Tochcha Lake map sheet (93K/13), British Columbia; in *Geological Fieldwork 1997*, *B.C. Ministry of Employment and Investment*, Paper 1998-1, pages 3-1 to 3-13.
- MacIntyre, D.G. and Struik, L.C. (1999): Nechako NATMAP Project, central British Columbia 1998 Overview; in *Geological Fieldwork 1998*, *B.C. Ministry of Energy and Mines*, Paper 1999-1, this volume.
- MacIntyre, J.F. and MacIntyre, R.F. (1995): Report on diamond drilling, Green 1-4 mineral claims, Omineca Mining Division; *B.C. Ministry of Energy, Mines and Petroleum Resources*, Assessment Report 24 094.
- Monger, J.W.H. (1976): Lower Mesozoic rocks in McConnell Creek map-area (94D), British Columbia; *Geological Survey of Canada*, Paper 76-1a, pages 51-55.
- Monger, J.W.H. and Church, B.N. (1977): Revised stratigraphy of the Takla Group, north-central British Columbia; *Canadian Journal of Earth Sciences*, Volume 14, pages 318-326.
- Monger, J.W.H., Richards, T.A. and Paterson, I.A. (1978): The Hinterland Belt of the Canadian Cordillera: New data from northern and central British Columbia; *Canadian Journal of Earth Sciences*, Volume 15, pages 823-830.
- Mowat, U. (1988a): Geochemical sampling on the Van Group, Klone Group, Mid claim, Omineca Mining Division; *B.C. Ministry of Energy, Mines and Petroleum Resources*, Assessment Report 17 173.
- Mowat, U. (1988b): Geochemical sampling, prospecting and mapping on the Van Group, Klone Group, Mid claim, Omineca Mining Division; *B.C. Ministry of Energy, Mines and Petroleum Resources*, Assessment Report 18 089.
- Mowat, U. (1990): Mapping and drilling program on the Mount Sidney Williams property, Omineca Mining Division; *B.C. Ministry of Energy, Mines and Petroleum Resources*, Assessment Report 20 541.
- Mowat, U. (1991): Drilling program on the Mount Sidney Williams property, Omineca Mining Division; *B.C. Ministry of Energy, Mines and Petroleum Resources*, Assessment Report 21 870.
- Mowat, U. (1994): Drilling program on the Mount Sidney Williams gold property, Omineca Mining Division; *B.C. Ministry of Energy, Mines and Petroleum Resources*, Assessment Report 23 569.
- Mowat, U. (1996): Drilling and sampling program on the Bornite property, Omineca Mining Division; *B.C. Ministry of Energy, Mines and Petroleum Resources*, Assessment Report 24 277.
- Mowat, U. (1997): A geochemical/petrographic report on the Mount Sidney Williams property, Omineca Mining Division; *B.C. Ministry of Employment and Investment*, Assessment Report 24 906.
- Orchard, M.J. (1996): Report on conodonts and other microfossils; *Geological Survey of Canada*, unpublished fossil report MJO-1996-10.

- Orchard, M.J., Struik, L.C. and Taylor, H. (1998): New conodont data from the Cache Creek Group, central British Columbia; in Current Research 1998-A; *Geological Survey of Canada*, pages 99-105.
- Paterson, I.A. (1974): Geology of Cache Creek Group and Mesozoic rocks at the northern end of the Stuart Lake Belt, central British Columbia; in Report of Activities, Part B, *Geological Survey of Canada*, Paper 74-1, Part B, pages 31-42.
- Pezzot, E.T. and Vincent, J.S. (1982): Geophysical report on an airborne VLF-EM and magnetometer survey, Cr 1 - Cr 6 Claims, Omineca Mining Division; *B.C. Ministry of Energy, Mines and Petroleum Resources*, Assessment Report 10 286.
- Sano, H. and Struik, L.C. (1997): Field properties of Pennsylvanian - Lower Permian limestones of the Cache Creek Group, northwest of Fort St. James, central British Columbia; in Current Research 1997-A, *Geological Survey of Canada*, pages 85-93.
- Schiarizza, P. (1998): The Sitlika assemblage in the Takla Lake area: Stratigraphy, external structural relationships and regional correlation; in New geological constraints on Mesozoic to Tertiary metallogenesis and on mineral exploration in central British Columbia: Nechako NATMAP Project, *Geological Association of Canada, Cordilleran Section*, March 27, 1998, Short Course Notes.
- Schiarizza, P. and Payie, G. (1997): Geology of the Sitlika assemblage in the Kenny Creek - Mount Olson area (93N/12, 13), central British Columbia; in Geological Fieldwork 1996, *B.C. Ministry of Employment and Investment*, Paper 1997-1, pages 79-100.
- Schiarizza, P., Massey, N. and MacIntyre, D. (1998): Geology of the Sitlika assemblage in the Takla Lake area (93N/3, 4, 5, 6, 12), central British Columbia; in Geological Fieldwork 1997, *B.C. Ministry of Employment and Investment*, Paper 1998-1, pages 4-1 to 4-19.
- Shaede, E. A. (1988): Geochemical report on Butter claim, Omineca Mining Division; *B. C. Ministry of Energy, Mines and Petroleum Resources*, Assessment Report 17 294.
- Stelling, D. (1975): A rock sampling and prospecting report on the Pauline mineral claims, Omineca Mining Division, British Columbia; *B.C. Ministry of Energy, Mines and Petroleum Resources*, Assessment Report 5648.
- Struik, L.C. (1998): Bedrock geology of the Fraser Lake (93K/SE) map area, British Columbia; *Geological Survey of Canada*, Open File 3559, 1:100 000 scale.
- Struik, L.C. and Erdmer, P. (1990): Metasediments, granitoids and shear zones, southern Babine Lake, British Columbia; in Current Research, Part E, *Geological Survey of Canada*, Paper 90-1E, pages 59-63.
- Struik, L.C. and Orchard, M.J. (1998): Cache Creek Group: Its stratigraphy, structural stacking and paleoenvironment, central British Columbia; in New geological constraints on Mesozoic to Tertiary metallogenesis and on mineral exploration in central British Columbia: Nechako NATMAP Project, *Geological Association of Canada, Cordilleran Section*, March 27, 1998, Short Course Notes.
- Tipper, H.W. and Richards, T.A. (1976): Jurassic Stratigraphy and History of North-Central British Columbia; *Geological Survey of Canada*, Bulletin 270, 73 pages.
- Villeneuve, M.E. and MacIntyre, D.G., 1997: Laser $^{40}\text{Ar}/^{39}\text{Ar}$ Ages of the Babine Porphyries and Newman Volcanics, Fulton Lake map area (93L/16), west central British Columbia; in Radiogenic Age and Isotopic Studies, Report 10, *Geological Survey of Canada*, Current Research 1996-F.
- Whittaker, P.J. (1983): Geology and petrogenesis of chromite and chrome spinel in alpine-type peridotites of the Cache Creek Group, British Columbia; unpublished Ph.D. thesis, *Carleton University*, 339 pages.
- Wright, D.M. (1997): Metamorphic geology of the Kenny Creek - Mount Olson map area: Implications for the relationship between the Sitlika assemblage and Cache Creek Group, central British Columbia; unpublished B.Sc. thesis, *University of Victoria*, 75 pages.



DESCRIPTION, U-PB AGE AND TECTONIC SETTING OF THE QUESNEL LAKE GNEISS, EAST-CENTRAL BRITISH COLUMBIA

by Filippo Ferri¹, Trygve Höy¹ and Richard M. Friedman²

KEYWORDS: Quesnel Lake Gneiss, geochemistry, U-Pb age, Kootenay Terrane, Barkerville Subterrane, tectonic setting, volcanogenic massive sulphides.

sic volcanics associated with important volcanogenic massive sulphide deposits in southern Kootenay Terrane and their study will better constrain the timing and tectonic setting of this important metallogenic event.

INTRODUCTION

The name 'Quesnel Lake Gneiss' has been applied to several bodies of Mid-Paleozoic orthogneiss found along the western margin of pericratonic rocks between Cariboo Lake and the southern arm of Quesnel Lake (Campbell, 1978; Figure 1). These represent the northern extent of Mid-Paleozoic intrusive rocks found intermittently along the Kootenay Terrane in the southern Canadian Cordillera (Okulitch, 1985).

The Quesnel Lake Gneiss has been the focus of several studies over the years which have detailed its geochemistry, geochronology and structural relationships with surrounding rocks (Rees and Ferri, 1983; Montgomery, 1985; Fillipone, 1985; Montgomery and Ross, 1989 and Mortensen *et al.*, 1987). Although the southern parts of the orthogneiss have been dated by U-Pb analysis of zircons, lead loss, together with inheritance, have produced a bracketed age of 335 to 375 Ma (Late Devonian to Mid-Mississippian; Mortensen *et al.*, 1987). Modal mineralogy and chemical analyses indicate compositions ranging from diorite to granite to syenite. The tectonic setting of these bodies based on chemical analysis is ambiguous suggesting arc or possibly within plate signatures, the latter implying an extensional setting (Montgomery and Ross, 1989).

The purpose of this study was to sample the Quesnel Lake Gneiss in areas where it is least metamorphosed in hopes of better constraining its intrusive age and origin. These bodies most likely represent the intrusive equivalents of fel-

REGIONAL GEOLOGY

The Quesnel Lake Gneiss intrudes the western margin of peri-cratonic rocks assigned to the Kootenay Terrane. Stratigraphic evidence has shown that these rocks represent the distal western edge of Ancestral North America. In this area, Kootenay rocks are locally assigned to the Barkerville Subterrane which is separated from more inboard rocks of the Cariboo Subterrane by the west-verging Pleasant Valley thrust fault (Struik, 1988). The oceanic Slide Mountain Terrane has been structurally emplaced along the western margin of the Barkerville Subterrane, carried on the east-verging Eureka thrust fault (Figure 1). It also structurally overlaps the Barkerville and Cariboo terranes along the Pundata thrust fault (Struik, 1988).

Strata in the Barkerville Subterrane have been assigned, almost entirely, to the Proterozoic to Paleozoic Snowshoe Group (Struik, 1986; 1988). This package of rocks is dominated by distal, fine grained siliciclastics with lesser carbonates and volcanics. The Slide Mountain Terrane is represented by the Late Paleozoic Crooked Amphibolite, a sheared and altered unit of mafic to ultramafic composition that probably has an ocean-ridge origin (Struik, 1988; Rees, 1987). It is structurally or stratigraphically succeeded by Middle to Late Triassic black phyllites of the basal Nicola Group ("Black Phyllite"; Panteleyev *et al.*, 1996). To the west these stratigraphically interfinger with volcani-

¹British Columbia Geological Survey Branch

²Department of Geological Sciences, University of British Columbia, 6339 Stores Road, Vancouver, British Columbia, Canada, V6T 1Z4

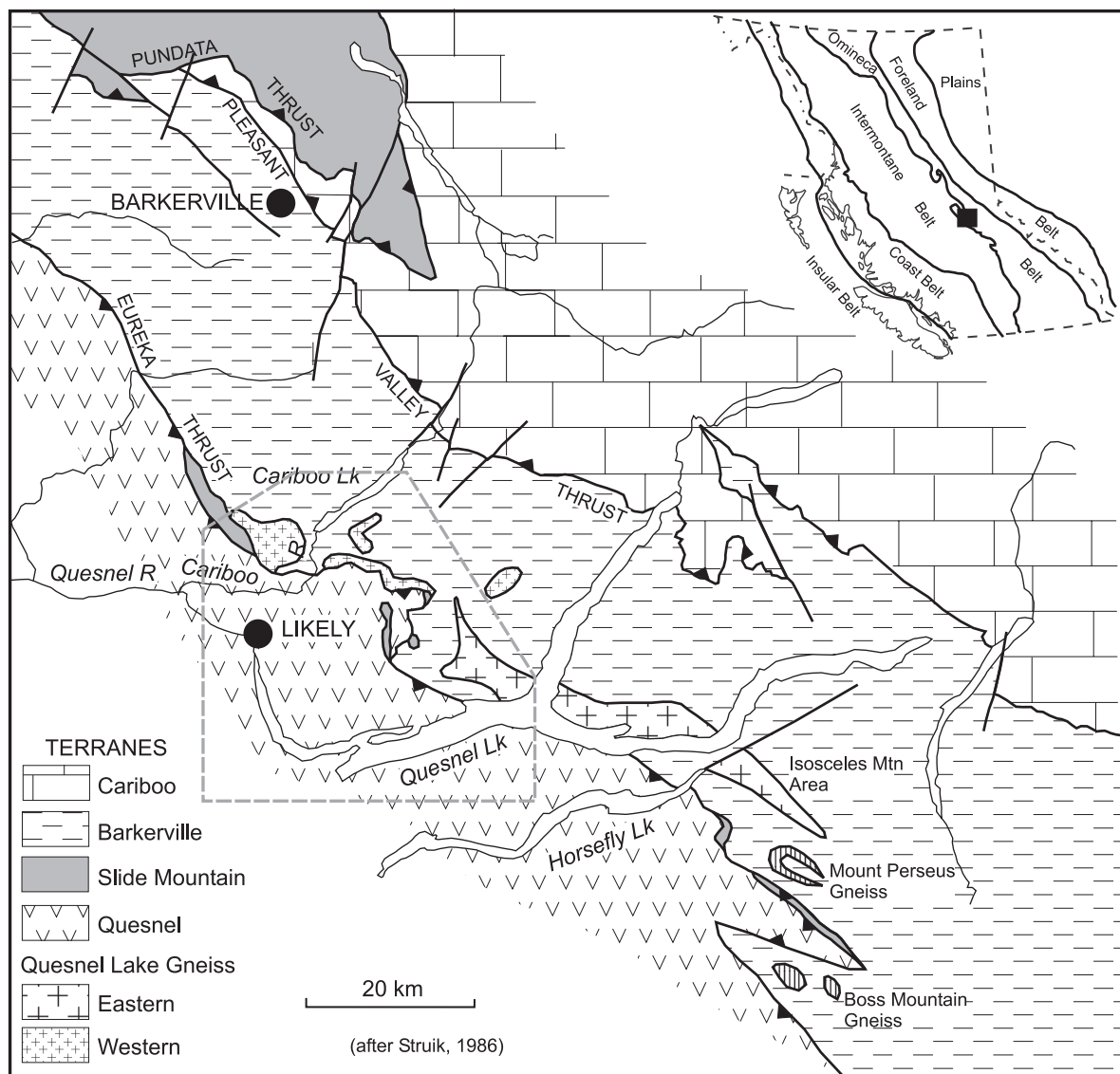


Figure 1. Distribution of Quesnel Lake Gneiss with respect to main geologic terranes. Dashed line shows area covered in Figure 2.

clastics of the Nicola arc which are as young as Early Jurassic.

Rocks in these terranes have been polydeformed and metamorphosed, possibly as early as middle Paleozoic time (Sutherland Brown, 1963) but certainly during the Mesozoic (Struik, 1981, 1988). Mesozoic deformation produced the dominant structures in the area and resulted from emplacement of oceanic and arc rocks of the Slide Mountain and Quesnel terranes against the western margin of the Kootenay Terrane (Eureka Thrust; Struik, 1988; Panteleyev *et al.*, 1996). This penetrative deformation was of a polyphase nature and was accompanied by regional metamorphism which reached amphibolite grade within the pericratonic rocks.

Quesnel Lake Gneiss

The Quesnel Lake Gneiss comprises approximately half a dozen separate intrusive bodies found between Cariboo Lake and the southern arm of Quesnel Lake (Figures 1 and 2). Immediately south of its eastern extent, similar bodies, referred to as the Mount Perseus and Boss Mountain gneisses, have been correlated with the Quesnel Lake Gneiss (Figure 1; Mortensen *et al.*, 1987; Montgomery and Ross, 1989).

Individual intrusions of the Quesnel Lake Gneiss vary in size from less than 1 to over 100 square kilometres. These are generally elongate and tend to follow the tectonic boundary between the Barkerville and Slide Mountain ter-

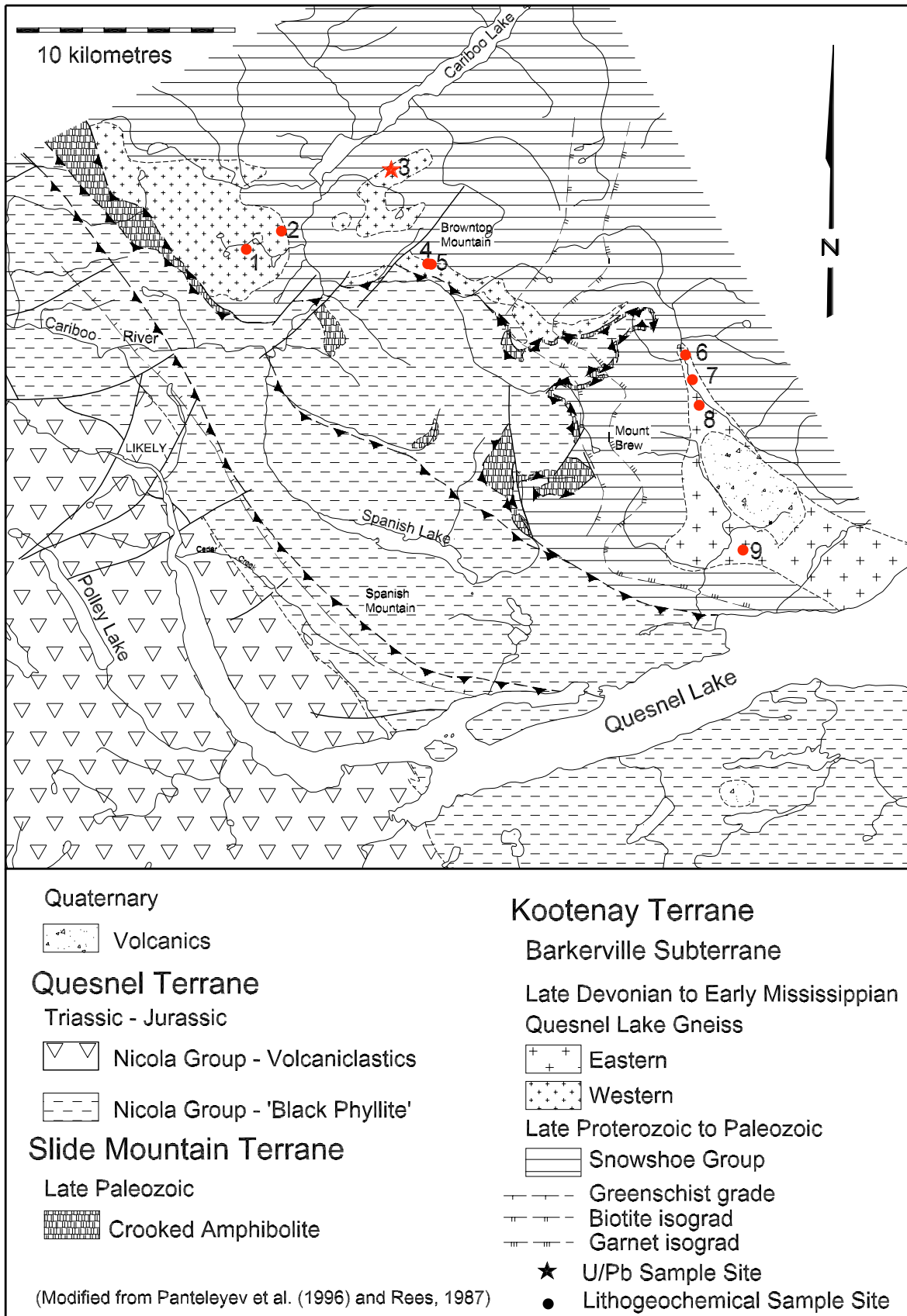


Figure 2. Simplified geology of the area between Cariboo Lake and the eastern part of Quesnel Lake.

ranes. Detailed mapping has shown the more elongate bodies are tabular or sill-like in nature (Mortensen *et al.*, 1989; Rees, 1987).

The Quesnel Lake Gneiss can be subdivided into two varieties which are compositionally and texturally distinct. These were noted by Rees (1987) who subdivided the gneiss into eastern and western subunits. Lithogeochemistry from this study re-enforces this distinction and his nomenclature will be used in this report.

The Western Quesnel Lake Gneiss is found northwest of Mount Brew and comprises 4 distinct intrusive bodies (Figure 2). The Eastern Quesnel Lake Gneiss is approximately 70 kilometres long and is dissected by the northern and eastern arms of Quesnel Lake (Figure 2). Both units invariably display a flattening fabric and associated lineation which, in Western Quesnel Lake Gneiss, is amplified by alignment of feldspar megacrysts (Photos 1 and 2). The intensity of deformation displayed by these units is quite variable, ranging from relatively undeformed to ultra-mylonitic at the contact with the Slide Mountain Terrane.



Photo 1. General picture of Western Quesnel Lake Gneiss showing large megacrysts of potassium feldspar. The view here is down the lineation such that the granite looks relatively undeformed.

Lithologically, the Western Quesnel Lake Gneiss is characterized by large megacrysts of potassium feldspar from 1 to over 5 centimetres in length, which can comprise up to 30 per cent of the rock (Photo 1). These are typically broken parallel to lineation with fractures healed by quartz. Quartz can form recrystallized masses up to 0.5 centimetre in diameter, although these are commonly flattened and can form “ribbons” several centimetres long. These porphyroclasts are set in a coarsely crystalline



Photo 2. Typical outcrop of foliated Eastern Quesnel Lake Gneiss. This gneiss typically lacks phenocrysts or porphyroclasts and, as shown here, can contain xenoliths.

matrix composed of quartz, plagioclase, potassic feldspar, muscovite, biotite (chloritized) and locally garnet. Feldspar is typically altered to muscovite.

In contrast, the Eastern Quesnel Lake Gneiss typically lacks megacrysts (Photo 2), although plagioclase(?) feldspar porphyroclasts up to 0.5 centimetres in size and totaling 5 to 15 per cent of the unit were seen at locality 8. This unit is composed of quartz, plagioclase, microcline, muscovite, biotite (chloritized), as well as epidote and clinozoisite. Feldspar is also altered to muscovite, particularly in highly strained localities. This unit is much more homogenous than the Western Quesnel Lake Gneiss and commonly contains sheared, schistose xenoliths of the country rocks. Gneiss in the area of localities 6 to 8 (Figure 2) was not previously recognized. It is tentatively shown connected to the main body, although it is possible that it is a separate body.

Table 1. Major, trace and rare earth element data for 9 samples of Quesnel Lake Gneiss.
See Figure 2 for sample locations.

Map No.	1	2	3	4	5	6	7	8	9	
Easting	601986	603626	608276	610615	610665	622301	622566	622650	624900	
Northing	5839963	5840803	5843637	5839965	5839990	5835413	5834126	5832700	5826280	
Field No.	H97									
Precision	BC-75	BC-74	BC-5	BC-33	BC-35	BC-13	BC-12	BC-15	BC-17	
SiO ₂	±0.01	72.89	73.19	74.05	73.07	73.72	70.67	64.83	64.74	68.76
TiO ₂	±0.01	0.26	0.25	0.22	0.24	0.29	0.3	0.47	0.52	0.39
Al ₂ O ₃	±0.01	13.85	13.83	13.59	13.82	14.27	14.45	14.8	14.83	14.54
Fe ₂ O ₃	±0.01	0.71	0.45	0.65	0.92	0.54	1.52	2.69	2.56	1.88
FeO	±0.01	1.14	1.45	0.51	0.93	1.58	1.2	2.22	2.63	1.67
MnO	±0.01	0.02	0.03	0.03	0.03	0.03	0.05	0.08	0.09	0.05
MgO	±0.01	0.69	0.58	0.64	0.58	0.54	0.76	2.48	2.67	1.24
CaO	±0.01	0.76	0.6	1.05	0.58	0.97	2.45	5.17	5.42	3.83
Na ₂ O	±0.01	2.83	2.29	3.72	2.9	4.04	3.49	2.33	2.13	2.94
K ₂ O	±0.01	4.92	5.04	2.85	4.71	2.13	3.57	2.85	2.36	2.76
P ₂ O ₅	±0.01	0.17	0.17	0.15	0.15	0.15	0.1	0.12	0.12	0.1
LOI	±0.01	1.22	1.39	1.99	1.36	1.33	0.94	1.35	1.45	1.25
SUM	±0.01	99.51	99.37	99.71	99.35	99.62	99.63	99.5	99.63	99.54
Nb	±5	18	21	23	18	21	35	16	16	26
Sr	±5	107	108	180	122	265	697	574	542	504
Y	±5	15	16	18	15	21	18	21	22	20
Zr	±5	112	116	101	118	118	159	142	149	140
V	±5	17	19	17	24	26	56	123	139	74
As	±0.5	2.9	4.5	2.9	3.1	1.9	3.1	2.8	2.7	2
Ba	±50	440	820	1800	430	290	1000	760	700	1000
Co	±1	4	4	-	3	3	4	13	10	7
Cr	±5	170	190	140	150	160	150	200	160	150
Cs	±1	6	6	2	3	6	3	2	2	2
Hf	±1	4	5	3	4	4	6	5	5	6
Rb	±15	210	170	110	160	77	100	91	72	82
Sc	±0.1	5.2	5.2	3.2	4.8	6.7	4.5	18	18	11
Th	±0.2	9.9	11	8.6	8.9	11	20	9.9	10	15
U	±0.5	3.2	5.5	1.5	3.9	7.1	3.4	3.4	3	3
La	±0.5	26	25	9.5	20	29	110	37	36	43
Ce	±3	48	49	22	38	53	140	58	53	69
Nd	±5	21	17	10	15	16	38	18	19	16
Sm	±0.1	3.8	3.5	2.5	2.8	3.9	5.2	3.5	3.3	3.6
Eu	±0.2	0.8	0.8	-	0.8	1	1.7	1.3	1.2	1.3
Yb	±0.2	1.9	2	1.8	2	1.9	1.5	1.8	1.7	2.1
Lu	±0.05	0.33	0.28	0.2	0.26	0.33	0.22	0.36	0.34	0.36

Notes

Major oxides and Nb to V determined at Cominco Research Laboratories, Vancouver, B.C.
As to Lu determined by thermal neutron activation analysis at ActLabs, Ancaster, Ontario.
All samples milled in a steel mill by Cominco Research Laboratories
Major oxides by X-ray fluorescence. Nb to V by pressed pellet X-ray fluorescence.
FeO determined by acid digestion /volumetric. LOI (Loss on ignition) by fusion at 1100°C
Major oxides as per cent. Elements Nb to Lu in parts per million

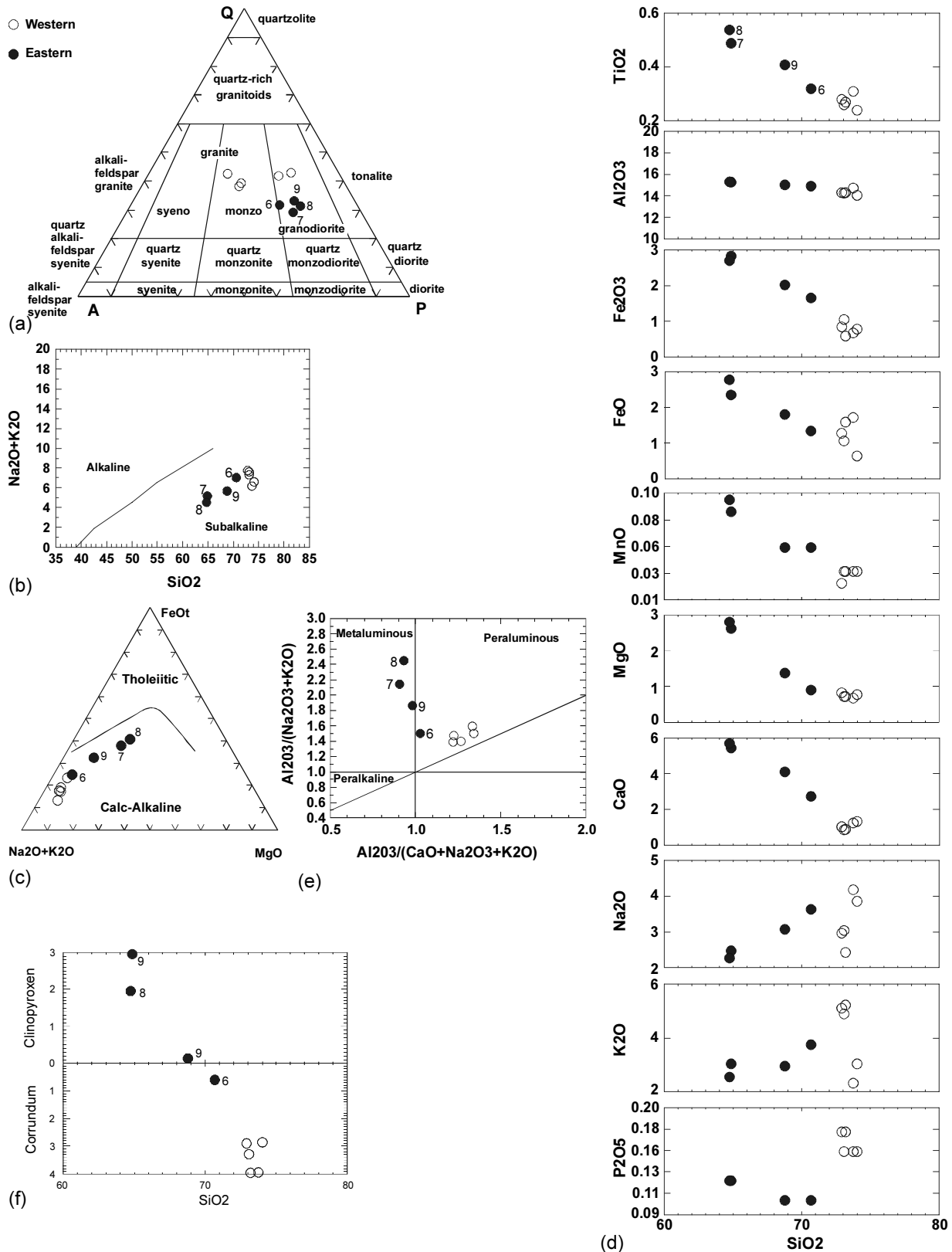


Figure 3. (a) Mesonormative plot of data from Table 1 for Quesnel Lake Gneiss. Ternary diagram from Streckeisen (1979). (b) Diagram showing alkalinity of Quesnel Lake Gneiss based on data in Table 1. Diagram by Irvine and Baragar (1971). (c) FeOt-MgO-Na₂O+K₂O plot for Quesnel Lake Gneiss based on data in Table 1. Diagram from Irvine and Baragar (1971). (d) Harker variation diagrams for Quesnel Lake Gneiss based on data in Table 1. (e) Plot of Shand's Indices for Quesnel Lake Gneiss based on data in Table 1. (f) Plot of normative corundum and clinopyroxene for the Quesnel Lake Gneiss for data from Table 1.

Litho geochemistry

Nine samples of the Quesnel Lake Gneiss were analyzed; five from the Western and 4 from the Eastern suite (Figure 2). Results include whole rock, trace and rare-earth element data (Table 1). As these bodies are locally highly strained, metamorphosed or altered, interpretation of some of the data, particularly the whole rock, should be viewed with caution. Although the Eastern and Western Quesnel Lake gneisses display distinct chemical, as well as lithological trends, they also share some similarities. (Table 1; Figure 3).

Mesonormative plots of this data indicate compositions ranging from granodioritic to granite (Figure 3a). They are subalkaline and fall within the calc-alkaline field as defined in the FeO-MgO-Na₂O+K₂O diagram of Irvine and Baragar (1971; Figures 3b and c). Harker variation diagrams of the major elements show typical igneous fractionation trends, however scatter in Na₂O and K₂O, particularly in the Western Gneiss, probably reflects the mobility of these elements during metamorphism and deformation (Figure 3d). In general, the Western Quesnel Lake Gneiss has a higher and more uniform silica content than the Eastern suite.

Greater distinction between the two gneiss varieties is shown in diagrams involving their aluminum content. Plots of Shand's Indices indicate that the Eastern Quesnel Lake Gneiss is metaluminous whereas samples from the Western suite are clearly peraluminous (Figure 3e). This is corroborated on a plot showing normative values of corundum and clinopyroxene (Figure 3f). Samples from the Eastern Quesnel Lake Gneiss are either clinopyroxene normative or produce less than 1 per cent corundum. In contrast, samples from the Western Quesnel Lake Gneiss are all corundum normative, with values as high as 4 per cent. This is reflected by the presence of igneous garnet in some of the samples south of Browntop Mountain and the indication that these were originally two-mica granites.

Radiogenic isotopes also distinguish the two parts of the Quesnel Lake Gneiss. ⁸⁷Sr/⁸⁶Sr ratios from Montgomery (1985) and tabulated by Rees (1987) show that the Western Quesnel Lake Gneiss is clearly more radiogenic than its Eastern counterpart. Values for the Western suite range from 0.7199 to 0.7478 whereas the Eastern gneiss has values

between 0.7030 and 0.7088.

Finally, geochemical, isotopic and petrographic data from these two suites indicates that the Western Quesnel Lake Gneiss has characteristics of an S-type granite whereas the Eastern Gneiss more closely approximates an I-type granite (Chappell and White, 1974; White and Chappell, 1983). Montgomery (1985), working in the Isosceles Mountain area, also found that the Eastern Quesnel Lake Gneiss, and the Mount Perseus Gneiss to the south, generally display I-type characteristics. These bodies, although similar in certain aspects with parts of the Eastern Quesnel Lake Gneiss in the present map area, tend to be less siliceous and more alkaline such that some parts of the Eastern Quesnel Lake Gneiss are syenitic in composition.

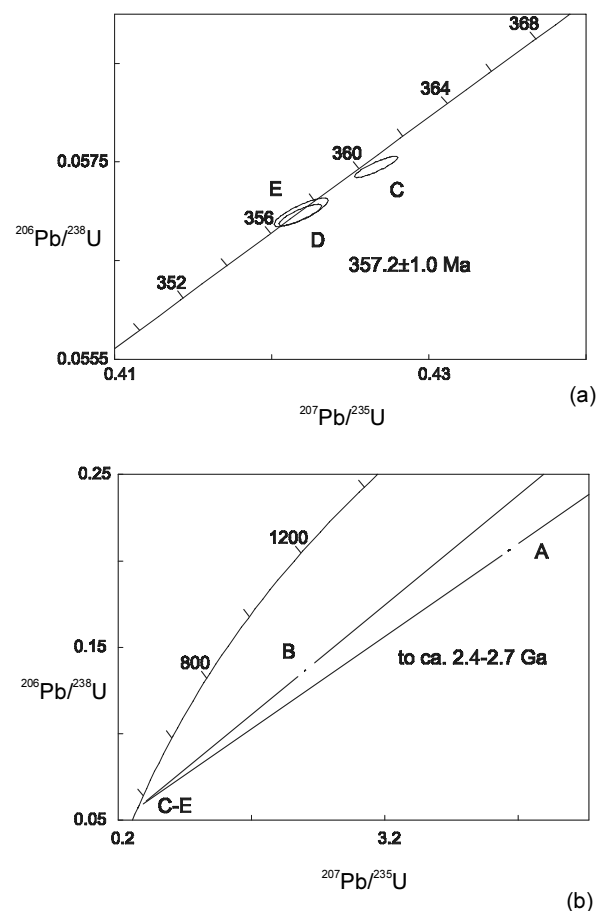


Figure 4. (a) U-Pb concordia plot for zircon from Quesnel Lake Gneiss at locality 5. Sample numbers correspond to Table 2. Error ellipses are plotted at the 2 δ level of uncertainty. (b) U-Pb concordia plot for zircon from Quesnel Lake Gneiss at locality 5. This diagram shows location of data points A and B and the corresponding upper intercepts. Sample numbers refer to Table 2. Error ellipses are plotted at the 2 δ level of uncertainty

Table 2. U-Pb analytical data for sample of Quesnel Lake Gneiss from locality 5.
See Figure 2 for location of sample.

Fraction ¹	Wt mg	U ²		Pb* ³		Pb ⁴		Pb ⁵		Pb ⁶		Isotopic ratios (1σ,%) ⁷			Apparent ages (2σ, Ma) ⁷	
		ppm	ppm	ppm	ppm	ppm	ppm	ppm	ppm	ppm	ppm	ppm	²⁰⁶ Pb/ ²³⁸ U	²⁰⁷ Pb/ ²³⁵ U	²⁰⁷ Pb/ ²⁰⁶ Pb	²⁰⁶ Pb/ ²³⁸ U
A c,p,eq ¹	12	259	64	15603	3	16.3	0.20610 (0.10)	4.5979 (0.15)	0.16180 (0.08)	1208.0 (2.1)	2474.6 (2.7)					
B f,p,eq ⁵	14	243	35	8153	4	8.2	0.13654 (0.09)	2.3035 (0.16)	0.12236 (0.08)	825.1 (1.5)	1990.9 (2.7)					
C c,p,e,m	20	409	22	7004	4	4.1	0.05745 (0.09)	0.4266 (0.16)	0.05386 (0.09)	360.1 (0.7)	365.2 (4.1)					
D c,p,e,n,m	26	422	23	7283	5	4.8	0.05696 (0.09)	0.4218 (0.16)	0.05370 (0.10)	357.1 (0.7)	358.7 (4.4)					
E f,p,e,n,m	14	406	22	4167	5	6.7	0.05699 (0.13)	0.4219 (0.20)	0.05369 (0.12)	357.3 (0.9)	357.9 (5.5)					

Notes: Analytical techniques are listed in Mortensen *et al.* (1995).

¹Upper case letter = fraction identifier; Zircon fractions A-D air abraded 10-30 volume%; E unabraded; Grain size, intermediate dimension: c=134mm to 104mm; f=104mm to 74mm; All fractions nonmagnetic on Franz separator at sideslope of 5° and field strength of 1.8A. Front slope for all fractions is 20°; Grain character codes: e=elongate, eq=equant multifaceted; p=prismatic; n=needles; Numeral=number of grains analysed; m=>10 grains.

² U blank correction of 1pg ± 20%; U fractionation corrections were measured for each run with a double 233U-235U spike (about 0.004/amu).

³Radiogenic Pb.

⁴Measured ratio corrected for spike and Pb fractionation of 0.0035/amu ± 20% (Daly collector) and laboratory blank Pb of 2-5 pg ± 20%. Laboratory blank Pb concentrations and isotopic compositions based on total procedural blanks analysed throughout the duration of this study.

⁵Total common Pb in analysis based on blank isotopic composition.

⁶Radiogenic Pb

⁷Corrected for blank Pb, U and common Pb. Common Pb corrections based on Stacey Kramers model (Stacey and Kramers, 1975) at the age of the rock or the 207Pb/206Pb age of the fraction.

U-Pb Geochronology

Samples of the Western Quesnel Lake Gneiss were collected south of Cariboo Lake for U-Pb geochronology (Figure 2). Gem quality, clear, pale pink zircon, varying in shape from equant multifaceted to very elongate prismatic was recovered from this sample. Fractions A and B were equant multifaceted grains, whereas C, D and E comprised elongate to needle-like prisms. The equant grains gave very discordant results and appear to contain significant Precambrian inherited zircon, while the fractions composed of elongate grains contain little or none of these old components (Figure 4a, Table 2). An interpreted crystallization age of 357.2±1.0 Ma is based on concordant fractions D and E. The average age of inherited components in analyzed

equant grains is about 2.4-2.7 Ga, based on the upper intercepts of two chords which extend from the magmatic age of the rock (defined by fractions D and E) through fractions A and B (Figure 4b). This age is consistent with results from samples of the Eastern Quesnel Lake Gneiss in the Isosceles Mountain area and the Boss Mountain Gneiss, which give bracketed ages of emplacement between 335 and 375 Ma (Mortensen *et al.*, 1987). This, together with a Rb/Sr age of 351±70 Ma for the eastern-most part of the Eastern Quesnel Lake Gneiss (Rees, 1987), suggests that these two suites are essentially of the same age.

DISCUSSION

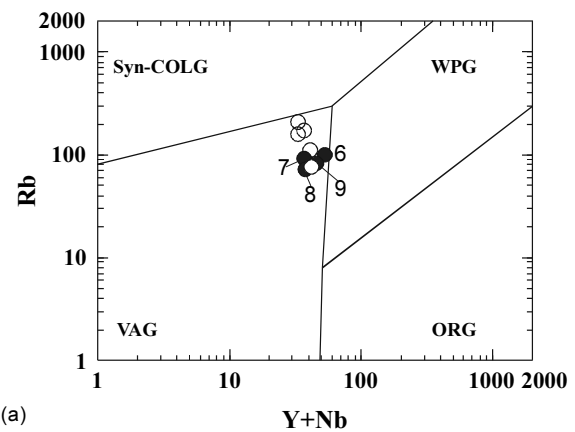
The distinct lithologic, geochemical and iso-

topic characteristics of these two essentially coeval suites reinforces the suggestion originally put forth by Rees (1987) that they represent different phases of a single intrusive event. The S-type characteristics of the Western Quesnel Lake Gneiss, together with its high $^{87}\text{Sr}/^{86}\text{Sr}$ ratios and strong inheritance in zircons, strongly suggest that it represents melting of the continental crust. In contrast, the Eastern Quesnel Lake Gneiss displays I-type attributes, although $^{87}\text{Sr}/^{86}\text{Sr}$ ratios and inheritance in zircons indicates some assimilation of continental material.

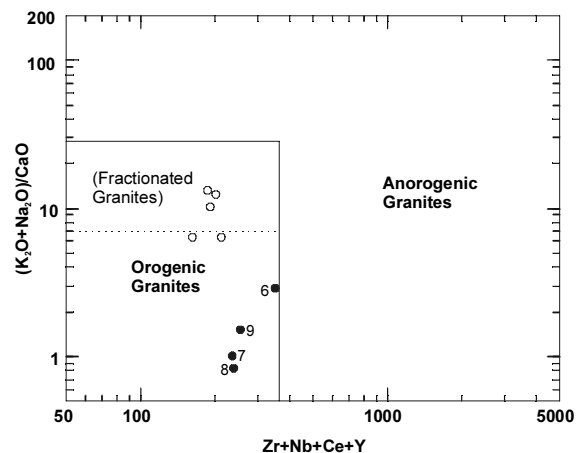
The origin of these granites has been debated by many workers. Some view these granites as being anorogenic in origin and related to rifting along the western edge of ancestral North America (Struik, 1987; Gordey *et al.*, 1987). Others have suggested that they were produced in an orogenic setting and are related to compressional tectonism documented within westernmost Ancestral North American miogeoclinal rocks along the southern U.S. Cordillera (i.e. Roberts Mountain Allochthon; Smith *et al.* 1993).

Early attempts at differentiating these two tectonic settings through use of geochemical data was attempted by Montgomery (1985) and Montgomery and Ross (1989) using information from the eastern-most part of the Eastern Quesnel Lake Gneiss in the Isosceles Mountain area. These authors used a discrimination diagram developed by Pearce *et al.* (1984) which utilized the elements Nb, Rb, and Y. Data plotted on this diagram was not conclusive with points forming an area straddling the volcanic arc granite and within plate granite fields. Montgomery and Ross (1989) interpreted this data to indicate the gneisses are calc-alkalic and/or tholeiitic granites intruded into continental crust during subduction of oceanic lithosphere, presumably along an east dipping zone to the west.

Data from this investigation plotted on the same diagram falls within the volcanic arc granite field similar to some of the data points from the Isosceles Mountain area (Figure 5a). The relatively low values of the elements Zr, Nb, Ce and Y also supports an orogenic setting for these granites. (Figure 5b). The data points for the Western Quesnel Lake Gneiss should be viewed with caution. These granites were most likely produced by melting of the continental crust (i.e. sediments) and the geochemistry would be a reflection of the source material and not the tec-



(a)



(b)

Figure 5. (a) Plot of Rb versus Y+Nb for Quesnel Lake Gneiss based on data in Table 1. Diagram from Pearce *et al.* (1984). Syn-COLG: syn-collisional granites; WPG: within plate granites; VAG: volcanic arc granites; ORG: ocean ridge granites. (b) Plot of $(\text{K}_2\text{O}+\text{Na}_2\text{O})/\text{CaO}$ versus $\text{Zr}+\text{Nb}+\text{Ce}+\text{Y}$ for Quesnel Lake Gneiss based on data in Table 1. Diagram from Whalen *et al.* (1987).

tonic setting. Furthermore, Pearce *et al.* (1984) indicate that average continental crust plots within the volcanic arc granite field of the Rb versus Nb+Y diagram, a feature also supported by granite of the Western Quesnel Lake Gneiss.

The same cannot be said of the Eastern Quesnel Lake Gneiss. Data for this granite suggests it was produced by melting of igneous source rocks (I-type granite). Subgroups of this granite type include A-type, or anorogenic granites, produced by melting of dehydrated continental crust and M-type resulting from melting of subducted oceanic crust or overlying mantle (Whalen *et al.*, 1987). Data for the Eastern Quesnel Lake Gneiss from the present study area

indicates this granite is most likely M-type (i.e. volcanic arc granites; Figures 5a and b).

In summary, these data suggests that the Quesnel Lake Gneisses are the products of arc volcanism. However, parts of the Eastern Quesnel Lake Gneiss from the Isosceles Mountain area have geochemical signatures that indicate a within plate or anorogenic setting (Montgomery and Ross, 1989). Data for syenitic phases in this area (Montgomery, 1985) have values of Zr+Nb+Ce+Y greater than 1000 which are well within the anorogenic field of Whalen *et al.* (1987; Figure 5b), which supports the within plate setting for this data indicated on the Rb versus Y+Nb plot of Pearce *et al.* (1984; see Figure 4 of Montgomery and Ross, 1989).

Clearly, the interpretation of the tectonic setting of the Eastern and Western Quesnel Lake gneisses based on geochemical abundances, is not straightforward. The Western Quesnel Lake Gneiss is probably the product of partial melting of continental crust in an arc setting. The bulk of the geochemical data suggests Eastern Quesnel Lake Gneiss granites were also produced in an arc-setting, although the alkaline nature of some of the phases is not fully understood. Whalen *et al.* (1987) suggested that alkaline or peralkaline granites can be formed in non-anorogenic settings, such as arc or transcurrently faulted subduction zones. The latter two settings would imply back-arc spreading or extension, a scenario envisioned by many workers during Late Devonian to Early Mississippian times along the western edge of Ancestral North America (Robback and Walker, 1995; Ferri, 1997; Gabrielse, 1991).

It is probable that these Early Mississippian plutonic rocks are comagmatic with Late Devonian to Early Mississippian? arc volcanics that are exposed intermittently along the western limit of the Kootenay and Cassiar terranes. These volcanics are most abundant in the Eagle Bay Assemblage north of Kamloops (Schiarizza and Preto, 1987), and may possibly occur in western exposures of the Snowshoe Group (Struik, 1988; Höy and Ferri, 1998). Eagle Bay volcanics are bimodal, calc-alkaline arc volcanics that locally contain alkaline phases (Höy, 1987) and are intruded by a number of ?Late Devonian orthogneisses that are similar to the Quesnel Lake gneisses. Devono-Mississippian calc-alkaline felsic volcanics are also found

along western exposures of the Cassiar Terrane in the Germansen Landing area of east-central British Columbia (Ferri and Melville, 1994; Ferri *et al.*, 1992, 1993).

The comparison between these terranes, and in particular, the recognition of subvolcanic magmatism related to arc volcanism in the Barkerville Subterrane and Cassiar Terrane, enhances the potential for discovery of base and precious metal mineralization similar to those that occur in the Eagle Bay Assemblage.

ACKNOWLEDGEMENTS

The authors would like to thank Graham Nixon for helpful discussions on the geochemical aspects of this paper and Nick Massey for reviewing an early version of the manuscript.

REFERENCES

- Campbell, R.B. (1978): Quesnel Lake (93A) map area, British Columbia; *Geological Survey of Canada*, Open File 574.
- Chappell, B.W. and White, A.J.R. (1974): Two contrasting granite types; *Pacific Geology*, Volume 8, pages 173-174.
- Ferri, F., and Melville, D.M. (1994): Bedrock geology of the Germansen Landing - Manson Creek area, British Columbia (93N/9, 10, 15; 94C/2); *B.C. Ministry of Energy, Mines and Petroleum Resources*, Bulletin 91.
- Ferri, F., Dudka, S., and Rees, C. (1992): Geology of the Uslika Lake area, northern Quesnel Trough, B.C. (94C/3,4 and 5); in *Geological Fieldwork 1991*, *B.C. Ministry of Energy, Mines and Petroleum Resources*, Paper 1992-1, pp. 127-146.
- Ferri, F., Dudka, S., Rees, C., and Meldrum, D.G. (1993): Geology of the Aiken Lake and Osilinka River areas, Northern Quesnel Trough (94C/2, 3, 5, 6 and 12); in *Geological Fieldwork 1992*, *B.C. Ministry of Energy, Mines and Petroleum Resources*, Paper 1993-1, pp. 109-134.
- Ferri, F. (1997): Nina Creek Group and Lay Range Assemblage, north-central British Columbia: Remnants of Late Paleozoic oceanic and arc terranes; *Canadian Journal of Earth Sciences*, Volume 34, pages 854-874.

- Fillipone, J.A. (1985): Structure and metamorphism of the Boss Mountain area, southwestern Cariboo Mountains, British Columbia; M.Sc. Thesis, *The University of British Columbia*, Vancouver, British Columbia, 130 pages.
- Gabrielse, H. (1991): Late Paleozoic and Mesozoic terrane interactions in north-central British Columbia; *Canadian Journal of Earth Sciences*, Volume 28: 947-957.
- Gordey, S.P., Abbott, J.G., Tempelman-Kluit, D.J. and Gabrielse, H. (1987): "Antler" clastics in the Canadian Cordillera; *Geology*, Volume 15, pages 103-107.
- Höy, T. and Ferri, F. (1998): Zn-Pb deposits in the Cariboo Subterranean, central British Columbia (93A/NW); in *Geological Fieldwork 1997*, B.C. Ministry of Employment and Investment, Paper 1998-1, pages 13-1 to 13-12.
- Höy, T. (1987): Alteration, chemistry and tectonic setting of volcanogenic massive sulphide-barite deposits at Rea Gold and Homestake, southeastern British Columbia; in *Exploration in British Columbia 1986*, B.C. Ministry of Energy, Mines and Petroleum Resources, pages B7-B19.
- Irvine, T.N., and Baragar, W.R.A. (1971): A guide to the chemical classification of the common volcanic rocks; *Canadian Journal of Earth Sciences*, Volume 8 pages 523-548.
- Montgomery, J.R. (1985): Structural relations of the southern Quesnel Lake Gneiss, Isosceles Mountain Area, southwest Cariboo Mountains, British Columbia; M.Sc. Thesis, *The University of British Columbia*, Vancouver, British Columbia, 96 pages.
- Montgomery, J.R., and Ross, J.V. (1989): A note on the Quesnel Lake Gneiss, Cariboo Mountains, British Columbia; *Canadian Journal of Earth Sciences*, Volume 26, pages 1503-1508.
- Mortensen, J. K., Ghosh, D.K. and Ferri, F. (1995): U-Pb geochronology of intrusive rocks associated with copper-gold porphyry deposits in the Canadian Cordillera; in *General Aspects of Porphyry Deposits of the Northwestern Cordillera of North America*, *CIM Special Volume 46*, p. 142-158.
- Mortensen, J.K., Montgomery, J.M. and Phillipone, J. (1987): U-Pb zircon, monazite, and sphene ages for granitic orthogneiss of the Barkerville Terrane, east-central British Columbia; *Canadian Journal of Earth Sciences*, Volume 24, pages 1261-1266.
- Okulitch, A.V. (1985): Paleozoic plutonism in south-eastern British Columbia; *Canadian Journal of Earth Sciences*, Volume 22, pages 1409-1424.
- Panteleyev, A., Bailey, D.G., Bloodgood, M.A. and Hancock, K.D. (1996): Geology and mineral deposits of the Quesnel River-Horsefly map area, central Quesnel Trough, British Columbia; B. C. Ministry of Employment and Investment, Bulletin 97, 156 pages.
- Pearce, T.H., Harris, N.B.W. and Tindle, A.G. (1984): Trace element discrimination diagrams for the tectonic interpretation of granitic rocks; *Journal of Petrology*, Volume 25, pages 956-983.
- Rees, C.J. (1987): The Intermontane - Omineca Belt boundary in the Quesnel Lake area, east-central British Columbia: Tectonic implications based on geology, structure and paleomagnetism; Ph.D. Thesis; *Carleton University*, Ottawa, Ontario, 421 pages.
- Rees, C.J. and Ferri, F. (1983): A kinematic study of mylonitic rocks in the Omineca-Intermontane Belt tectonic boundary in east-central British Columbia; in *Report of Activities, Geological Survey of Canada*, Paper 83-1B, pages 121-125.
- Roback, R.C., and Walker, N.W. (1995): Provenance, detrital zircon U-Pb geochronometry, and tectonic significance of Permian to Lower Triassic sandstone in southeastern Quesnellia, British Columbia and Washington; *Geological Society of America Bulletin*, Volume 107, pages 665-675.
- Schiarizza, P. and Preto, V.A. (1987): Geology of the Adams Plateau-Clearwater-Vavenby area; B.C. Ministry of Energy, Mines and Petroleum Resources, Paper 1987-2, 88 pages.
- Smith, M.T., Dickinson, W.R. and Gehrels, G.E. (1993): Contractual nature of Devonian-Mississippian Antler tectonism along the North American continental margin; *Geology*, Volume 21, pages 21-24.
- Stacey, J.S., and Kramers, J.D. (1975): Approximation of terrestrial lead isotope evolution by a two-stage model; *Earth and Planetary Science Letters*, Volume 26, pages 207-221.
- Streckeisen, A.L. (1976): To each plutonic rock its proper name; *Earth and Science Reviews*, Volume 12, pages 1-33.
- Struik, L.C. (1981): A re-examination of the type area of the Devonian-Mississippian Cariboo orogeny, central British Columbia; *Canadian Journal of Earth Sciences*, Volume 18, pages 1767-1775.

- Struik, L.C. (1986): Imbricated terranes of the Cariboo Gold Belt with correlations and implications for tectonics in southeastern British Columbia; *Canadian Journal of Earth Sciences*, Volume 23, pages 1047-1061.
- Struik, L.C. (1988): Structural geology of the Cariboo Gold Mining District, east-central British Columbia; *Geological Survey of Canada*, Memoir 421, 100 pages.
- Sutherland Brown, A. (1963): Geology of the Cariboo River area, British Columbia; *B.C. Ministry of Energy, Mines and Petroleum Resources*, Bulletin 47, 60 pages.
- Whalen, J.B., Currie, K.L. and Chapell, B.W. (1987): A-type granites: geochemical characteristics, discriminations and petrogenesis; *Contributions to Mineralogy and Petrology*, Volume 95, pages 407-419.
- White, A.J.R. and Chappell, B.W. (1983): Granitoid types and their distribution in the Lachlan Fold Belt, southeastern Australia; *Geological Society of America*, Memoir 159, pages 21-34.



NEW GALENA LEAD ISOTOPIC DATA FROM CARBONATE ROCKS IN NORTHEASTERN B.C. - IMPLICATIONS FOR REGIONAL MVT FLUID MIGRATION

JoAnne Nelson (Geological Survey Branch, B.C. Ministry of Energy and Mines),
Janet E. Gabites (Geochronology Laboratory, Department of Geological Sciences, U.B.C.),
Suzanne Paradis (Mineral Deposits Division, Geological Survey of Canada)

KEYWORDS: lead isotopes, Robb Lake, Pine Point, Northeastern B.C., carbonate-hosted deposits, Pb-Zn

INTRODUCTION

Outcropping Siluro-Devonian carbonate strata in the northeastern Rocky Mountains host a series of Mississippi Valley-type Zn-Pb deposits (Figure 1). The largest and most extensively explored of these is the Robb Lake deposit (Nelson *et al.*, this volume). Carbonate strata continue eastward into the subsurface as the Middle Devonian Presqu'ile barrier complex, which divides the Muskeg evaporite basin to the south from the McKenzie shale basin to the north. The world class Pine Point zinc-lead mine lies near the eastern end of the Presqu'ile barrier, where it overlies the McDonald-Hay River fault, a major Precambrian crustal break (Figure 1).

Mississippi Valley deposits are considered to form as the result of regional flow of basinal brines (Jackson and Beales, 1967). Recent models have emphasised the importance of tectonically-driven fluid flow in their formation (Leach and Rowan, 1986, Oliver, 1986). Sverjensky (1984) and Oliver (1986) proposed that the processes of hydrocarbon migration and metal transport were inseparable, both being the results of brine flow on a basin-wide scale.

Garven (1985) first applied regional hydrologic modelling to the Western Canada Sedimentary Basin, relating both petroleum migration and the formation of the Pine Point deposit to regional eastward fluid flow along the Presqu'ile Barrier, driven by post Early Cretaceous (Laramide) uplift of the Rocky Mountains. This model, although appealing, has been controversial ever since its publication, primarily because of the lack of absolute age constraints on major fluid transport events in the basin. There are two "end-member" hypotheses.

It is possible that Pine Point formed through a Devonian-Mississippian, "Antler orogenic" fluid event. This hypothesis is supported by the data of Nesbitt and Muehlenbachs (1994), who contrasted the characteristics of fluid inclusions in secondary saddle dolomites with those in later, cross-cutting, syn-Laramide veins. They considered the former to be certainly pre-Laramide and probably Devonian-Mississippian. Alternatively, Qing and Mountjoy (1992), in studies of fluid inclusions and saddle dolomites, observed systematic easterly-decreasing temperatures and west-to-east evolution in the isotopic character of brines, which they considered consistent with Garven's (1985) Laramide model.

The Pine Point deposit has recently been dated at 361 ± 16 Ma (Devonian-Mississippian) by Rb-Sr methods on sphalerite (Nakai *et al.*, 1993). Although this method and the interpretation of results from it are themselves still controversial (see discussion by Pettke and Diamond, 1996), it at least offers the possibility of an absolute age, which can be evaluated in terms of other indirect evidence. An Rb-Sr age for Robb Lake is currently being attempted (Nelson *et al.*, this volume).

LEAD ISOTOPIC MODELLING OF CARBONATE-HOSTED DEPOSITS

The isotopic composition of lead in deposits depends on the source reservoir (e.g., mantle, crust), the age of the deposit, and on the selectivity of the mineralisation process (Godwin *et al.*, 1988). Galena lead isotopic signatures of carbonate-hosted sulphide deposits tend to fall into one of two categories: either as a well-defined cluster, or as a linear trend to extreme enrichment in radiogenic lead (Gulson, 1986). Most deposits of the Mississippi Valley type fall into the second category (Heyl *et al.*, 1974, Vaasjoki and Gulson, 1986). Lead isotope analy-

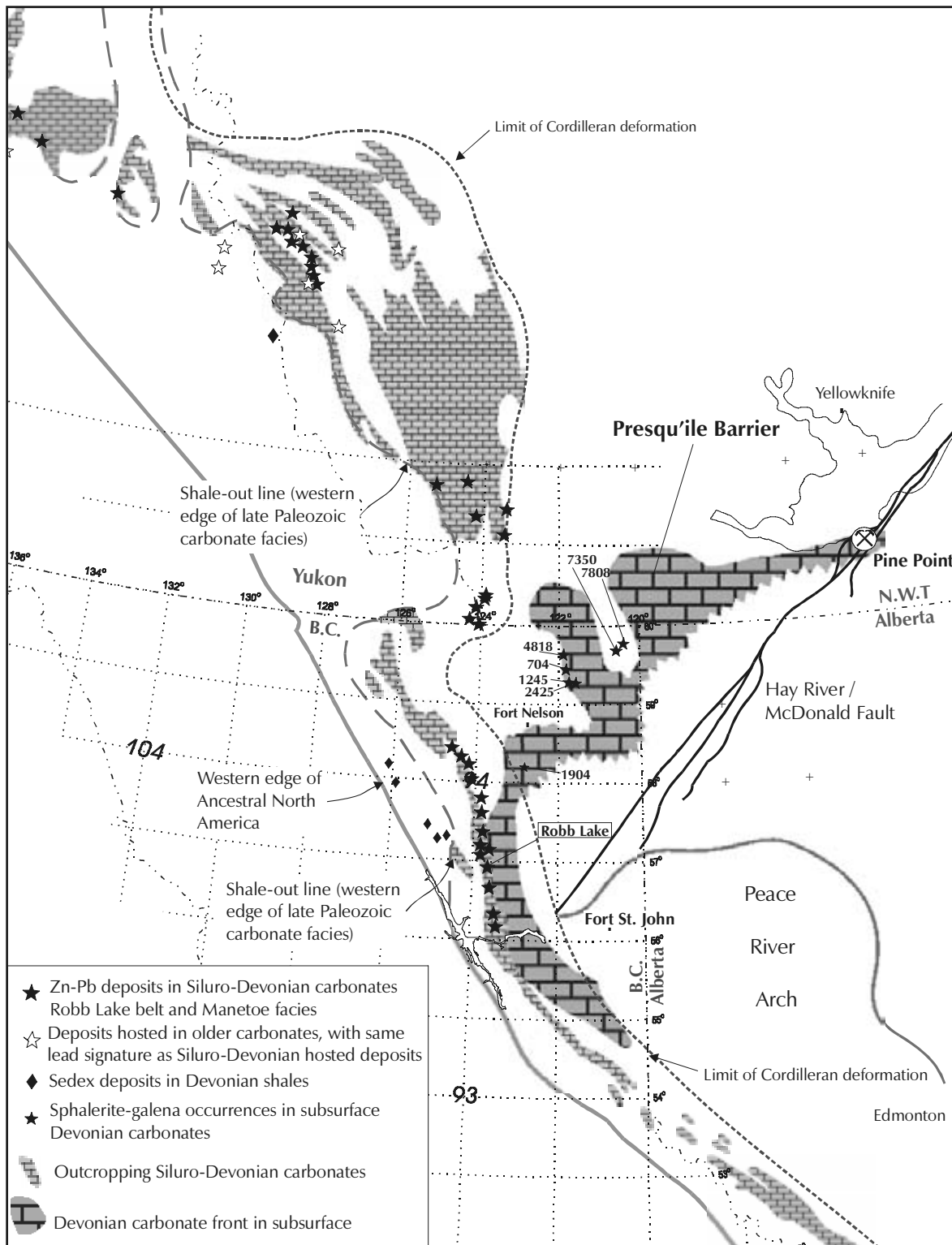


Figure 1. Location of outcropping and subsurface sulphide occurrences in Silurian-Devonian carbonates of northeastern British Columbia, N.W.T. and Yukon.

ses from the Pine Point district (Cumming *et al.*, 1990) form a very tight cluster, despite the deposits sampled being spread through an area of 15 by 60 km. The brines carrying lead to Pine Point had a very homogeneous isotopic composition (Cumming *et al.*, 1990), which implies that either the source was homogeneous or that the fluids homogenised during transport through large distances. By contrast, leads from Cordilleran carbonate-hosted deposits, including the Robb Lake belt and deposits in the Yukon (Morrow and Cumming, 1982, Godwin *et al.*, 1982, Morrow *et al.*, 1986), form a trend (or closely spaced trends) to very radiogenic values (Figure 2a). The least-radiogenic end of the trend intersects the “shale curve” of Godwin and Sinclair (1982). This model curve is a reference for the growth of lead in upper crustal environments in the Canadian Cordillera, defined using data from stratiform shale-hosted deposits in British Columbia and Yukon Territory. In terms of lead sources, Pine Point and the Cordilleran deposits therefore appear to represent two highly disparate fluid systems.

The regional extent of “Robb Lake” as opposed to “Pine Point” lead in the subsurface Presqu’île Barrier may outline the extent of these two fluid systems. Although an extensive lead isotopic database exists for surface sulphide occurrences in Paleozoic carbonate rocks of the northern Rockies and the Yukon (Morrow and Cumming, 1982, Godwin *et al.*, 1982, Morrow *et al.*, 1986), so far very few samples from the subsurface have been analysed. In 1998, we began a program of systematic sampling of galena-sphalerite occurrences from cored intervals of Devonian carbonates in the subsurface of B.C. and Alberta. As part of the Central Foreland NATMAP project, our study aims at a deeper understanding of MVT mineralization in the northeastern Rockies, and of the possible relationship between sulphide deposition and hydrocarbon formation in the Western Canada Sedimentary Basin.

PRESENT STUDY

This paper reports lead isotopic compositions of six samples collected in 1998 at the B.C. Ministry of Energy and Mines Core Storage Warehouse in Charley Lake, B.C. The locations of these samples are shown on Figure 1. Three of

them, and also sample 704, a previously unpublished analysis, are from dolostones of the Slave Point and Pine Point formations along the buried Devonian carbonate front in NTS sheets 94P/5 and 94P/12. Sample 1-98-1904-2 is from within the carbonate barrier in 94J/2; of the sample suite, it lies closest to the mountain front. Samples 1-98-7350-1 and 1-98-7808-1 are from the Jean Marie Formation in the Helmet North Field.

In all of them except sample 1-98-1904-2, galena and sphalerite occur in veins and patches with coarse secondary dolomite, and in open spaces with saddle dolomite and, in some instances, drusy quartz. Sample 1-98-1904-2 is unique in that it contains a 0.5 metre thick, bedding-parallel replacement body of massive pyrite, sphalerite and galena that grades out into heavily disseminated sulphides.

Analytical Techniques

Small clean cubes of galena were hand-picked, washed, and dissolved in dilute hydrochloric acid. Approximately 10 to 25 nanograms of the lead in chloride form was loaded on a rhenium filament, and isotopic compositions were determined using a modified VG54R thermal ionization mass spectrometer. The measured ratios were corrected for instrumental mass fractionation of 0.13% per mass unit based on replicate measurements of the N.B.S. 981 Standard Isotopic Reference Material. Errors reported in Table 1 were obtained by propagating all mass fractionation and analytical errors through the calculation.

Results

The results of lead isotopic analyses of galena are shown in Table 1, and plotted in Figures 2a, 2b and 2c. Figure 2a and 2b are standard $^{206}\text{Pb}/^{204}\text{Pb}$ versus $^{207}\text{Pb}/^{204}\text{Pb}$ and $^{206}\text{Pb}/^{204}\text{Pb}$ versus $^{208}\text{Pb}/^{204}\text{Pb}$ plots. Figure 2c is a plot of uranium and thorogenic lead, $^{207}\text{Pb}/^{206}\text{Pb}$ versus $^{208}\text{Pb}/^{206}\text{Pb}$. The small peak of ^{204}Pb is not used in the isotopic ratios in this plot, thus removing a major source of analytical error. The analyses have been plotted against the shale curve of Godwin and Sinclair (1982). The $^{206}\text{Pb}/^{204}\text{Pb}$ versus $^{207}\text{Pb}/^{204}\text{Pb}$ isotopic ratios of

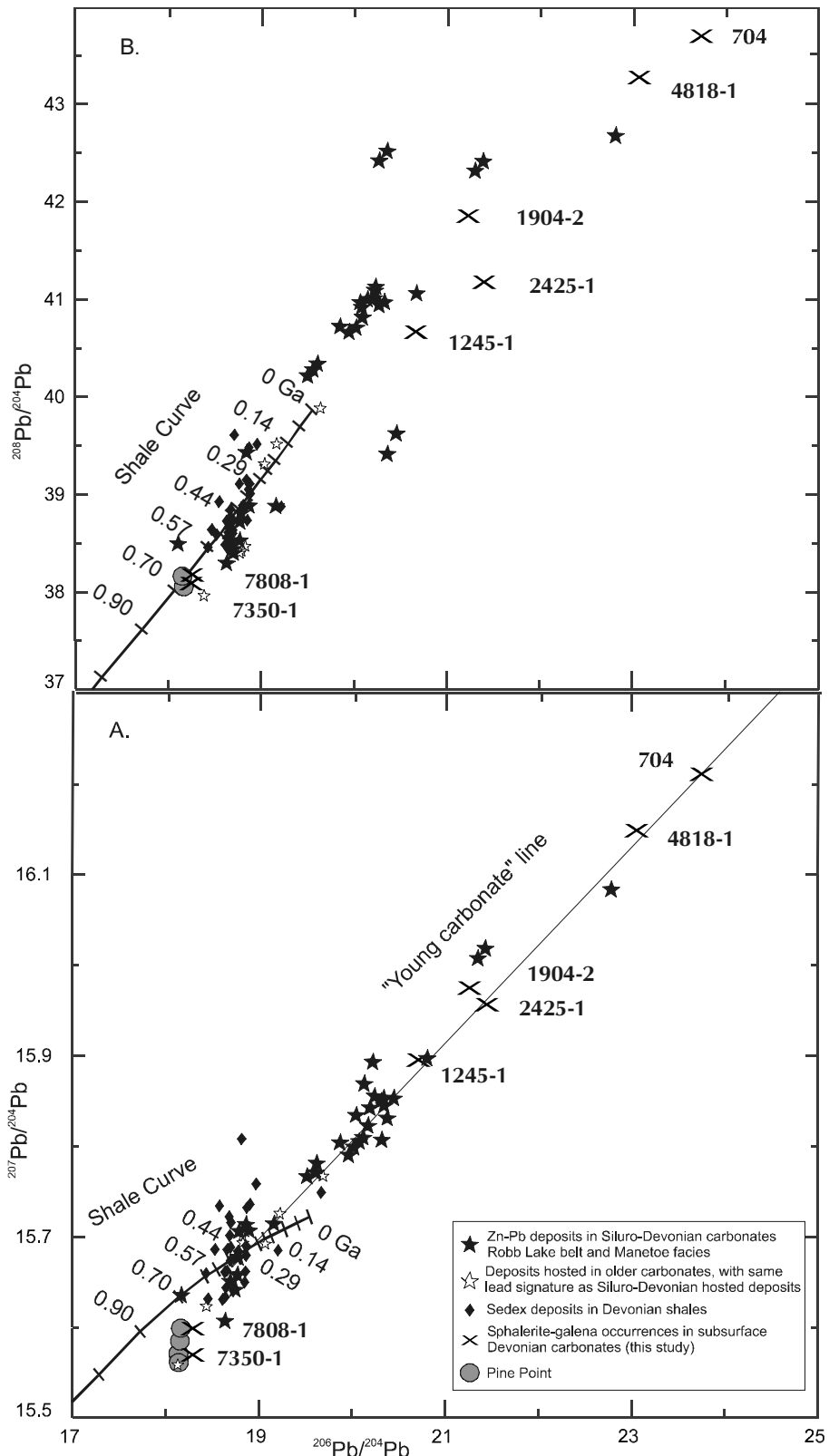
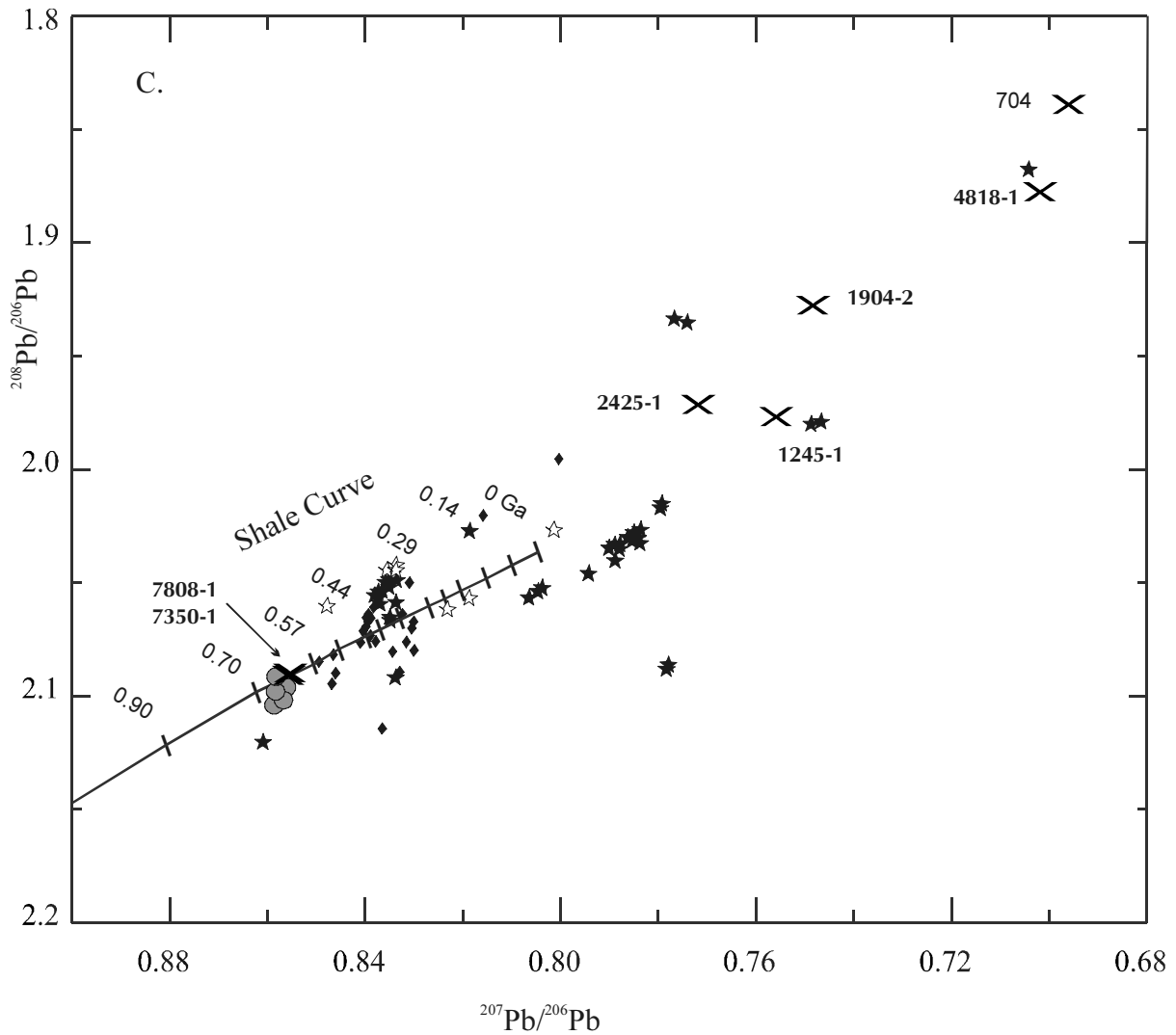


Figure 2A). Lead isotopic analyses of samples plotted on $^{207}\text{Pb}/^{204}\text{Pb}$ versus $^{206}\text{Pb}/^{204}\text{Pb}$ diagram, with shale curve (Godwin and Sinclair, 1982) for reference, the “young carbonate” line (Godwin *et al.*, 1982); additional data from Godwin *et al.* (1989), Morrow and Cumming (1982), Morrow *et al.* (1986) and Cumming *et al.* (1990). B). Lead isotopic analyses of samples plotted on $^{208}\text{Pb}/^{204}\text{Pb}$ versus $^{206}\text{Pb}/^{204}\text{Pb}$ diagram. Sources as for Figure 2a.



2C). Lead isotopic analyses of samples plotted on $^{208}\text{Pb}/^{206}\text{Pb}$ versus $^{207}\text{Pb}/^{206}\text{Pb}$ diagram. Sources as for Figure 2a.

samples 1-98-7350-1 and 1-98-7808-1, the Jean Marie samples, plot below the shale curve, but very near to the Pine Point cluster (Figure 2a). The other four samples are highly radiogenic, plotting above and to the right of the shale curve,

along the same trend as the Robb Lake belt (Morrow and Cumming, 1982), the “young carbonate” deposits of Godwin *et al.* (1982, 1988), and sulphides within the Devonian Manetoc Facies of southern Yukon (Morrow *et al.*, 1986).

Table 1. Lead isotopic analytical data

Lab Number	Sample Number	$^{206}\text{Pb}/^{204}\text{Pb}$	$^{206}\text{Pb}/^{204}\text{Pb}$ % 1* err	$^{207}\text{Pb}/^{204}\text{Pb}$	$^{207}\text{Pb}/^{204}\text{Pb}$ % 1* err	$^{208}\text{Pb}/^{204}\text{Pb}$	$^{208}\text{Pb}/^{204}\text{Pb}$ % 1* err	$^{207}\text{Pb}/^{206}\text{Pb}$	$^{207}\text{Pb}/^{206}\text{Pb}$ % 1* err	$^{208}\text{Pb}/^{206}\text{Pb}$	$^{208}\text{Pb}/^{206}\text{Pb}$ % 1* err
31198-001	1-98-1245-1	20.6715	0.01	15.8991	0.01	40.7209	0.013	0.7691	0.004	1.9699	0.009
31199-001	1-98-2425-2	21.4054	0.015	15.9603	0.014	41.2292	0.016	0.7456	0.006	1.9261	0.003
31200-001	1-98-7350-1	18.2667	0.004	15.5742	0.002	38.1483	0.005	0.8526	0.003	2.0884	0.003
31201-001	1-98-7808-1	18.2958	0.006	15.6044	0.005	38.2296	0.007	0.8529	0.004	2.0895	0.004
31202-001	1-98-4818-1	23.0992	0.006	16.1475	0.005	43.3369	0.006	0.6991	0.003	1.8761	0.003
31203-001	1-98-1904-2	21.2185	0.01	15.9786	0.006	41.9101	0.011	0.7531	0.007	1.9752	0.005
31205-001	95-704-1	23.707	0.005	16.212	0.005	43.73	0.005	0.68385	0.007	1.8446	0.005

Discussion

In this preliminary study, five galena lead samples from the subsurface Presqu'ile Barrier in northeastern B.C. show lead signatures similar to those of outcropping deposits in the northeastern Rockies and along the margins of the Selwyn Basin. These five highly radiogenic samples plot along the "young carbonate line" of Godwin *et al.* (1982), and are more radiogenic than most of the Robb Lake belt analyses (Figure 2a, b, and c). This suggests that the metal-bearing fluids scavenged radiogenic lead during transport, possibly from a zircon-rich source such as old basement or a sandstone aquifer (Godwin *et al.*, 1988). The lead sampled is heterogeneous, indicating either that the source was heterogeneous, fluid flow was relatively localised, and/or transport distances were not great enough to allow homogenisation. The location of these five deposits along the westernmost margin of the Presqu'ile Barrier supports the theory that metal-bearing fluids flowed eastwards from a western source until they intersected the carbonates, where sulphide-precipitating reactions occurred. The fact that there was no apparent mixing of Pine Point lead in the formation of these deposits suggests that the fluids forming the two systems were entirely separate.

On the plots of $^{206}\text{Pb}/^{204}\text{Pb}$ versus $^{208}\text{Pb}/^{204}\text{Pb}$ and $^{207}\text{Pb}/^{206}\text{Pb}$ versus $^{208}\text{Pb}/^{206}\text{Pb}$ (Figures 2b and 2c), which involve both thorogenic and urogenic lead, samples from the Jean Marie Formation lie in a tight cluster, apparently on the shale curve. The lead source for Pine Point and the two occurrences reported here was slightly enriched in thorium over lead compared to the shale curve, shown by the different relationships of the uranium and thorogenic isotopes to the growth curve. However, the model age at which the Pine Point - Jean Marie array projects onto the shale growth curve in $^{206}\text{Pb}/^{206}\text{Pb}$ versus $^{206}\text{Pb}/^{206}\text{Pb}$ space is close to 700 Ma (Figure 2a), significantly older than either the Middle Devonian age of the host rocks or the 361 Ma Rb/Sr age of the deposit itself. This shows that the shale curve is not an appropriate model for all northern Canadian carbonate-hosted deposits, only for those associated with the Cordilleran shale basins from which the shale curve data base was derived.

The similarity in lead signatures between Pine Point and the two Jean Marie samples

offers a surprise and a puzzle. These samples are located within an embayment in the Presqu'ile barrier, remote from Pine Point and also from the Hay River/McDonald Fault. Was there a physical barrier to fluid flow between the Helmet Field and the deposits along what is now the western margin of the Presqu'ile Barrier? Does their lead signature reflect the growth curve of the McKenzie shale basin, or fluids sourced directly from Precambrian basement? We intend to undertake further studies to expand the scope of the data set, in order to build a regional lead isotopic distribution for the Western Canada Sedimentary Basin.

REFERENCES

- Cumming, G.L., Kyle, J.R. and Sangster, D.F. (1990): Pine Point: a case history of lead isotopic homogeneity in a Mississippi Valley-type district; *Economic Geology*, Volume 85, pages 133-144.
- Garven, G. (1985): The role of regional fluid flow in the genesis of the Pine Point deposits, Western Canada Sedimentary Basin; *Economic Geology*, Volume 80, pages 307-324.
- Godwin, C.J. and Sinclair, A.J. (1982): Average lead isotope growth curves for shale-hosted zinc-lead deposits, Canadian Cordillera; *Economic Geology*, Volume 7, pages 675-690.
- Godwin, C.J., Sinclair, A.J., and Ryan, B.D. (1982): Lead isotope models for the genesis of carbonate-hosted Zn-Pb, shale-hosted Ba-Zn-Pb, and silver-rich deposits in the Northern Canadian Cordillera; *Economic Geology*, Volume 77, pages 82-94.
- Godwin, C.J., Gabites, J.E., and Andrew, A. (1988): LEADTABLE: A galena lead isotope database for the Canadian Cordillera; *B.C. Ministry of Energy, Mines and Petroleum Resources*, Paper 1988-4, 188 pages.
- Gulson, B.L., 1986: Lead isotopes in mineral exploration; *Developments in Economic Geology* 23, *Elsevier*, Amsterdam, 245 pp.
- Heyl, A.V., Landis, G.P., and Zartman, R.E. (1974): Isotopic evidence for the origin of Mississippi valley-type mineral deposits: a review; *Economic Geology*, Volume 69, pages 992-1006.
- Jackson, S.A. and Beales, F.W. (1967): An aspect of sedimentary basin evolution: the concentration of Mississippi Valley-types ores during the late stages of diagenesis; *Bulletin of Canadian*

- Petroleum Geology*, Volume 15, pages 393-433.
- Leach, D.L. and Rowan, E.L. (1986): Genetic link between Oachita foldbelt tectonism and the Mississippi Valley-type lead-zinc deposits of the Ozarks; *Geology*, Volume 14, pages 931-935.
- Morrow, D.W. and Cumming, G.L., (1982): Interpretation of lead isotope data from zinc-lead mineralization in the northern part of the western Canadian Cordillera; *Canadian Journal of Earth Sciences*, Volume 19, pages 1070-1078.
- Morrow, D.W., Cumming, G.L. and Koepnick, R.B. (1986): Manetoe facies - a gas-bearing, megacrystalline, Devonian dolomite, Yukon and Northwest Territories, Canada; *American Association of Petroleum Geologists Bulletin*, Volume 70, p. 702-720.
- Nakai, S., Halliday, A.N., Kesler, S.E., Jones, H.D., Kyle, J.R. and Lane, T.E. (1993): Rb-Sr dating of sphalerites from Mississippi Valley-type (MVT) deposits; *Geochimica et Cosmochimica Acta*, Volume 57, pages 417-427.
- Nelson, J., Paradis, S. and Zantvoort, W. (1999): The Robb Lake carbonate-hosted lead-zinc deposit, northeastern British Columbia: a Cordilleran MVT deposit; in *Geological Fieldwork 1998, B.C. Ministry of Energy and Mines*, Paper 1999-1, this volume.
- Nesbitt, B.E. and Muehlenbachs, K. (1994): Paleohydrology of the Canadian Rockies and origins of brines, Pb-Zn deposits and dolomitization in the Western Canada Sedimentary Basin; *Geology*, Volume 22, pages 243-246.
- Oliver, J. (1986): Fluids expelled tectonically from orogenic belts: their role in hydrocarbon migration and other geologic phenomena; *Geology*, Volume 14, pages 99-102.
- Pettke, T. and Diamond, L.W. (1996): Rb-Sr dating of sphalerite based on fluid inclusion-host mineral isochrons: a clarification of why it works; *Economic Geology*, Volume 91, pp.951-956.
- Qing, H. and Mountjoy, E. (1992): Large-scale fluid flow in the Middle Devonian Presqu'ile barrier, Western Canada Sedimentary Basin; *Geology*, Volume 20, pages 903-906.
- Sverjensky, D.A. (1984): Oil field brines as ore-forming solutions; *Economic Geology*, Volume 79, pages 23-37.
- Vaasjoki, M. and Gulson, B.L. (1986): Carbonate-hosted base metal deposits: Lead isotopic studies bearing on their genesis and exploration; *Economic Geology*, Volume 81, pages 156-172.



THE ROBB LAKE CARBONATE-HOSTED LEAD-ZINC DEPOSIT, NORTHEASTERN BRITISH COLUMBIA: A CORDILLERAN MVT DEPOSIT

JoAnne L. Nelson (Geological Survey Branch, B.C. Ministry of Energy and Mines),
Suzanne Paradis (Geological Survey of Canada, Mineral Resources Division, Sidney, B.C.),
Willem Zantvoort (SEOS, University of Victoria)

KEYWORDS: MVT, Lead-zinc, Northern B.C.,
Robb Lake, Silurian, Devonian

done during the summer of 1998, and introduces
the Rb-Sr analytical study that will be complet-
ed in 1999.

INTRODUCTION

The Robb Lake Pb-Zn deposit is hosted by platform carbonate rocks in the Rocky Mountains of northeastern British Columbia (56°56N, 123°43W; 94B/13; Fig. 1). The deposit, hosted by Silurian-Devonian dolostone of the Muncho-McConnell Formation, consists of a series of interconnected bedding-parallel and crosscutting breccia bodies with sparry dolomite, sphalerite, galena, pyrite, quartz, calcite, and pyrobitumen in their matrix. It is the most promising and the best developed lead-zinc occurrence in the northern Rockies, with significant showings over an 8 km² area.

The timing and mode of origin of the Robb Lake mineralization are controversial. The host breccias were attributed to early karst collapse by Taylor (1977) and to collapse related to evaporite dissolution by Manns (1981). In these models, mineralization was a late diagenetic or early post-diagenetic process of mainly passive infilling and replacement. On the other hand, Macqueen and Thompson (1978) advocated hydraulic cracking as the mechanism of brecciation. They hypothesised a Laramide age for the deposit based on the co-occurrence of metals and petroleum, and on the observation that burial depths necessary to produce temperatures greater than 200°C in Siluro-Devonian strata were not achieved until the Mesozoic time.

This re-evaluation of the Robb Lake deposit is a joint Geological Survey of Canada – British Columbia Geological Survey project, part of the Central Foreland Natmap Project. Its aims are: 1) to map the deposit area at a scale of 1:20,000, 2) to describe the surface showings and their host rocks and 3) to produce an absolute age by Rb-Sr methods on sphalerite (Christensen *et al.*, 1996). This paper summarizes the field work

PREVIOUS WORK

Lead-zinc mineralization was discovered near Robb Lake in 1971 by Arrow-Interamerican Corp., Barrier Reef Resources Ltd., and Ecstall Mining Ltd. This discovery sparked an exploration and staking rush in the northern Rocky Mountains of British Columbia that led to the discovery of numerous lead-zinc occurrences (Figure 1) and recognition of a potential new lead-zinc belt.

The geological resource at Robb Lake is quoted as 6.5 million tonnes at 7.11% combined lead and zinc, (2.4 metre mining width, 5% cut-off grade; Consolidated Barrier Reef Resources, Rights Offering Circular, November 29, 1984). Drilling between 1972 and 1975 led to the incomplete delineation of three prospective ore bodies, the “lower zone”, the East Webb ridge zone, and the West Webb ridge zone (Figure 2). Drilling was continued by Texasgulf in the summers of 1980 and 1981. Since then, no exploration work has been done. Core is stored at an airstrip at the confluence of Mississippi Creek and the Halfway River (Figure 2).

In 1959, Irish (1970) began reconnaissance mapping of the Halfway River map area, an area of the Canadian Rocky Mountains that is located between the Peace (lat. 56°00'N) and the Halfway (lat. 57°00'N) rivers. Four field seasons led to the first published geological map of the Halfway River area. This map was immediately used by mineral explorationists, who in the late summer of 1971 discovered lead-zinc mineralization at Robb Lake. This discovery sparked a staking and exploration rush that lasted until 1974. By that time, a host of new geological problems, requiring investigation at a more refined scale, needed attention, and R.I.

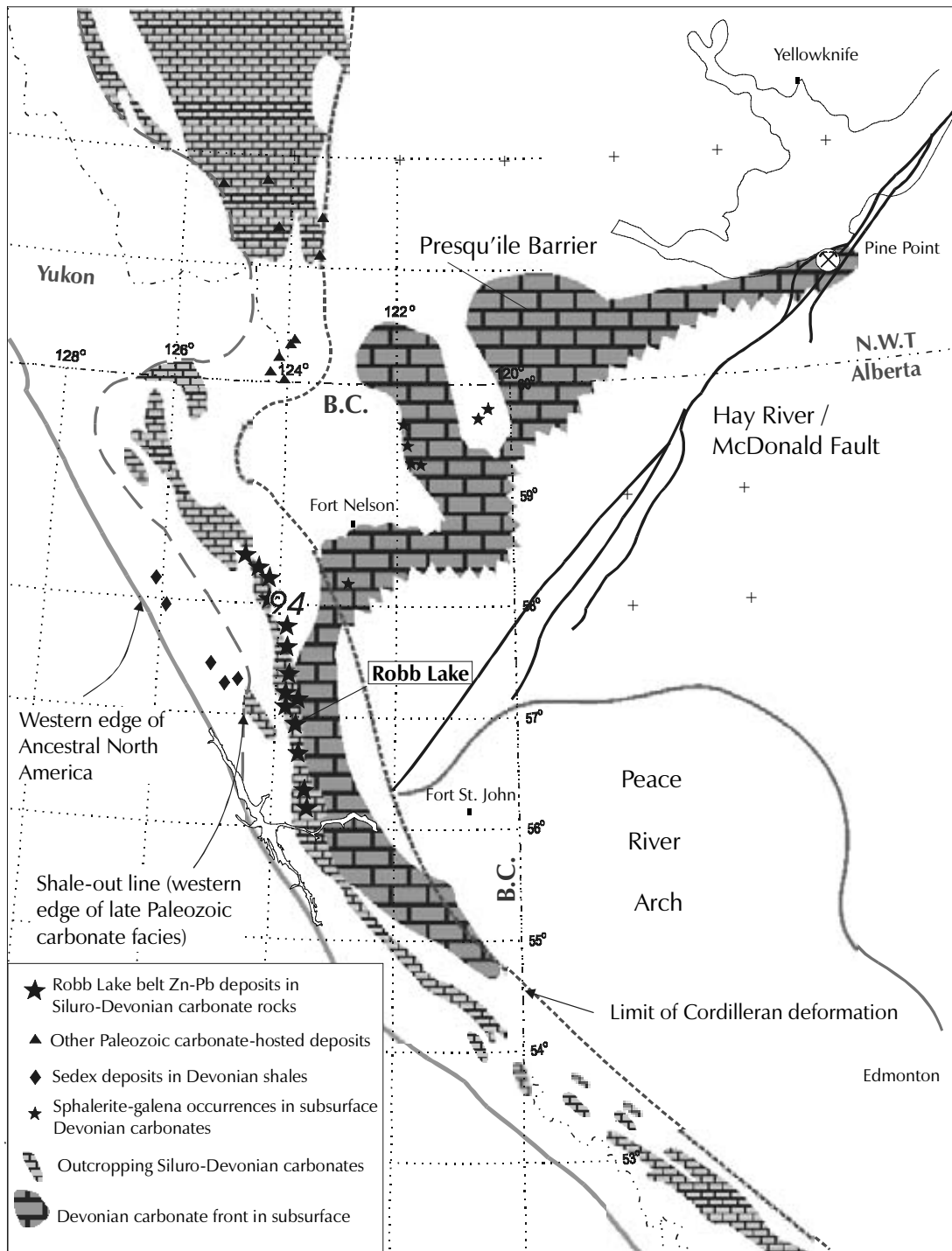


Figure 1. Location of Robb Lake and related deposits, and regional features of the North American continental margin in Siluro-Devonian time.

Thompson (1989) began mapping in 1975. Two theses were done in the course of the following years on specific geological problems. A. Taylor (1977) studied the carbonate stratigraphy and petrology, and suggested a peritidal environment for the sedimentary succession. He concluded

that the formation of breccias was due to intrastratal karst and that the mineralization occurred subsequent to brecciation from formation waters that issued from compacting shales. Manns (1981) studied the stratigraphic aspects of the Silurian-Devonian sequence hosting the

Robb Lake lead-zinc mineralization. He concluded that the host breccias were collapse structures due to solution of evaporite interbeds, and that mineralization resulted from migration of petroleum-bearing formation fluids into an evaporitic dolostone platform at an unknown time prior to the Laramide Orogeny. Sangster (1973, 1979), and Sangster and Lancaster (1976) favoured a paleokarst solution collapse origin, linked to an unconformities within and above the Siluro-Devonian carbonate sequence. Macqueen and Thompson (1978) rejected this hypothesis, and ascribed the breccias to hydraulic fracturing that resulted from compaction and dewatering of the shale basin to the west during Laramide deformation.

PROPERTY GEOLOGY

The Robb Lake Pb-Zn deposit is part of a belt of Mississippi Valley-type (MVT) deposits in the northern Rocky Mountains (Figure 1). The deposits are hosted by Silurian-Devonian platform dolostones that form part of the outcropping Paleozoic carbonate front (Thompson, 1989). In the subsurface, the Devonian carbonate front turns eastward to become the Presqu'île Barrier, which hosts the Pine Point lead-zinc deposit.

Most of the lead-zinc mineralization at Robb Lake occurs within the Muncho-McConnell Formation, although a few occurrences lie within a thin overlying sequence attributed to the Stone-Dunedin formations. As noted by Macqueen and Thompson (1978) and Thompson (1989), and documented in our detailed mapping (Figure 2), the deposit is located next to the tectonically telescoped shelf-slope facies boundary. The strata that host Robb Lake lie in the immediate footwall of a major thrust fault, which carries deep water early Paleozoic strata in its hanging wall.

The main stratigraphic units encountered in the Robb Lake area are described below, and their distribution is illustrated on Figures 2 and 3. They are divided into two disparate stratigraphic sequences, separated by the major thrust fault southwest of Mississippi Creek. Basinal units in the hanging wall of the fault include the Cambro-Ordovician Kechika Group, the Ordovician Skoki Formation, the Ordovician-

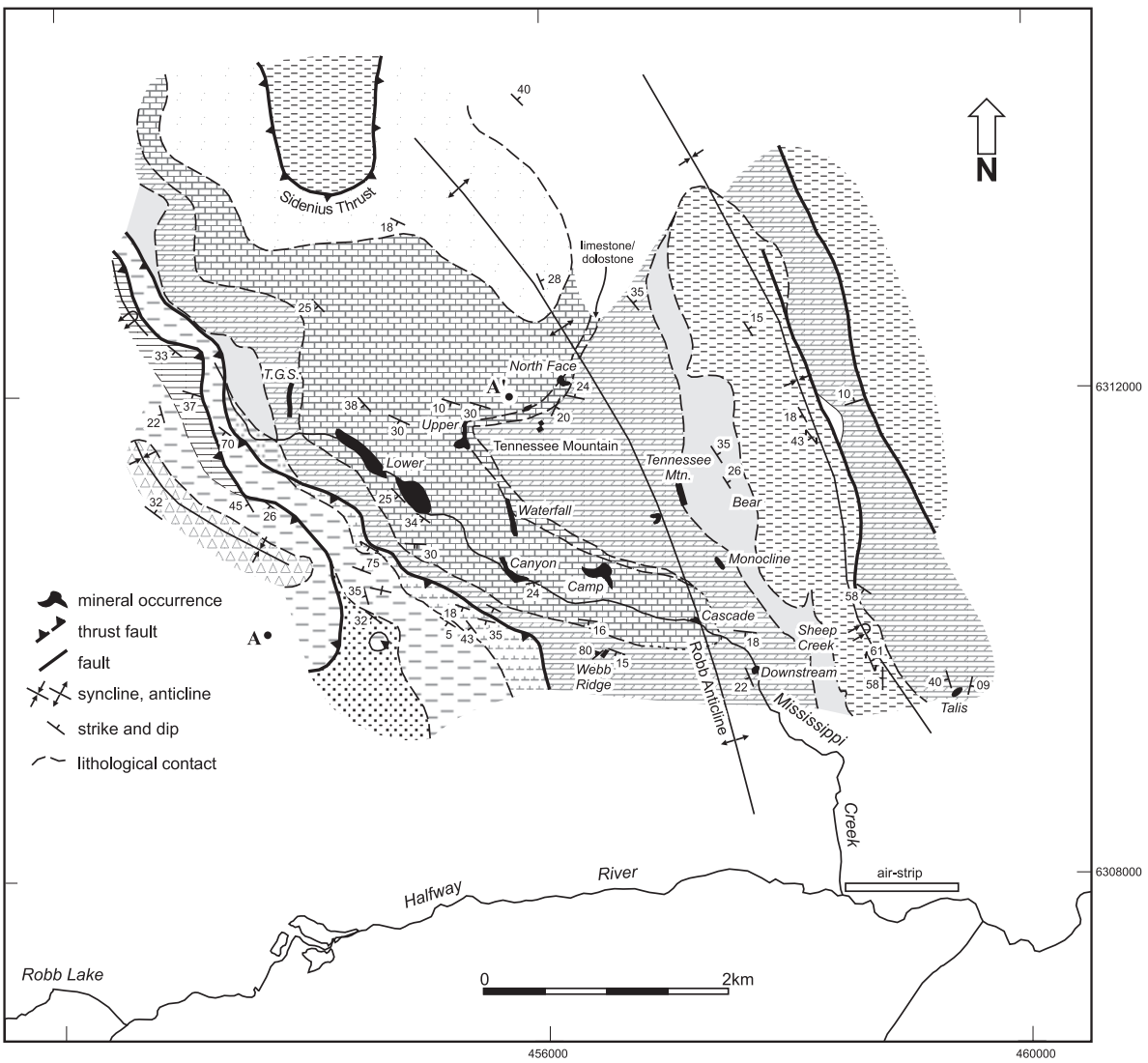
Silurian Road River Group, and unnamed Siluro-Devonian quartzite-dolomite and Silurian dolostone breccia units. Northeast of the fault a platformal succession includes the Silurian Nonda Formation, the Siluro-Devonian Muncho-McConnell Formation, very thin and mostly undivided Lower Devonian Stone and Middle Devonian Dunedin Formations, and Upper Devonian Besa River Formation.

Basinal Units

Kechika Group?

Strata here assigned to the Kechika Group are restricted to a single cliff and ridge top exposure in the immediate hanging wall of the major thrust fault southwest of Mississippi Creek. This sequence consists of medium to dark grey, orange-brown to olive weathered, calcareous shale and slate characterised by very distinct colour laminations in the millimetre to centimetre range. It is very well-cleaved, forming papery to slabby cleavage fragments. These rocks somewhat resemble the eastern facies of the Besa River Formation and were assigned to it by Thompson (1989); however we have assigned them to the Kechika Group based on a) their slaty, almost phyllitic character, which contrasts with the softer, muddier Besa River shales, b) their complete contrast with black Besa River siliceous argillites less than a kilometer along strike (Figure 2) and c) their contact with the underlying Muncho-McConnell Formation, which is non-outcropping and structurally discordant. If this contact is a thrust fault, then the complete absence of Stone/Dunedin strata along it is explained.

These strata are overlain directly by the Road River Group; the Skoki Formation, which outcrops in the overlying thrust sheet above the headwaters of Mississippi Creek, is missing. Since the Skoki Formation in northern Halfway River map area is over 600 metres thick, the assignment of these rocks to the Kechika Group poses a distasteful regional problem. They may belong to the upper part of the Beaverfoot Formation (A. Legun, personal communication 1998) or, in spite of the local contradictions that this engenders, to the Besa River Formation as previously mapped.



PLATFORMAL UNITS

Upper Devonian

- Besa River Formation
- Western facies: Black to dark grey siliceous argillite and shale, in part with silt laminae
- Eastern facies: Light brown to grey weathering, well laminated soft calcareous mudstone/siltstone

Lower to Middle Devonian

- Stone and Dunedin Formations, undivided
- Interbedded dark grey fossiliferous dolostone and light to medium grey non-fossiliferous dolostone

Silurian-Devonian

- Muncho-McConnell Formation
- Upper unit: Thick to medium bedded, light to medium grey dolostone that alternate with thin bedded dolostone
- Lower unit: Thick to medium bedded, light to medium grey dolostone. Limestone common near the top of unit, and fossiliferous beds present in the upper half of unit.

Silurian

- Nonda Formation
- Medium to dark grey fossiliferous dolostone

BASINAL UNITS

Silurian to Devonian

- Dolostone and quartzite

Silurian

- Dark grey dolostone breccia with secondary chert and fossil fragments

Ordovician to Silurian

- Road River Group
- Dark grey to black slate, calcareous slate; dark grey carbonaceous limestone; quartzite

Ordovician

- Skoki Formation
- Muddy, carbonaceous thick-bedded dolostone and thin-bedded, fossiliferous silty dolostone

Cambrian to Ordovician

- Kechika Group
- Laminated medium to dark grey, orange-brown to olive-weathering flaggy calcareous slate

Skoki Formation

The Skoki Formation, which outcrops on the southwest wall of the cirque that heads Mississippi Creek, is subdivided into two distinct units. The lower part of the Skoki is 70 metres of thickly bedded, cliff forming dolostone. It is light to medium grey, muddy and carbonaceous. The upper Skoki is a recessive unit of light brown to chalky orange weathering, light to medium grey, thinly bedded silty dolostone. Beds are up to 50 centimetres thick. This unit contains bivalves and abundant burrow structures; and one trilobite fossil was noted.

Road River Group

The Road River Group is dominated by sooty, non-fossiliferous flaggy slate and calcareous slate, and well cleaved, dark grey to black carbonaceous limestone. Less abundant are white quartzite, and beds several metres thick of highly fossiliferous, carbonaceous limestone that contain corals and brachiopods. Large carbonate concretions produce cleavage fragments the size of dinner plates. This highly heterogeneous section is typical of the Road River Group strata near shelf margins. It is overlain by unit SDdq in the lower of the two thrust sheets, and by the Silurian breccia in the upper one.

Siluro-Devonian dolostone and quartzite, unit SDdq

This unnamed unit lies in well-exposed stratigraphic contact above the Road River Group on the ridge southwest of Mississippi Creek. Its basal grey sandstone overlies black limy shale along a slightly undulating contact with a suggestion of load casting. The basal thick-bedded grey quartzite is overlain by light grey thick-bedded dolostone and quartzite. No fossils were seen. It is correlated with the Silurian-Devonian shelf dolostone-sandstone units farther northeast.

Silurian sedimentary breccia, unit Sbx

The Silurian breccia is a thin, cliff forming dolomite breccia that extends for 30 km from Lady Laurier Lake to Mt. Kenny, immediately west of Robb Lake (Thompson, 1989). The breccia overlies the Road River Group on ridge

tops at the headwaters of Mississippi Creek (Figure 2). Breccia beds consist of medium to dark grey, angular to subangular dolostone and black chert fragments in a grey dolomite cement. They also contain abundant and well-preserved fossil fragments of halysites, favosites, and colonial corals. The dolostone fragments exhibit grey-black colour laminations on the millimetre to centimetre scale. The breccia itself is bedded on the centimetre- to 10 metre-scale; sets of thin dolostone calcilutite and calcarenite and small-clast breccia alternate with thick units of unsorted, matrix-supported megabreccia.

According to Thompson (1989), the fragments are all derived from the Nonda Formation, and the unit is interpreted as a debris flow (or succession of debris flows) deposited on the foreslope of a Nonda reef.

Platformal Units

Nonda Formation

The Nonda Formation is a very distinctive medium grey to very dark grey weathering, fossiliferous dolostone. Fossils include crinoids, and the corals halycites and favosites. The alternating medium to dark grey coloured beds make the Nonda Formation unmistakable. Bedding thickness ranges from .15 to 2.0 metres. Locally fine calcareous laminations are observed. Chert nodules and silicified fossils are common throughout the unit.

The Nonda Formation exposed at Robb Lake forms the core of the Robb Anticline.

Muncho-McConnell Formation

The Muncho-McConnell Formation forms most of the high peaks adjacent to the mountain front (Thompson, 1989). It consists almost entirely of light grey weathering, resistant dolostone and sandy dolostone, except for few beds of dark grey micritic limestone. The Muncho-McConnell is over 400 metres thick in the Robb Lake area, and consists of fine-grained primary crystalline dolomite that formed largely in a low energy, high salinity lagoonal, intertidal and supratidal environment. Because of its completeness, and uniform fine grain size, the "regional" dolomitization is probably early diagenetic.

Although the Muncho-McConnell is generally unfossiliferous, large brachiopods (average 5 to 10 cm long) are prominent within some exposures along Mississippi Creek, and gastropods, amphiporids, stromatolites, fragments of bivalves, and other unidentified fossils have also been noted (Manns, 1981). Taylor (1977) links the presence of fossils within the Muncho-McConnell near Robb Lake to the proximity of the Silurian-Devonian facies front.

In the vicinity of the Robb Lake deposit, the Muncho-McConnell Formation can be subdivided into upper and lower units based on bedding thickness, and outcrop and bedding characters. The lower unit (SDM1) is a massive, cliff forming unit that has thick and subtly defined bedding, and is locally blocky in character. By contrast, the upper unit (SDMu) has well defined bedding with locally distinct very fine carbonaceous laminations.

The lower unit (SDM1) is a light to medium grey, thickly bedded dolostone approximately 250 metres thick. Sedimentary textures include abundant fenestrae, less common algal laminations and rare, thin intervals that show current laminations and rip-up clast breccias. A 10-15 metre thick sandstone unit, which marks the base of the lower unit, may be equivalent to a regional sandstone marker unit (Legun, this volume). Beds of silty dolostone, sandy dolostone, and shale are interspersed with the dolostone. A marker bed, known as the "angular sand marker" (ASM), occurs within the dolostone sequence about 110 metres below the top of the unit. According to Manns (1981), this marker is present in all drill holes but is rarely seen in surface rocks. It corresponds to a local disconformity. The general character of the lower Muncho McConnell Formation is consistent with a sabkha environment, as noted by Manns (1981).

The uppermost 30 to 50 metres of the lower unit are particularly thick-bedded and often form major cliffs. On Tennessee Mountain (i.e., near the North Face and Camp showings), parts of this upper section consists of thick-bedded to massive limestone pods that pass laterally and vertically into the typical thick dolostone beds. It is overlain by dark, thin-bedded, muddy dolostone of the upper unit. This unit is important to the Robb Lake deposit in that the stratabound-style showings on Tennessee Mountain are all located immediately below it (Figure 2).

The upper unit (SDMu) is a 200 metre thick, light to medium grey dolostone with well defined bedding and distinct carbonaceous current laminations. The rhythmic sequence of the upper unit is better developed than in the lower unit, and the thin bedded dolostone intervals are more extensive, giving outcrops a terraced appearance that contrasts with the cliffier lower unit. The basal sequence (0-25 m) of SDMu is composed of thick laminated dark grey silty dolomite mudstone with local sand concentrations (Manns, 1981). A marker bed known as the "pale sand marker" (PSM), 1-2 m thick, was identified in drill holes in Webb Ridge (Manns, 1981). The "TGS Breccia" (Manns 1981) is the lowermost unit of SDM2 on the eastern end of Texas Ridge. This breccia unit is over 20 meters thick. In it, large, subangular to subrounded clasts up to several metres across are surrounded by a matrix of fine dolomite mudstone. They show a diversity of colours and bedding characteristics: within the limited lithologic variation of local sources, this is a polymictic breccia. A series of large limestone clasts, probably fragments of a single disrupted bed, occurs along its base. Higher in the breccia, beds of fine-grained, thin-bedded dolostone drape over large breccia clasts. We interpret this unit as a synsedimentary slump deposit.

In unit SDMu, thicker, algal laminated beds alternate with thin, strongly current-laminated intervals. The latter may contain rip-up clast breccias, or current cross-laminae. Fenestrae are common, particularly near the tops of the algal-laminated beds. Mudcracks were observed in talus. These features indicate a sabkha environment affected by periodic strong wave action.

Taylor (1977) and Manns (1981) interpreted the top of the lower unit and at the top of the upper unit as disconformable. Evidence for significant erosion surfaces includes the presence of sand markers (ASM and PSM), scour surfaces, soft sediment deformation features, and local breccias such as the TGS.

Stone/Dunedin formations

The Lower to Middle Devonian Stone and Dunedin formations could not be distinguished in the Robb Lake area, so they are described together in this section. They consist of interbedded medium dark grey fossiliferous, partly cal-

careous, dolostone and light to medium grey buff weathering fossiliferous and non-fossiliferous dolostone. Some fossiliferous limestone occurs as a black (reef-front ?) breccia. Fossils include brachiopods, gastropods, crinoids, rugosa and colonial corals, and local crinoid wackestone.

This unit is thin and discontinuous (Figure 2). It is nowhere capped by a single thick dark grey fossiliferous carbonate unit assignable to the Dunedin Formation. Nevertheless it may be partly time-equivalent to the Dunedin. The position of Robb Lake next to the interpreted carbonate shelf margin may explain the anomalously thin Lower to Middle Devonian section.

Besa River Formation

The Besa River Formation outcrops in three areas: in the core of a syncline east of the main showing area, in the footwall of the Sidenius thrust fault in the core of the Robb Anticline, and in a narrow band in the immediate footwall of the major thrust fault exposed in the headwaters of Mississippi Creek (Figure 2). In its eastern exposures, the Besa River Formation consists of soft brown/grey weathering, finely laminated dark grey to black calcareous to noncalcareous argillite/shale and siltstone.

The western facies of the Besa River Formation includes dark grey to black, siliceous argillite and shale with silt laminae. In outcrop, the thrust fault is a zone of strong shearing that truncates bedding and cleavage in both the underlying black Besa River argillites and the overlying calcareous, carbonaceous shales of the Road River Group.

Mineralization

The Robb Lake deposit consists of numerous stratabound and cross-cutting lead-zinc showings hosted by the Muncho-McConnell Formation, and a few occurrences in the overlying Stone-Dunedin formations. Most of the showings occur along the valley of Mississippi Creek and adjacent mountain slopes (Fig. 2). Mineralization at Robb Lake takes two forms: mineralized breccias, and veins/vein stockworks. Breccia mineralization is by far the most important. The breccias are interconnected, bedding-parallel and/or crosscutting bodies in as much as 200 metres of stratigraphic section (Fig. 3). Not all the breccias are mineralized. The favorable mineralized sections form a broad stratabound zone occupying the upper 200 metres of the lower unit of the Muncho-McConnell Formation and the lower 130 metres of upper unit; a 70 metre thick, barren section separates the mineralized zones (Boronowski and James, 1982).

The mineralized zones have a northwesterly elongation and alignment, parallel to the strike direction and to the structural and paleofacies features. The breccia bodies form relatively thin and narrow horizons and pods that are both parallel to and crosscut bedding (Figs. 2, 3). The largest of these bodies may extend for more than 300 metres along bedding or crosscut more than 50 metres of section. The base of the upper cliff-forming unit exerted a strong control on the location of the main stratiform breccia bodies, as is illustrated on the cross-section of the valley of Mississippi Creek (Fig. 4). This cross section shows that the south slope of Tennessee Mountain is more or less a dip slope, and the

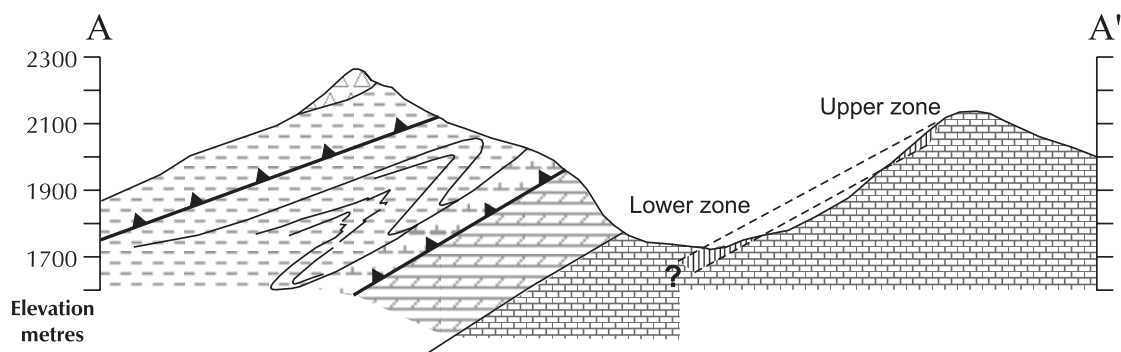


Figure 3. Cross-section A-A' of the Mississippi Creek valley, looking northwest. Shows that, assuming an average bedding dip of 30°, the upper and lower mineralized zone are at the same stratigraphic level. For legend and location of section see Figure 2.

showings along the creek, such as the Lower, Canyon, and Cascade zones, are stratigraphically equivalent to those on the south side of Tennessee Mountain (the Upper, Waterfall, and Camp zones, and also the North Face zone). In the East and West Webb zones on Webb Ridge, drilling has outlined up to four major mineralized horizons and numerous isolated pods in the lower and upper units of the Muncho-McConnell Formation. They are stacked and may be connected at different levels laterally and vertically (Boronowski and James, 1982).

A broad mineral zonation has been recognized in the distribution of the sulphides and other minerals at Robb Lake. The sphalerite/galena ratio decreases stratigraphically upward, with approximate ratios of zinc to lead of 7:1 at the Lower showing, 1.5:1 at the West Webb showing, and 4.5:1 at the East Webb showing (Manns, 1981). The best overall grade mineralization, intersected in hole 113-82, was 15.02% Pb+Zn over 3 metres, with a Zn:Pb ratio of 2:1: this was predominantly associated with the pyrobitumen- and carbonaceous-rich matrix of the rock-matrix ("trash") breccias (Boronowski and James, 1982).

Characteristics and morphology of the breccias

The breccias at Robb Lake have long been a focus of study (Sangster, 1973, MacQueen and Thompson 1978, Manns, 1981), although not a topic of consensus. There are a number of breccia types within the Muncho McConnell Formation of primary and of secondary origin; some are unrelated and some intimately related to sulphide mineralization. The most important ones with regard to the mineralization are the sparry dolomite-cemented crackle, mosaic and rubble breccias, and the rock-matrix ("trash") breccias. The following classification is texturally based.

Dolostone-chip breccias associated with current-laminated beds in SDM2. These thin layers, generally less than 10 centimetres thick, contain thin bedding fragments of dolostone roughly imbricated or stacked in a fine dolostone mud matrix. Their occurrence suggests that they are of syndepositional origin. No mineralization is associated with them.

Dolostone-matrix breccias in SDMI and SDM2, including TGS Breccia. In these breccia

layers, sparse to abundant, generally subangular clasts of dolostone contrast in color with their dolostone matrix. The matrix lacks internal bedding, except rarely within the TGS breccia. Breccias may be either monomict or polymict; in any case the clasts are all assignable to the Muncho McConnell Formation. A syndepositional origin is reasonable based on their character and occurrence. In a few cases - the TGS breccia and at the upper end of the North Face showing - mineralization is associated with these breccias.

Crackle and mosaic breccias. These terms represent end members of a continuum. The crackle breccias show little displacement of the fragments in coarse-grained sparry white dolomite cement (Fig. 5A). The fragments consist exclusively of highly angular clasts of the variably altered crosscut dolostone host-rock. The mosaic breccias have fragments that are largely but not wholly displaced (Fig. 5B). The fragments also consist of highly angular clasts of the dolostone host-rock in a coarse-grained sparry white dolomite cement. Generally, mosaic breccias grade out through crackle breccias into unfractured dolostone. It is notable that in these breccias, individual clasts tend to be of somewhat uniform size, typically 5 to 20 centimetres across; although the fragments can range in size from one millimetre to several metres in longest dimension. Megabreccias of this type are rare. A substantial portion of the mineralization at Robb Lake occurs within the dolomite cement of the mosaic and crackle breccias.

Rubble breccias. In contrast with the crackle and mosaic breccias, the rubble breccias are polymictic, and the fragments are completely displaced, showing no match with each other. By textural definition, this category includes the rock-matrix ("trash") breccias, which are rubble breccias with fragmental matrix instead of dolomite cement. The rubble breccias are by far the most volumetrically important types of breccias and the most varied. They contain a variety of clasts that are included in a fine-grained dark grey fragmental matrix or in white sparry dolomite cement or in a mix of both. The breccias are generally grain-supported and locally matrix-supported. The fragments consist of a variety of altered and unaltered dolostone (90 volume per cent), white sparry dolomite

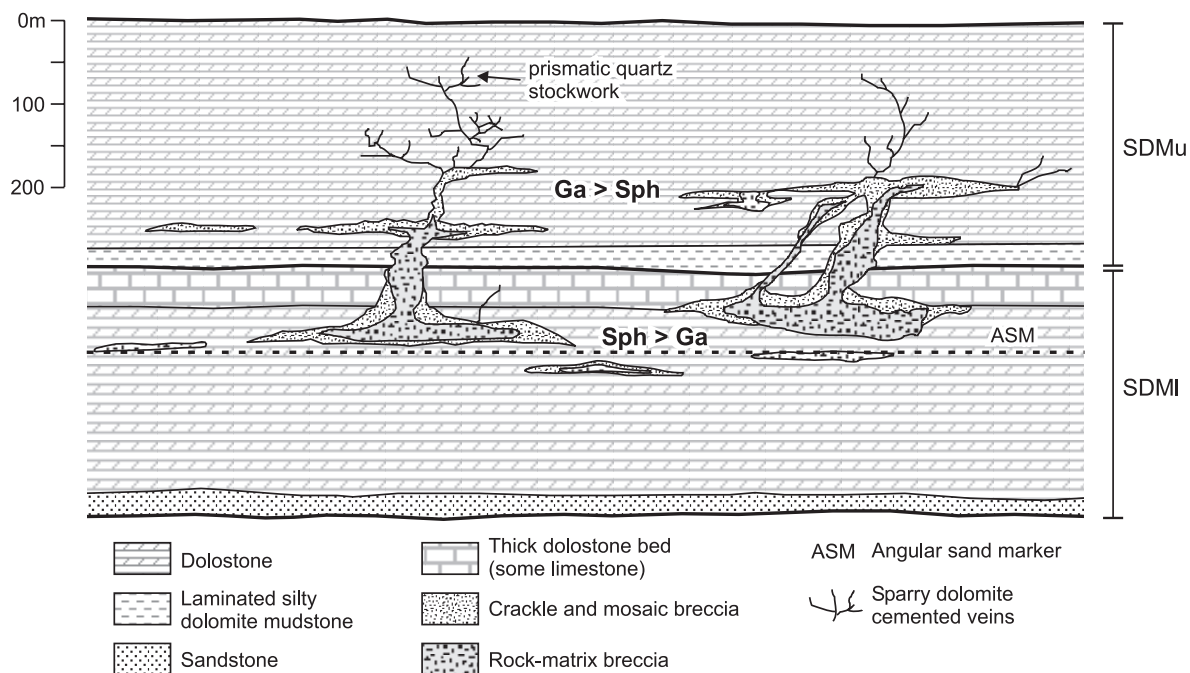


Figure 4. Textural and mineralogical zoning in the Robb Lake system.

(i.e., subangular fragments and thin curvilinear segments of vein selvages; 5 volume per cent), shale/mudstone (2 volume per cent), finely laminated shaly carbonate (1 volume per cent), chert (1 volume per cent), pyrobitumen-rich material (<1 volume per cent); sulphides (<1 volume per cent), individual rounded sand grains with overgrowths (<1 volume per cent), and fossils (brachiopods and gastropods; <1 volume per cent). The fragments are highly angular to subangular and vary in size from less than one millimetre to several metres. Most breccias are dominated by fragments less than 10 centimetres in diameter. The matrix of the “trash” breccias is a dark grey to black carbonaceous dolostone. On close inspection, this matrix is composed of fine fragments, cemented by overgrowths and interstitial dolospar and quartz. Some of the fine fragments are possibly pyrobituminous shale, however much of the dark colour of the matrix can be accounted for by the dark to medium grey dolostone fragments, occasional shale fragments, and the fine disseminated sulphides. The sulphides, sphalerite, galena and pyrite, are concentrated in the matrix as individual grains and clusters, and as fracture filling material.

In terms of relative paragenesis, the rock-matrix (“trash”) breccias crosscut the dolomite-cemented mosaic and crackle breccias; but con-

versely the dolomite cement of the crackle and mosaic breccias enclose fragments of the rock-matrix (“trash”) breccia, and dolomite veins crosscut the “trash breccia”. We interpret these apparently conflicting temporal relationships to mean that the breccias originated as an overlapping, multi-episodic sequence of events prior to and during mineralization. The incorporation of sulphide clasts in the rock-matrix (“trash”) breccias is evidence that brecciation and mineralization were at least in part contemporaneous.

Figure 4 depicts the spatial relationships between the different classes of mineralized breccias. The rock-matrix (“trash”) breccias with combined zinc-lead grades in the order of 6% (Boronowski and James, 1982) are preferentially located within the upper half of lower unit of the Muncho-McConnell. Some of these breccias are also found in the upper unit but they rarely achieve ore grade mineralization. In general, the rock-matrix (“trash”) breccias occur at the base of the breccia bodies and are overlain and fringed by the rubble, mosaic, and crackle breccias that are cemented by white sparry dolomite. Also, in the overall system, the rock-matrix (“trash”) breccias tend to be located within the lower unit, whereas the dolomite-cemented rubble, mosaic and crackle breccias tend to overlie the “trash” breccias and are more abundant in the upper unit.

Mineralogy, textural relationships, and mineralogical zonation

Sphalerite, galena, and pyrite are the main sulphide minerals; marcasite has been observed in thin sections by Taylor (1977), and Manns (1981). Sphalerite is pale yellow, dark orange, red, or brown. It occurs as fine to coarse single or aggregates of anhedral crystals (1 mm to 1 cm) in white sparry dolomite cement of the crackle, mosaic, and rubble breccia, and in the fine-grained carbonaceous dolostone matrix of the rock-matrix (“trash”) breccia. Anhedral crystals or aggregates of crystals of sphalerite occur as rims on one or several sides of the angular dolostone fragments, or as scattered crystals within the white sparry dolomite cement. According to Manns (1981), geopetal sphalerite (i.e., “snow on the roof” texture) is abundant at Robb Lake, but in our observations on the various showings, sphalerite was also seen to coat indifferently any or every side of fragments. “Snow-on-the-roof” is only well-developed in surface showings within the TGS breccia, where mosaic breccias cross-cut the original synsedimentary breccia. Sphalerite crystals and aggregates range from less than 1mm to 1.5 cm. Very fine-grained sphalerite (i.e., < 1mm) is only present in the matrix of the rock-matrix breccia. Sphalerite crystals are usually anhedral and are commonly fractured. Colloform sphalerite has been reported at the Waterfall showing (locality 3; Fig. 2) (Macqueen and Thompson, 1978; Manns, 1981).

Overall, galena is less abundant than sphalerite and pyrite. It commonly occurs as euhedral crystals (< 1cm to 2 cm) and less commonly as anhedral aggregates in the white sparry dolomite cement of the rubble, mosaic, and crackle breccias, and in the carbonaceous dolomite matrix of the rock-matrix (“trash”) breccia. Galena also occurs as fracture-filling, without sphalerite or quartz. Sangster and Carrière (1991) observed galena veinlets crosscutting sphalerite crystals, and grains of sphalerite completely enclosed by galena. In showings located in the lower sequence of the Muncho-McConnell (SDMI), galena is typically associated with sphalerite, and may have co-precipitated or precipitated slightly later. In the upper sequence (SDMu), galena often occurs by itself, as euhedral and anhedral crystals disseminated in the white spar-

ry dolomite, and in one instance filling fractures in sparry dolomite. It is also commonly associated with quartz. When quartz is present and associated with galena, it occurs as fractures cutting galena or as inclusions in galena (Sangster and Carrière, 1991).

Pyrite and marcasite occur as disseminated fine-grained euhedral to subhedral crystals and aggregates in the rock-matrix (“trash”) breccia, and as massive aggregates of fine-grained pyrite along stylolites and bedding planes, and as fracture fillings. Irregular pyrite veins cut the breccia at the “Lower zone”.

Pyrobitumen commonly occurs within the various breccias where it fills small cavities, and fractures. It locally forms a component of the rock-matrix breccia, giving the dark grey colour to its matrix.

Besides zoning stratigraphically upwards from stratabound to cross-cutting style of mineralization, the Robb Lake system exhibits mineralogical zonation (Figure 4). Sphalerite, the dominant sulphide mineral, is most abundant within breccias in the stratabound showings. Both locally and in the system as a whole, the galena-sphalerite ratio appears to increase upwards and outwards. On the scale of metres at the North Face showing, sphalerite-rich rock matrix (“trash”) breccia passes outwards into mosaic breccia cemented by sparry dolomite and galena. Regional zoning is demonstrated at one of the stratigraphically highest showings, the Bear, located within the Stone Formation high on the southeast ridge of Tennessee Mountain. There, sphalerite is insignificant, and large galena clumps in sparry dolomite veins pass outwards into drusy, crystalline quartz. Crystalline quartz appears to be the most distal expression of the Robb Lake system, occurring in veins and voids throughout the upper part of the Muncho McConnell Formation.

Alteration

Megascopically, three distinct phases of dolomitization affected the carbonate rocks in the Robb Lake area. An early phase consists of a light grey weathering, medium and dark grey replacement dolostone composed of fine-grained crystalline dolomite. This dolomite dominates the sequence regionally and is considered to be the result of very early diagenetic alteration of

primary calcite. A texturally later, coarse sparry and prismatic white to grey dolomite coats some dolostone fragments and is associated with zebra texture. Zebra dolomite, a common feature of carbonate rocks associated with MVT deposits, is well displayed at the Robb Lake deposit. It consists of thin dolostone layers (mm to cm scale) identical to, and connecting with, the surrounding homogeneous dolostone, but separated from each other by coarse sparry and prismatic white dolomite layers (mm to cm scale) or, in some cases, by voids of the same shape as the white layers, or by pyrobitumen, or by a combination of the three. The layering is either oriented parallel to bedding or in herringbone patterns that resemble cross bedding, the template for which is cryptic. It never extends continuously either vertically or laterally for more than 50 cm. Zebra texture affects all the dolostone units of the Robb Lake area, and fragments of the zebra texture are incorporated in the mineralized breccias. It forms broad altered selvages to vein-type mineralization, for instance around the showing on Webb Ridge. The third phase of secondary dolomite in the Robb Lake area is a white sparry dolomite that forms the cement of the breccias, and fills the joints, fractures, vugs, and primary porosity such as fenestrae and fossil interiors.

With the help of cathodoluminescence petrography, Manns (1981) was able to distinguish four generations of dolomite: (1) fine-grained inert dolomite forming the regional host-rock dolostone, (2) inert coarse white sparry and prismatic dolomite lining cavities, coating dolostone fragments in breccias, and associated with the zebra texture, (3) luminescent dolomite forming the cement of the mineralized breccias and associated with sphalerite, galena, pyrite, and local pyrobitumen, and (4) inert dolomite filling the central portions of large cavities.

Accompanying laboratory studies

A total of 10 samples from various lead-zinc showings of the Robb Lake area were submitted to the University of Michigan for Rb-Sr dating of sphalerite. Rb-Sr dating of the Robb Lake mineralization, if successful, will provide an absolute age on the mineralization and a constraint on the geochronology of ancient crustal fluid flow in the Presqu'île Barrier.

Until recently, radiometric geochronology

has been of little use in evaluating models for the formation of MVT deposits because of lack of alternative minerals that are amenable to dating by conventional isotopic methods (Halliday *et al.*, 1990). Over the past years, a handful of apparently robust radiometric ages for carbonate-hosted Pb-Zn deposits have become available. Rb/Sr dating of sphalerite is a technique that provides a direct age for the primary sulphides and consequently has a direct impact to the understanding of causes and effects of fluid migration in relation to basin evolution and tectonic events. This technique has been successfully used to date other MVT deposits, such as Pine Point (Nakai *et al.*, 1993), Polariss (Christensen *et al.*, 1995b), Blendevale in Australia (Christensen *et al.*, 1994, 1995a), and deposits in East Tennessee (Nakai *et al.*, 1990, 1993) and Upper Mississippi Valley (Brannon *et al.*, 1992). However Rb/Sr methods have not always been successful in dating certain MVT deposits, primarily because the low Rb content of sphalerite poses a sometimes unsurmountable analytical/interpretational challenge. The theory, methods, success, and pitfalls of the technique are explained in Christensen *et al.* (1996).

DISCUSSION

Brecciation and open-space filling are very important processes in the formation of Robb Lake as in most Mississippi Valley-type deposits. Temporal and genetic relationships between brecciation and mineralization at Robb Lake are controversial. Are the breccias that host mineralization the result of wall-rock dissolution by Mississippi Valley-type mineralizing brines or were they formed by other, earlier fluids, possibly related to regional weathering and karstification, which created an extensive paleoaquifer system for later MVT brines (Sangster, 1988)? Did alteration and dissolution of carbonate wall rock in the breccias cause ore deposition at Robb Lake? These questions largely remain unanswered at Robb Lake, as indeed at other MVT deposits around the world.

In some MVT districts, it is documented that solution of carbonate by ore-related brines has allowed collapse and brecciation of the overlying beds, and that gravity was an important force in the shattering. However, the fine median size and high degree of angularity of the fragments

within the trash breccias and of the breccia bodies at Robb Lake suggest that other forces such as hydraulic fracturing may have supplemented simple collapse. Although like other MVT deposits, Robb Lake is intimately associated with carbonate breccias, a number of key textures that in other cases have clearly linked brecciation to karsting and solution collapse are not observed in the deposit. These include intrakarst sediments, sagging of overlying strata, and open-space sulphide textures such as stalactites and sulphide-carbonate laminites. On the contrary, mineralization is intimately associated with brecciation, particularly with the synmineral trash breccias, both in time and in space.

One possible explanation for the textural differences between Robb Lake and, for instance, Pine Point, is that the Robb Lake deposit formed from fluids under higher confining pressure, with hydrostatic and lithostatic pressure equivalent, whereas Pine Point formed in a near-surface environment in which significant open spaces were maintained over time.

Questions that we will try to resolve in the future with respect to the Robb Lake deposit include the following:

The age of mineralization is unknown and could be as old as late Devonian (equivalent to Pine Point deposit) or as young as Cretaceous or even younger. It is hoped that the proposed Rb-Sr sphalerite study will illuminate this issue.

How did the rock-matrix ("trash") breccias form? How does solution collapse promote the fine clast size and highly angular clast shapes seen in these; and by what collapse mechanism are entire vein selvages detached? On the other hand, what other mechanism of brecciation could be operative in the context of relatively cool brines (87° to 154°C with a mean of 119°C; Sangster and Carrière, 1991)?

Why do the mineralized and unmineralized breccias preferentially favor a stratigraphic interval, the base of the upper thick unit, which is otherwise lithologically indistinguishable from others in the Muncho-McConnell Formation?

Are the deposits of the Robb Lake belt, Pb-Zn mineralization in the subsurface Presqu'île Barrier and Pine Point cogenetic, the result of a single eastward "flush" of MVT brines; or are they polygenetic? Are the MVT deposits of the Robb Lake belt genetically related to the SEDEX deposits of the Kechika Trough?

ACKNOWLEDGMENTS

The authors are very grateful to D.J. Robertson and J.M. Der Weduwen of Falconbridge Ltd. for lively exchange of ideas, and for providing access to property and data. We are grateful to Amy Thibeault for her assistance in the field. Drafting was done by Richard Franklin. R.I. Thompson, A. Legun and W. J. McMillan reviewed the manuscript.

REFERENCES

- Brannon, J.C., Podosek, F.A., and McLimans, R.K. (1992): A Permian Rb-Sr age for sphalerite from the Upper Mississippi zinc-lead district, Wisconsin; *Nature*, Volume 356, pages 509-511.
- Christensen, J.N., Halliday, A.N., and Kesler, S.E. (1996): Rb-Sr dating of sphalerite and the ages of Mississippi-Valley-type Pb-Zn deposits; *Society of Economic Geologists*, Special Publication No. 4, pages 527-535.
- Christensen, J.N., Halliday, A.N., Vearncombe, J., and Kesler, S.E. (1995a): Testing models of large-scale crustal fluid flow using direct dating of sulfides: Rb-Sr evidence for early dewatering and formation of MVT deposits, Canning Basin, Australia; *Economic Geology*, Volume 90, pages 877-884.
- Christensen, J.N., Halliday, A.N., Kesler, S.E., Liegh, K.E., and Randell, R.N. (1995b): Direct dating of sulphides by Rb-Sr - a critical test using the Polaris Mississippi Valley-type Zn-Pb deposit; *Geochimica et Cosmochimica Acta*, Volume 59, pages 5191-5197.
- Christensen, J.N., Halliday, A.N., Kesler, S.E., and Vearncombe, J. (1994): Age of MVT mineralization in the Canning Basin, Australia: Rb-Sr analysis of sphalerite from the Blendevale deposit; *Geological Society of America*, Abstracts with Programs, Volume 26, pages A381.
- Halliday, A.N., Ohr, M., Mezger, K., Chesley, J.T., Nakai, S., and DeWolf, C.P. (1990): Recent developments in dating ancient crustal fluid flow; *Reviews of Geophysics*, Volume 29, pages 577-584.
- Haynes, S.J. (1979): Carbonate-hosted lead-zinc occurrences in northeastern British Columbia with emphasis on the Robb Lake deposits: Discussion; *Canadian Journal of Earth Sciences*, Volume 16, pages 1641-1642.

- Legun, A. (1998): Geology of the Mt. McCusker area, northeastern British Columbia (94G/4W); in Geological Fieldwork 1998, *B.C. Ministry of Energy and Mines*, Paper 1999-1, this volume.
- Macqueen, R.W. and Thompson, R.I. (1978): Carbonate-hosted lead zinc occurrences in northeastern British Columbia with emphasis on the Robb Lake deposit; *Canadian Journal of Earth Sciences*, Volume 15, pages 1737-1762.
- Macqueen, R.W. and Thompson, R.I. (1979a): Carbonate-hosted lead zinc occurrences in northeastern British Columbia with emphasis on the Robb Lake deposit: Reply; *Canadian Journal of Earth Sciences*, Volume 16, pages 1634-1644.
- Macqueen, R.W. and Thompson, R.I. (1979b): Carbonate-hosted lead zinc occurrences in northeastern British Columbia with emphasis on the Robb Lake deposit: Reply; *Canadian Journal of Earth Sciences*, Volume 16, pages 2067-2068.
- Manns, F.T. (1981): Stratigraphic aspects of the Silurian-Devonian sequence hosting zinc and lead mineralization near Robb Lake, northeastern British Columbia; unpublished Ph.D. thesis, *University of Toronto*, Ontario, 252 pages.
- Nakai, S, Halliday, A.N., Kesler, S.E., Jones, H.D., Kyle, J.R., and Lane, T.E. (1993): Rb-Sr dating of sphalerites from Mississippi Valley-type (MVT) ore deposits; *Geochimica et Cosmochimica Acta*, 57, pages 417-427.
- Sangster, D.F. (1973): Geology of Canadian lead and zinc deposits; *Geological Survey of Canada*, Paper 73-1, Part A, pages 129-130.
- Sangster, D.F. (1979): Carbonate-hosted lead zinc occurrences in northeastern British Columbia with emphasis on the Robb Lake deposit: Discussion; *Canadian Journal of Earth Sciences*, Volume 16, pages 2063-2066.
- Sangster, D.F. and Lancaster, R.D. (1976): Geology of Canadian lead and zinc deposits; *Geological Survey of Canada*, Paper, 76-1A, pages 301-310.
- Sangster, D.F. and Carrière, J.J. (1991): Preliminary studies of fluid inclusions in sphalerite from the Robb Lake Mississippi Valley-type deposit, British Columbia; in *Current Research, Part E*; *Geological Survey of Canada*, Paper 91-1E, pages 25-32.
- Taylor, A.H. (1977): Carbonate stratigraphy and petrology: Robb Lake zinc-lead property, northeastern British Columbia; unpublished M.Sc. thesis, *Carleton University*, Ottawa, Ontario.
- Thompson, R.I. (1974): Geology of the Robb Lake property; *B.C. Department of Mines and Petroleum Resources*, Annual Report 1972, pages 463-467.
- Thompson, R.I. (1989): Stratigraphy, tectonic evolution and structural analysis of the Halfway River map area (94B), northern Rocky Mountains, British Columbia; *Geological Survey of Canada*, Memoir 425, 119 pages.



GEOLOGICAL SETTING OF THE KEMESS SOUTH AU-CU PORPHYRY DEPOSIT AND LOCAL GEOLOGY BETWEEN KEMESS CREEK AND BICKNELL LAKE (NTS 94E/2)

By Chris Rogers¹, and Jacques Houle²

KEYWORDS: Kemess South deposit, Early Jurassic, Maple Leaf pluton, gold-copper porphyry, Asitka Group, Takla Group, Toadogone Formation.

ships to, or controls on distribution of ore; to characterize the alteration and zoning; and to define mineral zoning in both the hypogene and supergene ore zones.

INTRODUCTION

The Kemess South gold-copper porphyry deposit is British Columbia's newest mine. With reserves of 170 thousand kilograms of gold and 441 million kilograms of copper, it is projected to be in production for sixteen years (Royal Oak Mines Inc., 1996). The deposit, discovered in 1983, is owned by Royal Oak Mines Inc. Production began from an open pit on May 19, 1998 and the first shipment of gold-copper concentrate was on June 23, 1998. The daily production in October, 1998 was 76 thousand tonnes of combined waste rock and ore per day.

During June and July of 1998 a detailed geological study of the Kemess South deposit and adjacent region was conducted by the principal author with the support of the B.C. Geological Survey Branch and Royal Oak Mines Inc. This study is part of a Master of Science thesis at the Ottawa-Carleton Geoscience Centre. The underlying purpose of this study is to determine the geological setting and genesis of the Kemess South gold-copper porphyry deposit. This objective will be approached as follows:

- ♦ Conduct detailed mapping at 1:10,000 scale in order to determine local stratigraphy and structure and their relationship to geology within the orebody;
- ♦ Study the orebody to identify important geological features: to determine their relation-

In addition, study of the Kemess deposit and surrounding prospects and geology will establish it as a representative example for comparison and evaluation of other potential porphyry-related intrusions in the region.

The study area covers 36 km² and is bounded to the south and west by the Omineca Mining Access Road, to the north by a major valley that connects Kemess and Duncan lakes and to the east by Kemess Creek (Figure 1). It is located on the western margin of the Swannell Ranges, an area characterized by gentle mountainous terrain and wide valleys that range in elevation from about 1200 to 1800 metres. The area is covered for the most part by trees, and swampy ground characterizes lower elevations. Rock exposures are scarce, comprising less than 5% of the study area. With recent development of the open pit at Kemess South, new exposures of the orebody provide an excellent opportunity to map internal and external stratigraphic and structural relationships.

The field program involved mapping both regionally and within the open pit and re-logging of selected drill core from the deposit to augment the surface work. This report presents only the results of mapping in and adjacent to the Kemess South orebody. This mapping will be incorporated with regional 1:20,000 scale mapping that has been ongoing for several seasons (Diakow and Metcalfe 1997; and Diakow and Rogers 1998), and is scheduled for publication at 1:50,000 scale.

¹ Ottawa-Carleton Geoscience Centre, Carleton University, 1125 Colonel By Drive, Ottawa, Ontario, K1S 5B6

² Royal Oak Mines Inc., Exploration Division, #9-3167 Tatlow Rd., Smithers, B.C., V0J 2N0

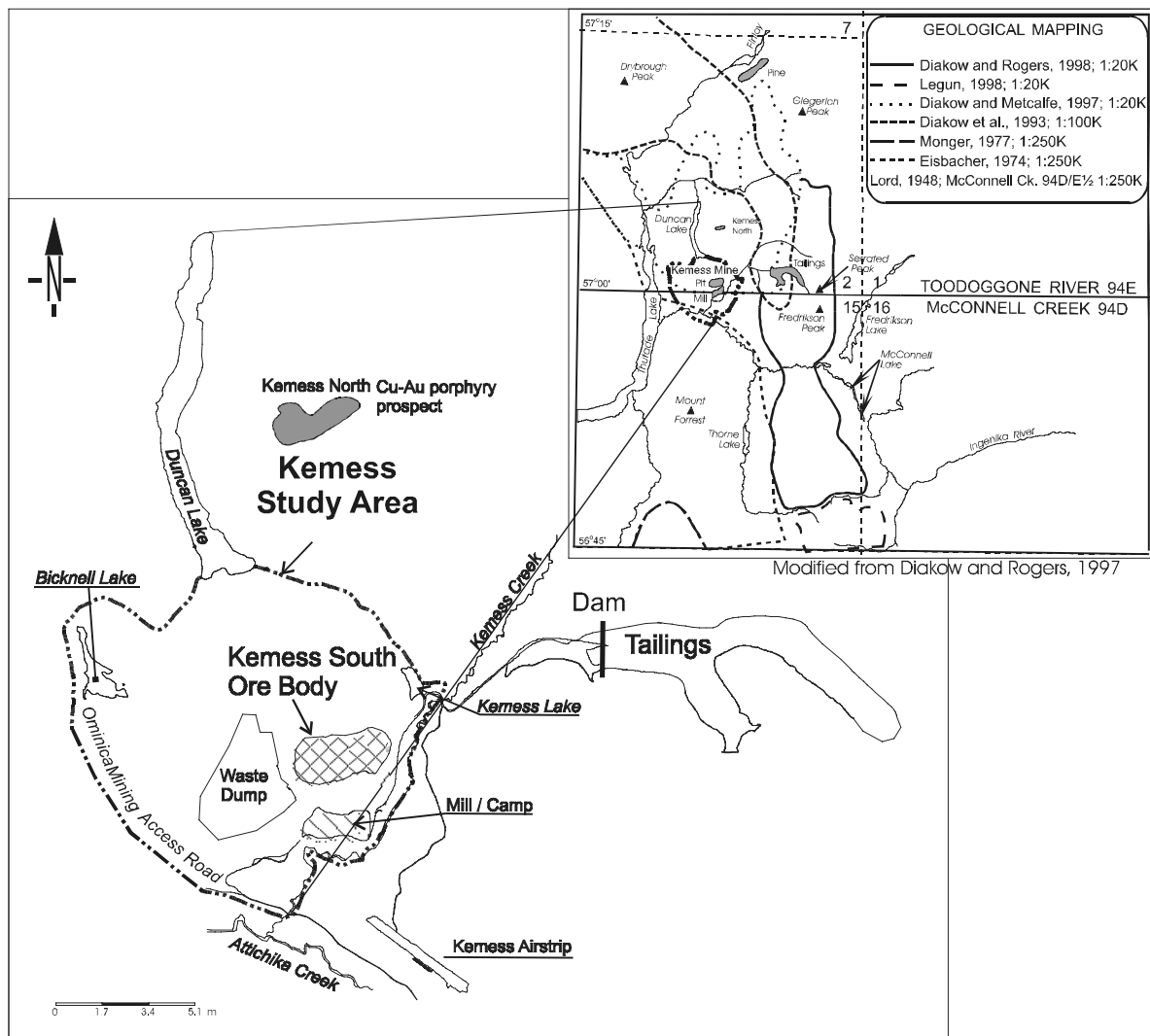


Figure 1. Location of the study area centered on the Kemess South deposit.

GEOLOGY BETWEEN KEMESS CREEK AND BICKNELL LAKE

Three distinct lithostratigraphic units are recognized in the Kemess map area and they can be correlated with major rock units that have been mapped regionally by Diakow and Metcalfe (1997) and Diakow and Rogers (1998). These major stratigraphic divisions include: the mid-Pennsylvanian to Lower Permian Asitka Group; the Upper Triassic Takla Group; and the Lower Jurassic Hazelton Group, specifically the Toodoggone Formation. In the study area the oldest rocks, the Asitka Group, consists of a sequence of rhyolitic to basaltic volcanic rocks that are succeeded by a limestone-chert succession. The Takla Group is dominated by augite-plagioclase pyritic basalts. Pyritic mudstone

locally marks the bottom of the Upper Triassic sequence, and volcanic sandstones comprise relatively minor, but diagnostic interbeds in an otherwise monotonous basalt flow sequence. Rocks of the Toodoggone Formation are mainly dacitic tuffs. Two previously unmapped units are exposed as a consequence of development of the open pit at Kemess. The lower unit, which rests directly on supergene ore, is composed of friable tuffaceous rocks and interspersed epiclastic beds. These were encountered in early definition drilling of the deposit, but are unlikely to be Upper Cretaceous Sustut Group as interpreted by Rebagliati and co-workers (1995); we tentatively correlate them with the Toodoggone Formation. The uppermost unit is an olivine basalt flow that directly overlies the tuff-epiclastic unit.

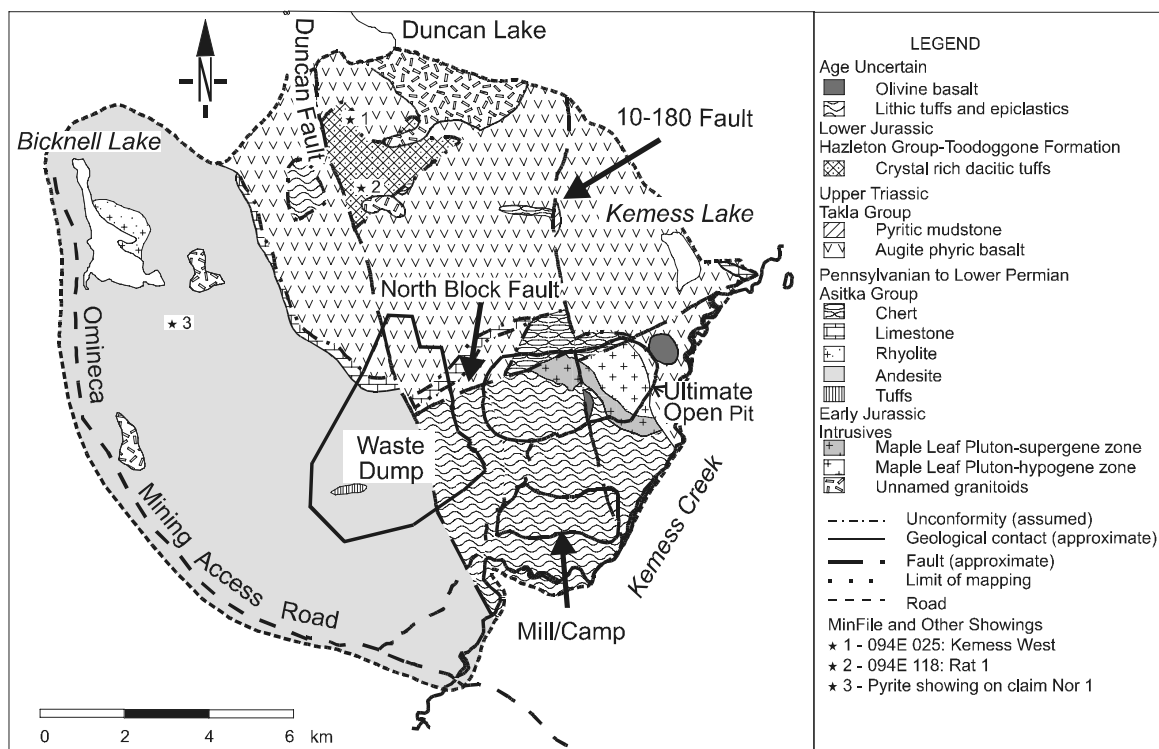


Figure 2. Geological sketch map of the Kemess map-area showing the location of the Kemess South mine.

Asitka Group

Rocks assigned to the Asitka Group underlie much of the topographically low part of the study area east of the Omineca road and west of the Duncan fault (Figure 2). In the region of the Kemess deposit, which is situated between two major faults - the Kemess fault and the Duncan fault, strata of the Asitka Group are scarce but sufficiently widespread to suggest they comprise basement. Good exposures of the Asitka Group, particularly, the upper sedimentary part comprise the foot-wall of the North Block fault, whose trace cuts across the highest benches of the open pit. The lower contact is not exposed either in the study area or regionally. However, the upper contact, which is probably an unconformity, is overlain by rocks of the Takla Group. At the contact, augite-phyric lavas lie above either distinctive andesite or limestone known to be Lower Permian and older. This contact can be traced along the south-facing slope of Duncan Ridge, southwest of Duncan Lake.

Lower Volcanic Unit

The stratigraphic subdivisions proposed for the Asitka Group in this report are based on sim-

ilar rocks mapped adjacent to the study area (Diakow and Metcalfe, 1997; Diakow and Rogers, 1998). In general, the Asitka Group comprises a lower, volcanic-dominated package that passes upward into a comparatively thinner unit composed of sedimentary rocks. Within the study area, rhyolitic tuffs, which are exposed only at a solitary site in the waste rock area, are believed to represent some of the oldest deposits in the Asitka Group. They are light greenish grey and contain flattened lithic fragments that range in size from lapilli to blocks. The lithic fragments are generally crystal poor and rhyolitic in composition. Regionally, similar lithic tuffs accompany rare, thin rhyolite flows that have been sampled at several widely spaced localities and have yielded U-Pb zircon ages of about 308 Ma (Diakow, personal communication, 1998).

Up section from these tuffs is a thick and widespread light green porphyritic andesite unit. Andesitic flows underlie the entire region between the Omineca road and the Duncan fault. These andesites contains 10 to 30% blocky plagioclase crystals approximately 1 to 3 millimetres in diameter, and trace amounts of quartz as subrounded phenocrysts about 1 millimetre in diameter. The andesite flows are generally light

green and contain variable amounts of epidote. Thinly bedded tuff and fine-grained sandstone layers are locally interbedded with these andesites. The tuffs are a few metres thick at two localities. They are light green and contain chloritized rhyolitic fragments. Sandstone beds inter-layered locally with andesitic flow may be up to 2 metres thick. Exposed in a single location along the Omineca road, they are fine grained, light green, internally graded, and thinly to thickly laminated.

Massive basalts that are found stratigraphically beneath the andesites regionally appear to be absent in the study area. However, on the west side of the open-pit there are several outcrops of massive basalt that exhibit characteristics of both Asitka Group and Takla Group basalts. These basalts crop out slightly upslope from a small isolated exposure of Asitka Group limestone. Because the intervening area between exposures is vegetated the contact relationship is equivocal. A sample of this basalt was collected for lithogeochemical analysis, and will be compared to other basalts representative of the Takla and Asitka groups, regionally.

Upper Sedimentary Unit

Limestone and chert, with or without black argillite interbeds comprise the upper, sedimentary division of the Asitka Group in the area (Diakow and Rogers, 1998). These rocks are easily recognized and regionally are typical lithologies comprising the top of the Asitka Group below an unconformable contact with the Takla Group. West of the Duncan fault, a discontinuous 50-metre thick band of limestone that is intermittently exposed for about 6 kilometres, stratigraphically overlies porphyritic andesite and local maroon tuff on the south-facing slope of Duncan Ridge. Neither chert nor argillite occurs with the limestone in this region. East of the Duncan fault, there is a solitary exposure of limestone that lies between the open pit and waste rock area. Around the open pit, chert interlayered with black argillite is the dominant Asitka Group unit exposed. Northeast of the pit, between Kemess Lake and Kemess Creek, limestone is once again exposed, presumably brought up along a strand of the Kemess fault that trends northwest through a major valley between Kemess Lake and Duncan Lake.

Limestone of the Asitka Group is typically white, recrystallized and weathers light grey. Limestone that is exposed between Kemess Lake and Kemess Creek has an uncharacteristic light green color and contains fine grained impurities. This limestone is adjacent to several mafic, hornblende-bearing hypabyssal dykes and carries some pyrite, chalcopyrite and sphalerite mineralization. A solitary outcrop at the south end of Duncan Ridge, exposes chert interbeds in the limestone. However, in the study area, chert is generally found in thick sections without associated limestone. The best exposures of chert are in the upper benches of the Kemess open pit where it is light to dark grey and thinly bedded. The chert has partings of black mudstone and local siliceous mudstone interbeds. In pit exposures the chert-argillite beds are intensely folded adjacent to the North Block fault. Graphitic argillite with polished slip surfaces marks the fault plane in places. Indeterminate bivalves have been found in strongly sheared siliceous and graphitic mudstone adjacent to the fault.

Takla Group

Lower Sedimentary Unit

Pyritic mudstone with or without volcanic sandstone comprises the base of the Takla Group. A solitary outcrop of the pyritic mudstone is exposed on the northeast side of the ridge, behind the Kemess open pit where it was brought up along a fault that is interpreted to represent the northern extension of the 10-180 fault, which cuts the Kemess orebody. It in turn is overlain by volcanic sandstone then basalt. The mudstone is friable, light to dark brown and contains rusty sections where disseminated pyrite is oxidized. This mudstone contains fossils that resemble the Upper Triassic bivalve *Halobia*.

Volcanic sandstone is found in two localities within the map area. The first is on the east side of the ridge immediately behind the Kemess open pit, where it rests directly on top of pyrite mudstone; the second is on the west side of the same ridge where the sandstone is surrounded by Takla basalt. These two relatively thin beds aver-

age six metres in thickness. Sections are characteristically graded from light green sandy beds at the base to darker green siltstone that exhibit fine cross-laminations near the top. Volcanic sandstone and siltstone containing pyroxene grains are diagnostic of sedimentary interbeds derived by erosion of local Takla Group basaltic rocks (Diakow and Rogers, 1998).

Upper Volcanic Unit

Where present, the Lower Sedimentary unit of the Takla Group is conformably overlain by a thick monotonous succession of augite-plagioclase phyric flows. Although the basalts of the Asitka and Takla groups are very similar, Asitka Group basalts are generally aphyric, whereas Takla Group basalts typically contain approximately 5 to 20% pyroxene crystals and 15 to 35% plagioclase crystals. Confusion arises locally because some Takla basalt members may also be aphyric and some Asitka basalts are porphyritic, containing pyroxene phenocrysts.

Takla basalts cover the two highest points of land within the study area, the ridge north of the Kemess South open pit, and the south end of Duncan ridge. Although exposure is spotty, there is enough evidence to indicate that Takla basalts form dip slopes on those ridges. Because no submarine features, such as pillowed basalt, have been recognized these basalts appear to have been subaerially deposited.

HAZELTON GROUP - Toodoggone Formation

Volcanic rocks of the Toodoggone Formation underlie a small area east of the Duncan fault. They consist of a grey-green, dacitic crystal-rich ash-flow tuff. Bounded on the west by the Duncan fault, these tuffs unconformably overlie Takla basalts and are cut by unnamed Early Jurassic ? intrusive rocks. The tuffs contain diagnostic quartz phenocrysts (2-5%) and approximately 30% plagioclase crystals that are 1 to 3 millimetres in size. Alteration in the tuffs is weak, identified by sericite, chlorite and pyrite.

INTRUSIVE ROCKS

The Black Lake suite consists of a series of

Early Jurassic calc-alkaline intrusions (Diakow and Metcalfe, 1997). Within the Kemess map area there are five intrusions that are thought to be part of the Black Lake intrusive suite. They include the Maple Leaf, which hosts the Kemess South gold-copper porphyry mineralization, and four other unnamed, very poorly exposed intrusions. One is located east of Bicknell Lake, another is south of the lake, and two are at the western end of the prominent ridge immediately to the south of Duncan Lake. The contacts of the intrusions have not been directly observed but some of the country rocks are recrystallized indicating an intrusive contact. The Maple Leaf pluton is discussed in a later section that deals with the Kemess South orebody.

Granitic plutons near Bicknell Lake

The largest of the intrusions, which covers less than 1 square kilometre on a knoll south of Bicknell Lake and east of the Omineca road, is near the south end of the map area west of the Duncan fault. Although no contact has been observed, andesite of the Asitka Group crop out both east and west of this intrusion. The intrusion has an equigranular texture of interlocking 2-4 millimetre crystals. It weathers light tan to buff and is pinkish white on a fresh surface. The intrusion is composed of roughly 15% quartz, 40% plagioclase, 25% potassium feldspar, 15% hornblende and 5% biotite. This mineral assemblage places the intrusion in the quartz-monzo-diorite field on the Streckeisen ternary diagram.

A second intrusion approximately 1 kilometre east of the southern tip of Bicknell Lake is exposed over a distance of about 200 metres. It intrudes porphyritic andesite of the Asitka Group. The intrusion is reddish brown and weathers tan to buff. It consists of 10 to 15% quartz, 10 to 15% plagioclase, 50 to 60% potassium feldspar, and 10 to 15% biotite, placing it in the quartz syenite field of the Streckeisen ternary diagram.

Granitic plutons south of Duncan Lake

Approximately 1 kilometre south of Duncan Lake, on the northwest end of the ridge that is immediately behind the Kemess South open pit, a granitic intrusion and a megacrystic quartz porphyry crop out. The granitic rock covers an area

of approximately 1 square kilometre, while the quartz porphyry is only 500 square metres in size. Disseminated pyrite is widespread in both intrusions and throughout adjacent country rocks of the Toodoggone formation and Takla Group. The intrusions cut distinctive quartz-phyric dacitic rocks of the Toodoggone formation. Also associated with these intrusions are magnetite veinlets that cut dacitic tuffs near the contact.

The granitic rock consists of 5 to 10% quartz, 50 to 60% plagioclase, 10 to 15% potassium feldspar, 10% hornblende and 5% biotite. Approximately 5% pyrite and 1 to 2% magnetite are disseminated through the intrusion. The mineral assemblage plots in the quartz-monzodiorite field of the Streckeisen ternary diagram.

The quartz porphyry contains 15 to 25% quartz crystals that are up to 15 millimetres across. The rock is altered; the original groundmass has been changed to a light green to beige mixture of clay minerals and silica that gives it a porcelaneous texture.

STRUCTURE

Two major high angle brittle faults have been mapped within the study area; the Duncan and Kemess faults. The assumed traces of these structures correspond with major valleys and have been located on the basis of significant discontinuities of lithostratigraphic units. Other important faults that provide evidence for more than one deformational event at the Kemess South deposit are well exposed in the open pit.

The trace of the most significant fault in the study area, the Duncan fault, projects to the north up the axis of Duncan Lake and presumably abuts the Early Jurassic Duncan pluton. To the south, the fault is covered by overburden for the most part, but it is believed to closely approximate the axis of a broad valley that also marks a significant change in the character of the Paleozoic rock units across the valley. West of the fault is a broad region underlain by andesitic rocks, whereas east of this structure mainly limestone and chert from the upper sedimentary division of the Asitka Group are exposed. Farther north, near the south end of Duncan Lake, the fault forms a prominent linear cleft in the slope. Here the fault places basalt of Late Triassic age west of the fault, against dacitic tuff of Early Jurassic age to the east. Juxtaposition of differing rock units along the Duncan fault is

consistent with a normal fault having east-side down displacement. The actual amount of displacement is not known.

The Kemess fault, located along the northern margin of the study area, is also aligned parallel to a major valley that extends northwest from Kemess Lake to the southeast corner of Duncan Lake. On the northeast side of this structure, a thick section of aphanitic basalt and rare argillite and some chert comprising part of the Asitka Group crops out (Diakow and Rogers, 1998). A series of en echelon, valley-parallel normal faults with south-side down motion have been documented cutting these rocks (Diakow, personal communication, 1998). To the southwest, across the fault, pyroxene basalt and rare *Halobia*-bearing mudstones that form part of the lowermost sedimentary division of the Takla Group are exposed along the ridge crest north of the Kemess pit. The northeast-facing slope below these Takla exposures was not traversed, but presumably is underlain, in part, by rocks of the Asitka Group. Projection of the Takla Group toward the southwest from the ridge crest suggests they form a dip slope, and could explain the distribution of stratigraphically underlying chert and argillite of the Asitka Group, which crops out in topographically lower areas in the immediate vicinity of the Kemess South deposit.

GEOLOGY OF THE KEMESS SOUTH OREBODY

The Kemess South gold-copper porphyry deposit is a recent discovery (Rebagliati *et al.*, 1995). Production began in 1998 and the projected mine life is 16 years. Kemess South is associated with an Early Jurassic sub-volcanic, calc-alkaline porphyritic quartz monzonite intrusion called the Maple Leaf pluton (Figure 3). Drill information indicates that the intrusion is a gently inclined sheet (Rebagliati *et al.*, 1995) that was intruded into Takla Group basalt and is in fault contact with Asitka Group chert. Its age, based on a U-Pb zircon analysis, is 199 ± 0.6 Ma (Diakow and Rogers, 1998). The majority of the mineralization is within the Maple Leaf intrusion. After emplacement and uplift, exposure and oxidation of the mineralized sill caused the supergene zone to form. This took place before deposition of a tuff-epiclastic sequence which directly rests on the supergene zone.

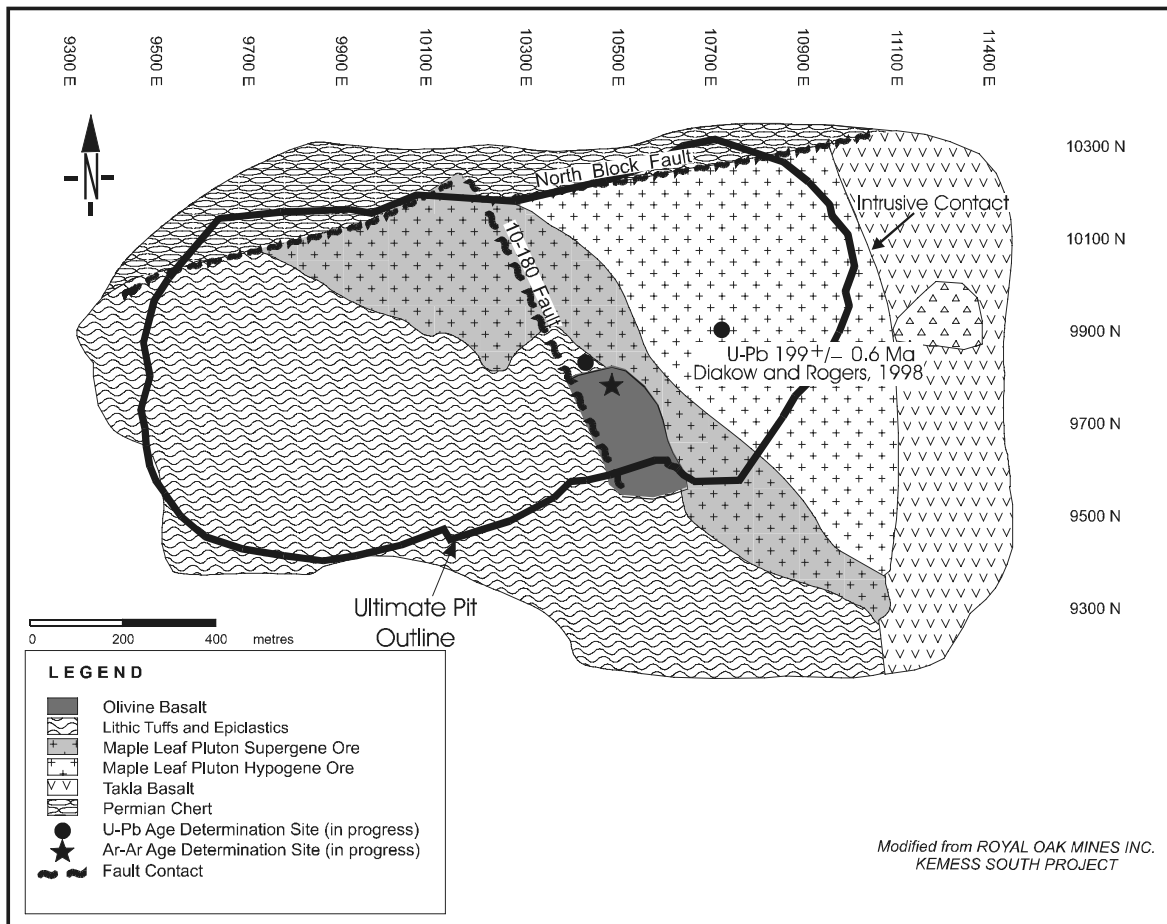


Figure 3. Simplified surface projection of major lithostratigraphic units and ore zones at Kemess South. The U-Pb date of 199 ± 0.6 Ma represents the emplacement age of the Maple Leaf intrusion (Diakow and Rogers, 1997).

The hypogene ore zone consists predominantly of pyrite, chalcopyrite, magnetite-hematite, bornite, with local molybdenite and important amounts of native gold. Weathering in an arid environment of the time produced the supergene cap where the overall grade is the same as that in the underlying hypogene zone (Rebagliati *et al.*, 1995). The supergene blanket is 10 to 70 metres thick (Rebagliati *et al.*, 1995) and contains native copper, native gold, chalcocite and oxides.

MAPLE LEAF PLUTON

The Maple Leaf quartz monzonite intrusion is a tabular body that dips to the south-west at approximately 30 degrees. The South Kemess ore zone measures 1.7 kilometres east to west, 650 metres north to south and varies in thickness from approximately 50 metres in the south to over 250 metres near the North Block fault (Rebagliati *et al.*, 1995). Gold-copper mineralization extends beyond the intrusion but is

uneconomic at present metal prices.

Samples of the Maple Leaf pluton seen on surface and in drill core are strongly altered. The least altered section of the deposit is near the east side of the open pit. At this locality the intrusion consists of approximately 10 to 15% quartz, 45% plagioclase, 10 to 15% potassium feldspar, and 20 to 25% mafic minerals, now mostly replaced by chlorite and local hydrothermal biotite. Also at this locality quartz veins make up approximately 5% of the rock.

One mafic dike cuts the Kemess orebody and therefore post dates mineralization at the Kemess South deposit. It is located on the east side of the deposit (herein called the East dike). The East dike was not detected in any of the four surrounding drill holes; it is assumed to be near vertical in its orientation. The dike is dark green and porphyritic in texture. It contains approximately 10 to 15% pyroxene phenocrysts that are 2 to 4 millimetres in diameter and 15 to 20% plagioclase less than 2 millimetres.

Hypogene Zone

The hypogene zone makes up approximately 75% of the Kemess South deposit and is mineralized with gold and copper. The Maple Leaf intrusion contains approximately 1 to 5% disseminated pyrite, chalcopyrite, magnetite-hematite and bornite, with minor amounts of molybdenite and traces of gold and other minerals (Rebagliati *et al.*, 1995). The sulphides are hosted mainly within the Maple Leaf sill. They occur on fractures, in veins and interstitial to the feldspar crystals.

Sericite is the dominant alteration mineral associated with Kemess mineralization. Locally it comprises up to 25% of the rock. It gives the intrusion a light greenish pink color but a dirty white appearance when associated with silica alteration. As the sericite content increases in the deposit there also tends to be an increase in silica content and greater destruction of the primary minerals and original textures.

The second most abundant alteration type is pink potassium feldspar. Potassic alteration with minor sericite forms selvages on the quartz veins that can range from several millimetres to 3 centimetres in width. Sulphide veins also have pink potassium feldspar alteration envelopes and these tend to be proportionally thicker than those associated with the quartz veins.

According to Rebagliati *et al.* (1995) drilling has shown alteration patterns that are subparallel to the contact of the Maple Leaf intrusion. In cross section, a lower hematite-clay-carbonate-silica zone gives way upward to a quartz stockwork zone with associated potassium feldspar alteration which gives way upward to a strong quartz stockwork zone with potassium feldspar selvages and interstitial sericite alteration. The highest copper and gold grades occur in the intense quartz stockwork zones.

As part of this study, alteration related to Kemess mineralization will be examined in detail. Samples have been taken at approximately 25 metre intervals from 13 individual drill holes across the deposit. These samples will be analyzed to study geochemical trends, and polished thin sections will be made to study the silicate and ore minerals and their chemistry.

Supergene Zone

The supergene zone is a red oxidized zone. It contains chalcocite and two forms of native copper, as large sheets, and as tiny disseminated flecks of native copper termed “pin prick copper” by workers at the Kemess South mine, who have subdivided the supergene zone into three sub-zones. The lowest zone overlies hypogene ore and contains the “pin prick” copper, in which flakes are less than 2 millimetres in diameter and disseminated throughout the oxidized, highly clay and hematite altered intrusive rock. This zone also contains secondary sulphides, consisting of chalcocite and minor hypogene sulphides - chalcopyrite and bornite. The middle zone contains slightly larger leaves of native copper, some of them reaching 10 centimetres in diameter, and 3 millimetres in thickness. Near the top of this zone the copper is associated with planes of weakness and sheets more than 3 metres long and 50 centimetres wide have been found. This zone is more highly altered and contains up to 30% hematite-stained clay. The upper zone has been termed the “Leach Cap” by the mine geological staff. It contains elevated levels of gold, and very little copper and is characterized by the intense alteration, and contains 5 to 10% quartz and relict plagioclase crystals.

Typical rocks from the supergene zone are reduced to a hematitic mud in drill core making an in-depth study difficult. However, 12 sample were collected from the Kemess South open pit for petrographic analysis. The samples were collected approximately 10 metres apart; three representative samples from both the top and bottom units, and three from the upper and three from the lower section of the middle unit.

POST-ORE LAYERED ROCKS

Tuff-epiclastic Unit

The supergene zone of the Maple Leaf pluton is overlain by poorly indurated lithic tuffs, and interbedded epiclastic rocks. This unit does not crop out at surface near the orebody, however, drilling has shown that it is widespread in the subsurface, thickening towards the southwest to more than 200 metres. Similar rocks also crop out along Kemess Creek, south of the mine site, where cut banks up to 60 metres high are domi-

nated by reddish brown to maroon epiclastic rocks. Farther downstream these rocks are covered by glacial till. West of the Duncan fault, bedded epiclastic rocks with similar lithologic characteristics crop out sporadically in a small area, approximately 100 by 200 metres. They consist of a relatively flat lying bedded sequence more than 25 metres thick exposed along an unnamed creek. The lower contact is not exposed, however, basalts of the Takla Group crop out nearby and suggest a probable unconformity.

At Kemess South, copper and gold assays from drill core indicate that the lower contact of the tuff-epiclastic unit is sharp against the supergene enrichment zone. Gold assays average 1 ppb in the tuff-epiclastic unit but 45 ppb in the supergene zone. Copper assays behave similarly, averaging 0.015% in the tuff-epiclastic unit but 0.3% in the supergene zone. Native copper is notably absent in the tuff-epiclastic unit. In the field the contact looks more gradational. This gradation occurs over approximately one metre with a decrease of quartz grain content from approximately 5% in the supergene zone to trace amounts in the tuff-epiclastic unit. Plagioclase increases from virtually none in the supergene zone to more than 5% in the tuff-epiclastic unit.

The tuffs form crudely layered, very thick beds that are maroon to brick red. The concentration of lithic fragments in the tuff ranges markedly, from 5 to 50%. The dominant fragments are aphanitic, very light green and scale-like, between 5 and 20 centimetres long and 1 to 4 millimetres thick. A diagnostic feature is their greasy feel and swelling habit when exposed to the atmosphere, suggestive of replacement by a clay mineral. A sample of one of these fragments has been collected for X-ray diffraction analysis. Locally the tuff contains rare quartz and biotite crystals. There are also a few sub-angular to sub-rounded basaltic-looking clasts. These clasts make up 1% of the unit and are dark green; some have pyroxene phenocrysts.

Grey-green and maroon epiclastic rocks comprise distinctive bedded intervals within the comparatively more massively bedded maroon tuffs. They are typically medium to thickly bedded with thinner, parallel laminated and graded sections. The epiclastic layers are composed mainly of sandstone and siltstone. Rounded pebbles and cobbles, varying in composition from

basalt to andesite, are randomly dispersed in some sandstone beds or form clast-supported conglomeratic interbeds. Pyroxene occurs as discrete grains and crystals in basaltic clasts. The provenance of this detritus is thought to be nearby basaltic rocks of the Takla Group. Despite the proximity of older Paleozoic chert and mudstone, clasts of these lithologies are not evident in the epiclastic beds.

The thin section of tuffs and epiclastic rocks exposed in an unnamed creek west of the Duncan fault are lithologically similar to those that overlie the supergene zone. Light grey epiclastic rocks dominate this section with approximately 20% broken plagioclase in the matrix. The sedimentary components are very similar to the reddish grey and brick red epiclastics and the tuffs are similar and although finer grained, and the lithic fragments have the same greasy texture as those found in the open pit. The rocks in Kemess Creek are tentatively assigned to the tuff-epiclastic unit despite the generally rubbly appearance of bedrock exposures that masks distinguishing features.

Rebagliati and co workers (1995) correlated the tuff-epiclastic unit at Kemess South with the Sustut Group. However, there are significant lithologic differences between typical rocks of the Sustut Group and those overlying the deposit that make this correlation improbable. The Sustut Group nearby is characterized by diagnostic well-rounded chert, vein quartz, and granitic clasts in thick, parallel bedded conglomerate-sandstone beds. In contrast, the maroon colored rocks found above the Kemess deposit are mainly subaerial tuffs with subordinate immature epiclastic rocks, more like rocks of the Toodoggone formation. Toodoggone tuffs typically contain quartz and quartz is present, albeit as rare grains, in the Kemess tuff-epiclastic unit. A tuff sample from this unit has been collected for a U-Pb zircon age determination. Because this unit overlies the supergene zone, a date from these rocks would aid in bracketing the time of uplift and oxidation of the Maple Leaf pluton that resulted in the development of the supergene blanket.

Olivine Basalt

A fresh olivine-bearing basalt, more than 30 metres thick, sharply overlies the tuff-epiclastic

unit and represents the youngest rock unit in the study area. It contains approximately 30 to 35% plagioclase, up to 10% glassy olivine, and pyroxene phenocrysts. Unlike any basalt mapped regionally, a sample is being processed for a whole rock ^{40}Ar - ^{39}Ar age determination.

LOCAL STRUCTURE

The North Block fault is the most prominent fault exposed in the open pit. The fault strikes roughly east and dips at about 70 degrees towards the south. It truncates the north side of the Kemess orebody and juxtaposes it against deformed chert and argillite of the Asitka Group. Some of the best grades reported in the hypogene zone are against the North Block fault. The fault also truncates the supergene zone and the overlying tuff-epiclastic unit. Fault gouge zones 5 to 10 metres wide are developed along the North Block fault. Other than milled pyrite, the fault zone is unmineralized. This is consistent with data from the exploration drill core logs, which show that mineralization is cut off by the fault. Offset on the fault is normal and sinistral, but the absolute amount of offset is not known.

The 10-180 fault, another important structure mapped within the open pit, cuts both the orebody and the North Block fault. Extrapolated to the north, the 10-180 fault connects with a fault that apparently uplifted and mildly folded Upper Triassic sedimentary rocks on the ridge crest north of the pit. This structure strikes due north and dips east at 80 degrees. Like the North Block fault, the fault zone is unmineralized, and most of the displacement apparently post-dates supergene enrichment. The 10-180 fault truncates both the tuff-epiclastic unit that overlies the supergene zone and the olivine basalt that conformably overlies the tuffs. It also cuts the orebody near the south wall of the open pit. The 10-180 fault also crosses and displaces the trace of the North Block fault by approximately 250 metres; offset is dextral. Approximately 150 metres north of the North Block fault, near the ring road around the open pit, the 10-180 fault crosses deformed chert layers that contain native copper mineralization. This mineralization may have deposited from groundwater that moved along the fault from where it cuts the supergene zone. The 10-180 fault also has a rotational component; the east block rotated clockwise relative

to the counterclockwise movement of the west block. Adjacent to the 10-180 fault, the tuff-epiclastic unit changes inclination. West of it the dip is approximately 60° southwest; to the east the dip is 20° southwest.

In the open pit, intensely folded chert and argillite of the Asitka Group are present in the foot-wall section of the North Block fault. Folded Permian chert in the foot-wall of the deposit is cut by the North Block fault. The folds are asymmetric and verge east-northeast. The axial planes strike on average 132 degrees and dip approximately 70 degrees southwest, oriented roughly 30 to 60 degrees relative to the strike of the North Block fault. Fold axes trend 145 degrees and plunge 16 degrees. Fold axes within the chert display small reverse faults that parallel axial planes of the folds.

Minor folds are also documented in a rare exposure of Takla Group mudstone that is located on the ridge crest north of the open pit. The mudstone unit is less than 5 metres thick and apparently faulted into place against augite-phyric basalts. Upright, open folds in these rocks have axial planes that strike north and dip east at approximately 80 degrees. The orientation of these folds is almost perfectly parallel to the projection of the 10-180 fault and the folds are interpreted as drag structures related to faulting.

MINFILE AND OTHER PROSPECTS

Kemess West (Minfile 094E 025)

The Kemess West showing was first explored in the late 1960s. The showing is situated along the west central portion of a broad positive IP chargeability anomaly which covers the 6 by 4 kilometres area between and including the Kemess North and South deposits. This anomaly is likely caused by pervasive disseminated pyrite mineralization in augite phyric basalts of the Upper Triassic Takla Group and dacitic ash flows of the Toodoggone formation, which have been intruded by quartz monzonite bodies of the Early Jurassic Black Lake Suite. Dominant structures in the area are steeply dipping faults which define a northerly fabric. Extensive gossanous, pyritic and potassically-altered outcrops contain occasional quartz-carbonate-magnetite-pyrite shear-hosted veins

with up to 5% sphalerite and traces of chalcopyrite and galena. Assay results of up to 252.5 g/t Ag, 9.9% Zn, 0.7% Cu, 0.18% Pb and 2.0 g/t Au have been reported from selected grab samples.

Rat 1 (Minfile 094E 118)

The Rat showing is situated 0.5 kilometres southwest of, and in a similar geological environment to, the Kemess West showing. Like the Kemess West showing, the Rat 1 showing is mainly hosted in dacitic ash flows of the Toodoggone formation and basalts of the Takla Group. In addition, quartz-feldspar porphyry bodies form locally gossanous and potassically-altered outcrops that host fractures, quartz veins and stockworks with 1 to 2% disseminated pyrite and traces of chalcopyrite. Assay results of up to 7.1 g/t Ag, 0.109% Cu, 0.005% Zn, 0.002% Pb and 0.315 g/t Au have been reported from selected grab samples.

Pyritic Showing on Nor 1 Claim (UTM 632360, 6321546)

This showing is located 5 kilometres west-northwest of the Kemess South deposit, and is hosted by relatively unaltered rhyolite of the Asitka Group. The rhyolite is underlain by light green andesitic flows. The showing consists of an outcrop approximately 5 metres in diameter of semi-massive pyrite, which appears to be replacing the rhyolite. A grab sample of the pyrite yielded an anomalous value of 530 ppm As.

SUMMARY

The map area is underlain by three major stratigraphic units. The oldest, the mid-Pennsylvanian to Permian Asitka Group consists of rhyolitic and andesitic tuffs and flows, chert, mudstone and limestone. It is mainly exposed west of Duncan Lake valley and in the Kemess South open pit. The Upper Triassic Takla Group consists mainly of dark green augite-plagioclase pyritic basalts. The Toodoggone Formation of the Lower Jurassic Hazleton Group consists of dacitic ash flows, lithic tuff and epiclastic rocks. The youngest rocks are olivine basalt that overlie the tuff-epiclastic unit, tentatively correlated

with the Toodoggone formation, in the Kemess South open pit.

The lithic tuffs interbedded with epiclastic sediments that overlie the supergene zone of the Kemess South deposit were originally correlated with the Upper Cretaceous Sustut Group. However, deposits of the Sustut Group in the region are predominantly pebble and cobble conglomerates composed of well-rounded chert, vein quartz and granitic clasts. This contrasts markedly with the constituents of the reddish brown tuff-epiclastic unit in which conglomerates are relatively scarce, composed of volcanic-derived clasts.

The deposit is cut off to the north by the east-west striking, south-dipping North Block fault. It has sinistral and normal motion; the magnitude of the offsets is uncertain. The deposit is also cut by a north-south fault named the 10-180. This fault, discovered during stripping of overburden in the open pit cuts and therefore post dates the North Block fault. There is approximately 250 metres of dextral offset and approximately 30 degrees of rotation on the 10-180 fault.

In the Kemess South open pit three sub-zones have been identified within the supergene zone. The lowest, above the hypogene ore contains "pin prick" native copper flakes. Locally the percentage of copper can be up to 5%. Rare hypogene sulphides can also be found in this zone. The middle zone is a redder color and contains approximately 50% hematite-stained clay altered material. This zone is characterized by small leaves of native copper at the base that become larger and more sheet-like upward.

As a new producing mine in British Columbia, the South Kemess Mine will have a significant impact on the economy of the province. A better understanding of the mine geology and the character of the deposit will have regional applications in the search for similar porphyry copper-gold deposits elsewhere.

ACKNOWLEDGMENTS

The authors would like to thank Larry Diakow for discussions that improved understanding of regional geology and the Kemess deposit, and both Larry and Bill McMillan for providing editorial review that significantly improved this manuscript. We are grateful to the

staff and especially the engineering and geological staff of Kemess Mines for their hospitality, use of the facilities at the mine site, and useful advice throughout the field season. The principal author is also grateful to the B.C. Geological Survey Branch and Royal Oak Mines Inc. for financial and logistical support during the field component of this thesis-related project.

REFERENCES

- Diakow, L.J. and Metcalfe, P. (1997): Geology of the Swannell Ranges in the vicinity of the Kemess copper-gold porphyry deposit, Attycelley Creek (NTS 94E/2), Toodoggone River map area; *in* Geological Fieldwork 1996, B.C. Ministry of Employment and Investment, Paper 1997-1, pages 101-116.
- Diakow, L.J. and Rogers, C. (1998): Toodoggone-McConnell Project: Geology of the McConnell Range - Serrated Peak to Jensen Creek, parts of NTS 92E/2 and 94D/15; *in* Geological Fieldwork 1997, B.C. Ministry of Employment and Investment, Paper 1998-1, pages 8a-1 to 8a-14.
- Diakow, L.J., Panteleyev, A. and Schroeter, T.G. (1993): Geology of the Early Jurassic Toodoggone Formation and gold-silver deposits in the Toodoggone River map area, northern British Columbia; *B.C. Ministry of Energy, Mines and Petroleum Resources*, Bulletin 86, 72 pages.
- Rebagliati, C.M., Bowen, B.K., Copeland D.J., and Niosi, D.W.A. (1995): Kemess South and Kemess North porphyry gold-copper deposits, northern British Columbia; *in* Porphyry Deposits of the Northwestern Cordillera of North America, T.G. Schroeter, Editor, *Canadian Institute of Mining, Metallurgy and Petroleum*, Special Volume 46, pages 377 – 396.
- Royal Oak Mines Inc. (1996): Annual Report; Kirkland, Washington U.S.A., 64 pages.

GEOLOGY OF THE MOUNT MCCUSKER AREA, NORTHEASTERN BRITISH COLUMBIA (94G/4W)

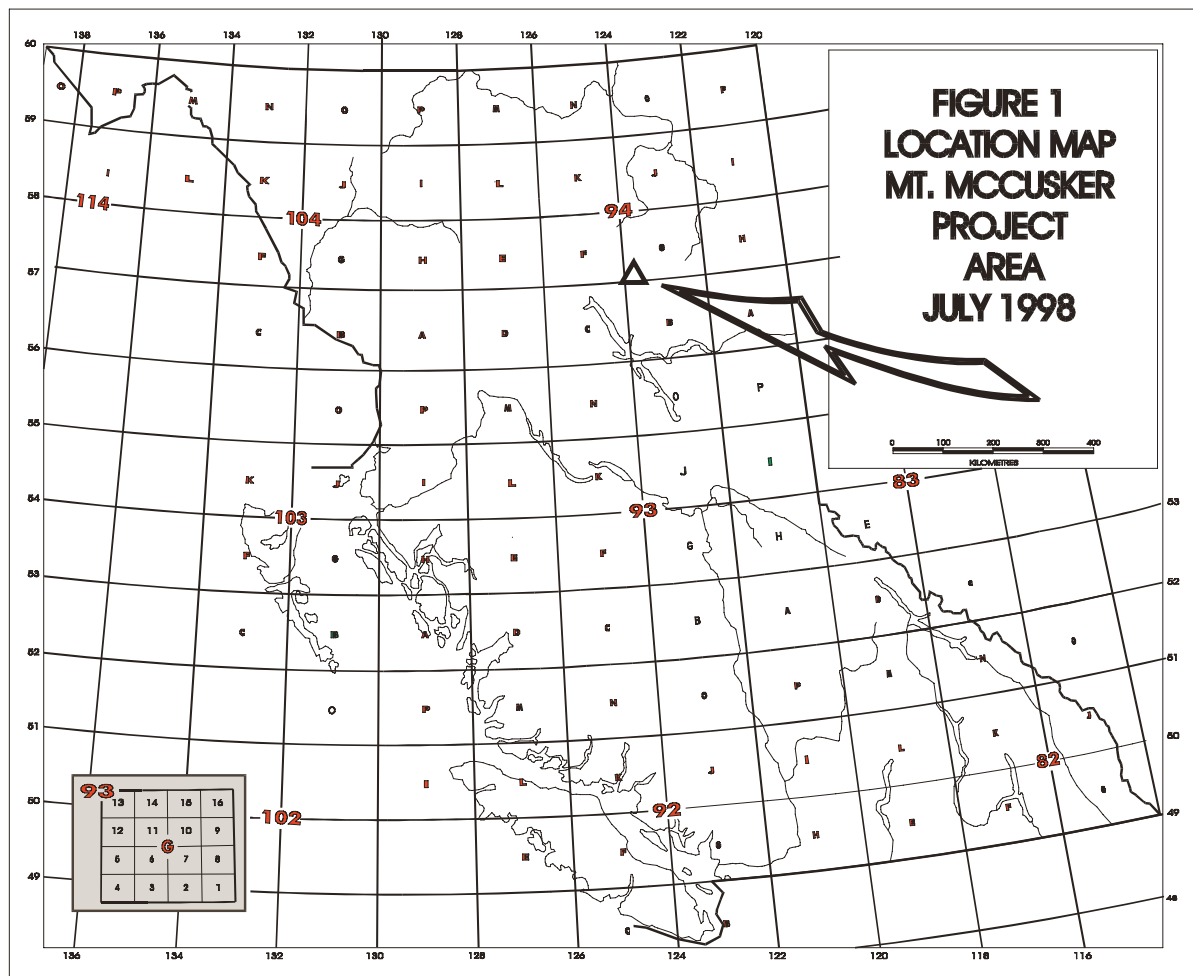
By A. S. Legun, B.C. Geological Survey Branch

KEYWORDS: Regional Geology, Paleozoic, Mississippi Valley type (MVT) deposits, Sidenius thrust, Skoki Formation, Beaverfoot Formation, Nonda Formation, Muncho-McConnell Formation, Robb Lake deposit, stratiform breccia, lead and zinc mineralization.

INTRODUCTION

This paper reports on mapping in a portion of NTS 94G/4W (Mt. McCusker west half), conducted during the month of July 1998 (Figure

1). This area, only accessible by air, lies 80 kilometres due west of the small settlement of Pink Mountain, 151 kilometres north of Fort St. John on Highway 97. The mapping program is part of the Central Foreland NATMAP Project, led by Mike Cecile of the Geological Survey of Canada (G.S.C.). The program objectives are to update the geology of the area, tie in with ongoing G.S.C. mapping to the north and east, and complement the Robb Lake mineral deposit study of JoAnne Nelson (Nelson *et al.* this volume. The G.S.C. offered considerable helicopter support



as well as occasional lodging at Pink Mountain lodge. The work was conducted from two fly camps; at Bartle Creek, and the headwaters of the valley immediately north of Sidenius Ridge.

Data from twenty-one traverses assisted in recompiling the geology of an area of a 10 x 30 km. area at a scale of 1:30000. Preliminary results are presented in Figures 2 and 3.

Mapping has suggested a rather sharp platform to basin facies transition in several Paleozoic Formations between the McCusker and Robb Lake areas. The transitions suggest a re-entrant, rather than a simple indentation to the Ospika Embayment in this area (Thompson 1989, Fig. 7,9). The Middle to Upper Devonian Besa River shale has been usually invoked as a source of metals and transporting fluids for the Robb Lake deposit (MacQueen, R.W. and Thompson, R.J. 1978). A local and thickened Late Ordovician to mid Devonian shale package may have been a more important factor in the subsequent location, size and relative richness of this lead-zinc deposit.

Regional Setting and Previous Geologic Mapping

The area of study lies at the eastern edge of the northern Rocky Mountains, about 20 kilometres north of the Robb Lake lead-zinc deposit. Main streams within the map area are the upper Sikanni Chief River and Sidenius Creek. Secondary drainages include Bartle, Embree and Gautschi Creeks.

Early work in the area dates from the 1960's and focused on the regional stratigraphic and structural framework of the Paleozoic rocks for assessment of oil and gas potential. Mineral exploration received its impetus from active assessment (drilling, sampling) of the Robb Lake prospect 20 kilometres to the south in the early 1970's. This led to spin-off exploration for Mississippi valley type deposits along the entire eastern border of the Northern Rockies. In the study area a number of showings were found and one, Mt. McCusker (Minfile 094B 005), was drilled.

The area has not been mapped in detail, except for the immediate vicinity of the McCusker prospect which was done at a scale of 1:12000 (McHale and Pearson 1974). The region is generally covered by a 1:250000 scale

compilation by the G.S.C. (Taylor 1979). Bob Thompson mapped and compiled the Halfway sheet south of the study area (Thompson 1989), publishing both 1:50,000 and 1:250,000 scale maps.

In the following geological description of the area major ridges are referenced by using the name of a nearby drainage (Figures 2,3). The ridge extending south from Sikanni Chief River, drained by Bartle and Embree Creeks, is Bartle Ridge. Sidenius Ridge is the east-west trending ridge on the north side of the Creek of the same name.

PROJECT AREA STRATIGRAPHY

The stratigraphic succession ranges from Ordovician to Devonian in age. Dolostones dominate the succession but quartzites, calcarenites, dolomitic siltstones, limestones, variegated shales and sandstone are also present. The succession in stratigraphic order (oldest to youngest), comprises the Ordovician Kechika, Skoki and Beaverfoot Formations, the Silurian Nonda Formation, and the Devonian Muncho-McConnell, Wokkash and Stone Formations.

The Sikanni Chief section on Bartle Ridge (Norford *et al.*, 1966) was walked out and used as a frame of reference for mapping. Units were mapped on lithologic grounds although specific fossils and biogenic features assisted in pinning down some units. For example the colonial coral *Halysites* assists in recognizing the Nonda, while algal oncolites and large gastropods (*Maclurites*) facilitate recognition of the Skoki. Units above the Muncho-McConnell are difficult to distinguish on lithology alone. Here further work on fossil assemblages would be useful.

A quartzite marker unit, up to 50 metres thick, is useful in the tracing of structures and stratigraphy within the dolostone dominated succession. The marker forms resistant ribs in outcrop, is paler in tone, and is traceable in the field with airphoto in hand.

Since the quartzite marker is mappable in the area, it is designated as a separate unit. Thompson (1989, Sections 3 and 4, p. 117) included it in the basal Muncho-McConnell while Norford *et al.* (1966, fig. 3) placed it in the upper part of the Nonda. It is probably equivalent to a thinner (15 metre) sandy interval noted at the base of the Muncho-McConnell by JoAnne Nelson (Nelson *et al.* this volume).

Kechika Group

The Kechika Group forms the ridge crest extending north and south of Mt. McCusker, the head of the ridge SSE of the confluence of Sikanni Chief River and Gautschi Creek (Figure 3), and most of the area immediately adjacent to the western limit of mapping. Large nearly recumbent chevron folds with axial planar cleavage are visible in rock walls of western peaks. The most common lithology is a well recrystallised thin to medium bedded calcareous shale to dolostone. Flaggy cleavage plates typically have a slight phyllitic sheen. It is perhaps more dolomitic in the McCusker area than seen regionally. On the ridge overlooking the south side of Sikanni Chief River, thick, massive beds appear to form the top of the Group. Normally a strong cleavage obscures bedding characteristics.

Skoki Formation

The Skoki Formation in the area comprises medium to thick beds of dark grey to tan dolostones. Oncolites (up to several centimetres long) and large coiled gastropods (up to 5 cm. long) are a characteristic feature of the formation. Solitary corals (*Bighornia*) are present, except in basal beds near the Kechika contact. A chert nodule facies was seen at more than one stratigraphic position but was best developed in stratigraphically high beds on Sidenius Ridge. Extensively burrowed and bioturbated beds are also interbedded at various stratigraphic levels. Trace fossils occur in a maze-like fashion both on bedding surface and in section. Most trace fossils appear to be subhorizontal grazing trails. Some branching was evident.

The contact with the Beaverfoot on Sidenius Ridge is marked by a change in lithology to orange dolostone, limestone, and dark calcareous shale. Skoki beds immediately below are pale, oncolitic in part and have a reddish to orange tone. This is due in part to red hematitic shale partings. The section is approximately 500 metres thick. These beds dip gently and the thickness can be estimated from the elevations of the upper and lower contacts.

Norford measured a minimum 406 metres of Skoki from the Kechika contact to the peak on the high ridge that overlooks the south side of the Sikanni Chief River (section 707). Along the ridge crest, the transition to Beaverfoot facies

occurs and thus the thickness measured is probably close to that of the entire formation. North of the river rather massive, oncolite-poor beds characterize the Skoki sequence.

On the northwest side of Gautschi valley, McHale and Pearson (1974) describe oncolitic grey to dark grey thin bedded dolostones with the planispiral gastropods *Maclurites* and *Palliseria* cf. *Robusta*. Though not named, these beds can be reasonably assigned to the Skoki Formation. According to McHale and Pearson (1974) the associated fossils are probably Late Ordovician.

Immediately south of the map area Thompson records 617 metres of Skoki near Mt. Kenny and 450 metres from a section ten kilometres west of Mt. Kenny (section 2-3, 2-4 of Thompson 1989).

Beaverfoot Formation

The Beaverfoot Formation is not the lithologic equivalent to the formation of the same name in the southern Rockies, but is approximately the same age (Thompson 1989). As the Beaverfoot is an areally significant unit on the G.S.C. map of the Trutch area, it seems useful to retain this nomenclature rather than several descriptive terms, pending redefinition of the stratigraphy. The Beaverfoot, as mapped, is equivalent to Upper Ordovician strata mentioned by Cecile and Norford (1979), the quartz dolostone unit of Thompson (1989); and his brown quartzite and shale unit of the Road River strata.

The Beaverfoot weathers in tones of brown, red and orange and is a more clastic detrital sequence in contrast to dolostones above and below. This is an interesting formation showing lateral and vertical facies variation worthy of further study.

Eastern area (Bartle Ridge, north side of Sikanni Chief River)

The Beaverfoot Formation in the Sikanni Chief section consists of a lower member of brownish beds (not accessible but visible on precipitous slopes), overlain by reddish (bioturbated) dolomitic siltstones. The upper member consists of laminated to cross-bedded quartz arenite, arenaceous dolostone and orange dolostone.

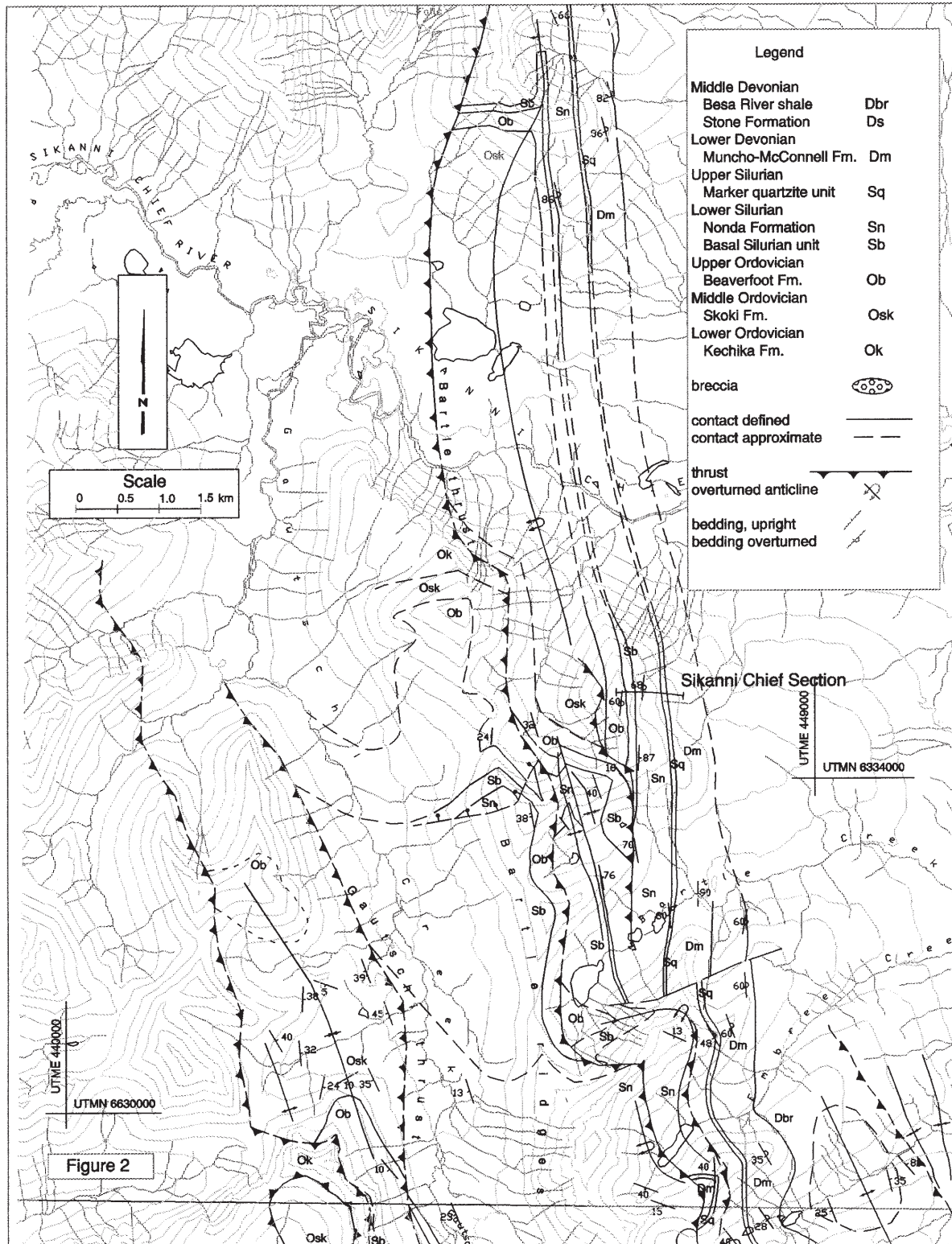


Figure 2. Geology of the northern portion of the study area.

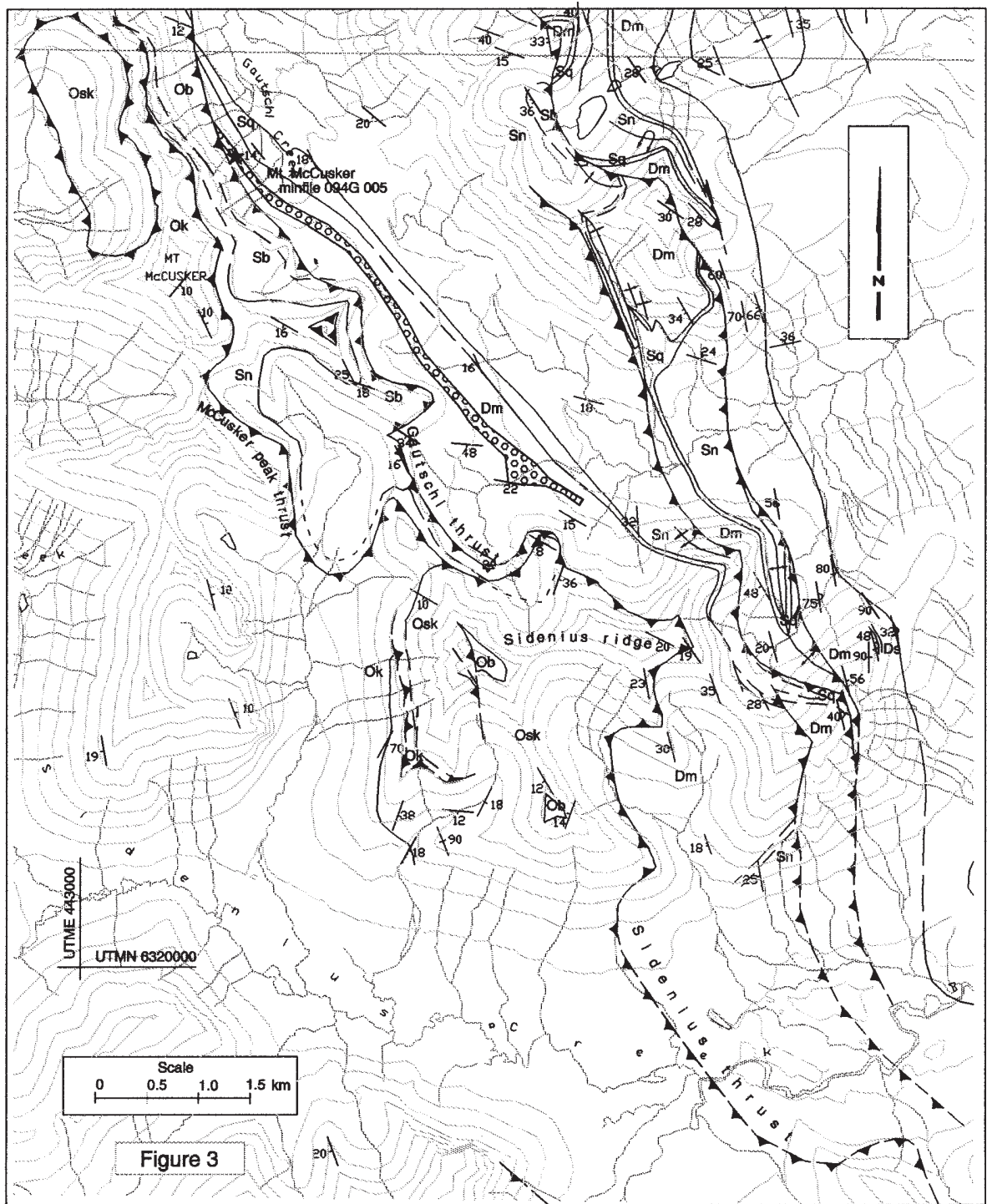


Figure 3. The southern border of Figure 2 adjoins the northern border of Figure 3. Geology of the southern portion of the study area.

Quartz arenite beds are horizontally laminated to cross-bedded. Cross bedding is low angle to medium and there are some scour and fill features in the form of shallow troughs filled with horizontally laminated sand. Individual quartz beds appear to thin rapidly along strike. Dolostones grade into arenaceous dolostones,

often cross-bedded with resistant “highlights” of sandy foreset laminae. Similarly quartz arenites grade to sandy dolostones with sandpaper texture. Dolomitic lenses may occur within arenite beds.

The upper contact is placed at the highest siliciclastic bed. In the Sikanni Chief section

this contact is a breccia with rounded dolostone clasts to 50 centimetres and hematite rich nodules within a sandy matrix. The breccia lies ten metres above a resistant sequence of quartzites. Just to the west, on a fold limb, the highest siliclastic bed is brown-grey laminated dolostone with quartz filled mudcracks. Further west, below the Bartle thrust, the highest bed is a five metre thick quartzite with an irregular top, containing mudchips and limonitic nodules. A few kilometres to the north, on the other side of the Sikanni Chief River, the top of the Beaverfoot comprises a gritty granule quartzite with dark chert and chips of dolostone.

The Beaverfoot in the eastern part of the map area appears to reflect an upward shallowing marine sequence capped by one or more unconformities. The environment of deposition includes exposed dolomitic mudflats and washover deposits of quartz sands. Some limonitic and hematitic nodules may represent ferricrete developed at the water table. A laterally restricted redbed quartz sandstone may be a subaerial deposit.

About 195 metres of section is estimated from map contacts and dip measurements on strata on Bartle Ridge. On the north side of the Sikanni Chief River the section is thinner, estimated at 110 metres.

Gautschi valley

To the west of Bartle Ridge, a synclinal structure along the west valley wall of Gautschi Creek exposes approximately 200 metres of interbedded dolomitic shale and shaly dolostone. The lithologic contrast between the brownish dolomitic shales and pale Skoki strata is discernible from across the valley. The formation outcrops on rugged slopes and was not examined in detail. Some minor pale resistant beds in lower cliffs of Mt. McCusker may be sandstones near the top of the formation. Otherwise it is recessive and obscured by scree. This section lies in the hangingwall of the Gautschi thrust.

Sidenius Ridge

A 15 metre section of brownish-red dolomitic siltstone and fine sandstone lies above

Skoki strata on a spur of Sidenius Ridge. The beds form a rather recessive flat tabletop to the spur and were mapped as basal Beaverfoot. At the base of the unit are a few metres of black calcareous shale with thin limestone bands, and minor phosphatic brown sandstone. Fossils in these beds were identified as an open coiled nautiloid cephalopod, orthid and inarticulate brachiopods, echinoderm fragments, bryozoan and minute gastropods by Brian Norford (G.S.C Paleontological Report 0-3-BSN-1998). Unfortunately the collection is not age diagnostic. A sample has been collected for conodont determination.

Basal Silurian facies

A basal Silurian facies of platy yellowish shaly dolostone and thin bedded mottled limy dolostone, lying below the Nonda Formation and above the Ordovician Beaverfoot Formation, forms a mappable unit in the study area. This basal Silurian facies appears to be equivalent to the carbonaceous limestone unit (Scl) of Thompson (1989). This rather recessive facies has been previously recognized by petroleum consultants (Riddell 1972) and Norford *et al.* (1966) in section descriptions.

The facies is typically thin bedded with a yellowish weathering cast. It varies from thin bedded mottled and "donut" nodular dolomitic limestone to laminated dolomitic siltstone to laminated calcareous shale. It represents an incompletely dolomitised facies. A few dark biostromal and rubbly bioclastic beds, which resemble stratigraphically higher Nonda beds, are found within the basal Silurian. Along Bartle Ridge and on the slopes north of the Sikanni Chief River, the thickness of these units is in the order of 100 metres. Thickness is difficult to compare from one section to another due to the transitional contact with the Nonda. The thickness to the west, in the hangingwall strata of the Gautschi thrust is estimated as 100 to 150 metres. Here basal Silurian, represented by shaly fossiliferous limestone, is underlain by Beaverfoot dolomitic shale and overlain by thick bedded dolostone containing abundant Halysites and Favosites which are assigned to the Nonda Formation.

The basal Silurian facies is easily confused

with the Kechika Group in exposures near thrusts or in the core of folds. Both units are similar lithologically in that they are thin bedded mixed clastic and carbonate off-shelf "calcareous shale" facies. Both develop strong axial plane cleavage during deformation, in contrast to more competent and massive carbonate and dolostone beds. In exposures where Silurian fossils are not present, designation of these platy, highly cleaved beds is problematic.

Nonda Formation

The Nonda Formation is mainly composed of grey, medium bedded dolostone. The unit is medium grey to dark grey for the most part, but pale subunits were noted during mapping. One pale subunit occurs locally in the middle of the formation, and often beds immediately below the quartzite marker unit are pale. Silicified fossils are common and there are beds of chert nodules and cherty dolostone layers. Fossils include corals, crinoids (usually in hash), brachiopods (dense colonies), corals and stromatoporoids. Some of these occur in discrete biostromal beds. Coral mounds were seen in growth position. The most diagnostic fossil is Halysites.

Norford measured 350 metres of Nonda in the Sikanni Chief section, but this included about 48 metres of the quartzite marker, which the writer has mapped separately. The writer calculates that the Nonda section is about 300 metres (minus quartzite) thick on the slopes north of Sikanni Chief River. Similar thicknesses are noted nearby Riddell (1972, section B-10-72).

The Nonda is relatively homogenous and uniform in thickness within the map area. Just below the southern border of the map area, towards Mt. Kenny, Thompson (1989) noted dramatic facies changes in the Nonda Formation. Tongues of carbonate debris are interlayered with off shelf carbonaceous limestone along the foreslope of a Nonda reef. In the Mt. McCusker area the slope breccia facies of the Nonda Formation is not present.

Quartzite marker unit

The quartzite marker unit, which is up to 50 metres thick and laterally persistent, is in sharp

contact with the rocks of the underlying Silurian Nonda Formation. At one locality, inclined quartzite filled burrow casts were noted at the top of Nonda dolostones; just below the base of the quartzites. Elsewhere quartz filled fracture networks of uncertain origin are present in the dolostone immediately below the first quartzite.

Locally the unit is composed of several massive quartzite beds, up to 10 metres thick. In other areas quartzites a few metres thick are interbedded with paler dolostones and sandy dolostone over 20 to 30 metres. The quartzite beds display abundant intersecting low angle crossbeds and trough crossbeds. The beds are interpreted as marine sand bars, subjected to strong waves and currents, possibly due to a low stand in sea level. According to McHale and Pearson (1974) Silurian fossils persist into overlying beds of the Muncho-McConnell for about 10 metres. The quartzite marker is therefore Silurian in age.

Muncho-McConnell Formation

The Muncho-McConnell Formation consists of pale, fossil-poor, massively bedded dololutes. Locally dolostone can contain discontinuous sand laminae. In other areas bedding is well laminated to crinkly or wavy laminated suggestive of algal origin. MacQueen and Thompson (1978) noted dessication features and flat pebble conglomerate indicative of exposure. The random distribution of spherical quartz grains in dololute suggests an aeolian component.

A breccia unit of potential economic interest lies within the Muncho-McConnell Formation. The unit was found in several locales on separate thrust blocks in about the same stratigraphic position, 70 metres above the quartzite marker. The breccia is described under Structure (see below).

Wokkash, Stone and Dunedin Formations

A thin discontinuous sandy dolostone was locally recognized about 350 metres above the base of the Muncho-McConnell Formation. It does not form a traceable unit, except in the immediate footwall of the Gautschi thrust near Sidenius Ridge, where it forms a crossbedded dolomitic sandstone, 10 to 15 metres thick. This unit typically forms a thin discontinuous interval of sandy dolostone with 10-20% dispersed

quartz. Locally a single half metre of quartzite is interbedded with it.

The Stone Formation is a pale crystalline dolostone that is difficult to distinguish from the Muncho-McConnell, into which it grades. Some alternation in dark and light (sometimes bluish) thick beds is apparent. The unit is most evident in the eastern areas of the map area where it is underlain by thin sandy (Wokkpash) beds.

A thin unit of dark fossiliferous dolostone and limestone is found at the contact with the Besa River shale and is tentatively assigned to the Dunedin Formation. South of Mt. Helen, the Dunedin thins and passes laterally into Besa River shales according to regional maps by Riddell (1972). About 40 metres of Dunedin equivalent dark grey dolomitised carbonate with *Amphipora* is reported near the Sikanni Chief section by Riddell (1972, pg. 28, section F-2-72). Conodont samples were taken in two areas to determine the age of the basal Besa River contact in the McCusker area.

STRUCTURE

The Northern Rocky Mountain front (Main Ranges) near Sikanni Chief River is marked by a large anticline, extending from Mt. Helen across the river to Bartle Creek (Figure 2). A significant section, from Ordovician Skoki to Devonian Stone Formation, is exposed on the east limb of the fold, on the topographic slopes draining southeast into Sikanni Chief River. In the north, the fold is box-like, with the eastern limb subvertical. South of the Sikanni Chief, the fold is overturned, tighter and chevron in form. The west limb of the chevron fold is crumpled into tight folds cut by steep axial plane faults. The Bartle thrust overrides the west limb continuing south of Bartle Creek to the headwalls of the cirques of Bartle Ridge.

Between Bartle Creek and Embree Creek an east northeast trending tear fault offsets quartzite marker beds on the east limb of the fold. The tear fault is related to a secondary, northeast verging, overturned fold.

South of Embree Creek, the eastern overturned limb persists but the amplitude and wavelength of the fold diminishes. Southward toward Sidenius Creek, an additional thrust is mapped west of the Bartle thrust (Figure 3). In essence, the ridges west of the eastern overturned limb consist of two to three thrust panels of repeating

Nonda Muncho-McConnell sequences with overturned folds in the footwalls and hangingwalls.

The Bartle and associated faults lying east of the Gautschi valley show little lateral displacement of hangingwall relative to footwall. The Bartle thrust juxtaposes Ordovician beds over Silurian rocks in the north, whereas in the south Silurian Nonda Formation overrides Devonian rocks. An oblique section across the Bartle thrust is present on the north end of Bartle Ridge overlooking Sikanni Chief River. The view from a vantage point on the north side of the Sikanni Chief suggests a westward steepening of dip in the thrust.

The eastern overturned to subvertical limb along the entire mountain front is much more persistent than individual fold elements. It probably originally constituted the eastern limb of a large south plunging anticlinorium whose western limb is preserved in the Gautschi valley. This crumpled anticlinorium forms the footwall to the Gautschi Valley thrust.

Several late small scale normal faults were noted. At one location, a normal fault displaces a nearly recumbent fold in the footwall of the Bartle thrust, indicating that the normal fault postdates the thrust.

Gautschi Valley thrust (figure 4)

A significant shallowly dipping thrust fault is exposed on the west side of the Gautschi valley. It juxtaposes Ordovician over Silurian rocks in the north, and basal Silurian over Devonian rocks in the south. The westernmost exposures of Devonian beds occur in the footwall of this thrust; they host the principal showing in the area.

McCusker Peak thrust (figure 4)

Topographically above the Gautschi thrust, on the high ridges extending north and south of Mt. McCusker, is a flat-lying thrust with Kechika Group strata exposed in the hangingwall and basal Silurian facies in the footwall. Variable erosion through the thrust has left a klippe to the east and a tectonic window to the west. The klippe indicates that the thrust is flat to the east. Its transect of contour lines in the west indicates that it steepens to the west. Projection of flat dips indicates the thrust should be present on valley walls of western drainages, but it is not. The western side of the tectonic window is

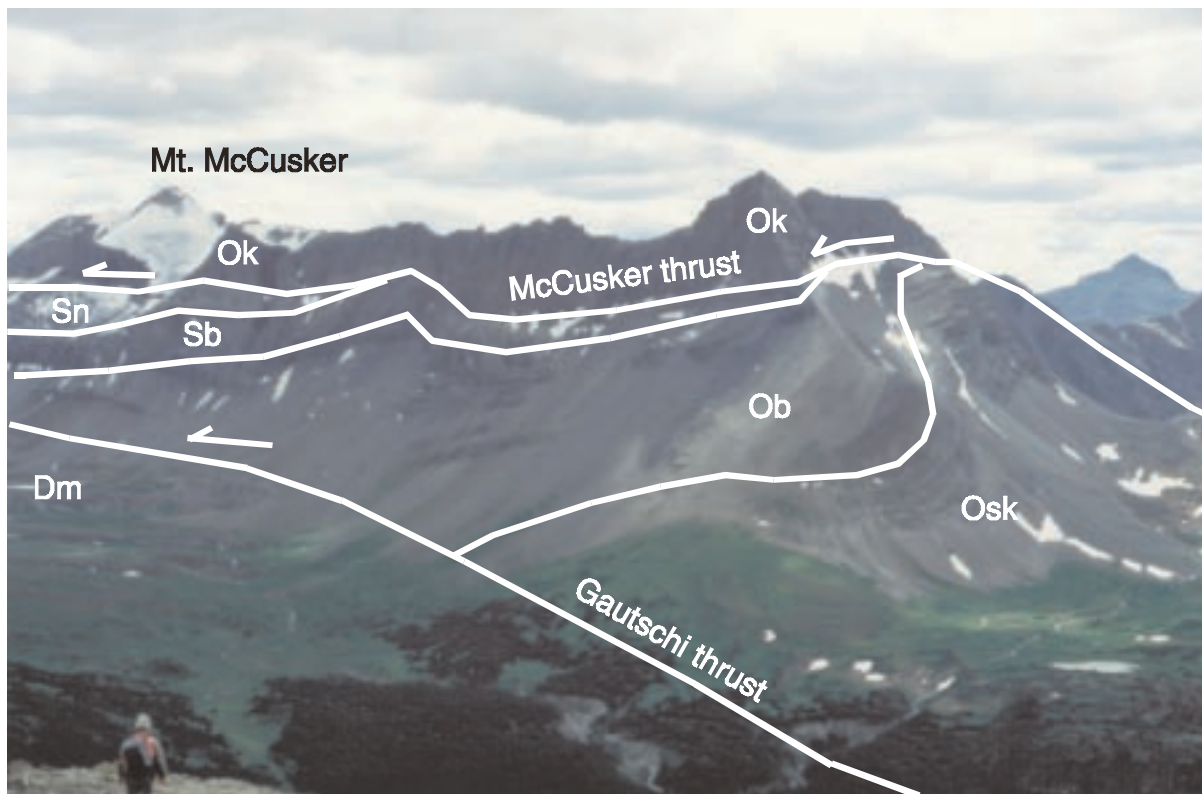


Figure 4. View southwest across Gautschi valley to thrusts at Mt. McCusker.

closed off, an observation that is also compatible with a steep fault dip in the west.

Sidenius thrust

The stratigraphic and vertical interval between the Gautschi and McCusker peak thrusts diminishes southward; in the saddle between Sidenius Ridge and Mt. McCusker the two thrusts are separated by less than a 100 metres of basal Silurian beds (figure 5). On the north side of Sidenius Ridge the thrusts appear to merge and a single west dipping fault cuts the ridge top. This single, possibly ramping thrust of Ordovician Skoki over Muncho-McConnell continues to the south side of Sidenius Ridge. Its strike extension across Sidenius valley appears to be the Sidenius thrust of Thompson (1989). The Sidenius thrust as depicted in cross-section (fig. 5 of MacQueen and Thompson 1978) is a folded thrust with a gentle undulating surface in the east and a steep segment to the west.

Breccias in Muncho-McConnell Formation

A breccia zone in the Muncho-McConnell is present about 70 metres stratigraphically above

the quartzite marker on the west side of the Gautschi valley. The McCusker Minfile showing is located in breccia exposures in the immediate footwall of the Gautschi thrust. To the northwest the breccia zone terminates against the thrust. The breccia zone continues to the southeast where it diverges in trend from the thrust but maintains its stratigraphic position. According to McHale and Pearson (1974) it becomes less prospective in this direction. Initially the Mt. McCusker breccia was thought to lie near a facies front. Subsequent work showed that a covered thrust (the Gautschi thrust) rather than a dramatic facies change was present near the showing. Figure 3 shows this cut off by the Gautschi thrust, an important indicator of its relative age (ie. pre-thrust).

Breccias were found on other structural panels. Evaluation of their position indicates that they are in a comparable stratigraphic position to the McCusker breccia. One of these was slightly gossanous and was sampled for assay with negative results. These particular breccias were not traced along strike due to time constraints. Their presence confirms some stratigraphic, rather than structural, control of brecciation.

The stratiform breccia unit at Mt. McCusker

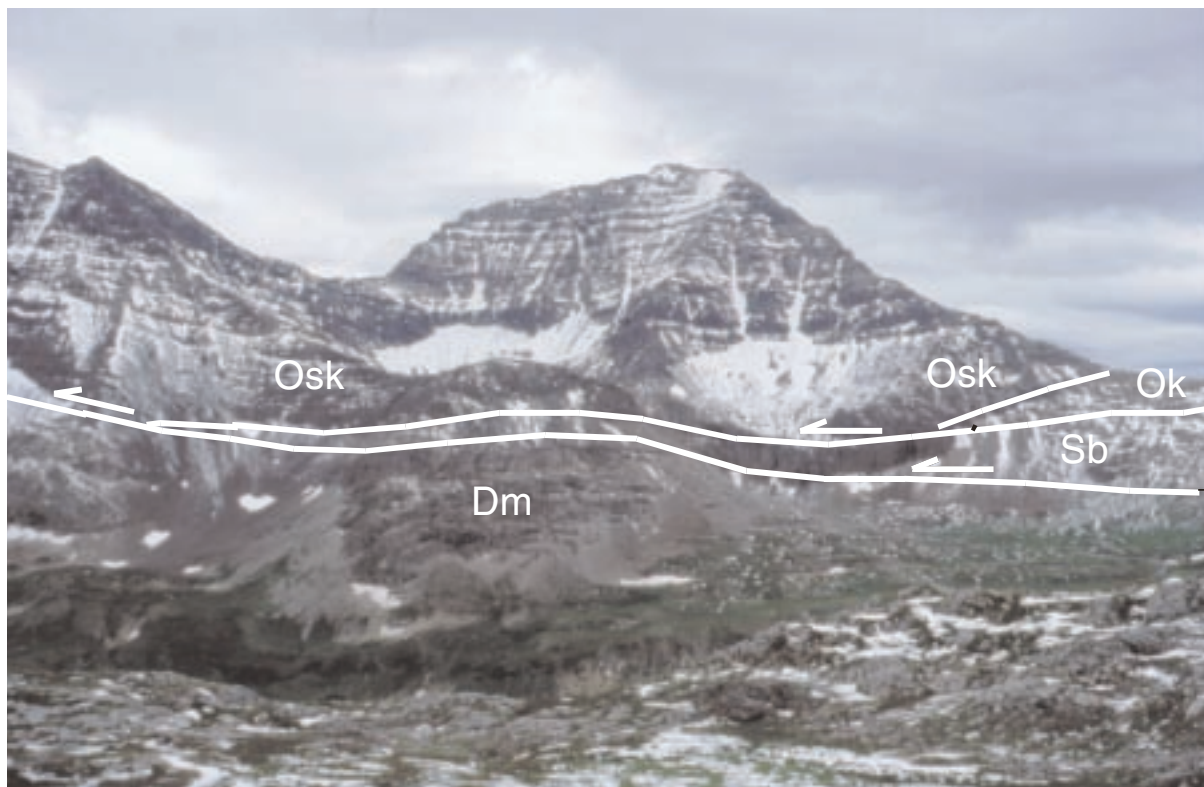


Figure 5. Looking southwest to merging thrusts on Sidenius Ridge.

was traced for several kilometres to the south-east. It varies from “mosaic angular” to “rounded rubble” type with fragments, up to half metre in dimension, enclosed in a coarser recrystallised, often iron stained, yellowish to pale orange-brown dolostone matrix. Brecciation varies widely in intensity. Locally it is pervasively developed across 5 to 15+ metres of stratigraphy, elsewhere it occurs as discrete veins filled with fragments that border undisturbed beds. A few crosscutting limonitic fractures are present. These are quite narrow but crosscut several tens of metres of section. Some fragments in vein breccias are rounded and rotated, the rounding difficult to reconcile with solution collapse.

The spectrum of breccias includes crackle breccias. These extend outside the main stratigraphic zone and into higher stratigraphy. Vug fillings of white calcite and quartz are more common in crackle breccias, with white calcite rinds about some fragments.

At the Mt. McCusker showing, one to two percent combined lead zinc over five to ten metres of section has been reported from chip samples. The best drilling results are 3.58% zinc with trace lead over 1 metre (Williams 1975).

This is a much less significant prospect than Robb Lake. The facies change from Munchon-McConnell dolostone to the brown siltstone unit described at Robb Lake, is not present in the map area. The platformal edge apparently lay further to the west. At this showing proximity to a thrust is not a controlling factor in brecciation, but it may be a factor in the development of weak mineralisation.

COMMENTS AND SPECULATIONS

The ongoing mapping program suggests that the east to west transition from platformal Beaverfoot to basinal Road River strata can be traced across three thrust panels from Bartle Ridge to the Mt. Kenny and the Robb Lake area of the Halfway sheet. On Bartle Ridge, in both the footwall and hangingwall of the Bartle thrust, a shelf edge quartz dolostone unit represents the Beaverfoot. An off shelf facies outcrops in the hangingwall of the Gautschi thrust. Near Robb Lake are equivalent Road River Group strata represented by the quartz graptolite facies of Thompson (1989). This facies is exposed in the hangingwall of a third, more westerly, thrust. The quartz graptolite facies is a deep

water facies that includes quartz turbidites. Thompson (1989) in a composite section indicated it is up to 600 metres thick but Nelson *et al.* (this volume, Fig. 2) found a much thinner interval between the Skoki and Silurian breccia unit at Robb Lake. Further work is warranted. Suffice to say a subsiding basin developed at the end of Skoki time. Thompson (1989) described this basin as the Ospika Embayment, essentially the southern termination of the Kechika Trough. He showed that the embayment endured for a considerable period of time (Late Ordovician to mid Devonian). Significantly his reconstructions (Fig. 7,9) show an indentation in this embayment in the immediate area of Robb Lake.

Work this summer suggests the indentation may be a re-entrant. Between Mount McCusker and Mount Kenny there seems to be a basinal facies trend in the Beaverfoot Formation, development of shelf break facies in the Nonda Formation, and off shelf facies development in the Muncho-McConnell. The re-entrant may have persisted to mid or even upper Devonian time given the anomalously thin Dunedin Formation. (see also Nelson *et al.*, this volume). A local and thickened shale package, rimmed on three sides by platformal carbonates may have been a factor in the subsequent location, size and relative richness of the Robb Lake prospect. It is the only significant prospect known along the Northern Rocky Mountain front.

The presence of a re-entrant shale facies may have facilitated eastern migration of thrusts along surfaces of reduced friction, for example the Sidenius thrust. The identification of re-entrant shales may be an exploration guide to locating other Mississippi valley type deposits in the Northern Rockies.

ACKNOWLEDGEMENTS

Many thanks to Mike Cecile and Larry Lane of the Geological Survey of Canada for an introduction to the geology of the area and Tom Gleeson for good cheer and assistance in the field. The manuscript benefited from review by JoAnne Nelson, Fil Ferri, Bill McMillan and Neil Church of the B.C. Geological Survey. Super thanks to helicopter pilot Duncan Heeren of TurboWest Helicopters who safely flies where only eagles dare.

REFERENCES

- Cecile, M.P. and Norford, B.S. (1979): Basin to platform transition, lower Paleozoic strata of Ware and Trutch areas, northeastern British Columbia; *Geological Survey of Canada*, Paper 79-1A, p. 219-226.
- MacQueen, R.W. and Thompson, R.J. (1978): Carbonate-hosted lead-zinc occurrences in northeastern British Columbia with emphasis on the Robb Lake deposit; *Canadian Journal of Earth Sciences*, volume 15, p. 1737-1762.
- McHale, K.B. and Pearson, B.D. (1974): Geological and Geochemical Report McCusker Claim Groups I,II and III, Liard/Omineca Mining Division; *B.C. Ministry of Energy, Mines and Petroleum Resources*, Mineral Assessment Report 4865.
- Nelson, JoAnne L., Paradis, Suzanne, Zantvoort, Willem (1998): The Robb Lake Carbonate-Hosted Lead-Zinc Deposit, Northeastern British Columbia: A Cordilleran MVT Deposit; in *Geological Fieldwork 1998*, *B.C. Ministry of Energy and Mines*, Paper 1999-1, this volume.
- Norford, B.S., Gabrielse, H. and Taylor, G.C. (1966): Stratigraphy of Silurian carbonate rocks of the Rocky Mountains, northern British Columbia; *Bulletin of Canadian Petroleum Geology*, Volume 14, p. 504-519.
- Riddell, C.H. (1972): Surface Geology, McCusker Area, Northeastern British Columbia; *B.C. Ministry of Energy, Mines and Petroleum Resources*, Petroleum Assessment Report 1761, 51 p.
- Taylor, G.C. (1979): Trutch (94G) and Ware East Half (94F, E1/2) map-areas, northeastern British Columbia; *Geological Survey of Canada*, Open File Report 606.
- Thompson, R.I. (1989): Stratigraphy, tectonic evolution and structural analysis of the Halfway River map area (94B), northern Rocky Mountains, British Columbia; *Geological Survey of Canada*, Memoir 425, 119 p.
- Williams, Michael G. (1975): Geological and geochemical report, LAD, LASS and EL DORADO mineral claims, Liard and Omineca Mining Division; *B.C. Ministry of Energy, Mines and Petroleum Resources*, Mineral Assessment Report 5725.



AGE CONSTRAINTS FOR EMPLACEMENT OF THE NORTHERN CACHE CREEK TERRANE AND IMPLICATIONS OF BLUESCHIST METAMORPHISM

By M.G. Mihalynuk¹, P. Erdmer², E.D. Ghent³, D. A. Archibald⁴, R.M. Friedman⁵,
F. Cordey⁶, G.G. Johannson⁷, and J. Beanish⁴

KEYWORDS: regional geology, Cache Creek terrane, blueschist, isotope geochronology, biogeochronology, fossil, tectonics, French Range Formation, Kutcho Formation, massive sulphide, structure

INTRODUCTION

Ophiolitic and accretionary units and associated blueschists of the Cache Creek terrane constitute the most complete evidence of a coherent subduction zone within the Canadian Cordillera. The rocks occupy a central position in the Intermontane Superterrane, a complex of arcs that includes most of the accreted crust in British Columbia (Figure 1). The Cache Creek terrane contains exotic fossil fauna interpreted to have originated in the equatorial Tethyan realm. In contrast, coeval rocks in adjacent terranes contain fossils endemic to ancestral North America. How this arrangement of terranes can be explained has been the focus of much speculation (see Mihalynuk *et al.*, 1994). It is clear that the Cache Creek terrane plays a central role. Data constraining its history bear on the geodynamic evolution of the Cordillera as a whole.

One of the most complete crustal sections is preserved in the part of the northern Cache Creek terrane known as the Atlin complex (Figure 1; Mihalynuk, 1999). Current understanding of the regional stratigraphy and fossil age

range derives from the work of Monger (1969, 1975). Northern parts of the Atlin complex have been mapped by Hart and Radloff (1990), Hart (1997), and Gordey and Stevens (1994). Studies with a topical focus include those on the origin of enclosed ultramafic rocks (Terry, 1977), their geochemical character, and their recognition as mantle tectonites (Ash, 1994). Isotopic characterization and detailed mapping in the northern Atlin complex by Jackson (1992) revealed that sandstones were derived from the Stikine terrane. Microfossil biostratigraphic studies by Cordey *et al.* (1991, and F. Cordey unpublished data, 1990) showed that the radiolarian-bearing strata range in age from Permian to Early Jurassic. In contrast, the southern portion of the Atlin complex has been less studied. Recent studies include a regional geological compilation by Gabrielse (1998) and detailed mapping of volcanic rocks in the French Ranges near Dease Lake by Mihalynuk and Cordey (1997). Data reported here complement work by Mihalynuk and Cordey (1997) in the French Ranges and Teslin Lake area, and by Mihalynuk *et al.* (1995a,b) in the Tulsequah area.

FRENCH RANGE

Regional units in the French Range were established by Gabrielse (1994) and Monger (1969). Units include Permian mafic volcanic flows and tuff (PFRv) and undifferentiated tuff

¹ British Columbia Geological Survey Branch, PO Box 9320, Stn Prov Govt, Victoria, B.C., V8W 9N3
email: mitch.mihalynuk@gems5.gov.bc.ca

² Department of Earth and Atmospheric Sciences, University of Alberta, Edmonton, Alberta, T6G 2E3

³ Department of Geology and Geophysics, University of Calgary, Calgary, Alberta, T2N 1N4

⁴ Department of Geological Sciences, Queen's University, Kingston, Ontario, K7L 3N6

⁵ Department of Earth and Ocean Sciences, University of British Columbia, Vancouver, British Columbia, V6T 2B4

⁶ Sciences de la Terre - Bat 402, Université Claude Bernard Lyon 1, 69622 Villeurbanne cedex, France

⁷ Decollément Consulting Limited, Suite 200, 1009-7th Avenue SW, Calgary, Alberta, T2P 1A8

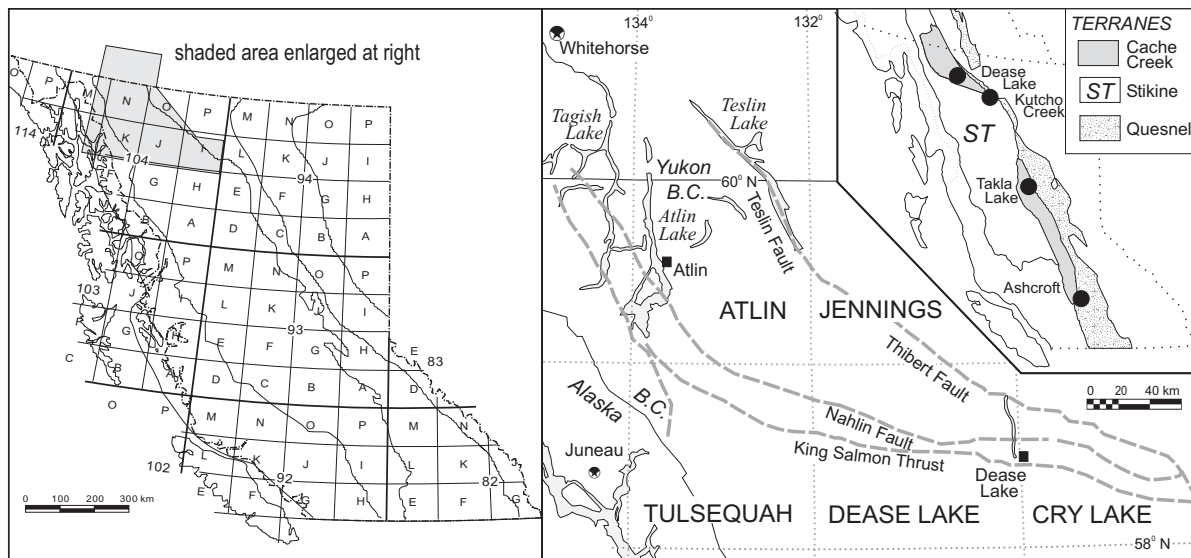


Figure 1. Study areas within and adjacent to the Northern Cache Creek Terrane, named here the Atlin complex. The inset shows the extent of the Cache Creek Terrane and adjacent Stikine (ST) and Quesnel (QN) terranes which together comprise most of the Intermontane Superterrane. Also shown are sites within the Cache Creek terrane where felsic volcanic rocks have been isotopically dated.

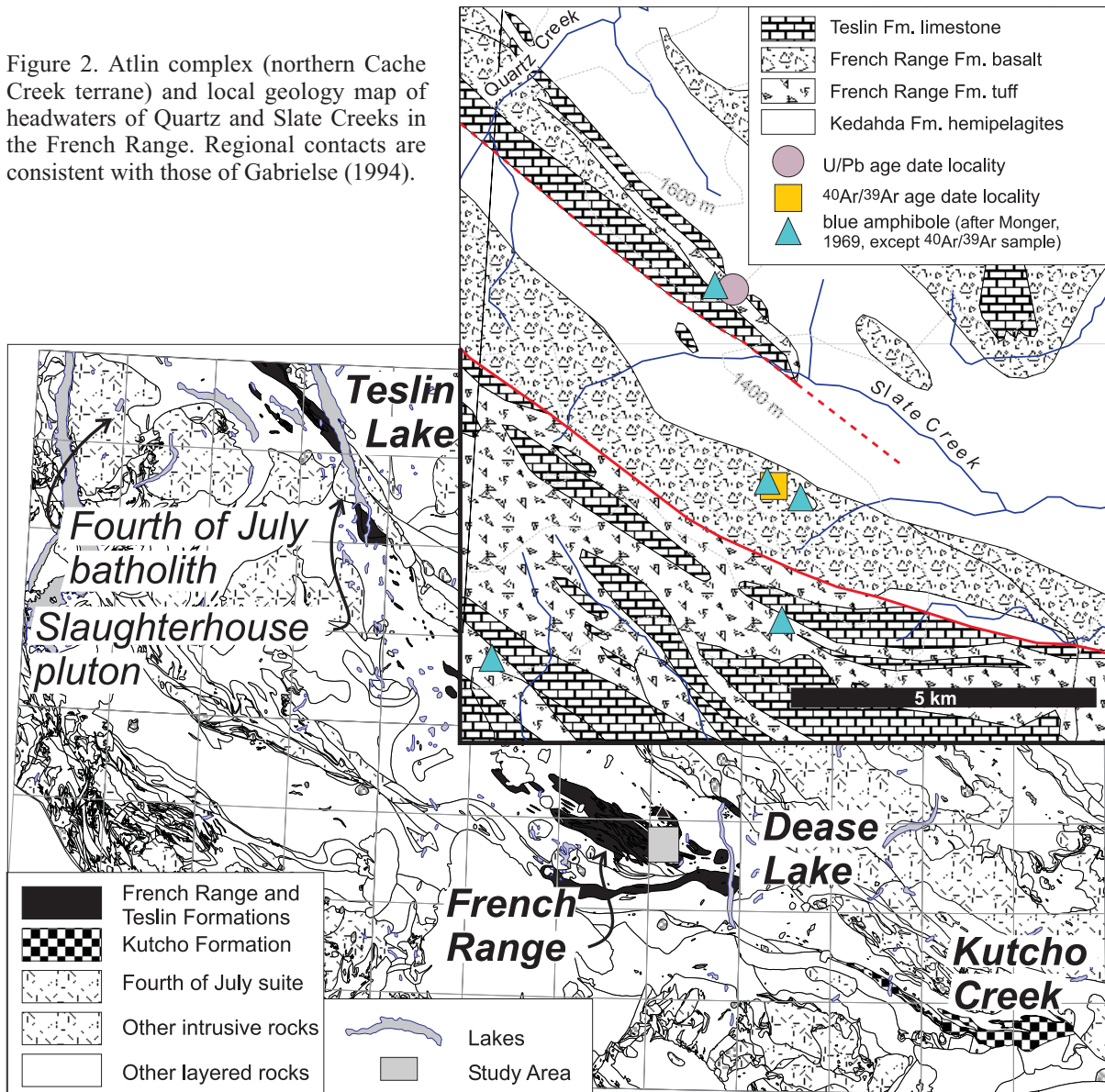
(PFRt) of the French Range Formation, Permian limestone of the Teslin Formation (PT) and stratigraphically and structurally underlying hemipelagic rocks of the Kedahda Formation (MTK, Figure 2). Rocks included regionally in the Kedahda Formation range from Carboniferous to Triassic in age (Gabrielse, 1994). Near the British Columbia - Yukon boundary similar rocks range up to Early Jurassic in age (Jackson, 1992). Over a small area studied in the French Range, radiolarians in the Kedahda formation are Guadalupian (Lower Late Permian) in age. Fusulinids extracted from the Teslin Formation are Leonardian to Guadalupian in age (Monger, 1969, uses the North American stage names *cf.* Figure 8). Detailed geological mapping in the French Range revealed the presence of tholeiitic rhyodacite, correlated on the basis of geochemistry and apparent stratigraphic age with the Kutcho Formation (Mihalynuk and Cordey, 1997). Such a correlation is economically significant because the Kutcho Formation includes cogenetic volcanogenic massive sulphide accumulations. U-Pb isotopic dating of the rhyodacite showed it to be Early Permian (*see* Isotopic Dating below) and significantly older than the Kutcho Formation, although within the range of age determinations (Table 1) from rocks belonging to a belt of felsic volcanic rocks deposited on the Cache Creek terrane that ex-

tends to Ashcroft in southern British Columbia (Figure 1, *see* Table 1 for references).

Basalt tuff, massive fine-grained flow and pillowed flow units are ridge-forming strata at the headwaters of Slate and Quartz Creeks. Individual units are typically 1m to 15m thick. Accumulations of basalt such as on the east end of the Slate Creek ridge attain thicknesses of several hundred metres. Basalt flow rocks contain sparse amygdalae of calcite, chlorite, and, outside the area detailed in Figure 2, stilpnomelane. Basalt to trachyandesite lapilli tuff is locally interlayered with flow units. Basalt tuff is mint green, locally with up to 20% highly vesicular clasts containing coarse bladed plagioclase. Trachyandesite tuff is generally red and displays a weak to moderate foliation. It locally has gradational contacts with limestone or carbonate debris flow units. Some tuffaceous layers appears reworked and display vague ripple cross-stratification.

Rhyodacite tuff contains fine embayed quartz phenocrysts. Clasts display a eutaxitic texture in outcrop (Photo 1). Alteration and blueschist metamorphism are inferred to have destroyed any relict pumice outlines that may have been present, and it is not possible to demonstrate that the banded and flattened nature of volcanic clasts is due to welding rather than to compaction following lithification.

Figure 2. Atlin complex (northern Cache Creek terrane) and local geology map of headwaters of Quartz and Slate Creeks in the French Range. Regional contacts are consistent with those of Gabrielse (1994).



Volumetrically minor but conspicuous ferruginous chert layers up to 0.5 metres thick occur throughout the tuff succession. A red ribbon chert layer about 8 metres thick containing abundant recrystallized radiolarians crops out at two localities within the mafic succession in the middle of the ridge southwest of Slate Creek. Argillaceous partings in the chert are blue as a result of abundant included fine-grained, blue amphibole (Photo 2; Figure 3). Samples of this unit dated by $^{40}\text{Ar}/^{39}\text{Ar}$ technique return a cooling age of about 173 Ma (see Isotopic Dating below).



Photo 1. An outcrop of rhyodacitic lapilli tuff that has eutaxitic textures.

Table 1. Comparison of age data from the Kutcho Fm., Sitlika Assemblage and French Range rhyodacite.

Sample No.	Lithology	Location	Age	Reference
<i>Oldest to youngest</i>				
MMI96-17-7	French Rg. Rhyodacite	Dease Lake	263.1 +1-1.4	This report
"locality C"	metadacite	Taseko Lakes	259±2	Read, 1993
SA-GC-01	Mount Bodine rhyolite	Takla Lake	258+10-1	Childe, 1997
see reference	granodiorite	Taseko Lakes	258±5	Friedman and Van der Heyden, 1992)
"locality B"	leucoquartz monzonite	Taseko Lakes	254±1.2	Read, 1993
97PSC97-22-2	Driver Lake rhyolite	Takla Lake	248.4 ±0.3	Schiarizza et al., 1999
KC-GC-04	footwall rhyolite	Cry Lake	246 +7-5	Childe and Thompson, 1997
KC-GC-03	quartz-feldspar porphyry	Cry Lake	244 ±6	Childe and Thompson, 1997
97PSC97-19-3	Maclaing Ck. tonalite	Takla Lake	243 ±3	Schiarizza et al., 1999
96A-7	tonalite	Ashcroft	242+/-2	Childe et al., 1997
KC-GC-01	hangingwall rhyolite	Cry Lake	242 ±1	Childe and Thompson, 1997
PSC95-16-4	Diver Lake tonalite	Takla Lake	241+/-1	Childe, 1997

Teslin Formation limestone occurs in generally poorly bedded sections that are 400m thick or less and have a combined strike length of at least 5 kilometres. Poorly-bedded sections weather white, buff or pink and are light to dark grey on fresh surfaces. Where sections are well bedded they tend to be dark grey to black with individual beds generally 3 to 15 cm thick. Interbeds of black or red chert and green or maroon ash tuff are common.

Kedahda Formation hemipelagites are dominated by grey-green to tan ribbon chert. In contrast to structurally and stratigraphically higher units, these rocks are strongly disrupted. High amplitude chevron folds (Photo 3) pass downward into strongly transposed layering in



Photo 2. Photomicrograph of argillaceous partings in ribbon chert showing the development of muscovite (Ms) and crossite (Cs) layers with polygonal quartz (Qtz). A weak crenulation folds, but does not recrystallize, the authigenic minerals. The sample is number MMI97-17-4, viewed under cross polarized light. Long dimension of the photograph represents 2.5 mm.

quartz-mica phyllite (Photo 4). This structural disharmony may be the locus of a regionally extensive, low to moderate-angle fault zone. Above the discontinuity, clear evidence of gradational contacts between Kedahda Formation chert and both French Range Formation volcanics and Teslin Formation limestone is present.

TESLIN LAKE AREA

The French Range, Teslin, and Kedahda formations are well exposed west of Teslin Lake where they display similar deformation and contact relationships as in the French Range. Within the broad valley occupied by the southern part of Teslin Lake, the southeast extension of this belt of rocks is mostly covered by thick glacial and alluvial deposits. It is apparently cut (Aitken, 1959) by an undeformed to moderately-foliated quartz diorite body, named the Slaughterhouse pluton (Mihalynuk *et al.*, 1998). Fabric within the pluton is parallel to Teslin Lake and to the Teslin fault, interpreted to underlie the lake. The pluton fabric is inferred to be related to motion on the Teslin fault. As suggested by the contact relationships shown on the map of Aitken (1959), the quartz diorite body is neither strongly elongate nor infolded with the sedimentary succession, and post-dates thrust emplacement of the Cache Creek terrane. The pluton has been dated in two localities by the

U-Pb technique with a Middle Jurassic age indicated (*see* Isotopic Dating below).

TULSEQUAH AREA

Dominantly arc-derived clastic strata of the Whitehorse Trough border the entire 450 kilometre long southwest margin of the Atlin complex, yet they offer no sedimentological indication of its proximity (Johannson, 1994), except in the youngest Laberge Group strata in the Tulsequah area. Thorstad and Gabrielse (1986) reported clasts of the Kutcho and Sinwa formations in the Cry Lake area, but correlation between these units and the Cache Creek Terrane *sensu stricto* is equivocal.

Whitehorse Trough strata in the Tulsequah area are dominated by the conglomerate facies of the Takwahoni Formation (Figures 4 and 5). Macrofossils collected mainly from fine-grained interbeds indicate an age range of Pliensbachian to Bajocian (Table 2, Figure 4). Successively younger conglomerate units contain volcanic, plutonic, and metamorphic clasts, in ascending order, indicative of progressive arc

exhumation (Figure 4). Paleoflow directions are dominantly eastward, consistent with location of the most probable source terrain to the west. A marked change in both paleoflow and provenance occurred in Early Bajocian time. West-directed currents delivered chert granules from the Atlin Complex. Numerous well preserved specimens of the ammonites *Chondroceras* cf. *allani* and *Chondroceras defontii?* from fine clastic units interbedded with chert granule conglomerate indicate an age of latest Early Bajocian (Table 2).

Radiolarians in chert clasts (Table 3) range from Early Permian through Lower Jurassic in age, which overlaps with the ages of all but the oldest (Carboniferous) chert of the Atlin Complex. A minimum age of the chert source is based on the radiolarian species *Praeconocaryomma* cf. *immodica* Pessagno and Poisson which ranges from Pliensbachian to Toarcian in age. Thus, in Early Bajocian time, all but the lowest levels of the Kedahda Formation appear to have been tectonically exhumed.

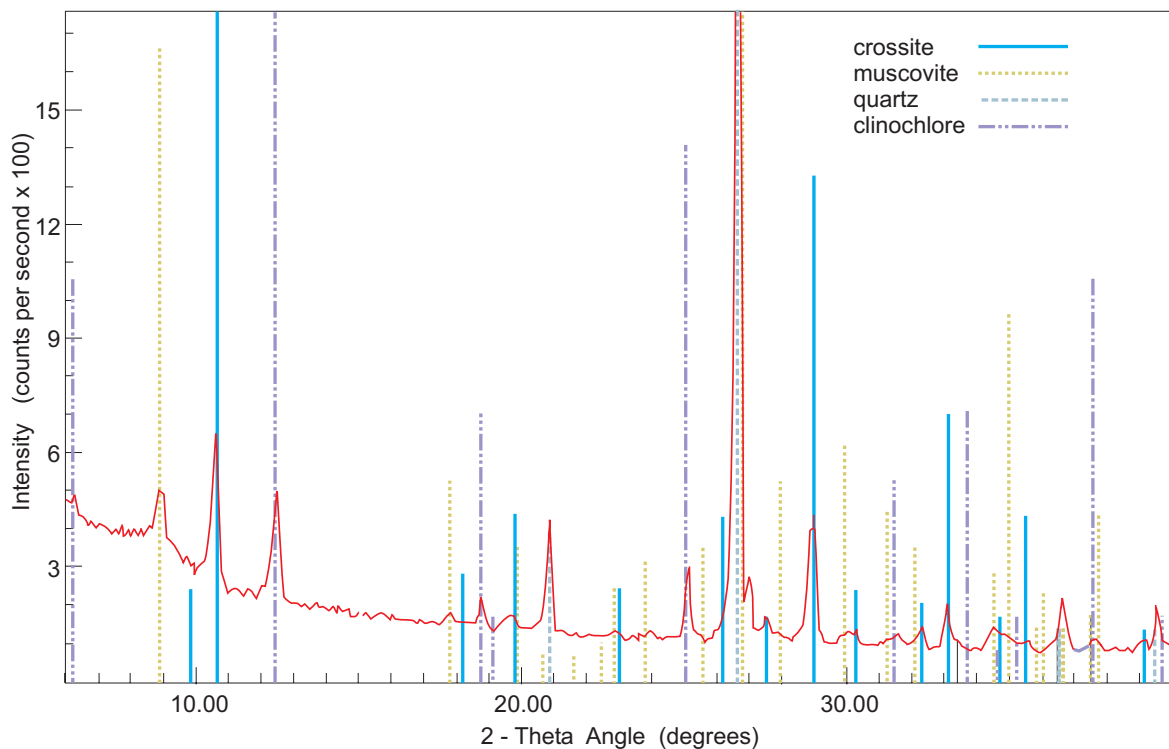


Figure 3. Interpreted X-ray diffraction spectrum from blueschist sample MMI96-17-4 showing that the mineralogy is dominated by quartz, muscovite, crossite and ferroan clinochlore.

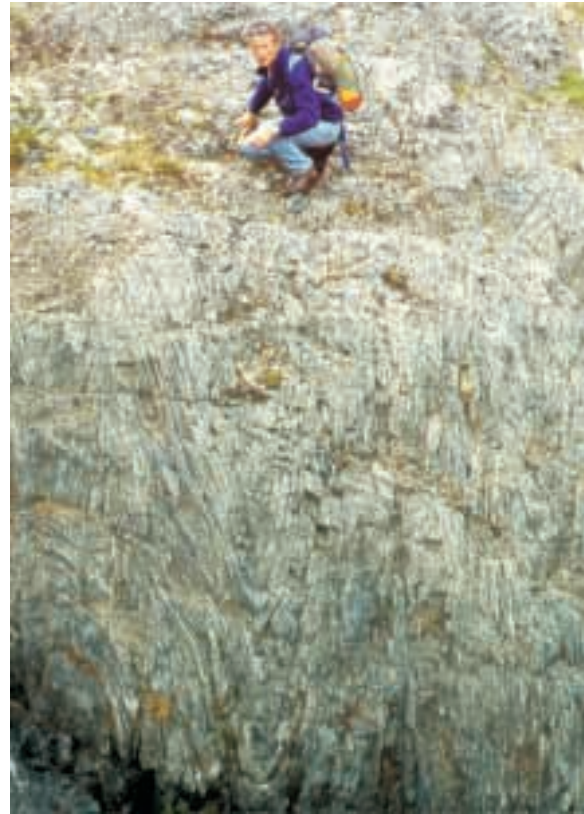
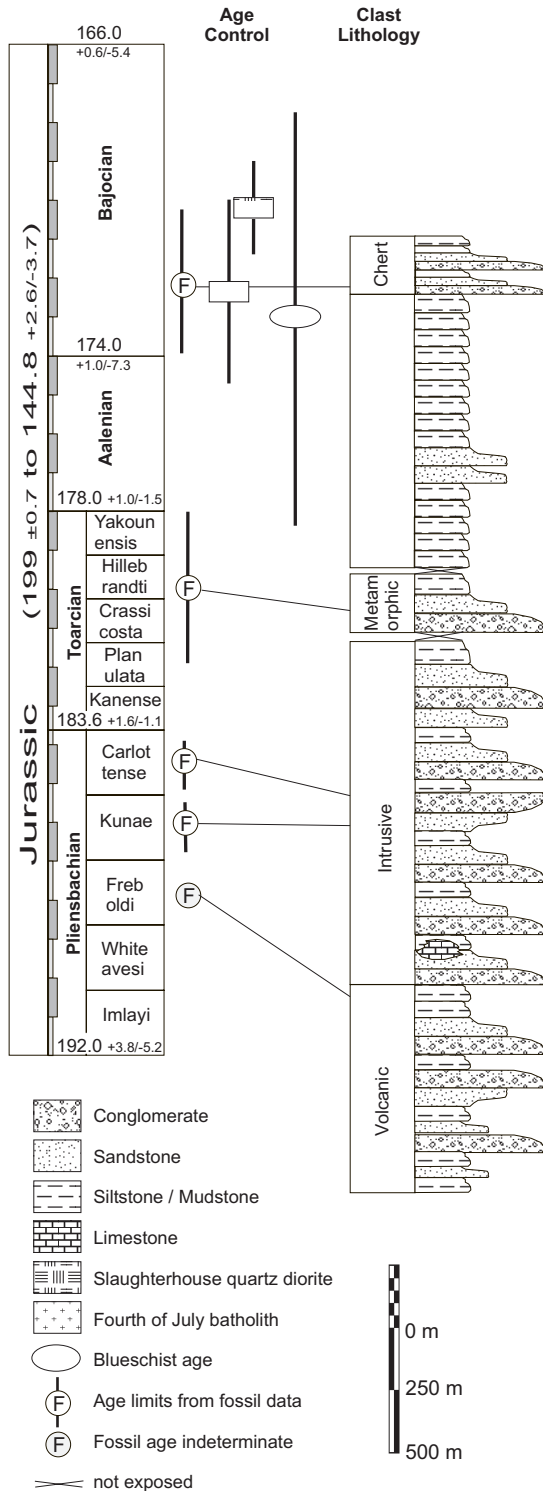


Photo 3. High-amplitude chevron folds deform ribbon chert near the contact with overlying, relatively weakly deformed French Range Formation mafic volcanics.

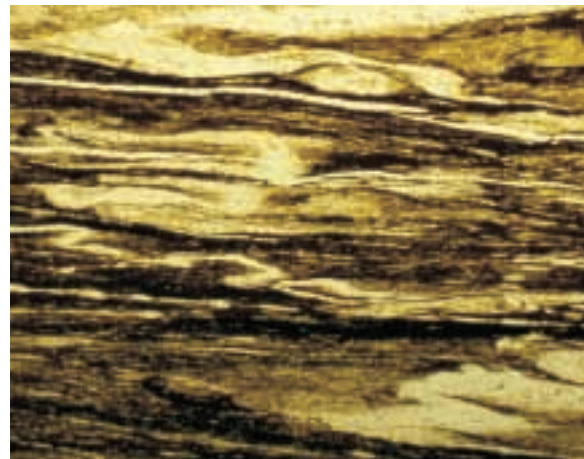


Photo 4. Photomicrograph of strongly transposed layering of deformed hemipelagite, now quartz-muscovite schist, located structurally below the rocks shown in Photo 3. Long dimension of the photograph represents 2.5 mm. Viewed in plane polarized light.

Figure 4. Laberge Group stratigraphy of the northeast Tulsequah area. Conglomerate composition records unroofing of the Stuhini arc. Youngest conglomerates are chert-rich and derived from the Cache Creek terrane. The fossil ages are calibrated against the revised Jurassic time scale of Pálffy *et al.* (1998).

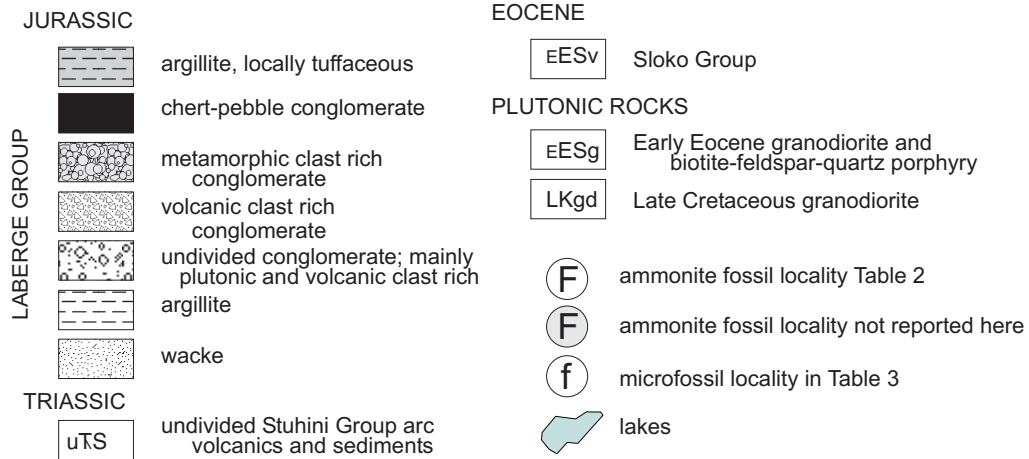
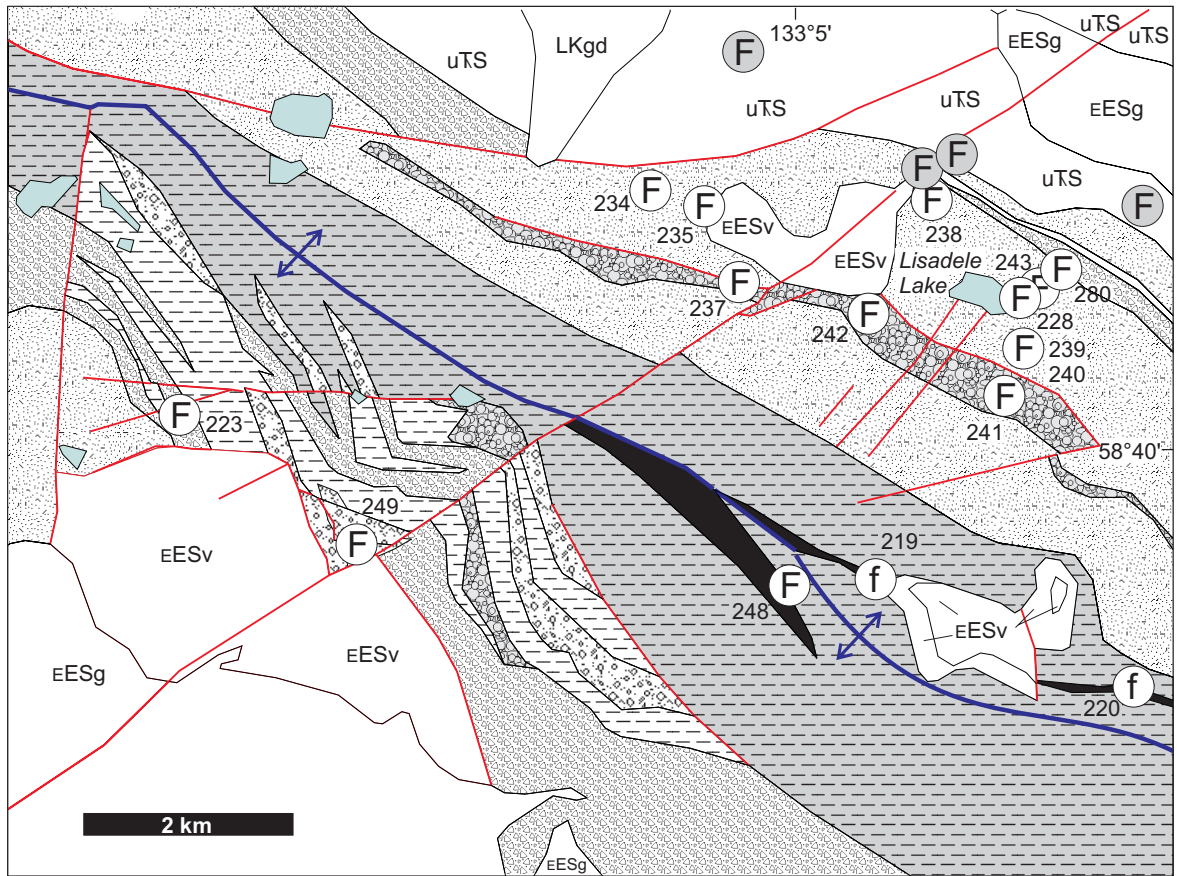


Figure 5. Simplified regional geology of the Lisadele Lake area, 104K/11NE, after Mihalynuk *et al.*, 1995b.

Table 2. Ammonite age determinations from the central Tulsequah area.

Field Number	Location	Fauna	Age
GJ094-41-8 GSC C208234	Bug Pk.	<i>Protogrammoceras paltum</i> , <i>Fieldingiceras fieldingii?</i> , <i>Lioceratoides</i> sp., <i>Arieticer</i> sp. Comments: Numerous specimens of complete and fragmentary ammonites. Poorly- to well-preserved	Upper Pliensbachian -Carlottense Zone
GJ094-41-9 GSC C208235	Bug Pk.	<i>Dactylioceras kanense?</i> , <i>Dactylioceras</i> spp., <i>Taffertia tafferentis?</i> , <i>Protogrammoceras paltum?</i> , <i>Ovaticeras?</i> Sp. Comments: ten specimens of poorly- to well-preserved whole and fragmentary ammonites.	Lower Toarcian - base? of Kanense Zone
GJ094-4 1 -10 GSC C208237	Bug Pk.	Ammonite gen. et sp. indet. Comments: one large moderately preserved ammonite fragment. Collected from talus 300 m. SE. of GJ094-41-9 (L. Toarcian) from similar stratigraphic level.	Lower? Toarcian?
GJ094-42-5 GSC C208238	Lisadele Lk.	<i>Arieticer</i> sp., <i>Fucinicer</i> sp., <i>Protogrammoceras?</i> sp. Comments: five complete and fragmentary ammonites. Poorly- to well-preserved.	Upper Pliensbachian
GJ094-42-12	Lisadele Lk.	<i>Protogrammoceras paltum?</i> Comments: two moderately- to well-preserved fragments.	Upper Pliensbachian probable Carlottense Zone
GJ094-43-1 GSC C208239	Lisadele Lk.	<i>Dactylioceras</i> sp., <i>Hildaites</i> cf. <i>murleyi</i> Comments: four moderately-preserved ammonite fragments.	Lower Toarcian -Kanense Zone
GJ094-43-1-2 GSC C208240	Lisadele Lk.	Ammonite gen. et sp. indet. Comments: seven poorly- to moderately-preserved whole and fragmentary ammonites. Collected - 80 m. upsection from GJ094-43 1 (Lower Toarcian).	Lower? Toarcian
GJ094-43-3 GSC C208241	750m S of Lisadele Lk.	<i>Pseudolioceras</i> cf. <i>lythense</i> Comments: two specimens: moderately-preserved whole ammonite + small fragment. Associated with 'metamorphic' conglomerate.	Middle Toarcian -possibly upper Planulata Zone
GJ094-43-6 GSC C208242	1km WSW of Lisadele Lk.	<i>Podogrosites latescens</i> Comments: one very well-preserved whole ammonite. Associated with 'metamorphic' conglomerate.	Upper Toarcian - Hilldebrandti Zone
GJ094-44-2 GSC C208243	Lisadele Lk.	<i>Tiltoniceras antiquum</i> , <i>Arieticer</i> sp., <i>Lioceratoides</i> spp. (including <i>L grecoi?</i>), <i>Protogrammoceras paltum?</i> , <i>Lioceratoides (Pacificer)</i> spp., <i>Fieldingiceras?</i> Sp. Comments: numerous specimens of complete and fragmentary ammonites. Poorly to well-preserved.	Upper Pliensbachian - Carlottense Zone
GJ094-44-3 N/A	Lisadele Lk.	<i>Leptaleoceras accuratum</i> , <i>Amaltheus stokesi?</i> , <i>Protogrammoceras</i> spp., <i>Fanninoceras?</i> sp. Comments: missing collection. Fauna listed are from field identifications and cannot be verified but are certainly Upper Pliensbachian (e.g. <i>Amaltheus</i> sp.).	Upper Pliensbachian - Kunae Zone
CHA94-46-1 GSC C211256		<i>Metaderoceras?</i> sp., <i>Weyla bodenbenderi?</i> , <i>Vaugonia</i> sp., belemnoid Comments: five moderately- to well-preserved fragmentary specimens (includes 2 ammonites).	Lower? Pliensbachian
MM194-19-8 GSC C211248	3km SSW of Lisadele Lk.	<i>Chondrocer</i> cf. <i>allani</i> , <i>Chondrocer defontii?</i> , Ammonite gen. et sp. indet. Comments: numerous specimens of moderately to well-preserved fragmentary ammonites. Associated with 'chert' conglomerate.	latest Lower Bajocian
MM194-20-6 GSC C211249	7km SW of Lisadele Lk.	<i>Tiltoniceras antiquum?</i> , <i>Protogrammoceras</i> spp., <i>Fontanelliceras</i> sp., <i>Lioceratoides</i> sp Comments: numerous specimens of complete and fragmentary ammonites. Poorly- to well-preserved.	Upper Pliensbachian - Carlottense Zone

Table 3. Radiolarian age determinations from chert granules in Bajocian conglomerate.

SAMPLE No	LOCATION	RADIOLARIAN TAXA	AGES REPRESENTED
MMI94-19-6 (clasts) GSC: C-208219	104K/11 Lisadele Lk.	<i>Canesium lentum</i> Blome, <i>Canoptum</i> sp., <i>Capnodoce</i> sp. - <i>Capnuchosphaera</i> sp., <i>Corum</i> cf. <i>perfectum</i> Blome, <i>Pachus</i> sp., <i>Pseudoeucyrd</i> (?) sp., <i>Praesarla</i> sp., <i>Praeconocaryomma</i> cf. <i>immodica</i> Pessagno and Poisson <i>Pseudostylosphaera</i> cf. <i>acrior</i> Bragin, <i>Xipha striata</i> Blome, <i>Yeharaia elegans</i> Nakaseko and Nishimura COMMENTS: preservation is good, geological unit is Laberge Group, lithology is chert pebble conglomerate. The association is a mixing of radiolarians of various ages extracted from several chert clasts and chips. Also contains sponge spicules (non diagnostic).	Middle Triassic (late Anisian-Ladinian) Middle Triassic (late Anisian-early Ladinian) Late Triassic (Carnian-middle Norian) Late Triassic (late Carnian- Middle Norian) Early Jurassic (Pliensbachian-Toarcian)
SSE94-48-9 (matrix) GSC: C-208220	104K/11	occurrence of radiolarians not established COMMENTS: geological unit is Laberge Group, lithology is chert pebble conglomerate	undetermined
SSE94-48-9 (clasts) GSC: C-208220	104K/11	<i>Canoptum</i> sp., <i>Capnodoce anapetes</i> De Wever, <i>Capnodoce</i> sp., <i>Oertlispongidae</i> -type rods, <i>Pachus</i> cf. <i>longinquus</i> Blome, <i>Plafkerium</i> sp., <i>Pseudoalballielia</i> aff. <i>scalprata</i> Holdsworth and Jones, <i>Pseudoeucyrd</i> (?) sp., <i>Praeconocaryomma</i> cf. <i>immodica</i> Pessagno and Poisson, <i>Pseudostylosphaera</i> cf. <i>acrior</i> Bragin, <i>Quinqueremis</i> sp. COMMENTS: preservation is moderate, geological unit is Laberge Group, lithology is chert pebble conglomerate. The association is a mixing of radiolarians of various ages extracted from several chert clasts and chips. Also contains sponge spicules (non diagnostic).	Early Permian (Sakmarian-Artinskian) Middle Triassic (late Anisian-Ladinian) Late Triassic (Late Carnian-Middle Norian) Early Jurassic (Pliensbachian-Toarcian)
SVA94-2-4 (matrix) GSC: C-208221	104K/11	occurrence of radiolarians not established COMMENTS: geological unit is Laberge Group, lithology is chert pebble conglomerate. Also contains arge sphaeromorphs.	undetermined
SVA94-2-4 (clasts) GSC: C-208221	104K/11	? <i>Capnodoce</i> sp., ? <i>Kalherosphaera</i> sp., ? <i>Plafkerium</i> sp., ? <i>Sarla</i> sp., <i>Thurstonia</i> sp. COMMENTS: preservation is poor, geological unit is Laberge Group, lithology is chert pebble conglomerate. The association is a mixing of radiolarians of various ages extracted from several chert clasts and chips.	possibly Middle or Late Triassic possibly Late Triassic (late Carnian-Middle Norian) Early Jurassic (Hettangian-Toarcian)

ISOTOPIC DATING

⁴⁰Ar/³⁹Ar age for blueschist

Phyllitic to weakly schistose red and blue ribbon chert interlayered with volcanic rocks of the French Range Formation was selected for ⁴⁰Ar/³⁹Ar age determination. Red layers are ferruginous chert. Blue layers are metapelite composed of quartz, muscovite, crossite, and ferroan clinocllore (Figure 3). Layer-parallel schistosity in the metapelite is weakly crenulated, and both muscovite and crossite display undulatory extinction (Photo 2). The grain size of these minerals is 40 microns or less. A magnetic method of separation of minerals produced a non-magnetic split that was quartz rich,

with resultant low overall potassium content and relatively high uncertainty for the ⁴⁰Ar/³⁶Ar age obtained.

Analysis of a non-magnetic fraction of sample MMI96-17-4Bwr produced the spectrum shown in Figure 6. Four of ten heating steps accounted for more than 50% of the ³⁹Ar released and were combined to define a plateau date of **173.2 ± 7.6 Ma (2σ)**, interpreted to be the closure age. Close correspondence between the plateau date, the integrated date of 175.2 ± 9.2 Ma (2σ), and the correlation date of 171.1 ± 9.6 Ma (2σ), as well as an ⁴⁰Ar/³⁶Ar ratio equal to atmospheric argon within error (325 ± 84) support the interpretation of a undisturbed closure notwithstanding the crenulation fabric of the blueschist minerals.

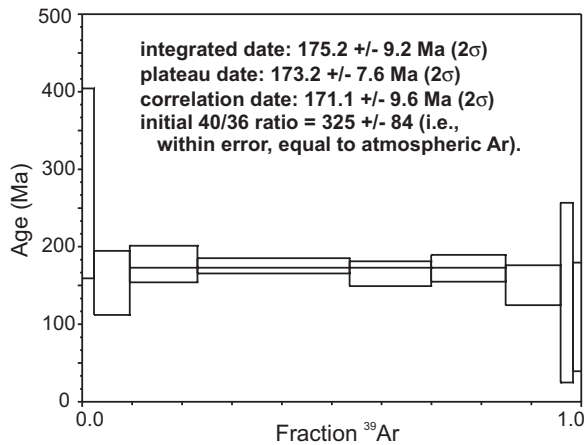


Figure 6. Step heating $^{40}\text{Ar}/^{39}\text{Ar}$ age spectrum for French Range blueschist sample MMI96-4Bwr.

U/Pb ages

Complete U-Pb age data for a sample of rhyodacite from the French Range Formation are reported here (Table 4). The data provide an absolute age for rocks of unequivocal Cache Creek Terrane affinity in the Atlin complex. A quartz porphyritic rhyolite at the Kutcho deposit in the Cry Lake area was dated by Childe *et al.* (1997), but its relationship to the Cache Creek terrane is equivocal.

Zircon recovered from French Range Formation rhyodacite tuff (sample MMI96-17-7) is clear, colourless to pale pink, and of stubby to elongate prismatic morphology. Three analysed fractions are concordant at about 260 to 265 Ma. An age of **263.1±1.0/-1.4 Ma**, is based on the average $^{206}\text{Pb}/^{238}\text{U}$ results for concordant fractions A and C (Figure 7, Table 4).

Two samples of the Slaughterhouse quartz diorite from the south end of Teslin Lake were dated. As discussed above, this body appears to cut the deformed, inboard edge of the Cache Creek terrane. Preliminary U-Pb isotopic data yielded dates of **170.2±1.2 Ma** (Mihalynuk *et al.*, 1998) and **168 to 175 Ma**. These provisional dates confirm age constraints provided by the 171.7 ± 3 Ma Fourth of July pluton, which cuts emplacement-related structures (Mihalynuk *et al.*, 1992) on the outboard edge of the Atlin complex.

AGE CONSTRAINTS: IMPLICATIONS AND DISCUSSION

Isotopic age data reported here have implications for the correlation of the French Range Formation, the position of the Guadalupian stage boundaries, the age of emplacement of the Atlin complex, and the mechanism of blueschist exhumation in the French Range.

Correlation of the French Range and Kutcho Creek formations was suggested by Mihalynuk and Cordey (1997) on the basis of: occurrence within the Cache Creek Terrane (*e.g.* Monger *et al.*, 1991), felsic volcanic character, comparative volcanic chemistry, and similar ages. However, absolute age constraints for Permian stage boundaries are poor (Harland *et al.*, 1990) and an isotopically determined protolith age for the French Range Formation was required to test the proposed correlation. The new U-Pb age data from the French Range rhyodacite show that the French Range rocks are significantly older than the Kutcho Formation (263 Ma versus 242 Ma; Table 1). Recent work on felsic strata of presumed Cache Creek terrane affinity revealed isotopic ages that range from 263 (the French Range Formation) to 241 Ma to (the Kutcho Formation (see Table 1). The French Range rhyodacite is the oldest dated felsic unit, making it the earliest evidence of an intra-oceanic arc built upon oceanic crust of the Cache Creek terrane. If Kutcho Formation volcanic rocks represent part of the same arc, that arc was active for at least 20 m.y.. This possibility carries significant metallogenic and paleogeographic implications. The age of Cache Creek terrane

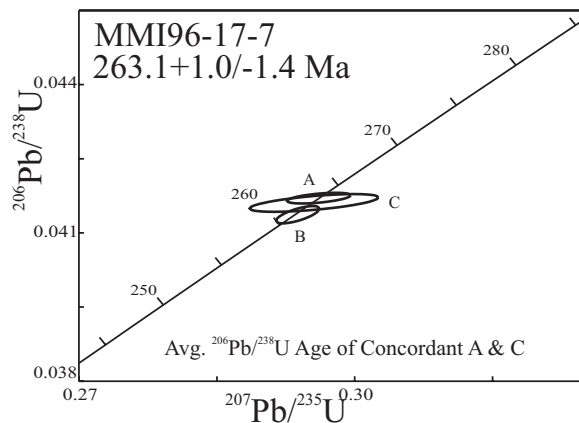


Figure 7. U-Pb concordia diagram for Sample MMI96-17-7.

Table 4. U/Pb isotopic data, French Range rhyodacite, sample MMI96-17-7.

Fraction ¹	Wt mg	U ² ppm	Pb* ³ ppm	²⁰⁶ Pb ⁴ ²⁰⁴ Pb	Pb ⁵ pg	²⁰⁸ Pb ⁶ %	Isotopic ratios (1σ, %) ⁷			Apparent ages (2σ, Ma) ⁷	
							²⁰⁶ Pb/ ²³⁸ U	²⁰⁷ Pb/ ²³⁵ U	²⁰⁷ Pb/ ²⁰⁶ Pb	²⁰⁶ Pb/ ²³⁸ U	²⁰⁷ Pb/ ²⁰⁶ Pb
MMI96-17-7											
A c,N20,p	0.080	117	5	556	46	17.3	0.04170 (0.13)	0.2961 (0.59)	0.05150 (0.53)	263.4 (0.7)	263 (24)
B m,N20,p	0.088	110	5	1237	21	17.0	0.04137 (0.21)	0.2938 (0.40)	0.05151 (0.29)	261.3 (1.1)	264 (13/14)
C c,N20,p	0.142	85	4	194	178	16.0	0.04160 (0.21)	0.2956 (1.2)	0.05152 (1.1)	262.8 (1.1)	264 (48/50)

Notes: Analytical techniques are listed in Mortensen et al. (1995).

¹ Upper case letter fraction identifier; All zircon fractions air abraded; Grain size, intermediate dimension: cc 180 μm and 134 μm, c 134 μm and 104 μm, m 104 μm and 74 μm, f 74 μm. Magnetic codes: Franz magnetic separator sideslope at which grains are nonmagnetic (N) or Magnetic (M); e.g., N1 nonmagnetic at 1 ; Field strength for all fractions 1.8A; Front slope for all fractions 20 ; Grain character codes: b broken fragments, e elongate, eq equant, p prismatic, s stubby, t tabular, ti tips.

² U blank correction of 1-3pg ± 20%; U fractionation corrections were measured for each run with a double ²³³U-²³⁵U spike (about 0.005/amu).

³ Radiogenic Pb

⁴ Measured ratio corrected for spike and Pb fractionation of 0.0043/amu ± 20% (Daly collector) and 0.0012/amu ± 7% and laboratory blank Pb of 10 pg ± 20%. Laboratory blank Pb concentrations and isotopic compositions based on total procedural blanks analysed throughout the duration of this study.

⁵ Total common Pb in analysis based on blank isotopic composition

⁶ Radiogenic Pb

⁷ Corrected for blank Pb, U and common Pb. Common Pb corrections based on Stacey Kramers model (Stacey and Kramers, 1975) at the age of the rock or the ²⁰⁷Pb/²⁰⁶Pb age of the fraction.

rocks with potential for felsic volcanic associated massive sulphide deposits can now include Late Permian as well as earliest Triassic. Also, a geodynamic problem that may be resolved is the apparent narrow time constraint for transporting Cache Creek terrane strata from a Tethyan realm in the Late Permian to a north American realm in the Late Triassic. An intra-oceanic Permian-Triassic subduction zone, in addition to the one inferred beneath the Stikine and Quesnel terranes, would double the consumption of oceanic crust and increase the amount of conveyor belt-like transport of Cache Creek strata.

Stage boundaries of the Late Permian time scale are imprecise and currently under revision. Rhyodacite in the French Range appears to be over- and underlain by Early and Late Guadalupian limestone (Monger, 1969). Guadalupian age limits are not considered *sensu stricto* in the time scale of Harland *et al.* (1990), but the Kazanian stage, which encompasses most of the Guadalupian, is restricted to 254 +18.8/-7.2Ma and 250.5 +3.5/-13Ma (Figure 8; this is within a “permissive” range of 273 to 237.5 Ma). Recent, U-Pb age dating of a volcanic ash unit at the Permian-Triassic boundary has yielded an age of 251 Ma (Renne *et al.*,

1995; Bowring *et al.*, 1998); resolution of other Permian stage boundaries is lacking.

Our petrographic analysis of samples collected from both the Slate Creek and Quartz Creek ridges augments data of Monger (1969), who reported blueschist minerals in the area. Crossite, lawsonite, riebeckite, and ferro-glaucophane occur over an area of at least 5 by 8 km. This areal distribution of min-

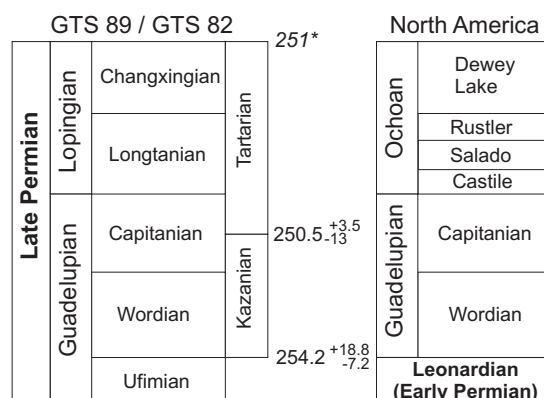


Figure 8. A comparison of International (Harland *et al.*, 1990) and North American stage boundaries for the Late Permian. A new Permian-Triassic boundary age from Renne *et al.* (1995, 251*Ma) is inconsistent with that of Harland and others.

eral assemblages indicates that a coherent crustal fragment several tens of square kilometres in size underwent blueschist facies metamorphism. Pressure and temperature conditions are shown in the shaded stability field of Figure 9.

The imprint of peak blueschist metamorphism is interpreted to have been recorded by the $^{40}\text{Ar}/^{39}\text{Ar}$ age spectra, and to be around 173 Ma. This is the youngest blueschist age in the Intermontane Superterrane (Erdmer *et al.*, 1998). On the basis of ages of crosscutting plutons, the blueschists must have been rapidly exhumed during emplacement of the Atlin complex along structures which ceased to be active by 172 to 170 Ma. Rapid exhumation at this time is recorded in sedimentation in the Whitehorse Trough with the introduction of chert pebbles derived from the Atlin complex. A late Early Bajocian age for this change is based on the occurrence of fossils in the Tulsequah area (see above, and Table 2). Revision of the Jurassic time scale (Pálffy *et al.*, 1998) placed the Bajocian lower boundary at $174 \pm 1.0/-7.3$ (Figure 4). By interpolation, late Early Bajocian would be about 171 Ma. The youngest chert clasts within the conglomerate are Pliensbachian to Toarcian ($192 \pm 3.8/-5.2$ Ma to $178 \pm 1.0/-1.5$ Ma), similar in age to the youngest chert dated by radiolarians in the Atlin complex

(Cordey *et al.*, 1991). The youngest chert-rich units display evidence of basin narrowing and instability. Wacke, rather than argillite, is interbedded with ribbon chert, and basin cannibalization is recorded by chert sharpstone conglomerate interbedded with chert layers. This time interval corresponds with a shift in either ocean current circulation or the paleolatitude of the Whitehorse Trough, as indicated by ammonite paleobiogeography. Late Pliensbachian ammonite faunas include the Tethyan taxa *Arietoceras*, *Leptaleoceras*, *Lioceratoides*, *Protogrammoceras*, *Fontanelliceras* and *Fieldingiceras*, and the Boreal taxa *Amaltheus* and *Tiltoniceras*, indicating a sub-Boreal paleogeography at this time (mixed faunal realm; Smith & Tipper, 1986). In contrast, Toarcian taxa are dominated by pandemic forms but include the Boreal species *Dactyloceras commune* and the high-latitude genus *Pseudolioceras*, indicating a Boreal paleogeography by Early to Middle Toarcian time.

Tectonic events causing changes in basin morphology and paleogeography recorded by changes in depositional and faunal character are speculative. However, the new data allow updating of the tectonic model presented by Mihalyuk *et al.* (1994). In that model, relicts of the Cache Creek ocean basin were consumed beneath two converging and oppositely polarized segments of the same subduction zone as a result of oroclinal bending of the arc complex (an updated model, which is constrained by the data presented here, is shown in Figure 10). As the basin narrowed, wacke derived from flanking arc segments clogged the trench and flowed toward the basin axis. Flexure of the old, colder oceanic crust formed horsts and grabens and widespread chert sharpstone deposition at fault scarps. Basin isolation in the Toarcian resulted in changes of ocean circulatory patterns, cooler water temperature, and a predominance of Boreal ammonite fauna, around 185 Ma. Increasing flexure could not be sustained, and the oceanic crust ruptured in the Early Bajocian, at approximately 173 Ma. (In north-central British Columbia, sediments of the Bowser Basin may preserve older evidence of incipient Cache Creek obduction. According to Ricketts *et al.* (1992) a condensed section of Aalenian shale records flexural subsidence due to earliest thrust-

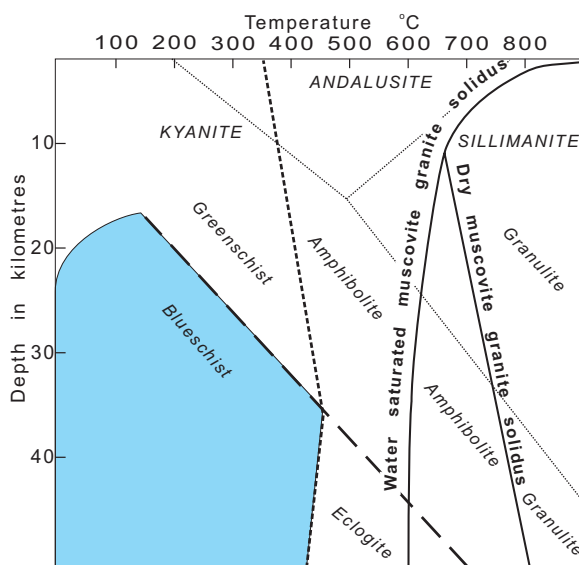


Figure 9. P-T stability limits for blueschists (shaded).

ing.) A rigid cratonic back-stop helped the inboard oceanic crustal fragment ride over hinterland rocks. Blueschists formed in the inboard subduction zone would have been rapidly exhumed by southwest-verging thrusts. The timing and sense of displacement of the structures inferred to have accommodated exhumation remain unclear but the process preserved the coherence of high-pressure metamorphosed rocks over areas of tens of square kilometres. The preserved coherent stratigraphy in the French Range rocks obviates the possibility of outcrop-scale structural dismembering commonly inferred for accretionary tectonic settings. Plutons cut emplacement fabrics at 172 and 170Ma. Clasts derived from chert of the exhumed oceanic crust invaded the Whitehorse Trough by about 171Ma.

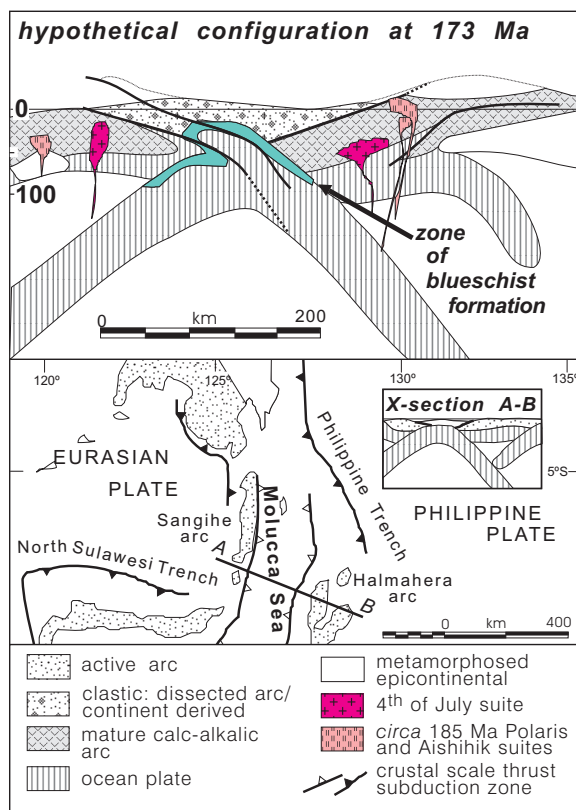


Figure 10. Model for blueschist emplacement at 173 Ma, modified after Mihalynuk *et al.* (1994). Top: a hypothetical cross section at about 173Ma shows rupture of doubly subducting Cache Creek oceanic crust. Bottom: a modern day analogue, the Molucca Sea region, in which a similar double subduction zone is interpreted.

REFERENCES CITED

- Aitken, J.D., (1959): Atlin Map-area, British Columbia; *Geological Survey of Canada*, Memoir 307, 89 pages.
- Ash, C.H. (1994): Origin and tectonic setting of ophiolitic ultramafic and related rocks in the Atlin Area, British Columbia (NTS 104N); *B.C. Ministry of Energy, Mines and Petroleum Resources*, Bulletin 94, 48 pages.
- Bowring, S.A. and Erwin, D.H. (1998): A new look at evolutionary rates in deep time: uniting paleontology and high-precision geochronology; *GSA Today*, Volume 8, Number 9, pages 1-8.
- Childe, F. and Thompson, J.F.H. (1997): Geological setting, U-Pb geochronology, and radiogenic characteristics of the Permo-Triassic Kutcho Assemblage, north-central British Columbia; *Canadian Journal of Earth Sciences*, Volume 34, pages 1310-1324.
- Childe, F., Friedman, R.M., Mortensen, J.K. and Thompson, F.H. (1997): Evidence for Early Triassic felsic volcanism in the Ashcroft (92I) map area, British Columbia; in *Geological Fieldwork 1996*, B.C. Ministry of Employment and Investment, Paper 1997-1, pages 117-124.
- Childe, F.C. (1997): U-Pb Geochronology, Geochemistry and Nd isotopic systematics of the Sitlika Assemblage, central British Columbia; in *Geological Fieldwork 1996*, B.C. Ministry of Employment and Investment, Paper 1997-1, pages 69-77.
- Cordey, F. (1990): Comparative study of radiolarian faunas from the sedimentary basins of the Insular, Coast and Intermontane belts; unpublished manuscript, 57 pages.
- Cordey, F., Gordey, S.P. and Orchard, M.J. (1991): New biostratigraphic data for the northern Cache Creek terrane, Teslin map area, southern Yukon; in *Current Research, Part E, Geological Survey of Canada*, Paper 91-1E, pages 67-76.
- Erdmer, P., Ghent, E.D., Archibald, D.A. and Stout, M.Z. (1998): Paleozoic and Mesozoic high-pressure metamorphism at the margin of ancestral North America in central Yukon; *Geological Society of America Bulletin*, Volume 110, pages 615-629.
- Friedman, R.M. and van der Heyden, P. (1992): Late Permian U-Pb dates for the Farwell and Northern Mount Lytton plutonic bodies, Intermontane Belt, British Columbia; in *Current Research, Part A; Geological Survey of Canada*, Paper 92-1A, pages 137-144.
- Gabrielse, H. (1994): Geology of the Cry Lake (104I) and Dease Lake (104J/E) map areas, north central British Columbia; *Geological Survey of Canada*, Open File 2779.

- Gabrielse, H. (1998): Geology, Dease Lake, British Columbia; *Geological Survey of Canada*, Map 1908A, scale 1:250 000.
- Gordey, S.P. and Stevens, R.A. (1994): Preliminary interpretation of bedrock geology of the Teslin area (105C), southern Yukon; *Geological Survey of Canada*, Open File 2886, scale 1:250 000.
- Harland, W.B., Armstrong, R.L., Cox, A.V., Craig, L.E., Smith, A.G. and Smith, D.G. (1990): A geologic time scale 1989; *Cambridge University Press*, Cambridge, 263 pages.
- Hart, C.J.R. (1997): A transect across Stikinia: Geology of the northern Whitehorse map area, southern Yukon Territory (105D/13-16); Exploration and Geology Services Division, Yukon, *Indian and Northern Affairs Canada*, Bulletin 8, 112 pages.
- Hart, C.J.R. and Radloff, J.K. (1990): Geology of the Whitehorse, Alligator Lake, Fenwick Creek, Carcross and part of Robinson map areas (105D/11,6,3,2 & 7), Yukon Territory; *Indian and Northern Affairs Canada*, Open File 1990-4, 113 pages plus 4 map sheets.
- Jackson, J.L. (1992): Tectonic analysis of the Nisling, northern Stikine and northern Cache Creek Terranes, Yukon and British Columbia; unpublished Ph.D. thesis, *The University of Arizona*, Tucson, 200 pages.
- Johannson, G.G. (1994): Provenance constraints on Early Jurassic evolution of the northern Stikinian arc, Whitehorse Trough, Atlin Lake, northwestern British Columbia; unpublished M.Sc. thesis, *The University of British Columbia*, Vancouver, 300 pages.
- Mihalynuk, M.G. (1999): Geology and Mineral Resources of the Tagish Lake Area, Northwestern British Columbia (NTS 104M/8, 9, 10E, 15, 104N/12W); *B.C. Ministry of Energy and Mines*, Bulletin 105 (in press).
- Mihalynuk, M.G., Smith, M.T., Gabites, J.E., Runkle, D. and Lefebure, D. (1992): Age of emplacement and basement character of the Cache Creek Terrane as constrained by new isotopic and geochemical data; *Canadian Journal of Earth Sciences*, Volume 29, pages 2463-2477.
- Mihalynuk, M.G., Nelson, J. and Diakow, L. (1994): Cache Creek Terrane entrapment: oroclinal paradox within the Canadian Cordillera; *Tectonics*, Volume 13, pages 575-595.
- Mihalynuk, M.G., Meldrum, D., Sears, W.A., Johannson, G. G. (1995a): Geology of the Stuhini Creek area (104K/11); in Geological Fieldwork 1994, B. Grant and J.M. Newell, Editors, *B.C. Ministry of Energy, Mines and Petroleum Resources*, Paper 1995-1, pages 321-342.
- Mihalynuk, M.G., Meldrum, D., Sears, W.A. and Johannson, G. G., Madu, B.E., Vance, S., Tipper, H.W. and Monger, J.W.H. (1995b): Geology and litho-geochemistry of the Stuhini Creek map area (104K/11); *B.C. Ministry of Energy, Mines and Petroleum Resources*, Open File 1995-5.
- Mihalynuk, M.G. and Cordey, F. (1997): Potential for Kutcho Creek volcanogenic massive sulphide mineralization in the northern Cache Creek Terrane: A progress report; in Geological Fieldwork 1996, *B.C. Ministry of Employment and Investment*, Paper 1997-1, pages 157-170.
- Mihalynuk, M.G., Nelson, J. and Friedman, R.M. (1998): Regional geology and mineralization of the Big Salmon Complex; in Geological Fieldwork 1997, *B.C. Ministry of Employment and Investment*, Paper 1998-1, pages 6-1 to 6-20.
- Monger, J.W.H. (1969): Stratigraphy and structure of Upper Paleozoic rocks, northeast Dease Lake map-area, British Columbia (104J); *Geological Survey of Canada*, Paper 68-48.
- Monger, J.W.H. (1975): Upper Paleozoic rocks of the Atlin terrane, Northwest British Columbia and south-central Yukon, *Geological Survey of Canada*, Paper 74-47.
- Monger, J.W.H., Wheeler, J.O., Tipper, H.W., et al. (1991): Part B. Cordilleran Terranes; in Chapter 8 of Geology of the Cordilleran Orogen in Canada, H. Gabrielse and C.J. Yorath, Editors; *Geological Survey of Canada*, Geology of Canada, Number 4, pages 281-327.
- Mortensen, J. K., Ghosh, D.K. and Ferri, F. (1995): U-Pb geochronology of intrusive rocks associated with copper-gold porphyry deposits in the Canadian Cordillera; in Porphyry Deposits of the Northwestern Cordillera of North America, Schroeter, T.G., Editor, *Canadian Institute of Mining, Metallurgy and Petroleum*; Special Volume 46, pages 142-158.
- Pálffy, J., Mortensen, J.K. and Smith, P.L. (1998): A U-Pb and ⁴⁰Ar-³⁹Ar time scale for the Jurassic. *5th International Symposium on the Jurassic System*, Vancouver, Canada, Abstracts and Program, page 72.
- Read, P.B. (1993): Geology of northeast Taseko Lakes map area, southwestern British Columbia; in Current Research, Part A; *Geological Survey of Canada*, Paper 93-1A, pages 159-166.
- Renne, P.R., Zhang, Z., Richards, M.A., Black, M.T. and Basu, A.R. (1995): Synchrony and causal relations between Permian-Triassic boundary crises and Siberian flood volcanism; *Science*, Volume 269, pages 1413-1416.
- Ricketts, B.D., Evenchick, C.A., Anderson, R.G. and Murphy, D.C. (1992): Bowser basin, northern British Columbia: Constraints on the timing of

- initial subsidence and Stikinia-North America terrane interactions; *Geology*, Volume 20, pages 1119-1122.
- Schiarizza, P. and MacIntyre, D.G. (1999): Geology of the Babine Lake-Takla Lake area, central British Columbia (93K/11, 12, 13, 14; 93N/3, 4, 5, 6); in Geological Fieldwork 1998, *B.C. Ministry of Energy and Mines*, Paper 1999-1, this volume.
- Smith, P.L. and Tipper, H.W. (1986): Plate tectonics and paleobiogeography: Early Jurassic (Pliensbachian) endemism and diversity; *Palaeo*, Volume 1, pages 399-412.
- Stacey, J.S. and Kramers, J.D. (1975): Approximation of terrestrial lead isotope evolution by a two-stage model; *Earth and Planetary Science Letters*, Volume 26, pages 207-221.
- Terry, J. (1977): Geology of the Nahlin ultramafic body, Atlin and Tulsequah map-areas, northwestern British Columbia; *Geological Survey of Canada*, Paper 77-1A, pages 263-266.
- Thorstad, L.E., and Gabrielse, H. (1986): The Upper Triassic Kutcho Formation, Cassiar Mountains, north-central British Columbia; *Geological Survey of Canada*, Paper 86-16, 53 pages.



DEVONO-MISSISSIPPIAN VMS PROJECT: CONTINUING STUDIES IN THE DORSEY TERRANE, NORTHERN BRITISH COLUMBIA

By JoAnne Nelson

KEYWORDS: Mississippian, Dorsey Terrane, Yukon Tanana Terrane, Northern British Columbia

INTRODUCTION

This project aims to trace out, within central northern B.C., stratigraphy favorable to the formation of Early Mississippian volcanogenic massive sulphide deposits similar to Kudzu, Ze Kayah, Wolverine, and Fyre Lake. Begun in 1997, the project has focussed on two areas, the eastern Dorsey Terrane near the headwaters of the Cottonwood River in central Jennings River map area (Figure 1; Nelson *et al.*, 1998a), and the Big Salmon Complex (Mihalynuk *et al.*, 1998). Mapping in the eastern part of the Dorsey Terrane continued in August 1998. The Big Salmon project, on hold for a year, will be completed in 1999.

The Dorsey Terrane has been divided into several assemblages (Harms and Stevens, 1996). The lower Dorsey Terrane in the southern Yukon comprises the Ram Creek and Dorsey assemblages. The structurally lowest Ram Creek Assemblage is a suite of mafic and intermediate to felsic metavolcanic rocks with lesser quartzite, marble and metaplutonic bodies. The overlying Dorsey Assemblage consists of quartzose, pelitic, mafic (to possibly felsic, muscovite-quartzite?) metavolcanic and intermediate metaplutonic rocks, which underwent high-temperature, high-pressure metamorphism (609-732°C, 7.7-14.1 kilobars) prior to emplacement of the mid-Permian Ram Stock (Stevens, 1996). The Dorsey Assemblage is overlain structurally by the Klinkit and Swift River assemblages, which show lower metamorphic grades and less penetrative deformation (Stevens and Harms, 1995, Harms and Stevens, 1996). Fossil ages in these upper assemblages of the Dorsey Terrane range from late Mississippian to Triassic (Harms and Stevens 1996). Limestones at different

structural levels contain Pennsylvanian conodonts (Abbott, 1981): this may indicate fault and/or fold repetition.

Mapping in 1997 indicated that the Dorsey Terrane near the headwaters of the Cottonwood River contains elements assignable to the Ram Creek, Dorsey, and Swift River assemblages (Nelson *et al.*, 1998a). Both the Ram Creek and Dorsey units contain felsic rocks of early Mississippian age (Nelson *et al.*, 1998a), comparable with the age of the suite that hosts VMS deposits in the Yukon-Tanana Terrane near Finlayson Lake, Yukon (Mortensen and Jilson, 1985, Hunt, 1997).

LOCAL GEOLOGY

In the central Jennings River map area, the lower part of the Dorsey Terrane rests structurally on metamorphosed basinal strata that are assumed to be the outer fringes of the Cassiar Terrane, the western edge of the North American passive continental margin (Figure 2).

Field mapping in 1997 and 1998 has resulted in subdivision of the Dorsey Terrane into a number of units (Figure 2 and Table 1). As none of them can be traced across Parallel Creek, it is assumed that a major high-angle fault is concealed within its valley.

Units northeast of Parallel Creek include, from structurally lowest to highest:

Unit 1: "Greenstone-intrusive unit": Greenschist-grade intermediate to mafic metatuff, pyritic felsic metatuff, and tonalite/quartz diorite.

Unit 2: "Metasediment-amphibolite unit": This unit consists of a lower, amphibolite (metabasite)-bearing part (2L on Figure 3) and an upper metasedimentary part (2U on Figure 3). The contact between the two, albeit tectonised, appears to be gradational. The lower part consists of amphibolite and garnet amphibolite,

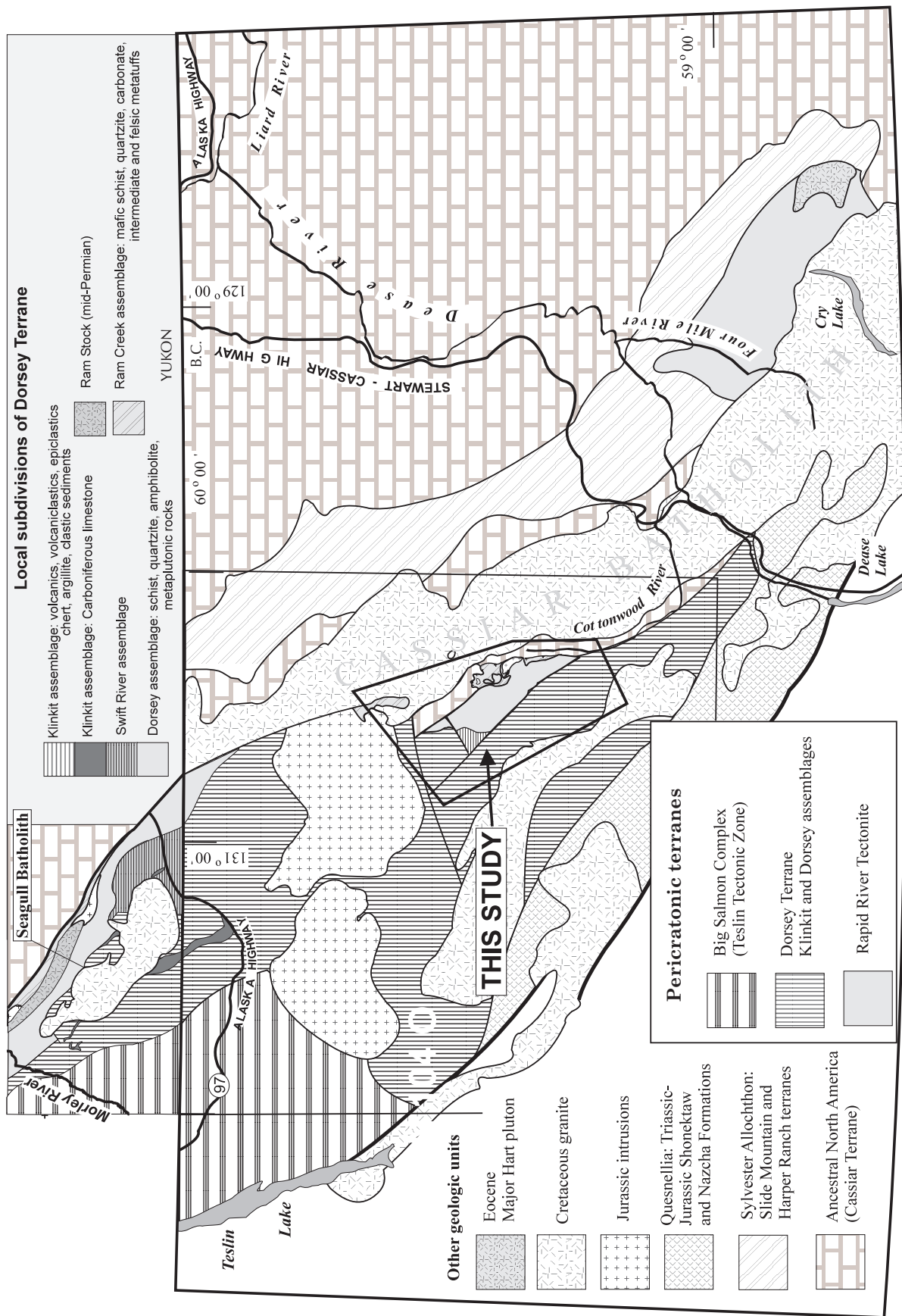


Figure 1. Location and tectonic setting of the Dorsey Terrane project. Regional Geology from Gabrielse (1963, 1969, 1994) and Steven and Harms.

Table 1. Lithostratigraphic units

Map Unit	Assemblage	Informal name
1	Ram Creek	greenstone-intrusive unit
2	Dorsey	metasediment-amphibolite unit
3	Swift River? Klinkit?	Quartzite-pelite unit
4	Swift River? Klinkit?	Metachert-metatuff-phyllite unit
5	Swift River	Dark phyllite-quartzite-marble unit
6	Swift River	Phyllitic metasedimentary unit
7	Klinkit	Limestone-chert-tuff unit

interlayered (interbedded?) with metatuffs, fine grained quartzite, biotite-muscovite+graphite schist, and quartzofeldspathic schist (metamorphosed chert, argillite and orthoquartzite, respectively), and marble. The upper part consists of thinly layered impure quartzite with biotite-muscovite partings (meta-argillite), thin bedded limestone, dark grey meta-chert; and interlayered chlorite+muscovite+garnet schist and quartz-muscovite schist that probably represent intermediate to felsic tuff protoliths. Both the upper and lower parts of this unit are intruded by pods of deformed tonalite, diorite and gabbro. Ultramafic pods are restricted to the lower, amphibolite-dominated unit.

Unit 3: “Quartzite-pelite unit”: quartzite, pelitic schist and phyllite, and one layer of quartz-plagioclase grit.

Unit 4: “Metachert-metatuff-phyllite unit”: thin bedded fine quartzite (metachert) interbedded with siliceous metatuff, dark grey meta-argillite, phyllite, chert-argillite-clast sedimentary breccia, and carbonate olistostromes.

Unit 1 is assigned to the Ram Creek Assemblage, unit 2 to the Dorsey Assemblage, and units 3 and 4 tentatively to the Swift River and/or Klinkit Assemblage.

Units southwest of Parallel Creek include:

Unit 5: “Dark phyllite-quartzite-marble unit”: Dark grey phyllite, white quartzite (quartz arenite), and one thick, continuous marble band.

Unit 6: “Phyllitic metasedimentary unit”: Siliceous green to grey phyllite, quartzite (quartz arenite), limestone, metatuff, and diorite.

Unit 7: “Limestone-tuff-chert unit”: Thick

pure limestone/marble, mafic metatuff, bedded chert.

Units, 5 and 6 are assigned tentatively to the Swift River and unit 7 to the Klinkit assemblage.

Many of these units have similar protoliths. The theme of basinal sedimentation accompanied by distal volcanism and persistent minor siliciclastic influx repeats from one to the other. For instance the contact between the “Metasediment-amphibolite unit” and the overlying “Metachert-metatuff-phyllite unit” was defined by the disappearance of garnet, as the protoliths of these two units - cherts, tuffs and argillites - resemble one another.

North American marginal strata

These rocks, described in Nelson *et al.*, 1998a, are dark grey to black slate, silty slate and argillite with minor quartzite and limestone, exposed in homoclinally southwest-dipping succession in the mountains north of the headwaters of the Cottonwood River (Figure 2).

Unit 1: Greenstone-intrusive unit

The “greenstone-intrusive unit” forms the lowest of the allochthons in the Cottonwood River area (Unit 1 on Figure 3), resting directly above inferred Earn Group-equivalent strata on a surface that is very gently dipping over tens of square kilometres and truncates steeper cleavage and bedding in the para-autochthonous rocks below. It consists of two lithologic suites: a supracrustal, metavolcanic suite, and a suite of

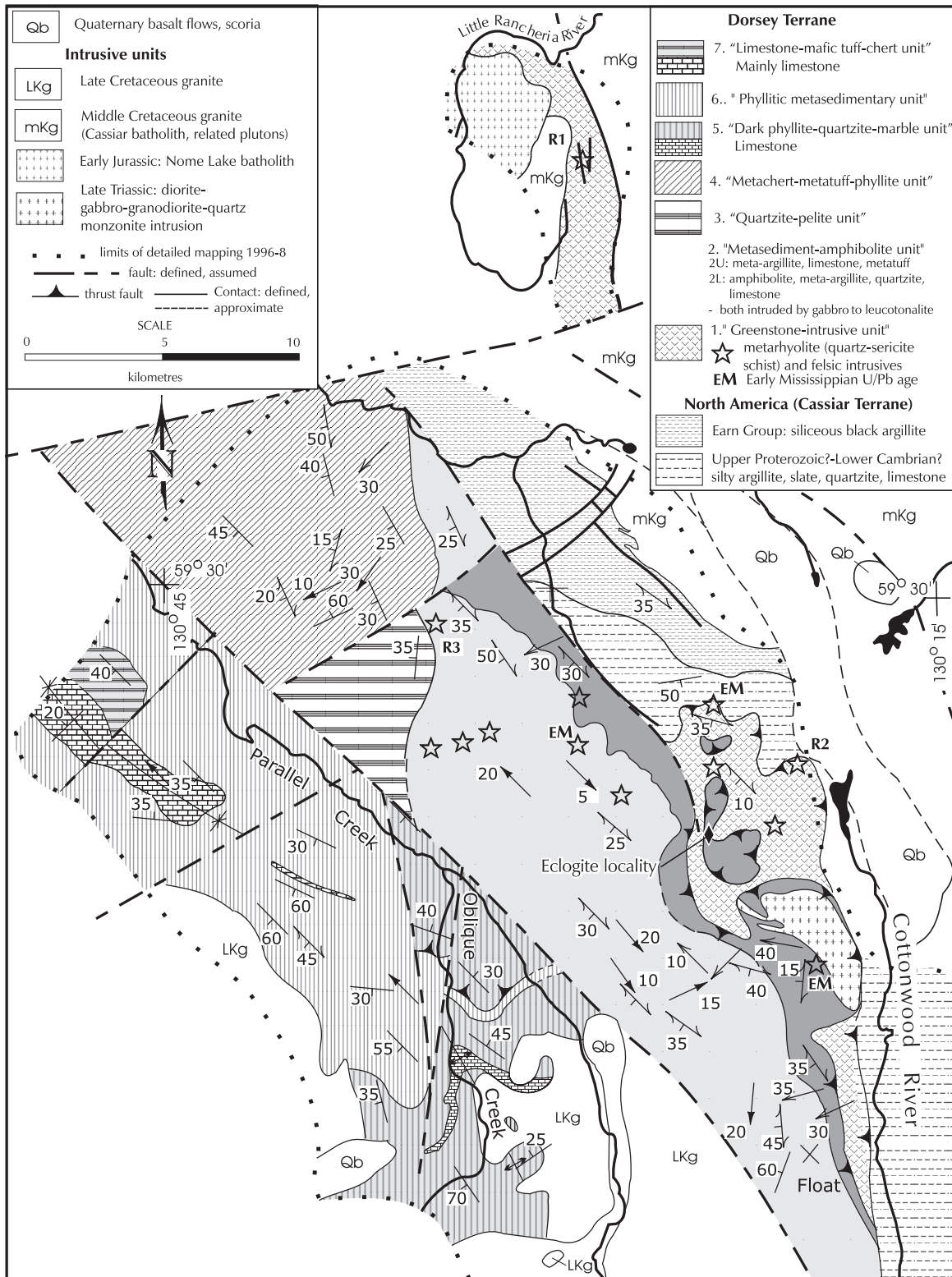


Figure 2. Geology of the area near the headwaters of the Cottonwood River and Parallel Creek (1040/7, 8, 9, 10). Based on 1998 mapping by J. Nelson, W. Zantvoort, T. Gleeson and K. Wahl; 1997 mapping by T. Harms, J. Nelson, and M. Mihalynuk; 1996 mapping by J. Nelson; and Gabrielse (1963).

heterogeneous intrusions. The metavolcanic suite consists primarily of metatuffs, mostly mafic to intermediate, but with pyritic quartz-sericite schist (meta-rhyolite tuff) in places. Some of the felsic metatuffs contain recognizable primary quartz and/or plagioclase phenocrysts. Quartz-sericite schist localities are shown on Figure 2 by stars. Sedimentary components of the “greenstone-intrusive unit” include volumetrically minor grey argillite and grey to sea-green chert. The metavolcanic-metasedimentary suite is intruded by deformed plutonic bodies. They range from gabbro and diorite to tonalite and quartz diorite. Foliation in them is variably developed. It ranges from weak to protomylonitic, particularly near the base of the allochthon. The thin southern extension of this unit is a polydeformed coarse-grained gabbro.

The “greenstone-intrusive unit” also includes a sequence of quartz-sericite schist-intermediate metatuff-limestone-chert near the headwaters of the Little Rancheria River, which contains a limestone that yielded early Mississippian conodonts (Nelson, 1997).

Three quartz-eye-bearing quartz-sericite and quartz-chlorite-sericite schists in the “greenstone-intrusive unit” were sampled in 1998 for U-Pb zircon analysis. One of the deformed tonalite bodies in it has returned a preliminary early Mississippian U-Pb age (R. Friedman, personal communication 1998).

Unit 2: Metasediment-amphibolite unit

This unit overlies the “greenstone-intrusive unit” above a sharp, nearly flat contact (Figure 2), and is distinguished from it by strong contrasts in metamorphic grade and lithologic components. The “metasediment-amphibolite unit” is divided into a lower part and an upper part (Units 2L and 2U on Figure 2). The lower part contains thick, dark green tabular amphibolite bodies and small pods of ultramafic rock, both of which are absent in the upper part. Both upper and lower parts contain very siliceous metasedimentary rocks and marble interbeds. Chlorite phyllite and quartz-sericite schist commonly occur together in the upper part. Based on their composition, they are interpreted as intervals of intermediate to felsic metatuff, although remnant primary textures are lacking to substantiate this. The contact between the upper and lower

parts is gradational, and is mapped at the top of the highest amphibolite body.

Thick bands of garnet and epidote amphibolite form prominent exposures in the lower part of the unit. They are interlayered and interfolded with quartz-rich to pelitic metasediments, some of which display protolith textures that identify them as meta-argillites, metacherts, and quartz sandstones. Microscopically, the amphibolites consist of aggregates of forest green, prismatic hornblende with interstitial albite and in some cases large splotchy garnet poikiloblasts; trains of rutile and ilmenite-magnetite are heavily overgrown by retrograde sphene.

The high metamorphic grade of the lower part of the unit is indicated by hornblende + garnet + epidote-sodic plagioclase-quartz-rutile in meta-basites. Assemblages of coarse biotite-muscovite-quartz-feldspar are developed in impure pelitic rocks, and garnet-clinozoisite-biotite-muscovite-plagioclase in intermediate to felsic orthogneisses. One of the garnet amphibolites contains relict sodic clinopyroxenes, and is interpreted as a heavily retrograded eclogite (P. Erdmer, personal communication 1998). Structural relationships show that some of the least deformed garnet amphibolites are garnetiferous gabbros that intrude the metasedimentary section. These bodies were folded and foliated prior to intrusion of the sill-like intermediate to felsic bodies. The intermediate to felsic intrusions themselves are highly foliated and affected by garnet-grade metamorphism. One of them has yielded early Mississippian zircons (349.9 + 4.2 Ma) (Nelson *et al.*, 1998a).

The contact between units 2L and 2U is a strongly sheared but lithologically gradational: it may be a structurally remobilized depositional contact. Above it, siliceous schists are the most abundant rock type, and amphibolite and ultramafites are rare. Three interlayered lithologic suites dominate the upper part of the unit: siliceous, platy-layered phyllites and fine grained quartzites, which are probably meta-argillites and metacherts; thin-bedded limestone; and interlayered chlorite, chlorite-sericite and quartz-sericite schist, which reflect a metamorphosed intermediate to felsic tuffaceous protolith. New mapping of the southern continuation of the upper unit shows an increase in the proportion of metatuff.

The metamorphic grade in 2U is somewhat lower than that in 2L: chlorite-muscovite + acti-

nolite assemblages predominate in metamorphosed intermediate tuffs, although this appears to be mainly due to strong retrograde metamorphism. Although large garnet porphyroblasts are common, both garnet and biotite are texturally unstable and both have partly reverted to chlorite. Cordierite occurs in a few metatuffs.

Both the upper and lower parts of the unit are intruded by small mafic to tonalitic pods and sills, typically coarse grained diorites, gabbros, and white leucotonalite and granite (leucosome?), which themselves are strongly foliated, folded and refolded. Their abundance decreases markedly upwards. One of these tonalite bodies contains some of the phases of deformation but not others, which are inferred to predate it (see Structure, below). U-Pb dating of this body is in progress, and if successful will help to constrain timing some of the tectonic events in the lower Dorsey Assemblage.

Unit 3: Quartzite-pelite unit

This unit underlies the western part of one ridge in the central part of the map area (Figure 2). It was previously included in unit 5, the "phyllitic metasedimentary unit"; however it is distinct from that unit, and geographically separated from it by the broad, overburden-covered valley of Parallel Creek. The lower 25 metres are dominated by quartzite with interlayered pelitic schist. This sequence contains one layer of quartz-plagioclase grit and monomictic, plutonic-clast conglomerate in a limey matrix. It appears to have been derived as an immature sediment from a coarse grained plutonic source. Towards the southwest in continuous exposure, the quartzite-pelite section passes gradationally upward into finer metasedimentary strata including grey, tan, greenish and white pelites, grey phyllite and metachert.

Relict garnet porphyroblasts enveloped by chlorite occur in the lower part of this unit, a feature that allies it with the underlying upper part of the "metasediment-amphibolite unit". However no garnet occurs in its upper part; therefore it is tentatively grouped with the units of Klinkit Assemblage affinity. Its contact with the "metasediment-amphibolite unit" is unexposed and structurally somewhat discordant (strikes change from approximately northwest, to north-northeast across the covered interval).

Preliminary detrital zircon data from the quartz-plagioclase grit indicates that the source pluton was Late Devonian (R. Friedman, personal communication 1998); this restricts the base of the unit to no older than Late Devonian.

Unit 4: Metachert-metatuff-phyllite unit

This unit underlies the broad highland in the north-central part of the map area. It consists of thin-bedded fine-grained quartzite (metachert) interbedded with green siliceous chlorite-muscovite phyllite, interpreted as metatuff, dark grey meta-argillite, phyllite, chert-argillite-clast sedimentary breccia, and carbonate olistostromes. The unit is characteristically highly variable on a small scale, but homogeneous on the scale of a regional map. Packages of ribbon-bedded cherts, including black-stained manganiferous chert, are common, and aquamarine "sea-green" cherts occur locally. In places, individual chert beds form white ribbons in green metatuff. There is a repeated association between dark grey meta-argillite, chert-argillite clast sedimentary breccia, and carbonate olistostromes with carbonate-breccia aprons.

The thin-bedded cherts are characteristically folded at outcrop-scale both into recumbent isoclines with M-folded cores, and upright chevron-style folds.

The lower contact of this unit above the "metasedimentary-amphibolite unit" is drawn above the highest occurrence of garnet in metamorphosed tuffaceous rocks, now chlorite-muscovite phyllites. Both it and the upper part of Unit 2 have similar protoliths, although some differences are seen. It lacks the thin-bedded limestones that typify parts of Unit 2. Metacherts are much more abundant in it, and the sedimentary breccias do not occur in Unit 2.

Unit 5: Dark phyllite-quartzite-marble unit

This unit is mainly exposed in the ridges surrounding the Oblique Creek valley. West of Oblique Creek, it overlies unit 6 across a strongly sheared zone shown as a thrust fault on Figure 2. It consists of dark grey phyllite and silty (?), siliceous phyllite, white quartzite (quartz arenite) and minor grit. One thick, continuous marble subunit outlines the limbs of a northwesterly plunging antiform.

The abundance of metamorphosed quartz sandstone and the presence of grit in this unit suggest a similarity to the “quartzite-pelite” of unit 3; however there is no structural continuity or age data to support a direct correlation, and the “look” of these two units is somewhat different: unit 3 lacks the overall dark coloring and flagginess of unit 5.

Unit 6: Phyllitic metasedimentary unit

This unit only occurs southwest of Parallel Creek. Although it is locally, and to a certain extent regionally, heterogeneous, no consistently mappable subdivisions of it could be made. It is dominated by grey, black and light green siliceous phyllite to phyllitic argillite with subordinate buff, dark grey, or white quartz grit and sandstone, and less abundant thin-bedded pale green to grey chert. A few prominent bands of recrystallized limestone are present. Meta-diorite, amphibolite and metatuff outcrop in one continuous layer, and appear to grade into one another. One dacite crystal tuff, a light green, comparatively uncleaved unit interfolded with green phyllite, was confirmed in thin section. Generally, however, igneous rocks are rare.

The “phyllitic metasedimentary unit” shows less development of metamorphic minerals and textures than the “metasediment-amphibolite unit”. Garnet is not seen, except where related to contact metamorphism.

Unit 7: Limestone-mafic tuff-chert unit

This unit, exposed on the subdued upland in the northwest corner of the map area, overlies unit 6, the “phyllitic metasedimentary unit”, across a well-exposed, concordant contact with no evidence of shearing or structural discontinuity. It consists of interbedded thick pure limestone/marble, mafic metatuff, and bedded chert. The limestone is partly replaced by pure white, coarse grained quartzite. The mafic metatuffs contrast strongly with other tuffs and metatuffs in the Dorsey Terrane. They range from large lapilli to laminated dust tuffs, all a rich, dark green color. They are interbedded with the limestone: mafic clasts occur in carbonate matrix, and dolomitized carbonate clasts occur in mafic tuff matrix; green tuff and orange-weathering carbonate are inter-laminated in dust tuffs. Ribbon-bedded chert lies

both above and below the limestone. Colors range from grey to green to white; some cherts are manganeseiferous, with black Mn-oxide coatings. Some cherts contain 3 to 10% disseminated pyrite.

Structural style of the allochthonous units

The following structural domains are recognized:

Domain A: Cassiar Terrane

Domain B: Unit 1, “greenstone-intrusive unit”

Domain C: Unit 2, “metasedimentary-amphibolite unit”; unit 3 “quartzite-pelite unit”

Domain D: Unit 4, “metachert-metatuff-phyllite unit”

Domain E: Units 5, 6 and 7 southwest of Parallel Creek

No new data is presented for the Domains A or B (see Nelson et al., 1998a). Structures from these domains are shown in Figure 3a.

Domain C: the metasedimentary-amphibolite unit

The “metasediment-amphibolite unit” was affected by several episodes of deformation over a protracted period of time. Near its base, early Mississippian sill-like intrusions follow and also cross-cut a pre-existing metamorphic foliation into which bedding was already transposed. The intrusions themselves were metamorphosed at garnet grade, carry a strong foliation subparallel to the earlier one, and are isoclinally folded. Well foliated to protomylonitic leucogranites cut foliations but are themselves folded. One of these has returned an Early Permian age (R. Friedman, pers. comm., 1998). Other nearby pegmatites, assumed to be part of the Permian suite, are very weakly foliated, and crosscut the ductile structures. Finally, the pluton near the base of the allochthon is discordant and only partly foliated, but some of its apophyses are folded. A preliminary U-Pb zircon age for this body is 211 Ma (R. Friedman, pers. comm., 1998).

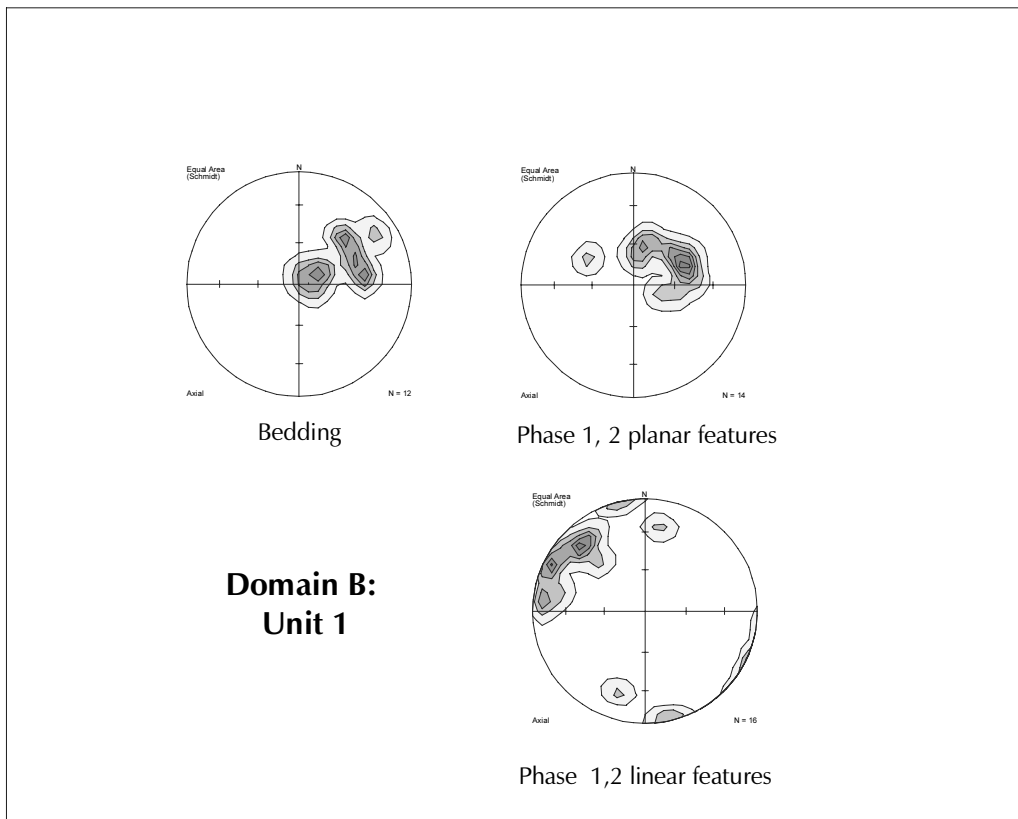
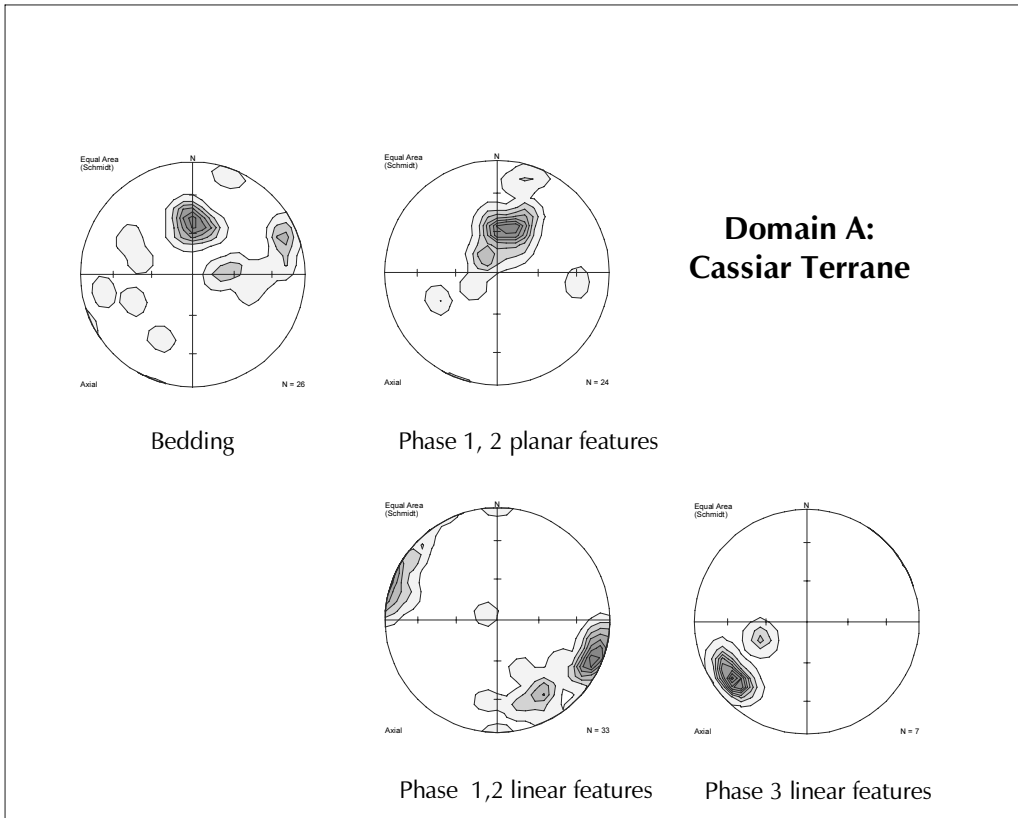


Figure 3a. Structural data from Cassiar Terrane and unit 1.

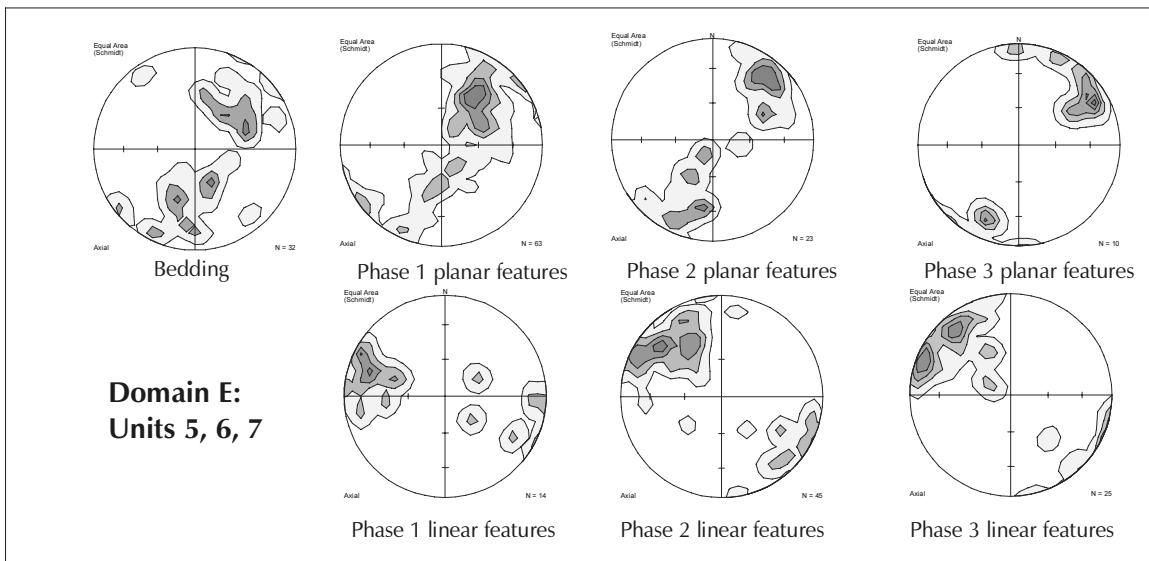
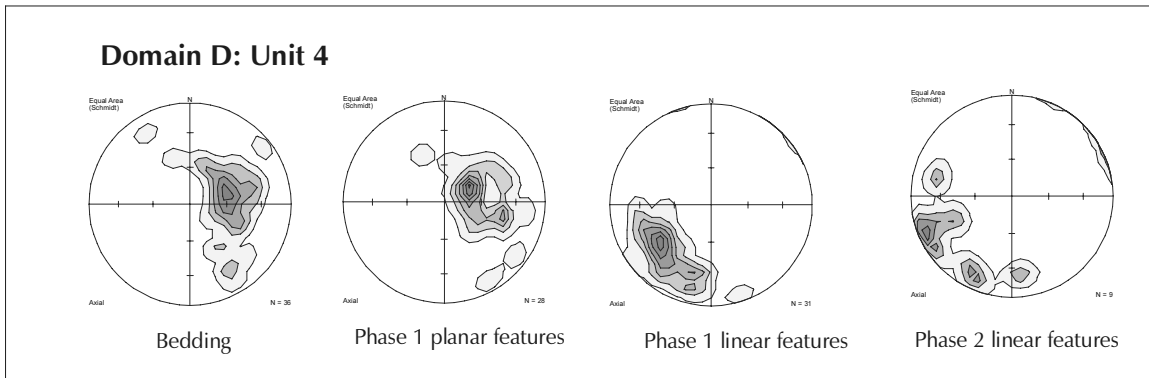
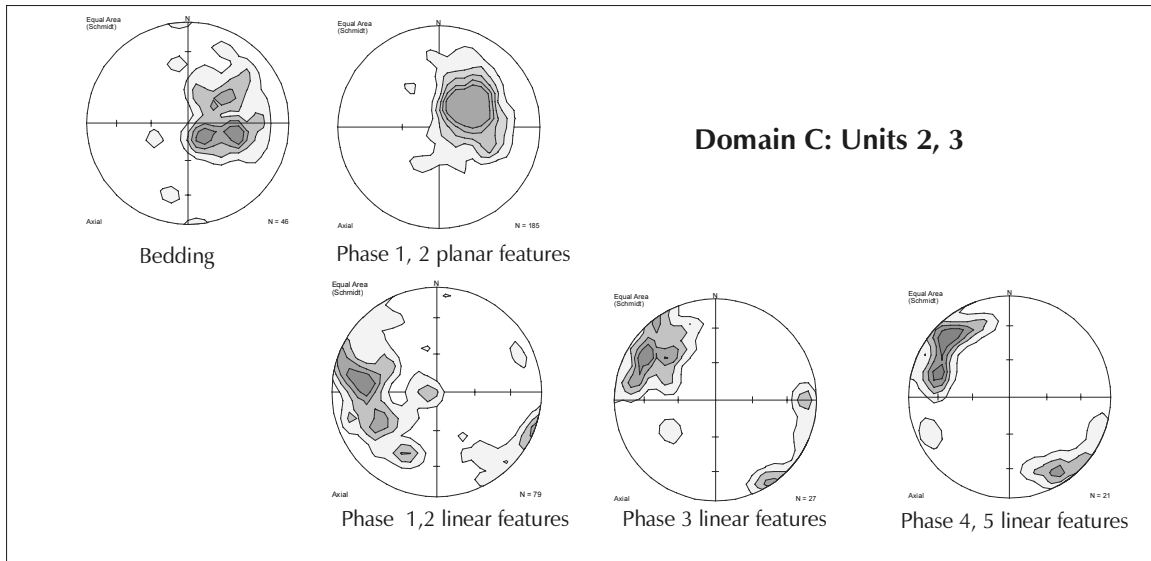


Figure 3b. Structural data from units 2 - 7.

Overall, foliation in Unit 2 tends to dip moderately southwest (Figure 3b). This attitude is discordant with its basal contact, which is nearly horizontal in exposures near the headwaters of the Cottonwood River.

Most minor folds are intrafolial isoclinal. They plunge gently in west-northwesterly or east-southeasterly directions (Figure 3b). Their attitudes are subparallel to the axes of kilometre-scale recumbent isoclinal folds, which fold the garnet amphibolite bodies. There is a small but significant population of minor folds, particularly in the lower part of the unit, that plunge 50° to 80° “downdip” to the west and southwest. This geometry is also seen in elongation and mineral lineations. Many of the “downdip”-plunging folds are rootless isoclinal folds outlined by quartzite layers, in a matrix of chlorite-muscovite phyllite. Within the same outcrop, folds of this type a few metres apart may have plunges that diverge by tens of degrees.

Timing and development of these “downdip” linear features is constrained by the structures in two small intrusive bodies. A sill-like muscovite-garnet-bearing felsic pluton, which outcrops fifty metres above the base of the unit, is strongly mylonitized and displays a well-developed, southwesterly-plunging quartz stretching lineation. A variety of strain indicators - asymmetric plagioclase porphyroclasts, displaced muscovite plates, mica fish, shear bands, and micro-thrust faults, indicate that shear sense was top-to-the-northeast. This mylonitization accompanied retrograde metamorphism in which chlorite-clinzoisite developed at the expense of biotite-garnet: it probably occurred during exhumation and cooling of the metamorphic complex.

Two hundred metres above the base of the “metasediment-amphibolite unit”, a well-foliated, intermediate sill-like body intrudes chlorite-muscovite-garnet schist and quartzite, locally cross-cutting an earlier foliation. The minor recumbent isoclinal folds in this body trend between 310 and 315 degrees; it lacks southwesterly-plunging minor structures. Both of these intrusive units are similar, in terms of composition and style of deformation, to the dated early Mississippian pluton that occurs 3 kilometres along strike to the north. A sample from the upper pluton is currently being processed for U-Pb dating.

During shearing, sheath folds can develop in which fold axes rotate towards the direction of tectonic transport (the extensional direction of the finite strain ellipse). The lower pluton underwent top-to-the-northeast shear after it was emplaced. The upper pluton, by contrast, was emplaced subsequent to rotation of local structures, since it only contains northwesterly, transport-normal folds. If they are indeed the same age, then these differences can be explained by strain gradients and progressive deformation: the stratified rocks were undergoing northeasterly transport and accompanying northwesterly folding during emplacement of the early Mississippian plutons, which continued after they cooled. Downdip structures formed in the lower pluton but not the upper one because shear strain increased with depth in the pile.

Later folds in unit 2, such as those that fold foliations, open folds and chevrons, also trend west-northwest to northwest. Northeasterly vergences are most common. It is notable that folds in unit 1, the Mississippian “greenstone-intrusive unit”, also trend west-northwesterly and verge to the northeast (Figure 3a). No downdip structures occur in unit 1, perhaps because it was too young (Mississippian) and too high structurally for them to develop.

Domain D: Unit 4, the metachert-metatuff-phyllite unit

This unit shows evidence for a unique structural history compared with the others. Foliations in it are variable, ranging in a continuum from northwesterly with southwesterly dips to southwesterly with northwesterly dips (Figure 3b). Linear features in this unit tend to southwesterly trends, in contrast to the other units. This orientation prevails, not only among quartz stretching lineations and rootless isoclinal folds, but also with respect to bedding-cleavage intersections, axes of outcrop-scale recumbent folds, and later upright fold axes. Northwesterly-trending fold axes are extremely rare. The structural history of this unit is anomalous; however, as noted in its description, it grades downwards into rocks indistinguishable from those in the “metasediment-amphibolite unit”. It represents an outstanding puzzle in the interpretation of the Dorsey Terrane.

Domain E: Units 5, 6 and 7 southwest of Parallel Creek

The structural style of the upper units 5, 6 and 7 reflects deformation at a higher crustal level than the units northeast of Parallel Creek. Mesoscopic recumbent and intrafolial folds are less common. Although bedding and cleavage are commonly parallel, axial planar cleavages that are steeper than bedding are also present, associated with concentric, open to tight upright folds. Phyllites are typically crenulated, and many outcrops display multiple sets of crenulations. Major fold axial surfaces strike west-northwest to northwest. Unit 7 occurs in the core of an open synform. Along the valley of Oblique Creek, a northwest-plunging antiform is disrupted by a steep, northerly-striking fault; limb attitudes of this structure outline the girdles in first and second phase planar features on Figure 3b. As in the other domains, early recumbent folds and later upright folds are coaxial, with northwesterly-plunging fold axes.

Two outcrops within unit 6 of this domain show southwesterly quartz stretching lineations, refolded by northwesterly crenulations and minor chevron folds. This temporal relationship, in which early “downdip” lineations are succeeded by northwesterly folding, constitutes a possible structural link between the rocks southwest of Parallel Creek and those of Domain C, the deeper, higher-grade “metasediment-amphibolite unit”.

Correlations and relationships between units

The Ram Creek Assemblage in the map area is represented by unit 1, the “greenstone-intrusive unit”. It is now known to be at least in part of early Mississippian age, on the basis of a U/Pb age on a deformed tonalite and conodonts from a limestone near the headwaters of the Little Rancheria River. It is interpreted as an early Mississippian arc edifice, with a varied volcanic to epiclastic suite ranging from andesite to dacite and rhyolite, accompanied by limestone banks and basinal chert/tuff sequences, all intruded by coeval intermediate plutons.

The Dorsey Assemblage is represented by unit 2, the “metasediment-amphibolite unit”. This unit, like the Ram Creek Assemblage, is intruded by early Mississippian intermediate (to felsic) plutons, which also display strong flatten-

ing fabrics. The presence of garnet grade metamorphic assemblages in them suggests that they either intruded at or were buried to mid-crustal levels, in contrast to Ram Creek plutons, which contain only greenschist-facies assemblages. The Dorsey Assemblage, unlike the Ram Creek, clearly records protoliths and metamorphic/tectonic events older than early Mississippian. Penetrative ductile fabrics in quartzite and metatuff are cut by the intermediate to felsic intrusions, and eclogite facies metamorphism predated garnet amphibolite conditions in at least one of the metabasites. One reasonable interpretation of the similarities and differences between the Ram Creek and Dorsey assemblages in this area is that the Dorsey Assemblage was basement to the Ram Creek Assemblage, but, through imbrication, now lies structurally above it. The comparative lack of volcanic rocks in the upper part of unit 2 may mean that unit 1 represents the core of the early Mississippian arc edifice, and unit 2 its flank. Reversal of top-to-the-northeast motion suggests that unit 2 once lay to the west of unit 1. If the presence of eclogite in unit 2 can be construed to indicate a subduction environment, then this western flank was the forearc, and the arc faced west.

Units 3 and 4, the “quartzite-pelite” and “metachert-metatuff-phyllite” units, are assigned to the Swift River or lower part of the Klinkit assemblage. Unit 4 overlies unit 2 across an apparently transitional contact. The principal differences between them, other than minor lithologic ones, are 1) unit 4 does not contain garnet grade assemblages, and 2) protolith textures in it are generally well-preserved. On the ridge immediately south of unit 4, unit 3 also overlies unit 2. The lowermost part of unit 3 is garnet grade, like the underlying unit 2. This part contains distinctive quartzose clastics and a pluton-derived grit with late Devonian zircons, which hint at an erosional interval. In southern Yukon near the Seagull Batholith, sequences of lower metamorphic grade that rest structurally above the Dorsey Assemblage are assigned to the Swift River and Klinkit assemblages (Figure 1); their basal contact is inferred to be a fault (Harms and Stevens, 1996). Here, however, the contact between units 2 and 4 appears to be gradational.

Units 5 and 6 southwest of Parallel Creek are similar to each other in metamorphic grade

(greenschist facies chlorite-muscovite), in the dominance of siliceous phyllite and in the presence of quartzose clastics as thick, discrete beds. These features ally them with the Swift River Assemblage, as noted by T. Harms (Nelson *et al.*, 1998a). Unit 6 is overlain concordantly by unit 7, the “limestone-mafic tuff-chert unit”. This unit resembles a lithostratigraphic triplet in the Big Salmon Complex, which consists of limestone, chert (locally highly manganese-bearing and piedmontite-bearing), and a thick, generally mafic greenstone unit that includes both flows and pyroclastic material (Mihalynuk *et al.* 1998). It also resembles limestones and associated volcanic rocks in the upper part of the Klinkit Assemblage of Stevens and Harms, 1995 and Harms and Stevens, 1996. In both of these cases, the carbonate is of mid- to late Carboniferous age (Stevens and Harms, 1995; Mihalynuk *et al.*, 1998).

Correlations with other allochthonous assemblages in southern Yukon and far northern B.C.

Unit 1, the Ram Creek Assemblage, contains an early Mississippian suite of arc affinity, like the host sequence for syngenetic deposits in the Finlayson Lake belt. Particularly noteworthy are the occurrences of metamorphosed pyritic felsic tuffs within it.

Unit 2, the “metasediment-amphibolite unit”, resembles not only the Dorsey Assemblage near the Seagull Batholith, but also the “Anvil allochthon” of the St. Cyr klippe (Fallas, 1997) and the Rapid River Tectonite in the Sylvester Allochthon (Gabrielse and Harms, 1989). All of these contain garnet-bearing amphibolites and interlayered metasedimentary rocks. Eclogite remnants in the St. Cyr klippe have yielded mid-Permian K-Ar muscovite ages (Fallas, 1997). Both the “metasediment-amphibolite unit” and the Rapid River Tectonite are intruded by Early Mississippian plutons, which cross-cut early ductile fabrics but are in part protomylonites (Nelson *et al.*, 1998b and unpublished data; Gabrielse *et al.*, 1993). This group of lithotectonic slivers that underwent late Paleozoic high-pressure metamorphism forms a distinct subset within terranes of general “Yukon-Tanana Terrane” affinity (Nelson *et al.*, 1998b): together with the set of Mississippian and Permian eclogite occurrences (Erdmer *et al.*, 1998), it may serve to outline

shifting mid- to late Paleozoic subduction zones that bordered or even segmented a composite pericratonic superterrane.

Mineral potential

Quartz-sericite schists, interpreted to be metamorphosed rhyolite tuffs, have been identified at numerous localities within the allochthons in the central Jennings River area. Several examples are found in the “greenstone-intrusive” unit, as shown by the Little Rancheria locality (R1 on Figure 2), and 2 kilometres northwest of the lake that forms the headwaters of the Cottonwood River (R2, Figure 2). Both occurrences are rusty and pyritic; and at R2, traces of chalcopyrite occur with pyrite in siliceous quartz-sericite schist. Quartz-sericite schists also occur at scattered localities associated with chlorite-muscovite phyllites (metatuffs) in the upper part of the “metasediment-amphibolite unit” (stars on Figure 2).

Interesting sulphide-bearing float was also discovered in a creek bed draining the lower part of Unit 1 (labelled “Float” on Figure 2). Pyrite and minor galena wisps occur in laminated metachert. Other float samples at the same locality contain laminated magnetite in a matrix of feathery actinolite and quartz. Although the feathery actinolite is clearly post-kinematic, the magnetite grains appear to be earlier: they are strongly aligned in the ductile fabric, and rimmed and penetrated by later titanite. Thus the origin of these rocks is equivocal: they may be either skarns, or banded magnetite such as is seen in the hanging wall at Wolverine. No bedrock exposure corresponding to them has yet been found.

ACKNOWLEDGMENTS

Much of the mapping for this project was executed by Willem Zantvoort, Tom Gleeson and Kim Wahl: this is reflected by their coauthorship of the open file map. Molly Wahl assisted with unflagging energy and enthusiasm. Jim Mortensen and Richard Friedman have aided this project with their insights, discoveries, and diligence. Philippe Erdmer identified and analysed the eclogite; his work is the topic of a forthcoming paper. Review by Mitch Mihalynuk and Bill McMillan is appreciated.

REFERENCES

- Abbott, J.G. (1981): Geology of the Seagull tin district; in *Yukon Geology and Exploration 1979-1980, Indian and Northern Affairs Canada*, pages 32-44.
- Fallas, K.M. (1997): Preliminary constraints on the structural and metamorphic evolution of the St. Cyr Klippe, south-central Yukon; *Slave-Northern Cordillera Lithospheric Evolution (SNORCLE) and Cordilleran Tectonics Workshop*, Report of the 1997 Combined Meeting, pages 90-95.
- Erdmer, P., Ghent, E.D., Archibald, D.A. and Stout, M. (1998): Paleozoic and Mesozoic high-pressure metamorphism at the margin of Ancestral North America; *Geological Society of America Bulletin*, Volume 110, pages 615-629.
- Gabrielse, H. (1963): McDame Map Area, Cassiar District, British Columbia; *Geological Survey of Canada*, Memoir 319.
- Gabrielse, H. (1969): Geology of Jennings River map area, British Columbia (104/O); *Geological Survey of Canada*, Paper 68-55.
- Gabrielse, H. (1994): Geology of Cry Lake (104I) and Dease Lake (104J/E) map areas, north central British Columbia; *Geological Survey of Canada*, Open File Map 2779.
- Gabrielse, H. and Harms, T.A. (1989): Permian and Devonian plutonic rocks in the Sylvester Allochthon, Cry Lake and McDame map areas, Northern British Columbia; in *Current Research Part E, Geological Survey of Canada*, Paper 89-1E, pages 1-4.
- Gabrielse, H., Mortensen, J.K., Parrish, R.R., Harms, T.A., Nelson, J.L., and van der Heyden, P. (1993): Late Paleozoic plutons in the Sylvester Allochthon, northern British Columbia; in *Radiogenic Age and Isotopic Studies, Report 7, Geological Survey of Canada*, Paper 93-1, pages 107-118.
- Harms, T.A. and Stevens, R.A. (1996): Assemblage analysis of the Dorsey Terrane; *Slave-Northern Cordillera Lithospheric Evolution (SNORCLE) and Cordilleran Tectonics Workshop*, Report of the 1996 Combined Meeting, pages 199-201.
- Hunt, J. (1997): Massive sulphide deposits in the Yukon-Tanana and adjacent terranes; in *Yukon Exploration and Geology 1996*, Exploration and Geological Services Division, Yukon, *Indian and Northern Affairs Canada*, pages 35-45.
- Mihalynuk, M. Nelson, J.L. and Friedman, R.M. (1998): Regional geology and mineralization of the Big Salmon Complex (104N NE and 104O NW); in *Geological Fieldwork 1997, B.C. Ministry of Employment and Investment*, Paper 1998-1, pages 6-1 to 6-20.
- Mortensen, J.K. and Jilson, G.A. (1985): Evolution of the Yukon Tanana Terrane: Evidence from Southeastern Yukon Territory; *Geology*, Volume 13, pages 806-810.
- Nelson, J.L. (1997): Last seen heading south: extensions of the Yukon-Tanana Terrane into Northern British Columbia; in *Geological Fieldwork 1996*, D.V. Lefebure, W.J. McMillan and J.G. McArthur, Editors, *B.C. Ministry of Employment and Investment*, Paper 1997-1 pages 145-156.
- Nelson, J.L., Harms, T.A. and Mortensen, J. (1998a): Extensions and affiliates of the Yukon-Tanana Terrane in northern British Columbia; in *Geological Fieldwork 1997, B.C. Ministry of Employment and Investment*, Paper 1998-1, pages 7-1 to 7-12.
- Nelson, J.L., Harms, T.A. and Mortensen, J. (1998b): The southeastern Dorsey Terrane: characteristics and correlations; *Slave-Northern Cordillera Lithospheric Evolution (SNORCLE) and Cordilleran Tectonics Workshop*, Report of the 1998 Combined Meeting; pages 279-288.
- Stevens, R.A. (1996): Dorsey Assemblage: pre-mid-Permian high temperature and pressure metamorphic rocks in the Dorsey Range, southern Yukon Territory; *Slave-Northern Cordillera Lithospheric Evolution (SNORCLE) and Cordilleran Tectonics Workshop*, Report of the 1996 Combined Meeting, pages 70-75.
- Stevens, R.A. and Harms, T.A. (1995): Investigations in the Dorsey Terrane, Part I: Stratigraphy, structure and metamorphism in the Dorsey Range, southern Yukon Territory and northern British Columbia; in *Current Research, Geological Survey of Canada*, Paper 1995 - A, pages 117-128.



THE DIGITAL TERRAIN MAP LIBRARY: AN EXPLORATIONIST'S RESOURCE

By I.C.L. Webster, P.J. Desjardins and W.E. Kilby

KEYWORDS: digital terrain maps, digital terrain stability maps, surficial geology, GIS, raster image, vector image

INTRODUCTION

The Digital Terrain Map Library provides terrain and related maps in digital format on the Internet at www.ei.gov.bc.ca/geology/. Vector and raster image maps presently in the library include early terrain maps produced by the Ministry of Environment, Lands and Parks and new Terrain and Terrain Stability maps that are currently being produced through B.C. Forest Practices Code Act requirements.

Terrain maps and their derivative products are becoming increasingly more popular and widely used in the province. Surficial materials displayed on terrain maps form the primary building blocks for many terrestrial mapping systems. In addition to their use in developing logging plans and road construction in the forest industry, these maps are routinely being used in engineering and geotechnical consulting, land-use planning, terrestrial ecosystem mapping, aggregate development, placer and glacial drift exploration. This paper is primarily directed to mineral explorationists that may be unfamiliar with terrain maps and their availability.

Since 1989 the British Columbia Geological Survey Branch has been responsible for Quaternary geology studies in the province. This includes mapping, drift exploration studies, geological hazard research and data inventory. The Geological Survey Branch is the custodian of digital map data and makes this information available over the Internet. The Digital Terrain Map Library project, which began in October 1996, is providing terrain information in an easily accessed format at no cost to the user. Funding for this project is provided by Forest Renewal B.C..

INTRODUCTION TO TERRAIN MAPPING

The terms terrain, surficial geology, Quaternary geology and the older term superficial geology are somewhat synonymous, however terrain maps do not differentiate units on a time-stratigraphic basis. Terrain refers to a tract or region considered as a physical feature, ecological environment or a site of planned activity; terrane is a tectono-stratigraphic grouping of bedrock formations.

To ensure data consistency between disciplines utilizing terrain information a standardized approach has been established through guidelines published by the Resources Inventory Committee (RIC). Information may be shared between all members of the terrain community. The B.C. Ministry of Environment, Lands and Parks (MELP) pioneered many of the early standards. The Terrain Classification System for British Columbia, Version 2 (Howes & Kenk, 1997) is designed to classify and inventory surficial materials, landforms and geomorphological processes. This document forms the basis for terrain mapping in British Columbia and can be either viewed or downloaded from the MELP Internet site located at <http://www.elp.gov.bc.ca/rib/wis/terrain/inventory/manuals.htm>. The objective of this website is to provide access to all material required and related to terrain mapping. Listed below are other publications located at this site.

- ♦ A User's Guide to Terrain Maps in British Columbia
- ♦ Guidelines and Standards to Terrain Mapping in British Columbia
- ♦ Terrain Stability Mapping in British Columbia: A Review and Suggested Methods for Landslide Hazard and Risk Mapping
- ♦ Standard for Digital Terrain Data Capture in British Columbia

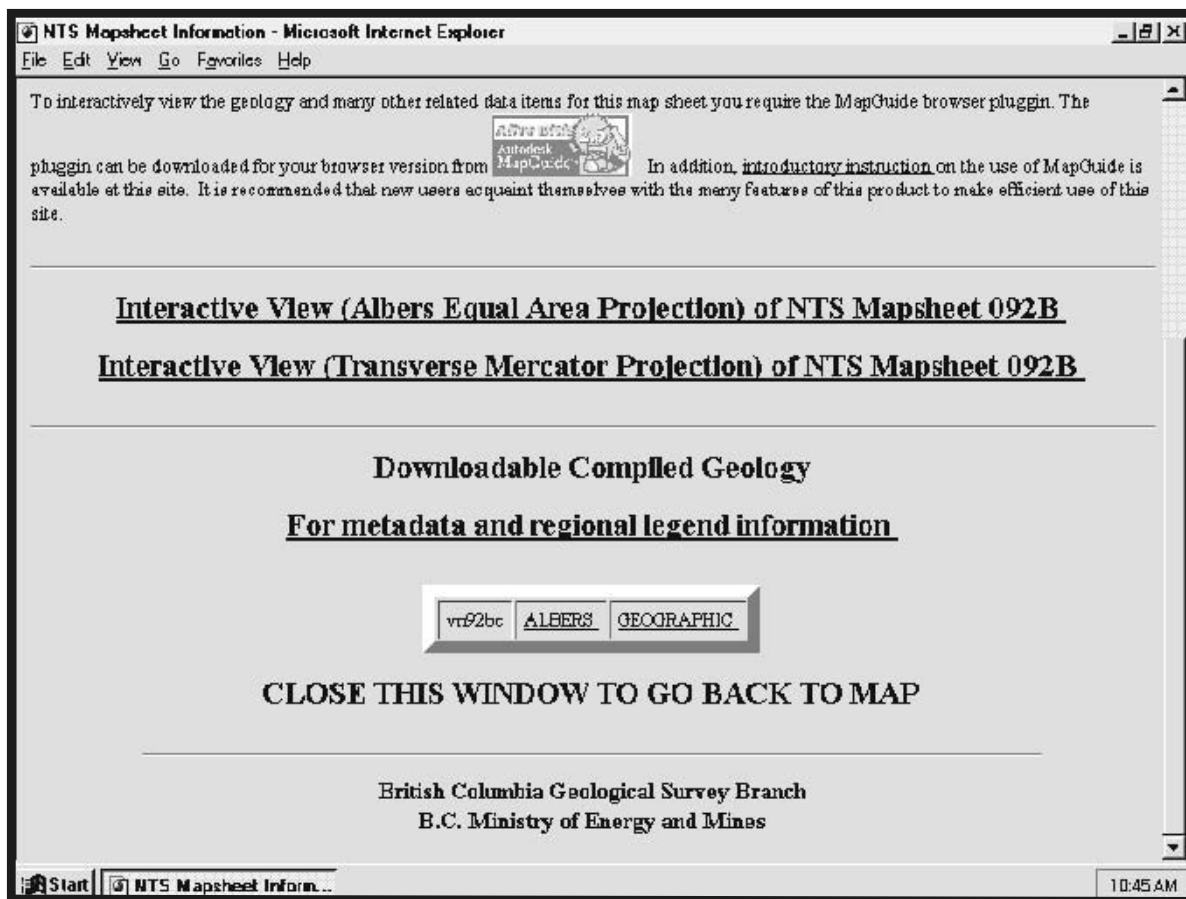


Figure 1. Digital terrain map library screen image showing options to view maps interactively with MapGuide or download as ArcInfo .E00 export file.

A variety of derivative maps are being produced that utilize information provided by terrain maps. Terrain stability maps are derived based on terrain polygon label information plus other criteria such as the frequency of occurrence of existing slope failures, drainage, anticipated usage and local knowledge. The Mapping and Assessing Terrain Stability Guidebook (1995), produced under the *Forest Practices Code Act*, contains information about derivatives such as the Slope Stability Classes I through V.

On-site symbols and line symbology are used extensively on terrain maps to represent features such as ice flow direction indicators, eskers, debris slides and avalanche tracks. A catalogue of all the features including a description and a feature code (number) can be found at the MELP website <http://www.env.gov.bc.ca/gis/featurecodes.html> and in The Standard for Digital Terrain Data Capture in B.C.. Terrain and derivative maps are well suited for Geographical Information

Systems (GIS) because of the variety and associations of information they contain.

ACCESSING MAPS AT THE LIBRARY

The B.C. Geological Survey home page is located at www.ei.gov.bc.ca/geology/. This site provides access to the entire provincial geoscience database available on the WWW and is expanding rapidly. Users are encouraged to explore the options available here for obtaining other geological information. The Terrain Map Library is reached by following the links on this page. The Terrain Map Library homepage contains the following links:

- ♦ General Project Description
- ♦ Surficial Geology Map Index of B.C. (GSB Open File 1992-13)
- ♦ Interactive and downloadable Terrain and Terrain Stability Maps
- ♦ Interactive Aggregate Potential Maps

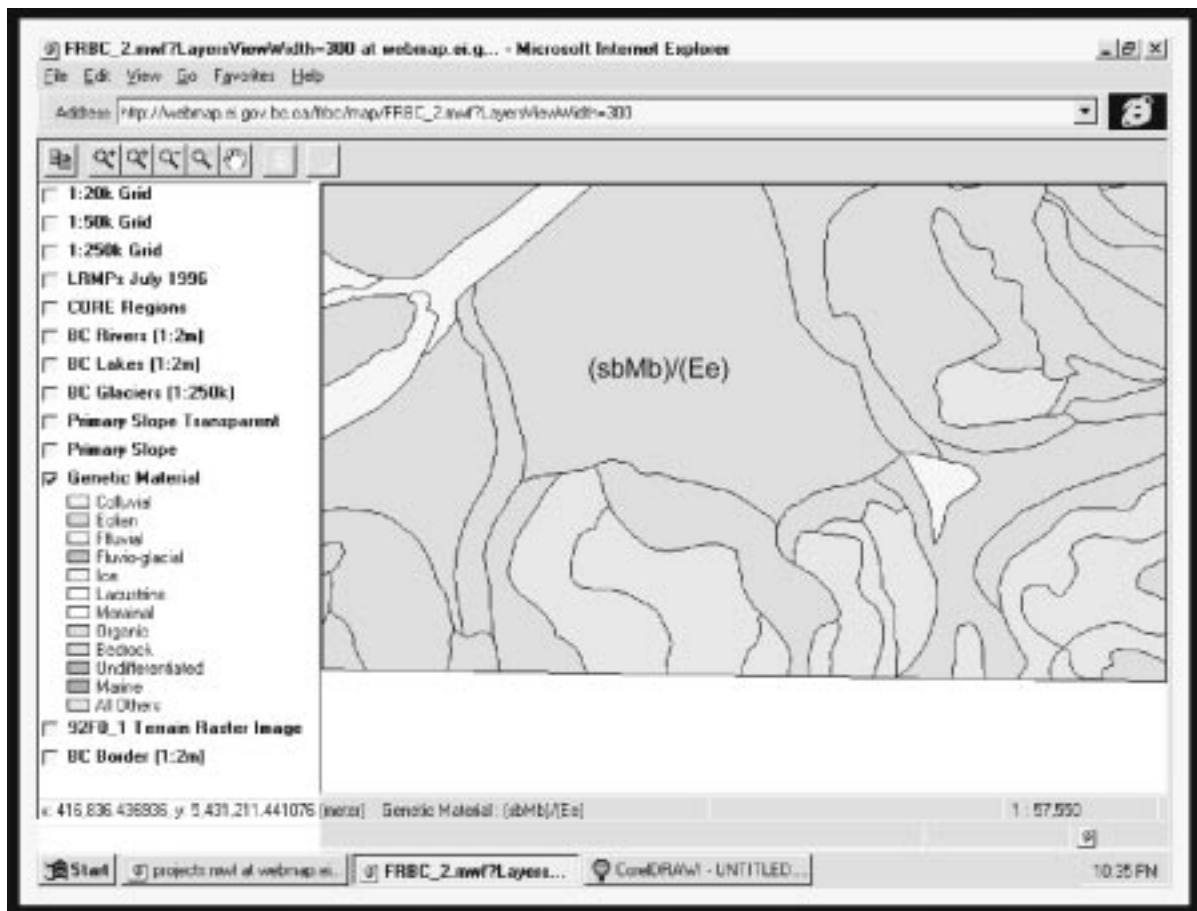


Figure 2. Terrain map library screen image showing example of vector image for part of Nanaimo Lakes mapsheet.

- ♦ Listing of new additions or changes
- ♦ Related WWW Sites

Follow the link to Interactive and downloadable Terrain and Terrain Stability Maps to view terrain maps or download the digital map files. The information provided at each step is comprehensive and should be read for a thorough understanding of the options available. The free MapGuide viewer must be downloaded and installed to enable the browser to display the maps. An outline of the province will appear with coloured areas indicating where digital coverage is available. Double click on an area. This leads to a page that provides an option to view the maps interactively using MapGuide or to download the files in zipped Arc Export (E00) format or raster image (Figure 1).

There are two digital formats that can be accessed in the Digital Terrain Map Library.

Vector Format

Vector data is available for viewing through

MapGuide or downloading in a standard GIS format. Vector objects can be associated with attribute information and are viewable at many scales (Figure 2). A number of queries can be performed on vector map data using MapGuide.

Raster format

Raster image maps are obtained by scanning the original map and as such, form a static copy of the original. These raster images are georeferenced for viewing with MapGuide in the Terrain Map Library or may be downloaded to produce copies of the original map (Figure 3).

MAP SOURCES

Existing hardcopy maps produced by Ministry of Environment during the 1970s and 1980s are being converted to digital format for inclusion in the library. There is coverage for approximately one half of the province at 1:50 000 scale (Figure 4). Soils and Landforms maps were included to provide coverage, where there

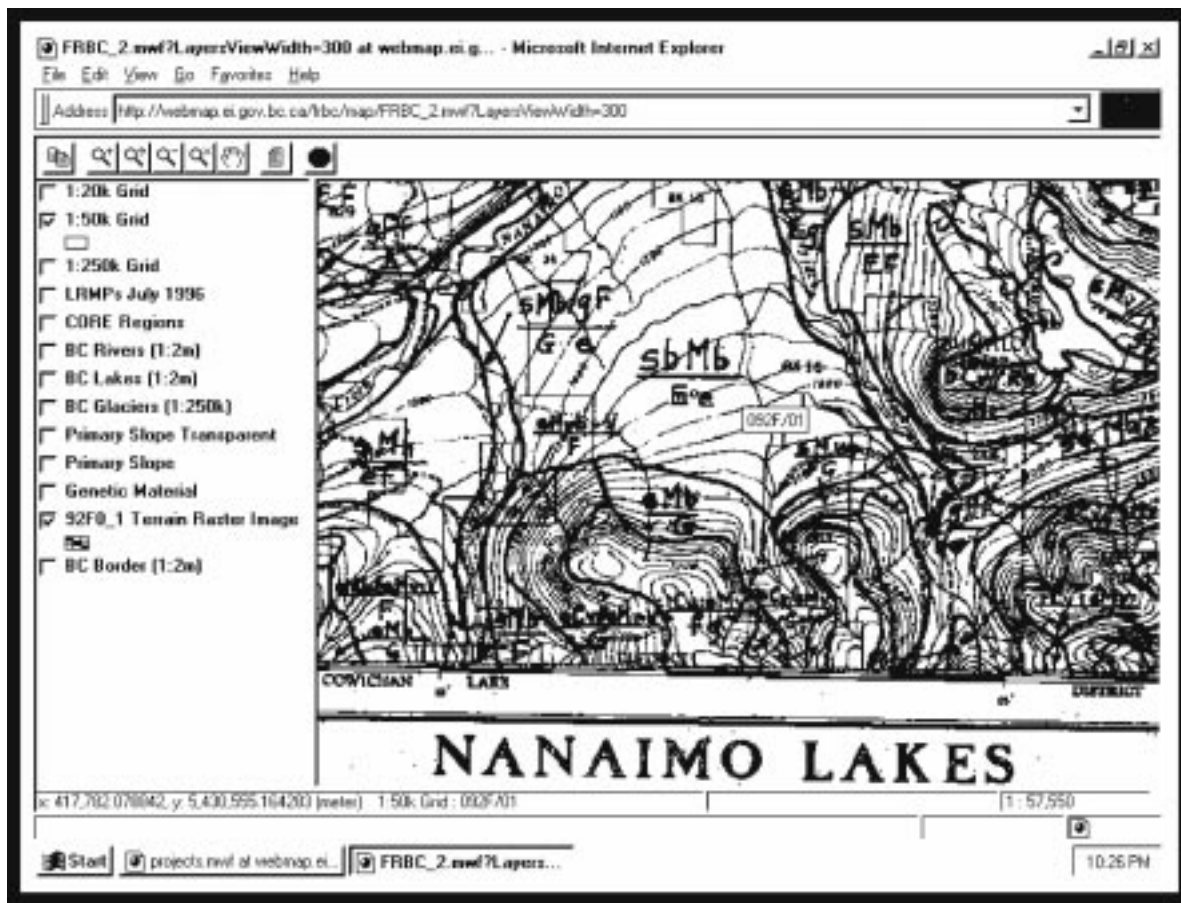


Figure 3. Raster image of original Ministry of Environment map showing the same area as in Figure 2.

were no terrain maps, because the soil types provide information about the parent (genetic) material. The converted digital maps reflect the original map information as closely as possible: no attempt is made to convert the older attribute information to comply with the new standards for terrain mapping. Data is captured in a georeferenced format in the same datum as the original. In most cases this is the NAD 27 datum, conversion to NAD83 is accomplished using the National Transformation Version 2 conversion grid. As digital vector based maps are useable at many scales and may be integrated with a wide variety of basemaps, special digitizing conventions were adopted to deal with the data capture of waterbodies. Existing waterbodies, oceans, lake shores and some large rivers, are not included. Instead terrain polygons are projected out into the waterbodies. This allows for data to be easily incorporated into many different basemaps. GIS operators can clip the terrain maps with the water bodies from their basemaps or simply overly the water features on the terrain data. Different scale digital basemaps have dif-

ferent shoreline positions and shapes and adoption of any one would have created significant problems for users of other basemaps.

Most maps contain inconsistencies in linework or labeling. Where obvious, these problems have been addressed, but in many cases they could not be resolved. Typical examples of these problems are; multiple labels in a polygon, no label in a polygon, labels that are not described in the legend and incomplete linework. Where possible, unresolved problems are left as documented on the map unless their inclusion is completely incompatible. The user does have the option to view the raster image of the original map.

All new FRBC funded terrain stability mapping that is being produced throughout the province under *B.C. Forest Practices Code Act* requirements is submitted to the library in hardcopy and digital format. This new mapping must adhere to RIC standards as outlined in Standard for Digital Terrain Data Capture in British Columbia. Most of these maps are at 1:20 000 scale and will be posted directly at the

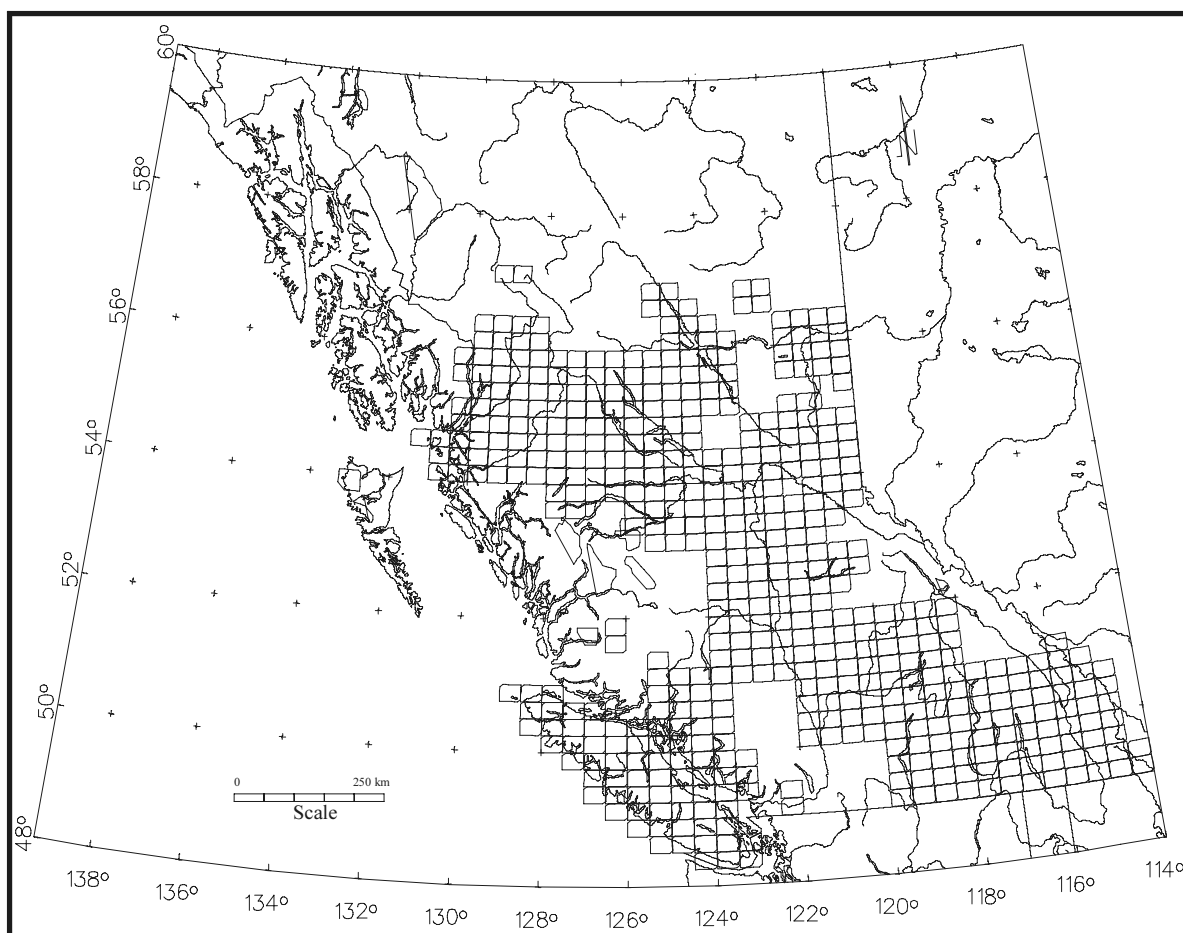


Figure 4. Map of B.C. showing 1:50 000 scale Ministry of Environment, Lands and Parks Terrain and Soils and Landforms coverage.

Terrain Map Library site for downloading and on-line access.

MAP USES

Terrain and terrain stability maps have many potential uses in mineral exploration. Knowledge of terrain materials distribution and processes in an area can assist in the planning and interpretation of geochemical programs such as drift and placer exploration. Terrain maps also provide information about the thickness and the direction from which materials may have been transported prior to deposition. This can assist in determining potential up-ice source areas for anomalous geochemical samples or mineralized float.

Work involving surface disturbance such as access or drill pad construction requires knowledge of slope stability in an area. The Mine Health & Safety Reclamation Code (Mineral Exploration Code) requires special considera-

tion in areas that are mapped as Slope Stability Class V, or class IV and V in community watersheds. Materials, processes and slope stability class can readily be determined at the Terrain Map Library. Other uses of terrain and terrain stability maps include providing information about areas with the greatest sediment delivery potential to fish bearing streams, baseline data for environmental considerations such as biodiversity and habitat possibilities and determining potential sources of aggregate.

SUMMARY

Terrain and terrain stability maps can be accessed from the Digital Terrain Map Library. This is a comprehensive site that provides the information required to understand, use and print maps. It is an important new resource of value to the explorationist.

BIBLIOGRAPHY

- Howes, D.E., Kenk, E. (1997): Terrain classification system for British Columbia; *B. C. Ministry of Environment*, Manual 10, Version 2, 102 pages.
- Resources Inventory Committee (1996); Guidelines and standards to terrain mapping in British Columbia; *Government of British Columbia*, 216 pages.
- Bobrowsky, P.T., Giles, T. and Jackaman, W. (1992): Surficial geology map index of British Columbia; *B. C. Ministry of Energy, Mines and Petroleum Resources*, Open File 1992-13, 147 pages.
- Ryder, J.M. and Howes, D.E. (1984): A user's guide to terrain maps in British Columbia; *B. C. Ministry of Environment*, 16 pages.
- Resources Inventory Committee (in press): Standard for digital terrain data capture in British Columbia; *Government of British Columbia*, 95 pages.
- Resources Inventory Committee (1996): Terrain stability mapping in British Columbia: a review and suggested methods for landslide hazard and risk mapping; *Government of British Columbia*, 80 pages.
- British Columbia Ministry of Forests (1995): Mapping and assessing terrain stability guidebook; *Forest Practices Code of British Columbia*, 34 pages.

THE BRITISH COLUMBIA SEDIMENT-HOSTED GOLD PROJECT

By David V. Lefebure, Derek A. Brown and Gerald E. Ray,
British Columbia Geological Survey

KEYWORDS: Economic geology, mineral deposits, Cordilleran geology, gold, Carlin-type deposits, sediment-hosted disseminated gold deposits.

INTRODUCTION

In 1997 the British Columbia Geological Survey (BCGS) initiated a project to identify prospective areas for sediment-hosted gold mineralization. The inspiration for the project came from presentations and articles by Howard Poulsen of the Geological Survey of Canada (1996a, 1996b). He pointed out that there is potential to find hypogene, sediment-hosted gold mineralization in Canada akin to deposits found in Nevada. He mentioned that if an intrusive association is important to generate the mineralization, then two different geological environments might host this style of mineralization. Accreted terranes with a basement containing carbonate lithologies intruded by Mesozoic or Cenozoic plutonism would be a prospective geological setting, specifically the Stikine and Quesnel terranes. The second favourable environment is within the sediments deposited along the continental margin of ancestral North America which have been cut by Mesozoic magmas, such as are found in the Kootenay Arc and Selwyn Basin (Figure 1).

Others have considered British Columbia as prospective territory for sediment-hosted gold. Early work by companies focused on the Insular Belt rocks exposed on Vancouver Island and the Queen Charlottes. These exploration programs were based largely on an epithermal-style model for the mineralization which was in favour at the time. The discovery of the Babe deposit (now called the Specogna or Cinola) in the Queen Charlotte Islands in 1970 increased the interest in this model because it was initially identified as a Carlin-type deposit (Richards *et al.*, 1976; Champigny and Sinclair, 1982). Subsequent

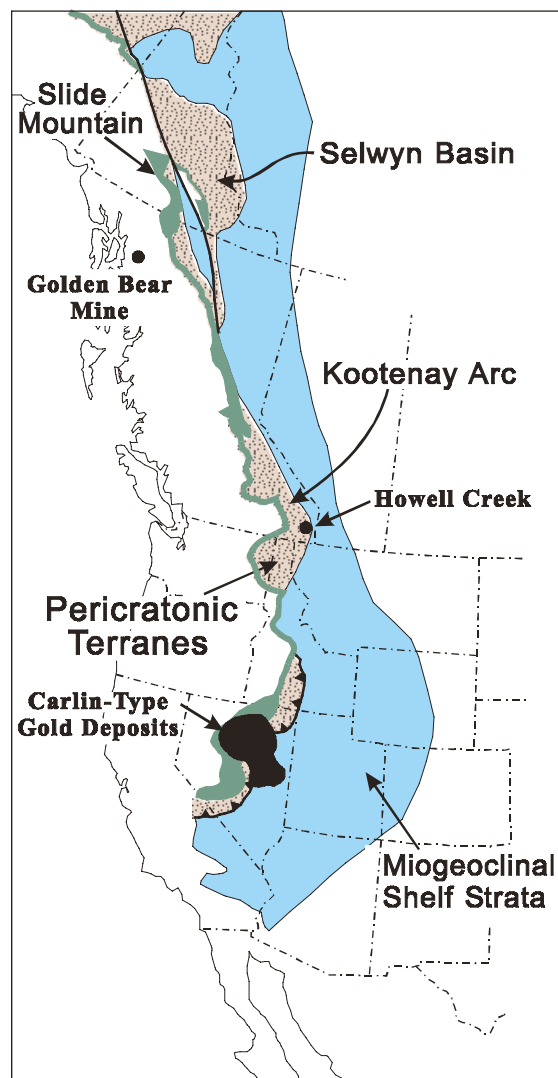


Figure 1. Map of western North America showing the sedimentary rocks deposited along the ancestral continental margin and the accreted terranes to the west (derived from Poulsen, 1996b). The Slide Mountain terrain consists of miogeoclinal sediments.

work showed that the Babe is a classic hot spring deposit and although some jasperoid occurrences were discovered on the Queen Charlottes, these programs did not result in any major sediment-hosted gold discoveries (Lefebure, 1998). Also in the early 1970s, Harry Warren of the

University of British Columbia became interested in exploring for Carlin-Cortez type deposits in the province (Warren and Hajek, 1973). He made the prophetic statement that the initiation of gold production at the Carlin deposit might prove to be as important a milestone for gold production as the first exploitation of a copper porphyry deposit was for copper.

A number of companies have carried out reconnaissance programs for sediment-hosted gold in British Columbia; but these are not part of the public record. In the early 1980s, Chevron searched for Carlin-type deposits in the Stikine terrane in the northwestern part of the province and found the Golden Bear deposit. Although initially discovered using exploration techniques applicable to Carlin-type deposits, the refractory style of mineralization and predominance of volcanic host-rocks delayed confirmation as this deposit type (Oliver, 1996).

During the first year (1997) of the BCGS project, Gerry Ray visited a number of gold occurrences, including Golden Bear, Watson Bar and Summit in British Columbia and Brewery

Creek in the Yukon. The following year, Derek Brown took over leadership of the project and carried out detailed studies of the Golden Bear and Howell Creek areas.

BACKGROUND

The State of Nevada has become the world's fourth largest gold producer after South Africa, Australia and the CIS. Much of this gold is being produced from sediment-hosted disseminated gold deposits. Many geologists call these deposits Carlin-type (Berger and Bagby, 1991) after the mine of the same name in Nevada. The Carlin mine was discovered in 1961 by Newmont Exploration Limited (Roberts, 1986) and subsequently was used to characterize a new class of deposits that are now identified as sediment-hosted deposits with microscopic gold. Subsequent discoveries around Carlin are now being mined and have made it the most prolific gold belt in North America with a current resource of more than 100 million ounces (Teal and Jackson, 1997). This belt, known as the

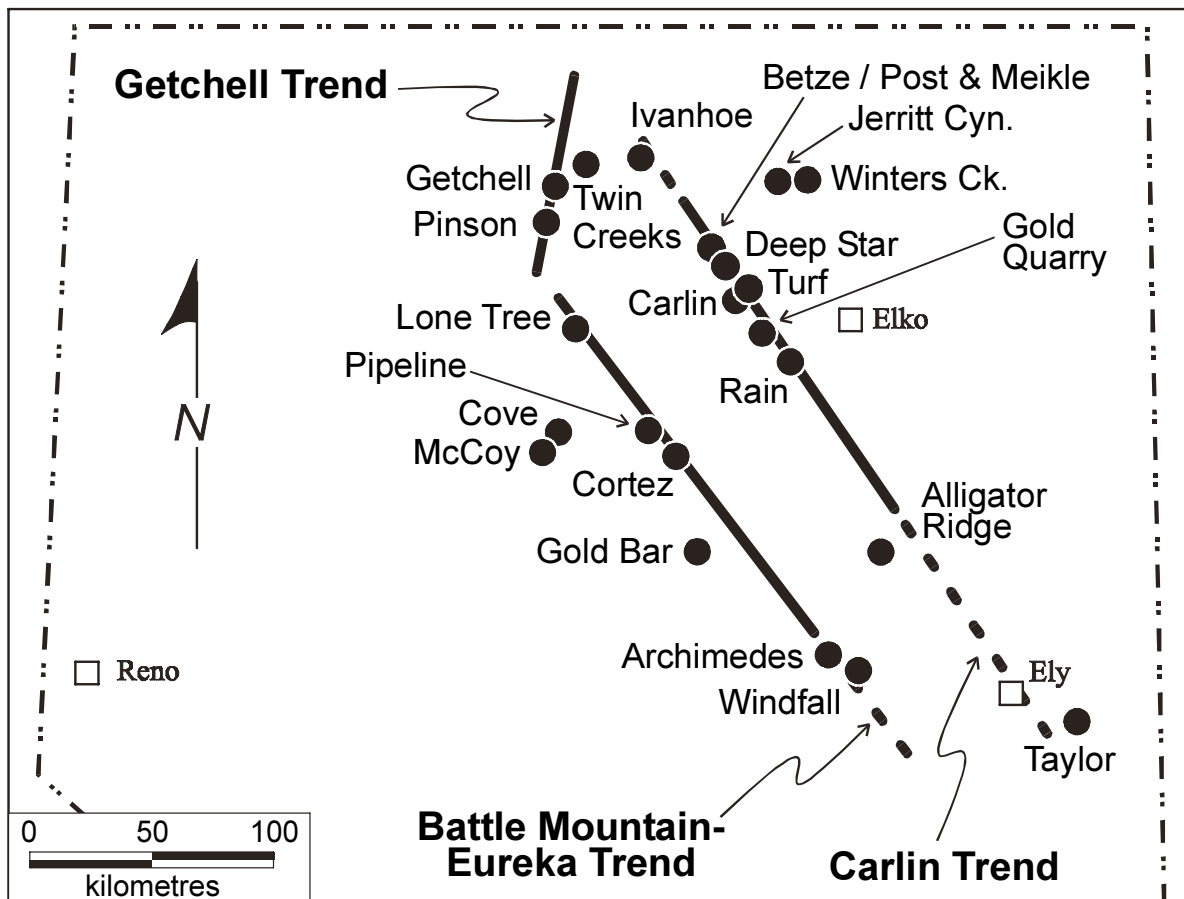


Figure 2. Location of Carlin-type gold deposits in Nevada showing the major trends.

Carlin Trend, is just one of the areas in Nevada with these types of deposits (Figure 2).

Since the gold mineralization is microscopic and associated features are often visually unspectacular at outcrop scale, these deposits are poorly understood and the mineralization is difficult to recognize. Fortunately, more than thirty years of exploration and mining in Nevada have resulted in a number of well described mines and documented the wide range of styles of mineralization. Some general information about Carlin-type deposits is presented in this article. For a more complete description of these deposits the reader is referred to the numerous articles published over the last ten years, including overviews by Arehart (1996), Teal and Jackson (1997) and Vikre *et al.* (1997) and numerous publications by the Nevada Geological Society (for example, Green and Struhsacker, 1996).

SEDIMENT-HOSTED DISSEMINATED GOLD DEPOSITS (CARLIN-TYPE)

Although initially called *Carlin-type*, many geologists have adopted other terms to facilitate developing a deposit model that is more generic, such as *disseminated gold* (Roberts, Radtke and Coats, 1971), *sediment-hosted disseminated gold*, *sediment-hosted micron gold*, *siliceous limestone replacement gold* and *invisible gold* (Schroeter and Poulsen, 1996). In this paper we use the terms *sediment-hosted disseminated gold* and *Carlin-type* interchangeably. With the discovery of many more mines over the last 20 years, a broader definition of Carlin-type deposits has emerged. They are now identified as 'sediment-hosted, disseminated, stratabound yet structurally controlled precious metal mineralization' (Ralph J. Roberts Research for Research in Economic Geology, web page, 1998).

Key Features

Carlin-type deposits contain micron-sized gold within very fine-grained disseminated sulphides in stratabound zones and in discordant breccias. The most common host rocks are impure carbonates, however, other sedimentary and igneous lithologies can host mineralization. Christensen (1993, 1996) points out that the gold mineralization appears to be disseminated at the

deposit scale, however, gold is structurally controlled at all scales. For a deposit to be considered a sediment-hosted disseminated gold deposit it usually has many of the following features:

- ♦ non-visible, micron gold within arsenicalpyrite or pyrite (refractory ore)
- ♦ non-visible, extremely fine native gold within iron oxide or attached to clay (oxide ore)
- ♦ anomalous values of silver, arsenic, mercury, and antimony and low base metals
- ♦ associated realgar, orpiment and/or stibnite sedimentary host sequences containing silty carbonate or calcareous siltstone
- ♦ intensely silicified zones, commonly called jasperoid
- ♦ carbonate dissolution (decalcification)
- ♦ associated brittle structures

Carlin-type deposits are difficult to find for a number of reasons. The gold is microscopic; visible gold is only very rarely reported from the highest grade zones. The lower grade deposits have low sulphide contents and even in higher grade hypogene deposits the gold is typically associated with a very fine-grained, black, sooty pyrite that can be difficult to identify macroscopically. Furthermore, surface weathering can convert all sulphides to iron oxides, such as hematite and limonite, and rarely produces significant gossans. Exploration for these deposits has tended to draw on empirical relationships observed in Nevada, such as the presence of thick sedimentary sequences along a paleo-continental margin, the presence of significant beds of impure carbonate, identification of jasperoids, and the presence of realgar, orpiment and stibnite. Yet even with the identification of these favourable features, it has taken numerous, systematic geochemical and drilling programs along known mineralized trends in Nevada to make new discoveries.

Since the gold is micron-sized, it cannot be identified by panning and Carlin-type deposits are normally not associated with placer gold workings. The alteration associated with these deposits is often inconspicuous (Christensen, 1994). It consists of carbonate dissolution (decalcification), pervasive silica replacement and deposition, alteration of aluminosilicates to

clay and sulphidation of iron to form pyrite. Gold is usually the only metal recovered from Carlin deposits. While minor sphalerite and galena are noted in some zones, the deposits rarely have any copper minerals. A more complete listing of the geological characteristics of Carlin-type deposits is given in Table 1.

The sediment-hosted microscopic gold deposits in Nevada are well known for the intense supergene alteration that occurs near surface. This feature is directly responsible for making heap leaching a viable process for treating low grade ores. It is generally attributed to the prolonged arid weathering of rocks in Nevada. It has been noted that oxidation features associated with the supergene alteration extend further below the surface in many deposits than in the surrounding areas (Christensen, 1994). Christensen postulates that this is because the host rock for these deposits has been structurally prepared and altered.

In the last ten years a number of deep deposits with higher grades have been discovered along the Carlin Trend. These high grade orebodies exhibit breccia features and vein-like ores (Figure 3) as well as low grade, stratabound replacement mineralization like the Carlin mine (Christensen *et al.*, 1996; Groves, 1996). The initial underground mining of these ore zones started with declines from open pit workings, such as are used for the Deep Star and Carlin

East deposits. However, in 1996 the Meikle mine started production utilizing a conventional shaft and has become the largest underground gold producer in the United States. These deep deposits are below the Miocene surface weathering and the ore is commonly refractory. Analysis of the orebodies along the Carlin Trend shows that stratabound replacement orebodies are less common than the vein-like and breccia mineralization styles.

Stratabound replacement mineralization is exemplified by the Carlin deposit. Large volumes of altered rock contain relatively low grade gold zones which have had minor structural disruption. Stratabound replacement deposits found at, or near surface, in Nevada are particularly amenable to heap leaching because the primary refractory ore has been oxidized by the arid climate that has existed since the Cretaceous. Using bulk mining techniques, relatively low grade surface material can be mined. Other examples of the stratabound replacement style of mineralization are the Pete, Deep West portion of Gold Quarry, West Leeville, Hardie Footwall, Goldbug and Screamer (Christensen *et al.*, 1996; Teal and Jackson, 1997).

The second style of mineralization is called stockwork (Christensen, 1993) or breccia ore (Groves, 1996) and is found near structural intersections which can produce complex relationships. An example of this deposit type is the

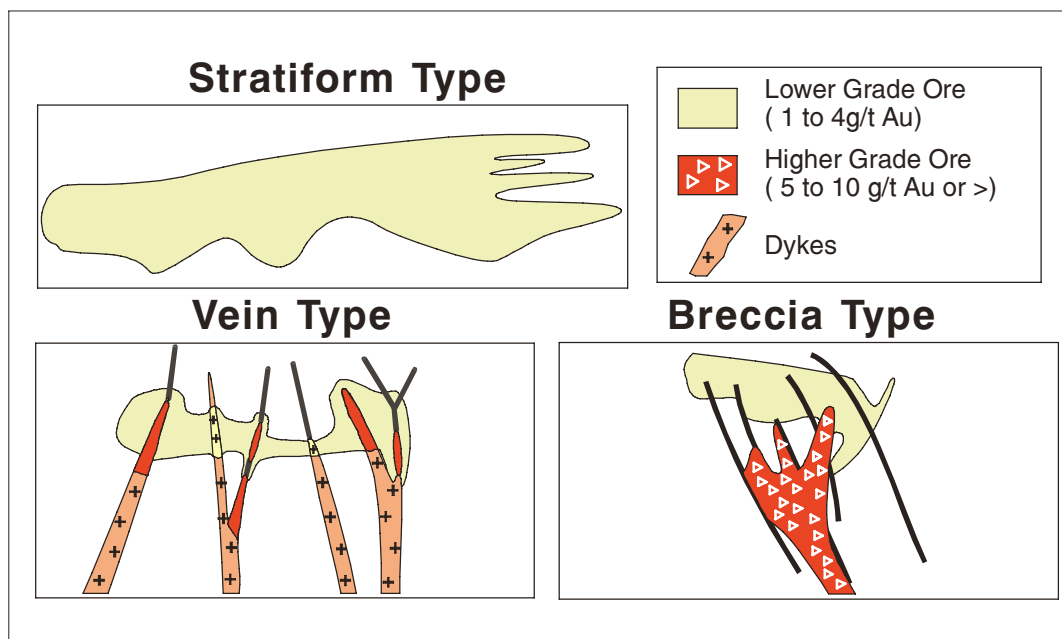


Figure 3. Different styles of Carlin-type mineralization (modified from Christensen, 1993, 1996). The heavy solid lines are faults.

Table 1. Geological Characteristics of Carlin-type Deposits.

TECTONIC SETTINGS: Passive continental margins with subsequent deformation and intrusive activity and island arc terranes.

DEPOSITIONAL ENVIRONMENT / GEOLOGICAL SETTING: Host rocks to the Nevadan deposits were deposited in shelf-basin transitional (somewhat anoxic) environments, formed mainly as carbonate turbidites (up to 150 m thick), characterized by slow sedimentation. These rocks are presently allochthonous in thrust fault slices and have been overprinted by Miocene basin and range extension. There are Mesozoic to Tertiary felsic plutons near many deposits.

AGE OF MINERALIZATION: Mainly Tertiary, but can be any age.

HOST/ASSOCIATED ROCK TYPES: Host rocks are most commonly thin-bedded silty or argillaceous carbonaceous limestone or dolomite, commonly with carbonaceous shale. Although less productive, non-carbonate siliciclastic and rare metavolcanic rocks are local hosts. Felsic plutons and dikes are also mineralized at some deposits.

DEPOSIT FORM: Generally tabular, stratabound bodies localized at contacts between contrasting lithologies. Bodies are irregular in shape, but commonly straddle lithological contacts which, in some cases, are thrust faults. Some ore zones (often higher grade) are discordant and consist of breccias developed in steep fault zones. Sulphides (mainly pyrite) and gold are disseminated in both cases.

TEXTURE/STRUCTURE: Silica replacement of carbonate is accompanied by volume loss so that brecciation of host rocks is common. Tectonic brecciation adjacent to steep normal faults is also common. Generally less than 1% fine-grained sulphides are disseminated throughout the host rock.

ORE MINERALOGY [Principal and subordinate]: Native gold (micron-sized), *pyrite with arsenian rims*, *arsenopyrite*, *stibnite*, *realgar*, *orpiment*, *cinnabar*, *fluorite*, *barite*, *rare thallium minerals*.

GANGUE MINERALOGY [Principal and subordinate]: Fine-grained quartz, barite, clay minerals, carbonaceous matter and late-stage calcite veins.

ALTERATION MINERALOGY: Strongly controlled by local stratigraphic and structural features. Central core of strong silicification close to mineralization with silica veins and jasperoid; peripheral argillic alteration and decarbonation ("sanding") of carbonate rocks common in ore. Carbonaceous material is present in some deposits.

WEATHERING: Nevada deposits have undergone deep supergene alteration due to Miocene weathering. Supergene alunite and kaolinite are widely developed and sulphides converted to hematite. Such weathering has made many deposits amenable to heap-leach processing.

ORE CONTROLS: 1. Selective replacement of carbonaceous carbonate rocks adjacent to and along high-angle faults, regional thrust faults or bedding. 2. Presence of small felsic plutons (dikes) that may have caused geothermal activity and intruded a shallow hydrocarbon reservoir or area of hydrocarbon-enriched rocks, imposing a convecting geothermal system on the local groundwater. 3. Deep structural controls are believed responsible for regional trends and may be related to Precambrian crystalline basement structures and/or accreted terrane boundaries.

from Schroeter and Poulsen, 1996

Main Gold Quarry deposit which has a variety of lithologies, including thin-bedded siltstone, shale, chert and limestone (Christensen *et al.*, 1996). Teal and Jackson (1997) also identify Meikle and Deep Star as deposits with significant breccia-style mineralization.

Vein-like mineralization occurs within and adjacent to high-angle faults. The structures contain intensely altered, igneous dikes and relatively high grade gold. The gold is largely restricted to the fault. Examples of this style of mineralization are the Turf, Sleeper, Boot Strap and Capstone (Teal and Jackson, 1997).

Median tonnages and grades for forty-three low-grade oxide and higher grade hypogene deposits in Nevada are 20 Mt grading 1.2 g/t Au and 6 Mt containing 4.5 g/t Au, respectively (Schroeter and Poulsen, 1996). Supergene deposits amenable to heap leaching typically grade 1-2 g/t Au; whereas, production grades for deposits with hypogene ore typically grade 5 to 10 g/t or greater.

Global Distribution

There have been remarkably few Carlin-type deposits found outside the western United

States. This could reflect the existence of special geological conditions in Nevada not found elsewhere or insufficient exploration in other parts of the world. Given the microscopic nature of the gold and the nondescript alteration features, it is likely that undiscovered deposits occur in areas not previously considered prospective for this type of deposit. This was the case in Nevada before mapping by the United States Geological Survey led Newmont Exploration Limited to carry out the exploration program which led to the discovery of the Carlin deposit in an area which had a long previous history of prospecting and mining.

Deposits with Carlin-type characteristics have been reported from Utah, South Dakota, southeast Asia, Mexico, South America and Canada (Figure 4). There are also a large number of these deposits in the southwest Guizhou and western Hunan regions of southeastern China (Cunningham *et al.*, 1988). The setting for these mines is generally similar to Nevada. The Chinese gold mineralization is hosted by Upper Permian to Middle Triassic shelf carbonates which have experienced broad, open folding and some high angle faulting (Christensen *et al.*,

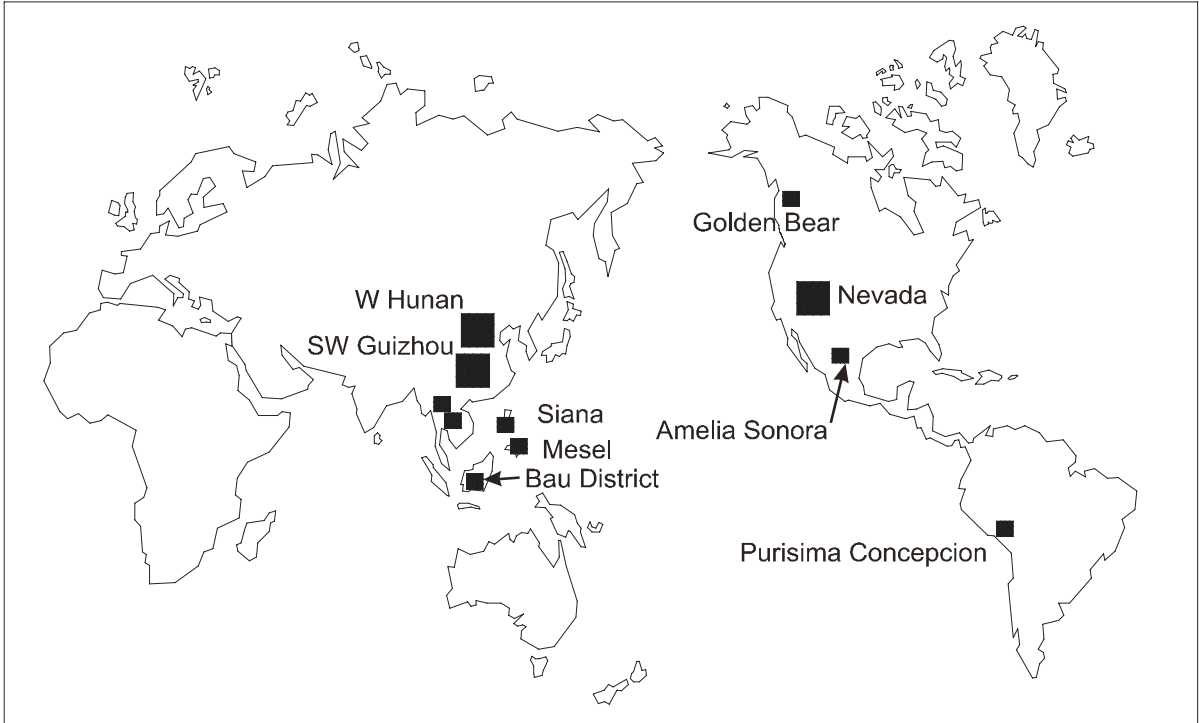


Figure 4. Global distribution of Carlin-type deposits (modified from Christensen *et al.*, 1996).

1996). Although the Guizhou area apparently lacks igneous rocks, they are reported at some other Chinese deposits (Griffin, personal communication, 1998).

There are relatively few Carlin-type deposits hosted by volcanic rocks (Lefebure and Ray, 1998). The best known examples are the Bau District of Sarawak, Malaysia (Sillitoe and Bonham, 1990) and the Mesel deposit of North Sulawesi, Indonesia (Turner *et al.*, 1994; Garwin *et al.*, 1995). The Mesel deposit, discovered in 1988, contains a reserve of 7.8 Mt grading 7.3 g/t Au and is currently in production. The Mesel deposit exhibits many characteristics of Carlin-type deposits, including decalcification, dolomitization and jasperoid development, accompanied by gold in disseminated fine-grained arsenian pyrite (Sillitoe, 1995).

In British Columbia, recent work by Jim Oliver as part of his Ph.D. thesis (1996) and field investigations by Howard Poulsen of the GSC and the authors have shown that the Golden Bear mine is a Carlin-type deposit.

Genesis

Currently, there is no clear understanding of the genesis of sediment-hosted microscopic gold deposits. Three general models have been proposed to explain the origin of the ore-forming fluids - magmatic, metamorphic and amagmatic. All three models involve generation of hydrothermal fluids at temperatures of 160 to 250 °C with low salinities and significant CO₂ contents, as found in fluid inclusions in Carlin-type deposits (Arehart, 1996; Ilchik and Barton, 1997). A more detailed listing of geological processes that could form sediment-hosted disseminated gold deposits is given by Adams and Putnam III (1992).

Carlin-type deposits were initially considered to be sediment-hosted, epithermal deposits (Radtke *et al.*, 1980; Radtke, 1985; Rye, 1985) because of a number of similar features including high gold, silver, arsenic, antimony and mercury values in mineralized zones, prevalence of silicification, presence of alunite, and spatial association with antimony and mercury occurrences. Given the abundance of epithermal gold-silver deposits hosted by volcanic rocks in Nevada, it seemed logical to assume that Carlin-type deposits formed at the roots of hot spring

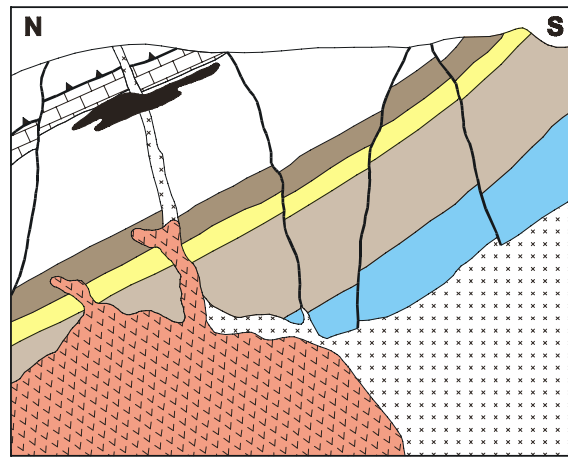


Figure 5. Early interpretations of Carlin-type deposits suggested that they were epithermal deposits that formed in sedimentary sequences (from Radtke, 1985).

systems related to shallow Miocene magmatism and basin and range extension (Figure 5). The subsequent discovery of deep orebodies and the documentation of overprinting of mineralization by basin and range deformation led most geologists to consider alternative models which are consistent with a deeper and older environment of formation (Arehart, 1996).

Magmatic systems are considered by many exploration and research geologists to play a key role in the formation of Carlin-type deposits (Arehart *et al.*, 1993). This model has been clearly conceptualized by Sillitoe and Bonham (1990). They suggested that hydrothermal fluids related to porphyry-type magmatic systems generated sediment-hosted disseminated gold deposits, somewhat akin to distal skarns (Figure 6). Some deposits, such as Post-Betze, Getchell, Bald Mountain and Archimedes, do occur near Jurassic or Cretaceous intrusions. Others are associated with, and partially hosted by, altered dikes that are controlled by faults. However, this model cannot explain all deposits because several districts (e.g. Jerritt Canyon) have no known related magmatism. Furthermore, in some locations the gold mineralization is a different age to the spatially associated intrusions.

Other workers have suggested models involving fluids generated either by deep-seated metamorphism (Seedorff, 1991), crustal extension (Ilchik and Barton, 1997), or the ancestral Yellowstone hotspot (Oppliger *et al.*, 1997). The regional metamorphic model derives the H₂O

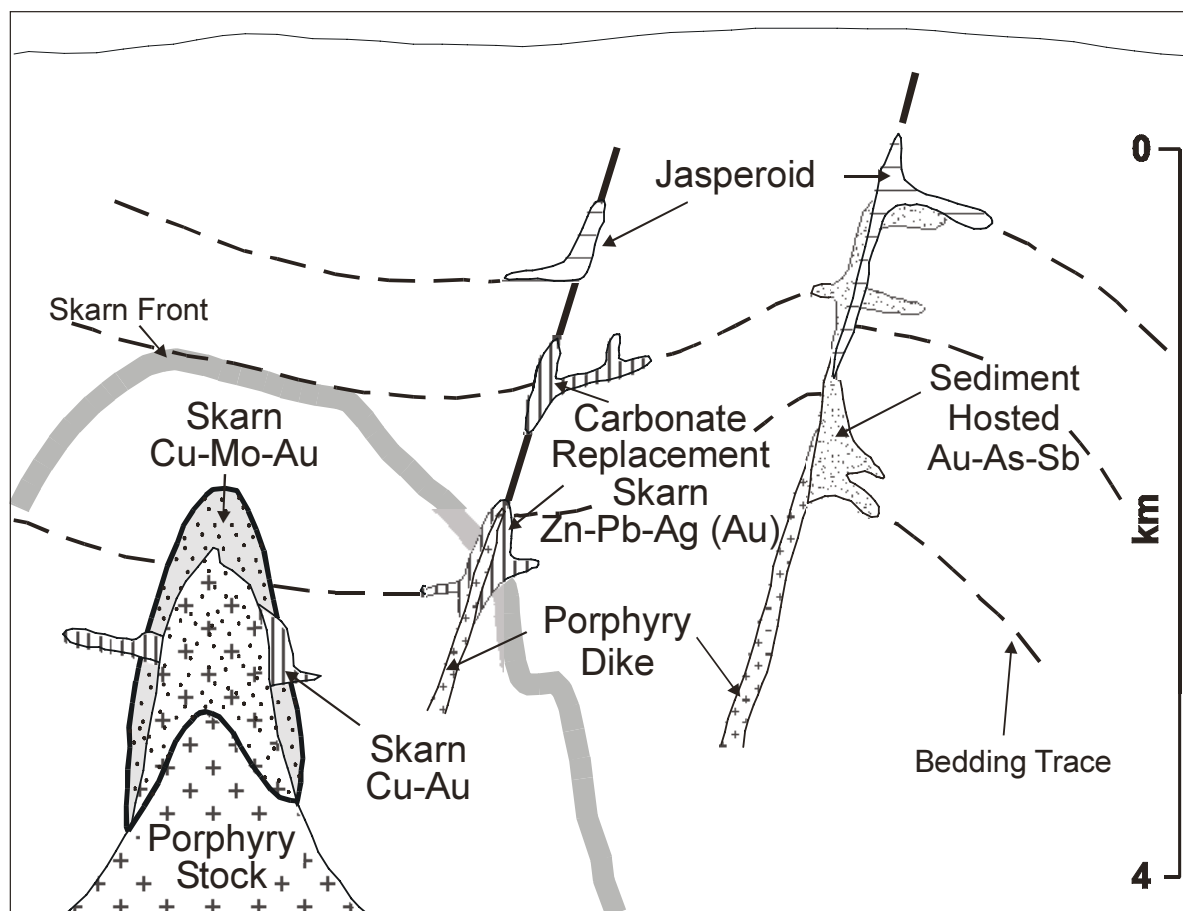


Figure 6. Magmatic systems are believed by some to play a major role in the formation of sediment-hosted microscopic gold deposits. Sillitoe and Bonham (1990) envisioned fluids emanating from porphyry-type magmatic systems.

and CO₂ from devolatilization of metasedimentary rocks which are also the source of metals and sulphur. While there may be associated magmatic activity, it is not a critical element to the model which emphasizes some of the similarities between mesothermal gold and Carlin-type deposits (Phillips and Powell, 1993).

More recently, Ilchik and Barton (1997) have proposed an amagmatic model with an anomalous thermal gradient caused by bringing more deeply buried, hotter rocks closer to the surface and allowing meteoric waters to penetrate to depths of ten to twenty kilometres before rising along major faults during mid-Tertiary extension in the Basin and Range province (Figure 7).

Another postulated source is metals derived from the core-mantle boundary and carried up into the crust by the plume associated with the ancestral Yellowstone hotspot (Oppliger *et al.*, 1997). The hotspot may have underlain the Great Basin of Nevada ca. 43-34 Ma and produced

hydrothermal fluids that formed the gold deposits. While these three models may explain some of the characteristics of the Carlin-type deposits, they also have some inconsistencies with published data. As well, all three models are tied to one geological event; therefore, they cannot explain deposits with significantly different ages. This is inconsistent with the widely held belief of many geologists working in the Great Basin that there are both Cretaceous (110-76 Ma) and Eocene (42-30 Ma) age deposits (Tosdal, personal communication, 1998).

Exploration Techniques

Geology is used to identify favourable stratigraphic units, related alteration zones and possible structural controls. Bedded silty carbonate and calcareous siltstone to dolomitic limestone are the most common hosts; although some deposits occur within sandstone, conglomerate, intrusive units and even volcanic rocks. In

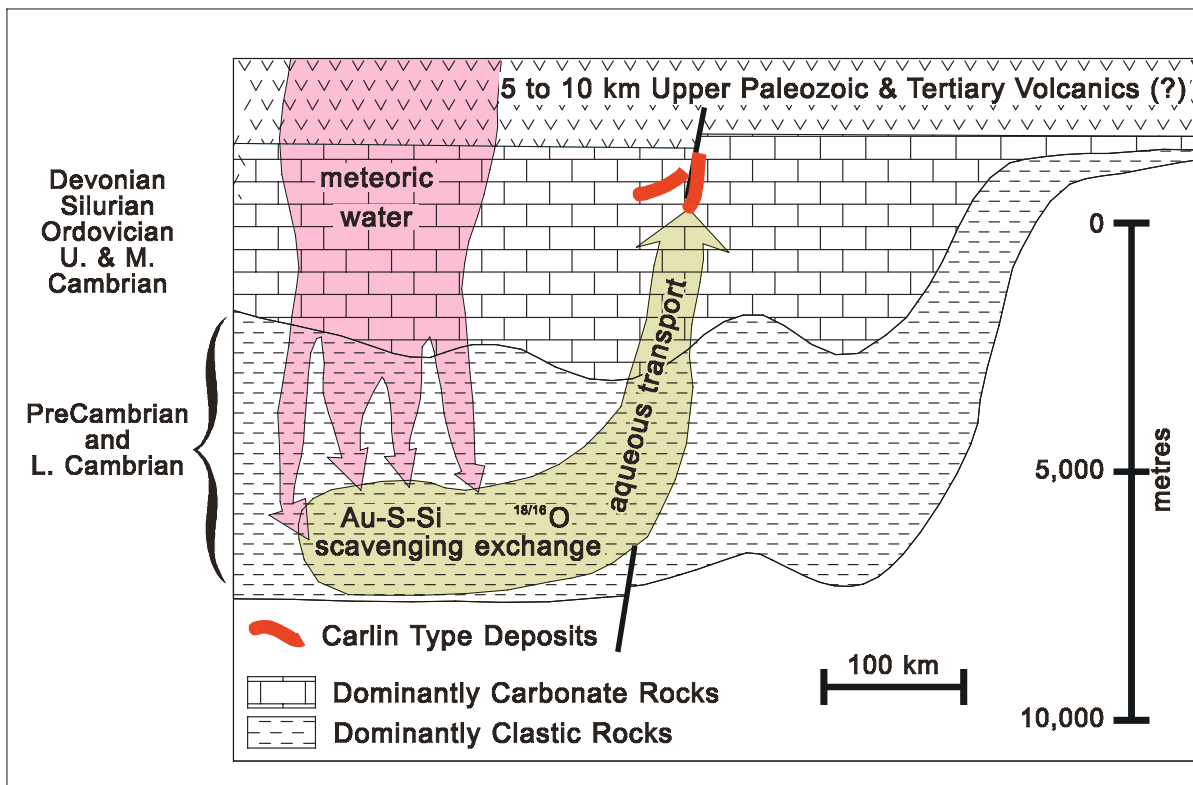


Figure 7. An amagmatic model to explain the genesis of sediment-hosted microscopic gold deposits (from Ilchik and Barton, 1997).



Photo 1. Bedded Roberts Mountain Formation from the Jerritt Canyon area, Nevada.

Nevada, bedded units, particularly thinly bedded sediments (Photo 1), have been found to be more likely to host mineralization.

Geochemistry has been the most important exploration technique following identification of geologically prospective districts. Initial field work often involves systematic sampling of soil or rock. Gold has been the most important element used in exploration programs, although anomalous values for the pathfinder elements arsenic, antimony and mercury have led to some discoveries (e.g. Golden Bear, L. Dick, personal communication, 1998). Schroeter and Poulsen (1996) identify two geochemical assemblages - (1) gold, arsenic, mercury and tungsten with or without molybdenum and (2) arsenic, mercury, antimony and thallium or iron. Common anomalous values in rock are 100 to 1000 ppm arsenic, 10 to 50 ppm antimony and 1-30 ppm mercury. Other elements that occur in anomalous amounts are silver, barium and thallium. Gold:silver ratios are generally greater than 8:1 (Adams and Putnam III, 1992; Roberts *et al.*, 1971).

Three principle alteration types are recognized: decarbonatization or decalcification of

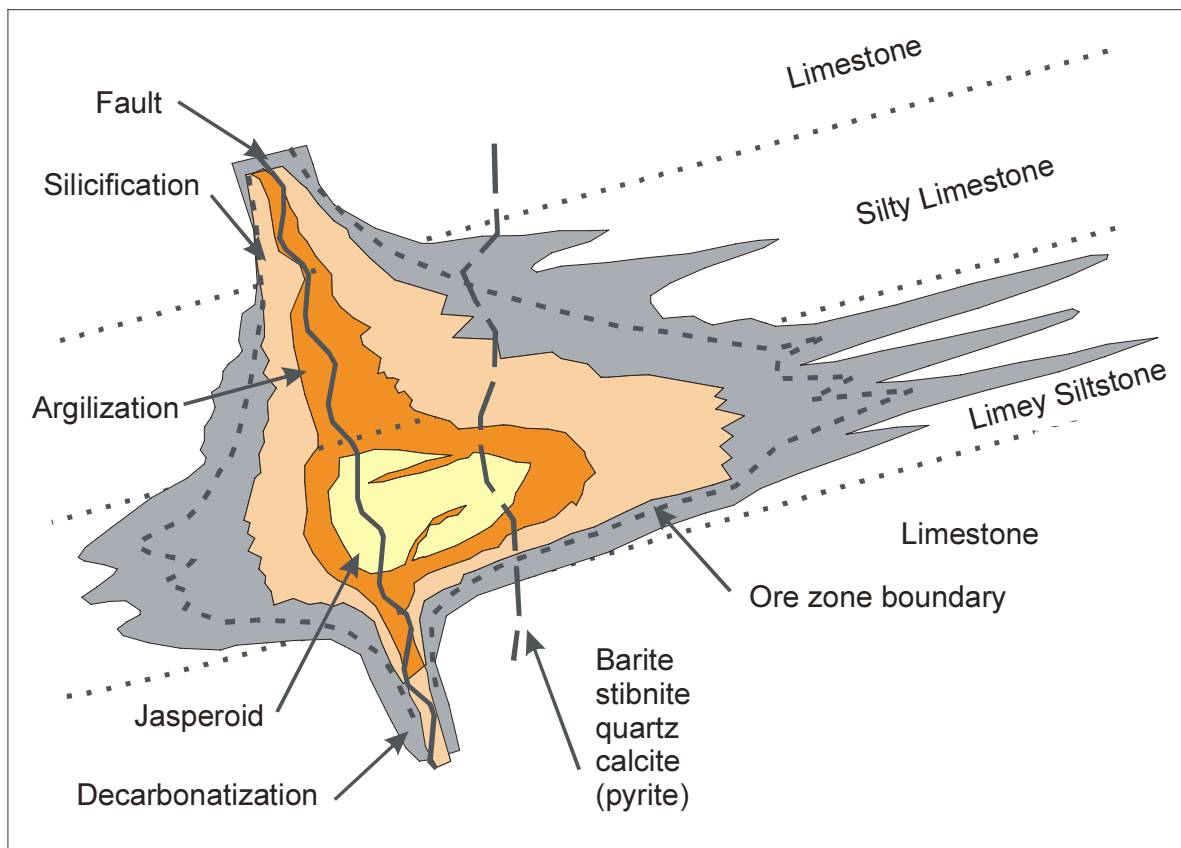


Figure 8. Schematic cross-section through a sediment-hosted disseminated gold deposit showing major alteration features adjacent to a fluid feeder structure (from Arehart, 1996).

carbonate rocks, silicification, and argillization. These types of alteration can display different relationships to gold mineralization. Arehart (1996) suggests that the most common zonation is decarbonatization on the fringes through silicification to argillization in the core of the deposit (Figure 8). Gold ore occurs in all three alteration types. However, in most deposits it is better developed in argillically or intensely silicified zones in the core of the system, often associated with a structural feature. The decarbonatized rocks are difficult to recognize unless alteration has been intense enough to produce a light, friable unit. These rocks can be brecciated because the volume loss associated with decarbonatization results in structural collapse. The clays in the argillized rocks are typically fine-grained and not particularly abundant, therefore, the alteration can be difficult to identify. Near surface, these altered rocks may be oxidized and are commonly brown, beige or reddish-brown with residual limonite or hematite after weathered pyrite. In a number of open pit mines the higher grades are associated with reddish-brown tabular zones which lie along structures (Photo 2).



Photo 2. The Jackrabbit Zone in the south wall of the Twin Creeks megapit, Nevada. The zone consists of reddish-brown iron oxides. It is 6 to 24 metres thick, extends laterally and vertically hundreds of meters and averages 3 g/t gold, but can grade up to 34 g/t Au (Bloomstein *et al.*, 1991).

One of the most obvious features of sediment-hosted disseminated gold deposits is an association with intensely silicified host rocks. In some cases the silicification contains little or no gold (Photo 3), however, it occurs proximal to a Carlin-type deposit. Frequently, the intense silicification is related to particular sedimentary bed or beds (Photo 4) or a fault zone. These rocks are particularly important exploration guide because they are a resistant lithology which is more likely to outcrop than other types of altered or unaltered host rocks (Photo 3). In Nevada, the intensely silicified rocks are commonly called jasperoid which is “an epigenetic siliceous replacement of a previously lithified host rock” (Lovering, 1972). This terminology has been rarely used in Canada, even for intensely silicified rocks. For this reason, there are few published references to jasperoid in the Canadian Cordillera.



Photo 3. Barren jasperoid boulders located approximately 100 metres from Gold Bar open pit in an area with no outcrop.

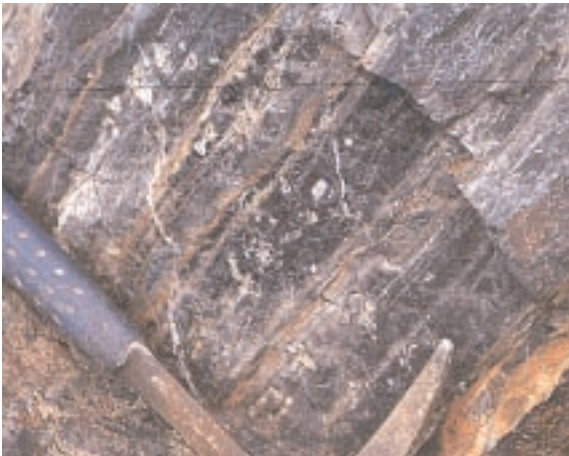


Photo 4. Jasperoid showing relict bedding, Jerritt Canyon, Nevada.

Many, if not all, sediment-hosted disseminated gold deposits are related to high-angle faults or shear zones (Adams and Putnam III, 1992) which acted as depositional sites for mineralization or provided a conduit for fluids to reach favourable lithological units. One aspect of Carlin-type deposits that receives considerable attention in Nevada is the alignment of known deposits along trends (Figure 2). The geological significance of these trends is not fully understood, however, they are widely used by the exploration community to promote properties and to identify prospective ground.

Geophysics are used, although usually as an indirect exploration method designed to provide information about structure and geology. Some deposits exhibit resistivity lows. Aeromagnetic surveys may identify associated intrusions and possibly regional trends (Schroeter and Poulsen, 1996). The high grade refractory ore zones should respond to electromagnetic techniques.

PROPERTIES EXAMINED

An initial investigation of the MINFILE database and discussions with government and industry geologists identified some possible occurrences which warranted investigation. In the last two years a number of mineral occurrences in British Columbia were examined and sampled, including the Greenwood Camp, Watson Bar, the Golden Bear mine, Slam and Howell Creek structure.

Information concerning the Watson Bar property is summarized by Cathro *et al.*, 1998; it is not a Carlin-type deposit. Initial reports on the Howell Creek structure and Golden Bear deposits are presented in this volume (Brown and Cameron, 1999; Brown *et al.*, 1999). The Slam property in northern British Columbia is located approximately eleven kilometers east-northeast of the Golden Bear mine. Gold mineralization is associated with a northeast-trending, silicified limestone unit which contains disseminations of fine, dark gray pyrite. Several rock samples from the silicified zone assayed over 1.0 g/t gold with anomalous values for mercury, arsenic and antimony (Walton, 1987). The Slam is similar to some of the Golden Bear deposits and is most likely a Carlin-type deposit. The Greenwood Camp does have a number of carbonate units with associated skarns which sug-

gest the area is potentially prospective for sediment-hosted disseminated gold, however, no sediment-hosted disseminated gold deposits have been identified in the area.

CONCLUSIONS

Carlin-type deposits are difficult to find because their setting and genesis are so poorly understood. Therefore, it is difficult to determine the key features to use for exploration. Furthermore, the gold is microscopic and many deposits have low sulphide contents (<1%). Even in the higher grade deposits the gold is typically associated with a very fine-grained, black, sooty pyrite that can be difficult to identify macroscopically. Surface weathering can convert all sulphides to hematite and limonite, and rarely produces significant gossans. In Nevada, it took sustained exploration over 20 years along the major mineralization trends to identify many of the new sediment-hosted disseminated gold deposits and discoveries continue to be made.

In the Canadian Cordillera there has been relatively little exploration for these deposits despite some geological similarities with Nevada. Poulsen (1996b) noted that two different geological environments in British Columbia might host Carlin-type mineralization. These are: 1) accreted terranes with a basement containing carbonate lithologies intruded by Mesozoic or Cenozoic plutonism, specifically the Stikine and Quesnel terranes, and 2) sediments deposited along the continental margin of ancestral North America which have been cut by Mesozoic magmas, such as are found in the Kootenay Arc and Selwyn Basin.

Initial results from the sediment-hosted gold project show that the Bear, Grizzly, Kodiak A, Kodiak B and Ursa are Carlin-type deposits and the Slam occurrence is similar. There is considerable potential to find other gold occurrences of this type in the Tatsamenie Lake region. Further work will probably identify other prospective regions in British Columbia.

ACKNOWLEDGEMENTS

Howard Poulsen assisted with the start up of the project and we continue to benefit from his expertise. All three authors have benefited from the full support of Andrew Hamilton and the

other staff during our visits to the Golden Bear mine of North American Metals Corp. Derek Brown and David Lefebure visited a number of sediment-hosted disseminated gold mines in Nevada in 1998. The many geologists we met during our travels shared information and ideas freely and helped us to understand Carlin-type deposits. We would like to especially thank Greg Griffin of Barrick Goldstrike Mines Inc. who first invited us to Nevada, Jim McDonald of White Knight Resources Ltd., Tommy Thompson of the Ralph J. Roberts Center for Research in Economic Geology and Stephen Peters of the USGS. Brian Grant of the BCGS provided useful comments on how to improve the article. The diagrams in this article have been drafted by Mike Fournier and Maurice Johnson.

REFERENCES

- Adams, S.S. and Putnam III, B.R. (1992): Application of mineral deposit models in exploration: a case study of sediment-hosted gold deposits, Great Basin, western United States; *in* Case Histories and Methods in Mineral Resource Evaluation, *Geological Society*, Special Publication Number 63, pages 1-23.
- Arehart, G.B. (1996): Characteristics and Origin of Sediment-hosted Disseminated Gold Deposits: a Review; *Ore Geology Reviews*, Volume 11, pages 383-403.
- Arehart, G.B., Foland, K.A., Naeser, C.W., and Kesler, S.E. (1993): $^{40}\text{Ar}/^{39}\text{Ar}$, K/Ar and Fission Track Geochronology of the Sediment-hosted Gold Deposits at Post-Betze, Carlin Trend, Northeastern Nevada; *Economic Geology*, Volume 88, pages 622-646.
- Berger, B.R. and Bagby, W.C. (1991): The geology and origin of Carlin-type gold deposits; *in* Gold Metallogeny and Exploration, R.P. Foster, Editor, *Blackie, Glasgow and London*, pages 210-248.
- Bloomstein, E.I., Massingill, G.L., Parratt, R.L. and Peltonen, D.R. (1991): Discovery, geology and mineralization of the Rabbit Creek gold deposit, Humboldt County, Nevada; *in* Geology and Ore Deposits of the Great Basin: Symposium Proceedings, G.L. Raines, R.E. Lisle, R.W. Schafer, and W.H. Wilkinson, Editors, *Geological Society of Nevada*, pages 821-843.

- Brown, D.A. and Cameron, R. (1999): Sediment-hosted disseminated gold deposits related to alkalic intrusions in the Howell Creek Structure, southeastern B.C. (82G/2/7); in *Geological Fieldwork 1999, B.C. Ministry of Energy and Mines*, Paper 1999-1, this volume.
- Cathro, M.S., Durfeld, R.M. and Ray, G.E. (1998): Mineralization on the Watson Bar property (92/01E), Clinton mining Division, Southern B.C., in *Geological Fieldwork 1997, B.C. Ministry of Employment and Investment*, Paper 1998-1, pages 21-1 to 21-13.
- Champigny, N. and Sinclair, A.J. (1982): The Cinola gold deposit, Queen Charlotte Islands, British Columbia; in *Geology of Canadian Gold Deposits*, Proceedings of the CIM Gold Symposium, September, 1980, R.W. Hodder and W. Petruk, Editors, *Canadian Institute of Mining and Metallurgy*, Special Volume 24, pages 243-254.
- Christensen, O.D., (1993): Carlin trend geologic overview; in *Gold Deposits of the Carlin Trend, Nevada*, O.D. Christensen, Editor, *Society of Economic Geologists*, Guidebook Series, Volume 18, pages 12-26.
- Christensen, O.D. (1994): Wall rock alteration in Carlin-type sedimentary-rock-hosted gold deposits; in *Models in Base and Precious Metals*, Short Course notes, *Northwest Mining Association*, 11 pages.
- Christensen, O.D. (1996): Carlin trend geologic overview; in *Field Trip Guidebook Compendium, Geology and Ore Deposits of the American Cordillera*, S.M. Green and E. Struhsacker, Editors, *Geological Society of Nevada*, pages 147-156.
- Christensen, O., Garwin, S.L. and Mitchell, P.A. (1996): Carlin-type sedimentary rock-hosted disseminated gold deposits around the Pacific; in *New Mineral Deposit Models for the Cordillera*, Short Course Notes, *Northwest Mining Association*, pages E1-E34.
- Cunningham, C.G., Ashley, R.P., Chou, I., Zushu, H., Chaoyuan, W. and Wenkang, L. (1988): Newly discovered sedimentary rock-hosted disseminated gold deposits in the People's Republic of China; *Economic Geology*, Volume 83, pages 1462-1467.
- Garwin, S.L., Hendri, D. and Lauricella, P.F. (1995): The Geology of the Mesel sediment-hosted gold deposit, North Sulawesi, Indonesia; in *Proceedings of the PACRIM Congress 1995, Australian Institute of Mining and Metallurgy*, pages 221-226.
- Green, S.M. and Struhsacker, E., Editors (1996): *Field trip guidebook compendium, geology and ore deposits of the American Cordillera; Geological Society of Nevada*, 501 pages.
- Groves, D.A. (1996): End members of the deposit spectrum on the Carlin Trend: examples from recent discoveries; in *New Mineral Deposit Models for the Cordillera; Cordilleran Roundup, Short Course Notes, B.C. Ministry of Employment and Investment*, pages D1-D35.
- Ilichik, R.P. and Barton, M.D. (1997): An amagmatic origin of Carlin-type gold deposits; *Economic Geology*, Volume 92, pages 269-288.
- Jackson, M. (1996): Geology of the West Leeville deposit: a high grade refractory gold deposit on the Carlin Trend, Nevada; in *New Mineral Deposit Models for the Cordillera, Short Course Notes, Northwest Mining Association*, pages C1-C25.
- Kuehn, C.A and Rose, A.W. (1992) Geology and geochemistry of wall-rock alteration at the Carlin gold deposit; *Economic Geology*, Volume 87, pages 1697-1721.
- Lefebure, D.V. (1998): Epithermal gold deposits of the Queen Charlotte Islands; in *Geological Fieldwork 1997, B.C. Ministry of Employment and Investment*, Paper 1998-1, pages 19-1 to 19-14.
- Lefebure, D.V. and Ray, G.E. (1998): Unconventional metallic deposits in arcs; *B.C. Ministry of Energy and Mines*, Open File 1998-8, pages I-1 to I-20.
- Lovering, T.G. (1972): Jasperoid in the United States — its characteristics origin, and economic significance; *United States Geological Survey*, Professional Paper 710, 164 pages.
- Oliver, J.L. (1996): Geology of Stikine Assemblage rocks in the Bearskin (Muddy) and Tatsamenie Lake District, 104K/1 and 104K/8, Northwestern British Columbia, Canada and characteristics of gold mineralization, Golden Bear mine, Northwestern British Columbia; Unpublished PhD thesis, *Queen's University*, Ontario, Canada, 213 pages.
- Oppliger, G.L., Murphy, J.B. and Brimhall Jr., G.H. (1997): Is the ancestral Yellowstone hotspot responsible for the Tertiary "Carlin" mineralization in the Great Basin of Nevada?; *Geology*, Volume 25, Number 7, pages 627-630.

- Phillips, G.N. and Powell, R. (1993): Link between gold provinces; *Economic Geology*, Volume 88, pages 1084-1098.
- Poulsen, K.H. (1996): Carlin-type gold deposits and their potential occurrence in the Canadian Cordillera; *in* Current Research 1996-A, *Geological Survey of Canada*, pages 1-9.
- Poulsen, K.H. (1996): Carlin-type gold deposits: Canadian potential?; *in* New Mineral Deposit Models for the Cordillera, Short Course Notes, *Northwest Mining Association*, pages E1-E34.
- Radtke, A.S., Rye, R.O. and Dickson, F.W. (1980): Geology and stable isotope studies of the Carlin gold deposit, Nevada; *Economic Geology*, Volume 75, pages 641-672.
- Radtke, A.S. (1985): Geology of the Carlin deposit, Nevada; *United States Geological Survey*, Professional Paper 1267, 124 pages.
- Raines, G.L., Lisle, R.E., Schafer, R.W. and Wilkinson, W.H., Editors (1991): Geology and ore deposits of the Great Basin; Symposium Proceedings, *Geological Society of Nevada*, Volumes I and II.
- Richards, G.G., Christie, J.S. and Wolfhard, M.R. (1976): Specogna: a Carlin-type gold deposit, Queen Charlotte Islands, British Columbia; *Canadian Institute of Mining and Metallurgy*, Volume 69, Number 733, page 64.
- Roberts, R.J. (1986): The Carlin story; *in* Sediment-hosted Precious Metal Deposits of Northern Nevada; J.V. Tingley and H.F. Bonham, Jr., Editors, *Nevada Bureau of Mines and Geology*, Report 40, pages 71-80.
- Roberts, R.J., Radtke, A.S. and Coates, R.R. (1971): Gold-bearing deposits in north-central Nevada and southwestern Idaho; *Economic Geology*, Volume 66, pages 14-33.
- Rye, R.O. (1985): A model for the formation of carbonate-hosted disseminated gold deposits based on geologic, fluid-inclusion, geochemical and stable-isotope studies of the Carlin and Cortez deposits, Nevada; *United States Geological Survey*, Bulletin 1646, pages 35-42.
- Schroeter, T.G. and Poulsen, K.H. (1996): Carbonate-hosted disseminated Au-Ag; *in* Selected British Columbia Mineral Deposit Profiles, Volume 2, D.V. Lefebure, and T. Hoy, Editors, *B.C. Ministry of Employment and Investment*, Open File 1996-13, pages 9-12.
- Seedorff, E. (1991): Magmatism, extension and ore deposits of Eocene to Holocene Age in the Great Basin - mutual effects and preliminary proposed genetic relationships; *in* Geology and Ore Deposits of the Great Basin, Symposium Proceedings, G.L. Raines, R.E. Lisle, R.W. Schafer, and W.H. Wilkinson, Editors, *Geological Society of Nevada*, Volume 1, pages 133-178.
- Sillitoe, R.H. (1995): Exploration and discovery of base- and precious-metal deposits in the Circum-Pacific region during the last 25 years; *Metal Mining Agency of Japan*, 127 pages.
- Sillitoe, R.H. and Bonham, H.F. Jr. (1990): Sediment-hosted gold deposits: distal products of magmatic-hydrothermal systems; *Geology*, Volume 18, pages 157-161.
- Teal, L. and Jackson, M. (1997): Geologic overview of the Carlin Trend gold deposits and descriptions of recent deep discoveries; *Society of Economic Geologists*, Newsletter, Number 31, pages 1, 13-25.
- Turner, S.J., Flindell, P.A., Hendri, D.; Hardjana, I., Lauricella, P.F., Lindsay, R.P., Marpaung, B., and White, G.P. (1994): Sediment-hosted gold mineralization in the Ratatotok District, North Sulawesi, Indonesia; *in* Mineral Deposits of Indonesia: Discoveries of the past 25 years, Theo-M. van-Leeuwen, J.W. Hedenquist, L.P. James and J.A.S. Dow, Editors, *Journal of Geochemical Exploration*, Volume 50, pages 317-336.
- Vikre, P., Thompson, T.B., Bettles, K., Christensen, O., and Parratt, R., Editors (1997): Carlin-type gold deposits; *Society of Economic Geologists*, Field Conference, Guidebook Series, Volume 28.
- Walton, G. (1987): Tats project, Tatsamenie Lake, British Columbia; Chevron Canada Resources Limited; *B.C. Ministry of Energy, Mines and Petroleum Resources*, Assessment Report 16276, pages 71.
- Warren, H.V. and Hajek, J.H. (1973): An attempt to discover a "Carlin-Cortez"; *Western Miner*, pages 124-134.



SEDIMENT-HOSTED, DISSEMINATED GOLD DEPOSITS RELATED TO ALKALIC INTRUSIONS IN THE HOWELL CREEK STRUCTURE, SOUTHEASTERN BRITISH COLUMBIA (82G/2, 7)

By Derek A. Brown and Robert Cameron¹

KEYWORDS: Sediment-hosted, disseminated gold, Carlin-type, Alkalic epithermal, Flathead syenite intrusions, Crowsnest Formation, Howell Creek Structure.

INTRODUCTION

This paper describes occurrences of low grade, disseminated gold in sedimentary rocks and alkalic intrusions in the vicinity of the Howell Creek Structure (HCS; Price, 1964) of southeastern British Columbia. The study is part of the B.C. Geological Survey's ongoing Sediment-hosted Gold Project, which is examining occurrences throughout the province which may have similarities to gold deposits in the Carlin district of Nevada. Brown spent two weeks examining the general setting of mineralization and sampling diamond drill core. Much of the paper is based on results of numerous exploration programs undertaken by Cameron for Dome Exploration Canada, Limited, Placer Dome Inc. (now Placer Dome Canada Limited) and Phelps Dodge Corporation of Canada, Limited (Cameron, 1989).

The geology map compiled at 1:1 000 scale, whole rock, trace element and rare earth element lithochemical data, PIMA short-wave infrared analysis results, and scanned photographs, are available in digital form from Brown.

Location and access

The study area lies 40 kilometres southeast of Fernie, British Columbia and 25 kilometres north of the British Columbia-Montana border, in the headwaters of Howell and Twentynine Mile creeks (Figure 1). The terrain varies from broad, U-shaped, drift covered valleys to precipitous headwalls of extensive outcrops (Plate 1),

between 1490 m and 2400 m elevation. This area lies within the MacDonald range of the Front Ranges of the southern Rocky Mountains. Access to the region is by logging roads leading from the locality of Morrissey, thirteen kilometres south of Fernie on Highway 3, for a distance of 50 kilometres following the Morrissey, Lodgepole and Harvey Forest Service roads. An extensive network of secondary logging roads and drill trails provides access to much of the study area.

History

The Flathead area is geologically unique within the Canadian segment of the Rocky Mountains and has sparked considerable interest and study since Price (1962) first mapped the area. The HCS in particular has been the subject of many studies including Jones (1964), Oswald (1964), Labreque and Shaw (1973) and others including a recent description by Legun (1993).

Gold exploration has been a focus of work since 1983 when Cominco Limited staked the Howell claim block along the ridge separating Howell Creek and Twentynine Mile Creek. Dome Exploration Canada, Limited completed regional sampling programs in 1984 and staked the Flathead claims covering Trachyte Ridge and the Howe claims adjacent to the Howell claim block. Additional work by Dome and Placer Dome Inc. in subsequent years led to drill programs on Trachyte Ridge, the Howell property, optioned from Cominco Limited, and the Howe property. Phelps Dodge Corporation of Canada Limited, acquired the properties in 1992 and continued with additional drill programs in 1993 and 1994. Recently, Eastfield Resources Limited conducted a prospecting program on the Trachyte Ridge area and staked the former Howe claim block south of Twentynine Mile Creek.

¹ Fox Geological Services Inc., 1409 – 409 Granville St., Vancouver, BC, V6C 1T8

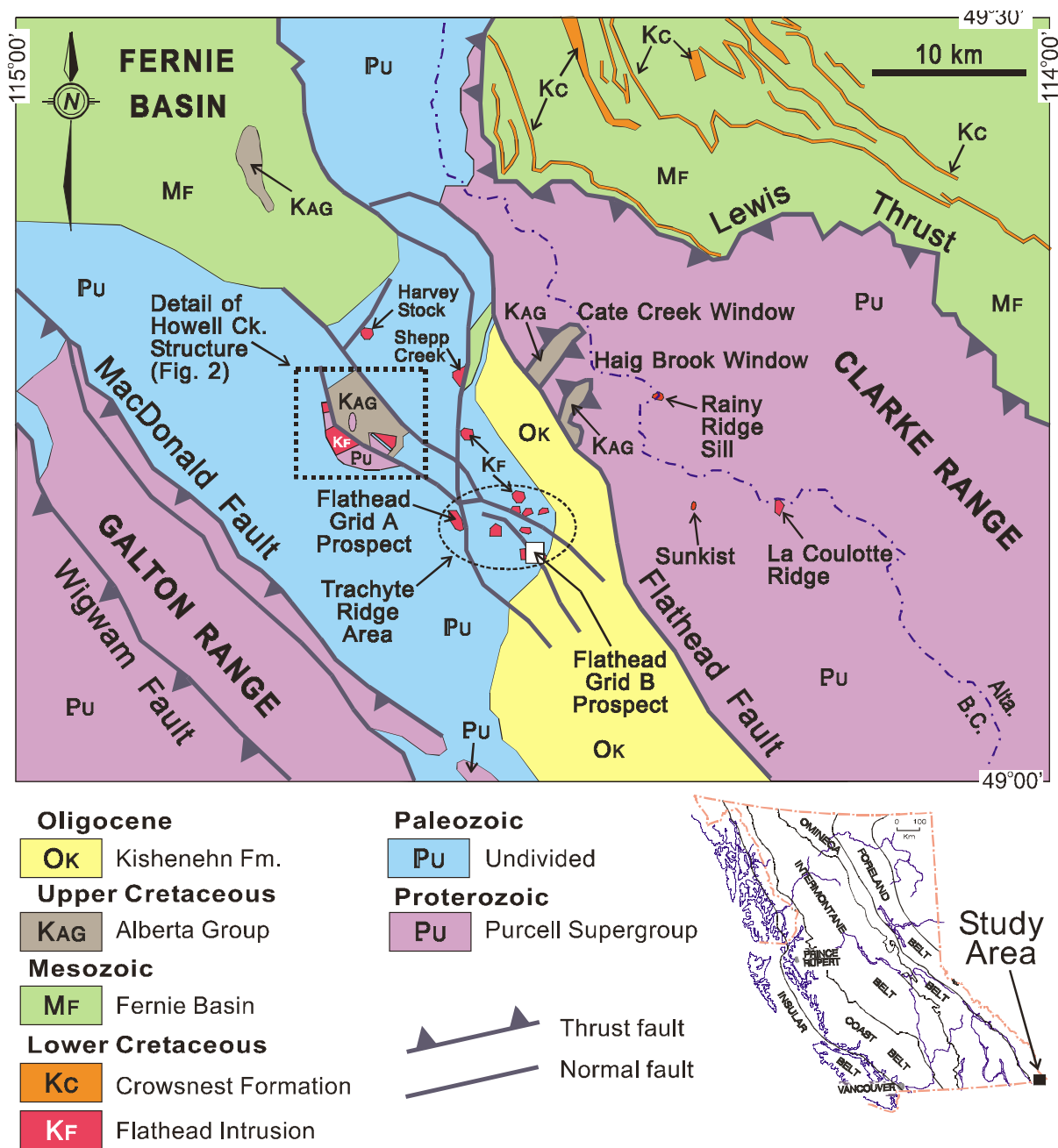


Figure 1. Regional setting of the Howell Creek Structure and distribution of Early Cretaceous syenite intrusions in southeastern British Columbia relative to the coeval Crowsnest Formation in Alberta (modified from Price, 1962).

REGIONAL GEOLOGICAL SETTING

The geology of the Flathead area is characterized by Laramide structures, comprising thrust faults and open folds that have been modified by Tertiary normal faults. Strata exposed in the Flathead area include Proterozoic Purcell Supergroup clastics, Paleozoic carbonate and clastic rocks, Mesozoic clastic sequences and coal beds and Tertiary fault scarp units related to normal faults. Cretaceous alkalic intrusions

comprising stocks, dikes and sills intrude layered rocks, and are generally restricted to areas of Tertiary faults.

The sediment-hosted gold occurrences in the region lie within the HCS, an enigmatic feature of the southern Rocky Mountain fold and thrust belt (Figure 1). The HCS is located southeast of the Fernie Basin in a zone of northwest-trending normal faults. The HCS described by Price (1965), Oswald (1964) and others is a feature in which Upper Cretaceous marine sedimentary

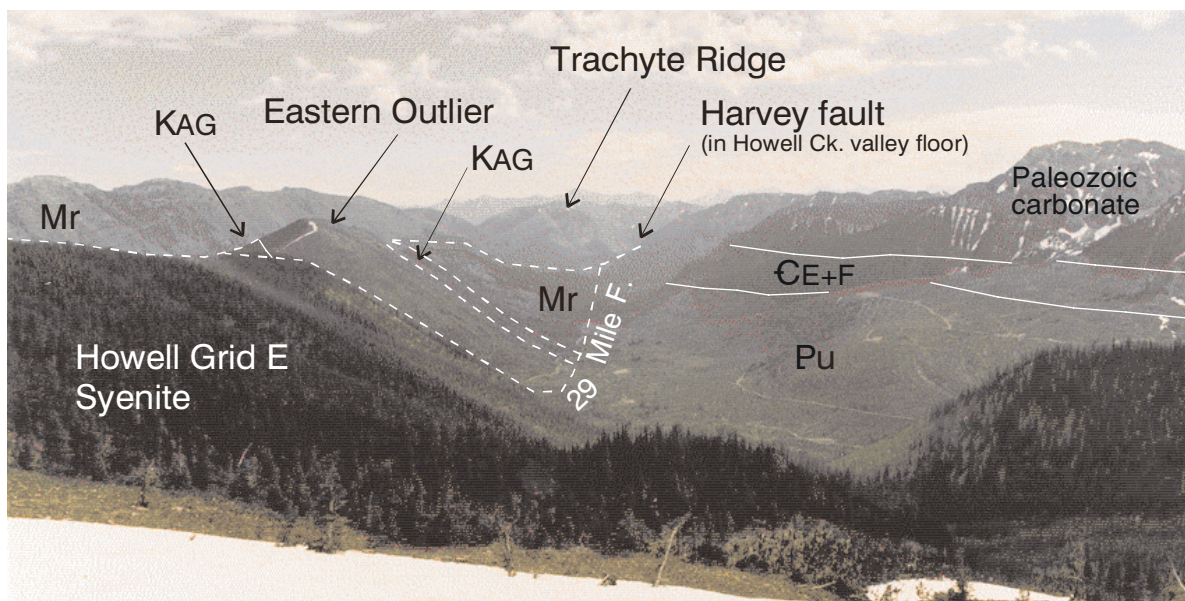


Plate 1. Overview looking east down Watluk and Twentynine Mile creeks to the southern portion of the Howell Creek Structure, the Eastern Outlier and Paleozoic carbonates to the south.

rocks of the Alberta Group occur within a fault-bounded window surrounded by Proterozoic to Mesozoic strata that have been intruded by bodies of Early Cretaceous syenite. The structural position of the Upper Cretaceous Alberta Group strata with respect to the regional Lewis Thrust fault is the subject of many studies and structural interpretations. The nature of the HCS is further complicated by the presence of two outliers of Proterozoic to Mesozoic rocks that structurally overlie the Alberta Group within the window.

GEOLOGY OF THE HOWELL CREEK STRUCTURE

Stratigraphy

Detailed descriptions of the regional stratigraphy are presented in Price (1962, 1965) and are summarized on Figure 2. The oldest unit exposed is the upper part of the Proterozoic Purcell Supergroup including the Gateway, Phillips and Roosville formations. These units are exposed south and west of Twentynine Mile Creek and within the Western and Eastern Outliers. More extensive Purcell Supergroup exposures lie to the west in the Galton Range and to the east in the Clark Range (Figure 2).

The Paleozoic sequence in the HCS includes the Cambrian Flathead Formation quartz arenite, the transitional Elko Formation green shale and

carbonate, massive middle to upper Paleozoic carbonate sequences, and ridge-forming dolomitic sandstone units of the Rocky Mountain Group. A single occurrence of Triassic Spray River Group siltstone with thin coal beds is present in the footwall of the Howell Creek fault.

Recessive weathering and poorly exposed Upper Cretaceous Alberta Group occupies the core of the HCS. The Alberta Group comprises fissile dark grey shale, siltstone (Plate 2), and minor quartz arenite. Lesser pebbly grit contains abundant dark coloured chert clasts and local clasts of alkalic intrusive rocks. Belly River Formation sandstone overlies the Alberta Group (Figure 2).

Flathead Intrusions

Intrusive rocks are commonly exposed in the valleys of Twentynine Mile Creek and Howell Creek and on Trachyte Ridge with a few outlying bodies in the Clark Range and on Shepp Creek to the east and north. Intrusions vary from equant stocks and plugs, ranging from 100 to >1200 m in diameter, to small irregular dikes and sills. The emplacement depth of the intrusions was relatively shallow, 3 to 5 kilometres, based on the minimum stratigraphic interval between the uppermost syenite at Shepp Creek, where it intrudes the Triassic Spray River Group, to the extrusive equivalents of the syenites, the Crowsnest Formation.

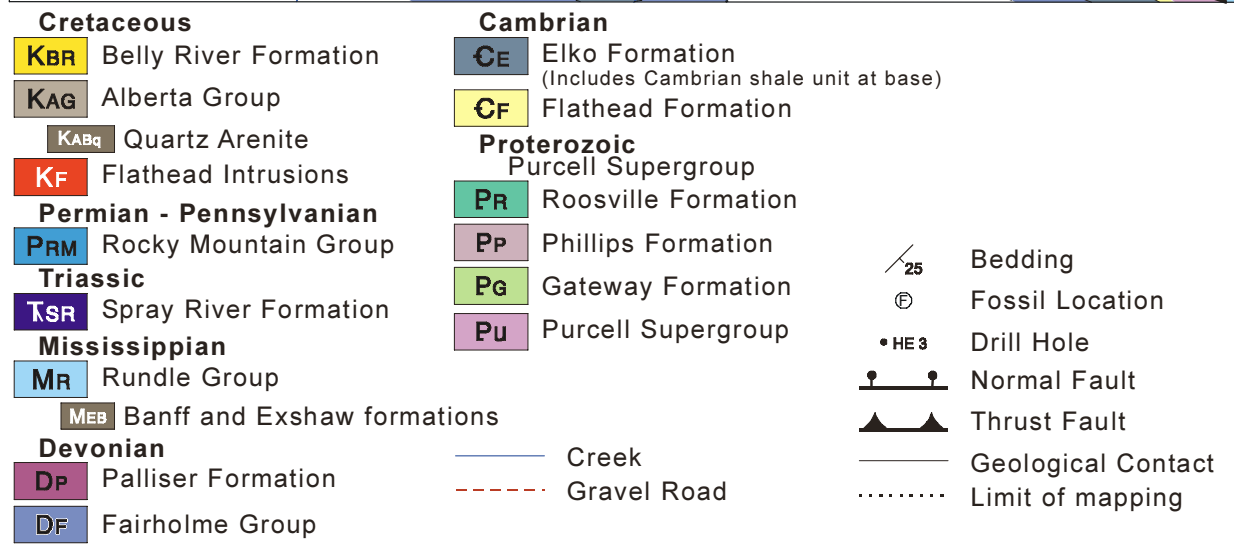
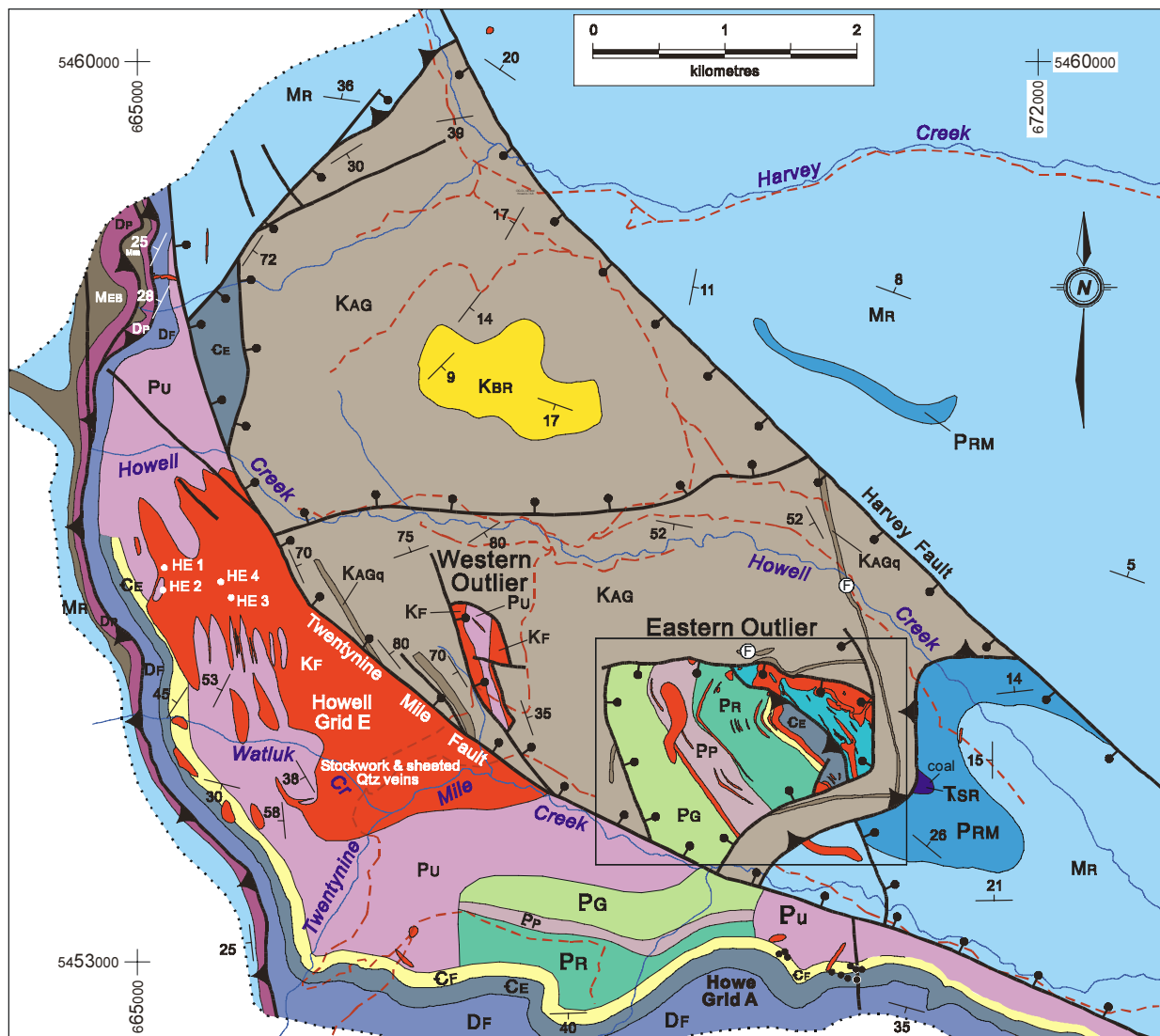


Figure 2. Geology of the Howell Creek structure and adjacent area (modified from Cameron *et al.* (unpub. map), Legun (1993) and Price (1965)).



Plate 2. View east to the sub-horizontal Mississippian Rundle Group on the northeast side of the Harvey Fault. Recessive Alberta Group shale and siltstone underlie the foreground within the Howell Creek Structure; the photograph illustrates the juxtaposition of these units. Inset: Typical Alberta Group, dark grey thin bedded siltstone exposure with prominent, widely-spaced limonitic concretions along a bedding plane.

The best age constraint for the Flathead intrusions comes from an unpublished U-Pb date of 98.5 ± 5 Ma from syenite collected from Trachyte Ridge (collected by Dave Grieve; reported in Skupinski and Legun, 1989). In addition, there are several conventional K-Ar dates that range from 72 to 119 Ma (in Treves *et al.*, 1993): Rainy Ridge sill 119 Ma (whole rock) and 111 Ma (hornblende); Trachyte Ridge 67 - 105 Ma (Gordy and Edwards, 1962); and Sunkist Mountain 79 - 95 Ma.

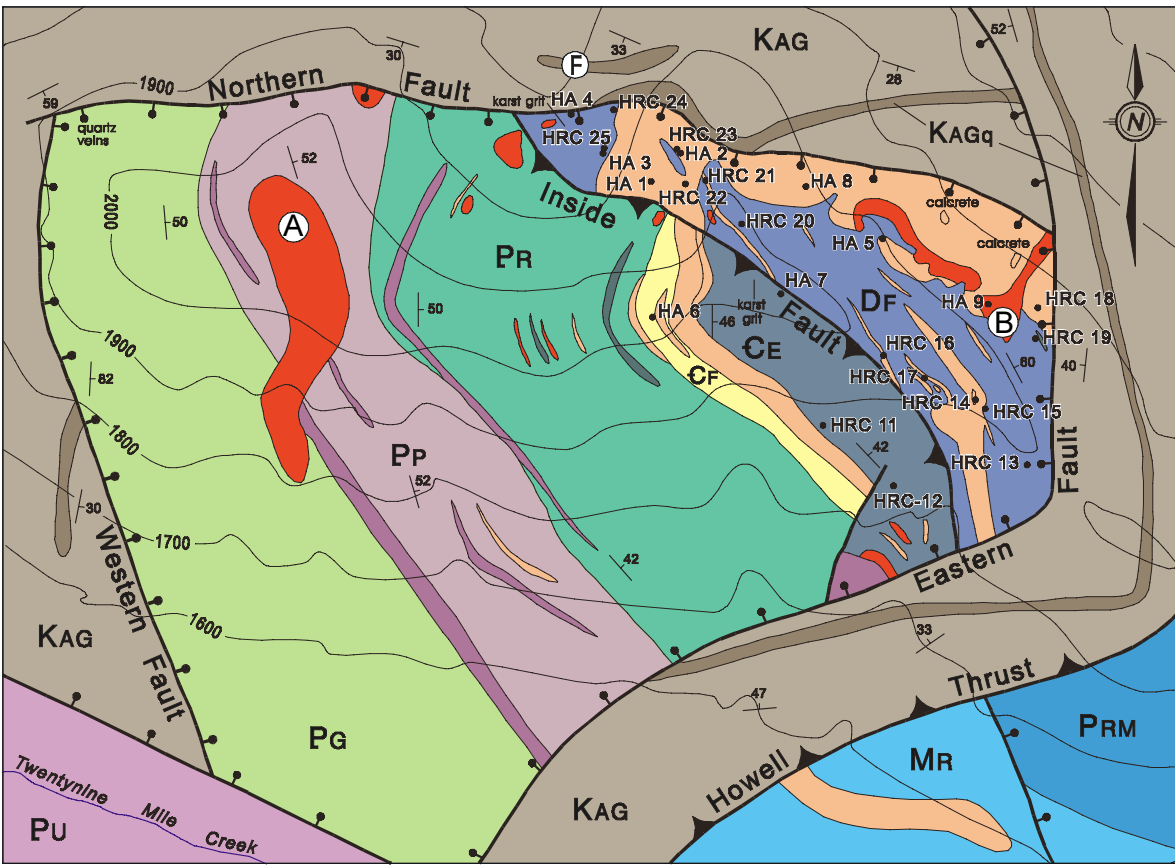
The Flathead Intrusions are coeval and have similar chemistry to the Lower Cretaceous Crowsnest Formation exposed 28 km to the northeast in Alberta. The Crowsnest Formation comprises pyroclastic and volcanoclastic rocks and flows of trachyte and phonolite composition (Adair and Burwash, 1996; Peterson *et al.*, 1997). Sanidine from these flows yielded a K-Ar age of 96 Ma (Folinsbee *et al.*, 1957) and bentonites of the Viking Formation produce an average K-Ar age (biotite and sanidine) of 98 Ma (Tizzard and Lerbekmo, 1975). Fossil determinations also constrain the volcanics to the Albian

(Norris *et al.*, 1965).

Intrusive rocks of the HCS are subdivided into five types: syenite and alkali feldspar syenite, foid syenite, megacrystic syenite, gabbro and intrusive breccia (Figure 3). These divisions use the plutonic nomenclature of Le Maitre *et al.* (1989), and therefore differ somewhat from those proposed by previous authors. A total alkali - silica variation diagram (Figure 4) illustrates the alkaline affinity of the syenites and petrographic descriptions can be found in Skupinski and Legun (1989).

Syenite, Alkali Feldspar Syenite

Fresh exposures of syenite are rare; most are rusty weathering, limonite and jarosite(?) stained, irregularly fractured and recessive. They are commonly pyritized and argillically altered (i.e. clay and carbonate-altered). Fracture-controlled fluorite and quartz stockworks are common in the Howell Grid E area. The syenites are porphyritic with aligned potassium feldspar phenocrysts from 5 mm to 2 cm or more in length.



Early Cretaceous
Flathead Intrusions differentiated

- Gabbro
- Intrusive Breccia
- Foid Syenite
- Syenite

F Fossil location

Drill Holes

- HRC Reverse Circulation Hole
- HA Diamond Drill Hole

0 500
metres

Figure 3. Detailed geology of the Eastern Outlier illustrating syenite and breccia distribution within the Proterozoic and Paleozoic strata (modified from Cameron *et al.* (unpub. map), and Legun (1993)). Drill hole locations are indicated. See Figure 2 for unit descriptions.

Foid Syenite

Foid syenite sills are characterized by a pale to dark green fresh surface with trachitoid texture defined by lath-shaped K-feldspar (1mm to 2 cm). Feldspathoids are present as equant subhedral crystals (1-5 mm, buff to red) that weather as recessive pits (Plate 3A and 3B). Analcime and nepheline have been positively identified (Skupinski and Legun, 1989) and nosean is suspected.

Megacrystic syenite

Megacrystic syenite comprises tan to grey, porphyritic syenite containing aligned ortho-

clase phenocrysts up to 7 cm in length (Plate 3C and 3D). Surface exposures are unaltered and the unit is observed crosscutting altered syenites.

Gabbro

Narrow sills of dark green to black gabbro are present on the Eastern Outlier and south of Twentynine Mile Creek and are volumetrically the least common intrusive rock. They are magnetic, display a felted texture and have a unique composition relative to the other syenite varieties, plotting in the alkali basalt (has normative nepheline), tephrite, and basaltic trachy-andesite fields of the total alkali vs. silica diagram (Figure 4).

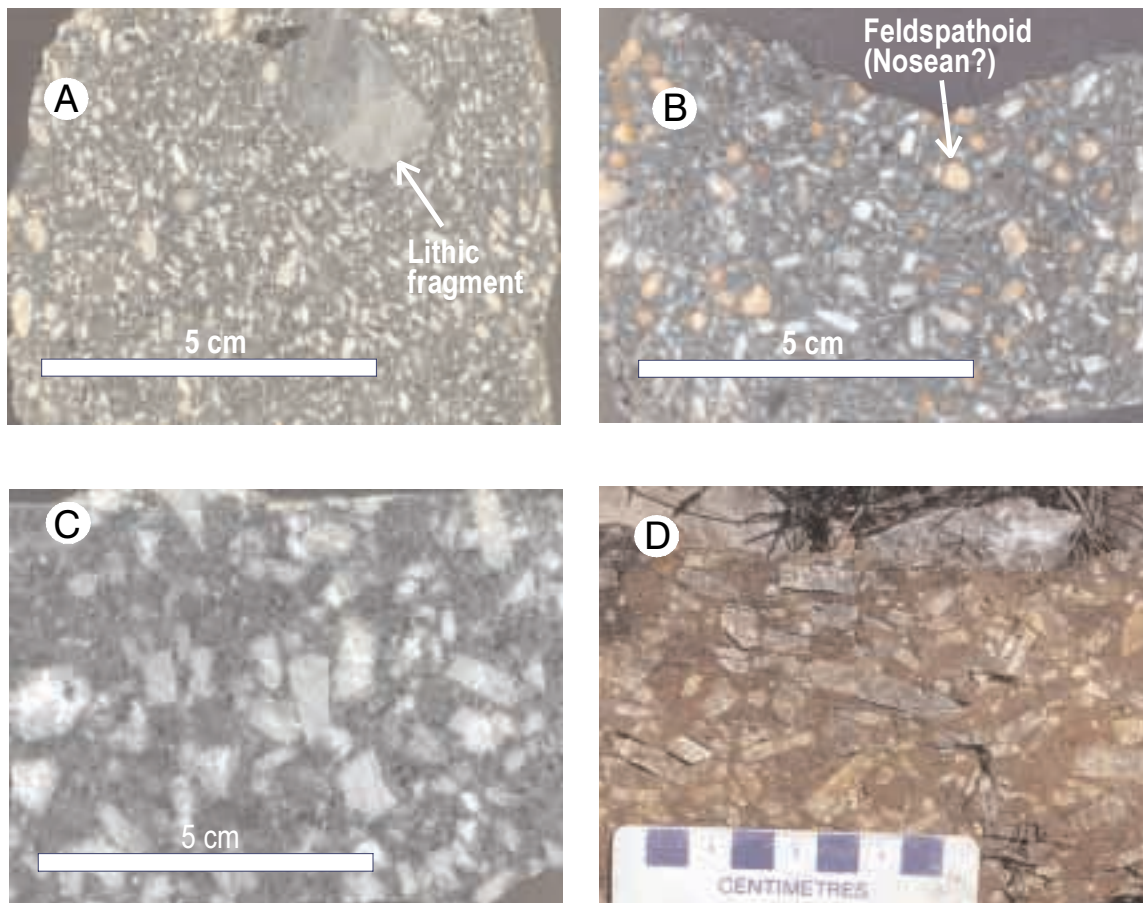


Plate 3. Syenite phases in and adjacent to the Howell Creek Structure: (A) Foid syenite from the Eastern Outlier with angular mudstone lithic fragment; (B) Foid syenite from Eastern Outlier with equant, brown rimmed mineral (possibly nosean?). Fine dark specks are probably melanite garnet; (C) K-feldspar megacrystic syenite that cuts syenite on Howell Grid E; and (D) Tabular K-feldspar megacrystic syenite sill in the Eastern Outlier.

Intrusive breccias

Intrusive breccia bodies are common throughout the HCS. Discordant and crudely stratabound breccia bodies characterize the Eastern Outlier. The largest breccia body, about 1000 m by 300 m, cuts strata at an acute angle but becomes semi-concordant in the middle of the Phillips Formation, at higher elevations (Breccia A on Figure 3). This body contains angular to rounded clasts of porphyritic syenite, and grey limestone.

A large, irregularly shaped reddish-brown weathering breccia, located at the northeast corner of the Eastern Outlier (Breccia B on Figure 3), also changes from discordant to concordant at higher elevations. The breccia cuts syenite and then flares out parallel to bedding within Fairholme Formation limestone below a prominent syenite sill. The competent core of the Breccia B pipe is composed of angular syenite

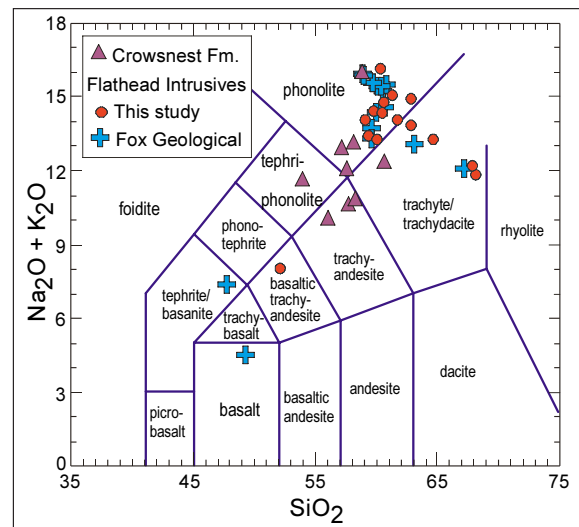


Figure 4. Total alkali versus silica variation diagram (after LeBas *et al.*, 1986) displaying the alkaline character of the Flathead Intrusions and how they compare with Crowsnest Formation volcanic rocks (Crowsnest data from Peterson *et al.*, 1997).

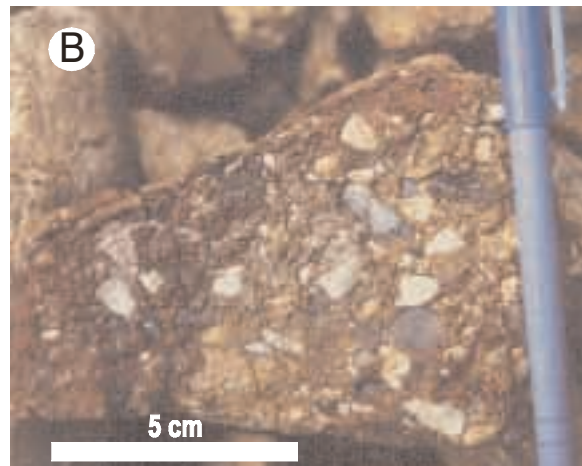
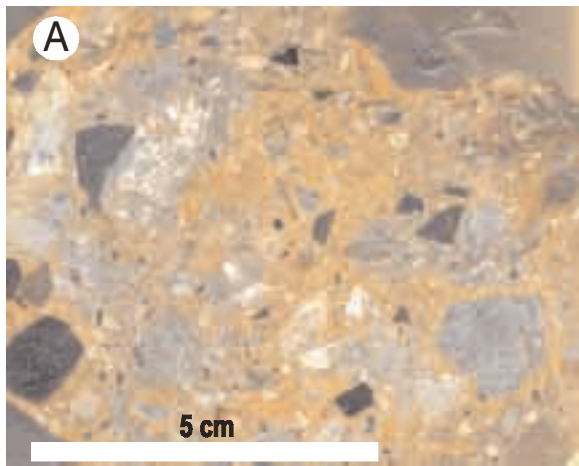


Plate 4. Examples of breccia types in Breccia B of the Eastern Outlier: (A) heterolithic intrusive breccia with angular, matrix-supported limestone and syenite fragments; (B) Discordant, limonitic weathering heterolithic breccia containing subangular limestone and lesser syenite fragments. Partially recessive matrix is carbonate-rich.

fragments within a feldspar crystal-rich matrix. Limestone fragments comprise less than 15% of this part of the breccia. This part of the breccia grades laterally and vertically into a heterolithic breccia with syenite, limestone, quartz arenite and siltstone fragments up to 30 cm (average 2-8 cm; Plate 4A). Peripheral to the main body is a hematitic weathering, limestone pebble breccia with a carbonate-rich matrix (Plate 4B). Adjacent country rock is fractured and locally crackle breccias have developed.

Structure

Detailed mapping of the HCS, in particular the Eastern Outlier, has documented the relationship between many of the bounding faults and the upper Cretaceous strata exposed in the core of the window. The current juxtaposition of units is attributed to high angle normal faults related to the Flathead Fault (Figure 1). The parallel eastern boundary fault of the Eastern Outlier and the Howell Thrust to the east could represent low angle structures.

ECONOMIC GEOLOGY

Gold mineralization related to the Flathead Intrusions has been an exploration focus in the area since 1983. Gold mineralization has been identified throughout this region defining a district scale mineralizing event. The sediment-hosted gold on the Eastern Outlier at Howell Creek is the focus of this paper. However, three

other areas of mineralization are also briefly discussed: Syenite-hosted quartz stockwork/sheeted veins (Howell Grid E), Pb-Zn manto-style mineralization (Howe Grid A), and Syenite-hosted Au (Trachyte Ridge).

Sediment-hosted Au: Eastern Outlier

Gold mineralization within the Eastern Outlier was explored extensively by detailed soil and rock geochemical surveys, induced polarization surveys and three drill campaigns. Key elements of the occurrence are summarized below. The focus of work was the carbonate rocks exposed on the eastern end of the outlier. Here, various syenite and breccia bodies intrude limestone of the Elko and Fairholme formations. A prominent gold, arsenic, silver and antimony soil anomaly coincides with the extent of the carbonate rocks and guided early drilling. Drilling in reverse circulation drill hole HRC 25 (Figure 3), near a soil sample station that graded 1800 ppb gold, returned a 58 m intersection grading 1.3 g/t Au from pyritic silicified limestone. Results from additional drilling, over an area of 1300 m by 800 m, returned widespread elevated gold within both limestone and intrusive rocks.

Key elements of sediment-hosted gold occurrences in the Eastern Outlier:

- ♦ extensive pyritization of syenite and sedimentary rocks, including carbonate and siliciclastic units;

- ♦ carbonatization of syenite;
- ♦ rare barite/fluorite veining;
- ♦ patchy silicification of limestone;
- ♦ argillic alteration of limestone (green clay, illite), syenite-destruction of feldspars;
- ♦ high zinc zones- manto or pod-like bodies adjacent to sills but in limestone;
- ♦ late hydrothermal or Intrusive breccias; soil anomalies- Au, Ag, As, Sb, Mo, V, Pb, Zn;
- ♦ best result: 59 m of 1.3 g/t Au in HRC 25 from weakly silicified limestone.

Alteration

Alteration of bedrock in the Eastern Outlier is pervasive. All layered rocks are pyritized including carbonate and siliciclastic lithologies as well as all intrusive varieties except the foid syenite sills. Pyrite within the intrusions is fine to medium grained with local concentrations to several percent occurring as disseminated grains and masses and along fractures. Pyrite within carbonate lithologies is generally fine grained and is present as disseminations and fracture-controlled concentrations (Plate 5A). Intrusive rocks, dominantly the syenite variety, are carbonate-altered and effervesce with dilute hydrochloric acid. Weak silicification is evident within the carbonate rocks where a general light coloured bleaching is observed emanating from fine fractures (Plate 5A). Argillic alteration is present in intrusive rocks where feldspar has been variably altered to clay and carbonate. Clay species identified by PIMA

short wave infrared analysis include illite and minor kaolinite with possible smectite (Thompson and Robitaille, 1998). Argillic alteration (illite) of carbonate host rocks imparts a pervasive pale green colour. Surface exposures of mineralized limestone are not visually distinct from unaltered varieties elsewhere.

Litho geochemistry

Downhole litho geochemistry for drill hole HA-3 is presented in Figure 5 and compiled in Table 1 (Figure 2 and 3 give drill hole locations). Elements were determined by ICP except for gold, which was determined by fire assay techniques. Results for some elements are partial and do not reflect total abundance. Gold correlates strongly with arsenic, antimony and tungsten and weakly with silver, vanadium and lead. A negative correlation with aluminum suggests gold mineralization is not introduced with argillic alteration. A silver to gold ratio between 6:1 (median) and 9:1 (average) exists for gold bearing rock containing greater than 200 ppb gold. These relationships hold true for both stream and soil geochemical results.

Syenite-hosted quartz stockwork/sheeted veins

A large syenite intrusion located west of the Twentynine Mile fault (Figure 2) and straddling the divide between Twentynine Mile and Howell

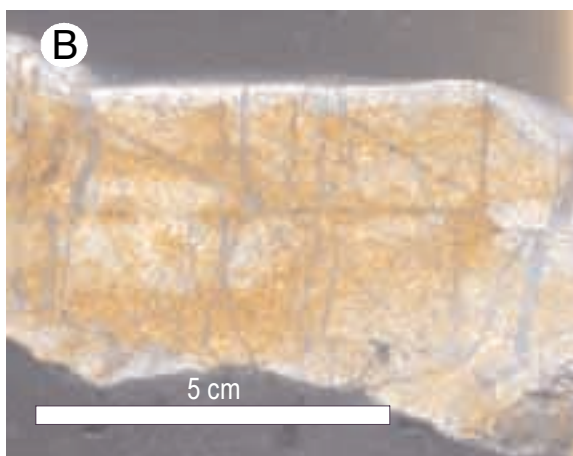
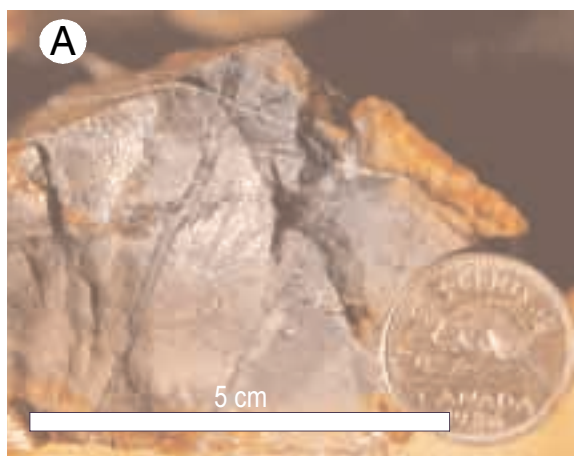


Plate 5. Examples of mineralized and altered rocks: (A) narrow quartz veinlets with partially silicified envelopes and very finely disseminated pyrite hosted in limestone; (B) Quartz stockwork developed in argillic-altered syenite offset by late fractures from Howell Grid E.

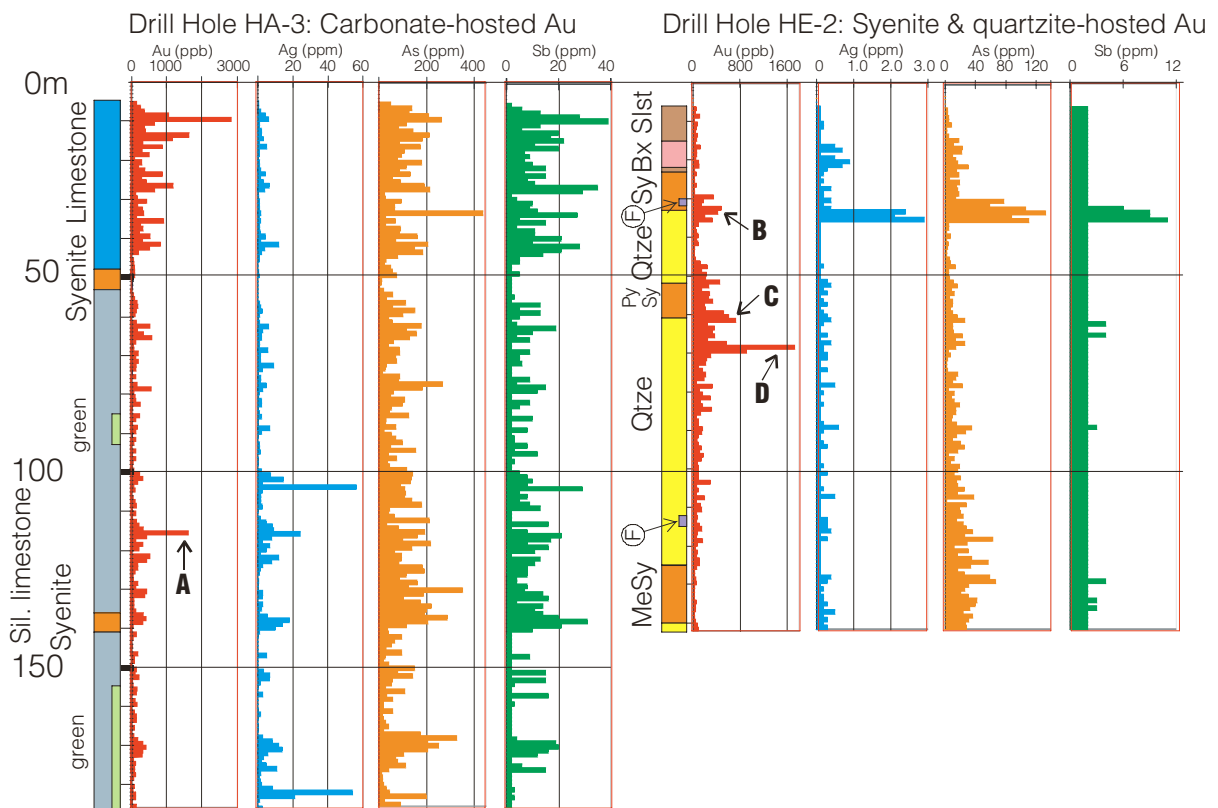


Figure 5. Comparison of downhole variations of Au, Ag, As and Sb values relative to lithology for a diamond drill hole from the Eastern Outlier (HA-3) and Howell Grid E (HE-2). One metre sample interval. The higher concentrations of As and Sb in carbonate units is clearly apparent. Lithologic detail for some of the anomalous gold intervals: (A) pyritic-clay gouge; (B) pyritized contact between syenite and quartzite and lesser crackle breccia; (C) bleached, clay-altered syenite adjacent to quartzite; (D) fluorite- and pyrite-rich quartzite. Abbreviations: Bx = breccia, F = fluorite, MeSy = megacrystic syenite, Sil = silicified, Slst = siltstone; Py = pyritic, Qtze = quartzite; Sy = syenite.

creeks hosts a large quartz stockwork. The stockwork is characterized by narrow, closely spaced quartz veins hosted by fine grained, bleached and argillically altered syenite, and megacrystic syenite. Silica forms stockworks and sheeted zones (Plate 5B), in which veinlets (<8 mm across) dominate with lesser large quartz veins up to 15 cm wide. The veins locally comprise up to 20% of rock volume. Elevated molybdenum in soils corresponds to the quartz stockwork zone.

The northwestern margin of the stock was the location of a four hole diamond drilling program designed to test a gold-in-soil geochemical anomaly associated with abundant fluorite veining within syenite (HE-1 to 4, Figure 2). On surface, the syenite is limonitic, rusty brown weathering with several zones of intense silicification. Drilling encountered silicified quartzite and siltite intruded by syenite, and minor dark purple fluorite-filled fractures (Figure 5).

Gold mineralization occurs within pyritic

syenite and in the adjacent quartzite (Figure 5; HE-2) associated with fracture-controlled and disseminated fine-grained pyrite. Locally, pyritic gouge carries gold (for example HE-2, 219 ppb Au @ 65.5 m depth). Coarse pyrite crystals locally fill irregular fractures in quartzite of the Phillips Formation but this pyrite is barren.

Pb-Zn manto-style mineralization

Elevated Au, Pb and Zn values in soils occur in the Howe Grid A area, south of Twentynine Mile Creek (Figure 2). The area is underlain by siltite of the Roosville Formation, quartz arenite of the Flathead Formation, and the basal green shale of the Cambrian Shale Unit. In addition, replacement-type mineralization, comprising local irregular zones of sphalerite ± fluorite and minor malachite occur in coarse-grained limestone (marble) of the Elko Formation.

Syenite-hosted Au veins: Trachyte Ridge Area

A cluster of small to medium sized (up to 1200 m across) syenite stocks and dikes intrude Paleozoic carbonate and clastic rocks 12 km southeast of the HCS, in the Trachyte Ridge area (Figure 1). The Flathead Grid A prospect, just west of Howell Creek, is centred on the largest of these syenite bodies. Here, soil sampling outlined a large area of gold-arsenic-copper rich soils coincident with the stock and peripheral dikes. Narrow zones of pyritic quartz veins several centimetres in thickness returned tenors greater than 31 g/t Au.

The Flathead Grid B prospect (Figure 1) located at the south end of Trachyte Ridge comprises a long glacial dispersion train which contains cobbles to 20 centimetres in diameter of quartz-magnetite-pyrite vein fragments, locally with syenite breccia still attached. Gold grades of these cobbles are exceptionally high with gold contents more than 30 g/t Au being common. The highest gold grade obtained to date is 620 g/t Au. A limonitic quartz vein in limestone near the up-ice origin of the soil anomaly returned over 300 g/t Au. Higher gold grades are accompanied by elevated contents of tellurium.

Mineral Zoning

Observations of the wide variability of gold mineralization styles from several widely separated areas of the HCS suggest a district wide mineral and alteration zonation as summarized below.

Central Zone: large syenite plugs and intrusive breccias

- ♦ central porphyry Mo-like system-quartz stockwork in Howell Grid E;
- ♦ intense silicification of siliciclastic rocks, disseminated and vein fluorite common, extensive intrusive breccia development, local galena, sphalerite, chalcopyrite;
- ♦ extensive pyritization.

Peripheral Zone: small syenite bodies, foid syenite sills, intrusive breccias

- ♦ multiple generations and varieties of intrusive bodies;

- ♦ alteration dominated by carbonatization of intrusives, pyritization, moderate to weak silicification, argillization;
- ♦ widespread low-grade gold in limestone and intrusive.

Distal Zone: isolated small dikes, syenite and foid syenite (i.e. Howe Grid A)

- ♦ isolated and volumetrically minor dikes of syenite and foid syenite;
- ♦ minor pyritization, rare barite veining, disseminated gold in sandstone and silt stone and green shale;
- ♦ manto-style base metal mineralization-colloform sphalerite in limestone, fluorite and pyrobitumin in limestone.

SUMMARY AND DISCUSSION

The Cretaceous Flathead Intrusions lie east of more extensive, coeval calc-alkaline plutons and batholiths, perhaps occupying an extensional setting inboard of the main magmatic axis during the middle Cretaceous. This broad setting is similar to the Tombstone Intrusive Suite in the Yukon with their associated Fort Knox and Brewery Creek styles of gold mineralization. The latter is related to syenite intrusions and has many features in common with the mineralization related to the Flathead Intrusions.

Removing the 65 to 75 km of post-Albian eastward displacement on the Lewis Thrust (van der Velden and Cook, 1994) would restore the syenites to a position west of the present southern Rocky Mountain trench, in the vicinity of the extension of the Vulcan Low magnetic anomaly. This feature is interpreted to mark the suture between two Archean structural blocks (Ross *et al.*, 1991), and would be an appropriate tectonic environment to localize alkalic intrusions.

Many features of the gold bearing mineralization within the HCS and surrounding area fall within the alkalic epithermal classification as described in Bonham (1988), Mutschler and Mooney (1993), and Richards and Kerrich (1993). Sillitoe (1993) prefers to categorize the alkalic epithermal class as a sub-type of the low-sulphidation epithermal deposits. The deposits of the Flathead region have also been described as alkalic intrusion-associated deposits in a con-

tinental setting by Schroeter and Cameron (1996). Similar but younger deposits can be found throughout Montana and South Dakota and include the Zortman and Landusky deposits (Wilson and Kaiser, 1988), the Golden Sunlight deposit and others within the central Montana Alkalic Province and deposits located in the Black Hills of South Dakota. Studies by Paterson (1990) and Paterson *et al.* (1989) of the Black Hills deposits describe fluids that are hotter and more saline than those attributed to typical epithermal deposits suggesting a regime transitional between mesothermal and epithermal environments.

Lefebure *et al.* (1999) describe key features of the sediment-hosted deposit type (i.e. Carlin-type) in an accompanying paper. The sediment-hosted mineralization of the HCS differs from the classic characteristics of the Carlin deposits in several respects including the direct and unequivocal association with intrusive rocks in the HCS deposits, the lack of mercury in the HCS and the higher silver to gold ratios. Whether this constitutes a fundamental difference between the deposit types is not clear.

CONCLUSIONS

This study has documented sediment-hosted gold occurrences in the Howell Creek Structure of southeastern British Columbia. The sediment-hosted mineralization is only part of a broader distribution of gold occurrences in the region related to syenite intrusions of Early Cretaceous age. The sediment-hosted occurrences are characterized by weak silicification of limestone accompanied by finely disseminated pyrite with an element association that includes arsenic, antimony, and silver. The occurrences do not directly compare with all features of the standard sediment-hosted or Carlin-type gold deposit model but enough similarities exist to warrant further study of the possible relationship.

ACKNOWLEDGMENTS

Andrew Legun provided unpublished field maps, airphotographs and lithogeochemical data for the study area. Jody Spence provided excellent field assistance in 1998 and contributed field data incorporated in this study. Cominco Ltd., Placer Dome Canada and Phelps Dodge

Corporation of Canada Limited conducted exploration programs and their data is used in this report. Petrascience Consultants Inc. (Anne Thompson and Audrey Robitaille) completed PIMA on selected samples to determine clay and carbonate mineralogy. Mike Fournier and Maurice Johnson produced several of the figures and scanned the plates. Reviews of this manuscript by Peter Fox and Jim Logan are appreciated and have improved the final product.

REFERENCES

- Adair, R.N. and Burwash, R.A. (1996): Evidence for pyroclastic emplacement of the Crowsnest Formation, Alberta; *Canadian Journal of Earth Sciences*, v. 33, p. 715-728.
- Bonham, H.F. (1988): Models for volcanic hosted epithermal precious metal deposits; in *Bulk Mineable Precious Metal Deposits of the Western United States*, Symposium proceedings, R.W. Schafer, J. J. Cooper, and P.G. Vikre, Editors, *Geological Society of Nevada*, p. 259-271.
- Cameron, R.S. (1989): Reverse circulation drilling report for the Howe claims, Fort Steele mining division, British Columbia; *B.C. Ministry of Energy, Mines and Petroleum Resources*, Assessment Report 18629.
- Folinsbee, R.E., Ritchie, W.D. and Stansberry, G.F. (1957): The Crowsnest volcanics and Cretaceous geochronology; in *7th Annual Field Conference Guidebook*, *Alberta Society of Petroleum Geologists*, p. 20-26.
- Gordy, P.L. and Edwards, G. (1962): Age of the Howell Creek intrusives; *Journal of Alberta Society of Petroleum Geologists*, v. 10, p. 369-372.
- Jones, P. B. (1964): Structures of the Howell Creek Area; in *Fourteenth Annual Field Conference*, *Bulletin of Canadian Petroleum Geology*, Special Volume 12, p. 350-362.
- Labreque and Shaw (1973): Restoration of Basin and Range faulting across the Howell Creek Window and Flathead valley of southeastern British Columbia; *Bulletin of Canadian Petroleum Geology*, v. 21, No. 1, p. 117-122.
- LeBas, M.J., LeMaitre, R.W., Streckeisen, A. L. and Zanettin, B. (1986): Chemical classification of volcanic rocks based on the total alkali-silica diagram; *Journal of Petrology*, v. 27, p. 745-750.

- Lefebure, D.V., Brown, D.A., and Ray, G.E. (1999): The British Columbia Sediment-hosted Gold Project; in *Geological Fieldwork 1998*, B.C. Ministry of Energy and Mines, Paper 1999-1, this volume.
- Legun, A. (1993): The Howell Creek structure, south-eastern British Columbia; in *Exploration in British Columbia 1992*, B.C. Ministry of Energy, Mines and Petroleum Resources, p. 117-120.
- Mutschler, F. E. and Mooney, T. C. (1993): Precious-metal deposits related to alkalic igneous rocks: provisional classification, grade-tonnage data and exploration frontiers; in *Mineral Deposit Modeling*, R. V. Kirkham, W.D. Sinclair, R. I. Thorpe, and J. M. Duke, Editors, *Geological Association of Canada*, Special Paper 40, p. 479-520.
- Norris, D.K., Stevens, R.D., and Wanless, R.K. (1965): K-Ar age of igneous pebbles in the McDougall-Segur conglomerate, southeastern Canadian Cordillera; *Geological Survey of Canada*, Paper 65-26, 11p.
- Oswald, D. H. (1964): The Howell Creek structure; in Fourteenth Annual Field Conference, Special Volume 12, *Bulletin of Canadian Petroleum Geology*, p. 363-377.
- Paterson, C. J. (1990): Magmatic-hydrothermal model for epithermal-mesothermal Au-Ag deposits in the northern Black Hills; in *Proceedings, 4th Western Regional Conference on Precious Metals and the Environment*, Lead SD, *Society for Mining, Metallurgy and Exploration*, p. 89-102.
- Paterson, C. J., Uzunlar, N., Groff J., and Longstaffe, F. J. (1989): A view through an epithermal-mesothermal precious metal system in the northern Black Hills, South Dakota: a magmatic origin for the ore-forming fluids; in *The geology of gold deposits: the perspective in 1988*, R.R. Keays, W. R. H. Ramsay, and D.I. Groves, Editors, *Economic Geology*, Monograph 6, p. 564-570.
- Peterson, T.D., Currie, K.L., Ghent, E.D., Bégin, N.J., and Beiersdorfer, R.E. (1997): Petrology and economic geology of the Crowsnest Volcanics, Alberta; in *Exploring for minerals in Alberta: Geoscience contributions, Canada-Alberta agreement on mineral development (1992-1995)*, R.W. MacQueen, Editor, *Geological Survey of Canada*, Bulletin 500, p. 163-184.
- Price, R.A. (1962): Fernie map-area, east half, Alberta and British Columbia (82G E1/2); *Geological Survey of Canada*, Paper 61-24, 65 p.
- Price, R.A. (1965): Flathead map-area, British Columbia and Alberta; *Geological Survey of Canada*, Memoir 336, 221 p.
- Ross, G.M., Parrish, R.R., Villeneuve, M. E., and Bowering, S. A. (1991): Geophysics and geochronology of the crystalline basement of the Alberta basin, western Canada; *Canadian Journal of Earth Sciences*, v. 28, no. 4, p. 512-522.
- Richards, J. P., and Kerrich R. (1993): The Porgera gold mine, Papua New Guinea: magmatic hydrothermal to epithermal evolution of an alkalic-type precious metal deposit; *Economic Geology*, v. 88, p. 1017-1052.
- Schroeter, T.G. and Cameron, R. (1996): Alkalic intrusion-associated Au-Ag; in *selected British Columbia mineral deposit profiles, Volume 2 - Metallic Deposits*, D.V. Lefebure, and T. Höy, Editors, *B. C. Ministry of Employment and Investment*, Open File 1996-13, p. 49-51.
- Sillitoe, R. H. (1993): Epithermal models: genetic types, geometrical controls and shallow features; in *Mineral Deposit Modeling*, R. V. Kirkham, W.D. Sinclair, R. I. Thorpe, and J. M. Duke, Editors, *Geological Association of Canada*, Special Paper 40, p. 403-417.
- Skupinski, A. and Legun, A. (1989): Geology of alkalic rocks at Twentynine Mile Creek, Flathead River area, southeastern British Columbia; in *Exploration in British Columbia 1988*, B.C. Ministry of Energy, Mines and Petroleum Resources, p. B29- B34.
- Thompson, A. and Robitaille, A. (1998): PIMA short-wave infrared analysis, Golden Bear Mine and Howell Property; Unpublished report for B.C. Ministry of Energy and Mines.
- Treves, S.B. Goble, R.J., Wampler, J.M. and Ghazi, A.M. (1993): Geochemistry and K-Ar ages of Cretaceous intrusions from the Lewis thrust sheet, Alberta, Canada; in *EOS Transactions, American Geophysical Union*, v. 74, 43, Suppl., p. 634.
- van der Velden, A.J. and Cook, F.A. (1994): Displacement of the Lewis thrust sheet in southwestern Canada: new evidence from seismic reflection data; *Geology*, v. 22, p. 819-822.
- Wilson, M. R., and Kaiser, T. K. (1988): Geochemistry of porphyry-hosted Au-Ag deposits in the Little Rocky Mountains, Montana; *Economic Geology*, v. 83, p. 1329-1346.



METALLOGENY OF THE BEATON — CAMBORNE MINING CAMP LARDEAU DISTRICT (082K 12 & 13)

By B.N. Church and L.D. Jones, B.C. Geological Survey

KEYWORDS: Beaton, Camborne, Trout Lake, veins, gold silver, lead, zinc, molybdenum, tungsten, Lardeau Group, Kootenay Arc.

INTRODUCTION

The Beaton area (NTS 082K12,13) comprises several former mines and dozens of mining prospects scattered across 200 square kilometres in the Lardeau district, West Kootenay region of southeastern British Columbia. The area is centred just north of the settlement of Trout Lake, 60 kilometres southeast of Revelstoke and 140 kilometres north of Nelson in the heart of Selkirk Mountains

Prospecting for metalliferous deposits in the Lardeau district began prior to 1890. A crew led by Peter Walker, following up on a rumor of new mineral discoveries, travelled down the Columbia River from Revelstoke to Upper Arrow Lake and overland to Trout Lake. Mining activity started in the late 1890's after more prospectors overflowed from the Slocan and Kootenay Lakes area. By 1899 mineral claims were located near Beaton on the Northeast Arm of Upper Arrow Lake and along the Incomappleux (Fish) River.

The history of the Lardeau district revolves about three mining camps - the Camborne camp on the Incomappleux River east of Beaton, the Ferguson camp east of Trout Lake and the Poplar Creek camp south of Trout Lake. This paper discusses the mines and mineral occurrences in the Beaton map area including the Camborne camp.

In the early years gold and silver-lead ores from the the Camborne camp attracted the most attention. Claims on Sable Creek, Lexington Mountain and at the head of Mohawk Creek, were responsible for much of the interest. In July 1899, good gold values were obtained from a quartz vein on the Eva claim on Lexington Mountain and a prospecting rush ensued. A

wagon road was built to Trout Lake from Thompson's Landing (renamed 'Beaton' in 1903) on the Northeast Arm of Upper Arrow Lake. In the succeeding eight years many gold claims were staked and developed. Four or five stamp mills were erected to process the quartz-rich vein ore and the town of Camborne, founded in 1901, grew rapidly. In 1902 the railway was extended to Gerrard at the south end of Trout Lake and steamer service began on the Arrow Lakes. Activity peaked in 1904 but the operations at Camborne soon proved unprofitable due to a combination of poor management, low ore grades and metallurgical problems. By far the greatest proportion of the ore that was shipped was hand sorted to produce a silver-lead product. Large quantities of ore containing sphalerite, accompanied by appreciable amounts of silver and gold, were left on mine dumps because of a penalty imposed for zinc by the smelters. By 1908 there was a decline in activity and by 1920 Camborne was practically a ghost town. In 1927 the area revived somewhat when the Multiplex Mining, Milling and Power Co. renewed work on their properties along Pool Creek. During the years 1935 to 1941 activity consisted mainly of mill cleanup and salvage projects. Then there was a resurgence of exploration and development in the 1950's. The Spider mine was brought into production in 1952 and continued operations until 1958.

During this period deposits other than just silver and lead were explored in the district. For example in 1942 the Lucky Boy mine on Trout Mountain produced 20 tonnes of scheelite (calcium tungstate) in addition to the previous production of important amounts of silver and lead. Although molybdenite was first reported on the property in 1917, it was not until 1969 and 1975-1982 that further exploration led to the delineation of major molybdenite reserves at what is now known as the Trout Lake deposit.



Figure 1. Location map, Beaton-Camborne mining camp.

Intermittent exploration activity continues in the area driven by changing market conditions for precious and base metals, new geophysical and geochemical methods and new geological interpretations.

GEOLOGICAL SETTING

The geology of the Beaton area (NTS 082K/12,13) comprises diverse lithological elements belonging to several tectonic terranes (Figure 2). On a regional scale, the Beaton-Camborne mining camp is within the Kootenay Arc which lies between the Windermere-Purcell anticlinorium on the east and the Monashee and Shuswap metamorphic complexes to the west and northwest (Reesor and Moore, 1971; Reesor, 1973).

The Kootenay Arc is a 400-kilometre-long curving belt of early Paleozoic to Mesozoic sedimentary, volcanic and metamorphic rocks. It trends northeast across Washington state into British Columbia, then north along Kootenay Lake and northwest into the Arrow Lake and Revelstoke area.

Along Kootenay Lake the arc succession comprises the Hamill, Badshot, Lardeau, Milford, Kaslo, Slokan and Rossland groups. The Hamill, Badshot and Lardeau constitute the early Paleozoic pericratonic Kootenay terrane; the Milford and Kaslo belong to the accreted late Paleozoic (and early Mesozoic) Slide Mountain terrane. The Hamill is mostly quartzite; the Lardeau comprises a lower calcareous section

overlain by phyllitic schists, quartzites and lenticular greenstone formations. The Milford and Kaslo groups are metamorphosed oceanic assemblages that include phyllites, thinly bedded calc-silicate metasedimentary rocks, chert beds, basic volcanic rocks and serpentinites (Fyles, 1967).

The Mesozoic formations constitute the Quesnel terrane that lies along the western side and within the curvature of the Kootenay Arc. The Kaslo and Rossland volcanics (Hoy and Dunne, 1997) and the Slokan argillite, slate and limestones are important units in this terrane and contain significant silver-lead-zinc deposits typical of the Lardeau and Slokan mining districts.

Many batholiths and arrays of small stocks interrupt the continuity of the older deformed stratigraphic succession throughout the Kootenay Arc. The Kuskanax and Nelson batholiths are the largest intrusions. They are predominantly granite and granodiorite in composition although diorite, monzonite and syenite are locally important phases. The age of these rocks is generally considered to be middle or late Jurassic age (Armstrong, 1988; Sevigny and Parrish, 1993).

The Nelson batholith and many of the related granitic stocks have local zones of intense deformation around their margins. Regional structures are deflected into near parallelism along the margins of these intrusions. It may be that antecedent structures controlled the emplacement of the granitic masses.

Cretaceous and Tertiary intrusions are common in the northern part of the arc and to the east. These include medium-size plutons and small stocks of fresh granite, monzonite and syenite such as the Battle Range, Fry Creek plutons and the Mount Toby and Glacier Creek stocks east of Kootenay Lake (Smith and Gehrels, 1992).

Lardeau Group

The Lardeau Group, as defined by Fyles and Eastwood (1962) in the Ferguson area, consists of 6 conformable Lower Paleozoic units named the Index, Triune, Ajax, Sharon Creek, Jowett and Broadview formations. This succession was believed to be an upright stratigraphic sequence having the Index Formation at the base and the Broadview

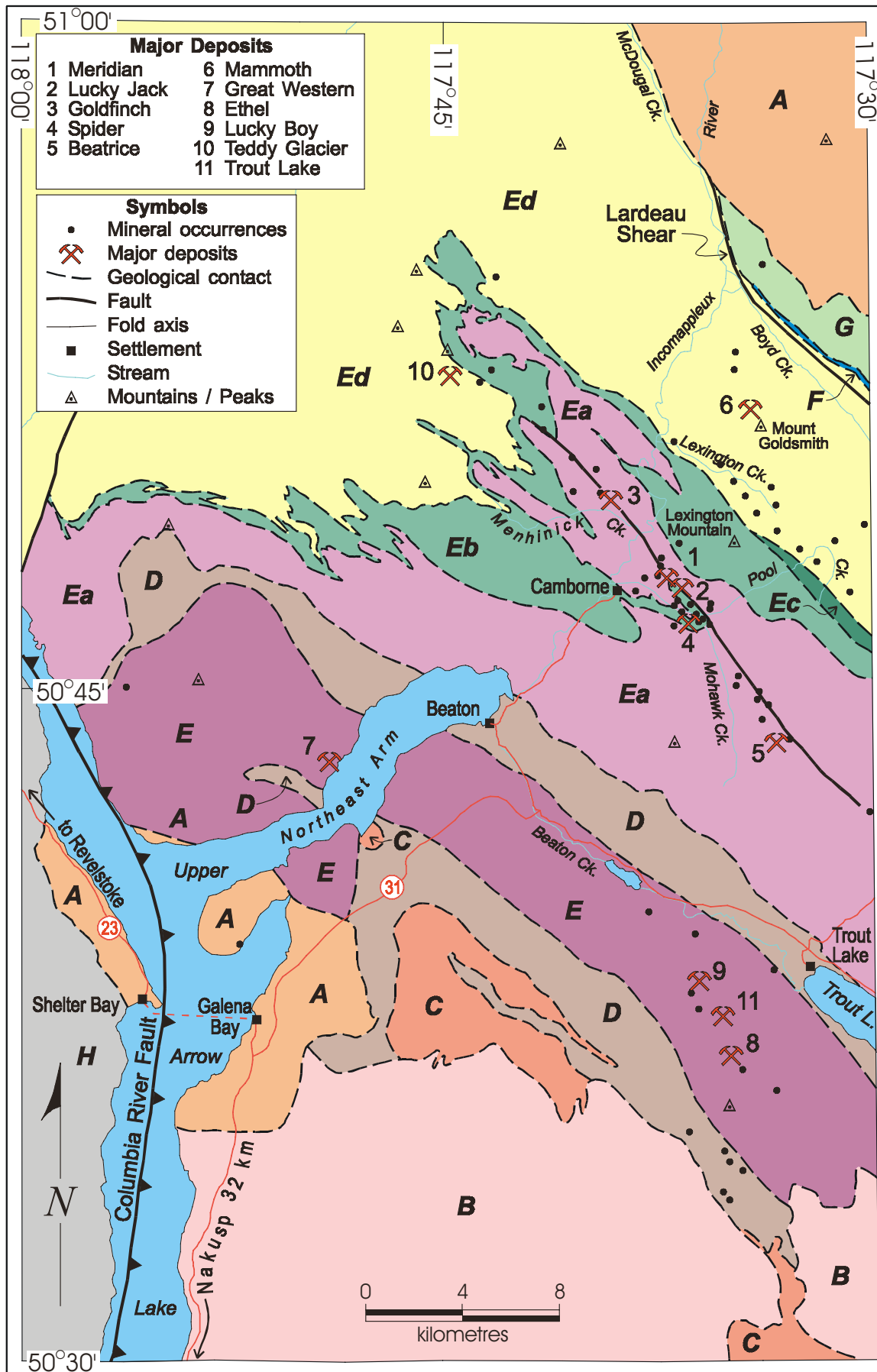


Figure 2. Geology of the Beaton area (modified after Read, 1976, and Read and Brown, 1981). See legend next page.

LEGEND

Cretaceous

A Galena Bay and Battle Range granodiorite, quartz monzonite, alaskite.

Jurassic

B Kuskanax batholith, monzonite, syenite

Permian to Triassic

C Kaslo Group, metavolcanics

D Milford Group, marble, metaconglomerate and sandstone

Lower Paleozoic

E Lardeau Group

Ea Broadview Formation, phyllite, limestone

Eb Jowett Formation, metavolcanics

Ec Sharon Creek Formation, siliceous phyllite

Ed Index Formation, phyllite, greenstone

F Badshot limestone

Hadrynian (Windermere)

G Hamill Group, quartzite, limestone

Precambrian

H Shuswap - Monashee, crystalline gneiss complex

Figure 2. Legend

Formation at the top. However, the highly folded condition of the beds, the lack of facing indicators and the presence of faulted contacts hindered verification of this interpretation (Smith and Gehrels, 1992).

The Index Formation is the most extensive unit in the Lardeau Group. The Index Formation comprises a thick sequence of grey, green and black phyllite, limestone and thick calcareous phyllite, tuff, tuffaceous greywacke, pillow basalt and rare quartzite and quartzo-feldspathic gritty sandstone. In vicinity of McDougal Creek, along the Incomappleux River, the formation consists of crystalline limestones and interbanded slates and phyllites (Figure 2). Many of the limestone bands are highly carbonaceous - some of them containing a considerable amount of graphite, while other bands contain sufficient chlorite to give a green colour to the rock. Although the

formation is highly variable, black and grey phyllite facies predominate near the base at the contact with the Badshot Formation, while green phyllite predominates in the upper part of the unit (Fyles and Eastwood, 1962). The Index Formation is overlain by a conformable assemblage of black siliceous argillite, grey quartzite and black siliceous argillite known respectively as the Triune, Ajax and Sharon Creek formations. The Jowett Formation is a greenstone unit intercalated with the Broadview Formation. The Jowett consists of volcanic breccias and pillow lavas (Photo 1) altered locally to chlorite schist. The predominant lithology of the Broadview Formation is grey green, gritty quartz wacke or subarkosic wacke with grey to black or green slate or phyllite interbeds. Two important bands of quartzite, assigned to the Broadview Formation, cross the valley of the



Photo 1. Deformed pillow lava sequence, Jowett Formation, Lardeau Group.

Incomappleux River – one a short distance below the mouth of Menhinick Creek and the other below the mouth of Sable Creek. This quartzite is an exceedingly hard, compact, dark blue rock invaded extensively by numerous quartz stringers. Size grading is occasionally seen, however, a consistent sense of facing could not be ascertained across the stratigraphy because of the intense deformation of these rocks.

Kuskanax and Nelson Intrusions

The Kuskanax batholith, named by Cairnes (1929), borders the southwest side of the Lardeau area from near the north end of the Kootenay Lake to the Northeast arm of Upper Arrow Lake. The rocks of the batholith are typically medium to fine grained, light coloured granite. Dikes and sills from the batholith vary from granite through syenite to granodiorite and diorite composition. Cairnes believed the Kuskanax batholith to be younger than the Nelson batholith, however, more recent studies

have established a somewhat older age range for these rocks (Smith and Gehrels, 1992).

The Nelson batholith underlies much of the western part of the Kootenay district where it is a complex of intrusives rocks differing in structure, texture and composition. The Nelson batholith is the principal rock type within the Slocan City camp and in this area it is subdivided into three phases (Cairnes, 1934) - granitic porphyry, crushed porphyry, and massive equigranular granite and granodiorite. The granitic porphyry is the predominant phase and hosts most of the ore deposits. Exposed surfaces of the rock are light grey with a flesh-colour hue due to weathering of the feldspar. It is characteristically coarse-grained and distinguished by rectangular phenocrysts (megacrysts) of potassium feldspar, commonly several centimetres long and comprising up to 50 per cent of the rock. These megacrysts are simple or Carlsbad twins of perthitic orthoclase replaced locally by microcline. The megacrysts are set in a coarse grained groundmass comprising subhedral plagioclase (An₃₀₋₅₀), anhedral quartz, irregular clots of amphibole and biotite, interstitial microcline, and minor amounts of apatite, sphene, magnetite and sulphides. Thin sections and chemical analyses indicate that the rock is a silica-poor granite verging to monzonite composition, having roughly equal amounts of alkali feldspar and plagioclase and an alkali/lime index greater than 1.

The various phases of the Kuskanax batholith are leucocratic and as such are readily distinguished from the neighbouring Nelson batholith. The Kuskanax rocks are, in general, medium to fine grained types which in places along the border of the intrusion show a well defined porphyritic texture. Syenite is well developed along the border of the batholith where it forms stock-like apophyses. Elsewhere the batholith is chiefly granite.

The Kuskanax rocks are mostly light coloured, although the syenite generally weathers brown and thus distinguished from the granite. The granite is also generally finer grained than the syenite. In thin section all phases show an abundance of both orthoclase and microcline. Plagioclase occurs chiefly as perthitic intergrowths; the abundance of perthitic intergrowths being a distinctive feature of these rocks. The amount of quartz varies from very little in the syenite to conspicuous proportions

in the granites. The quartz exhibits little evidence of strain or fracturing. Ferromagnesian minerals are few and occur as minute blackish specks throughout the rock. The chief mafic mineral is dark green to bluish green amphibole which is usually partly altered. Accessory minerals include sphene, apatite, magnetite, yellow garnet and occasional sulphide grains. Secondary minerals are mainly kaolin, chlorite and calcite.

A peculiar feature of the Kuskanax batholith is the paucity of mineralization associated with this body. This is in direct contrast to the Nelson batholith and, in particular, the Nelson granite whose relations to ore mineralization in the Slocan area have been previously indicated (Church, 1998). Except for occasional grains of pyrite, no significant mineralization was noted in the principal phases of the Kuskanax batholith.

Galena Bay Stock

The Galena Bay stock outcrops at the head of Upper Arrow Lake intruding the north end of the Kuskanax batholith along the eastern margin of the Monashee complex. The stock was originally considered to be Kuskanax (Cairnes, 1929; Walker et al., 1929), however, K/Ar dating on biotite and muscovite yielded 68 and 92 ± 8 Ma dates, respectively, (Leech et al., 1963) which is significantly younger than Kuskanax but similar to the Trout Lake intrusion, dated 76 Ma by K/Ar analysis of biotite (Boyle and Leitch, 1983).

The Galena Bay stock is a light coloured two mica granite similar to the muscovite - biotite bearing phase of the Battle Range pluton in the headwater area of the Incomappleux River. In thin section these rocks are hypidiomorphic granular and contain abundant quartz, plagioclase and significant amounts orthoclase and microcline. Biotite is an accessory mineral and occurs randomly or in clusters with minor ferromagnesian minerals and crosscutting muscovite laths. Determination of the normative mineralogy from major oxide chemical analysis of a typical sample of the granite yields 27% quartz, 69% feldspar and 4% ferromagnesian minerals (Table 1, no.1)

The main phase of the Trout Lake intrusion is a granitic microporphyry. The rock is charac-

Table 1. Chemical analyses of Galena Bay granitic rocks.

	1	2
SiO ₂	71.90	69.62
TiO ₂	0.18	0.27
Al ₂ O ₃	15.00	14.84
Fe ₂ O ₃	1.41	1.77
FeO	-	1.08
MnO	-	0.03
MgO	0.37	0.52
CaO	2.23	2.99
Na ₂ O	4.28	3.55
K ₂ O	3.18	3.22
BaO	0.18	0.14
LOI	0.66	0.98
P ₂ O ₅	0.05	0.12
Sum (%)	99.44	99.22
Normative Composition		
Qz	26.9	28.2
Or	19.1	19.6
Ab	39.0	32.8
An	11.2	15.3
Wo	-	-
En	1.0	1.5
Fs	2.0	0.1
Mt	-	1.9
Li	0.3	0.4
He	-	-
Cr	0.5	0.2

This table is based on fused disc x-ray fluorescence for the major oxides in rock powders and normative mineral calculations (molecular). Sample No. 1 is from the Galena Bay granitic stock located midway between Galena Bay and the junction of Highway 23 and 31. Sample No. 2 is typical of the granitic rocks hosting molybdenite-bearing veins at the Trout Lake Mine.

terized in thin section by oscillatory zoned, rectangular plagioclase and altered potassium feldspar laths (to 3 mm in diameter) set in a quartz-rich fine grained matrix with peppery biotite, magnetite, and molybdenite. The biotite flakes are partly altered to penninite, a variety of chlorite showing distinctive blue interference colour. Chemical analysis of the Trout Lake intrusion yields 28% normative quartz, 68% combined feldspar and 4% ferromagnesian minerals (Table 1, no.2), which is essentially the same as the Galena Bay granite.

A notable feature of some of these intrusions, relates to the occurrence of sulphides - i.e.

pyritiferous alaskite at the core of the Battle Range and disseminated molybdenite throughout the Trout Lake intrusion. This is in contrast to the Kuskanax batholith which contains no known mineralization, except for the occasional grains of pyrite, a feature that seems to explain why the host rocks intruded by this batholith have provided meager evidence of ore deposition (Cairnes, 1929).

Structural Geology

The Columbia River fault zone is a 250-kilometre long, linear detachment structure exposed along the Columbia River extending through Revelstoke and southward beyond Nakusp on North Arrow Lake (Figure 2). The Columbia River fault trends subparallel to the Slocan Lake fault and appears to be an offset or an en echelon northwest continuation of this structure. Both faults dip gently to the east and separate major tectonic elements. The footwall plate on both faults comprises the ductilely deformed gneissic rocks of the Monashee - Shuswap complex. The hanging wall plate in the Beaton area, known as the 'Selkirk allochthon', is composed of several tectonic slices comprising parts of the Lardeau, Milford and Hamill groups and associated intrusions (Read and Brown, 1981).

The Columbia River fault is a ductile-brittle break that records a history of movement extending from the Mesozoic to Eocene. According to Read and Brown (1981), early deformation resulted in a mylonitic zone up to one kilometre wide within which the rocks later recrystallized to the greenschist grade of regional metamorphism. The fault truncates the major folds and metamorphic zones that had developed in the middle Jurassic. Orientation of slickensides and strain features in the mylonite shows normal dip slip displacements with slices of hanging wall moving eastward. Late displacement in the Eocene, manifested by intense fracturing, folding of mylonite and the development of gouge zones, again shows dip-slip motion with the hanging wall moving eastward. As a result, the tectonic slices east of the Columbia River fault were transported tens of kilometres eastward over the gneissic complexes.

Between the head of Upper Arrow Lake at Beaton and Camborne, the largest tectonic slice,

the 'Selkirk allochthon', is comprised of dark carbonaceous phyllites, grey siliceous schists, greenschists assigned to the Lardeau Group and a green rusty-weathering schistose altered eruptive rocks (Jowett Formation?). These rocks generally have a southeasterly strike, dip northeasterly 50° to 80° and are cut by a series of joints dipping from 40° to 80° northwesterly (Figure 3).

North of Camborne the formations are mainly metasedimentary rocks represented by phyllites, talcose schists, calc-schists and quartzites interbanded with green chloritic schist and rusty weathering schistose eruptives. These rocks are folded forming a series of tight but gently southeast plunging, asymmetrical anticlinal and synclinal structures (Figure 4). The folds are inclined to varying degree, to the southwest and northeast, along the mid section of the Incomappleux River. According to Colpron et al. (1998) the diverse fold inclinations are part of the Selkirk fan structure that was developed regionally outboard of a pre-Cambrian basement ramp during the Columbian orogeny, from mid-Jurassic to Cretaceous.

At Boyd Creek, the Lardeau shear zone marks the boundary between the of the Lardeau Group and the older Badshot and Hamill miogeoclinal strata in the east part of the map-area. The Lardeau Group was deformed prior to mid-Mississippian time as shown by the basal conglomerate in the Milford Formation which contains foliated clasts of the underlying Broadview unit of the Lardeau. Regional constraints indicate probable Devonian - Mississippian timing of the orogeny (Antler-age tectonism) and juxtaposition of the Lardeau Group against the Badshot and Hamill strata along the Lardeau fault at this time. Further deformation (Columbian) produced large isoclinal folds with subhorizontal axes (Photo 2), and southeast (orogen-parallel) stretching lineations. This deformation was not synchronous everywhere and may have continued through late Jurassic time northeast of Trout Lake. This was followed by Cretaceous dextral strike-slip and normal movement on the Lardeau shear zone and other parallel faults. While apparently the locus of several episodes of faulting, the Lardeau shear zone does not record the accretion of far-travelled tectonic fragments. Clearly, the sedimentological evidence ties the Lardeau Group to the

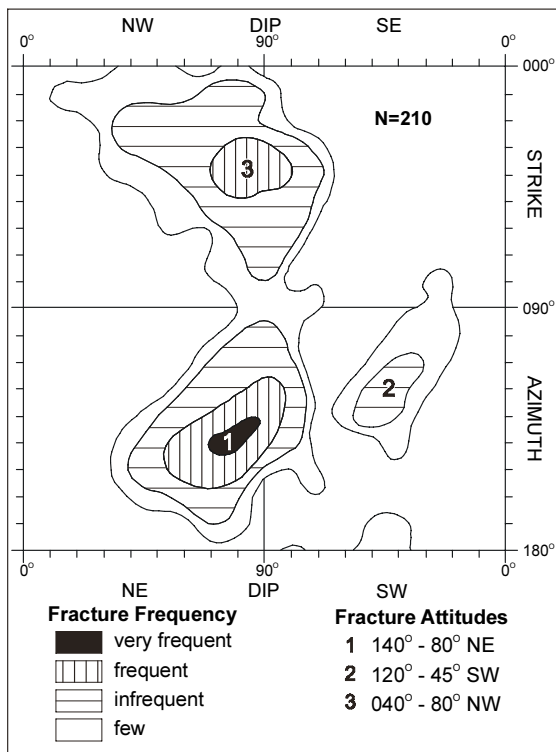


Figure 3. Fracture frequency plot, main belt, Lardeau Group.

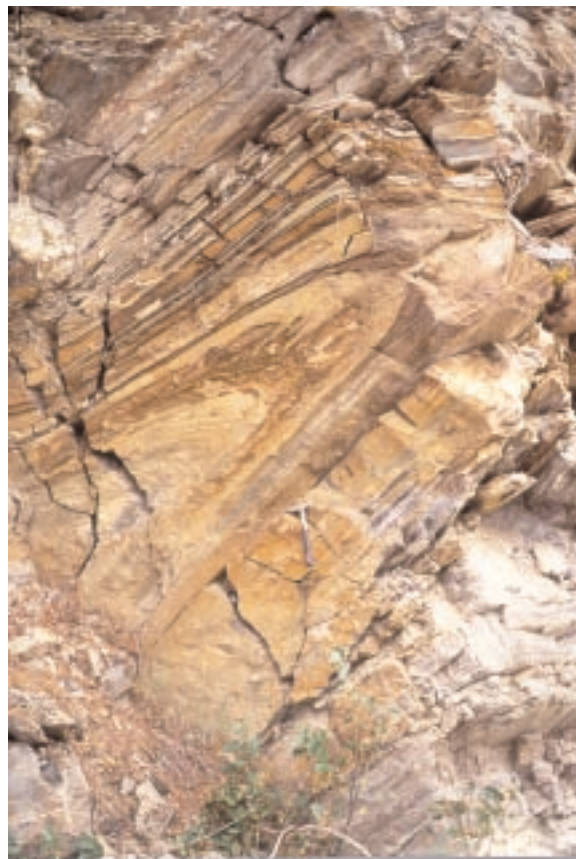


Photo 2. Isoclinally folded limestone, Index Formation, Lardeau Group.

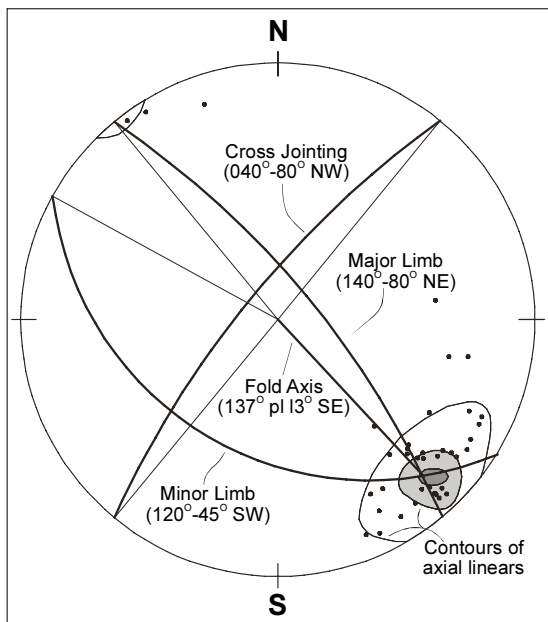


Figure 4. Stereographic projection of (lower hemisphere) of fracture and fold elements, main belt, Lardeau Group.

North American craton (Smith and Gehrels, 1987).

The lack of penetrative fabric distinguishes plutonic rocks of the Kuskanax batholith from the gneisses and schists of the surrounding areas. Fabrics in the shear zone associated with the Columbia River fault indicate easterly down dip displacement of the upper plate. Geochronological data suggest that some ductile strain exhibited in the gneisses and faulting is early Tertiary age and superimposed on considerably older deformation structures possibly related to the original emplacement of the Kuskanax and Nelson batholiths.

Carr et al. (1987) believe that uplift in the early Tertiary resulted in detachment along the Slocan and Columbia River faults and Monashee decollement causing downward movement of the overlying slab to the east. This listric process was accompanied by the development of a system of steeply dipping cross fractures (normal faults) in the hanging wall due to extension. The combined fracturing at this time provided convenient channels and repositories for mineralizing solutions (Beaudoin et al., 1991; Church, 1998).

MINERAL DEPOSITS

The Lardeau and Slocan sections of the Kootenay Arc are among the regions in British Columbia where small scale mining has remained viable for many years because of the richness of the ores. The Beaton - Camborne camp, near the northern extremity of the Kootenay Arc, includes 86 mineral deposits of which 18 are past mineral producers having a combined production of more than 60 million grams of silver and significant amounts of gold, lead and zinc (Table 2).

Comprehensive descriptions of the mineral deposits are provided by Brock (1904), Emmens (1915) and Walker et al. (1929), and Linnen et al (1995). The history of many of the various properties is also recorded in numerous assessment reports and the British Columbia Minister of Mines Annual Reports covering the area.

The following property descriptions are based on MINFILE reports and visits to the principal mines by the author during the summer of 1998.

Meridian (MINFILE 082KNW064, 066, 065, 063, 143)

The Meridian property consists of a consolidation of the Eva, Criterion-Oyster, Cholla, Lucky Jack and Red Horse claim groups. The property is situated on the southwest slopes of Lexington Mountain, northeast of Camborne near the confluence of Pool Creek and the Incomappleux River. The original access to the property was via a horse trail following the cable tram line beginning at a log bridge crossing the canyon of Pool Creek at Camborne. Later a switchback road was constructed to the Eva workings from flats of the Incomappleux River directly below the mine. The road, trail and mine working are presently overgrown and in total disrepair.

The first discovery of gold in the district was on the **Eva** claim (MINFILE 082KNW066). In 1900 an inexperienced prospector searching for silver-lead ores found what is now known as the Eva lode (Lat. 50°47.8', Long. 117°37.8'). Assays returned high gold values and a staking rush followed. By 1902 a group of 21 claims was assembled forming the nucleus of the proper-

ty and much surface work together with more than 490 metres of lineal underground development was completed by Imperial Development Syndicate Ltd. At the end of mine operations in 1908 development comprised 945 metres of drifting on seven levels, 610 metres of crosscuts, 115 metres of raises and 23 metres of shaft sinking.

The Eva mine explores and develops two veins ('A' and 'B') lying in and along two fault planes connected by numerous cross veins and stringers. The direction of the veins is about 135°, cutting the steeply dipping host rocks at a low angle. On the No. 6 level the confining faults are 53 metres apart and dip away from each other. Since the veins follow these faults and converge upward, they are only 27 metres apart on the No. 2 level (150 metres above).

The country rocks are spotted phyllite cut by yellow-weathering schistose diabase. The veins are quartz accompanied by siderite and a small amount of pyrite, galena and sphalerite and some free gold (Photo 3). The veins vary in width from a few centimetres to several metres. Gouge along the faults has evidently confined the ore-bearing solution within these planes and the crushed country rock between them.

The **Criterion-Oyster** claim group (MINFILE 082KNW065) adjoins the Eva on the southeast (Lat 50°47.6', Long 117°37.6'). In addition to a number of surface cuts on these claims, a total of 780 metres of underground development work has been done mostly on two levels following the Criterion vein. This vein is sub-parallel and appears to converge with the 'A' vein of the Eva mine. The ore was transported from the mine to the mill by a 1,066-metre-long aerial tram - the mill at Camborne was operated by water power taken from Pool Creek below the intake of the Eva flume.

The Criterion vein is a well defined and persistent structure that strikes 120° and dips 70° northeast. No. 1 level develops the vein 30 metres below its surface outcrop following a continuous ore-shoot 300 metres long, averaging 1.5 metres wide, from which about 12,700 tonnes of ore was extracted. The vein is the result of fissure filling with quartz and replacement of the brecciated country rock consisting of carbonaceous phyllite. In places the vein is solid

MINFILE Number	Name	Mined (tonnes)	Silver (grams)	Lead	Zinc (kilograms)	Copper	Other	First Year	Last Year
082KNW003	Lucky Boy (L.5423)	473	3097421	114703	1887	1997	Tungsten: 203	1902	1976
082KNW004	Copper Chief (L.4584)	26	135019	2728				1901	1917
082KNW040	Beatrice (L.4586)	618	1832369	182930	10894			1899	1984
082KNW041	Mohawk (L.4571)	8	13499	1358	1699			1963	1963
082KNW045	Spider (L.15752)	128063	53480800	10844750	11519402	85348	Cadmium: 60371 Antimony: 4261	1911	1958
082KNW059	Ethel	74	377839	8045				1899	1918
082KNW062	St. Elmo (L.4581)	5	19408	1098				1899	1899
082KNW064	Meridian	88763	165499					1903	1941
082KNW069	Teddy Glacier	5	2302	855	1351			1929	1929
082KNW071	Lead Star	12	19315	3104	1263			1930	1930
082KNW076	Goldfinch (L.5654)	4347	124215	31	31			1903	1989
082KNW077	Mammoth (L.6473)	76	483652	23167	1952			1905	1907
082KNW097	Mike	2	778	195	657			1973	1973
082KNW101	Silver Dollar	6	9860	1378	1009			1947	1947
082KNW127	Gillman	1	62	22	23			1933	1933
082KNW150	Silver Queen	24	40434	9435				1917	1917
082KNW187	Lucky Jack	462	373					1904	1908
Totals		222965	59802845	11193799	11540168	87345	Tungsten: 203 Cadmium: 60371 Antimony: 4261	1899	1989

Table 2. Mineral production in the Beaton-Camborne Camp



Photo 3. Pyrite, sphalerite, galena and chalcopyrite in vein quartz, ore feed, Meridian mill, Camborne (solid circle = 1 cm.)

quartz but elsewhere it is comprised of a mass of reticulating quartz veinlets with phyllite between. It has been suggested that the carbon in the phyllite has acted as a precipitating agent for the gold contained in the mineral-bearing solutions - the highest grade of gold occurring around the carbonaceous inclusions.

The Criterion vein is cut by a mineralized fault striking 043° known as the 'galena vein'. Where it cuts the Criterion it narrows from more than 1 to 0.3 metre wide, retaining well defined gouge seams along slickensided walls. This younger vein has been explored for 106 metres by drifting on the No. 1 level to a point where it is finally cut off by a shallow south-dipping east-west fault. At 160 metres into the tunnel a 2.4-metre wide quartz vein similar to the 'A' vein at

Eva was encountered. The No. 2 adit, 53 metres below the upper level, was driven 137 metres to intersect the Criterion vein, however, the continuation of the ore-shoot, mined out on the No. 1 level, was not encountered.

The Oyster vein outcrops 90 metres north of the Criterion. It strikes 145°, dips 65° northeast and extends onto the Lucky Jack property to the southeast. The only development on the vein is a series of trenches.

The **Cholla** claim group (MINFILE 082KNW143) on Lexington Mountain adjoins the west margin of the Eva and Criterion-Oyster groups (Lat. 50°47.6', Long. 117°38.0') and extends beyond Pool Creek to Camborne. The quartz veins on these claims are all gold bearing, however, there is little development other than two short adits, 38 metres apart, driven on the Cholla vein. The Cholla is a well defined vertical, north-trending quartz vein cutting phyllites that strike 110° and dip 85° northerly. A sample of a 1.5-metre wide section of the vein from the face of the upper adit assayed 18.5 grams per tonne gold and 13.7 grams per tonne silver. A manganese enriched, pyritic sample from the same general area assayed 41 grams per tonne gold and trace silver. A metre-wide channel sample across the vein in the lower adit, which contained many fragments of phyllite in the quartz, assayed 14 grams per tonne gold. (Emmens, 1915, page K256).

The **Red Horse** claim (MINFILE 082KNW063) is situated on Pool Creek 2.4 kilometres upstream from Camborne (Lat. 50°47.0', Long. 117°36.9'). The principal vein consists mostly of quartz and has been traced for a distance of 60 metres up the mountain side by a series of open cuts, trenches and an adit. The host rock is phyllite striking 135°, dipping vertically. The most prominent joint set strikes 045° and dips 80° northwesterly; a weaker set dips 15° northwesterly. At the adit, the vein strikes 155°, dips 70° northeast and is divided by a median seam of phyllite into a 2.4 metre wide footwall section and a 1.8 metre wide hangingwall section. Mineralization consists of discontinuous seams of massive and disseminated pyrite in the quartz. Sampling across the hanging wall section assayed trace gold and 20.5 grams per tonne silver. Sampling of the foot wall section assayed 0.7 gram per tonne gold, and 82 grams per tonne silver (Emmens, 1915, page K258).

Lucky Jack (L. 8715); (MINFILE 082KNW187)

The Lucky Jack property is situated on Lexington Mountain and adjoins the Criterion-Oyster and Cholla claim groups on the southeast (Lat. 50°47.5', Long. 117°37.1'). There are several veins on this property that have been prospected but the only significant development is confined to surface cuts and shallow underground workings which test the continuation of the 200 metre long Oyster vein. The vein ranges from 1 to 4.6 metres wide and consists mostly of quartz with bands of carbonaceous phyllite mineralized with pyrite. The vein has an average strike of 145° and a dip of 54° northeast. Close to the line of the Sleve Namon and Mascotte claims the vein has been opened by a large cut from which ore was mined and processed in a small two-stamp mill from 1904 to 1908. A crosscut driven through ore on the floor of the cut exposed a wide section of the vein. It dips 35° northeast and is divided into three bands by narrow seams of graphitic schist. Sampling and assay results across 1.5 metres on the hanging wall section yielded 6.9 grams per tonne gold, and 33 grams per tonne silver. Results from 1.8 metres of the central section assayed 10.3 grams per tonne gold and 17.1 grams per tonne silver; while 0.9 metre across the footwall section assayed 28 grams per tonne gold and 33 grams per tonne silver. About 38 metres southeast of this old cut, and 30 metres below it, a crosscut was driven into the hill to the vein and a drift extended for 12 metres to the northwest. Near this point, a sample of the 0.8 metre hanging wall section of the vein assayed 16.1 grams per tonne gold; the middle section across 0.85 metre returned 0.3 gram per tonne gold; and the footwall section across 1.7 metres returned 6.5 grams per tonne gold (Emmens, 1915, pages K257).

Goldfinch (L. 5654); (MINFILE 082KNW076)

The Goldfinch property, comprising the Goldfinch (L.5654), Walrus (L.5653), Dorothy (L.12481), Independence (L.12460) and 11 additional Crown granted claims and fractions, is centered on the west side of the Incomappleux River, 3.7 kilometres north-northwest of Camborne (Lat. 50°49.4', Long. 117°39.5'). Elevations on the property range from 488 metres at river level to 1,040 metres at the main

showings. Access to the property is from Camborne via a switchback logging road that ascends the ridge between Scott Creek and Menhinick Creek.

The property extends 1.5 kilometres following a series of gold-bearing quartz veins that strike southeast coincident with the regional structural trend. The claims were staked at the turn of the century and operated for several years by Northwestern Development Syndicate. The chief work was on the Goldfinch and adjoining Dorothy and Independence claims. Early reports mention numerous trenches and adits and a tramline connecting the Goldfinch mine with the mill at the mouth of Menhinick Creek.

The Goldfinch claim was the focus of the initial development work. In 1903 production of 726 tonnes of ore yielded 16.2 kilograms of gold and 4.98 kilograms of silver and, in 1904, an additional 590 tonnes returned 4.67 kilograms of gold and 633 grams of silver. Much of this production was from an open cut. The vein system is explored by two principal adits and a shaft. A short upper adit (Photo 4) was driven northeast to intercept a splayed vein striking 135° and dipping variably 20°-40° southwest and 75° northeast. The vein is 10 to 30 centimetres wide, and contains quartz, accessory pyrite, galena and visible free gold. Assays on selected samples range up to 62 grams per tonne gold and 21 grams per tonne silver (Emmens, 1915, page 251). The lower adit, located 20 metres below the upper adit, explores the area mostly west and south of the upper workings. A strong quartz vein at the shaft, dipping 80° southwest, is aligned with a similar vein striking 155° at the lower portal, located 130 metres to the southeast of the shaft. Assay results for several one metre sections taken across the shaft vein range up to 0.68 grams per tonne gold and 5.83 grams per tonne silver (Read, 1981).

There are two principal quartz veins on the Independence claim. These are hosted in phyllite and occur in, and adjacent to, a rusty-weathered diabase dike. The No. 1 vein was originally exposed by trenching which follow the bedding planes for 120 metres striking 135°, dipping 60° to 70° northeast. An assay sample taken across 0.9 metre of the vein returned 2.1 grams per tonne gold and 3.4 grams per tonne silver. The No. 2 vein has been opened and drifted on from a short adit. This vein strikes 155° and dips 70°

southwest. A splay of this vein, sampled across 4.9 metres, assayed 17.1 grams per tonne gold and 10.2 grams per tonne silver (Emmens, 1915, page 250).

After a long period of dormancy Eaton Mining and Exploration Co. Ltd. renewed exploration in 1971 and shipped ore in 1979. The property was then acquired by Windflower Mining Ltd. in 1985. Granges Exploration Ltd., in an option agreement with Windflower, completed additional work on the Dorothy zone which led to further production in 1989.

The Dorothy zone consists of a number of quartz lenses and pods on what appears to be an axial plane shear. This mineralized structure trends southeast for a several hundred metres from the Dorothy claim, across the western extremity of Goldfinch to the boundary of the Walrus claim. The main Dorothy structure has been tested by drilling to a depth of 99 metres and traced on strike for 546 metres. Width of the structure ranges between 1.8 and 9.1 metres. The East Zone, located 20 metres east and parallel to the Dorothy zone, is comprised of an echelon quartz veining containing visible gold and a minor amount of galena, sphalerite and a trace of chalcopyrite. The zone has a strike length of 150 metres, depth of 80 metres and width of 1.98 metres. The West zone, traced by drilling for 60 metres along strike, is a sulphide-rich lens containing coarse pyrite with native gold in quartz within graphitic phyllite, similar to the Dorothy zone. The Dorothy North is 80 metres in length and separate from the main zone. Best assay results returned 11.65 grams per tonne gold over 3.61 metres (George Cross Newsletter, # 224, 1987).

A soil sampling program in 1988 by Granges revealed a number of geochemical anomalies. Follow up prospecting resulted in the discovery of a new gold bearing quartz-carbonate vein near Scott Creek. The Scott Creek zone is located 500 metres north of the Dorothy zone and comprises quartz stockwork and quartz-carbonate veining averaging three to four metres and occasionally 10 metres in width. Assay results on grab and chip samples reportedly range from 3 to 27 grams per tonne gold (Northern Miner, Aug. 10, 1987).

Estimated ore reserves for the combined largest zones on the property reported by Granges Exploration Ltd., based on 60 diamond



Photo 4. Main portal, Goldfinch mine, Menhinick Creek area.

drill holes, is 180,000 tonnes grading 10 grams per tonne gold (Northern Miner, March 1987).

Spider (L. 15752); (MINFILE 082KNW045, 044, 048, 049)

The Spider mine (also known as the Sunshine Lardeau mine) is on the south side of Pool Creek, 2.7 kilometres by steep road southeast of Camborne (Lat. 50°46.8', Long. 117°36.5'). The Spider (L.15752), Spider No.1 (L.15753), Eclipse (L.5170) and Sandy (L.8719) are the nucleus of a group of Crown granted claims and fractions that extends from the valley of Pool Creek southeastly towards Mohawk Creek.

The first discovery of ore in this area was made in 1910 on the Spider claim. Development work continued until 1949 during which there were small intermittent shipments of hand-sorted ore (Photo 5). Sunshine Lardeau Mines Ltd. acquired the property and initiated a diamond drilling program which discovered Nos. 4 and 5 veins in 1950. A crosscut was driven to the veins

on No. 5 level and No. 6 adit was extended to intersect No.4 vein. A mill was installed in the old Meridian building on Pool Creek in May 1952. Concentrates were transported by truck to Beaton and thence by the Arrow Lakes barge to the rail-head at Nakusp and from there to smelters in the United States. Berens River Mines Ltd. provided additional funding to gain control of operations. In 1953 the No. 10 adit was driven. In 1956 the company was liquidated and operations passed to Newmont Mining Corp. Mining and milling operations were suspended on May 14, 1958.

The mine is underlain by southeasterly striking, steeply dipping volcanic and sedimentary rocks of the Lardeau Group. Sedimentary rocks of the Broadview Formation include medium grey to greenish quartzites, greywackes, carbonaceous phyllites and quartz sericite schist. The volcanic rocks of the Jowett Formation comprise massive fragmental lenses and lava flows, some chlorite schist and a few thin beds of banded iron formation. In the fragmental units, extreme elongation of the clasts, caused by synkinematic metamorphism, has imparted a crude secondary layering subparallel to the primary stratification.

The volcanic rocks are host to most of the ore. At the Spider mine the volcanic rocks underlie a lens-shaped area roughly 2,300 metres long by a maximum of 600 metres wide. As a unit, the volcanics are considerably more competent than the sedimentary rocks. The few schist zones that are found are generally only a few feet wide and are believed to represent strike or bedding parallel faults.

The major structures have been inferred from cleavage parasitic relationships in the volcanic and sedimentary rocks and the attitude of the minor folds. Large folds with many drag folds appear to be confined to the central part of the volcanic belt. In general the folds are tight isoclinal. The axes of all the folds strike northwesterly, and the axial planes are inclined steeply to the northeast. The folds plunge to the southeast at angles averaging from 25° to 30°.

A northwesterly trending fault, known locally as the Camborne fault, cuts the north limb of a southeasterly plunging anticlinal structure along the north side of Pool Creek.

The orebodies occupy four main veins on a system of steeply dipping, northerly trending

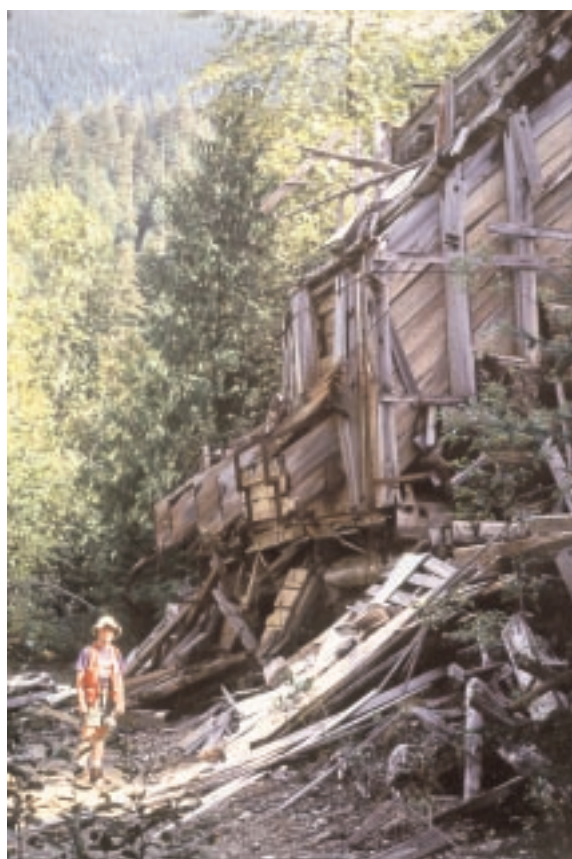


Photo 5. Ore bin, No. 8 Adit, Spider mine, Pool Creek area.

faults. The faults, spaced at ~ 275-metre intervals, cut across the bedding at about 50°, showing some dextral strike slip displacement. From northwest to southeast the veins are named the **Sandy** (MINFILE 082KNW048), **Barclay** (MINFILE 082KNW049), **No. 4** (MINFILE 082KNW045) and **Eclipse** (MINFILE 082KNW044).

Past development at the Spider mine consists of at least seven levels. Production by the end of 1957 was mainly from one ore shoot on the No. 4 vein. This vein, striking 170°, dipping 75° east, was developed from surface to a depth of 200 metres. Ore grade material was intersected in drilling an additional depth of 70 metres below this level.

The Eclipse vein (Lat. 50°46.6', Long. 117°36.3'), accessible via the No. 10 adit level of the Spider mine, produced 31,748 tonnes of ore in the period 1956-58. This development exposed the top of the ore body (005°/75° east) through a vertical range of 46 metres.

The principal showing on the Sandy claim (Lat. 50°46.9', Long. 117°37.1') is a quartz vein which strikes 160°. It is crosscut by four subparallel faults. The ore minerals occur as irregular

veinlets and small pockets along these faults. A small ore shoot discovered in this setting was explored but the limited tonnage indicated did not warrant production.

The Barclay vein is hosted by altered greenstone and exposed at the east end of a road cut. The vein consists of galena sparingly disseminated in quartz. Diamond drill programs in 1954 and 1956 failed to locate any extension of this mineralization. There is no record of ore production from this zone.

The orebodies range from 30 metres to 120 metres in length and from 0.45 to 4.5 metres in width. They are essentially tabular with some pinching and swelling. Tensional branch veins are fairly common. Some of these are more than 30 metres long and 100 metres deep - most of these pinch out within a metre of the main vein.

The main constituents of the ore bodies are quartz, pyrite, sphalerite and galena and minor amounts of ankerite, chalcopyrite, and rarely arsenopyrite and tetrahedrite. Sections composed essentially of pyrite, sphalerite and galena are common. The order of deposition of the vein minerals is ankerite, quartz, pyrite, sphalerite, chalcopyrite, galena. Fine and coarse grained varieties of galena are present.

Zones of carbonate alteration and oxidation, as much as several metres wide, occur along the faults principally on the eastern or hangingwall side with or without accompanying vein mineralization. These zones comprise altered remnants of the volcanic country rock, ankerite, disconnected quartz stringers and a small amount of chrome mica. In the oxidized zone, most of the pyrite, sphalerite and gangue has been leached, leaving a mixture of clay, limonite and galena. The No. 4 orebody shows vertical oxidation for 40 metres below the surface.

In summary, the main ore controls are a series of northerly trending fissures (splays or tension fractures?) that appear to be related to the through-going southeasterly trending Camborne fault along the valley of Pool Creek. Hydrothermal solutions were controlled by the intersection of the principal fissures with fold crests. Mineralization appears to have favoured the Jowett Formation because of the volcanic composition and the competent, fissure-sustaining characteristics of these rocks.

Total production to the end of 1958 was 370 kilograms of gold, 53,480 kilograms of silver, 85

tonnes of copper, 10,845 tonnes of lead and 11,519 tonnes of zinc from 128,063 tonnes of ore (MINFILE, also see Keys, 1956).

Measured geological reserves at the Spider mine are 25,398 tonnes grading 4.4 grams per tonne gold, 255 grams per tonne silver, 6.19 per cent lead and 6.34 per cent zinc (George Cross News Letter, April 26, 1987).

Beatrice (L. 4586); (MINFILE 082KNW040)

The Beatrice mine (Photo 6) is situated, at 2,103 metres elevation, near timber line, at the head of the southeast fork of Mohawk Creek (Lat 50°44.3', Long 117°33.5'). The property consists of six contiguous claims including the Beatrice (L.4586) and Folsom (L.4587). Access to the property is via the badly eroded and overgrown Spider mine road, 11 kilometres southeast of Camborne. Construction of a new logging road to Mohawk Creek has begun from a point just southwest of the canyon section on the Incomappleux River road, about five kilometres northeast of Beaton.

The Beatrice and Folsom claims were staked in 1897 and Crown granted about 1902. They were originally part of the Beatrice Group located on the southwest spur of Mount Pool.. The original discovery by two prospectors consisted of a small chimney of clean galena at the contact of schist and crushed slate. A 10-metre shaft was sunk on the ore, which was further developed by a 60-metre adit, known as the No. 1 level. The No. 2 level was driven from the opposite side of a shoulder (jutting north from the main ridge) to a vertical depth of 46 metres below the No. 1 level. In 1898 approximately 200 tonnes of silver-rich ore was hand mined.

The property was worked continuously from 1898 to 1906. In 1902 the Beatrice Mines Ltd. was organized. The company resumed operations in 1910, but ceased work in 1911. In 1918 the property was bonded to New Era Mines Ltd. and operations continued through 1920. At this point the workings consisted of a several hundred metres of drifts, crosscuts and raises on three levels. In 1921, a two-bucket tramway was installed to connect the No. 2 adit with ore bins on the main trail. However, the high zinc content of the ore prevented satisfactory market arrangements at the time and this discouraged further work. In 1954 a private company, Beatrice

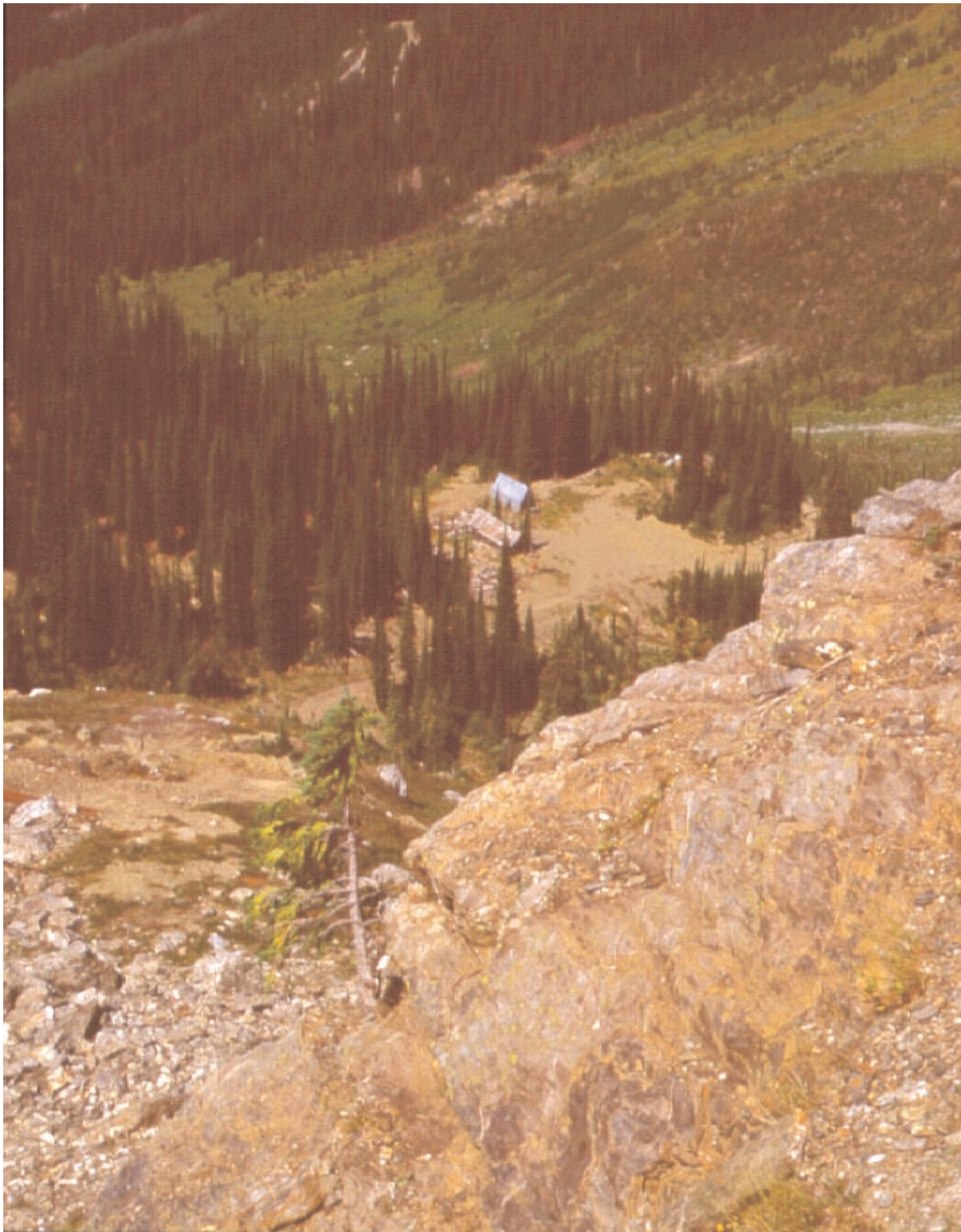


Photo 6. Panoramic view of the Beatrice camp site looking northeast from portal.

Mines Ltd., rehabilitated the mine and during the next few years rebuilt the road. In 1964 the property was optioned to Dakota Silver Mines Ltd. During this and the following years, limited work was carried out but the property and equipment was eventually abandoned.

The Beatrice is on the same belt of Lardeau metasedimentary rocks as the Silver Cup (MINFILE 082KNW027), Nettie L (MINFILE 082KNW100) and True Fissure (MINFILE 082KNW030) mines of the Ferguson camp to the southeast.

Black slates, carbonaceous schists, grey and reddish-brown weathering grits and quartzites and greenish grey talcose schists underlie the property. On average the rocks strike 140° and dip 65° northeast.

Ore occurs as irregular veins in shear zones, on bedding plane slips and crosscutting faults. The veins range from a few centimetres to a few metres wide and consist of sphalerite, galena, tetrahedrite and pyrite in quartz gangue with minor calcite. Replacement is considered to be an important factor in the formation of the ore.

The mine workings develop two principal vein-lodes - the Beatrice and the Main veins. The Beatrice vein, which was the original discovery at surface, strikes 050° and dips 65° southeast across the axis of the controlling synclinal structure. The Main vein, found only on the lower levels of the mine, strikes 140° and dips 65° northeast.

The No. 1 adit was crosscut to the Beatrice vein where considerable stoping was done. Above the level the vein was mined for a vertical distance of about 18 metres and horizontally for 20 metres. The ore appears to have been hand cobbled in the stope and backfilled with rejected subgrade debris. The mineralization consists of a solid band of pinching and swelling massive sulphides, ranging up to 50 centimetres wide. The hanging wall is a two metre wide siliceous zone carrying disseminated sulphides. Sampling at the face of No. 1 level across 0.6 metre yielded an assay result of 0.3 grams per tonne gold, 450 grams per tonne silver, 5.2 per cent lead and 7.8 per cent zinc (Ashton, 1977).

The Main vein on the No. 2 level consists of solid bands of sulphides and disseminations up to three metres wide, in a graphitic shear zone. In the most easterly workings of the intermediate level, the ore zone follows a parallel partly mineralized structure trending 138°, dipping 60° northeast.

A third vein, known as the 'Gold Lode' has been traced for a few hundred metres in open cuts below the main road. This vein, contains pyrite and a sprinkling of galena. It is 1.2 to 1.8 metres wide and strikes 155° and dips steeply to the northeast. Assay results returned 5.1 grams per tonne gold and 32.5 grams per tonne silver (Emmens, 1915, page K267).

Altogether, 618 tonnes of hand sorted ore was shipped from the property, mostly between 1899 and 1917, yielding 558 grams of gold,

1,832 kilograms of silver, 182,930 kilograms of lead and 10,894 kilograms of zinc (MINFILE).

Mammoth (L.6473); (MINFILE 082FNW077)

The Mammoth property comprises four Crown granted claims situated between 2,070 and 2,530 metres elevation, straddling the narrow northwest ridge extending from the summit of Mount Goldsmith (Lat. 50°51.4', Long. 117°34.5'). The original route to this remote mountain top property was by steep mountain trail from the Incomappleux River valley, however, the only practical access nowadays is by helicopter, 9.7 kilometres northeast of Camborne.

The property was worked from 1904 to 1907 by the Edward Baillie Syndicate of Nelson B.C. Production amounted to 76 tonnes of hand sorted ore that yielded 249 grams of gold, 484 kilograms of silver, 23 tonnes of lead and 1.95 tonnes of zinc (MINFILE).

The mine consists of an adit driven 180 metres southeast and several side tunnels crosscutting the main ridge. Some tunnels broke through to surface which now give views of the valleys of Boyd Creek to the east and the Incomappleux River to the northwest (Photo 7). These workings develop a seam of galena, pyrite and argentiferous tetrahedrite, up to 25 centimetres thick, on an essentially horizontal rolling fissure, dipping locally 5° to 10° northeast, in a fine grained, dark grey limestone bed that strikes 150°, and dips 80° northeast. These beds are succeeded to the southwest by other units of the Index Formation (Lardeau Group), including a bed of pure white crystalline limestone and west of that a thick band of green chlorite schist. The host rocks at the mine site are cut by a set of northeast striking vertical joints. Southeast from the adit, along the ridge, there are several small quartz veins and a band of limestone that has been heavily replaced by pyrite (with minor gold) and iron carbonates.

Lucky Boy (L. 5423); (MINFILE 082KNW003, 004)

The Lucky Boy property consists of a small group of Crown granted claims of which the **Lucky Boy** (L.5423), **Horseshoe** (L.5342) and **Copper Chief** (L.4584) (MINFILE 082KNW004) are the most important. The prop-



Photo 7. Main portal area, Mammoth mine, Mount Goldsmith.

erty is located on the northern shoulder of Trout Mountain overlooking Wilkie Creek (Lat. $50^{\circ}38.5'$, Long. $117^{\circ}36.2'$). Access to the property is by dirt road, five kilometres from the north end of Trout Lake.

The first claims in the area, the Lucky Boy and Copper Chief, were staked in 1897 and 1901, respectively. The property was worked originally for high-grade silver-lead ore. From 1901 to 1906 a total of 395 tonnes of this type of sorted ore was shipped and from 1911 to 1917 an additional 25 tonnes of similar ore was mined and shipped to smelters. In 1942 a further 20 tonnes of tungsten (scheelite) ore was hand sorted and shipped. In 1972 an additional 24 tonnes silver-lead-zinc ore was shipped. Total recovery from the claims was 3,232 kilograms of silver, 117,431 kilograms of lead and minor copper, zinc and gold.

The ore was developed by a number of surface cuts, adits and inclined shafts - most of the work was on the Lucky Boy claim and some of the remainder on the adjacent Horseshoe claim. The principal workings are accessible from an inclined shaft that extends downward southeasterly for 58 metres on the Lucky Boy claim. Drifts were developed east and west from this

shaft on three levels. The underground workings on the Horseshoe claim are accessible by two shafts collared 46 and 59 metres due west, respectively, from the Luck Boy shaft. Both of these shafts were driven as declines down dip about 50 metres on the extension of the Lucky Boy vein. The Copper Chief workings lie approximately 1.2 kilometres southwest from the main Lucky Boy and Horseshoe shafts (Lat. $50^{\circ}38.0'$, Long. $117^{\circ}36.5'$). The main showing, at the elevation of 1,575 metres, is exposed in an adit driven at 027° on a steeply dipping fault.

The geology of the area has been described by Read and Brown (1981). The area in the vicinity of Wilke Creek on Trout Mountain is underlain by schists, pelitic quartzites, calcareous phyllites and limestone beds of the Lardeau Group that underwent regional metamorphism and multiple episodes of deformation. The strike of beds across the claims is rather uniform at 150° . Bedding within the quartzite is obscured, but it and most limestone or skarn contacts dip from 65° to very steeply northeast. In several places small dragfolds plunge 20° to 30° northwest. This kind of folding, combined with gentle northwesterly plunging fold axes, seems typical of the area.

There are two types of mineral deposits on the property. One is typical of the main Lucky Boy and Copper Chief ore deposits and consists of nearly flat, drusy quartz veins which cut steeply dipping quartzites and limestones of the Lardeau group at nearly right angles. These veins carry galena, sphalerite, pyrite, tetrahedrite, minor native silver and scheelite in a quartz gangue. The second type is skarn mineralization in silicified limestone. The skarns contain garnet, pyroxene, pyrrhotite and considerable scheelite but little or no galena, tetrahedrite and only small amounts of sphalerite. They are rarely more than several metres in length and vary from 1 to 12 metres in width. The skarns usually crop out over exceedingly rugged and steep mountain sides.

The Lucky Boy vein has an easterly strike, with an average dip of 50° south that becomes almost horizontal in places. The vein apparently follows the major jointing of the enclosing silicified schist and quartzite. The sulphides reticulate through the vein quartz, sometimes occurring as almond-shaped masses. The following order of formation of the metallic minerals is suggested - galena, tetrahedrite, chalcopyrite and pyrite, galena, sphalerite. Galena is found both in and surrounding tetrahedrite; sphalerite encloses both. Chalcopyrite encloses and forms veins in the foregoing assemblage, and pyrite and galena form the matrix for the other sulphides. From the way chalcopyrite embays the tetrahedrite, it looks as if it was formed at the expense of the latter - perhaps the result of a reaction of tetrahedrite with pyrite.

From the shaft on the No. 1 level (100-foot level) drifts have been driven to connect with the Horseshoe workings and stopes opened at intervals along the strike of the vein. Near the face of the west drift, a ribbon of ore 15 centimetres wide, containing abundant tetrahedrite, assayed 5 grams per tonne gold, 6,500 grams per tonne silver and 3.3% copper. Also, a sample across a 25 centimetre width of the vein, at the head of the stope, assayed 13.7 grams per tonne gold, 2,600 grams per tonne silver and 47.2% lead (Emmens, 1915, page K 317).

The No. 2 level is driven eastward and westward from the shaft. To the east, the drifting was carried 75 metres without encountering significant ore. To the west, the vein was followed 37 metres and stoped throughout to the

No. 1 level. At 17 metres from the shaft, scheelite mineralization is present in the remaining pillars and exposed along the drift westward. In the vein, in the stopping face at 30 metres from the shaft, there is an attractive display of scheelite across 0.7 metre that contains an estimated 1.84% tungsten oxide (J.S. Stevenson, 1942, unpublished notes).

There is no development below the No. 3 level of the Lucky Boy mine. At that depth the vein fissure appears to cut a limestone bed but without significant accompanying mineralization. On the lowest level, the vein as exposed is narrow and contains little sulphides. However, scheelite mineralization extends nine metres up from the base of the shaft, and seven metres east on both walls of the drift - the drift having been driven 40 metres east and west from the shaft accessing raises that go through to the No. 2 level.

The distribution of scheelite mineralization indicates the existence of a shoot of several hundred tonnes of ore that rakes southeastward from the Horseshoe workings at surface, beginning by the east shaft, traversing through to the raise at the west end of No. 2 level and to the base of the shaft on No. 3 level, coinciding with the main shoot of sulphide mineralization which was previously mined. A grab sample of this scheelite ore assayed 1.41% tungsten oxide and 0.63% phosphorous (Stevenson, 1943, page 133).

There appears to have been a considerable tonnage of scheelite ore in place before the silver-lead quartz-sulphide vein was mined. Unfortunately, the sulphides and scheelite were in the same sections of the vein and, as a result of the original focus on precious metals, only the high grade silver-lead ore was mined and much of the scheelite was discarded. The bulk of this rejected material was used as fill in empty stopes or in surface waste dumps.

Other less mineralized veins can be found on parallel fissures. Locally, there is evidence of replacement of inclusions of country rock where the veins widen.

Skarn occurrences are principally southeast of Wilkie Creek. A total of 16 skarns have been found between elevation 1,090 metres (150 metres above the creek) and the crest of the northeast spur of Trout Mountain, at 1,630 metres elevation. The skarn mineralization consists of varying amounts of pyrrhotite and fine

grained scheelite. The skarn occurrences appear to coincide with three limestone beds or perhaps a single limestone bed that was intricately folded.

Several skarns lie on the southwest side of a steep gully extending from the Copper Chief adit at 1,475 metres elevation down to creek level. The lowest showing is about 150 metres below the old low trail that leads southwest from the Lucky Boy camp along the side of Wilkie Creek. The skarn is light coloured and composed mainly of calcite with small amounts of garnet and diopside. It occurs on the northeast side and close to the top of a band of grey limestone that extends uphill from the creek. The skarn is about 2.4 metres wide and is moderately well mineralized with scheelite. The skarn is below an anticlinal fold in quartzite that plunges 20° northwest.

Additional skarn exposures are located in the gully at 1,408 metres elevation on the high trail from the Lucky Boy camp to the Copper Chief adit. One exposure of dark coloured skarn in this area is 3.3 metres wide and contains some scheelite and abundant pyrrhotite. Another dark coloured skarn band, exposed on the southwest side of the gully, is 16 metres wide and contains a high proportion of diopside and epidote. Scheelite is disseminated through this skarn across four metres adjacent to a narrow enclosure of grey limestone. At the portal of the Copper Chief adit, the skarn is 0.6 to 1.2 metres wide and encloses several lenses of limestone. A sample across 1.2 metres of the skarn and limestone assayed 1.06% tungsten oxide (Holland, 1952, page A186).

Ethel (MINFILE 082KNW059)

The Ethel mine is situated northeast of the summit of Trout Mountain, between 1,800 and 1,900 metres elevation, overlooking Humphries Creek (Lat. 50°37.2', Long. 117°34.9'). It is reached by a switchback logging road that connects the property to the settlement of Trout Lake, four kilometres to the northeast.

The Ethel group, comprising the Ethel, Esther, May-Day, Frances and Noel claims, was located in 1898 on a silver-lead rich vein lode. In 1902 the property was purchased by a Philadelphia based company and, after lying idle for four years, the mine was worked on a small scale resulting in a shipment of 480 sacks of

high grade ore to the Trail smelter. Mining continued intermittently until 1918 resulting in a total production of 74 tonnes of ore yielding 378 kilograms of silver and 8,045 kilograms of lead. Underground development of the vein system extends over a vertical range of 50 metres and consists of one crosscut adit and seven drift adits - the longest of which is 90 metres. Since that time there has been no mining activity and the Crown granted claims have reverted. In the summer of 1965, the ground was restaked by Rexony Mining Co. Ltd., and a road was built connecting the property to an existing logging road. The workings were mapped and sampled and in June 1966 three holes were drilled that totalled 236 metres. In 1978 Cominco Ltd. staked the surrounding area and conducted detailed geochemical surveys, from 1979 to 1981, across the surrounding terrain. Subsequently there has been no additional development.

The showings at the Ethel mine are a series of closely spaced quartz veins hosted in dark grey phyllites and limestones of the Lardeau Group. A layer of fine grained limestone 15 to 23 metres thick contains the principal vein-lodes, however, some veins extend beyond the limestone into the phyllite. The veins strike 130° to 155° and dip 60° northeast essentially parallel to the schistosity of the phyllites. The quartz, containing scattered grains of galena, sphalerite, pyrite and tetrahedrite form lenses up to 46 centimetres thick following the schistosity. They have mostly been mined out, but judging from surface exposures and small underground stopes, they formed en echelon bodies with an average dip of 40° to the northeast. The old workings passed from one lens to the next, giving the appearance of a single continuous vein (Photo 8). Selected samples from the surface, containing sulphides or showing copper stain, assay as much as 2,800 grams per tonne silver (Fyles, 1966, page 230).

Teddy Glacier (MINFILE 082KNW069)

The Teddy Glacier property is located at 2200 metres elevation on Mount McKinnon, at the head of a tributary of Stephany Creek, 16 kilometres north of Beaton (Lat. 50°52.1', Long. 117°44.8'). Access is 30 kilometres by road from Beaton via the main Incomappleux River and Sable Creek roads.

The property was staked in 1924 by G. Ritchie and G. Edge. High grade float strewn for 300 metres downslope led these prospectors to the mineral occurrences at the foot of the receding 'Teddy' glacier.

Teddy Glacier Mines, Ltd. was incorporated in 1924 by Blockberger and Associates to acquire the important Rambler-Cariboo, Blackhead, Margaret and Mary Jane claims. A trail was opened to the property in 1925, and in late 1926 a crosscut adit was begun just below the main showing. The adit was advanced to the vein during 1927 and then work stopped. In 1929 the Bush and McCulloch interests provided funds for extending the crosscut to a second vein. A shipment of five tonnes of ore was made at this time yielding 2,302 grams of silver, 124 grams of gold, 855 kilograms of lead and 1,351 kilograms of zinc.

No further activity was reported until a syndicate, financed by Mines Selection Trust of London, began extensive development work in 1934. A considerable amount of money was spent on equipment, trails and camp buildings. Also, at this time, about 500 metres of drifting and cross-



Photo 8. Adit development, Ethel mine, Humphries Creek area.

cutting was done in the upper adit. In 1935, a lower adit, begun 55 metres below the upper adit, was driven 18 metres then abandoned because the upper level results were not encouraging.

The claims were allowed to lapse in 1942. The central claims of the group, covering the main showings, were then restaked in 1942 by A.D. Oakley who subsequently sold controlling interest to A.M. Richmond representing American Lead-Silver Mines Ltd. Richmond did a detailed re-evaluation of the property. The property was optioned to Columbia Metals Corporation Ltd. in 1952. However, no activity other than road building was reported and the option was abandoned.

In 1959 the property was acquired under joint ownership by Sunshine Lardeau Mines Ltd., Maralgo Mines Ltd. and Magnum Consolidated Mining Co. Ltd. - an indirect interest was secured by Transcontinental Resources Ltd. Work by this consortium during 1963 included geological mapping, sampling of the underground workings and 150 metres of diamond drilling in six holes. Road construction in 1964 disclosed new showings on the Bell No. 14 claim, located 900 metres southeast of the main workings. However, a drill program (which totalled 660 metres of diamond drilling) was somewhat discouraging and did not establish the continuity of the ore zones.

The Teddy Glacier property is underlain by tightly folded and sheared limestones, carbonaceous phyllites and grits of the Index Formation, Lardeau Group. These rocks trend southeast (115° - 135°), dip 50° - 60° northeast and are cut by steeply dipping cross-joints.

The ore zones are confined to quartz veins that vary from a few centimetres to 1.2 metres in width, are up to 40 metres long and occupy two adjacent fractures, striking 163° and 170° , and dipping steep easterly. On surface and in the upper adit level, these fractures join to form the 'Big Showing'. This showing comprises a large body of quartz roughly nine metres long carrying bodies of coarse sulphides up to 1.5 metres wide. Assay results across 4.9 metres at the widest point on the vein yielded 8.9 grams per tonne gold, 280 grams per tonne silver, 12.9% lead and 7.1% zinc (Richmond, 1949). Other showings occur 90 metres to the northwest ('Dunbar vein') and again at 180 and 300 metres on the same structure. Assay results on the Dunbar vein

across 0.7 metres returned 6.9 grams per tonne gold, 840 grams per tonne silver, 34.0% lead and 2.8% zinc (Richmond, 1949).

The sulphides occur as masses and bunches of almost clean (70-80%) galena, pyrite, sphalerite and minor chalcopyrite in quartz gangue and, less frequently, as intimately intermixed fine grained sulphides in narrow lenses in quartz. Tetrahedrite occurs as small inclusions in the galena. In most of the ore, silver is closely associated with galena and gold with pyrite (~29 grams of gold per tonne of pyrite). The wall rocks on both the foot and hanging wall sides of the orebodies are hard, competent limy-quartzitic sedimentary rocks that have been silicified, fractured and faulted during folding, and to a minor extent after sulphide mineralization.

The probable and inferred ore reserves at the Teddy Glacier mine are 44,212 tonnes of ore grading 161.1 grams per tonne silver, 4.4 grams per tonne gold, 7.9 per cent lead and 6.8 per cent zinc (Sunshine Lardeau Mines, Ltd., 1964 Annual Report).

Great Western (L.4503); (MINFILE 082FNW213)

The Great Western property, comprising the Great Western, June, Silver Tip and All Blue claims, is located two kilometres north of Whiskey Point on the shore of the Northeast Arm of Upper Arrow Lake (Lat. 50°43.4', Long. 117°49.3'). The claims extend from lake level, at 425 metres elevation, to 900 metres elevation on the southeast slopes of Mount Sproat. The property is reached from the shoreline of Arrow Lake and short access roads.

The rocks underlying the claim group are undivided units of the Lardeau Group consisting of grey to white crystalline limestone, green chloritic schist and a granodiorite body. The Lardeau rocks strike southeast at 120° on average. The large granodiorite body is generally concordant with these beds. The lowest showing located at 60 metres above the lake consists of a width of 3.5 metres of quartz in granodiorite. Galena and pyrite occur sparingly along the fractures and as disseminations in both the quartz vein and the dike. At 210 metres above the lake, at the face of a short adit, mineralization occurs across a width of 2.4 metres. Higher above the lake, at 440 metres, white and grey marble on

the east side of the dike contains small irregular masses of serpentinite and barite plus irregular galena replacements.

Trout Lake (MINFILE 082KNW087)

The Trout Lake deposit is located 60 kilometres southeast of Revelstoke on the northern spur of Trout Mountain between 1450 to 1520 metres elevation (Lat. 50°38.2', Long. 117°36.2'). Access to the property is by logging road, five kilometres west of the north end of Trout Lake.

The first claims in the area, the Lucky Boy and Copper Chief, were staked in 1897 and 1901, respectively. A total of 414 tonnes of hand-sorted ore was shipped from several small veins from the Lucky Boy between 1901 and 1917 - from which 2,898 kg of silver and 121 tonnes of lead were recovered; a further 18 tonnes of tungsten (scheelite) ore was shipped in 1942.

Molybdenite was first reported in 1917, but it was not until 1969 that a subsidiary of Scurry Rainbow Oil Ltd. carried out trenching and a diamond drill program. The property was optioned by Newmont Exploration of Canada in 1975. From 1976 to 1982, a joint venture project by Newmont and Esso Minerals Canada Ltd. delineated the deposit by surface drilling and subsequently by diamond drilling and bulk sampling from an exploration adit (Photo 9). Underground development on the property consists of about two kilometres of crosscuts and drifts. The pipe-like stockwork deposit extends from the surface to a depth greater than 1000 metres and contains estimated reserves of 49 million tonnes grading 0.19% MoS₂ (Linnen et al., 1995). The property has been inactive since 1982 and is now wholly owned by Newmont Mines Ltd.

The geology of the area has been described by Holland (1952, 1953), Boyle and Leitch (1983) and Linnen et al. (1995). The property is centred on the Trout Lake stock, a small granitic intrusion, in a belt of highly deformed metasedimentary rocks of the Lardeau Group (Lower Paleozoic).

The Lardeau Group is bowed around the eastern margin of the Kuskanax batholith. The group consists of argillite, quartzites, carbonate beds and schists that underwent middle Jurassic

regional metamorphism and deformation. Light grey to black argillite beds are interlayered with very fine grained grey to tan phyllites and brown biotite-chlorite-sericite schists with prominent segregated quartz layers and lenses. The carbonate beds are composed of massive and banded grey to white limestone and dolomite with variable skarn development. The skarnified rocks contain quartz, calcite, epidote, diopside, garnet, prehnite, phlogopite and minor amounts of idocrase, wollastonite, sphene and actinolite.

The Trout Lake stock is late Cretaceous age (76 Ma) and consists of four intrusive phases, the earliest of which is porphyritic granodiorite, comprising the bulk of the stock. This is followed by aplite dikes and a succession of somewhat younger dikes including porphyritic quartz diorite, granodiorite, and quartz diorite. These dikes cut off and are cut by mineralized quartz veins.

The porphyritic granodiorite is a grey, medium grey rock characterized by euhedral quartz eyes (10%) set in a seriate-textured groundmass of euhedral plagioclase (35%), anhedral quartz (35%), potassium feldspar (10%), and altered biotite relics.

The young porphyritic quartz diorite is medium to dark grey with a peppery appearance caused by fine biotite flakes in the groundmass. These rocks are composed of quartz (35%), plagioclase phenocrysts (45%), potassium feldspar (< 5%) and accessory biotite. The quartz diorite is also distinguished by hornblende phenocrysts and late magmatic potassium feldspar porphyroblasts.

The aplite dikes, commonly less than a metre thick, are gradational to pegmatitic quartz-potassium feldspar veins.

The regional metamorphic grade increases towards the southwest on the property, with chlorite, biotite and finally garnet and oligoclase appearing in the phyllite and schist facies of the Lardeau Group, as the Kuskanax batholith is approached. Superimposed on this regional metamorphic gradient is a thermal biotite hornfels surrounding the Trout Lake stock. This contact metamorphic aureole, measuring 1.2 x 2 kilometres, was developed during emplacement of the stock. The aureole is easily recognized in the calcareous lithologies where the appearance of clinozoisite defines the outermost isograd. At surface, the highest grade of contact metamor-



Photo 9. View of main portal, Trout Lake prospect.

phic assemblage in the phyllites and schists, consisting of muscovite- chlorite- tremolite-clinozoisite- plagioclase- potassium feldspar- and quartz, suggests a temperature of roughly 400°C.

Hydrothermal alteration at the Trout Lake deposit comprises; a central quartz- orthoclase-albite- (biotite)- 'potassic zone', coincident with molybdenum mineralization and overlapped by a slightly later antipathetic quartz-sericite-pyrite 'phyllitic zone'. The youngest alteration is quartz-muscovite- ankerite- pyrite- (microcline). This alteration is developed pervasively along faults or as halos around late subhorizontal quartz veins. Late chlorite and pyrite filled fractures are widespread but never pervasive. In detail many local variations and some retrograde effects are observed. The relationships of biotite, sericite and chlorite are complex due to the presence of regional metamorphic sericite, chlorite and biotite; the later development of hornfels biotite around the contacts of the stock; and the superimposed hydrothermal sericite and biotite related to vein margins.

Molybdenite mineralization is best developed in a quartz vein stockwork around the margin of the Trout Lake intrusion and dike offshoots of the same body. Molybdenite occurs as fine to medium grained flakes and rosettes accompanied by pyrite and pyrrhotite, mainly along the margins of the veins (Photo 10). In the highest grade zones, molybdenite is strongly disseminated on microfractures in areas of intense quartz vein flooding, some areas measuring as much as 200 metres long and 20 metres wide. Molybdenite grades drop off markedly towards

the centre of the large granodiorite mass and wherever the younger quartz diorite dikes are encountered.

Veins in the Trout Lake stockwork comprise several sets. The older veins trend southeast parallel to the major fold axes and most of the faults (135°, subvertical). Secondary vein sets occur on cross-joints striking 045° and dipping subvertical; and there are late subhorizontal veins. In addition, conjugate subvertical, shear-related veins, striking 005° and 095°, are prominent. The close spatial and temporal relationship between these veins and the Trout Lake stock suggests that hydraulic fracturing followed emplacement of magma. Furthermore, this suggests that the fracturing was caused either by the release of orthomagmatic fluids, or by hot overpressured metamorphic or meteoric fluids.

Post mineral faults observed in drill core cut off good grade molybdenite, but displacements, seen underground are clearly only minor readjustments between fault blocks. Only the 'Z' fault, which bounds the deposit on the east, appears to have significant dip-slip movement.

Tungsten mineralization is restricted to lenses of garnet-clinopyroxene skarn occurring as

replacements in limestone along faults adjacent to the Trout Lake stock. The tungsten occurs as scheelite, with pyrrhotite and minor chalcopyrite on the Copper Chief (MINFILE 082KNW004) and as scheelite in quartz veins with galena, sphalerite and tetrahedrite on the Lucky Boy (MINFILE 082KNW003).

Skarns, manifested mainly by clinopyroxene and garnet, and hosting minor scheelite, occur as replacements of marble along faults adjacent to the Trout Lake stock. Tremolite ± clinozoisite (calc-silicate alteration) locally replaces clinopyroxene and in turn is replaced by biotite and/or calcite, indicating that skarn predated potassic (biotite) alteration.

DISCUSSION

The most striking feature about the ore deposits in the Beaton-Camborne camp is that they occur in well defined linear mineral belts trending southeast parallel to the regional strike of the formations (Brock, 1904). These are referred to as the 'central', 'northeast' and 'southwest' belts. The central belt consists of an alignment of properties that extends southeaster-



Photo 10. Molybdenite-bearing quartz stringer in granite porphyry, Trout Lake prospect (solid circle = 1 cm).

ly from Scott and Menhinick Creek across the valley of the Incomappleux River near Camborne to the southwest slopes of Lexington Mountain and to Pool and Mohawk creeks. If extended further to the southeast, the trend aligns with the main mineral belt in the Ferguson area containing the Nettie, Triune and Silver Cup mines. The northeast mineral belt is less well defined and extends more or less along the divide between Lexington and Boyd Creeks and across the head of Pool Creek into the Ferguson area. The southwest belt consists of a few aligned deposits on the slopes of Trout Mountain, southwest of Trout Lake.

Control and Style of Mineralization

The belts are clearly controlled by regional structures and the physical characteristics of the deformed rocks. For example the central belt follows the axis of the Silvercup anticline and the trend of the Cup Creek fault from the Ferguson camp (Fyles and Eastwood, 1962). It appears that the favourable zones of mineralization along this belts developed at sites of intense fracturing where the fault approaches the crest of an anticline - local structures having formed subsequent to the folding. To the northeast the mineral deposits are scattered and the beds in which the deposits are found comprise relatively incompetent limestone units which were isoclinally folded, sheared and deformed again.

Silver-lead-zinc ores are typical of the central belt and occurrences to the northeast. The ore minerals are mainly pyrite, galena, sphalerite and smaller amounts of chalcopyrite and pyrrhotite. Silver is the most important commodity and it occurs in argentiferous tetrahedrite, galena and less commonly as native silver and sometimes in argentite, polybasite, ruby silver, stephanite and electrum. Gold is present in small quantities and is rarely seen as native gold or electrum. Quartz is the dominant gangue mineral, but carbonates such as ankerite, calcite and/or dolomite are significant gangue components in some veins. The deposits are characterized by open-space fillings with limited wall rock replacement. In a few places where replacement is important, carbonate gangue is relatively abundant.

The fracture frequency pattern in the central belt, underlain by the Lardeau Group, shows

three principal attitudes based on 210 measurements (Figure 3). These are (1) 140°/80°NE and (2) 120°/45°SW and (3) 040°/80°NW. Fracture set (1) is the principal layering, foliation and fissility of the sedimentary and volcanic rocks of the area; (2) is like (1) but a subsidiary fabric (short limb) in asymmetrical folds; (3) is the main cross joint direction. These fractures are mostly steeply inclined relative to the Columbia River fault and underlying Monashee gneiss complex that form the footwall of the Selkirk allochthon. Sets (1) and (2) are also the main fracture and vein direction (dipping mostly to the northeast) at the Meridian, Goldfinch, Ethel and Beatrice mines (Table 3). Cross joints (3) trend northeasterly subparallel to some of the veins at the Trout Lake and Meridian mines.

The southwest mineral belt is dominated by the Trout Lake molybdenum porphyry - tungsten skarn system. The deposit is temporally and spatially related to the emplacement of a small, late Cretaceous granodiorite intrusion. Molybdenite occurs in a quartz vein stockwork and as disseminations in the granodiorite and, to some extent, in the metasedimentary host rocks. In general molybdenite appears to accompany alkali feldspars, but in detail it is intimately associated with incipient muscovite replacing albite and potassium feldspar. Fluorite and barite are uncommon in this system.

Tungsten mineralization is found in skarn lenses in limestone bands peripheral to the main molybdenum zone. Scheelite occurs with pyrrhotite and minor chalcopyrite at the Copper Chief prospect and scheelite in quartz veins with galena, sphalerite and tetrahedrite at the Lucky Boy mine.

Veins associated with the Trout Lake deposit are diverse and complicated (Linnen et al., 1995). At least five orientations are recognized. The oldest veins are subvertical and strike southeasterly parallel to the regional foliation (135°), similar to (1) and (2) above. Orthogonal to this are steeply dipping veins striking 045°, similar to (3) and late subhorizontal veins. A conjugate set of subvertical shear related veins at 005° and 095° is also found. Although there is a close spatial and temporal relationships between the veins and the Trout Lake stock, no radial or concentric pattern occurs such as usually associated with hypabyssal intrusions. This suggests a moderately deep intrusion regime where hydraulic frac-

Table 3. Principal vein attitudes at mines and mineral prospects.

Occurrences (MINFILE No.)	Location		Vein Attitudes	
	Lat.	Long.		
Lucky Boy (003)	50° 38.5'	117° 36.2'	100°/25°SW	
Copper Chief (004)	50° 38.0'	117° 36.5'	150°/80°NE	
Beatrice (040)	50° 44.3'	117° 33.5'	138°/60°NE	155°/80°NE
			050°/65°SE	140°/65°NE
Mohawk (041)	50° 46.7'	117° 35.8'	155°/72°NE	120°/80°NE
			160°/80°NE	090°/60°NE
Excise (043)	50° 46.5'	117° 36.1'	155°/80°NE	
Eclipse (044)	50° 46.6'	117° 36.3'	005°/75°E	
Spider (045)	50° 46.8'	117° 36.5'	170°/75°E	
St. Joe (046)	50° 47.3'	117° 36.9'	135°/90°	
Sandy (048)	50° 46.9'	117° 37.1'	165°/90°	
Ethel (059)	50° 37.2'	117° 34.9'	130°/60°NE	
Red Horse (063)	50° 47.0'	117° 36.9'	155°/70°NE	
Meridian (064)	50° 47.4'	117° 37.2'	120°/70°NE	043°/90°
Oyster (065)	50° 47.6'	117° 37.6'	146°/65°NE	
Eva (066)	50° 47.8'	117° 37.8'	135°/80°NE	135°/80°SW
Teddy Glacier (069)	50° 52.1'	117° 44.8'	163°/80°NE	170°/80°NE
Lead Star (071)	50° 51.8'	117° 41.1'	145°/50°NE	
Burniere (072)	50° 51.2'	117° 41.7'	125°/80°SW	
Goldfinch (076)	50° 49.4'	117° 39.5'	152°/80°SW	135°/20°SW
Mammoth (077)	50° 51.4'	117° 34.5'	135°/10°NE	
Big Showing (078)	50° 52.7'	117° 34.9'	035°/50°SE	
Trout Lake (087)	50° 38.2'	117° 36.2'	135°/90°	045°/90°
Silver Dollar (101)	50° 44.7'	117° 33.9'	155°/60°NE	
Gillman (127)	50° 44.9'	117° 34.1'	165°/35°NE	
Agnes (132)	50° 51.8'	117° 42.5'	035°/45°SE	
Nelson (138)	50° 49.6'	117° 41.0'	120°/50°SW	
Cholla (143)	50° 47.6'	117° 38.0'	180°/90°	
Lucky Jack (187)	50° 47.5'	117° 37.1'	145°/54°NE	

turing within the existing structural framework, caused by the release of orthomagmatic fluids (perhaps combined with metamorphic and meteoric solutions), coincided with the emplacement of the magma. Linnen and William-Jones (1987) have interpreted the magmatization and the development of the orthogonal fracture system to be the result of release of elastic stresses during the late Cretaceous / early Tertiary uplift of the Kootenay arc.

Age of Mineralization

The age of mineralization in the Beaton-Camborne camp coincides with a major late Cretaceous through early Tertiary tectonic transition (to 59 Ma) that is marked by uplift, decollement and intrusion in the Kootenay Arc. This was followed by extensional exhumation of

the Monashee gneissic core complexes along the Columbia River and Slocan Lake faults. The Trout Lake intrusion dated 76 Ma (Boyle and Leitch, 1983) and associated Mo and W deposits represent the beginning, and the Ag, Pb, Zn veins, such as found at the Enterprise mine in the Slocan City area, dated 58.2 ± 0.7 Ma (Beaudoin et al., 1992), represent the culmination of the mineralizing cycle.

Source of Mineralization

The solutions that formed ore deposits ascended along whatever channels that were available in the host rocks such as bedding planes, shear zones and cross fractures (Walker et al., 1929). In the Beaton-Camborne camp predominant fissures are approximately parallel to the strike of the formations, and because the schistosity with few excep-

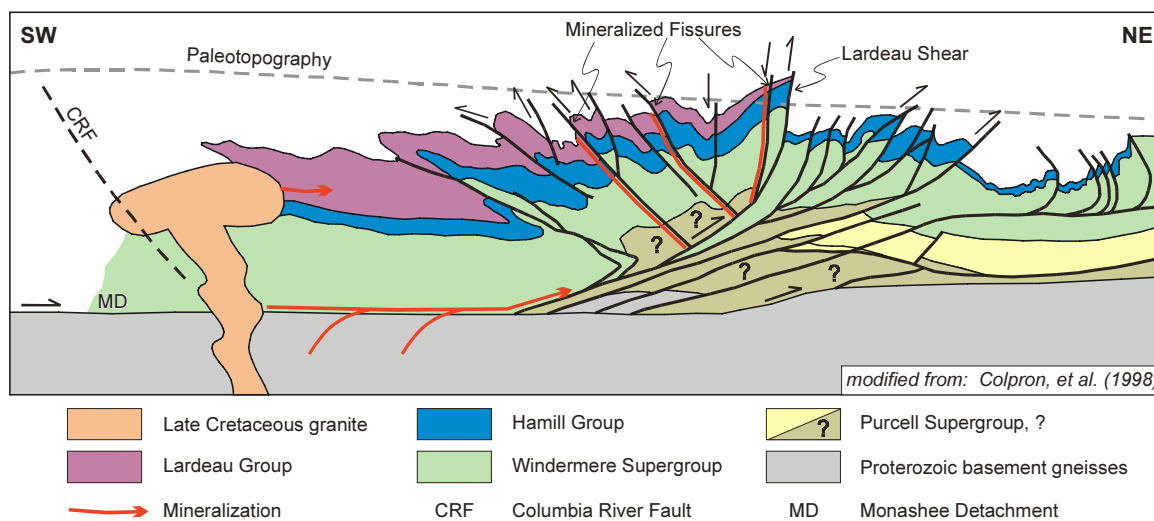


Figure 5. Schematic cross-section of the Selkirk fan structure, during late Cretaceous to early Tertiary time, showing mineralizing systems controlled by doubly verging assymetrical and isoclinal folds and trusts above Dogtooth crustal ramp.

tions also parallels the strike, it is clear that the solutions were forced to ascend along definite zones subparallel to bedding. Consequently, the ore deposits for the most part are aligned more or less along the strike of the beds.

A cross-section through the Selkirk allochthon shows a fan-like arrangement of southwesterly and northeasterly-verging tight folds with steeply dipping axial planes (Figure 5). These structures formed as a result of thrust-ramping of the covering beds along the Monashee decollement from mid-Jurassic to early Tertiary (Colpron et al., 1998). It is these structures that are also believed to have provided the main plumbing system and the regional control of mineralization.

The source of mineralizing solutions was believed by early workers to be the Kuskanax batholith. However, the deposits in the area are much younger and mostly remote from the nearest Kuskanax body. In the case of the southwest belt, which is closest to the Kuskanax, there is clear evidence that the late Cretaceous Trout Lake intrusion is the source of the Mo-porphyry, W-vein and skarn deposits.

The origin of the numerous Ag-Pb-Zn-Au deposits of the central and northeast belts is more complicated. Holk and Taylor (1997) support the general proposal of Beaudoin et al. (1992) that ascending metal-bearing aqueous fluids, derived from crystallizing granitic magma, mixed with deeply circulation meteoric ground waters. This produced numerous Ag-Pb-

Zn vein deposits in the Slokan area during Eocene extension related to the Slokan fault. This is similar to the model proposed (this study) for the Camborne area. Figure 5 shows the ore fluids tapped from magmatic and metamorphic sources, including the high grade gneisses of the underlying Monashee Complex.

CONCLUSIONS

The veins of the Beaton-Camborne camp are hosted by the Lardeau Group and consist mostly of galena, sphalerite and pyrite in quartz and carbonate gangue. Molybdenite and scheelite are associated with the Trout Lake intrusion.

Early workers regarded the granitic rocks as the singular magmatic - hydrothermal source of the mineralization, however, recent studies suggest a more complicated genesis. The veins are fracture fillings and replacements that appear to be related to the Columbia River fault and Monashee decollement that forms the footwall of the Selkirk allochthon. Prolonged movement on this fault system during the late Cretaceous and early Tertiary is believed to have sustained channelways for mineralizing solutions, which are the result of commingling of metamorphic and magmatic fluids and meteoric water.

ACKNOWLEDGMENTS

The writers are obliged to David Lefebure of the Geological Survey Branch for suggesting the

project, to Jim Logan for scientific improvements to this report, and Trygve Höy for his advice in the field. Thanks are also owing to Jody Spence for his field assistance and Mike Fournier and Verna Vilkos of the Branch for their technical advice, and to David Lefebure and Dorte Jakobsen for their technical editing duties.

REFERENCES

- Armstrong, R.L. (1988): Mesozoic and Early Cenozoic magmatic evolution of the Canadian Cordillera; *Geological Society of America*, Special Paper 218, pages 55-91.
- Ashton, A.S. (1977): Beatrice Property near Camborne; Unpublished private report, *Arch Mining and Milling Ltd.*, 13 pages.
- Beaudoin, G., Taylor, B.E. and Sangster, D.F. (1991): Silver-lead-zinc veins, metamorphic core complexes and hydrologic regimes during crustal extension; *Geology*, Volume 19, pages 1217-1220.
- Beaudoin, G., Taylor, B.E. and Sangster, D.F. (1992): Silver-lead-zinc veins and crustal hydrology during Eocene extension, southeastern British Columbia, Canada; *Geochemica et Cosmochemica Acta*, Volume 6, pages 175-196.
- Boyle, H.C. and Leitch, C.H.B. (1983): Geology of the Trout Lake molybdenum deposit, B.C.; *Canadian Institute of Mining and Metallurgy*, Bulletin 76, Number 849, pages 115-124.
- Brock, R.W. (1904): The Lardeau District, B.C.; *Geological Survey of Canada*, Summary Report, part A, pages 42A-81A.
- Cairnes, C.E. (1929): Geological reconnaissance in the Slocan and Upper Arrow Lakes area, Kootenay District, British Columbia; *Geological Survey of Canada*; Summary Report 1928, part A, pages 94A-108A.
- Carr, S.D., Parrish, R.R. and Brown, R.L. (1987): Eocene structural development of the Valhalla complex, southeastern British Columbia; *Tectonics*, Volume 16, pages 175-196.
- Colpron, M., Warren, M.J. and Price, R.A. (1998): Selkirk fan structure, southeastern Canadian Cordillera -Tectonic wedging against an inherited basement ramp; *Geological Society of America*, Bulletin, Volume 110, No.8, pages 1060-1074.
- Church, B.N. (1998): Metallogeny of the Solcan City Mining Camp (082F11/14); in *Geological Fieldwork 1997*, B.C. Ministry of Employment and Investment, Paper 1998-1, pages 22-1 to 22-13.
- Crosby, P. (1968): Tectonic, plutonic and metamorphic history of the central Kootenay Arc, British Columbia; *Geological Society of America*, Special paper 99.
- Eastwood, G.E.P. (1957): Spider, Eclipse etc. (Sunshine Lardeau Mines Ltd.); in Minister of Mines Annual Report 1956, B.C. Ministry of Energy, Mines and Petroleum Resources, pages 99-105.
- Emmens, N.W. (1915): Lardeau Mining Division; in Minister of Mines Annual Report 1914, B.C. Ministry of Energy, Mines and Petroleum Resources, pages K245-K283.
- Emmens, N.W. (1934): Report on the Meridian Mine, Camborne, British Columbia; Unpublished private company report, 33 pages.
- Fyles, J.T. (1966): Ethel; in Minister of Mines Annual Report 1966, B.C. Ministry of Energy, Mines and Petroleum Resources, page 230.
- Fyles, J.T. (1967): Geology of the Ainsworth-Kaslo Area, British Columbia; B.C. Department of Mines and Petroleum Resources, Bulletin 53, 125 pages.
- Fyles, J.T. and Eastwood, G.E.P. (1962): Geology of the Ferguson area, Lardeau district, British Columbia; B.C. Department of Mines, Bulletin 45, 92 pages.
- Gehrels, G.E. and Smith, M.T. (1987): "Antler" allochthon in the Kootenay Arc?; *Geology*, Volume 16, pages 769-770.
- Holk, G.J. and Taylor, H.P. (1997): 18O/16O homogenization of the middle crust during anatexis: Thor-Odin metamorphic core complex, British Columbia; *Geology*, Volume 25, pages 31-34.
- Holland, S.S. (1952): Lucky Boy and Copper Chief (Major Exploration Ltd.); in Minister of Mines Annual Report 1952, B.C. Ministry of Energy, Mines and Petroleum Resources, pages 183-187.
- Holland, S.S. (1953): Lucky Boy and Copper Chief (major Explorations Ltd.); in Minister of Mines Annual Report 1953, B.C. Ministry of Energy, Mines and Petroleum Resources, pages 144-145.

- Höy, T. and Dunne, K.P.E. (1997): Early Jurassic Rossland Group, southern British Columbia, Part 1 - stratigraphy and tectonics; *B.C. Ministry of Employment and Investment, Bulletin 102*, 124 pages.
- Klepacki, D.W. and Wheeler, J.O. (1985): Stratigraphy and structural relations of the Milford, Kaslo and Slocan groups, Goat Range, Lardeau and Nelson map areas, British Columbia; in *Current Research, part A, Geological Survey of Canada, Paper 85-1A*, pages 277-286.
- Keys, M.R. (1957): The Geology of the Sunshine Lardeau Mine; *The Canadian Mining and Metallurgical Bulletin*, Volume 50, Number 540, pages 218-221.
- Leech, G.B., Lowdon, J.A., Stockwell, C.H. and Wanless, R.K. (1963): Age Determinations and Geological Studies; *Geological Survey of Canada, Paper 63-17*, pages 24-25.
- Linnen, R.L. and Williams-Jones, A.E. (1987): Tectonic control of quartz vein orientations at the Trout Lake stockwork molybdenum deposit - implications for metallogeny in the Kootenay Arc; *Economic Geology*, Volume 82, pages 1283-1293.
- Linnen, R.L. and Williams-Jones, A.E., (1990): Evolution of aqueous-carbonic fluids during contact metamorphism, wallrock alteration, and molybdenum deposition at Trout Lake, British Columbia; *Economic Geology*, Volume 85, pages 1840-1856.
- Linnen, R.L., Williams-Jones, A.E., Leitch, C.H.B. and Macauley, T.N. (1995): Molybdenum mineralization in a fluorine-poor system: The Trout Lake stockwork deposit, southeastern British Columbia; in *Porphyry Deposits of the Northwestern Cordillera of North America; Canadian Institute of Mining and Metallurgy, Special Volume 46*, pages 772-780.
- Okulitch, A.V. (1985): Paleozoic plutonism in southeastern British Columbia; *Canadian Journal of Earth Sciences*, Volume 22, pages 1409-1424.
- Parrish, R.R. and Wheeler, J.O. (1983): A U-Pb zircon age from the Kuskanax batholith, southeastern British Columbia; *Canadian Journal of Earth Sciences*, Volume 20, pages 1751-1756.
- Read, P.B. (1973): Petrology and structure of the Poplar Creek map area, British Columbia; *Geological Survey of Canada, Bulletin 193*, 144 pages.
- Read, P.B. (1976): Lardeau map area (82K west half), British Columbia; *Geological Survey of Canada, Paper 76-1A*, pages 95-96.
- Read, P.B. and Brown, R.L. (1981): Columbia River fault zone - southeastern margin of the Shuswap and Monashee complexes, southern British Columbia; *Canadian Journal of Earth Sciences*, Volume 18, pages 1127-1145.
- Read, P.B. and Wheeler, J.O. (1976): Geology and Mineral deposits, Lardeau west half (82K); *Geological Survey of Canada, Open-File 432, Map 1:125,000*.
- Read, W.S. (1981): The 1980 Exploration Program on the Goldfinch Group Mineral Claims for Eaton Mining and Exploration Ltd.; *B.C. Ministry of Energy, Mines and Petroleum Resources, Assessment Report No. 9137*.
- Reesor, J.E. and Moore, J.M. (1971): Petrology and Structure of Thor-Odin Gneiss Dome, Shuswap Metamorphic Complex, British Columbia; *Geological Survey of Canada, Bulletin 195*, 149 pages.
- Reesor, J.E. (1973): Geology of the Lardeau map area, east half, British Columbia; *Geological Survey of Canada, Memoir 369*, 129 pages.
- Richmond, A.M. (1949): Report on the Teddy Glacier Mining Property of American Lead Silver Mines Ltd., Lardeau Mining Division, B.C.; unpublished private company report, 12 pages.
- Sevigny, J.H. and Parrish, R.R. (1993): Age and origin of late Jurassic and Paleocene granitoids, Nelson Batholith, southern British Columbia; *Canadian Journal of Earth Sciences*, Volume 30, pages 2305-2314.
- Smith, M.T. and Gehrels, G.E. (1990): Geology of the Lardeau Group east of Trout Lake, British Columbia (Silvercup Ridge, Mount Wagner and Mount Aldridge areas); *B.C. Ministry of Energy, Mines and Petroleum Resources, Open File 1990-24*.
- Smith, M.T. and Gehrels, G.E. (1991): Detrital zircon geochronology of upper Proterozoic to lower Paleozoic continental margin strata of the Kootenay Arc - implications for the early Paleozoic tectonic development of the eastern Canadian Cordillera; *Canadian Journal of Earth Sciences*, Volume 28, pages 1271-1284.
- Smith, M.T. and Gehrels, G.E. (1992): Stratigraphic comparison of the Lardeau and Covada groups - implications for revision of stratigraphic relations in the Kootenay Arc; *Canadian Journal of Earth Sciences*, Volume 29, pages 1320-1329.

- Stevenson, J.S. (1943): Tungsten deposits of British Columbia, *B.C. Department of Mines*, Bulletin 10, pages 130-133.
- Thompson, R.I. (1978): Geology of the Akolkolex River area; *B.C. Ministry of Energy, Mines and Petroleum Resources*, Bulletin 60, 77 pages.
- Walker, J.F., Bancroft, M.F. and Gunning, H.C. (1929): Lardeau map-area, British Columbia; *Geological Survey of Canada*, Memoir 161, 142 pages.
- Wheeler, J.O. (1968): Lardeau (west half) map area, British Columbia (82K W1/2); *in* Report of Activities, part A, *Geological Survey of Canada*, Paper 68 - 1A, pages 56-58.



MASSIVE SULPHIDE DEPOSITS OF THE EAGLE BAY ASSEMBLAGE, ADAMS PLATEAU, SOUTH CENTRAL BRITISH COLUMBIA (082M3,4)

by Trygve Høy, B.C. Geological Survey Branch

KEYWORDS: Kootenay Terrane, Eagle Bay assemblage, massive sulphide lead-zinc deposits, volcanogenic massive sulphide deposits, Mosquito King, Spar, Lucky Coon, Elsie, King Tut.

INTRODUCTION

The Eagle Bay assemblage in south central British Columbia contains numerous polymetallic massive sulphide deposits, mainly within highly deformed and metamorphosed Devonian felsic volcanic rocks. A number of these, including Rea and Homestake, have had limited past production, and others have undergone extensive exploration and development. Less known and understood are the sediment-hosted massive sulphide deposits that occur on Adams Plateau near the southern extent of exposures of the Eagle Bay assemblage. These deposits are thin sheets of dominantly lead and zinc sulphides within carbonaceous and calcareous phyllites. Their age is unknown, but based on regional correlations and geochemistry of underlying mafic volcanic rocks, host successions may be equivalent to phyllites and quartzites of the EoCambrian Hamill Group exposed farther east. This paper describes these deposits, their structural and stratigraphic setting, and compares them to other deposits in the Kootenay Terrane. The paper is part of a regional study of massive sulphide deposits and mineral potential of the Kootenay Terrane of southern British Columbia and the correlative Yukon-Tanana Terrane in the northern part of the province and Yukon Territory (see Lett *et al.*, 1999; Paulen *et al.*, 1999). It summarizes six weeks of regional mapping and deposit studies in July and August, 1998.

The Kootenay Terrane, and correlative rocks of the Barkerville subterrane farther north, comprise dominantly Paleozoic metasedimentary and metavolcanic rocks that are inferred to have

been deposited on the distal western edge of ancestral North America. Major rock packages of the Kootenay Terrane include the Lardeau Group, the Eagle Bay assemblage, eastern assemblages of the Late Paleozoic Milford Group, and equivalent rocks within the Shuswap metamorphic complex.

Massive sulphide deposits in the Kootenay Terrane include Besshi style volcanogenic massive sulphide deposits (VMS) of the Goldstream camp, formed during episodic extension along the western North American margin in Early Paleozoic time, and the Devonian polymetallic VMS deposits of the Eagle Bay assemblage, deposited in arc volcanic rocks in response to eastward subduction of a paleopacific ocean. Other important deposits or mineral camps within the Kootenay Terrane include numerous vein deposits in Lardeau Group rocks, such as the lead-zinc-silver veins of the Beaton-Camborne camp (Church, 1999), and within the Barkerville subterrane, the gold veins in the Wells-Barkerville area.

The Adams Plateau is a moderately high, low-relief plateau located southeast of Adams Lake in southern British Columbia (Figure 1). It is accessible by a well maintained gravel logging road that leaves the Scotch Creek road at Shuswap Lake park. The plateau is heavily treed, but with extensive logged areas. Numerous logging roads provide access to most of the area. Outcrops are relatively rare, and are largely restricted to roads and, less commonly, creeks.

Mineral exploration on the plateau has focused on the sediment-hosted massive sulphide deposits, and two of these, the Mosquito King and Lucky Coon have had limited past production. Published reserves of these, and others on the plateau, are listed in Table 1. These deposits have locally high gold and copper content and exhibit close spatial association with

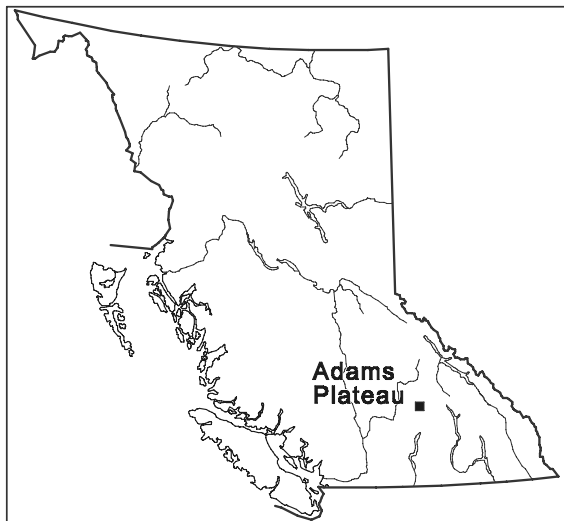


Figure 1. Location map

mafic volcanic rocks. Other occurrences on the plateau, mainly small massive sulphide copper deposits within mafic volcanic rocks, have had little exploration.

REGIONAL GEOLOGY

The Adams Plateau is underlain by rocks of the Eagle Bay assemblage, Late (?) Devonian orthogneiss, Late Cretaceous granites and numerous Tertiary dykes (Schiarizza and Preto, 1987). The Eagle Bay assemblage comprises Lower Cambrian to Mississippian metasedimentary and metavolcanic rocks that have been correlated with the Hamill and Lardeau Groups of the Kootenay arc (Schiarizza and Preto, 1987; Okulitch, 1977) and with rocks of the Barkerville subterrane in the Cariboo Mountains (Struik, 1986).

Paleozoic rocks of the Eagle Bay assemblage (Figure 2) are contained within four west directed thrust slices that collectively contain a

succession of Cambrian (and possibly Late Proterozoic) quartzites, grits and quartz mica schists (Units EBH and EBQ), mafic metavolcanic rocks and limestone (EBG), and overlying schistose sandstones and grits (EBS) with minor calcareous and mafic volcanic units (Schiarizza and Preto, 1987). These are overlain by a "...Devono-Mississippian succession of mafic to intermediate metavolcanic rocks (Units EBA and EBF) intercalated with and overlain by dark grey phyllite, sandstone and grit (EBP)" (Schiarizza and Preto, *op. cit.*). Many of the polymetallic VMS deposits in the Eagle Bay assemblage, including Rea and Homestake (Höy and Goutier, 1986; Höy, 1991), are within units EBA and EBF whereas the massive sulphide deposits of the Adams Plateau are within a sedimentary succession in Unit EBG.

The structure of the area underlain by Eagle Bay assemblage rocks and Fennel Formation has been described by Schiarizza and Preto (*op. cit.*). The earliest recognized structures are east-directed, essentially layer-parallel thrust faults that imbricated and emplaced Fennel Formation rocks, part of Slide Mountain Terrane, over Eagle Bay assemblage. Synmetamorphic southwest verging folds and thrust faults followed tectonic emplacement of the Fennel Formation. These folds are the most conspicuous macroscopic folds in the Eagle Bay assemblage, and the associated northeast dipping thrust faults separate the assemblage into the major structural-stratigraphic panels. Late folds are post-metamorphic, generally upright, northwest to west plunging structures with associated crenulation cleavage. In general, they are small structures that do not effect the regional distribution of lithologies (Schiarizza and Preto, *op. cit.*).

Table 1. Published reserves of lead-zinc massive sulphide deposits, Eagle Bay assemblage, Adams Plateau.

Deposit	Drill indicated tonnage	Zn %	Pb %	Cu %	Ag g/tonne
Spar adit	11,160	4.83	10.56		206
Mosquito King	33,740	2.09	0.83		13
Bowler Creek	171,500	2.43	0.53	0.19	50
Lucky Coon	68,033	"high	grade"		

Source of data: B.C. Minfile

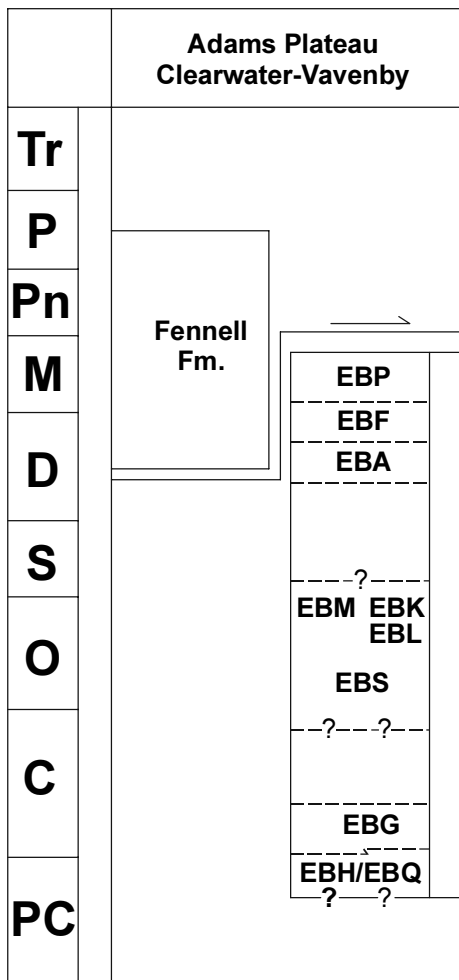


Figure 2. Stratigraphic column of the Eagle Bay assemblage (from Schiarizza and Preto, 1987).

These structures are cut by Jurassic-Cretaceous batholiths and stocks, including the Baldy and Raft batholiths and, on Adams Plateau, by granitic rocks exposed in Scotch and Nikwikwaia Creeks. Late quartz-feldspar porphyry dykes are locally conspicuous, and dark, commonly aphanitic dykes are less common. These are interpreted to be Tertiary in age (Schiarizza and Preto, 1987).

STRUCTURE

The earliest structures recognized on Adams Plateau are small, rootless isoclinal folds. Their vergence is unknown, but if correlative with the Phase 1 structures identified by Schiarizza and Preto (1987) west of Adams Lake, they may have an overall easterly vergence, related to the east-directed thrust faults that are prominent in the Fennell

Formation.

The Nikwikwaia synform, a Phase 2 structure, is the earliest map-scale structure identified on Adams Plateau (Figure 3). It is inferred to be a syncline because “the metasediments in its core are enclosed by chlorite schist which underlie them regionally” (Schiarizza and Preto, 1987, p. 56). It is outlined by a prominent sericitic quartzite, exposed in its limbs and hinge zone, and by repetition of the greenstones and metasediments of Unit EBG in its limbs. It closes to the southwest of Nikwikwaia Lake, and opens to the east towards Scotch Creek (Figure 3). The prominent foliation throughout the area parallels the axial plane of the syncline, and mineral lineations and bedding-cleavage intersections define its fold axis. In western exposures, the Nikwikwaia syncline has a northwest plunge, with a northeast trending axial plane that dips northwest at 30 to 40 degrees (Domain 1, Figure 4). Variable attitudes to the east reflect the effects of later north trending folds (Domain 2). Farther east, on the plateau northwest of Mosquito King, phase 2 axial planar foliations indicate that the syncline is essentially a recumbent fold that plunges variably to the north (Domain 3).

Units in the limbs of the Nikwikwaia synform are locally attenuated, but do not appear to be appreciably thickened in the hinge zone. Both the quartzite and an overlying thin chlorite schist retain a relatively constant thickness in its southern limb and in its closure to the southwest (Figure 3). Hence, it is assumed that the dramatic thickening of some units in the north limb north of Nikwikwaia Lake are due to original stratigraphic changes, particularly as they are accompanied by lithological changes.

A west-verging thrust fault, the Haggard Creek fault, that emplaced Unit EBG on Unit EBA, has been projected south to the Adams Plateau by Schiarizza and Preto (op. cit.). However, as there is little direct evidence for the existence of the fault on Adams Plateau, based on this mapping, it is not shown on Figure 3. Rather, this contact may be intrusive, with highly foliated metaplutonic rocks intruding greenstone of Unit EBG (see below).

The latest folds recognized in the area are broad, open, upright folds. These fold the limbs and axial plane of the Nikwikwaia synform, producing synform-antiform pairs that verge to the

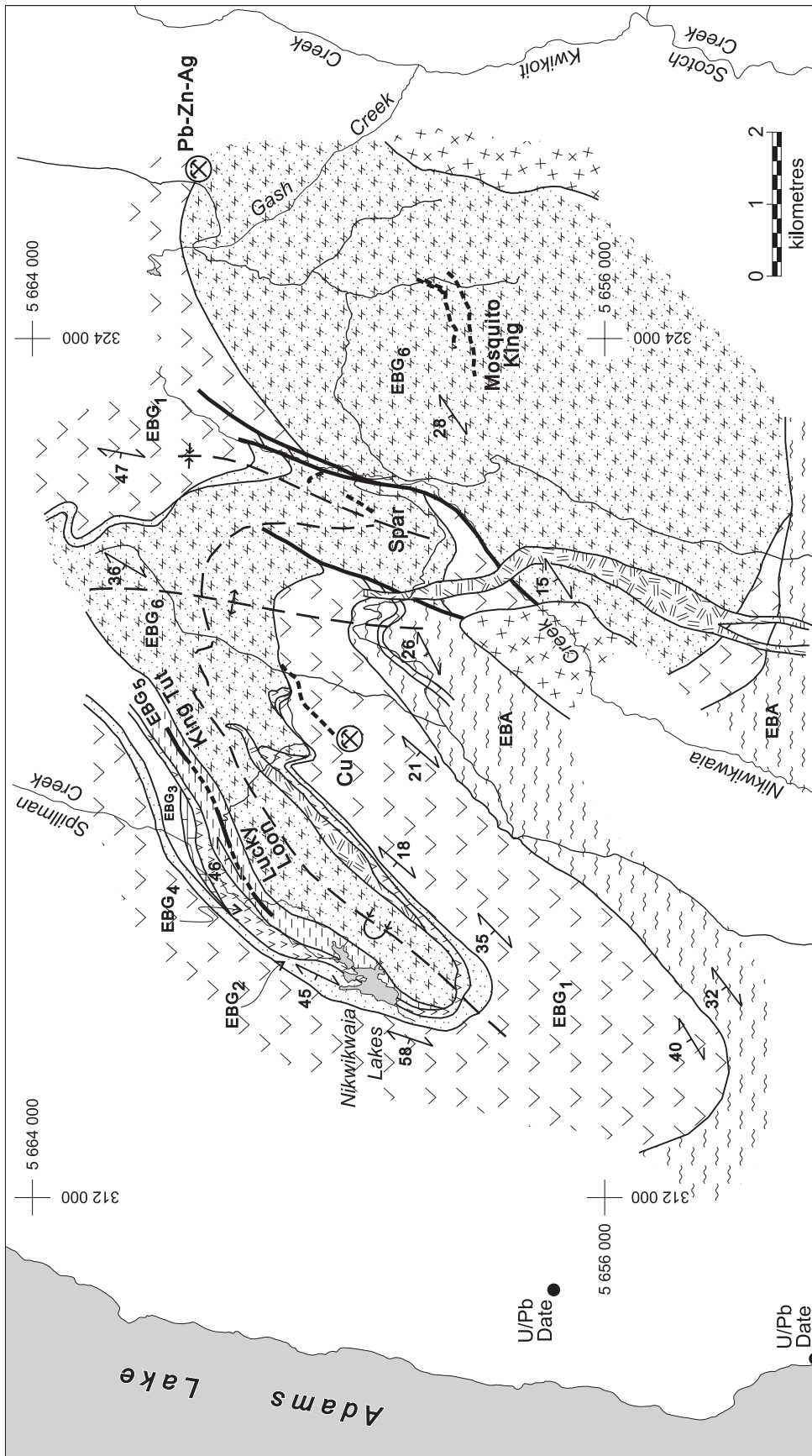
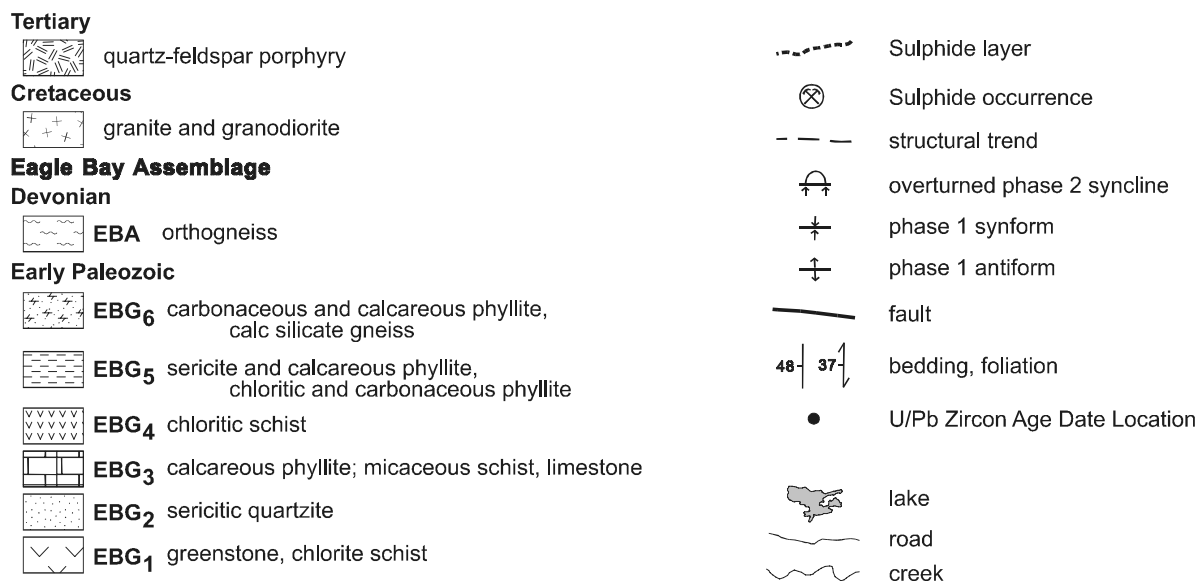


Figure 3. Geology of the Adams Plateau area (after Schiarizza and Preto, 1987 and this paper).



Legend for Figures 3, 8, 12.

east (Figure 3). The most western fold is a large, north-trending antiform, just west of the Spar deposit, with a northeast trending western limb and a northwest trending eastern limb. Steeply dipping, north to northeast trending faults appear to parallel the axial planes of these folds. These faults and related folds are cut by the Late Cretaceous intrusion in Nikwikwaia creek valley and by north-trending Tertiary dykes exposed to the east and north. Locally, minor lead-zinc or copper vein mineralization occurs along the faults.

A late, prominent crenulation cleavage and lineation trends to the west throughout the area (Figure 5). There are no macroscopic folds on Adams plateau associated with these structures. Their age is not known, but Schiarizza and Preto (1987) suggest they are the same age as mid-Cretaceous kink folds associated with emplacement of the Baldy and Raft batholiths.

STRATIGRAPHY

Units EBA and EBG of the Eagle Bay assemblage are exposed on Adams Plateau. Unit EBG comprises dominantly mafic volcanic rocks with interlayered metasedimentary units of Late Proterozoic to Early Cambrian age. EBA is dominated by plutonic orthogneiss that to the west, has a Late Devonian age.

Unit EBG

The basal part of Unit EBG comprises massive to foliated greenstone and chloritic phyllite exposed in the limb of the Nikwikwaia synform. The succession comprises dominantly mafic flows and pillow lavas, with a minor interbedded mafic tuffs and occasional calcareous phyllite and limestone layers. Some massive sulphide layers, comprising mainly chalcopyrite and pyrrhotite, occur within chlorite schists near

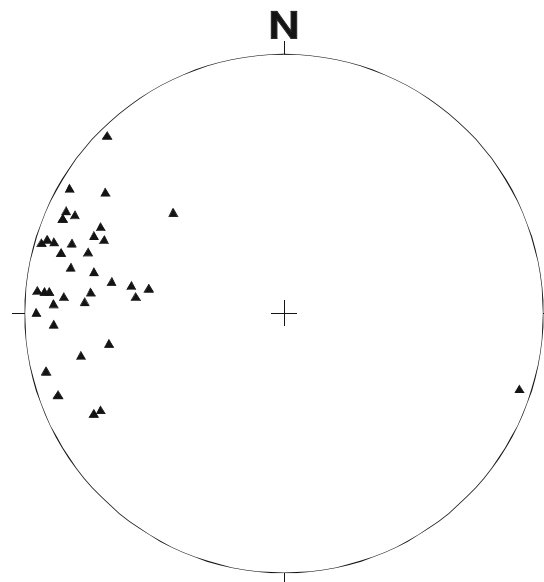


Figure 5. Stereoplot of "late" crenulation lineations, Adams Plateau.

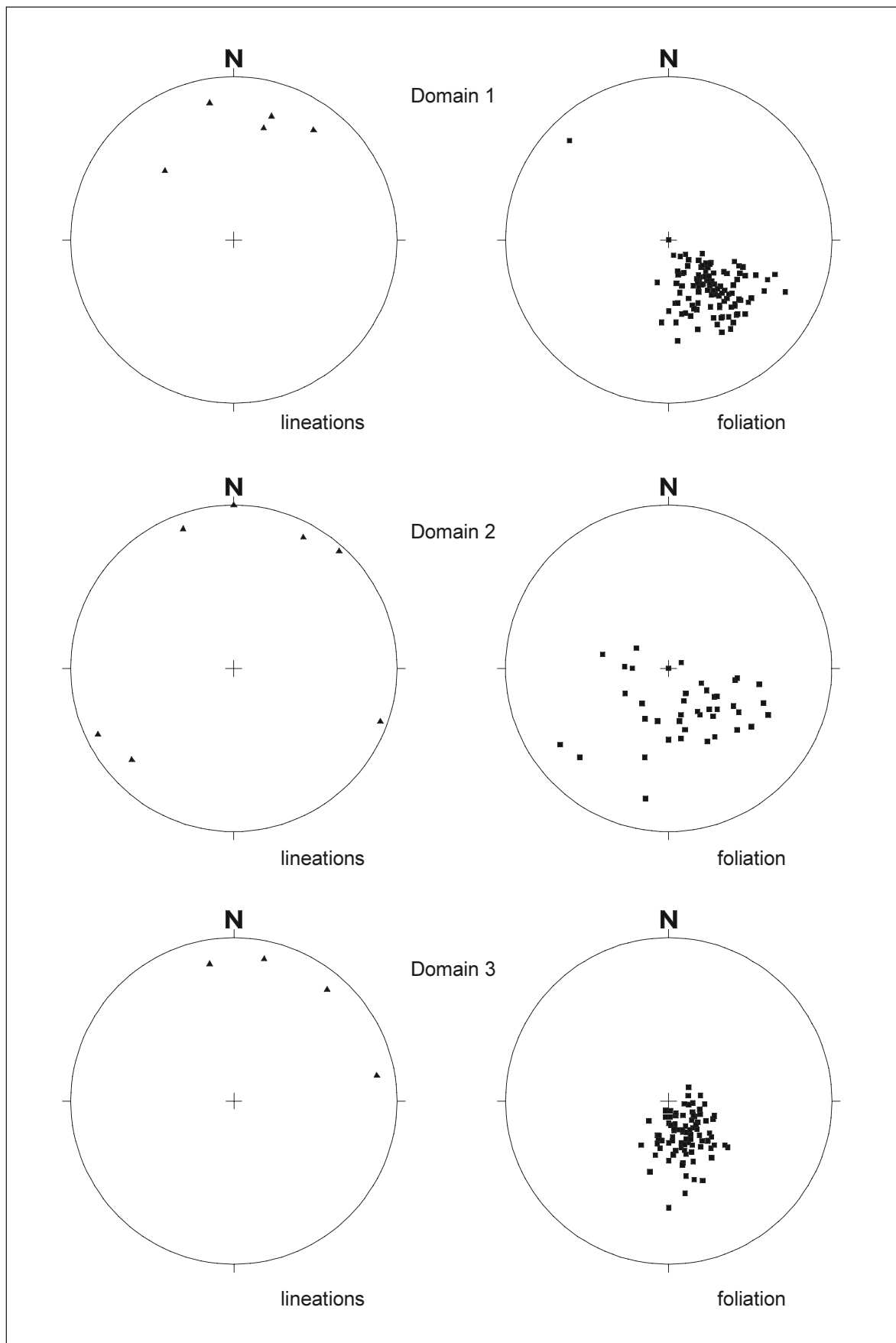


Figure 4a. Structural domains on the Adams Plateau, and stereoplots of Phase 2 foliation planes and mineral lineations (see next page).

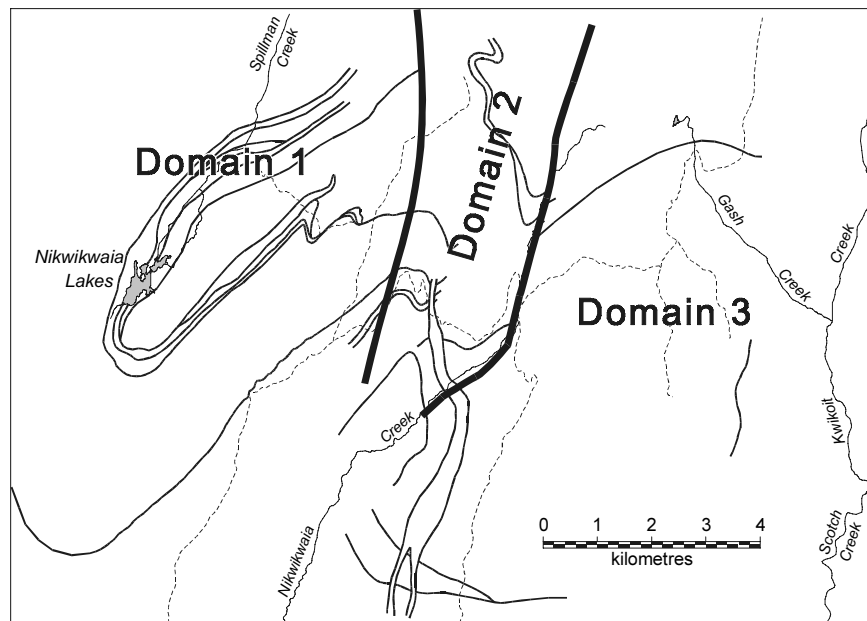


Figure 4. Structural domains on the Adams Plateau, and stereoplots of Phase 2 foliation planes and mineral lineations (see previous page).

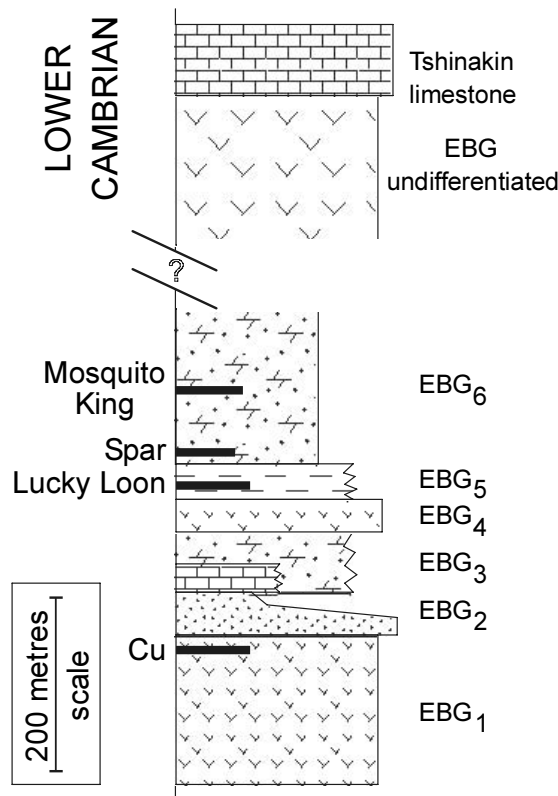


Figure 6. Stratigraphic succession of the Eagle Bay assemblage, Unit EBG, Adams Plateau.

the top of EBG1 (Figure 6).

North of these exposures of EBG1 is a thick limestone unit that has been correlated with the Lower Cambrian Tshinakin limestone exposed in the Vavenby area farther north (Schiarizza and Preto, 1987). An overturned antiform has been postulated to occur within Unit EBG1 (see Figure 4 and 5 of Schiarizza and Preto, *op. cit.*) thereby placing the Tshinakin limestone stratigraphically above the Adams Plateau succession. However, it is possible that the succession north of the Nikwikwaia synform is homoclinal and rocks hosting the stratabound mineralization on Adams Plateau is younger than the Tshinakin.

Major and trace element analyses of Unit EBG1 are given in Table 2 and plotted in Figure 7. Although these trace element data are assumed to be relatively immobile, the scatter in data may indicate some mobility during either regional metamorphism or hydrothermal activity related to mineralizing events. On a Zr/TiO₂ vs Nb/Y plot (Figure 7A), EBG1 metavolcanics plot mainly as sub-alkaline to alkaline basalts. Low vanadium/titanium ratios (Figure 7B) suggest ocean floor affinities, rather than arc basalts. Similarly, on a Ti-Zr-Y and Nb-Zr-Y plots (Figure 7C,D), these samples plot mainly as within plate, alkaline to tholeiitic basalts,

Table 2. Analyses of metavolcanic rocks of Unit EBG1, Eagle Bay assemblage, Adams Plateau.

Element	SiO2	TiO2	Al2O3	Fe2O3	MnO	MgO	CaO	Na2O	K2O	P2O5	Ba*	LOI TOTAL	Zr	Nb	Sr	Y	V	Cr2O3	
Units	%	%	%	%	%	%	%	%	%	%	%	%	ppm	ppm	ppm	ppm	ppm	%	
Method	XRF1	XRF1	XRF1	XRF1	XRF1	XRF1	XRF1	XRF1	XRF1	XRF1	XRF1	FUS	XRF2	XRF2	XRF2	XRF2	XRF2	XRF2	
Lab.	COM	COM	COM	COM	COM	COM	COM	COM	COM	COM	COM	COM	COM	COM	COM	COM	COM	COM	
Field No.																			
53769 AP98-26	45.97	1.85	16.47	13.6	0.2	7.96	8.56	3.05	0.4	0.21	0.01	1.64	99.92	120	18	470	25	287	0
53770 AP98-31	79.94	0.6	9.06	3.7	0.05	1.11	0.41	1.85	1.23	0.05	0.03	1.87	99.9	199	12	58	17	74	0.02
53771 Std. SY4	50.09	0.28	20.14	6.17	0.09	0.51	7.96	7.03	1.55	0.1	0.03	5.15	99.1	446	19	1135	113	8	0
53772 AP98-32	46	0.56	10.85	4.9	0.31	1.79	14.31	0.51	7.26	0.07	0.07	12.36	98.99	172	9	447	14	86	0
53773 AP98-36	36.77	0.18	3.54	26.71	0.85	1.84	25.87	0.03	0.25	0.15	0	2.53	98.72	38	5	35	9	118	0.01
53774 AP98-62	46.16	1.25	13.02	12.67	0.31	9.77	10.9	1.83	0.6	0.18	0.02	3.04	99.75	107	6	578	18	206	0.05
53775 AP98-90A	42.81	0.8	11.75	8.31	0.14	3.99	13.64	0.99	1.9	0.15	0.03	13.03	97.54	146	19	441	20	152	0.02
53776 AP98-95	45.68	2.44	16.53	12.52	0.14	7.5	3.51	4.28	0	0.25	0	6.86	99.71	123	16	152	20	243	0.03
53777 AP98-133B	48.86	2.65	14.82	13.21	0.12	4.65	8.43	3.75	0.81	0.56	0.01	2	99.87	146	33	841	25	201	0
53778 AP98-190	43	1.76	16.64	14.14	0.11	10.43	2.8	2.53	0.58	0.21	0.03	7.61	99.84	117	10	100	25	348	0.05
53779 AP98-250	49.84	1.03	15.52	14.14	0.43	4.25	6.76	2.35	0.07	0.25	0	5.09	99.73	91	5	512	26	324	0
53780 AP98-269	43.38	3.33	16.92	15.67	0.21	5.13	4.59	4.78	0.61	0.5	0.01	4.42	99.55	281	24	97	39	171	0

NOTES

Steel mill grinding @ Cominco

XRF1 = Fused Disc - X-ray fluorescence

Ba* = Fused disc analysis for XRF calibration. Values should be used with CAUTION.

XRF2 = Pressed pellet -XRF

COM = Cominco

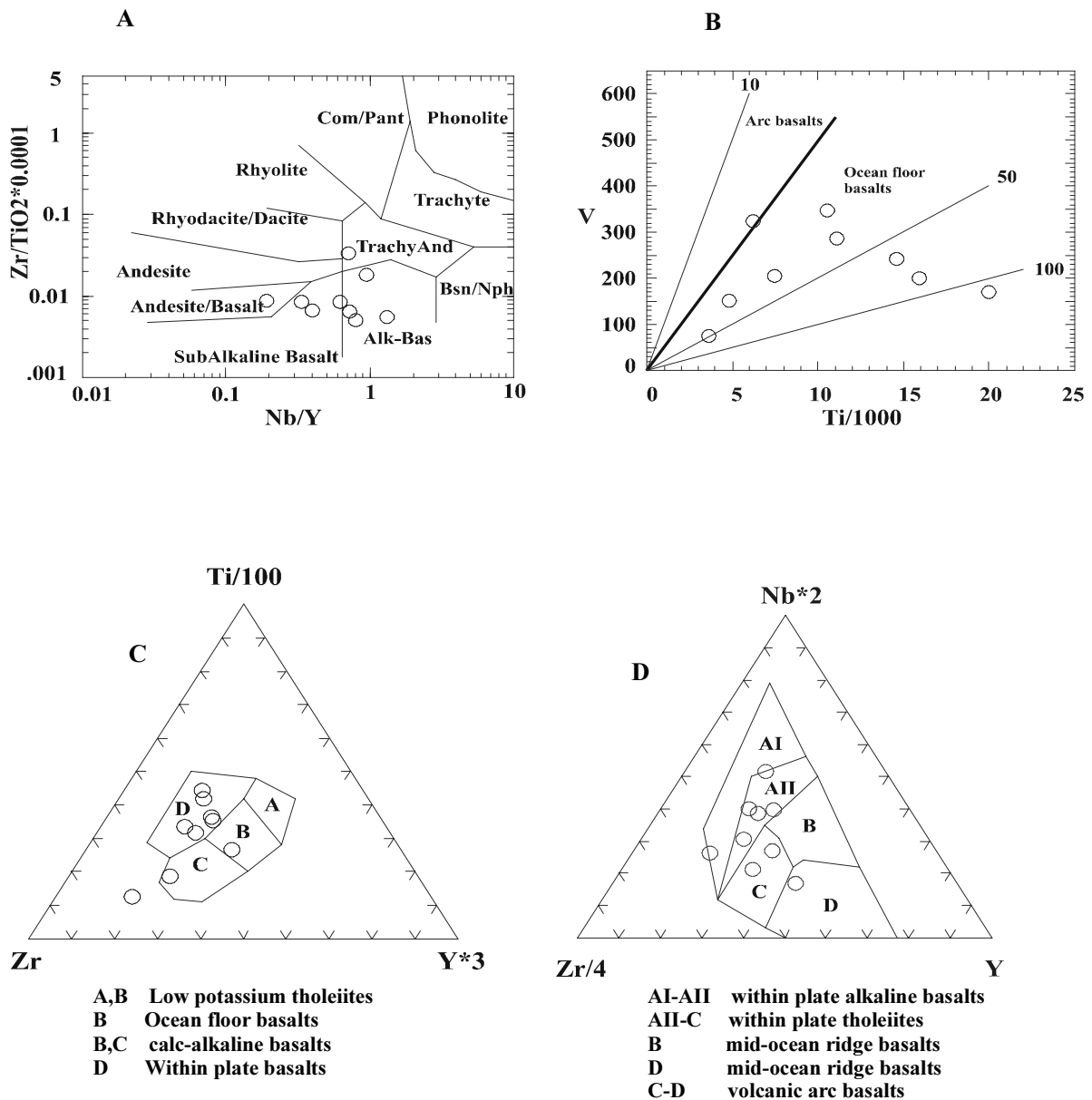


Figure 7. Plots of trace element data from metabolcanic rocks of Unit EBG1, Adams Plateau. A: after Winchester and Floyd (1977). B: after Shervais (1982). C: after Pearce and Cann (1973). D: after Meschede (1986).

recording extensional tectonics within the Kootenay Terrane in latest Proterozoic to Early Cambrian time.

A prominent white to pale grey quartzite marker unit, EBG2, overlies the greenstones of EBG1. It is a marker unit that outlines the limbs and closure of the Nikwikaia synform. It has a variable thickness, from a maximum of 250-300 metres immediately northwest of Nikwikaia Lake, to several tens of metres farther northeast on the north limb of the synform and a similar thickness on the south limb. Farther east, on both limbs, the quartzite apparently pinches out, and carbonaceous

and calcareous metasediments of EBG6 appear to directly overlie greenstones. This rapid thinning of the quartzite may be in part structural, but as it is associated with clearly defined facies changes in overlying units north of the Lucky Coon showing, and as the thickest succession does not occur in the hinge zone of the Nikwikaia synform, it is inferred to be mainly a stratigraphic thinning.

Unit EBG2 comprises white, pure to muscovite-rich quartzite, minor quartz-rich muscovite schist, and rare thin interlaminae of dark carbonaceous phyllite. It is typically foliated or has schistose textures due to variable muscovite

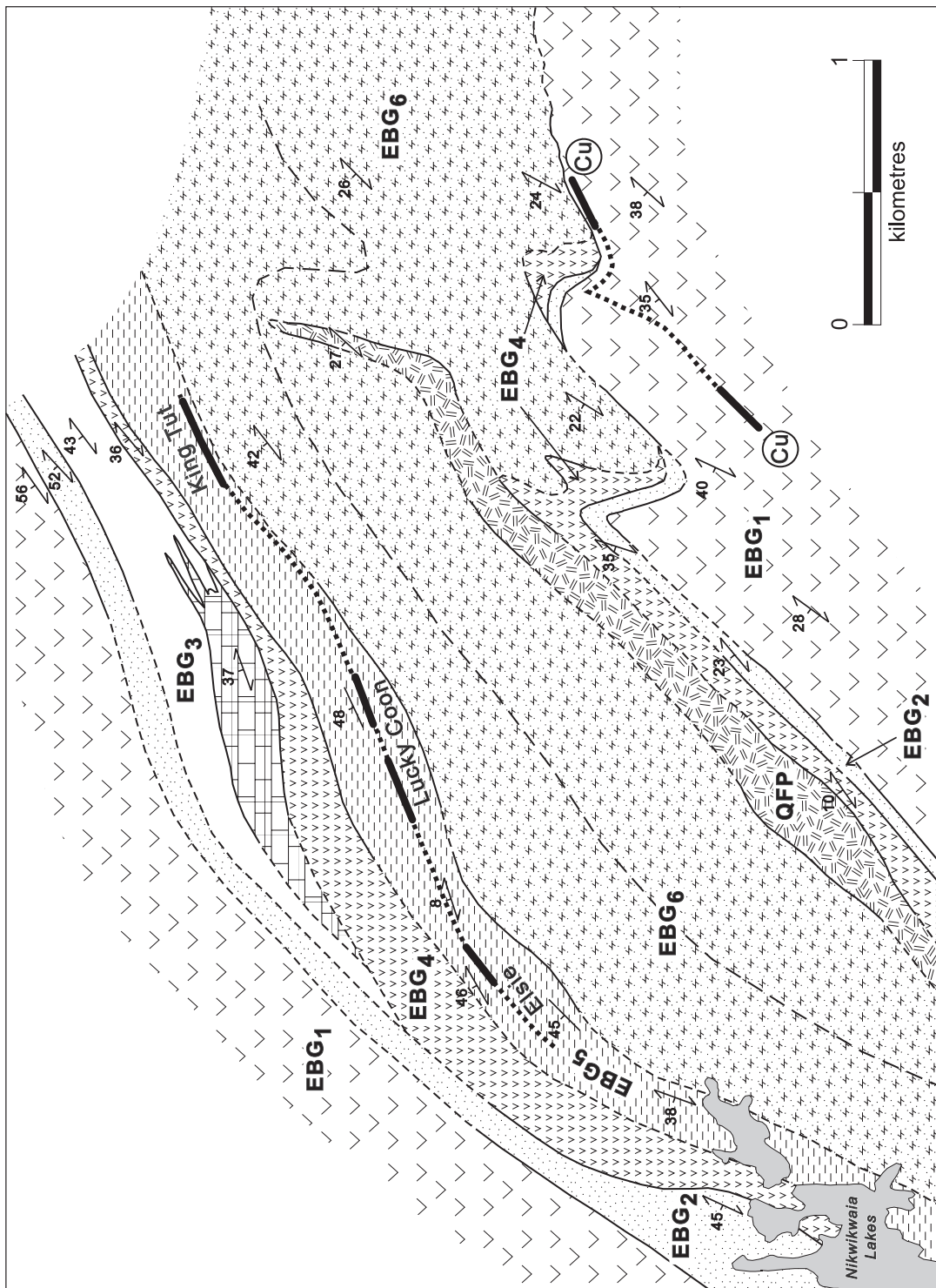


Figure 8. Geological map of the Lucky Coon, King Tut and Elsie deposit area, (legend; see Figure 3)

content. Intrafolial folds are common throughout, as are thin cross-cutting quartz-muscovite veins. The quartzite commonly forms small resistant white to grey outcrops. It has a sharp contact with underlying greenstone; in the south limb of the Nikwikwaia synform it appears to be in sharp contact with overlying chlorite phyllite, whereas in the north limb, the quartzite grades up into sericite schists of Unit EBG3.

EBG3, exposed only north of the King Tut showing, is characterized by rapid thickness and facies changes. Southwestern exposures comprise carbonaceous and sericite phyllite, overlain by several tens of metres of relatively pure grey limestone (Figure 8). To the northeast, EBG3 comprises a heterogeneous assemblage of carbonaceous, sericitic and chloritic phyllite, thin impure quartzite layers, "granular" quartz-feldspar phyllites and impure carbonates. The overlying limestone grades to the northeast into a succession of phyllites with thin interbeds of limestone and dolomite. These rapid facies changes, schematically illustrated in Figure 12, are suggestive of growth faults with deeper water, more basinal facies exposed in the northeast. Chloritic and feldspathic sericite-chlorite schists may record mafic to intermediate tuffaceous volcanism that followed deposition of the mafic volcanics of EBG1.

Chloritic schists of Unit EBG4 directly overlie either EBG3 or EBG2 in the core of the Nikwikwaia synform. The schists are thickest immediately north of Lucky Coon, thinning from several tens of metres to a few metres to the northeast (Figure 8). Only a few thin exposures were found south of Nikwikwaia Lake and to the east on the south limb of the synform where they occur immediately above the quartzite of EBG2. The chloritic schist was not recognized east of the north-trending faults, due either to lack of exposure or stratigraphic thinning. Unit EBG4 is similar to the greenstones of EBG1, comprising mainly chlorite schist or phyllite. Contorted layering is common within the schists. A few thin grey limestone layers occur within the thick section north of Lucky Coon. Unit EBG4 is interpreted to be a mafic tuff unit.

The succession hosting mineralization at the Lucky Coon, King Tut and Elsie deposits overlies EBG4. It comprises mainly sericitic or calcareous phyllite with common interlayers of chlorite or carbonaceous phyllite, and minor

limestone and granular quartz-feldspar phyllite interbeds. It contrasts with the immediately overlying units which are dominated by dark, carbonaceous phyllite and limestone. Sulphide host rocks are potassic and silica-altered producing sericite schists and thin bedded "quartzitic" units. Disseminated sulphides are locally common in Unit EBG5, resulting in rusty-weathering exposures; some of these have been extensively trenched in the vicinity of the folds in the south limb of the synform. Farther east, in areas of higher metamorphic grade, calcareous units within EBG5 have become a relatively massive diopside skarn.

A large part of the area underlying Adams Plateau comprises a mixture of carbonaceous and calcareous phyllite of Unit EBG6. It forms the core of the Nikwikwaia synform and appears to be the host to mineralization at the Mosquito King and Spar deposits. It has a variable lithology, but appears to comprise mainly carbonaceous phyllite with numerous thin interbeds of grey limestone at its base, the dominant lithology of western exposures, and grades up in more eastern exposures, to mixed carbonaceous and calcareous phyllites with occasional limestone, calcsilicate or chlorite phyllite layers. At higher metamorphic grades, grey to pale green diopside skarn layers and impure calcite marbles are common. Disseminated sulphides associated with silicification are common throughout the unit, but particularly in the dark carbonaceous layers, producing very rusty-weathering interbeds. The internal stratigraphy of EBG6 is not known, and it is possible that there is considerable infolding and repetition of layers within it. The sulphide layers occur at a number of structural levels, but their exact stratigraphic positions are not known due to the internal complexity of this unit. EBG6 appears to record deposition of dark calcareous muds and thin limestones with only very minor mafic tuffaceous volcanism.

Unit EBA

Unit EBA, a succession of mainly chlorite and sericite phyllites and schists derived mainly from felsic to intermediate volcanic rocks, hosts the VMS deposits northwest of Adams Lake. On Adams Plateau, rocks correlated with EBA occur in the south part of the map area (Figure

3). Only the basal part of the succession has been examined and it comprises mainly well foliated, locally rusty-weathering, orthogneiss.

Exposures of EBA are common along the logging access road southwest of the Spar deposit. They are dominated by grey to tan weathering, foliated quartz-feldspar porphyry, and quartz-feldspar schists and granitic orthogneisses. Aphanitic phases are less common. Hornblende and biotite are common throughout, and epidote alteration occurs near a few pyrite and chalcopyrite veins.

The contact with Unit EBG1 appears to be intrusive, rather than structural, as a number of layers of chloritic phyllite, similar to EBG1, occur in the basal part of EBA. As well, angular to subrounded xenoliths of chloritic phyllite of EBG1 occur in more massive phases of the orthogneiss, and occasionally foliated dykes, similar to EBA, cut EBG1 along its contact with the orthogneiss. U-Pb dates of metavolcanics of EBA, from exposures on the southwest slopes of the plateau (plotted on Figure 3), indicate a Middle Devonian age (Preto, 1981; Preto and Schiarizza, 1985).

Discussion and regional correlations

The exposed Eagle Bay stratigraphy on Adams Plateau comprises a succession of mafic volcanic rocks overlain by a relatively thin succession of metasedimentary rocks. These are intruded by granites that have been correlated with the Late (?) Devonian orthogneisses of Unit EBA.

The metasedimentary rocks of EBG include a basal quartzite overlain by dominantly carbonaceous and calcareous phyllites. Thickness and facies changes within the basal part of this metasedimentary succession are concentrated in the vicinity of stratabound lead-zinc mineralization in the Lucky Coon deposit area. These changes include rapid thinning of the quartzite (EBG2) and overlying mafic metavolcanics (EBG4), and associated thickening of the intervening metasedimentary schists of EBG3, as has been schematically shown in Figure 12. A change from grey limestone to interlayered phyllite and limestone within EBG3 accompanies these changes in stratigraphic thickness. These abrupt stratigraphic changes are characteristic of growth faulting that may have provided mineralizing conduits for overlying mineralization.

The age of the metasedimentary succession is not known. However, on the north slopes of Adams Plateau it is within a greenstone package that contains a thick limestone unit that has been correlated with the Early Cambrian Tshinakin limestone (Schiarizza and Preto, 1987). These authors suggested that an antiform occurs within the greenstones north of the map-area, thereby repeating the succession and placing EBG beneath the limestone.

The stratigraphic succession of the Eagle Bay assemblage and correlations with the Hamill, Lardeau and Milford Groups in the Kootenay arc, and with the Snowshoe succession in the Barkerville subterrane are shown in Figure 9. EBH and EBQ, comprising mainly quartzitic units, are correlated with the Late Proterozoic to Early Cambrian Hamill and Gog North American miogeoclinal rocks. Mafic volcanic rocks of EBG contain the Lower Cambrian Tshinakin limestone, as well as the metasedimentary succession that hosts massive sulphides on Adams Plateau (Schiarizza and Preto, *op. cit.*). As these are interpreted to be stratigraphically lower than the Tshinakin, they may correlate with the Mohican Formation, a succession of interbedded calcareous schists, pelites, limestones and quartzites at the top of the Hamill Group. Metavolcanic rocks of EBG are within plate, ocean floor basalts, similar to those that occur within the upper part of the Hamill Group (J. Logan, personal communication, 1998). Correlation of the Mosquito King - Lucky Coon succession with the Mohican Formation (or top of Hamill Group) indicates that these deposits are older than the massive sulphide deposits in the Goldstream camp (Höy, 1979; Höy *et al.*, 1984), hosted by Lower Paleozoic metavolcanics of the Index Formation (Logan and Colpron, 1995), or the stratabound sulphide deposits such as Ace (Höy and Ferri, 1998) in the basal part of the Snowshoe Group in the Barkerville subterrane (Struik, 1988).

EBS, EBL and EBK are mainly metasedimentary rocks that are inferred to stratigraphically overlie EBG and underlie Late Devonian rocks of EBA (Schiarizza and Preto, 1987). Their stratigraphic position and similar lithologies allow correlation with the Lardeau Group (Figure 9). A mafic volcanic unit within EBS may correlate with Index Formation volcanics. EBL, comprising limestone and calcareous phyllite, "is identical to the Sicamous Formation in

the Vernon map area” (Schiarizza and Preto, op. cit., p.23), and is apparently continuous with these exposures (Jones, 1959).

EBM, dominated by mafic metavolcanic rocks (Schiarizza and Preto, op.cit.), may correlate with similar basaltic rocks of the Jowett Formation in the Lardeau Group. It is inferred to be in stratigraphic contact with EBS and may be overlain unconformably by Devonian-Mississippian rocks of EBA, EBF and EBP (Figure 9).

Unit EBA, host to many of the volcanogenic massive sulphide deposits, is a succession of dominantly felsic to intermediate volcanic rocks that have been dated as Middle Devonian (Schiarizza and Preto, 1987). Gritty and fragmental rocks of EBF, derived in large part from intermediate tuffs and volcanic breccias, overlie EBA. Rea is a polymetallic volcanogenic massive sulphide deposit within dominantly mafic and minor felsic tuffs of EBF. Unit EBP, a succession of slates, phyllites and siltstone, with lesser sandstone, conglomerate and carbonates with Early and Middle Mississippian conodonts, is the youngest unit of the Eagle Bay assemblage. The contact of these Devonian to Mississippian rocks with underlying Lardeau correlative rocks may be unconformable, as a variety of different units of the Eagle Bay assemblage, including locally EBQ, underlie EBA (Schiarizza and Preto, 1987).

Unit EBP at the top of the Devonian-

Mississippian package may correlate, in part, with rocks of the Milford Group that unconformably overlies the Lardeau Group in the Kootenay arc (Figure 9). Similarities include their age and stratigraphic position, as well as some lithologic and metallogenic similarities; most notable of these are the occurrences of conglomeratic units in both, including quartz pebble conglomerates, and the recognition of felsic volcanics in both. Thin felsic tuffaceous units occur in Milford Group (?) rocks at Kootenay Lake, and some of these contain small polymetallic massive sulphide deposits such as True Blue and Copper Cliff (BC Minfile numbers 82F/SW002 and 82K/SW079). This correlation suggests that an unconformity may separate EBP from underlying units of the Eagle Bay.

MINERAL DEPOSITS

Three main deposit types are recognized on Adams Plateau: stratabound lead-zinc-silver deposits in metasedimentary rocks, stratabound copper occurrences in mafic volcanics and a variety of small vein occurrences. The lead-zinc deposits, including Mosquito King, Spar, King Tut, Lucky Coon and Elsie, have received considerable exploration activity while only limited work has been done on other occurrences. The following descriptions of these deposits are based on company reports, BC MINFILE descriptions as well as field visits and mapping

AGE	EAGLE BAY	KOOTENAY ARC	BARKERVILLE
Paleozoic	Permian		
	Mississippian	EBP	Snowshoe <i>Ramos</i>
	Pennsylvanian	EBF	
	Devonian	EBA	
	Silurian	EBM	Lardeau
Ordovician	EBS	<i>Jowett</i>	
Cambrian	EBQ <i>Tshinakin</i>	<i>Index</i> <i>Badshot</i>	
Proterozoic	EBH/EBQ	Hamill <i>Mohican</i> Horsethief Creek	

Figure 9. Regional correlation of rocks of the Eagle Bay assemblage with those in Kootenay Terrane rocks to the east, and Barkerville subterranean rocks to the north (after Schiarizza and Preto, 1987 with data from Struik, 1988; Höy and Ferri, 1998, and J. Logan, personal communication, 1998).

this past summer. Vein deposits, mainly lead-zinc-silver or copper-rich occurrences, are not described.

Mosquito King (082M 016)

Introduction

Mosquito King comprises a number of layers of stratabound Pb-Zn mineralization in a calcisilicate succession of Unit EBG6 of the Eagle Bay assemblage (Figures 3, 6). It is readily accessible via approximately 30 kilometres of logging access roads that leave the Scotch Creek road at Shuswap Lake park. The area is relatively flat and, as elsewhere on the plateau, exposures are largely limited to roads and trenches.

Recorded exploration on Adams Plateau dates back to 1927 with the discovery of the Spar deposit. Although records are scarce, considerable past work has been done in the Mosquito King area, including trenching, sampling, geological mapping, geophysical surveys and limited drilling. Orell Copper Mines Ltd., now Killick Gold Company Ltd., has held the

ground since the mid 1970's; in 1976 and 1977 it was optioned to Craigmont Mines Ltd. who drilled a series of short drill holes to test down dip extensions of known sulphide occurrences and geophysical anomalies (Vollo, 1977; 1978). Test ore shipments were sent to the Trail smelter in 1972 and 1980, with recovery of 22,721 kg lead, 18,328 kg zinc, 232 kg of silver and 281 grams of gold from 212 tonnes of ore (1972).

Noranda Exploration Company Ltd. optioned the claims in 1984, and conducted an airborne geophysical survey by Dighem Ltd., followed by considerable mapping, trenching and soil sampling. More recently, Minnova Ltd. drilled a northeast extension of the Mineral King, the Gash prospect. Reserves at the Mosquito King, based on drilling by Killick Gold Company in 1981, are summarized in Table 1.

Geology

Mosquito King is within a succession of calcareous and phyllitic rocks that trend approximately east-west and dip variably to the north. This succession includes mainly dark carbona-

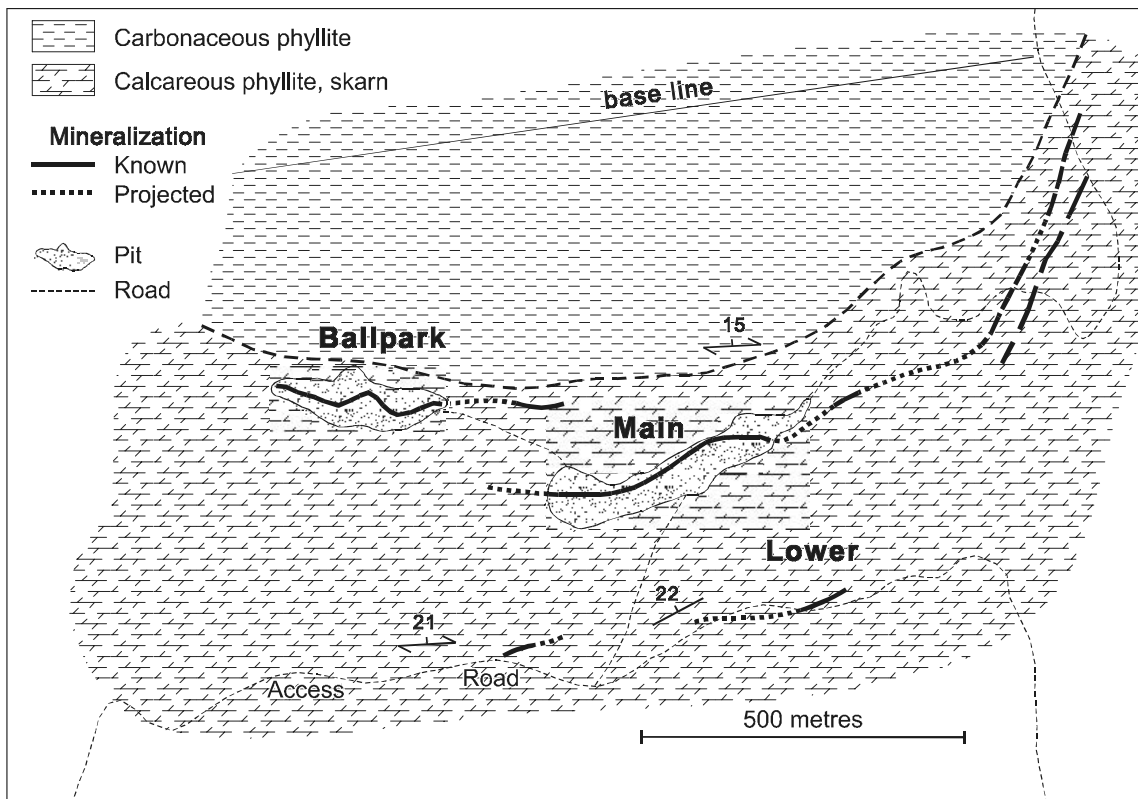


Figure 10. Geological map of the Mosquito King deposit area.

ceous phyllite, calcareous phyllite, thin impure grey limestone layers, and calcsilicate gneiss layers. It is not known if there are structural repetitions in the deposit area; where noted, bedding is essentially parallel with schistosity, and minor folds are generally late, affecting both bedding and the earlier foliation. However, the sulphide layers are interpreted to be separate and discrete layers, rather than fold repetitions, as associated thin limestone layers are not repeated.

At least three sulphide layers are recognized (Figure 10). A Lower zone is exposed in two trenched areas approximately 500 metres apart. It comprises banded, fine-grained galena and sphalerite with minor pyrrhotite in layers up to 30 centimetres in thickness hosted in interlayered diopside-rich calcsilicate gneiss, diopside-amphibole gneisses and thin marble layers. The total thickness of the mineralized calcsilicate layers is less than two metres. They are underlain by a grey calcite marble and overlain by calcsilicate gneisses and thin marble. Assays of two samples of the Lower zone, AP98-139 and AP98-385, are given in Table 3.

The Main showing consists of two thin sul-

phide layers, separated by calcsilicate gneiss and a prominent grey marble layer. The showings have been trenched along a strike length of approximately 300 metres, and are projected northeastward towards the Gap showings. The Ballpark showing occurs 400 metres west of the Main Mosquito King showing. The Mosquito King layers are separated from the structurally underlying Lower zone by several tens of metres of calcsilicate gneiss, dark carbonaceous and calcareous phyllite and thin limestone layers. They are overlain by less calcareous, dark carbonaceous phyllites. Immediate host rocks contain considerable disseminated pyrrhotite, producing very rusted outcrops.

A detailed section through the upper mineralized layer of the Main showing is illustrated in Figure 11. Layers vary from essentially massive, fine grained sphalerite, galena, pyrrhotite and minor chalcopyrite and magnetite (unit E), to semi-massive sulphides with variable diopside and quartz gangue (units A,B and C), to calcsilicate layers with dispersed to irregularly laminated sulphides (Unit D). Lead content in these layers varies from less than one to 4.5 per cent, zinc, to greater than 10 per cent, and silver to 34 grams/tonne

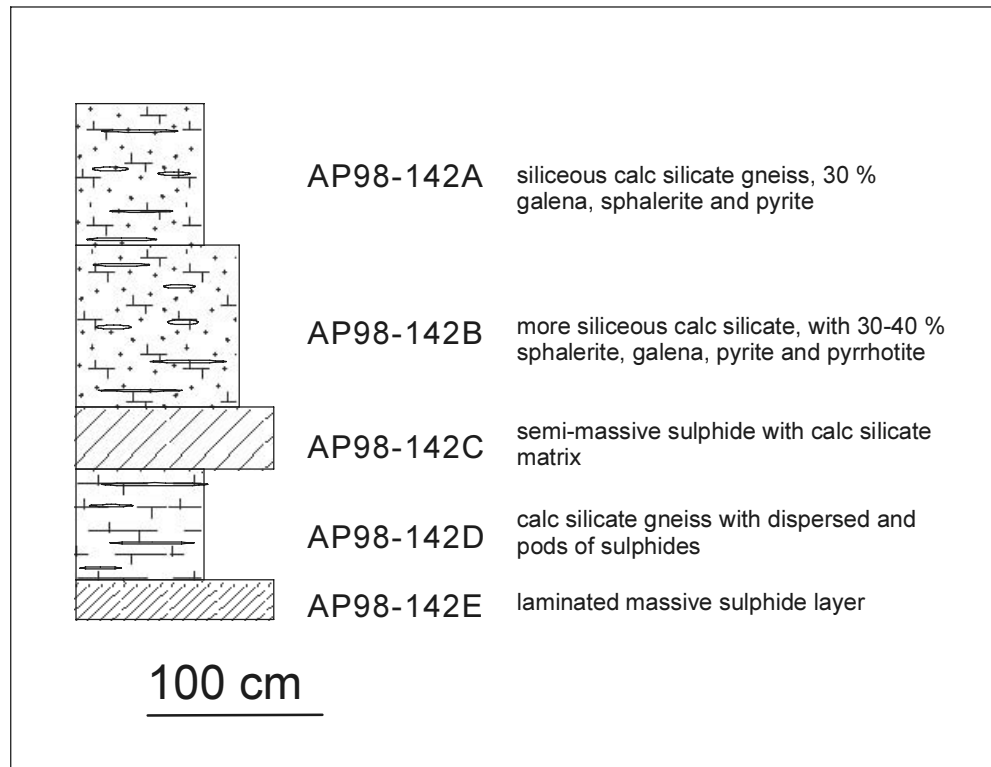


Figure 11. A detailed section through the Main sulphide layer, Mosquito King deposit; assays of sample numbers are given in Table 3.

Table 3. Analyses of selected hand samples of deposits and mineral occurrences on Adams Plateau. See next page.

Field No.	UTM E	UTM N	Mo	Cu	Pb	Zn	Ag	Ni	Co	Mn	Fe	As	Sr	Cd	Sb	Bi	V	P	La	Cr	Ba	Ti	W	Zr	Sn	Y	Sc	Au**			
	ppm	ppm	ppm	ppm	ppm	ppm	ppm	ppm	ppm	ppm	%	ppm	ppm	ppm	ppm	ppm	ppm	%	ppm	ppm	ppm	%	ppm	ppm	ppm	ppm	ppm	ppm	ppb		
King Tut																															
AP98-333	318274	5661860	< 2	179	34013	99999	497.1	30	15	23600	17.48	634	22	563.8	560	49	15	0.01	9	223	31	0.01	6	13	8	4	2	316			
AP98-334A	318432	5662119	< 2	172	41102	78667	593.6	17	7	53116	18.75	284	27	290.9	581	37	4	< 0.02	4	86	6	< 0.1	< 4	13	12	6	< 1	521			
AP98-334B	318493	5662023	< 2	248	31887	31868	101.8	30	< 2	79798	27.42	24	10	101.8	86	28	7	< 0.02	6	29	7	0.01	< 4	18	< 2	9	1	152			
AP98-334C	318493	5662023	2	180	44448	67011	127.9	14	14	332	6.38	2091	15	212.9	151	< 5	14	0.008	3	21	134	0.01	< 4	8	2	< 2	1	195			
Lucky Coon																															
AP98-88A	317377	5661379	< 2	1897	1722	9427	21.1	48	6	54392	27.74	< 5	52	31.4	< 5	< 5	20	0.039	10	30	26	0.04	< 4	24	2	8	5	62			
AP98-88B	317377	5661379	4	238	4320	50054	23.1	18	6	2065	17.87	4074	11	172.4	676	< 5	15	0.008	10	76	59	0.04	< 4	8	4	3	2	1692			
AP98-88C	317377	5661379	4	143	48121	68904	600.7	27	16	13232	13.13	1103	16	316.2	842	< 5	38	0.021	6	120	40	0.13	< 4	11	15	3	3	1387			
AP98-88E	317377	5661379	3	81	44107	99999	477.9	19	8	30180	11.96	710	101	494.4	381	29	18	0.011	4	210	9	0.03	4	9	11	4	3	1007			
AP98-150	322319	5658944	4	626	283	270	1	187	161	1054	12.93	15	481	1.2	< 5	< 5	63	0.047	15	49	46	0.3	< 4	19	2	24	10	6			
AP98-160	324658	5659526	< 2	398	4113	683	7.8	87	61	16492	23.93	9069	328	5.1	122	< 5	59	0.036	28	35	53	0.28	6	52	< 2	33	8	217			
AP98-198	322373	5658317	4	1467	35930	99999	28.6	26	39	17465	22.8	214	38	495.9	32	53	16	0.018	7	267	5	0.05	5	10	< 2	4	2	188			
AP98-200A	322441	5658512	< 2	137	608	588	2.3	20	69	42631	21.18	491	431	0.6	< 5	< 5	36	0.017	19	19	9	0.11	< 4	15	< 2	32	4	1132			
AP98-200C	322441	5658512	< 2	127	4638	23870	5.7	30	18	35367	13.54	22	202	87	< 5	< 5	48	0.025	17	52	154	0.23	9	16	3	19	5	73			
AP98-200E	322441	5658512	< 2	52	9833	31802	12.6	16	5	87411	20.69	13	243	130.4	7	< 5	24	0.024	18	54	17	0.13	6	28	2	16	3	186			
AP98-202	322617	5658950	3	269	8726	99999	26.8	13	29	25990	5.97	520	423	416.4	45	10	3	0.002	13	164	14	0.01	< 4	4	3	35	3	974			
AP98-203	322401	5658138	3	2194	25526	93772	440.5	112	49	1225	28.02	1761	4	351.5	482	303	< 2	< 0.02	< 2	173	4	< 0.1	< 4	< 2	< 2	< 1	772				
AP98-220	315917	5660773	3	228	26187	99999	60.5	23	13	38199	17.73	114	12	1295.9	48	< 5	30	0.01	5	900	97	0.05	< 4	9	< 2	3	2	39			
Mosquito King																															
AP98-139	323929	5657833	2	514	35060	99999	34.1	15	21	5655	14.45	370	117	1174.2	41	15	14	0.012	3	720	71	0.05	< 4	3	4	9	3	198			
AP98-142A	324167	5658078	3	196	41186	1313	24	24	6	1558	4.72	107	121	7.2	50	< 5	37	0.018	30	32	176	0.11	< 4	5	2	11	5	81			
AP98-142B	324167	5658078	3	580	9649	12175	11	49	24	1522	16.59	20	93	42.8	14	< 5	57	0.029	11	45	60	0.1	8	7	3	8	7	126			
AP98-142C	324167	5658078	3	749	16611	19286	19	30	9	2376	7.33	35	524	71.8	21	< 5	81	0.044	42	61	160	0.25	< 4	12	2	19	11	108			
AP98-142D	324167	5658078	3	177	3203	4418	10.5	28	8	5144	7.23	279	256	16.3	26	< 5	84	0.04	29	63	71	0.34	6	37	3	22	10	231			
AP98-142E	324167	5658078	3	2089	44659	44835	54.6	97	31	3433	24.92	97	158	193.5	49	26	23	0.015	13	81	156	0.07	9	3	4	12	3	80			
AP98-146A	322608	5657880	4	74	43305	99999	397.1	7	13	934	4.54	129	70	1128.7	436	12	29	0.022	15	99	175	0.17	< 4	8	11	8	4	425			
AP98-166	324798	5658596	4	387	41385	43503	109.4	60	114	2418	13.1	303	135	177.2	53	117	40	0.027	15	99	175	0.17	< 4	4	10	8	4	25			
AP98-167	324741	5658522	3	1793	320	7337	2.9	36	67	8703	20.75	93	31	26.9	5	< 5	15	0.005	3	25	4	0.06	6	5	3	4	2	54			
AP98-167A	324741	5658522	3	1408	45105	57156	104.5	80	172	11969	24.04	968	111	257.7	77	96	15	0.006	9	117	76	0.06	< 4	4	10	8	2	879			
AP98-168	324741	5658522	4	297	9285	99999	18.5	99	167	1688	16.14	1082	196	492.2	18	44	60	0.027	28	211	83	0.13	4	13	4	7	5	717			
AP98-169	324656	5658343	4	1334	2475	15795	20.7	81	113	1925	17.58	211	79	75.4	14	45	27	0.013	3	35	98	0.08	< 4	3	2	2	3	83			
AP98-208A	323745	5658188	< 2	3702	26747	855	140	95	53	5575	44.67	263	47	5.3	40	204	9	0.002	2	14	27	0.03	< 4	3	< 2	5	1	424			
AP98-208B	323745	5658188	< 2	840	802	494	4.2	73	38	3565	28.75	947	45	< 4	10	< 5	22	0.004	6	19	82	0.05	< 4	4	< 2	2	2	429			
AP98-209	323745	5658188	< 2	1985	6378	9734	28	162	61	6752	23.8	15	35	42.1	< 5	31	56	0.023	27	34	39	0.12	< 4	11	6	5	5	54			
AP98-211	323745	5658188	2	695	23649	24114	84.2	66	24	1804	16.02	98	55	11.8	49	99	65	0.027	19	30	190	0.07	< 4	14	13	4	6	414			
AP98-212	323745	5658188	3	448	5284	99999	< 5	9	< 2	2107	34.32	64	3	357.7	11	< 5	2	< 0.02	11	193	8	< 0.1	< 4	< 2	6	< 1	550				
AP98-385	324384	5657903	< 2	91	38138	84745	164.6	23	6	16666	13.14	< 5	435	405.3	154	11	54	0.032	20	102	8	0.23	52	16	2	18	7	197			
Spar																															
AP98-235	321731	5659417	2	1731	24699	26866	42.5	41	53	2287	20.23	70	71	122	43	20	48	0.023	9	51	107	0.16	19	14	5	6	4	111			
AP98-235A	321731	5659417	2	1708	25555	38338	155.6	47	16	2170	25.07	95	46	156.1	55	239	36	0.014	14	71	102	0.06	6	8	6	6	4	84			
AP98-235B	321731	5659417	2	1790	25420	99999	283.2	26	28	4926	17.7	182	26	533	261	45	6	0.002	4	461	22	0.02	< 4	2	5	3	< 1	177			
AP98-236	321725	5659420	2	853	22814	39894	485.2	57	29	502	12.04	1075	7	151.9	572	< 5	10	0.004	6	36	30	0.04	< 4	2	10	< 2	1	856			
AP98-237	321660	5659610	3	261	356	683	2	76	41	10692	14.29	12	438	3.2	< 5	< 5	76	0.065	28	35	123	0.22	< 4	27	< 2	25	7	8			

All elements but Au by TIGP = HClO4-HNO3-HCl-HF digestion - inductively coupled plasma emission spectroscopy; Au by flameless AAS; A.C.M.E. Analytical

Table 3. Analyses of selected hand samples of deposits and mineral occurrences on Adams Plateau.

Field No.	UTM E	UTM N	Mo	Cu	Pb	Zn	Ag	Ni	Co	Mn	Fe	As	Sr	Cd	Sb	Bi	V	P	La	Cr	Ba	Ti	W	Zr	Sn	Y	Sc	Au**			
			ppm	ppm	ppm	ppm	ppm	ppm	ppm	ppm	%	ppm	ppm	ppm	ppm	ppm	ppm	%	ppm	ppm	ppm	%	ppm	ppm	ppm	ppm	ppm	ppm	ppb		
Miscellaneous occurrences																															
AP98-8	321703	5656281	2	45	26	60	< 5	40	15	1634	3.54	< 5	385	0.4	< 5	< 5	102	0.055	41	70	592	0.31	< 4	31	2	23	13	3			
AP98-14A	322058	5658377	< 2	150	43	127	0.5	87	45	2801	8.77	6	806	0.7	< 5	< 5	112	0.113	31	81	127	0.53	12	43	3	32	14	3			
AP98-37	321113	5660434	2	41	66	69	1.6	30	12	871	3.43	12	492	< 4	< 5	< 5	64	0.022	26	33	489	0.19	11	12	< 2	18	7	2			
AP98-38	321113	5660434	< 2	91	55	204	1.6	24	14	2583	5.34	12	996	1.2	6	< 5	63	0.037	20	41	260	0.19	9	14	< 2	18	7	3			
AP98-46	320327	5660228	< 2	7277	13	65	3.1	104	181	3067	30.36	< 5	134	0.5	< 5	< 5	26	0.027	10	20	7	0.18	42	11	30	14	3	22			
AP98-46A	320327	5660228	< 2	4831	19	59	2	123	276	2564	33.55	< 5	141	1.5	< 5	< 5	27	0.037	12	22	7	0.19	44	11	26	15	3	13			
AP98-63	619184	5659606	4	377	16	17974	1.2	17	51	4188	12.78	< 5	457	137.8	< 5	8	210	0.074	10	114	52	0.92	< 4	27	< 2	24	20	5			
AP98-67	319620	5661177	5	199	6	79	1.6	27	19	982	6.38	8	329	0.7	7	< 5	186	0.313	36	17	439	2.01	8	21	11	39	17	< 2			
AP98-133A	323184	5658037	4	76	713	417	3.6	26	31	1155	9.13	37	948	1.6	12	< 5	205	0.26	30	21	92	1.61	< 4	19	< 2	32	15	3			
AP98-307	320082	5655156	5	604	165	175	3.2	54	232	2757	17.5	32	33	< 4	7	16	45	0.098	150	49	75	0.12	< 4	12	4	11	3	81			
AP98-365A	318433	5659803	2	9878	547	4893	10	30	79	3012	14.27	6	266	19.4	< 5	28	94	0.062	20	108	81	0.61	< 4	14	9	17	10	111			
AP98-365B	318433	5659803	< 2	12336	689	2486	10.4	91	239	2257	22.91	< 5	237	8.6	< 5	40	49	0.041	14	30	28	0.3	< 4	12	5	14	6	96			
AP98-408	326137	5661783	2	2111	20272	11015	30.1	139	125	766	32.71	< 5	39	40.6	< 5	65	10	< .002	3	15	28	0.02	< 4	2	< 2	2	< 1	152			

(samples AP98-142a,b,c,d,e; Table 3). Gold content varies from approximately 80 to 230 ppb. AP98-212, a more pyritic sample in a small trench farther west and on strike with the Main showing contains 550 ppb gold. The sulphide succession of the Main showing is within a pale greyish-green sericitic and siliceous rich calcsilicate unit, that may reflect both potassic and siliceous alteration. Footwall rocks comprise dark green, diopside-rich calcsilicate gneiss with approximately 10 per cent disseminated pyrrhotite.

The Ballpark showing is a very heavily rusted and extensively trenched area west of the Main showing. It is structurally higher, and may represent a separate sulphide layer. However, mineralization is similar to the Main showing, comprising massive to poorly banded pyrrhotite with sphalerite and galena, and minor pyrite and chalcopyrite, within a siliceous calcsilicate host. The footwall consists of fine-grained granular quartz with minor dispersed pyrrhotite, and the hangingwall, a thin silicified zone overlain by siliceous sericite phyllite. Analyses of samples from the Ballpark sulphide layer (samples AP98-208a,b) are given in Table 3, and indicate locally high silver (140 ppm) and gold (>400 ppb) contents. Copper (0.37 per cent) is also high in one of the samples. Samples AP98-209 and 211 (Table 3) are just east, on strike with the Ballpark sulphide layer.

In summary, Mosquito King comprises a number of thin, laterally extensive massive pyrrhotite-sphalerite layers, with locally high precious metal content, in a highly deformed and metamorphosed calcsilicate gneiss succession. Potassic and siliceous alteration are reflected in silicified sericitic zones in the immediate hangingwall and footwall.

Spar (082M 017)

Introduction

The Spar massive sulphide deposit is located near the headwaters of the east branch of Nikwikaia Creek (Figure 3). Access is via 29 kilometres of logging roads that leave Shuswap Lake at Shuswap Lake park.

Spar, discovered in 1927, was the first deposit located on the plateau. Due to lack of exposure in the area, as well as elsewhere on the plateau, most subsequent exploration has

involved geochemical and geophysical surveys, followed by trenching and limited drilling. In the 1960's, Giant Metallics mapped the area and undertook some trenching and drilling. The property was acquired in 1974 by the present owners, Killick Gold Company Ltd. (formerly Orell Copper Mines Ltd.). It was optioned to Craigmont Mines Ltd. in 1977 and 1978, Brinex Limited in 1980, and Noranda Exploration in 1984 and 1985. The Noranda exploration program consisted primarily of following-up airborne geophysical anomalies through geological mapping, soil geochemistry, geophysical ground surveys, trenching, considerable sampling, and some drilling (Shevchenko and Bradish, 1986). Minnova optioned the property in 1991, conducted an IP and magnetometer survey and drilled three holes, totaling 350 metres. Drill indicated reserves at the Main showing are 12,300 tonnes containing 4.83 per cent zinc, 10.56 per cent lead, and 206 grams/tonne silver.

Geology

The Spar deposit is a massive lead-zinc-silver layer near the base of Unit EBG6 of the Eagle Bay assemblage. Unit EBG6 in the vicinity of the deposit comprises dominantly calcsilicate schists, calcsilicate gneiss and thin marble layers in the footwall and dark carbonaceous phyllites, with interlayered calcareous schists in the hangingwall. This succession is believed to be stratigraphically lower than rocks that host Mosquito King.

The Spar massive sulphide layer trends northeast and dips 30 to 40 degrees to the northwest. The layer can be traced and extrapolated from the Main adit showing approximately 600 metres to the north where it is folded into an open, north plunging antiform whose east limb is truncated by a north-trending fault (Figure 3). Late, open minor folds, common in the immediate deposit area, verge to the east, supporting this antiformal closure. An exposure of a massive sulphide layer, 300 metres west of the Main showing, may be a fold repetition or a second sulphide layer.

The thickness of the sulphide layer is highly variable, due mainly to structural attenuation or thickening. In 1976 Hesca Resources Ltd. drilled 8 short vertical holes within a radius of 35 metres of the Main adit to determine the extent and thickness of the mineralized zones (Gutrath, 1978). DDH76-1 intersected 5 metres of massive

sulphides that assayed 18.9 per cent lead, 8.5 per cent zinc, 0.23 per cent copper, 380 g/tonne silver and 0.79 g/tonne gold. A hole drilled to the south, to intersect the "southwest plunge" of the mineralization, intersected a considerably thinner intercept, and holes to the north, along strike, did not intersect "mineralization of economic interest". It is critical to recognize the controlling structures in these deposits; the west-plunging Phase 3 structures do not appreciably thicken mineralized layers, whereas the less obvious Phase 2 structures typically control the distribution and plunge of massive sulphide zones.

Spar comprises crudely banded sulphides with siliceous and calcareous interbeds. Exposed mineralization at the Main showing comprises approximately 2 metres of coarse grained galena, with finer grained sphalerite and pyrrhotite in a granular quartzitic matrix, overlain by a variable but generally thin pyritic layer, and 2 metres of sphalerite with galena, pyrite and pyrrhotite. Chalcopyrite and trace arsenopyrite are also observed in the massive sulphide layers.

Assays of samples of the Spar sulphide layers are given in Table 3. A sample of the lower layer (AP98-235A) contains 2.5 per cent Pb, 3.8 per cent Zn and 155 ppm Ag whereas the more zinc-rich upper sulphide layer contained 2.5 per cent Pb, greater than 10 per cent Zn, 283 ppm Ag and 177 ppb Au. Copper content, 0.17 per cent, is similar in all samples. AP98-236, a sample from a thin sulphide layer in the immediate hangingwall, contained lead and zinc values similar to the main sulphide layers, but higher arsenic (1075 ppm), gold (856 ppb) and silver (485 ppm) content.

The hangingwall of the sulphide layers includes very rusty-weathering, hornfelsed argillite, dark limestone, minor granular, siliceous or chloritic phyllite and crudely layered calcsilicate gneiss. Pyrrhotite occurs throughout these units, either finely disseminated or forming discontinuous lamellae. The main alteration minerals are quartz, pyrrhotite and minor sericite.

Lucky Coon (082M 012), Elsie (082M 213) and King Tut (082M 013)

A layer of massive sulphides has been traced discontinuously for approximately 2.5 kilometres along the north limb of the Nikwikwaia synform. The southwest end of the sulphide layer is referred to as the Elsie deposit, the central part

where most exploration has been focused, the Lucky Coon, and its northeastern extension, King Tut. The Elsie and Lucky Coon deposits are accessible by a four-wheel drive road that crosses the ridge southeast of the deposit or by a logging road northwest of Gilfrid Lake that was opened this past September. The access road to the King Tut is largely overgrown. Sulphide exposures are restricted to numerous trenches and open cuts; however, cliffs on the slopes of Spillman Creek just to the north expose considerable outcrops of structural hangingwall rocks.

Recorded exploration on these properties was first described in 1927, and considerable trenching and minor drilling by the Granby Consolidated Mining, Smelting and Power Company undertaken in 1928 and 1930. In 1977, two pits were mined and 1360 tons of mineralization shipped to the Trail smelter (Spencer, 1985). In 1981, Adams Silver Resources undertook a program of mapping, soil geochemistry and diamond drilling to test the near-surface extension of the Lucky Coon mineralization, and in 1987, Esso Minerals Ltd. mapped approximately 1125 hectares at a 1:5,000 scale, relogged drill core and did some additional soil geochemistry (Holbek and Thiersch, 1987).

Geology

The Lucky Coon, King Tut and Elsie deposits are parts of a massive sulphide layer that has been traced or extrapolated more than 2500 metres along the north limb of the Nikwikwaia synform (Figure 8). The sulphide layer is generally thin, with typical widths ranging up to 30 centimetres; a maximum thickness of 2.8 metres is reported in a 1981 drill hole just below the main pit of the Lucky Coon (Tough, 1981; reported in Holbek and Thiersch, 1987). In detail, the sulphides can occur at several intervals, separated by thin phyllitic or calcareous units; these probably represent separate layers, similar to the Mosquito King and Spar occurrences, rather than structural repetitions. The sulphide layer is within a heterogeneous succession of thin bedded carbonaceous, calcareous and sericitic phyllites, chloritic schist, grey limestone and granular phyllite of Unit EBG5. It occurs stratigraphically lower than the sulphide layers of Mosquito King and Spar.

Lucky Coon is the central and largest sulphide zone in the area. A number of open pits and extensive trenching have exposed the mineralized layer for a strike distance of several hundred metres.

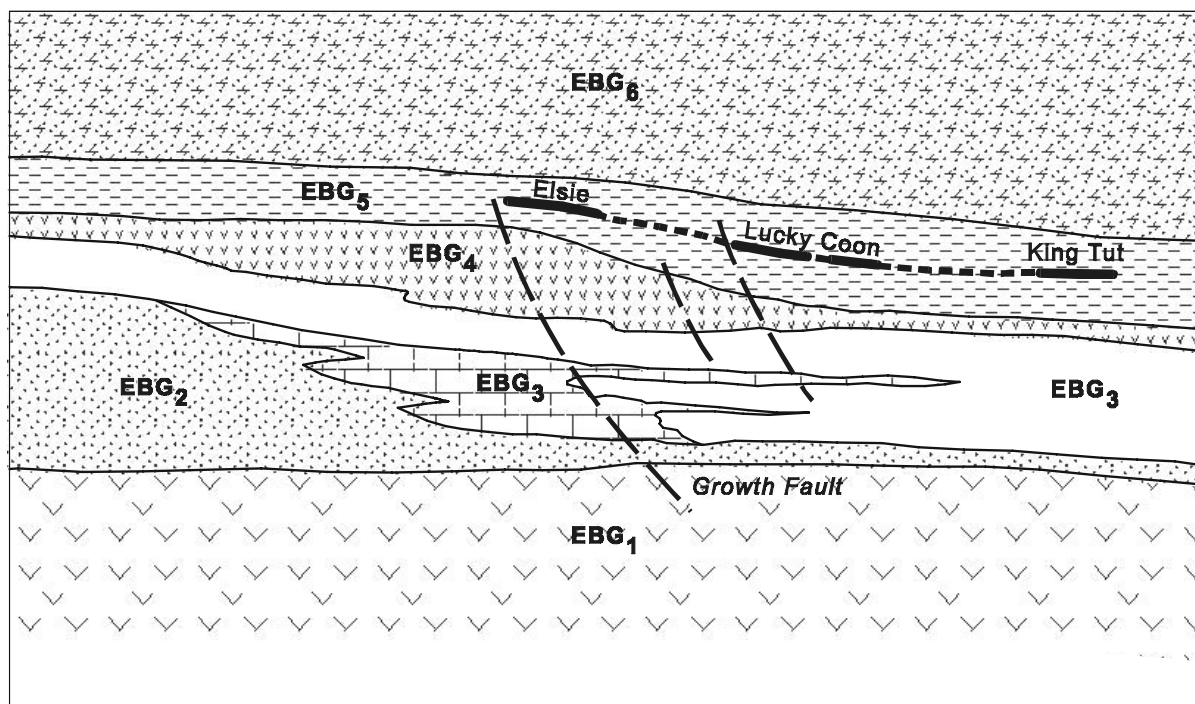


Figure 12. Schematic diagram showing facies and thickness variations in Eagle Bay rocks in the vicinity of the Lucky Coon, King Tut and Elsie occurrences; (legend, see Figure 3)

The massive sulphide layer comprises banded pyrite, sphalerite, galena, minor arsenopyrite, and trace argentite, tetrahedrite and chalcopyrite in a quartz \pm carbonate gangue. Its mineralogy is described in some detail by Hedley (1936). Pyrite and arsenopyrite are commonly euhedral, suggesting post-strain recrystallization, sphalerite and galena are typically closely intergrown, and argentite occurs only within galena. The high precious metal content of Lucky Coon is shown in analyses of selected hand samples in Table 3, with one sample containing greater than 600 ppm Ag and another, approximately 1.7 ppm Au.

Sulphides are usually enclosed in an alteration envelope of sericite, silica, minor carbonate and disseminated pyrite. The most common, persistent and widespread alteration is a tan to pale grey sericite in phyllite in both the hangingwall and footwall of the Lucky Coon. Silicification is closely associated with the sulphides, occurring as gangue, fine laminae and thin quartz veinlets within the sulphides and in both the hangingwall and footwall. Carbonate alteration, recognized by the typical brown weathering of iron-rich dolomite, is also closely associated with sulphides. It forms small spots or foliation parallel laminae, best developed in more chloritic units, and thin dolomitic beds in the immediate footwall. These beds may be dolomitized limestone units, as limestones are recognized along strike.

Elsie has been explored by a short underground adit. Although it is difficult to trace sulphides between these two deposits, they are at approximately similar stratigraphic levels. Samples in the dump comprise mainly pyrite with minor dispersed galena and sphalerite in a granular sericite-quartz matrix.

Exposures at King Tut are within a trench that trends 075 degrees, parallel to the strike of the sulphide layer. Sulphides comprise massive to banded galena, sphalerite and pyrite, with minor pyrrhotite in a granular to gneissic quartz, siderite, sericite and minor chlorite gangue. Analyses of selected hand samples (Table 3) returned approximately 10 per cent combined Pb+Zn and high silver content. Footwall rocks are commonly siliceous and sericitic schists with minor disseminated pyrite, whereas hangingwall rocks are dark carbonaceous phyllites.

The sulphide layer and Unit EBG5 are underlain by units that are characterized by prominent facies and thickness changes as are

schematically illustrated in Figure 12. EBG2, an impure quartzite succession, thickens considerably immediately south of the Elsie occurrence. EBG3 is characterized by rapid facies and thickness changes that are concentrated immediately below Lucky Coon mineralization. The most prominent of these is a change from thick-bedded, grey limestone near the base of the unit to thinly interbedded limestones and phyllites to the northeast (Figure 8). As well, chloritic schists of the overlying Unit EBG4 are also thicker in the immediate deposit area. These changes are indicative of growth faulting that may have controlled the discharge of basinal fluids leading to deposition of massive sulphide mineralization.

AP98-408 (082M 268 - new)

A small trench at the northeast end of the map area has exposed a massive pyrrhotite layer with minor chalcopyrite, sphalerite and galena. The sulphide layer has an exposed thickness of 80 centimetres and a length of a few metres. It is within a very rusted, siliceous calcsilicate gneiss. Based on its base and precious metal content, and location relative to the projected eastern extension of EBG1, it may be at approximately the same stratigraphic level as the Lucky Coon sulphide layer. A high pyrrhotite content, relative to pyrite, may reflect higher metamorphic grade.

STRATABOUND COPPER OCCURRENCES

A number of small showings of copper mineralization, including veins and massive sulphides, occur in metavolcanic rocks of EBG1 (Figure 8). The massive sulphide occurrences typically comprise pyrrhotite and chalcopyrite, with variable silver and gold content.

AXL 1 (082M 068)

This occurrence is within a trenched and cleared area several tens of metres in diameter. Bedrock is not exposed, but numerous large rusted boulders indicate a bedrock source. Host rocks are chloritic phyllites of Unit EBG1.

Boulders comprise very rusted, pyrrhotite rich chloritic phyllite as well as semi-massive sulphides. The sulphides are dominated by pyrrhotite rich layers with variable but generally

minor chalcopyrite and sphalerite. Sulphides are highly foliated, with a chlorite, quartz and minor sericite gangue.

Analyses of the two samples of the massive sulphides (AD98-365A,B; Table 3) yielded 0.1 and 1.2 per cent Cu, 0.5 and 0.2 per cent Zn, and low lead content.

AP98-46 (082M 269 - new)

A small pod of very rusty-weathering massive sulphides is exposed within amphibolite of Unit EBG1 several kilometres northeast of AXL 1. The sulphide exposure is several metres in length and up to a metre in thickness. It comprises mainly pyrrhotite and chalcopyrite, with subrounded granular quartz eyes, in a dark green chlorite-amphibole-quartz matrix. Sulphides are typically banded, commonly swirled and cut by late, thin chalcopyrite veinlets. Small euhedral pyrite grains may overgrow the massive sulphides.

Assays of two samples of the massive sulphide layer returned 0.48 and 0.23 per cent copper, with low lead and zinc content and only trace silver and gold (Table 3)

SUMMARY AND DISCUSSION

The Adams plateau is underlain mainly by highly deformed metasedimentary and metavolcanic rocks of Unit EBG of the Eagle Bay assemblage. The age of these are not known, but based mainly on the lithochemistry of the mafic volcanic rocks, and their stratigraphic position relative to the Tshinakin limestone, as established elsewhere in the Adams Lake-Vavenby area (Schiarizza and Preto, 1987), they are correlated with the Late Proterozoic to Early Cambrian Hamill Group or Mohican Formation.

EBG comprises massive to foliated greenstones and chloritic phyllites, derived from mafic volcanic rocks, overlain by a metasedimentary succession of phyllites, thin limestone layers, chloritic, calcareous and carbonaceous schists, and, at the base, a prominent marker quartzite unit. These are intruded by a variety of felsic plutonic rocks, including a Late (?) Devonian orthogneiss, Late Cretaceous granitic rocks, and a number of Tertiary quartz porphyry dykes.

The structure of Adams Plateau is dominated by a tight, north plunging syncline, the Nikwikwaia synform that closes in the western

part of the area. Its axial plane, defined by synmetamorphic fabrics, trends approximately east-west and dips north, shallowing to almost horizontal in the east. The limbs and axial plane of the synform are folded into a number of broad, upright north-trending folds. These folds and associated north-trending faults postdate the metamorphic fabric but are cut by the Late Cretaceous intrusions.

Three main deposit types were examined on the plateau: stratiform massive lead-zinc sulphide layers, stratabound massive copper-pyrrhotite lenses, and a variety of veins. The copper occurrences are generally small, comprising massive pyrrhotite and chalcopyrite in mafic metavolcanic rocks of Unit EBG. Most veins appear to be located near the north trending faults; they include a number of small lead-zinc-copper-silver occurrences and a small massive fluorite occurrence.

Most exploration and development has been directed towards the massive lead-zinc layers, including the Mosquito King, Spar, Lucky Coon, Elsie and King Tut. These comprise mainly layered galena, sphalerite, and pyrrhotite or pyrite within a calcsilicate gneiss or schist host. They occur at a number of horizons, within a stratigraphic interval of probably less than a few hundred metres. In all deposits, immediate host rocks are silicified and sericitized, reflecting potassic and silica alteration; locally (Lucky Coon) dolomitization of host limestone layers is important. More western deposits are characterized by higher lead/zinc ratios and higher silver contents. More eastern deposits are in rocks of higher metamorphic grade, and contain mainly pyrrhotite rather than pyrite.

Prominent facies and thickness changes in rocks stratigraphically underlying the Lucky Coon, King Tut and Elsie deposits indicate that growth faulting may have controlled the location of these deposits. These faults may have been the conduit for the discharge of hydrothermal fluids that led to the formation of massive sulphide deposits in overlying rocks. These deposits may be related to a period of regional extension, marked by rifting, volcanism and submergence, along the North American continental margin in EoCambrian time. Other deposits associated with this extension include sedex deposits such as Cottonbelt and Big Ledge in high grade metamorphic rocks of the

Monashee Complex farther east.

ACKNOWLEDGEMENTS

I would like to thank Paul Schiarizza, Jim Logan and Dave Lefebure and for their critical review of this paper. Discussions with Kevin Kane and the late Cecil Kane are much appreciated. M. Fournier is thanked for drafting most of the diagrams, R. Lett for expediting and preparing samples for geochemical analyses, and A. Yeow for her help in the field.

REFERENCES

- Church, B.N. (1999): Metallogeny of the Beaton-Camborne mining camp, Lardeau District; *in Geological Fieldwork 1998, B.C. Ministry of Energy and Mines*, Paper 1999-1, this volume.
- Fyles, J.T. and Eastwood, G.P.E. (1962): Geology of the Ferguson area, Lardeau District, British Columbia; *B.C. Ministry of Energy, Mines, and Petroleum Resources*, Bulletin 45, 162 pages
- Gutrath, G. (1978): Diamond drill logs on the Spar Group 1, Adams Plateau, Kamloops Mining Division; *B.C. Ministry of Energy, Mines and Petroleum Resources*, Assessment Report 6645.
- Hedley, M.S. (1936): Adams Plateau area; *in Annual Report of the Minister of Mines, B.C. Department of Mines*, pages D39-D43.
- Holbek, P. and Thiersch, P. (1987): Report on the Adams Plateau, Kamloops Mining Division; *B.C. Ministry of Energy, Mines and Petroleum Resources*, Assessment Report 16024.
- Höy, T. (1979): Geology of the Goldstream area; *B.C. Ministry of Energy, Mines and Petroleum Resources*, Bulletin 71, 49 pages.
- Höy, T. (1991): Volcanogenic massive sulphide deposits in British Columbia; *in Ore deposits, tectonics and metallogeny in the Canadian Cordillera; B.C. Ministry of Energy, Mines and Petroleum Resources*, Paper 1991-4, pages 89-123.
- Höy, T. and Ferri, F. (1998): Stratabound base metal deposits of the Barkerville subterranean, Central British Columbia (93A/NW); *in Geological Fieldwork 1997, B.C. Ministry of Employment and Investment*, Paper 1998-1.
- Höy, T., Gibson, G. and Berg, N.W. (1984): Copper-zinc deposits associated with basic volcanism, Goldstream area, British Columbia; *Economic Geology*, volume 79, pages 789-814.
- Höy, T. and Goutier, F. (1986): Rea Gold (Hilton) and Homestake volcanogenic sulphide-barite deposits, southeastern British Columbia; *in Geological Fieldwork 1985, B.C. Ministry of Energy, Mines and Petroleum Resources*, Paper 1986-1, pages 59-68.
- Jones, A.G. (1959): Vernon map-area, British Columbia; *Geological Survey of Canada*, Memoir 296, 186 pages.
- Lett, R.E., Jackaman, W. and Yeow, A. (1999): Detailed Geochemical Exploration techniques for base and precious metals in the Kootenay Terrane (NTS 82 L/13, 82M/4, 82M/5, 92P/1); *in Geological Fieldwork 1998, B.C. Ministry of Energy and Mines*, Paper 1999-1, this volume.
- Logan, J.M. and Colpron, M. (1995): Northern Selkirk project - geology of the Goldstream River map area (82M/9) and parts of 82M/10; *in Geological Fieldwork 1994, B.C. Ministry of Energy, Mines and Petroleum Resources*, Paper 1995-1, pages 215-242.
- Meschede, M. (1986): A method of discriminating between different types of mid-ocean ridge basalts and continental tholeiites with the Nb-Zr-Y diagram; *Chemical Geology*, volume 56, pages 207-218.
- Okulitch, A.V. (1979): Lithology, stratigraphy, structure and mineral occurrences of the Thompson-Shuswap-Okanagan Area, British Columbia; *Geological Survey of Canada*, Open File 637.
- Okulitch, A.V. (1985): Paleozoic plutonism in southeastern British Columbia; *Canadian Journal of Earth Sciences*, volume 22, pages 1409-1424.
- Paulen, R.C., Bobrowsky, P.T., Lett, R.E., Bichler, A.J. and Wingerter, C. (1999): Till geochemistry in the Kootenay, Slide Mountain and Quesnel Terranes; *in Geological Fieldwork 1998, B.C. Ministry of Energy and Mines*, this volume.
- Pearce, J.A. and Cann, J.R. (1973): Tectonic setting of basic volcanic rocks determined using trace element analysis; *Earth and Planetary Science Letters*, Volume 19, pages 290-300.
- Shevchenko, G. and Bradish, L. (1986): Assessment report, geochemical, geophysical and trenching survey on the Fox, Hiltec 1 & 2, Spar 1, MK 1, 2 & 3 and Bee 3, 4 & 5 claims, Kamloops Mining Division; *B.C. Ministry of Energy, Mines and Petroleum Resources*, Assessment Report 14,439.
- Schiarizza, P. and Preto, V.A. (1987): Geology of the Adams Plateau-Clearwater-Vavenby area; *B.C. Ministry of Energy, Mines and Petroleum Resources*, Paper 1987-1, this volume.

Resources, Paper 1987-2, 88 pages.

- Spencer, B.E. (1985): Report on a drill programme on the Adams Plateau property, Kamloops Mining Division; *B.C. Ministry of Energy, Mines and Petroleum Resources*, Assessment Report 13,542.
- Struik, L.C. (1986): Imbricated terranes of the Cariboo gold belt with correlations and implications for tectonics in Southeastern British Columbia; *Canadian Journal of Earth Sciences*, volume 23, pages 1047-1061.
- Struik, L.C. (1988): Structural geology of the Cariboo gold mining district, east-central British Columbia; *Geological Survey of Canada*, Memoir 421, 100 pages.
- Vollo, N.B. (1977): Diamond drilling report on the 82M/4 MK group of Craigmont Mines Limited on Adams Plateau; *B.C. Ministry of Energy, Mines and Petroleum Resources*, Assessment Report 6349.
- Vollo, N.B. (1978): Diamond drilling report on the 82M/4 MK group of Craigmont Mines Limited on Adams Plateau; *B.C. Ministry of Energy, Mines and Petroleum Resources*, Assessment Report 6788.
- Winchester, J.A. and Floyd, P.A. (1977): Geological discrimination of different magma series and their differentiation products using immobile elements; *Chemical Geology*, Volume 20, pages 325-342.



THE EFFECT OF COAL PREPARATION ON THE QUALITY OF CLEAN COAL AND COKE

By Barry Ryan (B.C. Geological Survey Branch), Ross Leeder (Industrial Leader - Canadian Carbonization Research Association and Teck) and John T. Price and John F. Gransden (CETC, CANMET Energy Technology Centre)

KEYWORDS: Plant circuits, maceral fractionation, coal quality, coal petrography, thermal rheology, coke quality, coke strength after reaction (CSR).

INTRODUCTION

Coal preparation plants are designed to control clean coal quality to meet contract quality specifications and normally focus on ash, sulphur, calorific value, size and moisture contents of the clean coal. The coking quality of clean metallurgical coal is evaluated, but generally only limited attempts are made to influence it by changing operating conditions in the plant.

Plants size the feed coal into different fractions, which are processed in individual circuits before being combined into the final clean coal. In western Canada, the coarsest (+0.6mm) coal is cleaned in combinations of heavy media vessels, drums and cyclones, while the finer coal (-0.6mm by 0.0mm) is cleaned using water-only-cyclones (WOC), spirals and/or froth flotation (FF) (Romaniuk, 1986). These processes are chosen to maximize the recovery of clean coal and for ease of control. Run-of-mine coal delivered to a plant is more complex than a mixture of three uniform materials (coal, rock and water). The coal is composed of a mixture of macerals and the rock a mixture of minerals with different chemical compositions. The type of association of the minerals and macerals, and the ability of each to be liberated by crushing, influences the size fraction and therefore the circuit into which they are concentrated. It is possible to adjust coal recovery from individual circuits to decrease ash content, and improve maceral composition and/or ash chemistry in the clean coal product. Whether this is economic depends in part on the characteristics of the run-of-mine coal and on the washing circuits available in the plant.

BACKGROUND

In the mid 1970's, the Canadian Carbonization Research Association (CCRA) undertook laboratory-scale coal washing (float/sink) tests of Canadian metallurgical coals to investigate changes in coal quality and petrographic and thermal rheological properties at varying ash concentrations for clean coal (Price and Gransden, 1987). It was found that as ash content decreased, the reactivities content of the coal increased and thermal rheological properties improved. However, it has been known for some time that using laboratory scale results to predict the coking quality of western Canadian coals is difficult (Gransden *et al.*, 1980). Four bulk samples of western Canadian coals were subsequently washed in a pilot plant and both the coal and coke quality determined for clean coals with varying ash contents (Gransden and Price, 1982). The results were similar to the earlier laboratory scale studies and there was a general improvement in coke quality. Generally finer sized coal produced from the pilot scale tests had higher reactivities content and better thermal rheological properties than coarser clean coal fractions, however, their relative influence on the coking quality of the coal was not investigated.

Following these two programs, the CCRA initiated the a detailed investigation of the performance of several coal preparation plants belonging to member companies. The objectives of the program were:

- ♦ to determine if it is technically possible to improve the coking characteristics of the over-all product coals;
- ♦ to determine if general trends occurred that would assist coal preparation engineers design or modify plant methods of operations to improve the clean coal coking characteristics.

This paper presents and discusses the results

of the CCRA study.

VARIATIONS IN COAL QUALITY AND ASH CHEMISTRY IN PLANT CIRCUITS

Maceral trends in wash plants

If all circuits in a plant recover all the coal, then the product coal will have the maceral composition of the run-of-mine coal but will be accompanied by less ash. However, if there is some coal loss, then it is possible to influence the maceral composition of the clean coal. Vitrinite is more friable than inert coal macerals and concentrates in the finer sizes. Therefore feed for coarse circuits is enriched in inert macerals compared to run-of-mine coal and feed to fine coal circuits is progressively enriched in vitrinite. Coarse circuits are generally not good at retaining vitrinite in clean coal. It appears that in these circuits some vitrinite is present in fine vitrain bands associated with in-seam splits. There is therefore a tendency for it to be lost in the rejects and the vitrinite content of the clean coal is less than that of the feed coal.

Vitrinite is less dense than the inert macerals, and once liberated in the feed coal, concentrates in the clean coal from the finer circuits, which use density separation. Bustin (1982) found that the maceral composition of washed coal varies based on the specific gravity (SG) of the split (Figure 1). The inert macerals tend to concentrate in the intermediate SG splits and the vitrinite in the lower SG splits. In detail there is a weak tendency in plants for vitrinite to concentrate in the clean 0.6 to 0.15 mm size fraction, and a stronger tendency for it to concentrate in the clean minus 0.15 mm material compared to the amount in the feed coal to these circuits (Table 1, Figure 2). In contrast the inert macerals concentrate in the clean coal from coarse circuits. It is therefore possible to influence the maceral composition of the clean coal by varying the cut points in the various circuits.

When documenting maceral trends, data can be presented as macerals in the total sample, which can be misleading because of varying ash content, or as maceral content as a percentage of the coal only part of the sample (mineral matter free basis). This second method is more representative of maceral changes in the various prod-

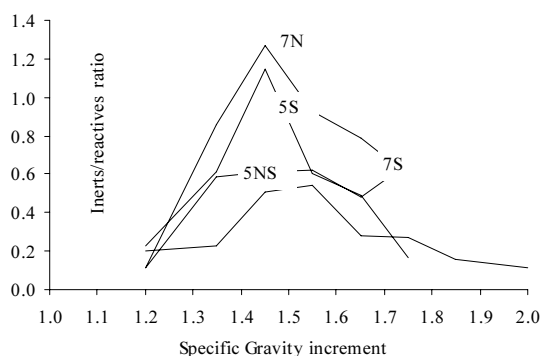


Figure 1. Variation of the reactivities/inerts ratio with specific gravity split for a number of Mist Mountain Formation coals. Numbers refer to specific seams (data from Bustin, 1982).

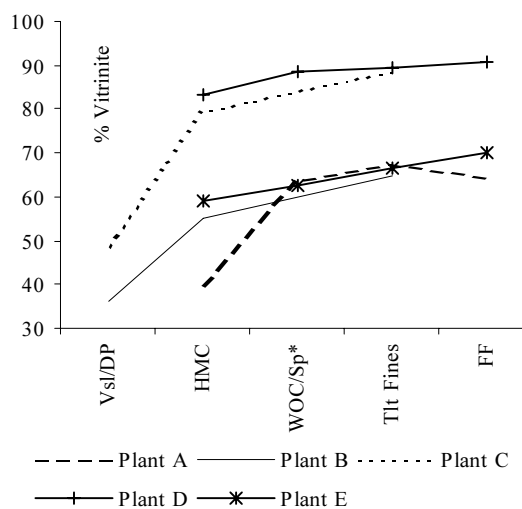


Figure 2. Variations in vitrinite content (total sample) in clean coal from the various circuits of the 5 plants studied, VsVDP=heavy medium vessels and drums, HMC=heavy medium cyclones, WOCSP=water only cyclones and spirals, Tlt Fines=total fines, FF=froth floatation.

ucts. Also it is possible to track vitrinite as the main reactive maceral or to track vitrinite plus reactive semifusinite as the total reactivities in the sample. The later method requires an assumption on how to divide the semifusinite into reactive and non-reactive components.

Controls on ash chemistry in wash plants

Coal wash plants cannot reduce the ash content of the clean coal to zero, there is therefore, always the possibility of improving the ash chemistry of the clean coal. Ash chemistry has

Table 1. Petrography and ash chemistry; Plant A.

<u>FEED COAL</u>				
Size mm	50x0.0	50x0.6	.6x0.15	0.15x0
percentage	100	66	18	16
	FEED	CLEAN	REJECT	
<u>HEAVY MEDIUM 50x0.6 mm</u>				
% Weight	100	68	32	
Ash%	29	10.5	68	
total reactives	68	65.5	70	
base/acid ratio	0.098	0.082	0.09	
Al ₂ O ₃ /SiO ₂	0.44	0.55	0.43	
S%	0.2	0.36	0.09	
coal rec%	-	90	-	
<u>WOC 0.6x0.15 mm</u>				
% Weight	100	69	31	
Ash%	18.7	8.3	41.5	
total reactives	79.5	79.6	73.3	
base/acid ratio	0.081	0.048	0.106	
Al ₂ O ₃ /SiO ₂	0.49	0.5	0.46	
S%	0.37	0.33	0.4	
coal rec%	-	80	-	
<u>WOC + Floatation 0.15x0.0 mm⁽¹⁾</u>				
% Weight	100	64	36	
Ash%	21.3	8.5	43.9	
total reactives	76.7	84.9	78.2	
base acid ratio	0.099	0.038	0.23	
Al ₂ O ₃ /SiO ₂	0.46	0.51	0.37	
S%	0.52	0.4	0.74	
coal rec%	-	76	-	
WOC =water only cyclones				
(1) data calculated from 0.6 by 0.0mm and 0.6 by 0.15mm material				
total reactives =% of organic material				
coal rec= ratio coal recovered / coal in raw sample				

always been an important parameter for thermal coals but it is also becoming an important parameter for metallurgical coals. This is because ash chemistry influences coke reactivity and

coke strength at high temperatures. The coke strength after reaction (CSR) test is used to evaluate coke strength at high temperatures and is used to assess the coking quality of hard coking coals, with ranks in the range 1.0% to 1.7% Rmax. In fact as PCI replaces coke in the blast furnace even more emphasis is likely to be placed on CSR values. A number of authors (Goscinski *et al*, 1985, Price *et al.*, 1988) have illustrated that CSR is strongly influenced by ash chemistry measured as alkalinity, base/acid ratio (B/A) or the modified basicity index (MBI) (Table 2).

There are a number of empirical equations, many listed in Coin (1995), that use only coal quality parameters to predict CSR. Generally the equations use rank, coal ash chemistry, rheology, and petrography, in that rough order of significance. It is important to recognize that rheology and petrography are in fact not independent variables and that CSR has a non linear relationship to rank, decreasing at high and low ranks and reaching a maximum value in the range Rmax%=1.35-1.43% (Coin, 1995). There appears to be an optimum amount of inerts, at a given rank, for maximum CSR and this amount increases as rank increases (Gill, 1982). This means that any linear regression of CSR against rheology, petrography and rank can only be effective over a limited range. CSR probably has a better linear correlation to ash basicity than any other factor, depending on how it is defined. Todoschuk *et. al.* (1998) uses coke basicity and other coke derived properties to predict CSR over a wide range of rank.

Table 2. Abbreviations for plant data.

<u>Gieseler Plastometer</u>	
startC° =temp of softening, fusC°=temp of fusion, max C°=temp of max fluidity, finalC°=temp at end of fluidity	
solidC°=temp at solidification, maxC°= fluid temp range, ddpm= max fluidity	
<u>Dilatometer</u>	
sf TC°= temperature of start of fusion in a dilatometer, max C C° = temperature at maximum contraction,	
max D C° = temperature at maximum dilatation, C=maximum contraction, D=maximum dilatation,	
<u>Ash Chemistry</u>	
B/A=base/acid ratio = (CaO+MgO+Fe ₂ O ₃ +Na ₂ O+K ₂ O)/(SiO ₂ +Al ₂ O ₃ +TiO ₂), MBI=B/A x Ash/ (100-MV) x 100	
Alkalinity=base/acid ratio x Ash/100	
<u>Petrography</u>	
vit =vitrinite, ex=exinite, SF=semifusinite, Mic=micrinite, Fus=Fusinite, MM=Mineral Matter, TR=total reactives	
<u>Plant</u>	
cl=clean, hm=heavy medium, sb=sieve bend, sbo=sieve bend oversize, bp=bird product, woc=water only cyclone, m=mesh	
Carbonization	
H ₂ O=moisture of charge, ASTM BD=bulk density of charge kg/m ³ , Max w l P kPa=max wall pressure, SI=Stability Index	

There have been a number of studies investigating the relationship of CSR to ash chemistry. Some studies have attempted to differentiate alkalis in terms of their ability to effect CSR and to determine whether mineral form influences the ability of an alkali element to effect CSR. Price *et al.*, (1992) found that additions of pyrite (FeS_2), siderite (FeCO_3) or calcite (CaCO_3) to coal samples decreased CSR in proportion to the amount they increased MBI. Goscinski and Patalsky (1989) emphasize the importance of Fe_2O_3 and CaO contents. When these oxides are present in eutectic proportions the ash fusion temperature is lowered and the catalytic effect of the ash on coke reactivity is enhanced.

The oxides CaO and Fe_2O_3 may be released by the dissociation of carbonates or pyrite in the coke oven. If the carbonates are finely dispersed in coal macerals the resulting oxides will be highly reactive. A plot of the concentration of Fe_2O_3 versus CaO in the total samples for 3 of the suits of medium-volatile coals studied in this paper (Figure 3) illustrates the devastating effects of iron and calcium on CSR and the tendency of CaO to be more harmful than Fe_2O_3 . Suite B contains increased concentrations of CaO, probably occurring as calcite (CaCO_3) on cleats in vitrinite. The Fe_2O_3 total sample concentrations in coals A, B and C do not correlate with sulphur (Table 3) and many of the samples plot above the pyrite line (Figure 4) indicating that the iron is probably present as siderite not as pyrite. Microscope work has identified siderite (FeCO_3) dispersed as oolites through the coal. Apparently the dispersion of calcite in vitrinite

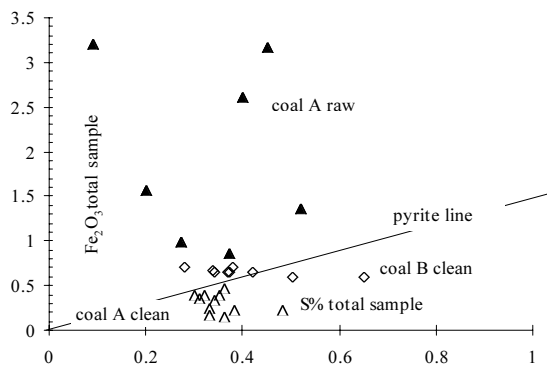


Figure 3. Fe_2O_3 total sample versus S% for plants A, B illustrating lack of relationship; plot indicates a siderite origin for most of the iron and an organic origin for the sulphur. Samples containing only pyrite plot on pyrite line.

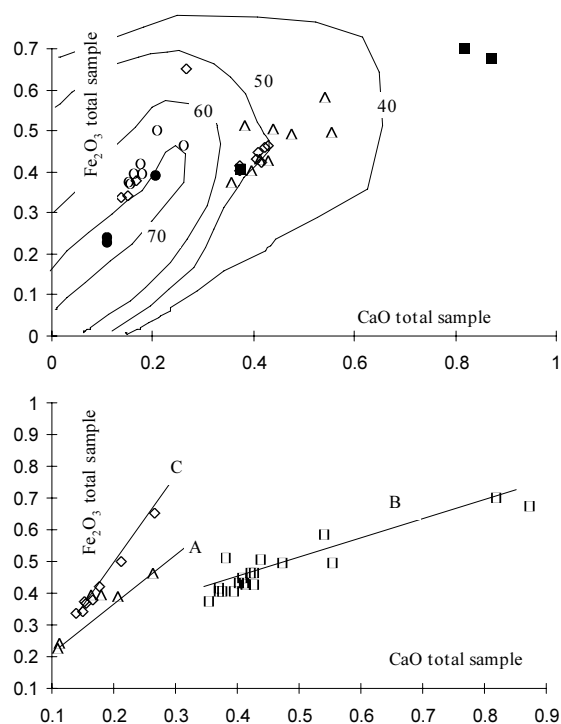


Figure 4. Fe_2O_3 and CaO data for plants A, B and C illustrating relative effect of oxides on CSR. CSR values are divided as follows Squares<40,triangles 40-50, diamonds 50-60, circles 60-70 solid circles>70. Plant B ash contains calcite plant C ash contains siderite.

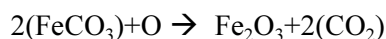
has increased the reactivity of CaO over that of Fe_2O_3 , which is not as finely dispersed in the coal macerals.

It is possible using a CSR predictive equation to illustrate the effects on CSR of additions of small amounts of calcite or siderite. The equation derived by Price *et al.* (1988) is a relatively consistent empirical approach to estimating CSR

Table 3. Linear correlation matrix for clean coal data, Plant C, illustrating effect of Fe_2O_3 on base/acid ratio (B/A).

×	SiO_2	Al_2O_3	Fe_2O_3	TiO_2	P_2O_5	CaO	MgO	B/A	K_2O	Ash	CSR
SiO_2	1.0										
Al_2O_3	-.51	1.0									
Fe_2O_3	-.19	-.33	1.0								
TiO_2	-.11	.56	-.93	1.0							
P_2O_5	-.50	.04	.69	-.60	1.0						
CaO	-.21	-.29	.98	-.92	.78	1.0					
MgO	.42	.01	-.94	.79	-.80	-.94	1.0				
B/A	-.24	-.42	.98	-.89	.64	.96	-.88	1.0			
K_2O	.31	.14	-.97	.87	-.81	-.98	.98	-.92	1.0		
Ash	.61	-.93	.34	-.58	-.19	.28	-.04	.40	-.14	1.0	
CSR	-.70	.35	-.39	.54	-.03	-.38	.28	-.24	.40	-.52	1.0

values, though it tends to predict on the high side (Coin, 1995). The equation emphasizes the sensitivity of CSR to changes in ash chemistry. It can be used to illustrate the effect of adding 1% calcite to a raw coal. If the original sample has values of 10% ash, 50 ddpmm fluidity, base/acid ratio 0.07 and a rank of $R_{max}=1.3\%$ then the calculated CSR is 67. The CSR value drops to 49 and the base/acid ratio changes to 0.13 after addition of 1 weight % calcite. The 1% addition of calcite added about 0.56% CaO to the sample but all of this is concentrated into the 10% ash changing the CaO % in ash from 1.4% to 6.6%. It is not uncommon to find 1% calcite in coal either along cleat surfaces in vitrain bands or in cells in semifusinite. The situation is even more extreme if siderite ($FeCO_3$) is added to the sample, because this will report to the ash as Fe_2O_3 and requires addition of oxygen because it is present in calcite as Fe+2 but is oxidized to Fe+3 in the ash:



This means that 1 gram of siderite in the samples adds 0.7 grams of Fe_2O_3 to the ash producing an increase in the percentage of Fe_2O_3 in the ash of over 7%. Or conversely surprisingly high Fe_2O_3 concentrations in ash result from quite small concentrations of siderite in the total sample.

It is important to know what minerals are influencing the ash chemistry and where they are located in the coal, before attempting, in a plant, to change the ash chemistry of the product coal. Coals with no marine influence generally contain high proportions of kaolinite and quartz; coals with some marine influence contain less degraded clays and more pyrite. Most of the Cretaceous coals in western Canada have kaolinite based ash, which ensures low base/acid ratios, unless there have been syngenetic or epigenetic additions of carbonate minerals. Scanning electron microscope work indicates that there are three primary locations for difficult to remove mineral matter in coal.

- ♦ Finely dispersed mineral matter occurs in desmocollinite (vitrinite B). In western Canadian coals this appears to be kaolinite rich though quartz and sometimes crandillite (aluminum phosphate) occur. If pyrite is pre-

sent it is often finely dispersed in reactive macerals (Ryan and Ledda, 1998) because it usually forms by bacterial reduction of SO_4 in moderate pH anaerobic conditions favourable to the preservation of vitrinite.

- ♦ A number of minerals (kaolinite, carbonates and sometimes apatite) fill the cell voids in semifusinite and fusinite. In some coals with high macrinite contents the amount of inherent mineral matter is low because these sites are not available.
- ♦ Some minerals are external to maceral grains but are too finely dispersed to be easily liberated by crushing. Calcite and other carbonates sometimes coat cleat and microfracture surfaces in vitrain bands. Calcite can be unexpectedly difficult to remove because it impregnates the vitrinite along microfractures associated with cleats. Oolites of siderite can occur randomly dispersed in the coal. Siderite can also coat cleat surfaces.

It is important to realize that these minerals are associated with the coal and not with the in-seam rock splits.

Calcite is one of the most important minerals influencing the ash chemistry of British Columbia coals. It is deposited on cleats and in the cell structure of semifusinite. The deposition of calcite into semifusinite cells must occur as the coal is forming and before compaction closes the cell openings. It has been suggested that fires in the coal swamps form charred vegetation, latter to form semifusinite and at the same time increase the pH of the swamp water, probably by deposition of soluble ash (Lamberson and Bustin, 1996). The higher pH causes calcite to precipitate into the porous semifusinite. This often effects upper parts of seams, producing a hard dull looking coal in outcrop. The occurrence of calcite-rich semifusinite will vary based upon depositional features. Once filled with calcite the semifusinite cells are protected from compaction and deformation and provide a location, from which it is almost impossible to remove the calcite. A similar problem can occur in some coals where apatite fills semifusinite cells.

If the calcite coats the surfaces of cleats, it must have been deposited after the coal was sufficiently indurated to fracture. Probably calcium rich water percolated down through the coal

from marine strata higher in the section. In this case the calcium will be associated with the bright vitrinite rich bands in the coal and may, on the regional scale, vary based on the extent of cleat development related to folding. Crushing the coal to a finer size may help to liberate some of the calcite.

Based on the association of minerals with coal and the type of minerals present, the base/acid ratio of ash changes with the size consist of raw coal and by specific gravity of wash fractions. This leads to the possibility of changing the ash chemistry of the clean coal. Coals that have carbonates on cleats and micro fracture surfaces have higher base/acid ratios in coarser sized coal, caused by increased contents of calcium, iron and magnesium associated with the minerals calcite (CaCO_3), dolomite (CaMgCO_3), ankerite (CaMgFeCO_3) and siderite (FeCO_3). These minerals are associated with coal rather than in-seam rock splits. They report to SG splits based on the average SG of the coal plus mineral matter plus carbonate mixture. The maximum amount of carbonate can occur in any SG split when it is associated only with pure coal. As the inherent mineral matter content increases in the sample the carbonate content has to decrease to maintain the same SG. In coals with high inherent ash contents, the carbonate is forced into the higher SG splits and tends to be removed with the rejects. In coals with low inherent mineral matter contents it can occur in lower SG splits and end up in the product coal.

A previous study looked at the distribution of calcite in a high-volatile bituminous coal (Ryan, 1994). Using washability data it is possible to convert analyses of CaO content by SG increment into approximate concentrations of calcite in the total sample (Table 4). Estimated contents of calcite increased to the range 10% to 20% in SG splits 1.45 to 1.7. These high concentrations were achieved because this coal has a low inherent mineral matter content. The reported ash concentrations include the CaO from the calcite, which has to be removed before calculating the content of non calcite derived ash in the coal. It should be noted that when carbonate concentrations are high, ash values are very deceptive because of the loss of CO_2 from carbonate component of the non coal part of the sample during ashing. In fact in the calcite distribution study (Ryan, 1994) the reported ash

Table 4. Calcite distribution by size and SG increment. Data from a high-volatile bituminous coal (Ryan, 1994).

SIZE mm	100-25	25-10	10-0.5	0.5-0.15
Weight%	23.5	24.3	40.2	4.5
Ash%	32.8	32.6	31.3	21.4
CaO% Ash	8.8	4.9	5.9	15.0
Wt% calcite	4.6	2.3	2.7	5.4
Vol% calcite	2.4	1.2	1.4	2.8

S.G.	wt% calcite		wt% calcite		wt% calcite		wt% calcite	
	Ash%	wt% calcite						
1-1.3	6.0	0.9	4.0	1.0	4.8	1.1	4.2	0.5
1.3-1.35	6.4	2.6	5.7	2.0	5.5	1.2	6.2	0.6
1.35-1.4	10.5	6.5	9.9	5.6	9.9	2.6	7.7	0.9
1.4-1.45	14.4	9.7	15.0	6.4	14.3	4.4	10.4	1.0
1.45-1.5	17.7	12.7	18.7	10.0	18.4	7.1	15.1	1.5
1.5-1.6	21.8	16.3	24.2	13.9	23.4	9.5	19.4	2.1
1.6-1.7	30.8	9.7	33.7	10.5	30.7	10.6	28.2	3.1
1.7-1.8	44.4	9.9	45.3	5.8	38.9	13.5	36.8	5.4
1.8-2.0	51.2	3.3	53.9	1.0	51.8	9.3	47.9	8.1
2.0-2.17	65.9	0.5	66.8	2.7	61.5	10.6	58.9	11.9
2.17-2.5	80.5	0.0	80.9	-0.5	81.4	1.0	79.3	21.3

concentrations for intermediate SG values and coarse size fractions are 23% and 36%; these values are actually closer to 30% and 42% mineral matter when the oxides are reconstituted to make carbonates.

It is also possible to estimate the SG of the material in each split by assigning densities to coal, mineral matter and calcite. When this is done in the study (Ryan, 1994), it is found that in order to derive an average SG for the material in each SG split that is bracketed by the SG increment range, a low density for calcite has to be used in the calculations. It is difficult to derive an accurate number but the effective density of the calcite appears to be low by about 20%. It appears that the actual density for carbonates on cleats and micro fractures may be less than the ideal density of the pure minerals. Possibly larger coal fragments (i.e. >5 mm), which contain microfractures have increased porosity, which is only partially filled by carbonate material. This could help explain the difficulty in removing carbonate material from coal, unless it is crushed to a fine (<1 mm) size. Obviously it is easier to remove calcite from finer sized coal, as more calcite is liberated. Also because the grains are smaller more of them contain higher amounts of

included calcite so that the calcite occurs in higher SG splits (Table 4).

Variations in ash chemistry are very important and can only be fully understood in the context of the mineralogy of the mineral matter in the coal. A powerful and cost effective way of doing this is to use a linear correlation matrix of oxide data. This is illustrated using data from a detailed study, which analyzed all major oxides in a bulk sample by size and SG increment. Data from this study are used to infer the mineralogy of the ash in each increment (Table 5). It should be noted that because Al_2O_3 and SiO_2 are major components of the ash they will always tend to be negatively correlated and this does not necessarily reflect changes in mineralogy. Calcium, iron and magnesium are concen-

Table 5. Linear correlation matrix for ash chemistry and petrographic data for incremental wash samples from 3 size ranges; TR=total reactivities.

x	Ash	SiO ₂	Al ₂ O ₃	Fe ₂ O ₃	TiO ₂	P ₂ O ₅	CaO	MgO	SO ₃	Na ₂ O	K ₂ O	TR
Ash	1.0											
SiO ₂	-.90	1.0										
Al ₂ O ₃	-.07	.45	1.0				plus 12.5 mm					
Fe ₂ O ₃	.62	-.86	-.57	1.0								
TiO ₂	.63	-.33	.25	-.18	1.0							
P ₂ O ₅	.59	-.53	.31	.60	-.04	1.0						
CaO	.72	-.91	-.74	.78	.29	.14	1.0					
MgO	.56	-.86	-.78	.95	-.12	.34	.90	1.0				
SO ₃	.72	-.51	.49	.41	.31	.93	.12	.16	1.0			
Na ₂ O	.38	-.07	.83	-.03	.26	.77	-.34	-.30	.88	1.0		
K ₂ O	-.96	.90	.03	-.73	-.43	-.78	-.65	-.61	-.83	-.49	1.0	
TR	-.76	.75	.15	-.77	-.13	-.70	-.57	-.63	-.69	-.31	.81	1.0
Ash	1.0											
SiO ₂	.88	1.0										
Al ₂ O ₃	-.85	-.86	1.0				12.5 - 0.6 mm					
Fe ₂ O ₃	-.79	-.96	.72	1.0								
TiO ₂	-.91	-.99	.91	.92	1.0							
P ₂ O ₅	-.84	-.78	.91	.72	.83	1.0						
CaO	-.62	-.84	.48	.87	.78	.35	1.0					
MgO	.09	-.12	-.39	.29	.02	-.41	.62	1.0				
SO ₃	-.82	-.90	.59	.95	.85	.64	.86	.40	1.0			
Na ₂ O	-.65	-.63	.89	.54	.69	.93	.13	-.64	.38	1.0		
K ₂ O	.88	.99	-.89	-.96	-.99	-.85	-.78	-.05	-.88	-.71	1.0	
TR	.52	.73	-.30	-.85	-.66	-.31	-.93	-.74	-.88	-.04	.70	1.0
Ash	1.0											
SiO ₂	.81	1.0										
Al ₂ O ₃	-.86	-.97	1.0				0.6 - 0.15 mm					
Fe ₂ O ₃	-.68	-.55	.73	1.0								
TiO ₂	-.71	-.92	.83	.25	1.0							
P ₂ O ₅	-.81	-.98	.92	.42	.96	1.0						
CaO	-.47	-.65	.54	.04	.85	.68	1.0					
MgO	.84	1.0	-.98	-.59	-.91	-.98	-.65	1.0				
SO ₃	-.41	-.29	.16	-.31	.59	.42	.73	-.29	1.0			
Na ₂ O	-.80	-.98	.94	.50	.90	.98	.58	-.98	.29	1.0		
K ₂ O	.86	.95	-.99	-.78	-.76	-.89	-.44	.95	-.06	-.92	1.0	
TR	.13	.14	-.27	-.60	.24	-.04	.64	.14	.80	-.19	.39	1.0

trated in the coarser sizes and in these sizes they correlate with each other and not with SiO_2 or Al_2O_3 indicating that they are present as carbonates. In the fine size, concentrations of these elements decrease; CaO correlates with P_2O_5 indicating an apatite connection; MgO correlates with ash and not with Fe_2O_3 or CaO indicating a clay connection; Fe_2O_3 does not correlate with CaO, MgO or ash indicating a probable pyrite connection. Maximum carbonate content of the samples can be estimated by combining the oxides of Ca, Mg and Fe with CO_2 and recalculating the weights as carbonates (XCO_2). This indicates that in the coarser sizes carbonate contents are in the range 1 to 15% but in the fine size, contents decrease to less than 3% except in the plus 2.17 SG split.

It is obvious, that for the coal represented in Table 5 the base/acid ratio is controlled by carbonate material on cleats. It is not easily liberated because a lot of the carbonate material is contained in particles with SG values in the middlings range. Small increases in the cut point of the coarse circuit or crushing the coal to a finer size may remove more carbonate material, reduce the base/acid ratio of the clean coal and improve the CSR values, with out a major decrease in plant yield.

In coals that do not contain carbonates on cleats, carbonate material can occur as cell filling in fusinite and semifusinite; though the amount present will be much less than in cleated

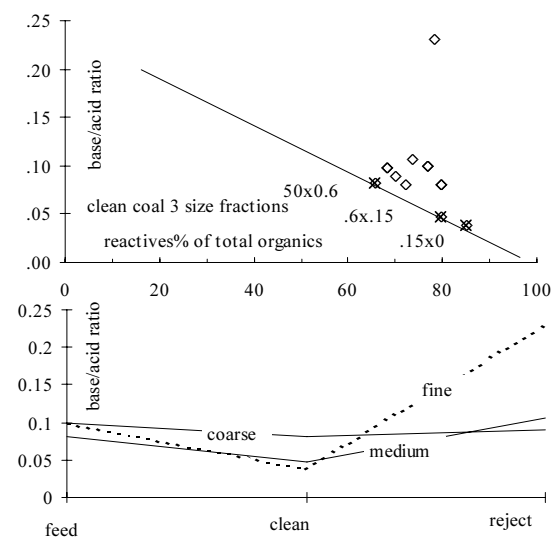


Figure 5. Relationship of base/acid ratio to size, clean, raw or reject coal and petrography in plant A. Diamonds are raw and reject samples.

coals. In these coals base/acid ratios have a negative correlation with reactive maceral contents and also decrease in the fine circuits because coal in these circuits tends to be enriched in reactive macerals (Table 1). A plot of reactivities content (mineral matter free basis) versus base/acid ratio for clean coal from a number of circuits (Figure 5) provides a good negative correlation indicating a zero base/acid ratio for reactivities and a ratio of about 0.2 to 0.25 for the organic inerts plus ash. A zero base/acid ratio suggests a mineralogy of kaolinite and quartz in the vitrinite. The ratio can be decreased by adjusting the cut point of coarse circuits to retain less inertinite.

CCRA PLANT EVALUATION PROGRAM

Coal was sampled from five Canadian coal preparation plants. The size fractions treated in the individual circuits of these five plants are summarized in Table 6. The sampling program varied at each plant because of somewhat different objectives and varying plant design and as the program unfolded the sampling program at each plant tended to become more detailed as information from the previous plants became available. Attempts were made to sample product coal, coal from each circuit as well as a number of blends of material from different circuits at each plant. Sampling at each plant occurred over a relatively short period and therefore quality does not necessarily reflect average product coal quality. It should also be noted that this CCRA project has been on going for a number of years and product quality from the plants has changed considerably since the project started.

Table 6. Coal sizes treated in the five plant circuits.

Plant	Plant Circuits			
	Heavy Media		Fines	
	Vessels or Drum	Cyclones	WOC/Sp*	Froth Flotation
A	-	50x0.6	0.6x0.15	0.15x0
B	50x16	16x0.65	0.65x0.15	0.15x0
C	40x10	10x0.65	0.65x0.15	0.15x0
D	-	50x0.65	0.65x0.15	0.15x0
E	-	40x0.65	-	0.65x0

*Water-only-cyclones (WOC) and/or Spirals (Sp)

Each of the bulk samples taken from the plants was evaluated for both coal and coke quality, and the impact of the coal produced from individual circuits on the coking quality of the overall clean coal was also evaluated. Testing of samples for coal and coking quality was conducted in the laboratories and pilot scale coke ovens at the CANMET laboratories (Ottawa). Because of differences in the sampling programs, the detailed results for each plant vary somewhat and are discussed separately. All the abbreviations used in tables containing the plant results are in Table 2.

Plant A

Basic analytical data for Plant A (Tables 7,8) indicate the distribution of ash and variations in petrography between the three size circuits in the plant. The coal is screened to 50mm by 0.6 mm and 0.6mm by 0.0mm. The coarse size is washed in heavy medium cyclones. The finer coal is partially cleaned in water only cyclones then screened to 0.6 by 0.15 mm and 0.15 mm by 0.0 mm. The 0.6 mm by 0.15 mm material goes to clean coal and 0.15 by 0 mm material is cleaned in floatation cells.

Some general comments can be made about the plant. Raw coal ash concentration is minimum in the 0.6 mm by 0.15 mm size; sulphur and reactive macerals concentrate in the finer sizes. Ash chemistry varies little with size, though there seems to be a concentration of kaolinite, probably associated with vitrinite, in the fine coal. The cleaning efficiency of the circuits decreases as the size decreases and this provides some flexibility to influence the petrography of the clean coal. The 0.15 mm by 0.0 mm clean coal, which is a combination of material from water only cyclones and floatation is enriched in vitrinite, possibly because these circuits reject about 25% of the feed coal. Consequently the reject coal must be enriched in inertinite.

Base/acid ratios are generally low and decrease as coal size decreases and as the amount of vitrinite increases (Figure 5). They tend to increase as the amount of inertinite or ash increase in the sample Figure 6. An indication of the ability of a plant to effect the base/acid ratio of the product coal is given by the percent-

	plant feed	hm feed	woc feed 0.15 x 0	hm reject	bird reject 0.6 x 0.15	bp reject 0.15x0.0	cl coal #1	cl coal #2	hm prod	sbo 0.6 x 0.15	bird prod 0.6 x 0	bird prop 0 x 0.15	cl c 0x0.15 only	new cl c 0x0.15 only	90%hm+10%sb	75%hm+25%sb	85%nci+15%bp 0x.15	bird -100m n dried	cl -100m thru drier	nci -100m thru drier
Ash%	23.5	29	18.7	21.3	68	41.5	43.9	10.1	10	10.5	8.3	9.6	9.1	10.6	10.3	9.9	9.9			
S%	0.27	0.2	0.37	0.52	0.09	0.4	0.4	0.32	0.33	0.36	0.36	0.48	0.34	0.31	0.3	0.35	0.38			
VM%	18.8	18.3	20.5	19.8	13.3	17.6	17.1	20.5	21.1	20.2	21.8	21.4	21.7	21.4	20.2	20.2	20.8			
VM%daf	24.58	25.77	25.22	25.16	41.56	30.09	30.48	22.8	23.44	22.57	23.77	23.9	23.87	23.94	22.52	22.42	23.09			
FC%	57.7	52.7	60.8	58.9	18.7	40.9	39	69.4	68.9	69.3	69.9	69.4	69	69.2	69.2	69.5	69.3			
H%	3.5	3.3	3.8	3.7	1.6	2.7	2.6	3.9	4.2	3.9	4.2	4.1	4.3	4.3						
O%	4.2	4.6	4.5	4	5.5	5.7	5.4	4.3	3.7	4.1	4.3	4.1	4	3.6						
FSI	2.5	1.5	7.5	4	0.5	1		3.5	7	3	8	7.5	8	7.5	3	3.5	7	7.5	8	7.5
startC°	455	450	434	437				453	445	457	433	443	445	441	451	452	446	444	445	441
fusC°			450	467				463	463	449	459			464	464	465	465	470	469	464
max C°	470	467	471	469				467	472	468	470	470	469	471	468	468	470	470	469	471
final C°	479	477	492	482				476	484	479	486	483	481	486	480	478	484	483	481	486
solid C°	488	483	495	486				485	490	489	492	490	487	491	486	486	490	490	487	491
range C°	24	27	58	45				23	39	22	60	43	39	45	29	26	38	39	36	45
ddpm	1.8	1.9	39	5.4				2.1	9.2	1.6	14.4	4.4	3.8	7.5	1.3	2.1	5.4	4.4	3.8	7.5
sf TC°	426	429	416	417				416	411	422	410	417	416	417	423	422	419	417	416	417
max C C°	492		467	474				483	469	485	459	467	469	466	483	483	474	469	467	466
max D C°			491	483				490	490		489	491	492	493	491	490	490	492	493	491
C	20	17	28	23				27	28	21	30	25	28	24	25	25	27	28	28	24
D	-20	-17	-1	-22				-27	-7	-21	19	6	-7	5	-25	-25	-19	-7	-8	5
vit%	46	38.5	58.4	55.4	23.8	41.7	46.8	42.5	50	39.6	63.6	67.4	64.2	65.8	47	49.8	58.5	64.2	65.8	71.8
SF%	32	34.6	24.8	23	15.4	22.4	16	37.4	36	44.2	24.6	20.8	21.6	21.2	37.2	37	27	21.6	21.2	17.5
Mie%	3.3	4.4	3.7	3.7	1.7	3.1	2.7	5.2	3.7	4.7	3.8	2.4	3.9	3.2	4.8	3.2	4.1	3.9	3.2	2.2
Fus%	4.6	4.6	2.2	5.2	4.1	5	4.6	9.3	4.7	5.6	3.4	4.5	4.9	4.7	5.2	4.5	4.9	4.9	4.7	2.6
MM%	14.1	17.9	10.9	12.7	55	27.8	29.9	5.6	5.6	5.9	4.6	4.9	5.4	5.1	5.8	5.5	5.5	5.4	5.1	5.9
Rmax%	1.34	1.34	1.36	1.35	1.32	1.35	1.34	1.35	1.34	1.35	1.35	1.33	1.33	1.33	1.37	1.34	1.33	1.33	1.33	1.33
TR%	62	55.8	70.8	66.9	31.5	52.9	54.8	61.2	68	61.7	75.9	77.8	75	76.4	65.6	68.3	72	75	76.4	80.55

Table 7. Proximate, ultimate, rheological and petrographic data for Plant A.

	plant feed	hm feed	woc feed .6x.15	woc feed .15x0	hm reject	bp reject .6x.15	bp reject .15x0	cl coal #1	new cl c #2	hm prod	sbo 0.6 x 0.15	bird prod (bp) 0.6 x 0.0	bird prop 0x.15	c cl 0x0.15 only	new c cl 0x0.15 only	90%hbm+10%sb	75%hbm+2.5%sb	85%ancl+15%bp 0x.15
<u>Proximate and ash chemistry</u>																		
Ash	24	29	19	21	68	42	44	10	10	11	8.3	8.8	9.6	9.1	11	10	9.9	9.9
S%	0.3	0.2	0.4	0.5	0.1	0.4	0.5	0.3	0.3	0.4	0.3	0.4	0.5	0.3	0.3	0.3	0.4	0.4
S% in Ash	1.15	0.69	1.98	2.44	0.13	0.96	1.03	3.17	3.30	3.43	3.98	4.09	5.00	3.74	2.92	2.91	3.5	3.8
SiO ₂	62	62	60	61	64	60	60	59	60	58	61	61	61	60	61	57	58.7	61.3
Al ₂ O ₃	27	27	29	28	28	27	25	31	31	32	31	31	31	30	29	31	31.5	31.4
Fe ₂ O ₃	4.2	5.4	4.6	6.4	4.7	6.3	7.2	3.9	2.4	4.4	2	1.7	2.4	3.7	3.3	3.8	4.0	2.3
TiO ₂	1.3	1.2	1.5	1.5	1.1	1.1	1	2.1	1.8	1.5	2.2	2.3	2.3	2.3	2	1.5	1.2	1.9
P ₂ O ₅	0.5	0.6	0.6	0.6	0.4	0.3	0.4	1.1	1	1.6	1	0.9	0.9	0.8	0.3	1.5	1.4	0.9
CaO	0.8	0.9	0.9	0.7	0.6	0.7	0.9	1.6	1.1	2.5	1.4	1.2	1.3	1.3	0.6	2	1.8	1.1
MgO	0.6	0.7	0.5	0.5	0.7	0.6	0.5	0.2	0.2	0.2	0.2	0.2	0.3	0.3	0.3	0.1	0.2	0.3
SO ₃		0.1			0.1		0.3	0.1	0.1	0.3				0.2	0.5			
Na ₂ O						0.1	0.1	0.1	0.1	0.1	0.1	0.1	0.1	0.1	0.1	0.1		
K ₂ O	1.7	1.8	1.4	1.4	2.3	1.7	1.6	0.8	0.8	0.3	0.8	0.9	1	1	1.3	0.3	0.4	0.8
BaO				0.1		0.1	0.2	0.1	0.1	0.1	0.1	0.1	0.1	0.1	0.1	0.1	0.1	0.1
LOF	0.5	1.4	1.6	0.9		0.8	1.6	1.2	0.5	0.2		2.1		0.6		3.8		0.2
B/A	0.08	0.10	0.08	0.10	0.09	0.11	0.13	0.07	0.05	0.09	0.05	0.04	0.06	0.07	0.07	0.07	0.07	0.05
<u>Carbonization results</u>																		
H ₂ O								3.4	3.5	3.3						3.1	3.1	3.4
wt charge								271	267	268						272	270	263
ASTM BD								777	775	777						778	778	777
Max w/ P kPa								4.7	3.8	2.1						1.9	2.8	4.1
coke yld%								79	80	79						79	79	78
mean coke size mm								50	48	52						50	47	48
coke ash%								12	12	13						13	12	12
coke VM%								1	0.8	0.8						0.9	1.1	0.8
coke S%								0.3	0.3	0.3						0.3	0.3	0.3
Stability								43	56	38						43	47	53
hardness								63	70	61						64	65	69
CSR								68	75	66						70	68	72
CRI								23	19	24						22	24	22
<u>Coke Petrography</u>																		
mosaic								19	18	19						21	21	20
flow								15	12	11						15	22	19
domain								13	12	17						12	17	14
total inerts								53	58	53						52	40	47

Table 8. Ash chemistry and carbonization data for Plant A.

age spread in base/acid ratios defined as:

$(baC-baF)/bacoal \times 100$: Where baC is base/acid ratio of product from the coarse circuit, baF is ratio for fine circuit and bacoal is the ratio for product coal.

The value for Plant A is about 70%. This is quite high though in general the ratios are low for all circuits. The ratios correlate strongly with the presence of Fe_2O_3 and are high in the coarse circuit because of the presence of siderite, which is inferred from the lack of correlation of Fe_2O_3 with Al_2O_3 , SiO_2 or sulphur (Table 9). Siderite is removed by crushing but probably does not have a strong maceral association in the coal and therefore may not be concentrated with the inert macerals in the intermediate SG splits.

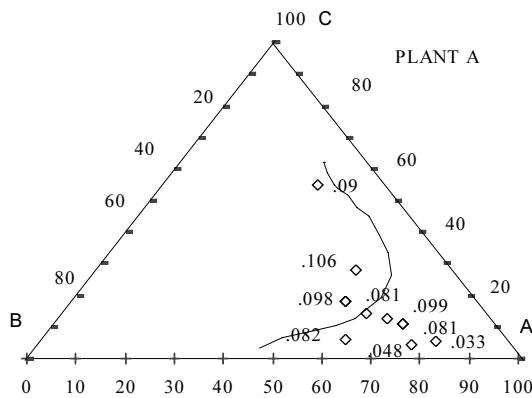


Figure 6. Triangular plot for Plant A data illustrating that base elements tend to be associated with mineral matter and inert macerals. Posted values are base/Acid ratios. A=reactives%, B=inerts%, C=ash%.

x	SiO_2	Al_2O_3	Fe_2O_3	P_2O_5	CaO	MgO	B/A	K_2O	Ash	S/ash
SiO_2	1.									
Al_2O_3	-.42	1.								
Fe_2O_3	-.02	-.77	1.							
P_2O_5	-.59	.85	-.55	1.						
CaO	-.70	.68	-.35	.94	1.					
MgO	.61	-.82	.69	-.82	-.70	1.				
B/A	-.02	-.79	.99	-.53	-.29	.70	1.			
K_2O	.76	-.83	.55	-.91	-.84	.94	.56	1.		
Ash	.55	-.73	.60	-.71	-.56	.78	.65	.85	1.	
S/ash	-.53	.84	-.72	.78	.63	-.96	-.75	-.92	-.86	1.

Table 9. Linear correlation matrix for ash chemistry data, Plant A.

Phosphorus contents in coals from Plant A are moderately high and have an ambiguous association with ash. At high ash concentrations there is some correlation with ash contents, but at low ash concentrations phosphorus content is not related to ash content. Phosphorus is concentrated in the coarse size fraction and is in part removed with the ash from this fraction. In the finer fractions it is not removed by washing and in the clean coal its concentration correlates with the fusinite plus semifusinite content (Figure 7). Most of the phosphorus is in these macerals and very little is associated with reactive macerals or ash. This means that phosphorus will concentrate in the intermediate SG splits (Figure 1) and in the coarser size fractions tracking the inertinite concentrations in the coal.

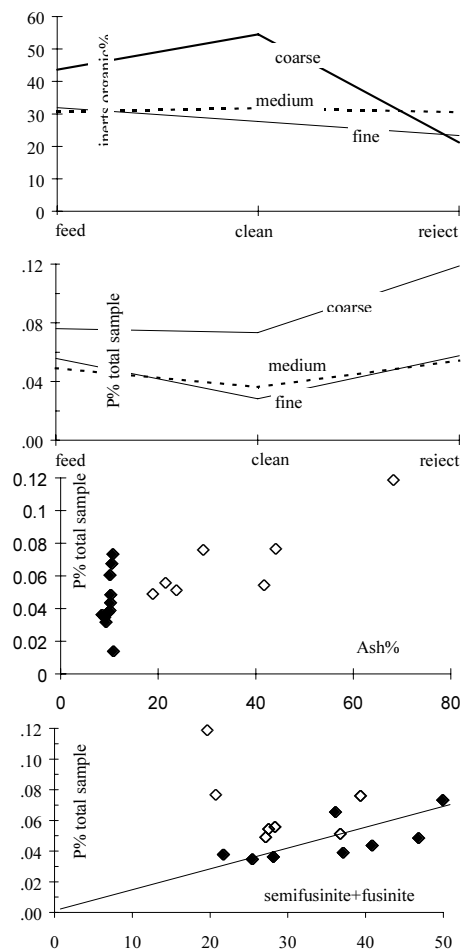


Figure 7. Phosphorus in Plant A. Phosphorus and inerts distribution by circuit and phosphorus relationship to ash and semifusinite+fusinite. Solid points are clean coal samples.

Fluidity and FSI values for the product 0.6 mm by 0.15 mm and 0.15 mm by 0.0 mm material are generally better than for the 50 mm by 0.6 mm material. This is to be expected based on the increased vitrinite content of this material (Figure 8). However on closer inspection it appears that fluidity and to a lesser extent FSI values of the 0.6 mm by 0.0 mm material are less than anticipated based on the high total reactivities content (Figure 8). This is important because it had been assumed that the fine coal with its increased reactivities content was important in maintaining and improving the coking quality of the product coal.

A partial explanation may relate to the fine size of the coal particles. A number of papers have indicated that fluidity and to a lesser extent FSI values are decreased if the coal is crushed to a finer size (Price and Gransden, 1987). It also appears that vitrinite in the fine coal forms a different population in terms of oxygen content than vitrinite in the product and coarse coal. The oxygen content of macerals increases from semifusinite to vitrinite and possibly from desmocolinite to tellinite (Mastalerz and Bustin, 1993). The fine coal samples plot to the left of a line of positive slope drawn through the product samples in the vitrinite versus oxygen plot implying that these samples are deficient in oxygen based on their vitrinite content. One would

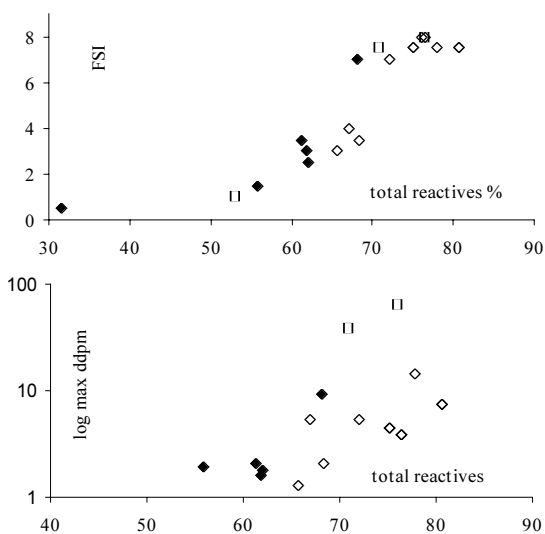


Figure 8. Relationship of FSI and fluidity to total reactivities content for Plant A. Solid diamonds =total product or 50 by 0.6 mm material, open diamonds=samples with all or some additional 0.15 mm material, open squares=0.6 by 0.15 material.

expect the opposite trend because tellinite is more friable and contains more oxygen than desmocolinite. If the fine coal samples are deficient in oxygen, then probably some of the fine vitrinite is more inert than coarse vitrinite. This may be because it experienced shearing, which increased its friability and decreased its reactivity, or it may be of higher rank. The effect is not related to the thermal drier because the samples were collected before the drier, nor is it related to ash because the effect is apparent in samples of similar ash content. The differences must therefore originate in the raw coal.

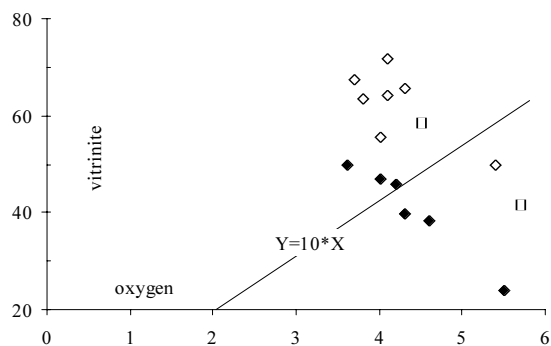


Figure 9. Oxygen versus vitrinite relationship.

When coal is coked there are some changes in the mineralogy of the mineral matter, which result in a volume decrease, but the main effect is loss of volatile matter, mostly from the reactive macerals. This has the effect of decreasing the relative percentage of reactive macerals in the coke compared to the coal. The effect is greater for coals with high inertinite contents and decreases to zero as the reactive maceral content approaches 100%. In the mid range it can account for a 5% to 10% increase in the inertinite content in coke compared to coal. For plant A, a comparison of coke and coal petrography indicates that when 15% 0.15 mm by 0.0 mm material is added to the clean coal, the coal reactivities maceral content increases but decreases in the coke (solid arrow in Figure 10) whereas when 0.6 by 0.15 mm material was added to heavy medium coal and coke reactivities increased (dashed arrow). Obviously petrography of fine samples is miss leading. It appears that the fine size and lower (?) oxygen content of vitrinite in the fine circuits makes it, in part, act like an inert coke maceral.

In an attempt to determine the contributions

of each size fraction to coke quality, additional fine coal was added to product coal and to product 50 by 0.6 mm coal. Despite increased vitrinite content, stability factor values appear to reach a maximum and then decrease as additional fine coal is added to the blend (Figure 10). This is not unexpected based on predictions by Schapiro and Gray, (1964) and Pearson (1980), who indicate that for a rank of about $R_{max}=1.35\%$ the optimum amount of reactive macerals is about 85%. Coin (1995) suggests the stability factor maximum occurs over a broader range of inerts content at constant rank. The

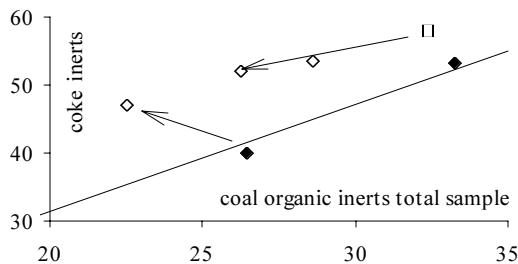


Figure 10. Relationship between coke and coal inerts for Plant A data. Open square=coarse fraction, solid diamond=clean coal, open diamond=additional fines.

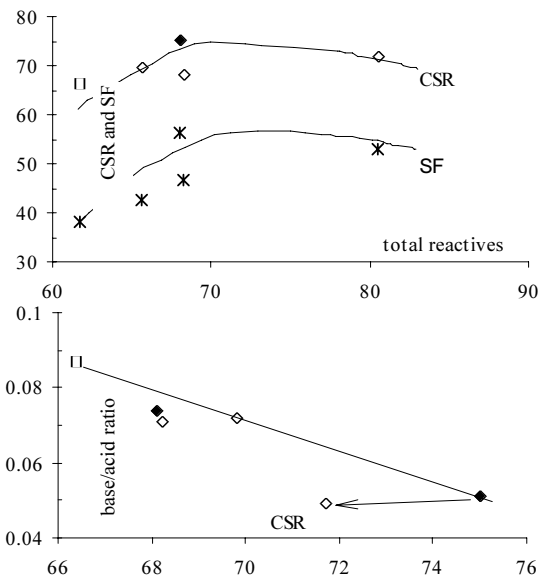


Figure 11. Relationship of coke strength and stability factor to total reactives and relationship of CSR to base/acid ratio. Plant A data, data symbols same as in Figure 10.

value of 85% reactives was not reached in blends of coal A and the stability factor maximum may occur in part because the vitrinite added was fine and therefore not as reactive as coarse vitrinite. CSR values also decrease as additional fines are added to product coal and the effect is not related to increasing base/acid ratios (Figure 11).

Plant B

Plant B uses wemco heavy medium drums to wash the 150 mm by 8 mm material, heavy medium cyclones to wash the 8 mm by 0.6 mm material, water only cyclones to wash the 0.6 mm by 0.15 mm material and froth floatation to wash the 0.15 mm by 0.0 mm material. Analytical data are in Table 10 and 11. In this plant emphasis was placed on sampling clean coal from the various circuits and recombining material from different circuits to make a number of new blends. Most of the samples therefore have similar ash contents of about 10% +/- 1%.

As with plant A, the vitrinite content increases in the clean coal in the fine circuits (Figure 12), however FSI and fluidity values increase less than predicted based on the increased vitrinite content. This may be because vitrinite in the fine circuits contains less oxygen and is less reactive than that in coarse circuits. A plot of oxygen *versus* vitrinite content indicates a weak tendency for the fine samples to contain less oxygen (Figure 12). Coke petrography provides an alternate estimate of the inert maceral content of the coal. In general it appears that coal petrography provides similar estimates of inert material in the various sizes as coke petrography though coke inerts are consistently higher (Figure 13).

Stability factor values for blends of coal from Plant B increase as the reactive contents increase, though there is a suggestion that values for the reactive rich bird product are lower than expected. Based on rank of about $R_{max}=1.35\%$ the maximum stability factor should occur at about 85% reactives, which was not reached in blends of coal B (Figure 14). When increasing vitrinite content is achieved by adding fine coal it is difficult to distinguish the effect of optimum vitrinite content from the decreased rheology of fine vitrinite additions. Additions of drum, heavy medium and belt press

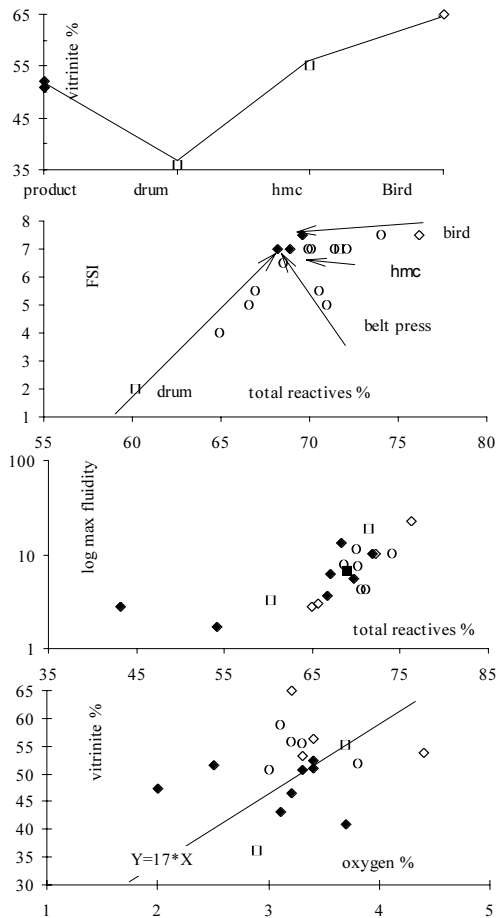


Figure 12 . Plant B, vitrinite content versus size, FSI, maximum fluidity and Oxygen content for clean coal and clean coal blends. Solid diamonds=product coal, open circles=blends, open diamond=fine coal and open square=coarse coal.

clean material to product coal decreased Stability Factor, only additions of bird product increased it.

Base/acid ratios decrease as size decreases (Figure 14). A correlation analysis of oxide data for all samples (Table 12) indicates that base/acid ratios correlate with the oxides CaO, MgO and Fe₂O₃. These oxides correlate with each other and not with SiO₂ or Al₂O₃. They probably occur in carbonates in the coarse coal, but are more likely associated with ash minerals in the fine coal, where individual oxide concentrations are lower. Carbonate minerals on fractures increase the base/acid ratios in the coarse material, but in the finer sized samples carbonate material is liberated and washed out so that base/acid ratios are lower. An indication of the ability of a plant to effect the base/acid ratio of the product coal is given by the percentage

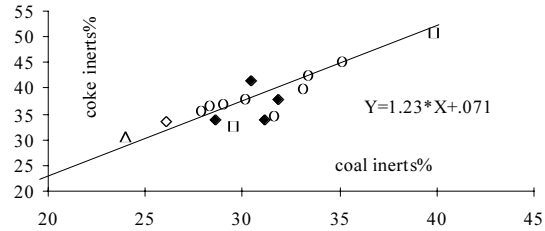


Figure 13. Coal inerts versus coke inerts for Plant B.

spread in base/acid ratios, defined previously, which is about 70% for Plant B.

CSR values are strongly correlated to ash chemistry and have a good negative correlation to modified basicity index (MBI) (Figure 14). Despite the lower base/acid ratio of the bird product its MBI value is higher and its CSR value lower than that of product coal because the bird product has a higher ash content. Also Additions of product from drum, heavy medium, bird or belt press material to product coal generally do not improve CSR (Figure 14). Only the heavy medium material has similar CSR values to product coal. In fact despite similar base/acid ratio and lower reactivities content it has a better CSR value than the bird product, probably because of the better rheology of coarser vitrinite.

The CSR values of coal from plant B are mainly limited by the base/acid ratio of the drum product (Figure 14). Removal of drum product from the product coal, or washing techniques that increase the removal of carbonate material from this circuit will lead to a decrease in base/acid ratio and improved CSR values of the product. Carbonates can be removed by crushing to a finer size with additional liberation or by washing to a lower cut point in the drum circuit. Washing to a lower cut point will reduce ash content and yield; these effects can be countered by increasing the cut point in the heavy medium circuit. This will have the effect of adding back ash with a lower base/acid ratio and increasing the yield. The effect on the product coal quality of over washing in the drum circuit and under-washing in the heavy medium circuit will be to reduce the base/acid ratio, probably cause a minor decrease in yield and have a marginal effect on ash content.

Phosphorus concentrations are not high in coal from Plant B. An association of phospho-

Table 10. Proximate, ash chemistry and rheological data for Plant B.

	test/clean prod coal #1	clean prod coal #2	75% clean coal+25% drum	75% cl coal+25%hmc	100% drum plant	100% hmc	75%cl coal+25%bird	100% bird	5%bltp+20%cl+d+25%b+50%hmc	75% cl coal+25% belt P	100% clean	100% clean	100% drum	100% hmc	100% bird	50% clean+50% drum	50% clean+50% hmc	50% clean+50% drum	50% clean+50% bird	60% clean+40% belt	5%b+25%brd+50%hmc+20%	100% clean	100% raw coal fines	100% raw coal	75% clean+25%raw fines	100% clean	
Ash%	9.7	9.8	10.4	9.6	10.9	8.8	10.1	11.2	10.3	11.2	9.7	9.8	10.8	9.1	11.2	10.4	9.4	9.7	10.4	11.9	9.9	9.9	9.6	23	38.2	13.2	9.8
VM%	21.2	21.5	21.4	19.7	18.4	21.3	21.1	22	21.5	21.4	21.8	20.9	20	21.6	22.2	20.6	22	19.9	20.8	20.9	21.6	21.7	19.2	16.4	20.9	21.2	
FC%	69.1	68.7	68.2	70.7	69.9	68.3	66.8	68.2	68.2	67.4	68.5	69.3	69.2	69.3	66.6	69	65.6	70.4	68.8	67.2	68.5	68.7	57.8	45.4	65.9	69	
H%	4.1	4.2	4.1	4.1	4.1	4.3	4.3	4.2	4.3	4.1	4.3					4.2	4.4	4.2	4.3	4.1	4.2	4.2	3.7	2.9	4.1		
S%	0.37	0.36	0.33	0.39	0.29	0.41	0.41	0.47	0.4	0.4	0.39	0.38	0.34	0.39	0.45	0.33	0.38	0.38	0.41	0.4	0.41	0.39	0.44	0.34	0.39		
O%	3.4	2.5	2	3.4	2.9	3.7	3.3	3.2	3	4.4	2.5					3.1	3.2	3.2	3.1	3.3	3.8	3.3	3.4	3.7	3.5		
SiO ₂	59.5	60	58.1	59.9	56.7	59	61.1	62.2	58.5	59	58.6					57.1	58.6	56.9	60	60.3	59.9	59.2	64.1	67.3	61		
Al ₂ O ₃	21.7	22	20.6	22.2	17.8	22.9	22.3	22.6	21.3	21.9	21.4					19.8	22.5	20.9	22.2	23.8	23.2	21.6	20.9	18.6	21.1		
Fe ₂ O ₃	4.8	4.7	5.6	4.5	6.2	4.6	4.2	3.7	4.8	4.5	4.6					5.3	4.4	5.1	3.6	4.3	4.3	4.2	3.2	3.1	3.9		
TiO ₂	1.3	1.3	1.2	1.2	1	1.2	1.3	1.4	1.2	1.2	1.2					1.1	1.2	1.2	1.3	1.3	1.2	1.2	1	0.9	1.1		
P ₂ O ₅	0.6	0.7	0.6	0.6	0.8	0.7	0.5	0.4	0.6	0.5	0.6					0.7	0.6	0.9	0.4	0.3	0.6	0.6	0.3	0.3	0.4		
CaO	4.4	4.3	5.2	4.2	8	4.2	4.1	3.3	4.6	3.9	4.2					6.2	4.2	5.7	3.4	3.2	4.3	4.1	3.1	2.6	3.6		
MgO	1.3	1.3	1.4	1.2	2	1.1	1.3	1.2	1.4	1.4	1.3					1.7	1.2	1.6	1.2	1.4	1.5	1.3	1.3	1.4	1.3		
SO ₃	3.5	3.1	3.5	2.9	3.8	3.1	2.9	2.4	3.7	2.9	3.2					4.8	3.8	4.6	3.1	2.4	2.7	4.1	2.4	1.6	3.1		
Na ₂ O	0.6	0.6	0.6	0.6	0.7	0.6	0.6	0.5	0.6	0.5	0.6					0.6	0.6	0.6	0.6	0.5	0.6	0.6	0.4	0.3	0.4		
K ₂ O	1	1	0.9	0.9	0.5	0.8	1.2	1.7	1.1	1.4	0.9					0.7	0.9	0.8	1.3	1.7	1.2	1	2.2	2.3	1.5		
BaO	0.6	0.6	0.6	0.6	0.5	0.7	0.6	0.6	0.6	0.6	0.6					0.6	0.6	0.6	0.6	0.6	0.7	0.6	0.5	0.3	0.5		
B/A	0.16	0.15	0.18	0.15	0.24	0.15	0.14	0.13	0.16	0.15	0.15					0.2	0.15	0.19	0.13	0.14	0.15	0.15	0.13	0.12	0.14		
start C°	435	436	436	429	449	429	432	432	433	435	435	434	439	432	430	441	431	436	432	441	433	433	438	440	435	432	
fusion C°	451	451	455	452	447	447	449	447	453	453	453	452	452	449	447	48	48	450	450	450	453	456	453	451	451		
max C°	462	462	461	463	459	465	462	462	460	463	463	459	458	462	461	460	480	458	462	461	461	458	460	459	455	459	
final C°	483	483	478	481	471	483	480	481	477	475	479	478	469	480	481	473	478	478	479	475	476	477	472	466	475	477	
solid C°	489	486	483	488	480	486	485	485	482	484	483	483	478	486	485	482	486	482	485	479	486	483	481	475	480	483	
range	48	47	42	52	22	54	48	49	44	40	44	44	30	48	51	32	47	41	47	34	43	44	43	26	40	45	
ddpm	13.5	10.3	6.2	11.6	3.3	19	10.2	22.8	7.9	4.4	5.6	8.7	2.2	11.4	16.4	2.8	10.3	3.7	10.1	4.2	7.6	6.8	3	1.7	5.1	7.5	
soft T	402	412	415	411	421	406	401	401	402	399	399	411	399	399	411	399	405	399	402	408	411	405	406	416	428	404	
max C C°	452	457	458	452	479	447	454	448	455	454	456	454	473	452	449	470	454	464	456	457	458	456	479	500	465	456	
max D C°	481	481	482	479	481	479	479	479	477	477	479	480	478	476	478	480	478	480	479	482	481	482	481	483	480	483	
C	28	24	25	26	21	27	29	29	26	29	27	30	27	29	29	26	28	26	26	28	27	28	22	6	26	30	
D	-3	-8	-16	-1	0	7	-4	8	-11	-12	-8	-5	0	-7	5	0	-5	-25	-3	-10	-11	-7	0	0	-21	-10	
FSI	7	7	5.5	7	2	7	7	7.5	6.5	5	7.5	7	2.5	7	7.5	4	7	5	7.5	5.5	7	7	4	0	0	-10	

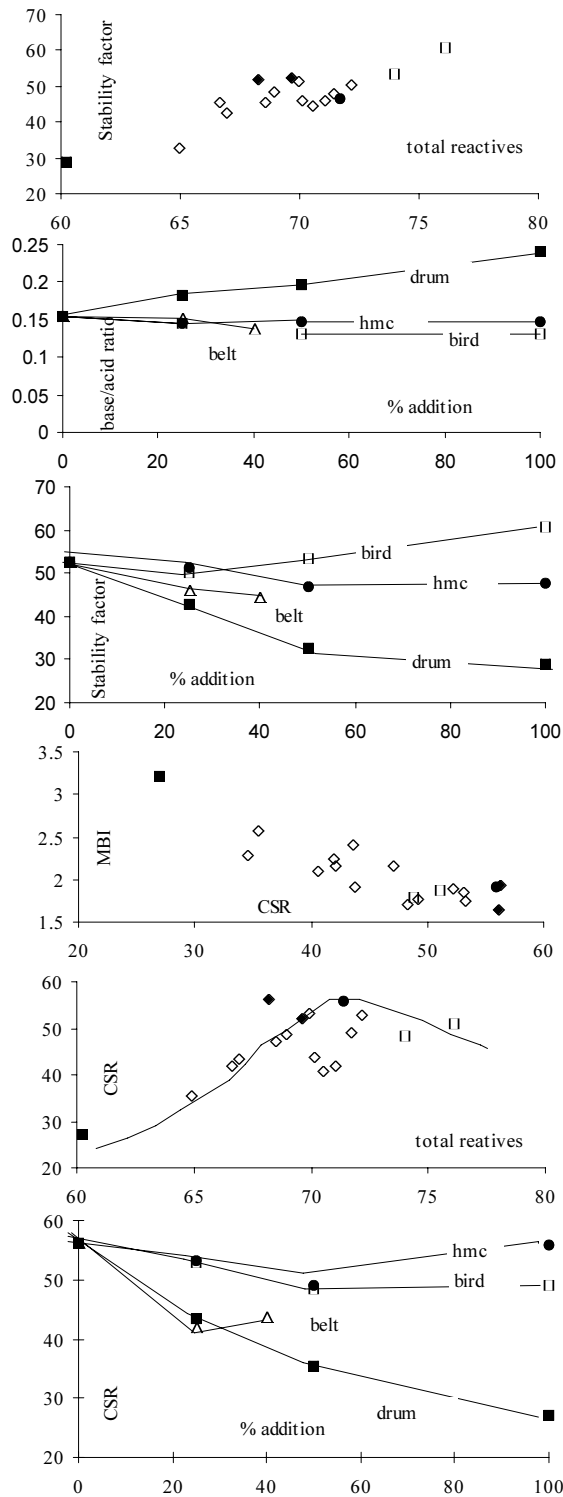


Figure 14. Stability Factor and CSR versus total reactivities and MBI, CSR, B/A and SF versus additions to clean coal of material from different circuits; Plant B. Drum=solid square, bird=open square, hmc=solid circle, belt press=open triangle, blend=open diamond, clean coal=solid diamond.

Table 12. Linear correlation matrix for clean coal ash chemistry, Plant B.

x	SiO ₂	Al ₂ O ₃	Fe ₂ O ₃	TiO ₂	P ₂ O ₅	CaO	MgO	SO ₃	Na ₂ O	K ₂ O	B/A
SiO ₂	1.0										
Al ₂ O ₃	.81	1.0									
Fe ₂ O ₃	-.76	-.95	1.0								
TiO ₂	.64	.89	-.77	1.0							
P ₂ O ₅	-.73	-.46	.42	-.37	1.0						
CaO	-.85	-.98	.92	-.91	.60	1.0					
MgO	-.89	-.97	.88	-.86	.62	.98	1.0				
SO ₃	-.82	-.47	.33	-.31	.57	.50	.62	1.0			
Na ₂ O	-.49	-.78	.74	-.88	.38	.82	.73	.01	1.0		
K ₂ O	.70	.83	-.74	.95	-.59	-.91	-.85	-.35	-.86	1.0	
B/A	-.86	-.99	.95	-.88	.56	.99	.98	.49	.80	-.87	1.0

rus with semifusinite plus fusinite in the clean coal is apparent (Figure 15). The high phosphorus contents in two raw samples (star and cross) indicate that there is some easy to remove phosphorus in the ash but in the clean samples the phosphorus correlates positively with semifusinite+fusiinite and negatively with ash. Therefore concentrations are higher in coarse and intermediate sized fractions and in intermediate SG splits where the inert macerals tend to concentrate, and lower in the fine coal and low SG splits.

Plant C

Plant C uses a tromp bath to wash the plus 10 mm material and heavy medium cyclones for

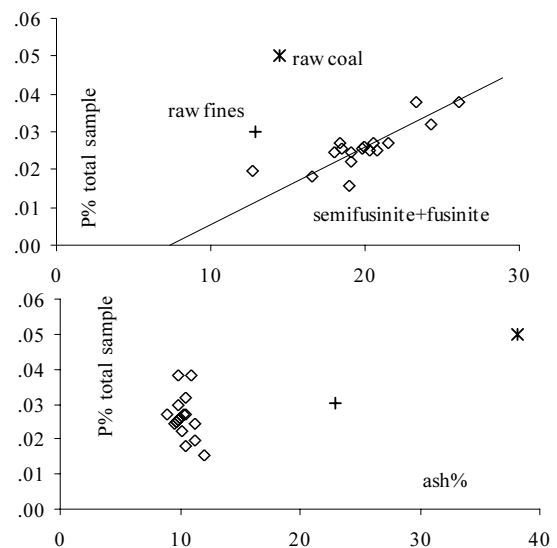


Figure 15. Relationship of phosphorus to ash and inerts content of coal, Plant B. Most of the samples are cleaned to about 10%.

Table 13. Coal quality, ash chemistry, rheology and carbonization data for plant C. A=clean coal, B=tromp clean coal, C=heavy medium cyclones clean coal, D=filter cake.

	A	85%A+15%D	50%A+50%D	85%A+15%B	50%A+50%B	A	C	B	D	50%C+50%B	50%C+50%D
Ash%	6.9	6.8	7.2	7	7.5	6.7	6.1	8.8	7.5		
VM%	29.6	29.8	29.4	28.6	28.1	29.2	29.5	27.3	28.9		
VMdaf	31.79	31.97	31.68	30.75	30.38	31.30	31.42	29.93	31.24		
FC%	63.5	63.4	63.4	64.4	64.4	64.1	64.4	63.9	63.6		
H%	4.9	4.9	4.9	4.9	4.9	5	5	4.7	4.9		
S%	0.65	0.66	0.67	0.65	0.6	0.66	0.7	0.59	0.71		
O%	3.9	4.2	3.8	4.2	4.3	4	4.1	4.1	4.4		
SiO ₂	59.4	58.9	61.5	60.1	60.4	56.4	58.6	61.1	62.3		
Al ₂ O ₃	23.9	23.8	24.1	23.6	23.1	24	24.8	22.5	23.3		
Fe ₂ O ₃	5.4	5	4.7	6	6.7	5.5	6.2	7.4	3.7		
TiO ₂	1.7	1.8	1.9	1.6	1.3	1.8	1.5	1	1.9		
P ₂ O ₅	2	1.9	0.7	2.1	2.2	1.9	2.6	2.1	1.3		
CaO	2.2	2.2	1.9	2.5	2.8	2.3	2.7	3	1.7		
MgO	0.5	0.6	0.7	0.5	0.4	0.5	0.3	0.3	0.9		
SO ₃	0.8	0.7	0.5	0.5	0.5	0.7	0.7	1	0.9		
Na ₂ O		0.1	0.1								
K ₂ O	1.3	1.4	1.9	1	0.7	1.3	0.5	0.3	2.4		
BaO	0.3	0.3	0.3	0.3	0.2	0.3	0.4	0.2	0.3		
B/A	0.114	0.114	0.110	0.121	0.127	0.120	0.119	0.132	0.103		
start C°	411	408	412	409	412	409	402	413	413	412	409
fus C°	422	421	425	422	424	421	420	426	427	425	424
max C°	448	445	451	447	448	447	446	450	450	448	449
final C°	478	477	481	475	474	477	478	474	451	474	477
solid C°	481	480	484	478	477	481	482	478	486	478	480
range C°	67	69	69	66	62	68	76	61	68	62	68
ddpm	690	760	660	530	410	580	915	190	430	225	365
FSI	9	9	9	8.5	8.5	8.5	8.5	6	9	8	9
sf TC°	375	377	380	378	383	378	371	384	378	377	376
max C C°	424	426	426	427	431	427	425	436	425	434	428
max D C°	467	470	468	468	466	468	466	467	465	464	465
C	32	31	32	31	27	31	30	28	29	33	31
D	148	139	146	109	62	127	137	10	145	50	109
Vit%	77.4	77.3	81.9	75.6	67	73.8	79.2	48.4	88.7	63.6	79.4
ex%	1.9	0.9	0.8	1.1	1.1	2.2	1.6	1.5	1	1.1	1.2
SF%	13.5	13.8	10.1	15.3	22.6	15.2	12.5	36	4.3	25.6	11.7
Mic%	1.4	1.9	1.9	1.4	2	2.3	1.4	2.8	1	3	1.7
Fus%	1.9	2.2	1.2	2.6	3.1	2.7	1.8	6.3	0.7	2.6	2.2
MM%	3.9	3.9	4.1	4	4.2	3.8	3.5	5	4.3	4.1	3.8
Rmax%	1.06	1.06	1.05	1.06	1.06	1.06	1.06	1.04	1.05	1.05	1.04
SI	49.2	50.4	43.3	52.2	53.2	51.5	47.7	51	34.4	54.1	46
H ₂ O	3.5	3	2.8	3.2	3	3.4	2.8	2.7		2.8	2.9
ASTM BD	778.4	776.8	776.8	780	780	775.4	781.6	778.4		778.4	778.4
max wall Kpa	7.86	7.72	7.72	6.14	4.48	7.65	6.27	1.59		5.24	10.55
coke yld	73.1	72.4	73.9	73.9	74	72.8	72.7	74.3		73.9	73
Ash%	9.1	9.2	9.7	9.5	10.2	9.1	8			1.03	9.8
VM%	0.5	0.5	0.5	0.4	0.2	0.3	0.5			0.5	0.5
S%	0.55	0.55	0.55	0.55	0.52	0.55	0.44			0.6	0.59
mean coke size	55.6	53.2	53.9	54	50.3	51.6	52.3	53.3		50.5	53.1
Stability	54.3	54.4	53.3	55.6	55	55.6	52.8	46.4		52.3	52.1
hardness	64.8	65.2	63.1	65.2	64.8	65.9	63	65.8		66.8	65.6
CRI	21.4	23.1	22.3	22.8	22.4	19.3	22.2	28.3		24.4	22
CSR	62.1	58.9	59.4	60.6	62	67.2	58.8	54.6		61.9	61.4

the 10.0 mm by 0.6 mm material. The 0.6 mm by 0.0 mm material is classified using water only cyclones and the 0.15 mm by 0.0 mm material is washed in flotation cells. Spirals are also used to clean the fine coal. The sampling program was similar to that at plant B. Product coal, clean coal from the various circuits, and several combinations of product coal and coal from various circuits were analyzed (Table 13).

The reactive maceral content of the clean coal increases and base/acid ratios decreases as the size decreases and consequently base/acid ratios have a good negative correlation with reactive maceral content (Figure 16). This is not because of an association of alkali rich minerals with inert macerals, but rather because the vitrinite concentrates in the fine circuits and the base/acid ratio is influenced by the probable presence of siderite and ankerite occurring in the coarse clean coal. This is inferred from the strong correlation of Fe_2O_3 with CaO and lack of correlation with ash (Table 3).

The stability factor reaches a maximum at about 80% reactives and despite additions of fine coal that increase the reactive content, it then decreases as reactive content increases (Figure 17). In fact the best stability factor appears to be achieved with the present mix of material from

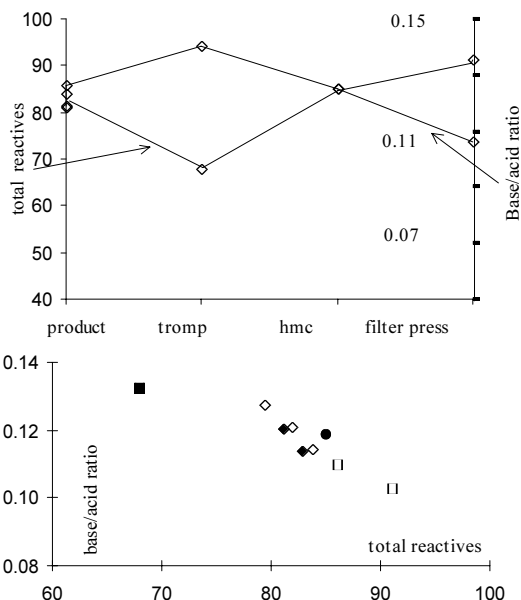


Figure 16. Plant C; Variation of petrography and base/acid ratio with size. Solid diamond=clean coal, solid circle=hmc, open square=fines or additional fines, solid square=drum, open diamond=additional coarse coal.

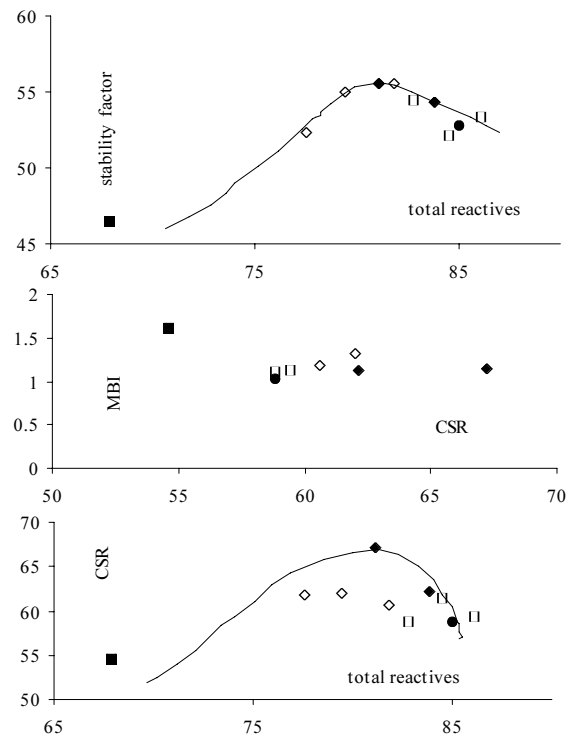


Figure 17. Stability Factor and CSR versus total reactives and CSR versus MBI for coal from Plant C. Solid diamond=clean coal, solid circle=hmc, open square=fines or additional fines, solid square=drum, open diamond=additional coarse coal.

the various circuits. It is not clear if this is because 80% is the optimum amount of reactives or the fine vitrinite has poor rheology. The vitrinite versus oxygen relationship is ambiguous and there is no clear evidence that the fine vitrinite contains less oxygen than the coarse vitrinite. Removal of drum product from the clean coal may increase stability factor by increasing the reactives content of the product but it is possible that at about 80% reactives the coal is close to the optimum reactives content for maximum stability factor.

Decrease in base/acid ratio in the fine coal (Figure 17) does not translate into a noticeable improvement in CSR, probably because the percentage spread in base/acid ratios is only 25% and also in part because the main oxide effecting MBI values is Fe_2O_3 , which may be less detrimental to CSR than CaO. CSR values are more sensitive to changes in ash content than ash chemistry (Table 3) and ash content in the clean coal is not correlated to base/acid ratio. This means that a noticeable improvement in CSR values may be achieved by reducing the ash content of the clean coal. Indications are that a 1%

decrease in ash content could increase of CSR values of up to 5.

Phosphorus correlates with the inert maceral content of the clean coal and is therefore concentrated in the coarse and intermediate sizes (Figure 18). Because phosphorus minerals (mainly apatite) occur in cells in the inert macerals, crushing the coarse coal to a finer size will not liberate much apatite. Over washing the coarse material and underwashing the fine material may reduce the phosphorus content. Based on the calculated distribution of phosphorus between inerts, reactives and ash in similar coals (Ryan and Grieve, 1995) and the variation of the reactives/inerts ratio by SG (Figure 1), it is possible to model the distribution of phosphorus by size and SG and compare the results to the actual phosphorus versus inerts distribution (Figure 18). The model washability data predicts a similar phosphorus distribution to that seen and can therefore be used to estimate the effect of over washing the coarse circuit. The predicted product coal has 7.1% ash, 0.062% phosphorus and a yield of 66%. If the SG in the coarse circuit is lowered the new product is predicted to have 6.6% ash, 0.059% phosphorus and a yield of 47%

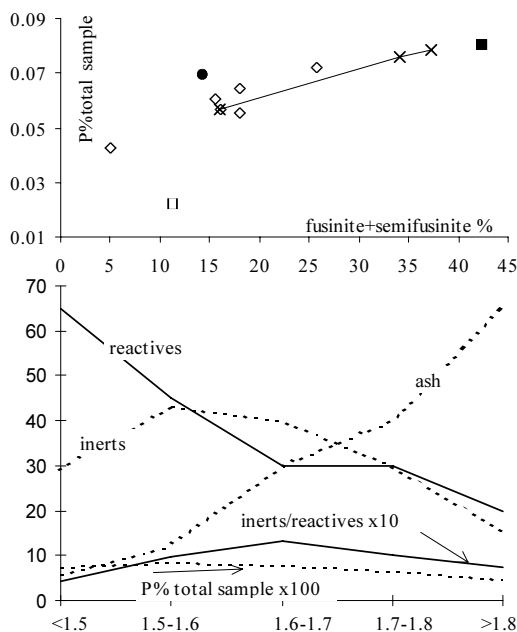


Figure 18. Phosphorus versus fusinite+semifusinite for Plant C, with model washability data and calculated theoretical phosphorus contents for three circuits (solid line and crosses). Symbols same as Figure 17.

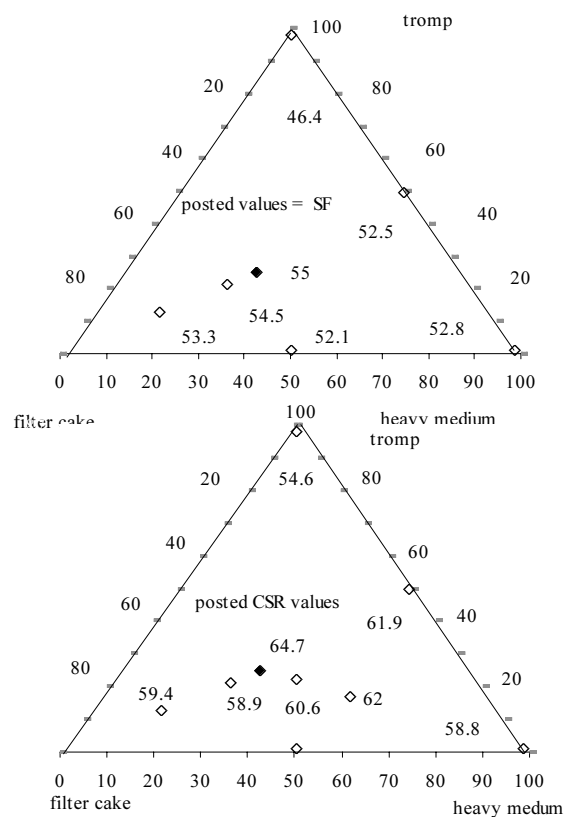


Figure 19. Variations of Stability Factor and CSR for blends of material from different circuits, Plant C.

59%. These numbers are based on modeling ash, phosphorus and inerts distributions and therefore only reflect trends. It appears that phosphorus can only be reduced a little by changing cut points in circuits, which incurs a yield penalty.

The various blends of product, tromp, heavy medium and filter cake coals are displayed in a triangular plot (Figure 19) from which it is apparent that the best quality is obtained from a mixture of all three components (the plotted position of the product coal is approximate).

Plant D

Plant D uses heavy medium cyclones, water only cyclones and froth flotation to produce thermal and metallurgical grade products by washing medium-volatile bituminous coal from two mines (coal A and coal B). The plant operating strategy is to produce acceptably low sulphur metallurgical and thermal coal products by blending the products from the various plant circuits and the two source coals, which generally

Table 14. Coal quality, ash chemistry, petrography and rheological data for Plant D. ASCF=secondary cyclone feed, SCOF=screen over flow, TP=thermal product, FT=float tails, FC=filter cake, PC=primary cyclone.

	RAW COAL				PC feed	MET PRODUCT				SCF 50x0.07	Coarse reject	TP				SCOF 0.07x.015	FC <0.015	FT <0.015
	size mm 50x0	25x12.5	12.5x3.35	<3.35		50x0.7	50x6.3	6.3x0.2	10x0.2			50x0.07	50x6.3	6.3x0.2	0.2x0.0			
Ash%	28.9	36.8	20.6	14.5	32.7	2.2	2.7	2	2.1	67.1	89.3	7.7	9	7.1	6	6.4	4.7	65.7
VM%	28.4	26.5	31.5	32.4	27	37	37.7	37.4	36.2	17.1	8	35.2	35.4	35.6	35.5	35.3	34.4	16.7
FC%	42.7	36.7	47.9	53.1	40.3	60.8	59.6	60.6	61.7	15.8	2.7	57.1	55.6	57.3	58.5	58.3	60.9	17.6
H%	3.9	3.4	4.4	4.6	3.7	5.3	5.3	5.4	5.3	2.1	0.7	5.2	5.1	5.2	5.2	5.1	5.2	2.1
S%	1.85	2.14	2.11	2	2.1	1.32	1.65	1.19	1.18	2.32	1.66	3.53	3.82	3.5	2.89	1.67	1.51	1.35
O%	3.4	3.6	4.1	3.9	3	5	4.5	4.7	4.6	1.8	3.9	3.7	3.3	3.5	3.9	4.3	4.5	3.3
SiO ₂	60.9	53	55.2	49.4	56.1	25.9	22.8	27	26.1	53.9	60.4	27.3	29.8	24.8	25.8	40.4	35.3	52.1
Al ₂ O ₃	21.6	24.1	23.5	23.3	24.1	17.4	14.6	19.2	16.9	23.2	22.7	15.9	16.3	14.8	16	20.1	18.3	23
Fe ₂ O ₃	10.5	10.4	14.1	16.8	10.9	49.5	58.5	48	49	16.4	6.9	49.4	48.1	54.2	52	28.9	31.7	13.3
TiO ₂	0.9	0.9	0.9	0.9	1	0.9	0.8	0.9	0.9	1.2	0.9	0.7	0.8	0.6	0.6	0.9	1	1.2
P ₂ O ₅	0.1	0.1	0.1	0.2	0.1	0.4	0.4	0.3	0.4	0.1	0.1	0.3	0.5	0.4	0.4	0.2	0.3	0.1
P%	.013	.016	.009	.013	.014	.004	.005	.003	.004	.029	.039	.010	.020	.012	.010	.006	.006	.029
CaO	0.3	0.1	0.4	1.2	0.4	1.2	0.9	0.2	1.8	0.2	0.1	1	0.9	1.1	1.6	2.2	3.4	1.8
MgO	1.4	1.4	1.3	1.3	1.3	0.6	0.5	0.6	0.7	1.3	1.4	0.5	0.4	0.4	0.5	1.1	1.2	1.3
SO ₃	0.5	0.4	0.6	1.2	0.6	0.8	0.8	0.9	1.3	0.6	0.4	1.3	0.8	1.3	1.3	1.2	2.6	2.3
Na ₂ O	0.5	0.4	0.5	0.8	0.6	0.8	0.5	0.8	1.3	0.3	0.4	0.3	0.3	0.3	0.6	1.4	2.2	0.9
K ₂ O	3.2	3.5	3.4	3.1	3.5	0.6	0.4	0.6	0.7	3.4	3.5	0.8	0.8	0.8	0.9	2.1	1.8	3.3
B/A	0.19	0.20	0.25	0.32	0.21	1.19	1.59	1.07	1.22	0.28	0.15	1.18	1.08	1.41	1.31	0.58	0.74	0.27
Vit%	78.5	75.2	81.9	85.5	81.9	82.3	76.8	80.1	83.3	73.4		78.3	68.2	78.6	83.7	85.6	88.5	78.0
ex%	5.4	5.2	4.0	3.9	4.6	5.5	7.1	5.3	4.2	7.2		5.2	8.8	4.7	3.5	3.3	2.8	4.2
SF%	8	9	6.1	3.7	5.9	5.2	7.2	6.8	4	8.6		9.6	12.3	7.6	4.9	5	2.6	6.2
Mic%	5.6	8	5.1	4	4.9	4.5	5.8	5.4	4.9	6.2		3.5	7	5.8	4.6	2.9	4	4
Fus%	2.5	2.6	2.9	2.9	2.7	2.5	3.1	2.4	3.6	4.6		3.4	3.7	3.3	3.3	3.2	2.1	7.7
TR%	87.9	84.9	89.0	91.3	89.5	90.4	87.5	88.8	89.5	84.9		88.3	83.2	87.1	89.7	91.4	92.6	85.3
Rmax%	0.96	0.95	0.98	0.98	0.95	0.97	0.96	0.95	0.98	0.94		0.96	0.94	0.96	0.95	0.98	0.96	0.95
SI	48.5	35	48.8	42.4	45.7	32.1	38.3	34	34			41.1	46.1	41.9	36.3	35.3	28.9	
startC°	386	384	383	389		379	377	380	379			379	379	381	383	381	387	
fusC°	400	400	399	402		398	395	397	397			397	396	398	399	398	404	
max C°	438	440	437	435		436	436	437	436			438	436	439	436	438	438	
final C°	475	474	480	479		477	480	480	479			478	478	479	479	480	480	
solid C°	478	477	483	482		480	483	483	482			481	481	482	482	483	483	
range C°	89	90	97	90		98	103	103	103			102	99	98	96	102	93	
ddpm	21300	20300	28000	23800		28000	28000	28000	28000			28000	28000	28000	28000	28000	28000	
sf TC°	354	368	356	356	366	348	344	351	351			347	347	345	350	348	351	
max C C°	414	419	408	409	417	398	398	398	398			402	404	402	402	402	403	
max D C°	464	462	463	462	462	465	463	467	465			461	461	461	463	464	462	
C	27	24	29	28	25	28	30	26	26			28	28	28	28	25	26	
D	118	42	198	203	76	270	290	274	265			246	247	252	249	259	238	
FSI	4.5	3	4	7	4.5	7.5	7	7	7.5			6.5	5.5	7	8	8	7.5	

have quite high run of mine sulphur contents. The sampling program was comprehensive involving sampling of raw coal, feed coal and product coal from the circuits. Samples were taken while the plant was washing the two source coals (A and B) separately. This enabled different qualities and washing characteristics of the two coals to be determined. Previously it was assumed that the two coals had similar washing characteristics, but data from this study revealed a number of differences. The analytical data for coals A and B and the coal quality and carbonization data for blends are in Tables 14, 15.

The petrography of the two coals is slightly

different both are vitrinite rich, but coal A contains less vitrinite and more micrinite than coal B and consequently has a lower reactive maceral content. Though both coals contain about the same amount of exinite in the raw feed, coal A retains more exinite in the various component clean coals and this partially explains the higher fluidity. Most samples of coal A have maximum fluidities over 28 000 ddpm (Table 14). Fluidity for coal B is generally lower and values correlate with total reactives content, though the vitrinite enriched finer coals tend to have lower than expected fluidities.

Raw coal A contains slightly less sulphur than

Table 15. Coal quality, ash chemistry, petrography and rheological data for Plant D. BSCF=secondary cyclone feed, SCOF=screen over flow, P=thermal product, FT=float tails, FC=filter cake, PC=primary cyclone

size mm	RAW COAL			PC	MET PRODUCT			SCF	Coarse	TP			FC	FT			
	50x0	25x12.5	12.5x3.35		50x0.7	50x6.3	6.3x0.2			10x0.2	50x0.7	50x0.7			50x6.3	6.3x0.2	0.2x0.0
Ash%	40.9	48	35.3	26.6	40.9	2.5	3.5	2.2	2.5	90.3	8.1	12.8	8.4	7.1	9.9	13.1	90.4
VM%	23.4	21.5	25.4	27.4	23.3	35.1	35.5	36	34.9	7.7	33.3	33.6	33.7	33.7	32.7	30	9.6
FC	35.7	30.5	39.3	46	35.8	62.4	61	61.8	62.6	13.7	2	58.6	58	59.2	57.4	56.9	0
H%	3.1	3	3.5	3.9	3.1	5.3	5.3	5.3	5.2	0.6	4.9	4.7	4.9	4.9	4.7	4.4	0.7
S%	2.05	1.78	1.81	2.09	1.7	1.2	1.21	1.13	1.19	1.66	3.15	3.82	3.35	3.03	1.94	2.04	0.7
O%	4.6	4.3	4.2	4.3	3.8	6.9	6.1	6.6	6.1	4	5.5	4.2	5.5	5.3	6.5	4.8	3.3
SiO ₂	59	61.2	59.5	54	60	41.1	52.4	46.1	41.2	56.6	61.1	34	34.6	32.5	45.8	45.3	55.9
Al ₂ O ₃	22.6	22.9	22.8	21.9	22.6	18.1	19.9	19.8	17.7	21.5	23	14.9	16.6	14.8	15.1	19.2	22
Fe ₂ O ₃	9.9	8.4	9.6	11.6	8.9	26.5	20.2	23.6	29.3	7.3	40.3	34	41.8	43.3	19.8	18	8.9
TiO ₂	1	1	1	1	1.1	1.2	1.2	1.2	1.4	1.2	1	0.9	1.1	0.9	0.8	0.9	1.1
P ₂ O ₅	0.2	0.4	0.2	0.3	0.2	0.5	0.4	0.5	0.5	0.2	0.1	0.5	0.6	0.5	0.6	0.3	0.2
P%	.036	.084	.031	.035	.036	.005	.006	.005	.005	.063	.018	.034	.018	.019	.013	.011	.039
CaO	1	0.6	0.8	2.5	0.7	3.9	2.2	3.8	4.4	0.5	0.4	2.6	1.9	2	3.1	4.6	3.2
MgO	1.7	1.7	1.7	1.6	1.7	0.7	0.9	0.7	0.8	1.6	1.7	0.5	0.6	0.5	0.6	1.2	1.6
SO ₃	1.4	0.9	0.9	3.1	1	3.2	1.2	2	2.4	1	1.2	3.3	1.9	1.9	3.4	4.1	2.2
Na ₂ O	0.5	0.4	0.5	0.7	0.5	1.2	0.8	1.1	1.3	0.4	0.4	0.5	0.3	0.5	0.6	1	0.7
K ₂ O	3.8	3.7	3.8	3.4	3.7	1.3	1.9	1.4	1.3	3.6	3.9	1.2	1.5	1.2	2.5	2.6	3.5
B/A	0.21	0.18	0.20	0.26	0.19	0.57	0.36	0.46	0.63	0.24	0.16	0.92	0.64	0.93	1.03	0.44	0.23
Vit%	85.5	82.7	84.6	87.3	87.4	88.2	86.6	86.9	89.8	80.4	77	78.3	67	79.3	83.1	87.3	88.4
ex%	5.3	4.4	4.7	2.4	2.6	2.2	3.8	3.9	1.8	4.6	7	4.5	8	4.7	2.3	3.5	1.6
SP%	4.6	6.3	4.9	4.6	5.1	3.9	4.7	3.1	3.7	8.2	9	10.2	13	7.4	6.5	2.7	3
Mic%	2.3	2.7	3.1	3.3	2.1	2.5	1.3	2.4	2.7	3.2	6.0	2.0	5.4	2.7	3.0	3.9	5.1
Fus%	2.3	3.9	2.7	2.4	2.8	3.2	3.6	3.7	2	3.6	1	5	6.6	5.9	5.1	2.6	1.9
TR%	93.1	90.3	91.8	92.0	92.6	92.4	92.8	92.4	93.5	89.1	88.5	87.9	81.5	87.7	88.7	92.2	91.5
Rmax%	0.94	0.94	0.95	0.97	0.96	0.97	0.95	0.96	0.97	0.96	0.96	0.94	0.94	0.95	0.94	0.97	0.96
SI	41.6	24.4	47.1	49.6	43.7	26.7	24.8	23.8	21.2	21.2	42.2	47	41.7	38.6	37.1	39	39
startC°	398	398	397	403	398	393	391	395	393	393	394	396	393	394	388	403	403
fusC°	407	407	406	413	408	405	403	403	407	407	407	409	404	405	402	413	413
max C°	436	436	435	440	437	438	432	432	438	438	437	437	438	436	438	439	439
final C°	465	466	467	468	467	473	473	474	472	472	467	468	468	469	471	466	466
solid C°	468	469	470	471	470	476	476	477	475	475	470	471	471	472	474	469	469
range C°	67	68	70	65	69	80	82	79	79	79	73	72	75	75	83	63	63
ddpm	900	1110	1510	690	1120	6640	15590	12150	4300	1680	2120	2120	2750	1810	3450	400	400
sfTC°	390	408	387	383	399	369	368	371	368	362	366	363	363	363	369	372	372
max C C°	438	444	424	424	438	409	408	410	411	411	417	413	413	413	414	423	423
max D C°	447	448	454	447	447	449	452	449	449	450	450	450	449	449	452	455	455
C	18	13	24	27	17	31	28	30	30	30	32	31	29	30	29	30	30
D	-13	0	6	18	-11	151	174	167	144	144	73	28	71	78	110	33	33
FSI						8	8	8	8.5	8.5	8	8	8	8	8.5	8	8

coal B, but washes to a slightly higher sulphur content and contains much more Fe₂O₃ than coal B. The Fe₂O₃ probably occurs in the mineral siderite. Sulphur is liberated somewhat into the fine feed but less than half is removed by washing, producing product metallurgical coals with sulphur contents in the range of 1% to 1.5% and thermal coals in the range 3% to 4%. Plots of S%

versus Fe₂O₃ % in total sample (Figure 20) provide some indication of how much of the iron and sulphur are combined as pyrite, how much excess iron exists as siderite and the concentration of organic sulphur. The slope of the line in Figure 20 (1.245) is that of the ratio of Fe/S in pyrite (FeS₂), taking into account that the Y axis is Fe₂O₃ and not Fe. The band, defined by the two lines, inter-

sects the X axis from 0.0% sulphur to about 0.6% sulphur and encloses samples containing pyrite and 0.0% to 0.6% organic sulphur. Points to the left and above this band contain excess Fe_2O_3 , which probably occurs as siderite, because Fe_2O_3 does not correlate with Al_2O_3 or SiO_2 (Table 16). The raw coal B appears to contain more siderite than A, though siderite tends to be removed by all circuits and is concentrated in the coarse and fine reject material (square symbols). Clean blends of each coal are represented by crosses and feed coal by solid symbols.

Coking tests were performed on number of blends each composed of one of the coals but made from different combinations of size fractions (Table 17). Maximum wall pressure was distinctly higher for blends using coal B. The blend composition, rank and bulk density were the same for the two coals, though the charge moisture for coal B was about 1% higher and the ash about 2% absolute higher. Usually a higher ash content will reduce pressure. In this case various sizes of washed coal A, which produced less

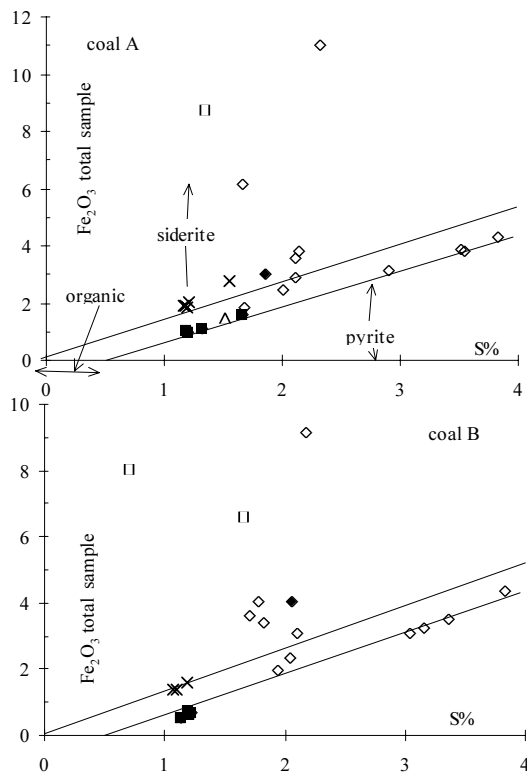


Figure 20. Approximate distribution of sulphur and iron between siderite, pyrite and organic sulphur. Coals A and B plant D. Open squares= reject material, solid diamonds=raw coal, open points =individual circuits, x= blend of sizes, solid squares=metalurgical coal.

Table 16. Linear correlation matrix for ash chemistry and CSR data, blend coals A and B from Plant D.

x	SiO_2	Al_2O_3	Fe_2O_3	Ash	P_2O_5	CaO	MgO	SO_3	Na_2O	K_2O	A	SA	CSR
SiO_2	1.0												
Al_2O_3	.97	1.0											
Fe_2O_3	-.7	-.6	1.0										
Ash	.92	.96	-.37	1.0									
P_2O_5	.80	.89	-.55	.84	1.0								
CaO	.95	.87	-.70	.81	.61	1.0							
MgO	.90	.82	-.62	.77	.55	.96	1.0						
SO_3	.96	.89	-.74	.81	.69	.97	.96	1.0					
Na_2O	.88	.88	-.59	.82	.68	.84	.89	.86	1.0				
K_2O	.91	.83	-.64	.77	.55	.97	.99	.97	.87	1.0			
A	.39	.47	.41	.68	.30	.32	.37	.27	.36	.36	1.0		
SA	.97	.93	-.61	.89	.68	.98	.95	.95	.90	.96	.45	1.0	
CSR	-.9	-.8	.9	-.6	-.6	-.9	-.9	-.9	-.8	-.9	.0	-.9	1.0

Note A=alkalinity (base/acid ratio*ash/100)

Note SA= Sum($\text{K}_2\text{O}+\text{MgO}+\text{CaO}+\text{Na}_2\text{O}$)*ash/100

pressure, contain more exinite and less vitrinite than coal B and this has the effect of increasing the VMdaf value for coal A by 1.5% absolute (VMdaf 37.5% for coal A and 36% for coal B). Increased vitrinite content increases pressure, whereas exinite reduces pressure and because of its very high volatile content will decrease coke yield. The exinite contents of the raw coals are similar and it appears that more exinite is lost from coal B during washing, possibly indicating a fundamental difference in the lithotypes. Exinite in both coals tends to concentrate in the coarser size fractions. The exinite content of high-volatile coals probably plays an important role in reducing maximum wall pressure. In this study a small average increase in the exinite content of the washed blends of coal A seems to be responsible for a pressure decrease from 7.3 kPa for blends of coal B to 1.1 kPa for blends of coal A.

Generally CSR has a negative correlation to the alkalinity of samples, but in this case there is a positive correlation between MBI and CSR (Figure 21). Compared to coal B, Coal A has higher CSR values associated with higher concentrations of Fe_2O_3 and lower concentrations of Ca, Mg Na and K. The Fe_2O_3 probably occurs as pyrite and it appears that in this form it is less damaging to CSR than the other alkalis especially CaO, which dominates Mg, Na and K in the chemistry of coals A and B and probably occurs as calcite on cleats in vitrinite. In experiments additions of pyrite to coals produced the same relative decrease in CSR as additions of calcite on a CSR versus MBI plot (Price *et al.*, 1992) so it appears that the association of these

Table 17. Plant D, Coal quality, ash chemistry, rheology, carbonization and coke texture data for blends of coals A and B. HV= high volatile blend coal, E=coal from Plant E.

size mm	A	A	A	A	A	B	B	B	B	HV	HV+E
3.8x0.07	75	75	65	85	56.25	75	75	65	85		
0.07x0.015	15	10	21	9	11.25	15	10	21	9		
0.015x0.0	10	15	14	6	7.5	10	15	14	6		
middlings 3.8x0.07					2.5						
Ash%	3.2	2.9	3.6	2.9	4.3	4.4	4.4	5.2	3.8	4.3	5.2
VM%	37.1	36.4	36.2	36.2	36	34.1	34.2	33.9	34.7	35.2	30.5
FC%	59.7	60.7	60.2	60.9	59.7	61.5	61.4	60.9	61.5	60.5	64.3
S%	1.41	1.4	1.45	1.44	1.97	1.29	1.3	1.36	1.23	1.34	1.08
SiO ₂	31.5	29.6	32.5	28.7	28.8	43	43.2	44.3	44.4	41.6	47
Al ₂ O ₃	18.5	17.6	18.3	17.5	16.7	18.8	19.4	19.3	18.9	19.2	22.6
Fe ₂ O ₃	43.2	45.6	40.9	47.2	49.1	21.7	22	21.1	23.2	25.3	16.8
TiO ₂	0.9	0.9	0.9	0.9	0.8	0.9	1	1	1	0.9	1.1
P ₂ O ₅	0.3	0.2	0.3	0.3	0.3	0.3	0.4	0.3	0.3	0.4	0.6
CaO	2.1	2.1	2.2	1.9	1.7	4.7	4.5	4.6	4.2	3.5	3.6
MgO	0.9	0.7	0.9	0.7	0.6	1.1	1.1	1.1	1	1.1	0.8
SO ₃	1	0.8	2.1	1.1	0.8	4	4.2	3.9	3.6	3.9	3.4
Na ₂ O	1.3	1	1.2	1	0.8	1	1	1	1	1	1
K ₂ O	1.3	1	1.4	1	0.9	1.9	2.1	2.1	1.9	1.9	1.4
LOF	0.6	2	0.6	0.5	1.4	2	2.2	2.1	0.8	2.2	2.3
startC°	384	385	382	382	378	395	395	396	394	392	397
fusC°	399	401	399	400	398	407	407	406	405	405	409
max C°	440	438	440	439	436	437	439	437	437	439	438
final C°	480	481	480	480	478	470	469	468	468	474	471
solid C°	483	484	483	483	481	473	472	469	471	477	474
range C°	96	96	98	98	100	75	74	70	74	82	74
ddpm	28000	28000	28000	28000	28000	2900	1970	1995	2460	6150	880
FSI	7.5	7.5	7	7.5	8	8	8.5	8.5	8	8.5	8
sf TC°	348	350	354	353	356	369	363	363	363	360	374
max C C°	402	402	404	402	403	404	401	400	401	404	420
max D C°	465	465	464	464	464	455	446	449	479	454	467
C	28	30	29	32	32	30	39	29	31	29	27
D	257	256	252	254	233	132	129	129	128	151	47
Coke Ash%	4.3	4.2	5	4	5.7	6.4	6.4	7.5	5.5	6	6.8
VM%	0.7	0.8	0.9	0.8	0.7	0.9	0.7	0.9	0.9	0.8	1
S%	1.2	1.18	1.21	1.17	1.55	1.1	1.07	1.18	0.98	1.07	0.83
H ₂ O	2.3	2.4	2.1	2.3	2.3	3.2	3.4	3.3	3.4	2.9	3.2
ASTM BD	776.8	776.8	776.8	778.4	776.8	778.4	780	778.4	776.8	780	778.4
linear expn	-25	-22.3	-25	-24.8	-23.8	-1.5	-7.2	-3	-4.7	-13.1	-8.1
max wall Kpa	1.24	1.24	1.24	0.62	1.02	8.3	9.41	5.5	6.1	3.4	9.6
max gas Kpa	0.69	1.18	1.38	0.62	0	19.3	11.4	13.8	18.1	6.3	18.3
coke yld	68	69.7	69.5	69.1	68.9	72.9	72.1	70.7	70.6	69.9	74.3
mean coke size	49.4	47.36	47.11	47.17	46.18	44.65	44.65	45.13	44.14	46.3	49.79
stability	34.3	36.1	38.6	32.7	38.9	33.8	16.9	39.8	33.1	40.2	57.1
hardness	62	62.1	61	63	62.6	68.9	34.2	68.8	68.5	68	68.7
CRI	40.3	38	38.8	38	40.5	53.8	55.5	55.1	50.6	50.9	45.7
CSR	33.7	39.1	35.5	38.3	45.1	21.5	24.2	22.8	28	26.3	26.1
mosaic	69.7	67	73.2	75.6	78	80.7	84.1	86.3	88		
flow	14.9	15.7	11.1	9.3	5.5	7.8	4.5	2.7	1.7		
domain	0.4	0.5	0.1	0.1	1	0	0	0	0		
inerts	15	16.8	15.6	15	15.5	11.5	11.4	11	10.3		

minerals in the natural samples influences how they effect CSR. The empirical rule seems to be that iron minerals are less destructive to CSR than calcite.

The best correlation for CSR is with SO_3 (Table 16, Figure 21), probably because SO_3 represents the formation of sulphates in the ash from organic sulphur and alkalis as they are released during the destruction of carbonates and other minerals. Obviously this is an approximate measure of the more mobile alkali components in the ash. For this particular plant it might offer the best way of estimating the CSR values of possible production blends. A similar though not as well defined trend is apparent in coals from the other plants (Figure 21).

Plant E

Plant E washes a low-volatile coal using 2 circuits, a heavy medium cyclone circuit to process the plus 0.6 mm material and froth floatation to process the minus 0.6 mm material. Product coal and a number of blends of product coal with coal from individual plant circuits were analyzed (Table 18).

Vitrinite is concentrated in the clean coal and fine coal feed (Figure 22). Despite the mod-

erate enrichment of vitrinite in the froth floatation feed and product, adding 10% product froth material to clean coal did not increase vitrinite content and did no improve stability factor (Figure 22). It appears that the best improvement in stability can be achieved by removing the inert rich plus 20 mm material from the clean coal, which accounts for about 5% of product.

The coal washes to a low ash (6% to 7%). Some blends were constructed to see what effect increased product ash content would have on coke quality. Blends composed of product coal plus additional feed or reject material were analyzed to see if ash content and yield could be increased without causing a major decrease in coke quality. It appears that a 2% increase in ash content reduces stability factor by about 20 points (Figure 23). Obviously at this rank ($R_{max} = 1.6\%$) coking properties are easily destroyed by the addition of inert material.

The maximum wall pressure of the product coal is quite high, as expected based on the high rank of the coal, but additions of small amounts of clean fine coal decrease pressure substantially while having only a minor negative effect on stability factor (Figure 23). In terms of pressure this is probably a good compromise but the increased fines content will make the coal more

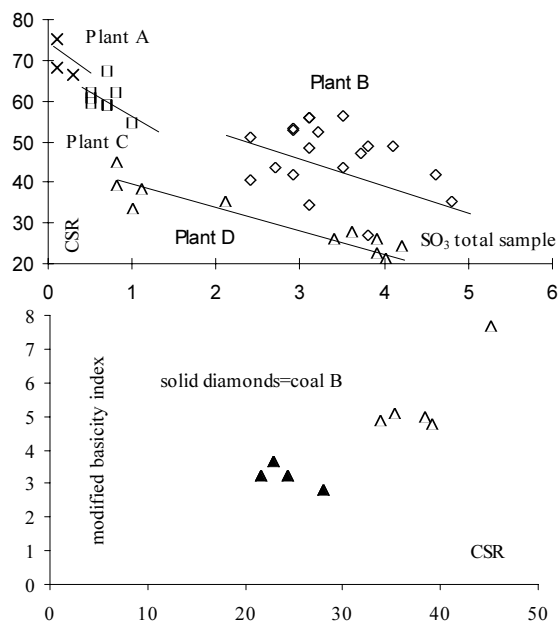


Figure 21. Relationship of CSR to SO_3 for different coals with different sulphur contents from plants A,B, C and D and relationship of CSR to MBI for coals A and B from Plant D.

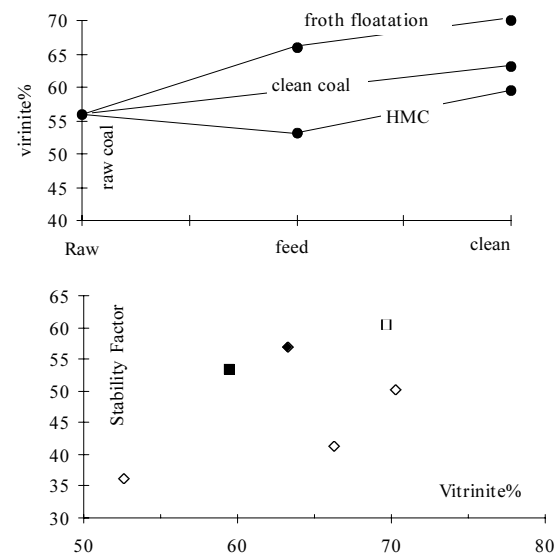


Figure 22. Vitrinite versus size and raw, feed and clean coal. Vitrinite versus stability factors, open diamonds=blends, open square=clean coal with plus 20 mm material removed, solid diamond=clean coal, solid square=clean coal with additional fines. Data from Plant E.

Table 18. Coal quality, rheology, petrography and carbonization data, Plant E.

	raw coal	cl coal	cl < 20 mm	hm prod	hm feed	hm reject	float prod	float feed	float reject	breaker reject	90% cl+10% cl fines	95% cl+5% reject	80% cl+20% feed	90% cl+10% rj fines	30% feed E+70% HV	24% E cl+6% E feed + 70%HV	30% cl E +70% HV
Ash%	19.4	6.7	6.4	6.6	19.1	61.7	7.4	14.5	29.6	78.3	6.8	10.7	8.9	7.5	10	7.2	6.4
VM%	16.3	17.4	17.5	17.3	16.6	13.3	17.5	16.8	15.6	14.2	17.6	17.5	17.5	17.8	29.4	29.8	29.9
S%	0.42	0.35	0.35	0.32	0.32	0.40	0.34	0.35	0.40	0.22	0.35	0.21	0.26	0.45	0.57	0.50	0.58
FSI	4	6.5	7	7	4		7.5	5.5			6.5	6	6.5	7.5	7.5	7.5	8
start C°		467	460	463	466		472	478			466	474	469	466	402	403	402
max C°	478	474	478	478	475		479	480			475	479	474	478	440	441	439
final C°		482	489	487	483		483	487			483	486	483	488	478	477	478
solid C°	496	493	497	493	492		498	495			492	497	496	501	481	481	481
range C°		15	29	24	17		11	9			17	12	8	22	76	73	76
ddpm	0.8	1.3	2.8	2	1.4		1.3	1.2			1.5	1.3	1.2	1.6	2150	2140	2520
sf TC°	441	438	429	434	437		432	441			435	437	434	435	363	363	362
max C C°		486	480	484			481	486			483	491	493	483	427	428	427
max D C°		495	498	495			497							495	466	468	468
C	16	24	26	24	22		23	23			24	26	27	24	27	27	26
D	0	-23	-13	-21	0		-19	0			0	0	0	-21	49	49	49
Vit%	56	63.2	69.7	59.4	52.6		70.2	66.2			61.5	62	61	61.5	65.3	65	63.7
ex%	0	0	0	0	0		0	0			0	0	0	0	5.5	4.4	5.8
SF%	22.4	24.8	17.8	26.8	24.6		16.6	17.2			12.8	23.8	25.2	22.8	11.5	17.4	16.2
Mic%	3.6	5.3	4.1	5.7	6		6.6	5			7	4.1	2.9	7	7.4	5.9	7.4
Fus%	6.6	3	4.9	4.5	5.6		2.5	3.3			4.9	4.1	5.9	4.9	4.6	3.2	3.3
MM%	11.4	3.7	3.5	3.6	11.2		4.1	8.3			3.8	6	5	3.8	5.7	4.1	3.6
Rmax%	1.63	1.63	1.62	1.65	1.64		1.64	1.64			1.62	1.63	1.63	1.62	1.1	1.13	1.08
H ₂ O coke		3.4	3.4								3.4	3.6	3.4	3.6	3	3	3.1
ASTM BD		784	790								784	778	782	787	781	786	783
max wall Kpa		30.8	42.1								8.8	3.8	4.7	4.07	2.41	4.55	4.9
coke yld		76.6	79.4								74.4	74.1	70.6	72.9	74.7	74.3	75.1
Coke Ash		8	7.6								7.9	11.7	9.7	7.8	11.8	9.1	8.3
VM%		0.8	0.9								1	0.9	0.8	1	0.9	1	0.8
S%		0.25	0.35								0.35	0.21	0.26	0.31	0.57	0.52	0.56
Stability		56.8	60.4								53.5	36.3	39.6	50.3	41.2	57.6	60.2
Hardness		63.7	67.2								62.3	49.6	52.3	59	62.4	68.4	69.1
CRI		24.2	21.3								24.5	31.8	28		29.4	28.8	27.5
CSR		66.8	70								65.2	40.9	47.9		47.9	56.1	58.9

hm = heavy medium, cl = clean, rj= reject, HV = high-volatile blend coal

difficult to transport and handle.

CONCLUSIONS

Generally economics dictate that plants have to maximize yield at a given specified clean ash content. Plants can not remove all the ash from the clean coal. This means that if the ash chemistry varies by size consist or specific gravity, then there is the possibility of changing the ash chemistry of product coal while at the same time having only a marginal effect on ash content and

yield. Before this is attempted it is important to know what minerals are effecting the ash chemistry and where they hide in the coal matrix. This can be achieved using standard microscope techniques, but the process is helped by using linear correlation matrixes of oxide data. In some coals, carbonates in the clean coal increase the base/acid ratio and decrease CSR values. A better understanding of the coal plus carbonate association with regards to size and SG splits gives the plant operator some flexibility to reduce base/acid ratios without incurring a major loss of yield and

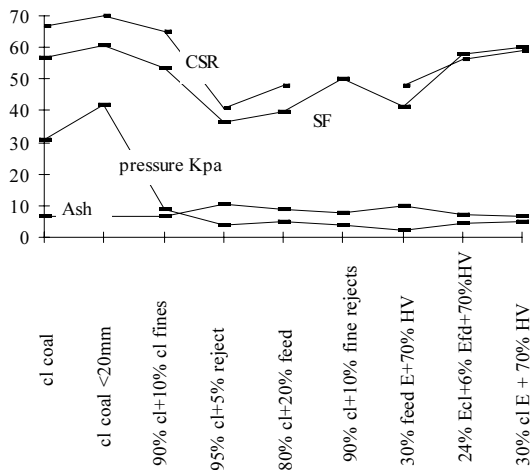


Figure 23. Variation of Stability Factor, CSR, ash and pressure (Kpa) for different blends of coal from plant E.

this has the potential to improve CSR values.

Coal macerals fractionate in plants in at least two ways. Firstly the vitrinite tends to concentrate in the finer sizes and secondly if the macerals are separated by crushing and washed using density separation, then the inert macerals tend to concentrate in the intermediate SG fractions and the vitrinite in the low density fractions. This pattern is confused in the coarser coal by incomplete liberation of the macerals and it is suspected that vitrinite tends to remain attached to in-seam rock material while the inert macerals tend to be liberated. Fine coal is washed by froth floatation using a wetting principle and it is not clear how this effects concentration of vitrinite into the clean coal. It appears that compared to fine feed coal there is an enrichment of vitrinite in the fine clean coal.

Plants are becoming very efficient at recovering coal from the various circuits and it is therefore difficult to influence the maceral composition of the clean coal. However it may be possible to increase the recovery of vitrinite rich coal from the fine circuit while decreasing the recovery in the more inert rich coarse circuit. This will probably require accepting a lower yield and it appears that increasing the content of fine vitrinite in the clean coal does not necessarily improve coke quality. Vitrinite enriched coal from fine circuits does not have the coke making properties that one would expect based on its reactive content. The problem does not seem to relate to the predicted optimum amount of reac-

tives in a sample because most of the coals studied are inert rich. Part of the effect may be size related but there may also be a chemical component to the problem. It is possible that altered non reactive vitrinite is concentrating in the fine material. There is some indication that fine vitrinite is oxygen deficient and may have experienced devolatilization or increase in rank caused by shearing or other geological process.

The size consist or Hardgrove Index of run of mine coal may indicate quality problems not apparent in proximate or petrographic analyses. Handling may not be the only problem associated with sheared coal. Shearing may increase the friability of vitrinite and decrease the rheology of some fine vitrinite grains. This is not unlike what is seen in artificial oxidation or alteration in underground mines where there have been fires. Over production of fines at the mine site may degrade coke quality by separating reactive and non reactive vitrinite, with the non reactive vitrinite concentrating in the fine coal. Addition of fine vitrinite rich coal is not guaranteed to increase coke quality despite the fact that it improves FSI and possibly fluidity of the product.

In addition to the above general conclusions, a number of other more coal specific insights were gained during the study.

Phosphorus is associated with the inert coal macerals in the coarse and intermediate sized circuits. Unfortunately the fractionation of phosphorus into the inert macerals is not complete and it is difficult to alter the washing characteristics of the various circuits to effect a decrease in phosphorus contents with out causing a substantial decrease in yield.

Sulphur content is a concern in some high-volatile coals studied. Washing these coals separately illustrates what each coal is contributing to the clean coal blend and by changing blend proportions possibly reduce the sulphur content. The sulphur is associated with high iron concentrations indicating the presence of siderite.

In most coals there is a good negative correlation between base/acid ratio and CSR. However in coals rich in Fe_2O_3 this is not true because high iron concentrations in the ash, have a positive correlation with CSR. In fact in these coals the SO_3 content in the sample is the best indicator of the CSR value.

The low-volatile coal washes to a low ash

content, and yield could be improved if a higher ash product were produced. Unfortunately coke properties decrease markedly when the ash content of the clean coal increases. Coke oven wall pressure is reduced with only small decreases in stability factor values when small quantities of clean fine coal are added to the product coal.

ACKNOWLEDGMENTS

Data for this study was collected as part of a Canadian Carbonization Research Association project and though not mentioned individually many members past and present of the technical committee of the CCRA have provided ideas. As is apparent from the amount of data presented, the project represents the efforts of many people from plant engineers who helped collect bulk samples from difficult locations in the plants to the staff at the CANMET laboratories who performed the analyses. The fact that the project proceeded emphasizes the importance that coal mining companies in Canada place on these types of cooperative industry government projects. The paper benefited from the editorial comments of Dave Lefebure.

REFERENCES

- Bustin, R.M. (1982): The effect of shearing on the quality of some coals in the southeastern Canadian Cordillera; *Canadian Institute of Mining and Metallurgy Bulletin*, Volume 75, pages 76-83.
- Coin, D.A. (1995): Statistical analysis of industrial plant data of coke production; *ACARP Project C1605*, Report Number OCA-0320, pages 1-10.2.
- Gransden, J.F., Price, J.T. and Leeder, W.R. (1980): Coke making with Canadian medium and high-volatile commercial coking coals; *CANMET*, Report 80-4E.
- Gransden, J.F., Price, J.T. (1982): Effect of mineral matter on the coking properties of four western Canadian coals; in *Proceedings of the Second Technical Conference on western Canadian coals*, *Canadian Institute of Mining*, Paper 10, Edmonton June 2-4 1982.
- Gill, W. W. (1982): Coke quality production models; Unpublished Report, *BHP Central Research Laboratories*, TC/39/82.
- Goscinski, J.S., Gay, R.J. and Robinson, J.W. (1985): A review of American coal quality and its effects on coke reactivity and after reaction strength of cokes; *Journal of Coal Quality*, Volume 2 Part 1, pages 21-29.
- Goscinski, J.S., Gay, R.J. and Robinson, J.W. (1985): A review of American coal quality and its effects on coke reactivity and after reaction strength of cokes; *Journal of Coal Quality*, Volume 4 Part 2, pages 35-43.
- Goscinski, J.S. and Patalsky, R.M. (1989): CSR control: a coal producers point of view; in *Iron Making Proceedings, Iron and Steel Society/American Institute of Mining, Metallurgical and Petroleum Engineers*, Volume 48, pages 50-65.
- Lamberson, M.N. and Bustin, R.M. (1996): The Formation of inertinite-rich peats in Mid Cretaceous Gates Formation: implications for interpretation of Mid Albian history of paleowildfire; *Paleogeography, Paleoclimatology, Paleocology*, 120, pages 235-260.
- Mastalerz, M. and Bustin, R.M. (1993): Variation in elemental composition of macerals, an example of the application of electron microscope to coal studies; *International Journal of Coal Geology*, Volume 22, pages 83-99.
- Pearson, D.E. (1980): The quality of western Canadian coking coal; *Canadian Mining and Metallurgical Bulletin*, pages 1-15.
- Price, J.T. and Gransden, J.F. (1987): Metallurgical coals in Canada: resources, research, and utilization; *Canadian Centre for Mineral and Energy Technology*, Report Number 87-2E, pages 1-71.
- Price, J.T., Gransden, J.F., Khan, M.A. and Ryan, B.D. (1992): Effect of selected minerals on high temperature properties of coke; *Proceedings of the 2nd International Cokemaking Congress*, Volume 1, pages 286-292.
- Price, J.T., Gransden, J.F. and Khan, M.A. (1988): Effect of the coking properties of western Canadian coals on their coking behaviour; in *Proceedings of the 47th Ironmaking Conference, Iron and Steel Society/American Institute of Mining, Metallurgical and Petroleum Engineers*, 47, pages 1545-1562.
- Romaniuk, A.S. (1986): Canadian coal preparation plants; *CANMET Energy and Mines Canada*, Report Number 86-5, pages 1-45.
- Ryan, B.D. and Price J.T. (1993): The predicted coke strength after reaction values of British Columbia coals, with comparisons to international Coals; in *Geological Fieldwork 1992, B.C. Ministry of Energy, Mines and Petroleum Resources*, Paper 1993-1, pages 507-516.

- Ryan, B.D. (1995): Calcite in coal from the Quinsam coal mine, British Columbia, Canada, origin, distribution and effects on coal utilization; *in Geological Fieldwork 1994*, B. Grant, and J.M. Newell, Editors, *B.C. Ministry of Energy, Mines and Petroleum Resources*, Paper 1995-1, pages 245-256.
- Ryan, B.D. and Grieve, D.A. (1996): Source and distribution of phosphorus in British Columbia coal seams; *in Geological Fieldwork 1995*, B. Grant, and J.M. Newell, Editors, *B.C. Ministry of Energy, Mines and Petroleum Resources*, Paper 1996-1, pages 277-294.
- Ryan, B.D., Gransden, J. and Price, J. (1998): Fluidity of western Canadian Coals and Its relationship to other coal and coke properties; *in Geological Fieldwork 1997*, *B.C. Ministry of Employment and Investment*, Paper 1998-1, pages 27-1 to 27-17.
- Ryan, B.D. and Khan, M. (1998): Maceral affinity of phosphorus in coals from the Elk Valley coal-field, British Columbia; *in Geological Fieldwork 1997*, *B.C. Ministry of Employment and Investment*, Paper 1998-1, pages 28-1 to 28-19.
- Ryan, B.D. and Ledda, A. (1998): A review of sulphur in coal: with specific reference to the Telkwa deposit, northwestern British Columbia; *in Geological Fieldwork 1997*, *B.C. Ministry of Employment and Investment*, Paper 1998-1, pages 29-1 to 29-21.
- Schapiro, N. and Gray, R.J. (1964): The use of coal petrography in coke making; *Journal of the Institute of Fuel*, Volume 11, pages 243-242.
- Todoschuk, T.W., Price, J.T. and Gransden, J.F. (1998): Simulation of industrial coking Phase 2; *in Iron Making Proceedings, Iron and Steel Society/American Institute of Mining, Metallurgical and Petroleum Engineers*, Volume 57, pages 1-17.

AGGREGATE POTENTIAL PROJECT FOR THE NANAIMO AREA, VANCOUVER ISLAND (NTS 92B, C, F and G)

By Peter T. Bobrowsky², Alex Matheson², Roger Paulen¹ and Nick Massey²

KEYWORDS: Aggregate potential, Nanaimo, sand and gravel, inventory, database.

INTRODUCTION

The Nanaimo Area Aggregate Potential Project was initiated in 1998 by the Geological Survey Branch of the Ministry of Energy and Mines as part of an ongoing government effort to assist municipal planners and local developers in their management of aggregate resources. This particular study represents a direct response to the regional needs of the Nanaimo Regional District which currently recognizes the importance of assessing aggregate inventory data and aggregate potential data in future land use deci-

sions. The 1998 Nanaimo project as well as the previous 1997 Okanagan Aggregate Potential Mapping Project (Matheson *et al.*, 1997, 1998) and 1996 Prince George Aggregate Potential Mapping Project (Bobrowsky *et al.*, 1996a) all reflect efforts by local government to respond positively to the provincial Growth Management Strategies Act which encourages local governments to manage their own aggregate resources.

The primary project objective was to examine existing aggregate resources and known occurrences, and define potential aggregate resources for the Nanaimo Regional District following the methodology of Bobrowsky *et al.* (1996b). It is reasonable to assume that increased demand for gravel resources in this area has been brought about

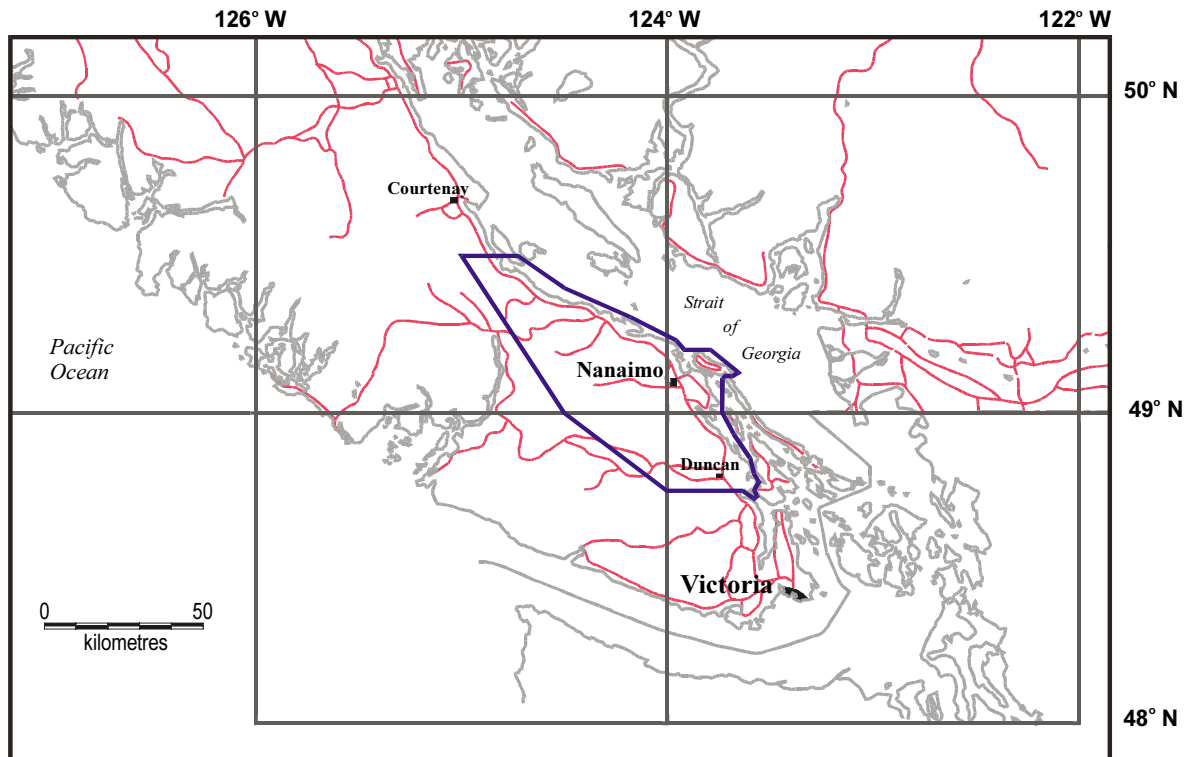


Figure 1. location of the study area on Vancouver Island.

¹School of Earth and Ocean Sciences, University of Victoria

²British Columbia Geological Survey Branch (BCGS)

by the pressures resulting from the construction of the Island Highway, coupled with continuing urban development and population growth. More specifically, the aim of the 1998 study was to evaluate the aggregate potential of the region as defined by parts of nine 1:50 000 scale map sheets: NTS sheets 92B12, 92B13, 92C09, 92C16, 92F01, 92F02, 92F07, 92F08 and 92G04. The exact boundaries are georeferenced in our digital product but roughly corresponds to the coastal areas beginning directly south of Duncan and continuing northwestwards to about Qualicum Beach (Figure 1). The field work was completed over a two week period, and a total of 117 pits were examined along this coastal strip of Vancouver Island.

PREVIOUS STUDIES

A number of studies relevant to aggregate resources have been completed in this area during the past few decades. One of the earliest mapping projects in the northern part of the study area was that of Fyles (1963) who detailed surficial deposits and evaluated the economic potential of the aggregate resources in the coastal areas from Parksville north to Denman

Island. Later a study by Leaming (1968) provided the most complete assessment on the status of sand and gravel bordering the Strait of Georgia. The detail of this work has yet to be repeated, and although the stratigraphic interpretations remain valid, the pit descriptions and reserve estimates have long since passed their usefulness. More recently, casual observations by Galbraith and Beswick (1982) have further confirmed the need for better aggregate information in this area and academic studies by Manson (1995) have provided an update of Ministry of Transportation and Highways aggregate activity in the region. Finally, the region was inventoried using Notice of Work files managed by the Ministry of Energy and Mines in Victoria and published by Matheson *et al.* (1996a).

FIELD ACTIVITIES

The first stage of this project was to identify and evaluate all active and inactive aggregate operations still evident in the district. The existing aggregate inventory database of Matheson *et al.* (1996a) was further supplemented by relying upon and verifying features denoted on NTS maps, current Notice of Work applications and



Photo 1. Gravel sizing operations - 800 meter conveyor built from jaw to crushers (Cassidy Pit).

pits discovered during field work through the region. Each known sand and gravel pit was visited by staff of the Geological Survey Branch. Pits identified in the study area were first photographed (Photo 1), and described according to the following parameters: name of pit, unique identity number and license, licensee or operator, and development status. Additional technical data included stratigraphic descriptions, measurements of exposed sections that allowed for the interpretation of facies, depositional history and quarry type, including these parameters: activity, (producing, reclaimed or abandoned) landform type, environment of deposition, stratigraphic units, structures, and thickness, pit lithology, clast size and roundness, etc. A hand held global positioning system (GPS) unit and 1:50 000 NTS maps were used to accurately define the pit location which was then plotted using UTM coordinates on the NTS maps and terrain maps used in the field.

METHODOLOGY

A field derived database using an Excel spreadsheet was first compiled consisting of the licensing information, all field observations, air-photo interpretations, as well as delineation and identification of the involved landforms. In the office, a digital database for use in ArcView was generated when individual aggregate pits were digitized as points on the nine map sheets.

Additional data were collected and compiled including water well records from the Ministry of Environment, Lands and Parks (location and stratigraphic data), isolated geotechnical records from the Ministry of Transportation and Highways, airphotographic interpretation of surficial geology, digitization of landform polygons and sediment thickness.

The primary element used in aggregate potential maps relies on “polygons” (areas containing similar surficial deposit type and landform genesis) as defined by the surficial geology. Within the Nanaimo Regional District study area, 1394 individual terrestrial polygons were assessed for hosting potential natural aggregate resources. An additional 50 aquatic (lakes, rivers, etc.) polygons were not included in this analysis. Manipulation of other layers of data

was accomplished by reference to these surficial polygons. The data were managed and manipulated in a PC-based GIS environment using ArcView and dBase software. In the Nanaimo study, which comprises nine 1:50 000 scale NTS map sheets, the following variables (mostly geological) were compiled for each polygon:

- ♦ Landform type.
- ♦ Texture of surficial material.
- ♦ Area of landform polygon.
- ♦ Presence/absence of aggregate pits.
- ♦ Overburden and aggregate thickness (from 4625 water well records).
- ♦ Aggregate resource volume (estimated from pits).

All 1394 polygons were then ranked for aggregate potential following the methodology of Bobrowsky *et al.* (1996b). We applied a weighted algorithm defined as follows to the terrestrial polygons:

$$\text{Total Rank} = \{3 \times \text{Landform1}\} + \{3 \times \text{Landform2}\} \\ + \{3 \times \text{Thickness(well)}\} + \{2 \times \text{Overburden(well)}\} \\ + \{3 \times \text{Pit}\} + \text{Area}$$

where Landform1 = primary landform present in the polygon, Landform2 = secondary landform in the polygon, Thickness(well) = gravel thickness in the polygon as estimated from water well records, Overburden(well) = overburden thickness in the polygon as estimated from water well records, Pit = presence or absence of an aggregate pit in the polygon, and Area = total area in hectares of the polygon. Details regarding algorithm generation, weighting and application appear in detail elsewhere (Bobrowsky *et al.*, 1996b; Bobrowsky *et al.*, 1998b; Massey *et al.*, 1998a)

Briefly, individual parameters were independently categorized and assigned a rank score. A two-step process was used to determine a final aggregate potential ranking. First, unfavorable polygons were screened based on the rankings considered most important for indicating resource potential (e.g. landform type, thickness of overburden, etc.). Eliminated polygons (those with virtually no possibility of aggregate) were designated ‘unclassified’. For the remaining polygons, the individual parameter rankings were ‘weighted’ according to significance in

assessing aggregate potential and then summed to determine an overall ranking. This weighting method and the reasoning behind the schema is discussed at length in Bobrowsky *et al.* (1996b). Finally, the significance of a polygon for aggregate resources was assigned. All polygons containing active or historical (inactive pits) were removed from the tally (48 in total) and classified as “H” for historic producers. These represent 7.04% of the total area or 3.44% of the total number of polygons. In the study, the following sub-groups were designated:

- H. Areas of present or recent aggregate production
- U. Unclassified or eliminated polygons.
 - 1. Areas of primary potential
 - 2. Areas of secondary potential, and
 - 3. Areas of tertiary potential.

RESULTS

From the original 1394 polygons the following distribution of categories resulted:

- H - 48 polygons, 6.75% of the total area and 3.44% of the total number,
- U - 395 polygons, 23.26% of the total area and 28.34% of the total number,
- 1 - 75 polygons, 7.31% of the total area or 5.38% of the total number,
- 2 - 229 polygons, 12.84% of the total area or 16.43% of the total number,
- 3 - 647 polygons, 49.85% of the total area or 46.41% of the total number.

The final aggregate potential map for the Nanaimo study has now been released, at no cost to users, in digital format, including the full parameter and ranking-score database, and is available from the Branch’s website: Open File 1998-12, <http://www.ei.gov.bc.ca/geosmin/mapinv/surfical/aggmap.htm> (Massey *et al.*, 1998b).

CONCLUSIONS - DISCUSSION

Locating Future Deposits

Exploration for future deposits should be focused in the low lying coastal areas where various glaciofluvial deposits tend to be common



Photo 2. Fan-delta outwash (Cassidy Pit).

(Photo 2). This area corresponds to the historic distribution of aggregate pits recorded as part of the inventory field work. When urban development and expansion have limited the aggregate potential for these areas, smaller but similar deposits located adjacent to the large valleys should be examined. Such landforms may be first recognized on the aggregate potential maps produced here, and with further ground truthing and additional detailed air photo interpretation, will allow accurate identification of aggregate resources for future use. Proportionately, just over 8% of the total number of polygons or 14% of the total area has favorable aggregate potential. Large parts of the H category polygons have yet to be mined for sand and gravel and these areas should be protected and explored first before land use sterilization occurs. Category 1 polygons also have very good potential to host suitable sources of sand and gravel, but polygons in this category do not yet support any operations. These polygon areas should also be given significant attention for protection against competing land use options.

The ranking of polygons will enable prospective producers and operators to target

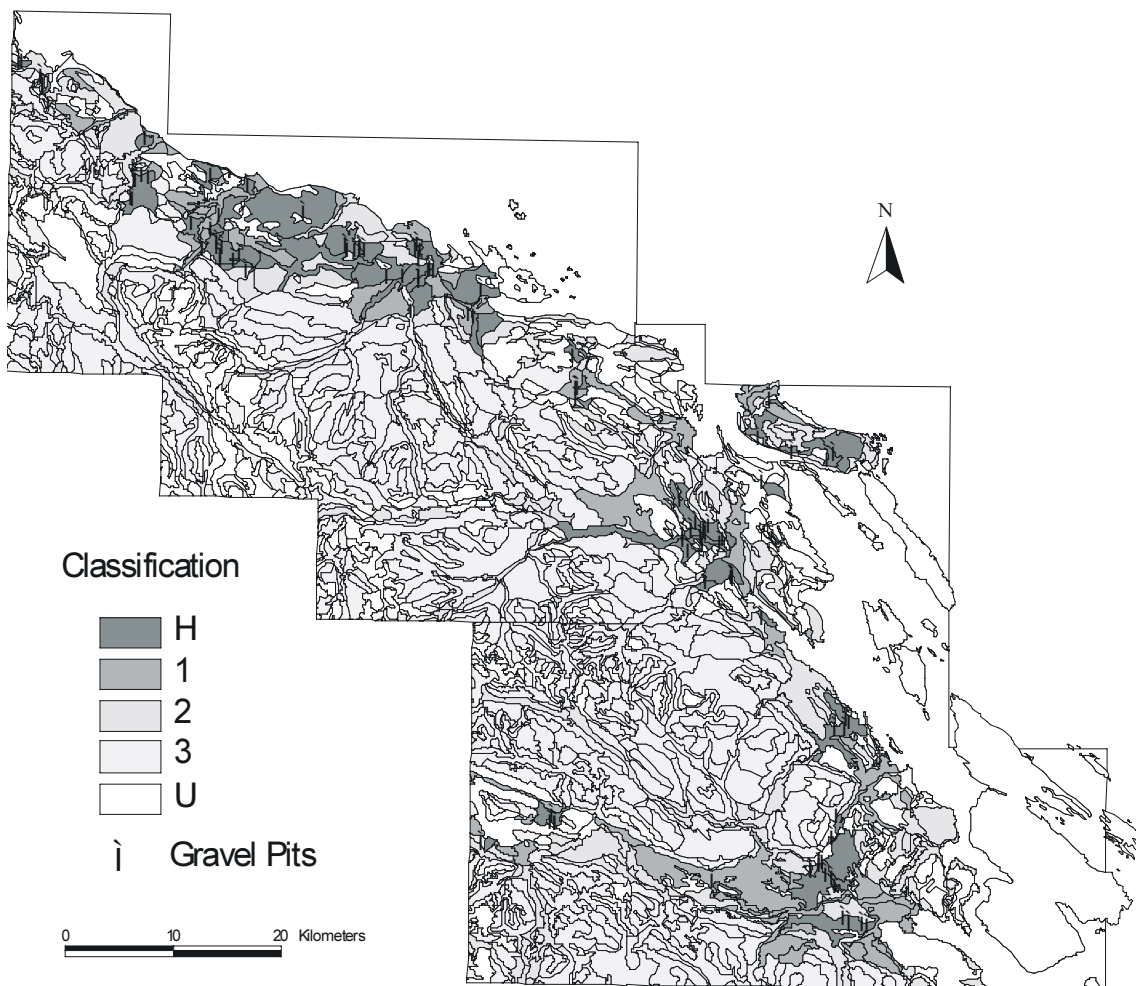


Figure 2. Nanaimo Aggregate Potential Map. Legend: H are historical or proven aggregate resources; 1 are primary or high potential polygons; 2 are secondary or medium potential polygons; 3 are tertiary or low potential polygons and U are unclassified or least favorable polygons for aggregate resources.

areas of greatest potential for future development. Equally important, such information can be used by planners to ensure that long term land use strategies take into account limited or high potential aggregate resources and thus minimize the opportunity for sterilization of the nonrenewable resources (Figure 2). Moreover, the digital data are ideally suited for importation into GIS systems, thus enabling the user groups to further integrate, compare and analyze aggregate data relative to other geographic and socioeconomic data sets.

Value of Aggregate Program

It is axiomatic that there will always be a demand for aggregate and consequently it is essential to have a well documented inventory and evaluation for future use in general develop-

ment planning, for construction purposes and the consequent infrastructure of transportation networks (Bobrowsky 1998). In short, an inventory and an evaluation of potential aggregate resources should be completed in areas of British Columbia where aggregate consumption is increasing rapidly or where present supplies are now exhausted.

The current series of nine partial 1:50 000 scale maps illustrating aggregate potential for the Nanaimo Regional District (Massey *et al.*, 1998b) can now be added to the five Prince George digital maps (Bobrowsky *et al.*, 1996a) and the 16 Okanagan digital maps (Bobrowsky *et al.*, 1998a). Collectively, these data provide an excellent information source for multi-client user groups interested in sand and gravel, surficial geologic and geotechnical information.

ACKNOWLEDGMENTS

The authors would like to thank the many owner-operators of gravel pits who kindly allowed access to their operations, and to Rod Zimmerman of the Ministry of Environment, Lands and Parks and Sheldon Harrington of the Ministry of Transportation and Highways for providing useful information. Ted Hall (MEM) was the principal factor in ensuring this project was initiated. His support is greatly appreciated. This project was funded jointly by the Nanaimo Regional District, Ministry of Municipal Affairs and Housing and the Ministry of Transportation and Highways. Extensive support was provided by the Ministry of Energy and Mines. The authors appreciate the editorial improvements offered by our manager Gib McArthur.

REFERENCES

- Bobrowsky, P.T. (editor) (1998): Aggregate Resources: A global perspective; *A.A. Balkema*, Netherlands.
- Bobrowsky, P.T., Massey, N.W.D., and Matheson, A., (1996a): Aggregate resource potential of the Prince George area; *B.C. Ministry of Energy, Mines and Petroleum Resources*, Open File 1996-24, 5 maps, Scale 1:50 000.
- Bobrowsky, P.T., Massey, N.W.D., and Matysek, P.F. (1996b): Aggregate Forum: Developing an inventory that works for you!; *B.C. Ministry of Energy, Mines and Petroleum Resources*, Information Circular 1996-6, 61 pages.
- Bobrowsky, P.T., Massey, N.W.D., and Matheson, A. (1998a): Aggregate resource potential of the Okanagan area (NTS 82E (west) and 82L (west)); *B.C. Ministry of Energy and Mines*, Open File 1998-5, 16 maps, Scale 1:50 000.
- Bobrowsky, P.T., Massey, N.W.D., and Matheson, A. (1998b): Aggregate resource potential mapping; in *Proceedings of the 8th Congress of the International Association of Engineering Geology and the Environment*, 21-25 September, Vancouver, Canada, D. Moore and O. Hungr, Editors, Volume 4, pages 2817-2824.
- Fyles, J.G. (1963): Surficial geology of Horne Lake and Parksville map areas, Vancouver Island, British Columbia 92F/7, 92F/8; *Geological Survey of Canada*, Memoir 318.
- Galbraith, D.M. and Beswick, J. (1982): Nanaimo to Qualicum Beach observations, unpublished field notes; *B.C. Ministry of Energy, Mines and Petroleum Resources*.
- Leaming, S.F. (1968): Sand and gravel in the Strait of Georgia area; *Geological Survey of Canada*, Paper 66-60.
- Manson, G.K. (1995): Modeling sand & gravel deposits and aggregate resource potential, Vancouver Island, B.C.; B.Sc. Thesis, School of Earth and Ocean Sciences, *University of Victoria*, pages 1-53.
- Massey, N.W.D., Matheson, A. and Bobrowsky, P.T. (1998a): Aggregate resource potential maps - a planning tool useful for explorationists; *B.C. Ministry of Energy and Mines*, Industrial Minerals in Canada 1998, pages 7-9.
- Massey, N.W.D., Matheson, A. and Bobrowsky, P.T., (1998b): Aggregate resource potential of the Nanaimo area (parts of NTS 92B12, 92B13, 92C09, 92C16, 92F01, 92F02, 92F07, 92F08, 92G01); *B.C. Ministry of Energy and Mines*, Open File 1998-12, 9 maps, Scale 1:50 000.
- Matheson, A., Massey, N.W.D., Bobrowsky, P.T., Kilby, C.E. and Manson, G.K. (1996a): Aggregate inventory of British Columbia: private pits; *B.C. Ministry of Energy, Mines and Petroleum Resources*, Open File 1996-5, 2 maps, Scale 1:2 000 000.
- Matheson, A., MacDougall, D., Bobrowsky, P.T., and Massey, N.W.D. (1996b): Okanagan aggregate potential project; in *Geological Fieldwork 1996*, D.V. Lefebure, W.J. McMillan and J.G. McArthur, Editors; *B.C. Ministry of Employment and Investment*, Paper 1997-1, pages 347-352.
- Matheson, A., Paulen, R., Bobrowsky, P.T., and Massey, N.W.D. (1998): Okanagan aggregate project; in *Geological Fieldwork 1997*, *B.C. Ministry of Employment and Investment*, Paper 1998-1, page 29a-1.



PRECIOUS OPAL IN THE WHITESAIL RANGE, WEST-CENTRAL BRITISH COLUMBIA, CANADA (NTS 93E/10W AND 93E/11E)

By G. J. Simandl (B.C. Geological Survey), S. Paradis (Geological Survey of Canada),
L. J. Diakow, P.J. Wojdak and A. J. Hartley (B.C. Geological Survey)

KEYWORDS: Precious opal, common opal, agate, new showings, debris flows, Ootsa Lake Group, Whitesail Range.

INTRODUCTION

The search for gemstone deposits in British Columbia has attracted very limited attention in the past. For example, precious opal deposits were not known in B.C. before the discovery of the Klinker deposit near Vernon in 1991 (Simandl *et al.*, 1996). This despite the fact that common opal occurrences are relatively widespread within Tertiary volcanic rocks (Leaming, 1973; Church and Hora, 1996). Another precious opal occurrence has been recently discovered in the Whitesail Range and is described in this article. The senior author is aware of two other new and confirmed precious opal localities in British Columbia that are not yet being made public. The Eagle Creek occurrence, located 6.5 kilometres from Burns Lake, is also reported to contain precious opal, however we were not able to confirm this information (Paradis and Simandl, 1998). The discovery of more precious opal localities since 1992 underlines the importance of the initial discovery and dissemination of information on how to look for more. This report is based on a two day property visit by the senior author, in combination with limited laboratory work and bibliographic research. The main objective of this study is to contribute to the systematic documentation of the precious opal deposits in the province and to develop a deposit model and exploration guidelines for prospectors.

WHAT IS OPAL?

Opal is a hydrated amorphous silica with between 3 and 20 percent water and a lattice structure of ordered or disordered α -cristobalite

microcrystallites. Electron microscope studies show that the precious opal consists of close packed silica spheres ($\text{SiO}_2 \cdot n\text{H}_2\text{O}$) and interstitial silica, water or CO_2 gas-vapour air. Opal is characterized by a conchoidal fracture, and it occurs in a variety of background colours. It is transparent to nearly opaque, and may be distinguished from chalcedony and cryptocrystalline varieties of quartz by its higher water content and lower hardness. Opal is brittle, sensitive to heat, and easily scratched. Furthermore, opal from some localities, is "unstable" and may craze or self-destruct through the loss of water. Despite these faults, opal's beauty is supreme, and it has been recognized for the past thousand years as a "highly prized" gemstone.

The terminology currently used to describe opal for lapidary applications is quite complex. The three most commonly used terms are "precious", "common", and "fire" opal. Precious opal is defined as opal with a bright, internal play of colours that may be red, orange, green or blue. This play of colours is caused by diffraction of white light by the regular packing of silica microspheres within the mineral structure. The diameter and spacing of the microspheres control the colour range of an opal (Darragh *et al.*, 1966). Precious opal may be subdivided further by colour modifiers, white, black, pink, and blue, which describe the body colour of the opal. Australia is famous for its white and black precious opal. The term "common opal" groups all opals without a play of color (including the fire opal). The lack of a play of colours may be due to a less ordered packing of the silica microspheres. Fire opal is defined as a solid opal with transparent orange to red-orange base colour. It belongs to the precious opal variety if it shows a play of colour, or to the common one if it lacks play of colour. Some of the best fire opal comes from Mexico.

The opal may be deposited by silica-bearing hydrothermal solutions in hot spring or geyser environments, from meteoric waters, or as the accumulation of tests of silica-secreting organisms called diatoms. These organisms live in marine or lacustrine environments.

Deposits that contain precious opal are divided into sediment or volcanic-hosted deposits (Simandl and Paradis, 1998 and Paradis *et al.* 1998). Most of the world's gem opals are from the Australian deposits of the Coober Pedy, Andamooka, and Mintabie areas, which are excellent examples of sediment-hosted fields. These deposits are believed to have formed by descending silica-bearing meteoric waters. The silica is derived from the intense and deep weathering of the sediments overlying the opal deposits. Silica in the meteoric water is concentrated by evaporation, resulting in the formation of colloidal silica gel and ultimately opal. The remaining opal production comes from volcanic-hosted deposits such as those of the Querétaro region of Mexico, Gracias à Dios area in Honduras, and the Spencer deposit in Idaho, USA. The volcanic-hosted opal deposits are believed to be genetically associated with hydrothermal activity.

REGIONAL GEOLOGY

The Whitesail Range is located near the boundary of the Coast and Intermontane belts (Van der Heyden, 1982). The Mesozoic through Tertiary Coast Belt is mainly composed of granitic rocks with variably metamorphosed and deformed peninsular and slivers of island arc terranes. The Intermontane Belt at the latitude of the study area is underlain by island and continental margin arc strata and comagmatic plutons that vary in age from Late Triassic to Paleogene. Block faults are numerous, juxtaposing rocks of contrasting age and tilting layered sequences (Diakow and Mihalyuk, 1987a,b).

A regional geologic synthesis of the Whitesail Lake map area was first published by Duffell (1959). Woodsworth (1978, 1980) remapped this area. Map sheets 93E/10W and 93E/11E, which contain the opal deposits, were mapped at 1:25,000 scale by Diakow and Mihalyuk (1987a) and the results were published at 1:50,000 scale by Diakow and

Mihalyuk (1987b). Stratigraphy of the Ootsa Lake Group (Figure 2) in the region between the Whitesail Range and Whitesail Lake map area is described in Diakow and Mihalyuk (1987a) and Drobe (1991). Radiometric dating of the Eocene rocks that host the opal are given in Diakow and Koyanagi (1988) and Drobe (1991).

NORTHERN LIGHTS OPAL OCCURRENCES

Location

The newly discovered opal showings are located in west central British Columbia in the Whitesail Range, north of Whitesail Lake (Figure 1). Access is either by helicopter or by surface transportation and hiking. By air, the property is approximately 130 kilometres from Smithers and 90 kilometres from Houston. One travels west by road from Prince George to Burns Lake and then southwest to the west end of Francois Lake. From there, a set of logging roads lead to Tahtsa Reach, where a private barge operated by Houston Forest Products affords passage to the few logging roads south of the Reach. From the nearest logging road, it is approximately a 12 kilometre walk southwest along the valley of Slide Creek towards Troitsa Peak to get to the Northern Lights claims. The claims are located well above the tree-line on the eastern spur of the Troitsa Peak.



Figure 1. Location of the precious opal occurrences, Northern Lights claims, Troitsa Peak area, Whitesail Range.

Geological Setting

The precious and common opal showings on the Northern Lights claims are hosted by Ootsa Lake Group volcanics (Figure 2). These volcanics were described by Drobe (1991) as well-layered, coarsely plagioclase- and pyroxene-phyric andesite flows, approximately 130 to 200 metres thick, that conformably overlie flows of rhyodacitic composition. The andesite flows are characterized by abundant plagioclase and pyroxene phenocrysts. In the area of the opal occurrences the andesite flows are subhorizontal and sheet-like, each of which range from 1 to about ten metres thick (Drobe, 1991). These flows resemble near-source compound lavas, consisting of a number of relatively thin lens-shaped flows separated by poorly sorted, debris flow deposits. Individual flows are typically massive at their base and grade upwards into oxidized and strongly vesicular tops (over 50% vesicles in the uppermost 20-40 cm). Vesicles are scarce in the center of the larger flows, but in some thinner flows the vesicular texture may persist throughout. Vesicles are filled with a variety of minerals that generally include a combination of chalcedonic quartz, celadonite, zeolites, and carbonates. Chabazite may occur locally (Diakow and Milhalynuk, 1987a). Volcanic rocks of the Ootsa Lake Group, with the exception of one sample, can be classified as subalkaline using the $(\text{Na}_2\text{O}+\text{K}_2\text{O})$ versus SiO_2 plot of Irvine and Baragar (1971). These rocks also belong to the calcalkaline field on an AFM diagram. Based upon the K_2O - SiO_2 plot of Ewart (1982), they are classified as high-K andesites and basaltic andesites (Drobe, 1991).

The debris flows are commonly up to two metres thick and interfinger with the compound flows (Drobe, 1991). These deposits are lenticular and composed of unsorted, subrounded to subangular clasts of andesite that locally may average 20 to 30 centimetres in diameter.

A broad zone of pervasive alteration developed in volcanic rocks assigned to the Lower Jurassic Hazelton Group is situated to the south of the opal-bearing area (Diakow and Mihalynuk, 1987a). The zone was not examined during this study and was not specifically described by Diakow and Mihalynuk. It is one of several broad areas they mapped with clay minerals, fine grained silica, pyrite, and in places barite, that replaces both underlying sedimenta-

ry rocks of the Smithers Formation (Hazelton Group) and unconformably overlying volcanic strata of the Ootsa Lake Group. It is not known if the precious opal on the Northern Lights claims is genetically linked to this zone of silicification. These silicification zones are probably due to hydrothermal alteration associated with high-level intrusions (Diakow and Mihalynuk, 1987a). No precious opal was found within this zone by the prospectors.

Opal-bearing lithologies

The dominant opal-bearing lithologies in the area are the debris flows. Less abundant opal-bearing lithologies are massive lava flows and associated flow top breccias and minor, possibly waterlain, ashfall tuffs. Massive flows are commonly dark green and mostly porphyritic, although aphyric flows were also observed. The phenocrysts are predominantly plagioclase (up to 2 cm) and pyroxene (<6 mm). Most of the flows are either strongly vesicular or amygdaloidal. The debris flows consist of subangular to subrounded, vesicular, amygdaloidal or massive clasts that typically vary in size from 2 to 100 centimetres, but some may be several metres in size. The flows are matrix- or clast-supported (Figure 3b). Some of the debris flows are polymictic, others are oligomictic. The colour of the clasts varies from dark green, brown, and beige to deep brick-red, a feature that is probably related to the degree of oxidation, and possibly permeability. The scoraceous clasts appear most oxidized. The colour of the matrix varies from yellow to red to gray. Reworking of the debris flows is common, as seen by the rounded heterolithic clasts making up the flows. Some of the flows are truncated by thin bedded, possibly waterlain tuffs, but more commonly by younger debris flows. In thin section most of the opal-bearing rocks consist of 10 to 30 percent plagioclase phenocrysts (up to 15 millimetres in length), amphiboles (0-2%), pyroxene (<2%), opaque oxides (<2%), apatite and opaques (trace). Vesicles may account for more than 20 volume percent of some rocks. The vesicles may be partially or completely filled by common and precious opal or agate and coated by celadonite or zeolites.

Locally, shallowly inclined compound flows and debris flows, including the opal-bearing

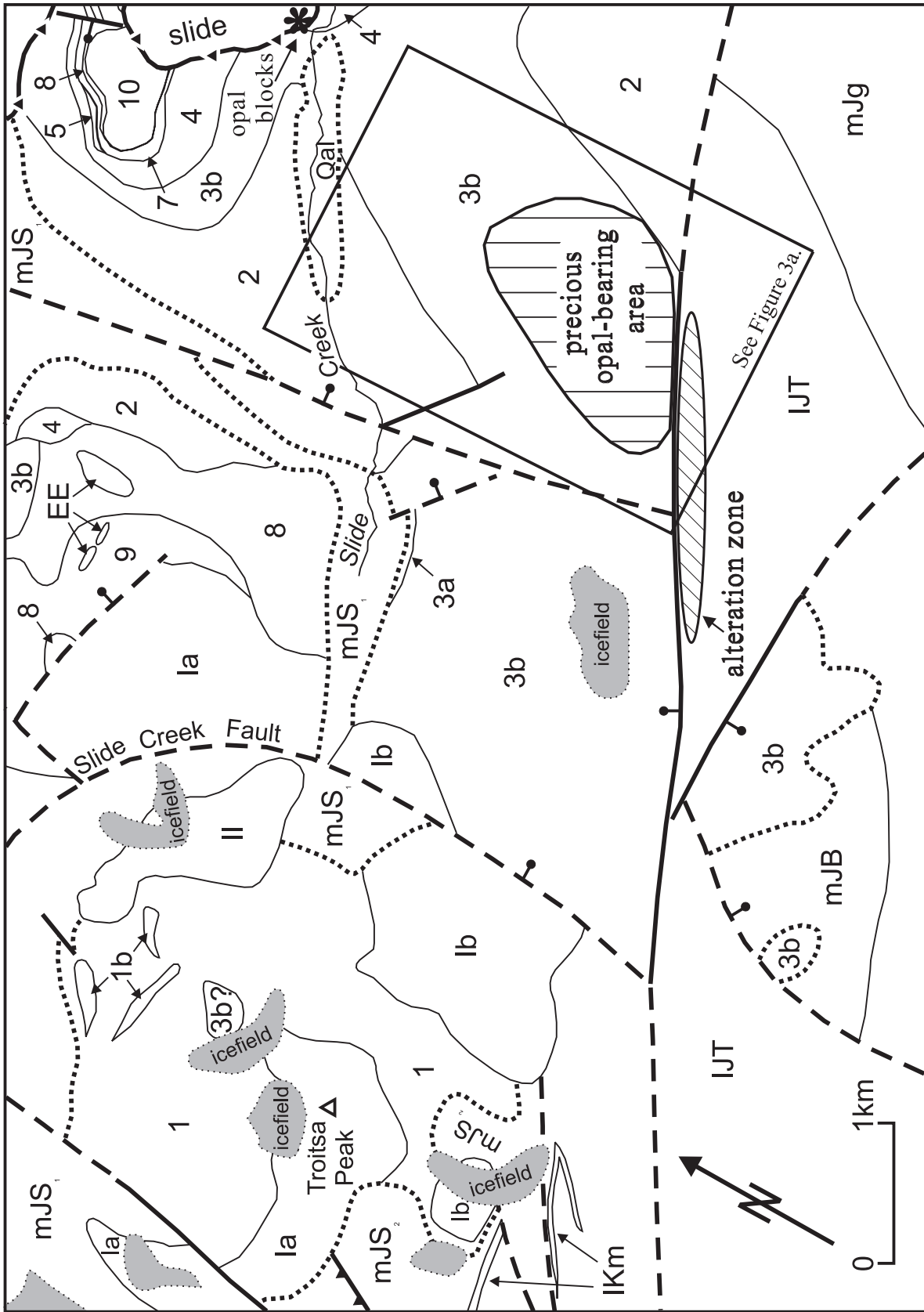


Figure 2. Geological setting of precious opal occurrences in the Whitesail Range (modified from Diakow and Mihalnyuk, 1987a,b and Drobe, 1991).

VOLCANIC AND SEDIMENTARY ROCKS

QUATERNARY

Qal Glacial till and alluvium

EOCENE

EE ENDAKO GROUP: Plagioclase and olivine phyric basalt

10 OOTSA LAKE GROUP: Plagioclase and biotite phyric rhyodacite flows, mauve and grey

9 Coarse plagioclase and pyroxene phyric well-layered andesite flows

8 Buff to tan airfall tuff

7 Intensely welded and minor weakly welded maroon devitrified and black vitrophyric ashflow tuff

6 Stratified and graded thickly bedded debris flows (not present)

5 Plagioclase and pyroxene phyric andesite

4 Sparsely plagioclase phyric dacite flows and debris

3b Coarse plagioclase and pyroxene phyric, well-layered basaltic andesite and andesite flows

3a Crystal lapilli air-fall tuff

2 Plagioclase-biotite-hornblende phyric rhyodacite flows

1 Intensely welded dacitic ash-flow tuff, minor weakly welded block and lapilli tuff, dacite lava flows

MIDDLE JURASSIC

mJB BOWSER LAKE GROUP
Ashman Formation: Siltstone, shale, feldspathic sandstone, lithic arkose; medium to thickly bedded; fossiliferous

LOWER AND MIDDLE JURASSIC

mJS₂ HAZELTON GROUP
Smithers Formation: Lapilli tuff, accretionary lapilli tuff, brownish-red to dark grey

mJS₁ Siltstone, feldspathic sandstone, lithic arkose, greyish-green, minor shale, chert, limestone

IJT TELKWA FORMATION: Maroon and green andesitic to basaltic tuffs and flows; rhyolitic flows, lapilli tuff and tuff breccia

INTRUSIVE ROCKS

TERTIARY

II Equigranular and quartz-biotite-feldspar porphyry granodiorite and quartz monzonite stocks

Ia Plagioclase porphyry diorite sills, plugs, and dykes

Ib Hypidiomorphic-granular diorite plugs and dykes

MESOZOIC

IKm Equigranular diorite and negmatitic monzonite

mJg Middle Jurassic equigranular granite and quartz monzonite stock

SYMBOLS

..... unconformity

▲▲▲▲▲ landslide

—●— fault (solid circle on downthrown block)

▲▲▲▲▲ thrust or reverse fault

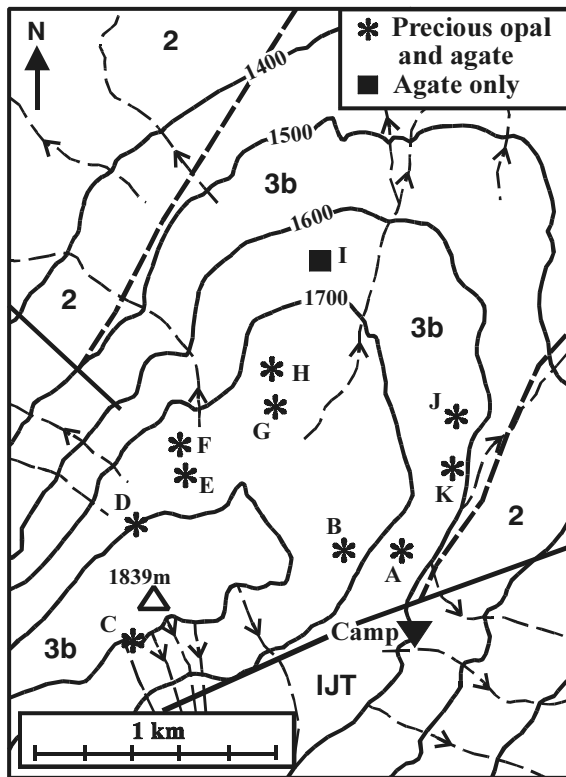


Figure 3a: Distribution of precious opal and agate occurrences on the Northern Lights claims situated on a ridge extending east-northeast from the Troitsa Peak. For geological legend see Figure 2. Star - precious opal and common opal ± agate; square - agate occurrence; A-Zona Rosa, B- Northern Lights, C- Great Wall, D-Bright Lights, E-Ptarmigan, F-New Lights, G-New Lights (East), H-Side Lights, I-No Lights, J-Agate Alley (North), and K-Agate Alley (South); Inverted triangle - camp. Contours are in metres.



Figure 3b: Typical debris flow, Agate Alley showing. Hammer for scale.

ones, may be repeated by displacement along recent, crescent shaped, steeply dipping slump planes in the southern part of the opal-bearing area. A mica-bearing, subvertical dike oriented N65E, cuts the opalized country rocks. The dike is about 60 centimetres wide and is traceable for 2000 metres as a distinctive positive weathered spine that protrudes as much as 6 metres above the surface. According to the prospectors, the dike itself contains a small amount of precious opal and was the initial opal discovery on the property. Common opal can be seen as thin fracture filling along the intrusive contact with the country rock. Prospectors refer to this dike as the Great Wall (Figure 3a). Chemical analysis would be required to determine if this dike is a feeder to the biotite-bearing rhyodacite unit described by

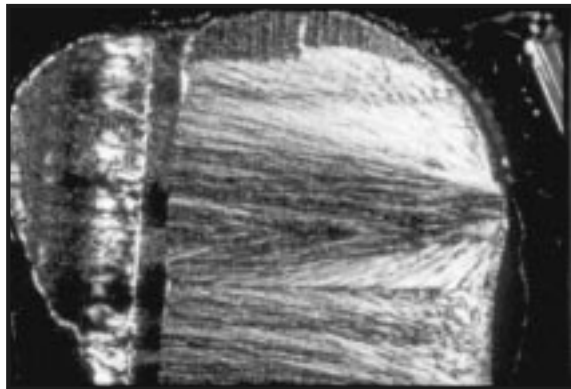


Figure 3c: Agate-filled vesicle in polarized light, showing multiple nucleation sites and nature of horizontal layering. The longest dimension of the photograph is approximately 4mm.

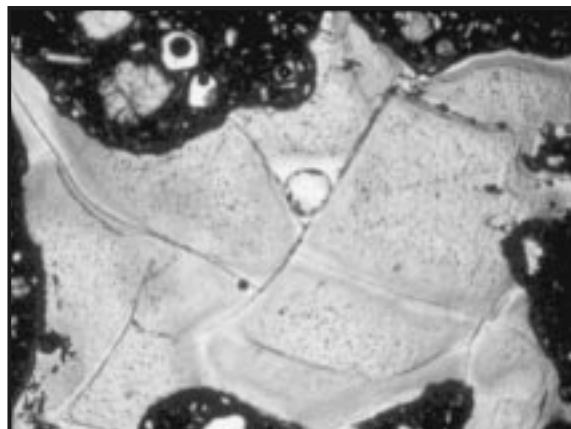


Figure 3d: Precious opal-filled vesicle in plain light. The center of the amygdule is more cloudy and greenish. Edges of the amygdule are slightly brownish, as well as salvages along the desiccation cracks. The longest dimension of the photograph is approximately 4mm.

Drobe (1991). The dike's mafic content appears too low to be described as a lamprophyre.

Opal and Agate Occurrences

The opal occurrences are located near the brim of a flat-topped ridge within an area 1200 by 2000 metres. (Figures 2 and 3a). There are at least 10 precious opal occurrences. Most of the precious opal extracted for testing purposes by the prospectors was from the Zona Rosa and Ptarmigan occurrences.

In general, opal and agate occur most commonly as open space fillings in the matrix and vesicles of clasts and rarely as thin films along fractures in debris flows and flow top breccias. It occurs also as amygdules in massive flows. Due to the complex history of some of the reworked flows, agate may be present only in the vesicles of individual clasts. In such flows only one clast out of fifty may contain agate fillings. Geopetal indicators generally suggest that the agate and opal formed when the lithological units acquired their present orientation. However, in rare cases they suggest that the strata has been tilted approximately 15 degrees south since the agate was formed. Celadonite, a soft, green, earthy mineral of the mica group, is present throughout the area as a vesicle filling and in some places it is so abundant that it gives the rocks a bright green colour. Celadonite commonly forms the rims of empty or agate filled vesicles, suggesting that celadonite predated agate.

Two of the metre-scale clasts within the same debris flow at the Agate Alley showing, display concentric layering (zoning) in terms of the vesicle fillings. The vesicles within the core zone (central portion) of these clasts are empty (silica-free). The core is surrounded by 10 to 15 centimetres thick zone containing individual vesicles coated by a one millimetre thick celadonite layer. This is in turn surrounded by an outer zone characterized by agate partially or completely filling the vesicles, suggesting that the fluids that deposited the celadonite and agate were penetrating the clast from the more porous matrix and moving inward. The high concentrations of celadonite on the property do not appear to coincide geographically with the high opal concentrations. As at the Klinker deposit, the presence of zeolites within the area indicates a favorable geological environment for opal

preservation. The opal stability field is similar to that of clinoptilolite and chabasite.

Most of the agate is colorless, gray or white. The largest agate eggs observed at the site measured up to 15 centimetres in longest dimension. The agate deposition may be in layers or it may form from several nucleation sites simultaneously (Figure 3c).

Precious opal occurs as irregular zones filling individual vesicles or fractures in some of the common opal and agate-bearing debris and compound flows. The size of the opal-bearing zones is difficult to evaluate, but the best exposed occurrence is Ptarmigan. At this location the opal occurs within a trench at least one metre deep, 2 metres wide and 5 metres in length. It appears genetically unrelated to the degree of oxidation, filling vesicles in both hematized and unoxidized lava flows. In most cases, vesicle fillings result in small flecks of opal being densely distributed throughout the rock, similar to examples of Honduran opal. Where the vesicles are large, solid opal recovery is possible. In places, the host volcanic material appears fresh and hard, and will probably take a good polish if polished simultaneously with the matrix opal. In other areas it appears porous and soft and may not give adequate support for the opal during processing. Uncommonly thin (<1mm) fractures filled by precious opal have also been observed. Some of these appear suitable for production of assembled stones as doublets and triplets.

The typical precious opal body colours observed at the sites are white, brown and honey yellow, although black is present but scarce. Most of the opal is opaque to translucent (semi-crystal). The play of colours within the precious opal are green, red, blue and yellow (no systematic study was attempted). The stones appear average or better than average in terms of brightness, although, the detailed evaluation is typically done on individual stones and it will commonly vary within a deposit. In general, the bright play of colour remained after the samples were extracted. The brightness of the samples from the "Bright Lights" locality (Figure 3a) appears strongly enhanced in humid or wet environments. The opal from this occurrence is probably hydrophane, a variety of common opal with a change in opacity and indirectly, intensity of colour, with a corresponding change in water

content. Under transmitted light the precious opal typically appears cloudy brownish or greenish in the central portions of the vesicles and it may contain some dehydration fractures (Figure 3d). It appears isotropic under polarized light.

Economic Potential

Based upon field observations, most of the stones extracted by the prospectors in 1998 may be described as matrix opal of specimen or gem quality. Some of the opal may be suitable for doublets and triplets. Material suitable for "solid opal" cabochon-making is relatively rare. The stability of the opal from the Northern Lights claim remains to be assessed. Some of the opal is hydrophane, however, the owners of the claims indicate that precious opal cut two or three years ago did not craze or undergo other undesirable changes. The appraisal of rough or finished stone from the Northern Lights claims is beyond the scope of this study. Test marketing of the precious opal jewelry from this deposit is in progress and several artists are determining if the opal is suitable for carving purposes. The Whitesail area has many similarities with the Klinker deposit in terms of lithologies, age of the host rocks, mineralogy of vesicle fillings, and the presence of zeolites and celadonite.

The precious opal exploration potential of the area is not limited to the Northern Lights claim. For example, slide scree on the north side of Slide Creek, approximately 3 kilometres north of the camp site (Figure 2), contains angular blocks up to 30 centimetres across consisting of cream colored, translucent, common opal crosscut by black opal veinlets. On the weathered surface these blocks are white. Although no precious opal was observed at this location, there is no doubt that more precious opal will be found in the Whitesail Range.

CONCLUSIONS

- ♦ Northern Lights precious opal is an important discovery that warrants more detailed evaluation.
- ♦ Ootsa Lake volcanic rocks in the Whitesail Range, and possibly even further afield in central B.C., have good exploration potential in terms of precious opal.

- ♦ Permeable lithological units such as debris flows are the most favourable host rocks.
- ♦ Known common opal- and agate-bearing areas in the above described geological settings should be carefully reexamined for the presence of precious opal.
- ♦ More precious opal will likely be located in other areas of British Columbia in similar geological settings as more prospectors and rockhounds are introduced to this type of deposit.

ACKNOWLEDGMENTS

The senior author is grateful to François Berniolles for his able field assistance. We thank Mr. Randy Lord, Mr. Bruce Holden and Larry (Hoopy) Hamula for inviting us to visit this property and for showing us around, their hospitality was very appreciated. Whitesail Ale produced from local ice fields at the elevation of 1600 metres tasted better than any other beer that the senior author tested in the last 40 years. We also appreciate reviews of this paper by Dr. David Lefebure and Dr. Neil Church of the B.C. Geological Survey.

REFERENCES

- Church, B.N. and Hora, Z.D. (1996): New Splitstone and opal occurrences, Nipple Mountain, Beaverdell area; *in* Geological Fieldwork 1996, B. C. Ministry of Energy, Mines and Petroleum Resources, Paper 1997-1, pages 329-332.
- Darragh, P.J., Gaskin, A.J., Terrell, B.C. and Sanders, J.V. (1966): Origin of precious opal; *Nature*, January 1, 1966, Number 5018, pages 13-16.
- Diakow, L. J. and Mihalynuk, M. (1987a): Geology of the Whitesail Reach and Troitsa Lake map areas (93E/10W, 11E); *in* Geological Fieldwork 1986, B.C. Ministry of Energy, Mines and Petroleum Resources, Paper 1987-1, pages 171-179.
- Diakow, L.J. and Mihalynuk, M. (1987b): Geology of Whitesail Reach and Troitsa Lake map areas, B.C.; B. C. Ministry of Energy, Mines and Petroleum Resources, Open File 1987-4.

- Diakow, L. J. and Koyanagi, V. (1988): Stratigraphy and mineral occurrences of Chikamin Mountain and Whitesail Reach map areas (93E/06, 10); in *Geological Fieldwork 1987, B.C. Ministry of Energy, Mines and Petroleum Resources*, Paper 1988-1, pages 155-168.
- Drobe, J.R. (1991): Petrology and petrogenesis of the Ootsa Lake Group in the Whitesail Range, west-central British Columbia; Unpublished M.Sc. Thesis, *Queens University*, Kingston. 200 pages.
- Duffell, S. (1959): Whitesail Lake map-area, British Columbia; *Geological Survey of Canada*, Memoir 299, 119 pages.
- Ewart, A. (1982): The mineralogy and petrology of Tertiary-Recent orogenic volcanic rocks: with special reference to the andesitic-basaltic compositional range; in *Andesites*, R.S. Thorpe, Editor, *John Wiley and Sons*, pages 25-83.
- Irvine, T.N. and Baragar, W.R.A. (1971): A guide to the chemical classification of the common volcanic rocks; *Canadian Journal of Earth Sciences*, Volume 8, pages 523-546.
- Leaming, S. (1973): Rock and mineral collecting in British Columbia; *Geological Survey of Canada*, Paper 72-53, 138 pages.
- Paradis, S. and Simandl, G.J. (1998): Precious opal in British Columbia; *Wat on Earth*, Volume 11, Number 2, page 8.
- Paradis, S. Townsend, J. and Simandl, G.J. (1999): Sedimentary-hosted Opal; in *Geological Fieldwork 1998, B.C. Ministry of Energy and Mines*, Paper 1999-1, this volume.
- Simandl, G.J. and Paradis, S. (1999): Volcanic-hosted Opal; in *Geological Fieldwork 1998, B.C. Ministry of Energy and Mines*, Paper 1998-1, this volume.
- Simandl, G.J., Hancock, K.D., Callaghan, B. and Paradis, S. (1996): Klinker precious opal deposit, south central British Columbia, Canada - Field observations and potential deposit-scale controls; in *Geological Fieldwork 1996, B.C. Ministry of Energy, Mines and Petroleum Resources*, Paper 1997-1, pages 321-327.
- Van der Heyden, P. (1982): Tectonic and stratigraphic relations between the Coast Plutonic Complex and Intermontane Belt, west-central Whitesail Lake map area, British Columbia; Unpublished M.Sc. Thesis, *The University of British Columbia*, 172 pages.
- Woodsworth, G.J. (1978): Eastern margin of the Coast Plutonic Complex in Whitesail Lake map-area, British Columbia; *Geological Survey of Canada*, Current Research, Part A, Paper 78-1A, pages 71-75.
- Woodsworth, G.J.(1980): Geology of Whitesail map-area; *Geological Survey of Canada*, Open File Map 708.



DETAILED GEOCHEMICAL EXPLORATION TECHNIQUES FOR BASE AND PRECIOUS METALS IN THE KOOTENAY TERRANE (82L/13, 82L/14, 82M/4, 82M/5, 92P/1)

By R.E.Lett, W. Jackaman and A.Yeow¹

KEYWORDS: Kootenay Terrane, Geochemistry, Sulphide deposits, Pathfinder Elements, Soil, Till.

INTRODUCTION

There is high potential for economic gold and polymetallic sulphide mineralization in the Cambrian to Mississippian rocks that form the Eagle Bay Assemblage within the Kootenay Terrane. These rocks presently host a number of gold-base metal sulphide deposits such as Homestake (MINFILE 82M025) and Samatosum (MINFILE 82M244). There are, however, a number of challenges to exploration for new deposits including the relatively small size of massive sulphide bodies, misleading electromagnetic response due to graphitic interbeds in sulphide-bearing host rocks, and limited bedrock exposure due to extensive drift cover. As part of an integrated project to better understand mineral potential of the Kootenay Terrane a regional stream water survey, detailed geochemical studies, regional till geochemical surveys, surficial mapping and mineral deposit studies have been undertaken between 1996 and 1998 by the Geological Survey Branch. The till geochemical surveys have covered NTS sheets 82M/4 and 82M/5 (Bobrowsky *et al.*, 1997), the western half of NTS sheets, 92P/1 and 8 (Paulen *et al.*, 1998) and parts of NTS P/9, 82M/3, 82L/13 and 82L/14 (Paulen *et al.*, 1999).

Stream sediment and basal till geochemistry successfully detected the larger massive-sulphide deposits such as Samatosum (Matysek *et al.*, 1991; Dixon-Warren 1998) because anomalous dispersal plumes for copper, cobalt, gold, lead and zinc in the till and copper dispersion patterns in drainage sediment are well developed. Till geochemical patterns can be a misleading indication of mineralization because there can be multiple bedrock sources for glacially transported materi-

al. Also, high pH conditions created by weathering of carbonate interbeds will inhibit the secondary geochemical dispersion of more mobile elements (e.g. zinc) in surface water, streams sediments and soil. Consequently, element patterns formed in soil over thick till may be small and more difficult to detect without a detailed sampling program. The identity of a sulphide mineral source can be better defined using pathfinder elements such as arsenic for gold and mercury or cadmium for copper-lead-zinc sulphides.

The objectives of the detailed geochemical studies described here are to:

- ♦ Discriminate between different sources of mineralized material reflected in the geochemistry of down-ice dispersal plumes.
- ♦ Compare the geochemical expression of different types of base and precious-metal mineralization in soil and underlying till to establish the most effective and economical follow-up geochemical technique (e.g. sampling strategy, analytical methods, ore indicator metals, mineralization pathfinder elements).
- ♦ Compare the effectiveness of different geochemical methods such as stream sediment, stream water, till and soil for detecting base and precious metal mineralization in the Kootenay Terrane.

As far as possible the detailed geochemical studies have been integrated with the regional till surveys and mineral deposit studies. Detailed geochemical studies in 1997 (Lett *et al.*, 1998) focused on the Cam-Gloria (MINFILE M266) gold-bismuth prospect and two base metal sulphide occurrences north-west of North Barriere Lake. Selenium and arsenic were identified as useful pathfinders for precious-base metal massive sulphide mineralization. High

¹ *GeoViro Engineering Ltd, Vancouver.*

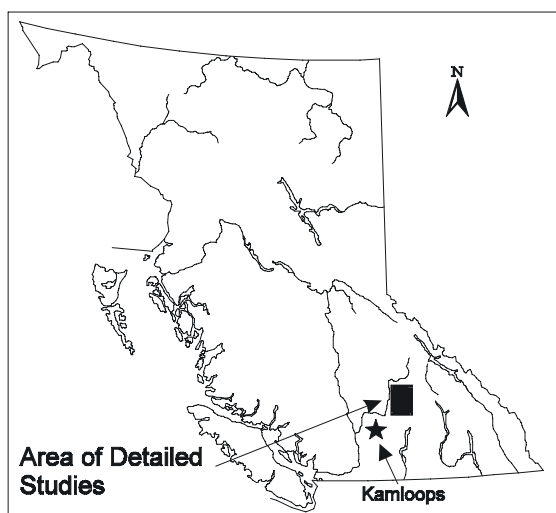


Figure 1. Location of detailed studies.

gold, bismuth, lead and arsenic in the till near Honeymoon Bay on Adams Lake originated from gold-sulphide mineralization in the Cam-Gloria quartz-vein.

Detailed studies carried out in 1998 centered on the area shown in Figure 1. This paper provides a summary of detailed geochemical studies to date including new areas investigated in 1998. In addition, till and soil geochemical data from the area around the Samatosum, and Rea deposits are compared to show how pathfinder element signatures can distinguish between different types of gold-base metal sulphide deposits.

GEOCHEMICAL SIGNATURES OF MINERALIZATION

Each mineral deposit type has a distinct primary trace element signature that, depending on the degree of weathering, may be closely reflected in till, soil or stream sediment geochemistry. These signature or pathfinder elements can be particularly useful in distinguishing between multiple sources of mineralized bedrock in glacial dispersal plumes. Minor and trace element associations typical of gold and base-metal sulphide deposits in the Kootenay terrane around Adams Lake (Nelson *et al.*, 1997; Höy, 1991, 1996, 1998, 1999; Schiarizza and Preto, 1987) are:

- ♦ Volcanogenic gold-copper-lead-zinc-sulphide and barite deposits hosted predominantly by felsic volcanic rocks of the Eagle Bay Assemblage. Examples of this type are

the Homestake (MINFILE 82M025), Rea Gold (MINFILE 82M191), Samatosum (MINFILE 82M244), Harper (MINFILE 82M060), and Scotch Creek (MINFILE 82LNW046). Pathfinder elements for this type of deposit are arsenic, barium, mercury, cadmium, selenium, tin, bismuth and potassium.

- ♦ Massive, volcanogenic copper-zinc sulphide deposits hosted predominantly by metasediments of the Eagle Bay Assemblage. The Mount Armour occurrence (MINFILE 92P050) is an example of this type of deposit. Pathfinder elements for this type of deposit are sodium, magnesium, cobalt, nickel and arsenic.
- ♦ Massive, volcanogenic copper-zinc sulphide deposits in mafic volcanic rocks. The Chu Chua deposit (MINFILE 92P140) hosted by mafic flows and tuffs of the Fennell Formation is an example of this type. Pathfinder elements for this type of deposit are cobalt, chromium and nickel.
- ♦ Massive, lead-zinc-silver sulphide deposits hosted by metasedimentary rocks of the Eagle Bay Assemblage. An example of this type is the Spar occurrence (MINFILE 82M017). Pathfinder elements for this type of deposit are potassium, barium and manganese.
- ♦ Disseminated copper-molybdenum sulphide deposits hosted by metavolcanic and metasedimentary rocks of the Eagle Bay Assemblage adjacent to Devonian orthogneiss. Examples of this type of deposit are Harper Creek (MINFILE 82M017) and the EBL prospect (MINFILE 82M017). Pathfinder elements for this type of deposit are potassium, magnesium, arsenic, antimony, cadmium, fluorine, bismuth, molybdenum and tungsten.
- ♦ Gold mineralized quartz veins in biotite quartz monzonite of the Cretaceous Baldy Batholith. An example, discovered by follow-up of the 1996 regional till geochemical survey is the Cam-Gloria prospect (MINFILE M266). Pathfinder elements for this type of mineralization are bismuth, lead, molybdenum, fluorine and tungsten.

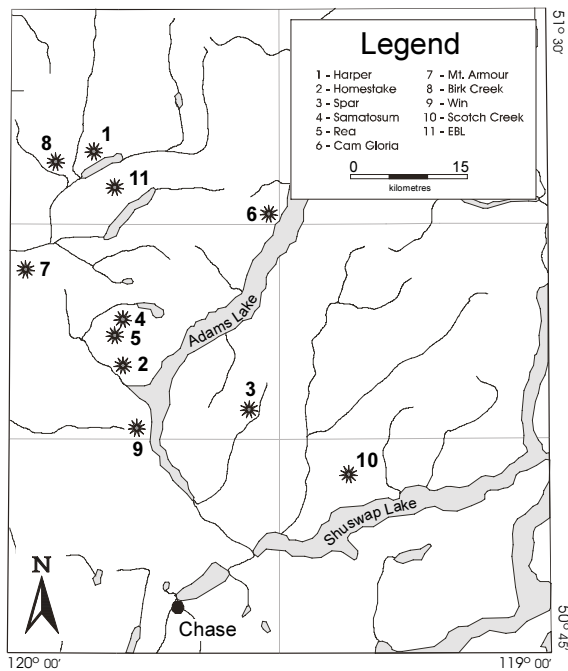


Figure 2. Location of orientation sites.

GEOCHEMICAL ORIENTATION SITES

Detailed geochemical orientation studies were conducted at eleven locations shown in Figure 2. The locations were selected to include the different types of gold and base metal sulphide mineralization and associated till geochemical dispersal trains. Mineralization, host rocks, surficial geology and types of sample collected at each site are summarized in Table 1.

SAMPLING AND ANALYSIS

Soil and till samples were collected from road cuts or pits at intervals ranging from 20 to 200 metres depending on the size of the mineralized zone or the glacial dispersal plume. Soil and till samples (minus 63 micron fraction) and pulverised rock samples were analysed for over 50 elements including antimony, gold, arsenic, barium, bismuth, cadmium, cobalt, copper, gallium, lead, molybdenum, nickel, mercury, silver, selenium, thallium, tellurium and zinc by a combination of thermal neutron activation (INA), aqua regia digestion-inductively coupled plasma emission spectroscopy (ARICP) and aqua regia digestion-solvent extraction and ultrasonic nebulizer-inductively coupled plasma emission spectroscopy (UARICP). Selected soil and till samples were analysed for major oxides, loss on ignition, carbon, sulphur, barium, scandium, ni-

bium, nickel, strontium, yttrium and zirconium by lithium metaborate fusion-inductively coupled plasma emission spectroscopy and leco combustion. Detection limits for INA, ARICP and UARICP are compared in Table 2. Detection limits for major oxides (e.g. aluminium oxide), carbon and sulphur are typically 0.01 per cent and for barium, scandium, niobium, nickel, strontium, yttrium and zirconium typically 10 ppm. The rock, soil and till samples were prepared by Eco Tech, Laboratories, Kamloops. Neutron activation analyses were carried out by Actlabs, Ancaster, Ontario and the inductively coupled plasma emission analyses were carried out by ACME analytical laboratories, Vancouver.

Each geo-analytical method has certain advantages and limitations. Neutron activation is non-destructive to the sample and provides a "total" estimate of an element concentration. It cannot, however, measure ore-indicator elements such as lead and copper. These can be determined on a separate sample by an aqua regia digestion and inductively coupled plasma emission spectroscopy. An aqua regia digestion, while very effective for dissolving gold, carbonates and sulphides in a sample, cannot completely break down aluminosilicate, oxide and other refractory minerals such as barite. Consequently, element concentrations determined by ARICP are "partial" rather than "total". Aqua regia digestion followed by ultrasonic nebulizer inductively coupled plasma emission spectroscopy (UARICP) enables detection limits for certain elements such as silver, arsenic, bismuth, tellurium and thallium to be improved by an order of magnitude. High levels of copper and other base metals can, however, interfere and decrease the sensitivity of other elements determined by this method.

Reliable interpretation of geochemical data depends on separating real geochemical trends caused by geological changes from those variations due to sampling and/or analytical variations. These variations are typically measured by monitoring the quality of the data through routine analysis of reference standards and duplicate samples. The standards and duplicates are inserted into each batch of 20 prepared samples analysed to measure accuracy and precision. Each batch of 20 samples contains seventeen routine samples, a field duplicate sample

Table 1. Mineralization, geology and samples collected at each study site

Site	Mineralization	Host Rock	Surficial Geology	Samples
1. Harper	Massive pyrite, galena, pyrrhotite, chalcopyrite, sphalerite.	Eagle Bay Assemblage (EBA) phyllites and schist.	Lodgment till veneer derived from Eagle Bay and Baldy Batholith rocks.	Soil-till (69) Rock (10) Vegetation (15)
2. Homestake	Lenses containing barite, pyrite, tetrahedrite, galena, sphalerite, argentite with native silver and gold.	Eagle Bay Assemblage (EBA) quartz-talc-sericite schist; sericite-quartz-phyllite; sericite-chlorite-quartz phyllite.	Colluvium and rock.	Soil-till (16) Rock (2) Vegetation (10)
3. Spar	Banded and massive, pyrite, galena, pyrrhotite, chalcopyrite, sphalerite.	Eagle Bay Assemblage (EBG) siliceous and graphitic phyllites, limestone and greenschist.	Lodgment till blanket derived from Eagle Bay rocks.	Soil-till (25) Rock (5) Vegetation (5)
4. Samatosum	Coarse-grained tetrahedrite, sphalerite, galena, gold chalcopyrite associated with quartz veining.	Eagle Bay Assemblage (EBG) cherty sediment within sequence of mafic volcanics and turbidites.	Lodgment till blanket derived from Eagle Bay rocks, locally anthropogenic (mine site).	Soil-till (30) Rock (10)
5. Rea	Massive sulphide lenses of pyrite, sphalerite, galena, arsenopyrite, quartz, gold and barite.	Eagle Bay Assemblage (EBF) mafic tuff, chert, dark grey tuffaceous sediments.	Lodgment till blanket derived from Eagle Bay rocks, locally anthropogenic (mine site).	Soil-till (30)
6. Cam-Gloria	Pyrite, galena, chalcopyrite bismuth and gold in massive quartz veins.	Baldy Batholith biotite, quartz monzonite.	Ablation till derived from Baldy Batholith.	Soil-till (30) Rock (5)
7. Mount Armour	Massive lenses of pyrite, chalcopyrite, sphalerite.	Eagle Bay Assemblage (EBS) chert, argillite, conglomerate and limestone.	Lodgment till veneer derived from Eagle Bay and Fennel Formation rocks.	Soil-till (70) Rock (5)
8. Broken Ridge	Banded pyrite, chalcopyrite, sphalerite, galena.	Eagle Bay Assemblage (EBA) actinolite schist and gneiss.	Lodgment till veneer derived from Eagle Bay rocks. Colluvium on steeper slopes.	Soil-till (36) Rock (5)
9. Win	Minor disseminated pyrite, chalcopyrite, sphalerite, galena in quartz veins.	Eagle Bay Assemblage (EBA) mafic tuffs, graphitic argillite, and siltstone.	Lodgment till blanket derived from Eagle Bay rocks.	Soil-till (9)
10. Scotch Creek	Massive pyrrhotite, pyrite, galena, chalcopyrite, sphalerite.	Eagle Bay Assemblage (EBA) sericite-chlorite phyllite, graphitic argillite, marble, schist, and iron formation.	Lodgment till blanket derived from Eagle Bay rocks.	Soil-till (16)
11. EBL	Disseminated pyrrhotite, pyrite, chalcopyrite.	Eagle Bay Assemblage (EBQ) biotite-chlorite schist and limestone.	Lodgment till blanket derived from Eagle Bay rocks.	Soil-till (22) Rock (5)

Table 2. Detection limits for aqua regia digestion-inductively coupled plasma emission spectroscopy (ARICP), aqua regia digestion-solvent extraction and ultrasonic nebulizer-inductively coupled plasma emission spectroscopy (UARICP) and neutron activation (INA). nd = not detected by method

Element		ARICP	UARICP	INA
Aluminium	Al	0.01%	0.01%	nd
Antimony	Sb	2 ppm	0.2 ppm	0.1 ppm
Arsenic	As	2 ppm	0.5 ppm	0.5 ppm
Barium	Ba	1 ppm	1 ppm	50 ppm
Bismuth	Bi	2 ppm	0.1 ppm	nd
Boron	B	3 ppm	3 ppm	nd
Bromine	Br	nd	nd	0.5 ppm
Cadmium	Cd	0.2 ppm	10 ppb	nd
Calcium	Ca	0.01%	0.01%	1.00%
Cerium	Ce	nd	nd	3 ppm
Cesium	Cs	nd	nd	1 ppm
Chromium	Cr	1 ppm	1 ppm	5 ppm
Cobalt	Co	1 ppm	1 ppm	1 ppm
Copper	Cu	1 ppm	0.2 ppm	nd
Europium	Eu	nd	nd	0.2 ppm
Hafnium	Hf	nd	nd	1 ppm
Gallium	Ga	nd	0.5 ppm	nd
Gold	Au	2 ppm	100 ppb	2 ppb
Iron	Fe	0.01%	0.01%	0.01%
Lanthanum	La	1 ppm	1 ppm	0.5 ppm
Lead	Pb	3 ppm	0.3 ppm	nd
Lutetium	Lu	nd	nd	0.05 ppm
Magnesium	Mg	0.01%	0.01%	nd
Manganese	Mn	2 ppm	2 ppm	nd
Mercury	Hg	1 ppm	10 ppb	1 ppm
Molybdenum	Mo	1 ppm	0.1 ppm	1 ppm
Nickel	Ni	1 ppm	1 ppm	20 ppm
Neodmium	Nd	nd	nd	5 ppm
Phosphorus	P	10 ppm	10 ppm	nd
Potassium	K	0.01%	0.01%	nd
Samarium	Sm	nd	nd	0.1 ppm
Scandium	Sc	nd	nd	0.1 ppm
Selenium	Se	nd	0.4 ppm	3 ppm
Silver	Ag	0.3 ppm	30 ppb	5 ppm
Sodium	Na	0.01%	0.01%	0.01%
Strontium	Sr	1 ppm	1 ppm	500 ppm
Tantalum	Ta	nd	nd	0.5 ppm
Tellurium	Te	nd	0.2 ppm	nd
Terbium	Tb	nd	nd	0.5 ppm
Titanium	Ti	0.01%	0.01%	nd
Thallium	Tl	5 ppm	0.2 ppm	nd
Thorium	Th	2 ppm	2 ppm	0.2 ppm
Tungsten	W	2 ppm	2 ppm	1 ppm
Uranium	U	5 ppm	5 ppm	0.5 ppm
Vanadium	V	1 ppm	1 ppm	nd
Ytterbium	Y	nd	nd	0.2 ppm
Zinc	Zn	1 ppm	1 ppm	50 ppm

Table 3. Analytical precision at the 95 per cent confidence limit for elements by ICP and INA. ne = not estimated.

Element		ICP (%)	INA (%)
Aluminium	Al	10.20	ne
Antimony	Sb	14.00	ne
Arsenic	As	26.10	6.20
Barium	Ba	18.80	29.00
Bismuth	Bi	90.20	ne
Bromine	Br	ne	ne
Cadmium	Cd	29.00	ne
Calcium	Ca	14.20	26.00
Cerium	Ce	ne	11.20
Cesium	Cs	ne	34.60
Chromium	Cr	9.00	10.10
Cobalt	Co	10.20	7.80
Copper	Cu	8.20	ne
Europium	Eu	12.80	ne
Hafnium	Hf	ne	29.20
Gallium	Ga	13.20	ne
Gold	Au	ne	100.00
Iron	Fe	11.40	5.60
Lanthanum	La	ne	9.30
Lead	Pb	9.60	ne
Lutetium	Lu	ne	14.80
Magnesium	Mg	16.00	ne
Manganese	Mn	6.60	ne
Mercury	Hg	22.80	ne
Molybdenum	Mo	25.40	ne
Nickel	Ni	12.60	ne
Neodmium	Nd	ne	21.00
Phosphorus	P	5.40	ne
Potassium	K	11.20	ne
Samarium	Sm	ne	10.60
Scandium	Sc	ne	7.60
Silver	Ag	16.00	ne
Sodium	Na	71.00	8.10
Strontium	Sr	ne	ne
Tantalum	Ta	ne	ne
Tellurium	Te	ne	ne
Terbium	Tb	ne	ne
Titanium	Ti	12.20	ne
Thallium	Tl	25.80	ne
Thorium	Th	48.80	16.00
Tungsten	W	ne	ne
Uranium	U	ne	43.00
Vanadium	V	6.40	ne
Ytterbium	Y	ne	15.00
Zinc	Zn	5.10	18.00

collected adjacent to one of the routine samples, a blind duplicate sample split from one of the 17 routine samples prior to analysis and a control reference standard containing material of known element concentrations (either Canada Centre for Mineral and Energy Technology certified standard or a Geological Survey Branch 'prepared' bulk soil). The locations of blind duplicate and control reference samples are selected prior to sampling, whereas field duplicate sites are chosen randomly during field-work. The analytical precision (at the 95 per

cent confidence limit) for elements determined by ARICP, UARICP and INA from fourteen replicate analyses of a Geological Survey Branch reference standard is shown in Table 3. The precision for some elements (e.g. boron) has not been calculated because all values are below detection limit. Also, low precision indicated by a high value in Table 3 does not necessarily mean that the analysis of a particular element is unreliable because the concentration of that element in the standard can be close to or below detection limit.

GEOCHEMICAL EXPRESSION OF THE SAMATOSUM AND REA DEPOSITS

Bedrock, soil and till geochemical data produced from the 1997 detailed sampling program in the area south east from the Samatosum and Rea deposits serves to illustrate how pathfinder elements can distinguish between different sources of mineralized bedrock. Surficial and bedrock geology of the area between Johnson Creek and Adams Lake are shown in Figure 3. Geology of the area around the Samatosum and Rea deposits comprises a northwest trending, northeast dipping sequence of mafic volcanics, mixed cherty argillites, black distal turbidites, minor amounts of felsic volcanics and recrystallized limestone. The Samatosum deposit occurs in cherty mixed sediments close to the contact between greenstone to the northeast and metasediments to the south-west. Mineralization at Samatosum consists of coarse-grained tetrahedrite, sphalerite, galena and chalcopyrite associated with quartz veining whereas at Rea the mineralization is dominated by fine grained arsenopyrite, pyrite, sphalerite, galena, quartz and barite.

Terrain mapping (Dixon-Warren, 1998) has identified that the surficial sediment in the area between Johnson Creek and Adams Lake is predominantly a single, locally derived, basal till deposited by ice that moved from the north or northwest to southeast. The distribution of gold, arsenic, silver, copper, cadmium, lead and zinc in basal till samples collected during the 1996 regional survey (Dixon-Warren, 1998) reveals high element concentrations forming ribbon-shaped plumes down-ice from the Samatosum and Rea deposits. These plumes trend parallel to the

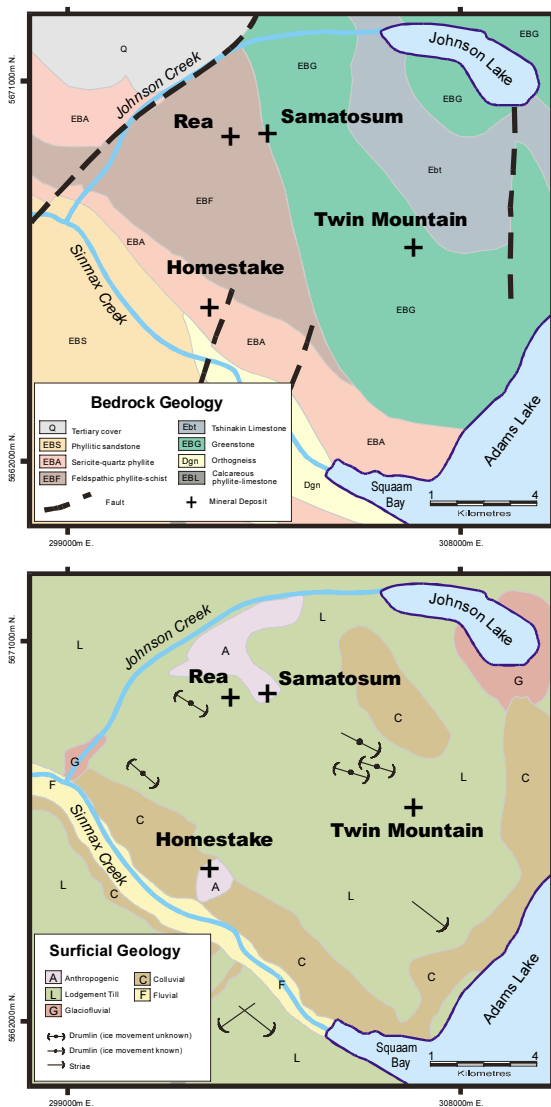


Figure 3. Bedrock Geology (from Schiarizza and Preto, 1987) and Surficial Geology (from Dixon-Warren, 1998).

direction of ice flow or form isolated clusters of values. Regionally, there is a moderate correlation between arsenic and gold in the till and maximum concentrations occur near known mineral occurrences. Down-ice from the Samatosum deposit till-clast plumes extend up to 5 kilometres in length whereas the gold-arsenic geochemical dispersal train can be detected up to 10 kilometres.

Examination of element data for 33 till samples collected in 1997 along profiles crossing the down-ice dispersal plume confirms a moderate statistical correlation (+0.7 coefficient) between gold and arsenic and a much stronger correlation (> +0.80 coefficient) between: cadmium-zinc-thallium-tellurium (sphalerite), copper-cobalt-iron (sulphides), magnesium-nickel-cobalt-

chromium-vanadium (mafic bedrock), mercury-antimony-silver (sulphides) and barium-molybdenum-selenium (barite-sulphides).

The spatial distribution of gold, lead, barium and mercury in the till samples (Figure 4) reveals dispersal plumes extending down-ice from the Samatosum and Rea deposits. Gold values fall sharply immediately southeast of the Samatosum deposit and then increase to a maximum concentration at 1.8 kilometres down-ice. The variation of lead, arsenic, antimony, cobalt, copper, chromium, silver and zinc along the down-ice profile is similar to gold and the fluctuation of values most likely reflects the influence of bedrock topography and till thickness on the dispersal of elements (Yeow, 1998). These elements are typical of those associated with the Samatosum mineralization. In contrast to the till geochemical signature of the Samatosum deposit, higher barium and mercury values occur with gold and arsenic down-ice from the Rea deposit. This element association most likely reflects the different mineralogy of the Rea mineralization. The full extent of the down-ice dispersal plumes from Samatosum and Rea is difficult to determine, however, due to the wide distribution of sample locations. As a result, the cluster of high gold, copper, mercury, barium and silver in the till about 5 kilometres southeast from the Samatosum deposit may reflect local dispersal of mineralized material from the Twin Mountain galena-sphalerite-chalcopyrite-barite occurrence.

A comparison between metals in the B-soil horizon and till is illustrated by gold and arsenic in Figure 5. While both elements can be detected in the B-soil horizon concentrations in soil are lower and there is a much weaker expression of the Rea mineralization compared to that in the till. Other elements (e.g. mercury, lead, zinc) also show smaller patterns in the soil. This difference can be explained by the expression of mineralized bedrock at different locations along an idealized dispersal plume (Figure 6). Close to the bedrock source a long, thin geochemical signature can be expected in the till whereas at a greater distance down-ice from the source the patterns detected will be smaller because of dilution. Secondary dispersion of more mobile elements (e.g. copper and zinc) can further distort and displace the soil geochemical anomaly away from the till dispersal plume.

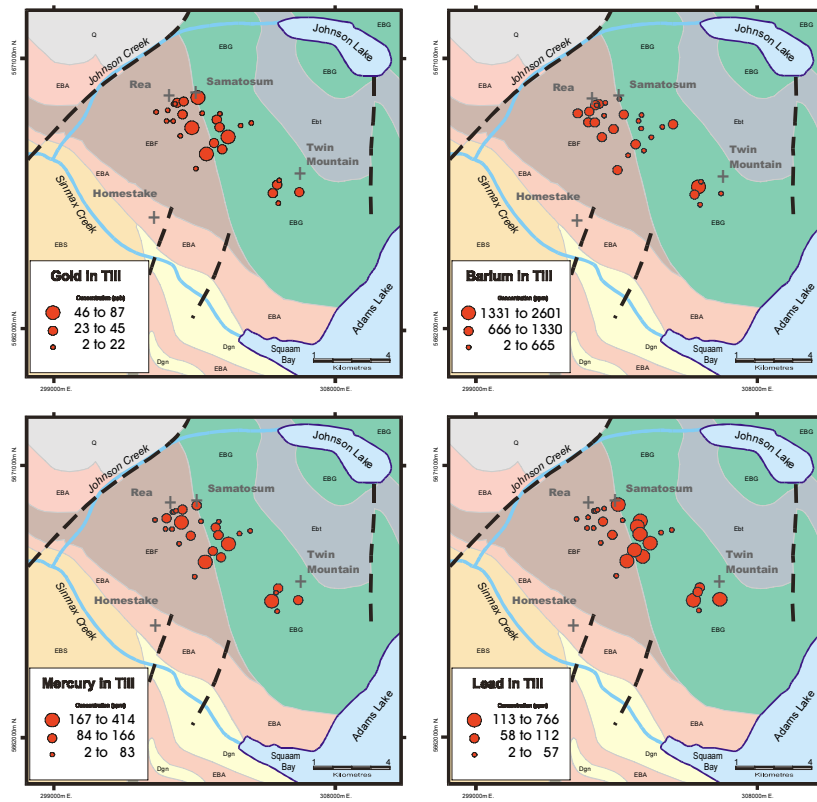


Figure 4. Gold, lead, barium and mercury in till samples.

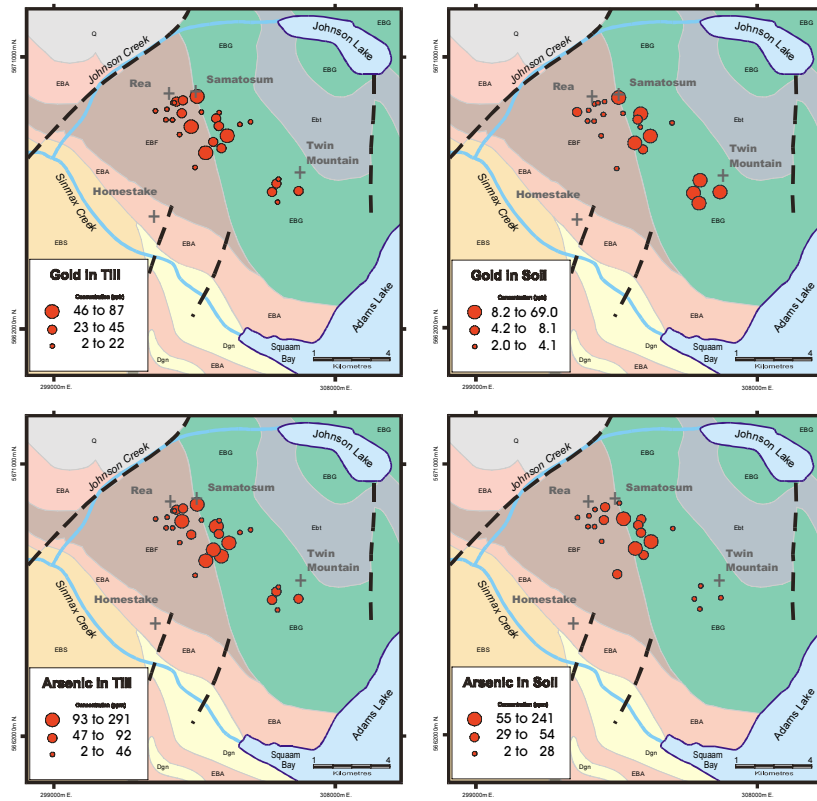


Figure 5. Comparison of gold and arsenic distribution in till and B-soil horizon samples.

Ice Flow

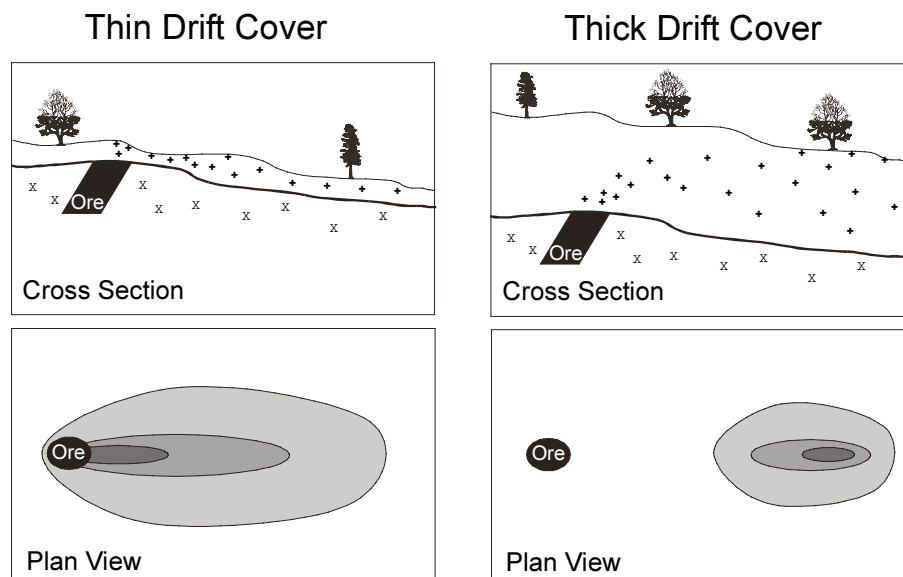


Figure 6. Geochemical signatures for mineralized bedrock in till.

CONCLUSIONS

Detailed geochemical till, soil and rock sampling has been completed at eleven locations in an area of the Kootenay Terrane, including the Samatosum gold-base metal sulphide deposit. The aim of the studies has been to improve geochemical exploration methods for base and precious metals in the Kootenay Terrane. Detailed sampling east of the Samatosum-Rea deposits has confirmed down-ice geochemical dispersal plumes for gold, arsenic, silver, copper, cadmium, lead and zinc originally identified by a regional till survey. The detailed sampling also revealed that higher barium appears to be a pathfinder for the Rea mineralization. Soil geochemical patterns are smaller than those for corresponding elements in till due to dilution of mineralized material in the dispersal plume down-ice from the bedrock source.

ACKNOWLEDGMENTS

The authors would like to thank Steve Sibbick, now with Norecol, Dames and Moore Inc., Vancouver, for initiating this project in 1996. Trygve Höy and Mike Cathro are thanked for their helpful comments on the geology of Eagle Bay Assemblage and the different styles of mineralization found in the Kootenay Terrane. Editing of this paper by Gib McArthur is very much appreciated.

REFERENCES

- Bobrowsky, P.T., Leboe, E.R., Dixon-Warren, A., Ledwon, A., MacDougall, D. and Sibbick, S.J. (1997): Till geochemistry of the Adams Plateau-North Barriere Lake area (82M/4 and 5); *B.C. Ministry of Employment and Investment*, Open File 1997-9.
- Bobrowsky, P.T., Leboe, E.R., Dixon-Warren, A. and Ledwon, A. (1997): Eagle Bay Project: Till geochemistry of the Adams Plateau-North Barriere Lake area (82M/4 and 5); in *Geological Fieldwork 1996*, D.V. Lefebure, W.J. McMillan and G. McArthur, Editors, *B.C. Ministry of Employment and Investment*, Paper 1997-1, pages 413-422.
- Dixon-Warren (1998). Terrain mapping and drift prospecting in south central British Columbia; Unpublished M.Sc. Thesis, *Simon Fraser University*, 184 pages.
- Dixon-Warren, A., Bobrowsky, P.T., Leboe, E.R. and Ledwon, A. (1997): Eagle Bay Project: Surficial geology of the Adams Plateau (82M/4) and North Barriere Lake (82M/5) map areas; in *Geological Fieldwork 1996*, D.V. Lefebure, W.J. McMillan and G. McArthur, Editors, *B.C. Ministry of Employment and Investment*, Paper 1997-1, pages 405-412.

- Höy, T. (1997): Harper Creek: A volcanogenic sulphide deposit within the Eagle Bay Assemblage, Kootenay Terrane, Southern British Columbia; *in Geological Fieldwork 1996*, D.V. Lefebure, W.J. McMillan and G. McArthur, Editors, *B.C. Ministry of Employment and Investment*, Paper 1997-1, pages 199-210.
- Höy, T. (1991): Volcanogenic massive sulphide deposits in British Columbia; *in Ore Deposits, Tectonics and Metallogeny in the Canadian Cordillera*, W.J. McMillan, Editor, *B.C. Ministry of Energy, Mines and Petroleum Resources*, Paper 1991-4, pages 89-199.
- Höy, T. (1999): Massive sulphide deposits of the Eagle Bay Assemblage, Adams Plateau, south central British Columbia; *in Geological Fieldwork 1998*, *B.C. Ministry of Energy and Mines*, Paper 1999-1, this volume.
- Lett, R.E., Bobrowsky, P., Cathro, M. and Yeow, A. (1998): Geochemical pathfinders for massive sulphides in the Southern Kootenay Terrane; *in Geological Fieldwork 1997*, *B.C. Ministry of Employment and Investment*, Paper 1998-1, pages 15-1 to 15-9.
- Matysek, P.F., Jackaman, W., Gravel, J.L., Sibbick, S.J. and Feulgen, S. (1991): British Columbia Regional Geochemical Survey, Seymour Arm (NTS 82M); *B.C. Ministry of Energy, Mines and Petroleum Resources*, RGS 33.
- Nelson, J., Sibbick, S.J., Höy, T., Bobrowsky, P. and Cathro, M. (1997): The Paleozoic massive sulphide project: An Investigation of the Yukon-Tanana correlatives in British Columbia; *in Geological Fieldwork 1996*, D.V. Lefebure, W.J. McMillan and G. McArthur, Editors, *B.C. Ministry of Employment and Investment*, Paper 1997-1, pages 183-186.
- Paulen, R., Bobrowsky, P.T., Little, E.C., Prebble, A.C. and Ledwon, A. (1998): Drift exploration in the southern Kootenay Terrane; *in Geological Fieldwork 1997*; *B.C. Ministry of Employment and Investment*, Paper 1998-1, pages 16-1 to 16-12.
- Paulen, R., Bobrowsky, P.T., Lett, R.E., Bichler, A.J. and Wingerter, C. (1999): Till geochemistry in the Kootenay, Slide Mountain and Quesnel Terranes; *in Geological Fieldwork 1998*, *B.C. Ministry of Energy and Mines*, Paper 1999-1, this volume.
- Schiarizza, P. and Preto, V.A. (1987): Geology of the Adams Plateau-Clearwater-Vavenby area; *B.C. Ministry of Energy, Mines and Petroleum Resources*, Paper 1987-2, 88 pages.
- Sibbick, S.J., Runnels, J.L. and Lett, R.E. (1997): Eagle Bay Project: Regional hydrogeochemical survey and geochemical orientation studies; *in Geological Fieldwork 1996*, D.V. Lefebure, W.J. McMillan and G. McArthur, Editors, *B.C. Ministry of Employment and Investment*, Paper 1997-1, pages 423-426.
- Yeow, A. (1998): Parthfinder elements in soil and till, Samatosum Mountain, British Columbia; Unpublished B. Sc. Thesis, *University of British Columbia*, 81 pages.



TILL GEOCHEMISTRY IN THE KOOTENAY, SLIDE MOUNTAIN AND QUESNEL TERRANES

By Roger C. Paulen², Peter T. Bobrowsky¹, Ray E. Lett¹,
Ahren J. Bichler², and Candice Wingerter²

KEYWORDS: Quaternary, surficial geology, till, drift exploration, geochemistry, exploration, prospecting, North Thompson River, Adams Plateau, Shuswap, Eagle Bay, Fennell, Nicola.

INTRODUCTION

A regional till sampling survey was undertaken during the summer of 1998 as year three of the Eagle Bay Project (Paulen *et al.*, 1998a; Bobrowsky *et al.*, 1997a; Dixon-Warren *et al.*, 1997a); an integrated regional exploration program centred on Devonian-Mississippian rocks of the Eagle Bay Assemblage and Permian to Devonian rocks of the Fennell Formation. Interesting results from the 1997 till geochemistry survey (Bobrowsky *et al.*, 1998) encouraged a further extension of the program into the Upper Triassic-Jurassic rocks of the Nicola Group. Volcanogenic massive sulphide (VMS) deposits hosted in the Fennell Formation, volcanogenic sulphide-barite deposits hosted in the Eagle Bay Formation, tombstone-style gold prospects hosted in the Baldy Batholith and the highly mineralized package of Nicola Group volcanic, sedimentary and associated intrusive rocks all suggest that the region has considerable mineral potential. Polymetallic gold-bearing veins hosted in volcanic assemblages of the Fennell Formation and the anomalous gold values in altered quartz vein float near the margin of the Thuya River Batholith also suggest a high potential for gold in the area. Related exploration studies included, mineral deposit studies in volcanogenic sediments of the lower Eagle Bay Assemblage (Höy, 1999), detailed property scale ice flow dispersal studies (Lett *et al.*, 1999), till geochemistry sampling and reconnaissance mineralized boulder tracing.

The till geochemistry sampling covered

approximately 1000 square kilometres within five 1:50000 scale map sheets (Figure 1). This being year three of the project, the purpose of the sampling program was to cover the remaining area of the Eagle Bay Formation north of Shuswap Lake and the Adams River, within the NTS sheets 82M/3, 82L/13 and 82L/14 and to extend the till geochemistry coverage north and west of the North Thompson River Fault into the poorly explored and poorly understood rocks of the Quesnel Terrane within the NTS sheets 92P/8 and 92P/9.

The objectives of the project were:

- ♦ to stimulate new exploration and economic activity in the area; especially in the poorly explored Quesnel Trough.
- ♦ to define new anomalies which may be used in the discovery of mineralization targets;
- ♦ to document ice flow indicators and both local and regional ice flow patterns to aid drift prospecting in the area;
- ♦ to document the dispersal of pathfinder elements down-ice from a known source;
- ♦ to provide information where mineral exploration has been hampered by thick glacial drift cover, and where traditional prospecting and exploration techniques have proven unsuccessful despite indications of high mineral potential.

The purpose of this paper is to summarize the till geochemistry activities of the 1998 summer field season and to present the results of the ice-flow indicator studies. Discussions of the paleo-ice flow history, Quaternary stratigraphy and the primary sampling media are provided to supplement the analytical results of the survey that will be released later.

¹British Columbia Geological Survey Branch (BCGS)

²School of Earth and Ocean Sciences, University of Victoria

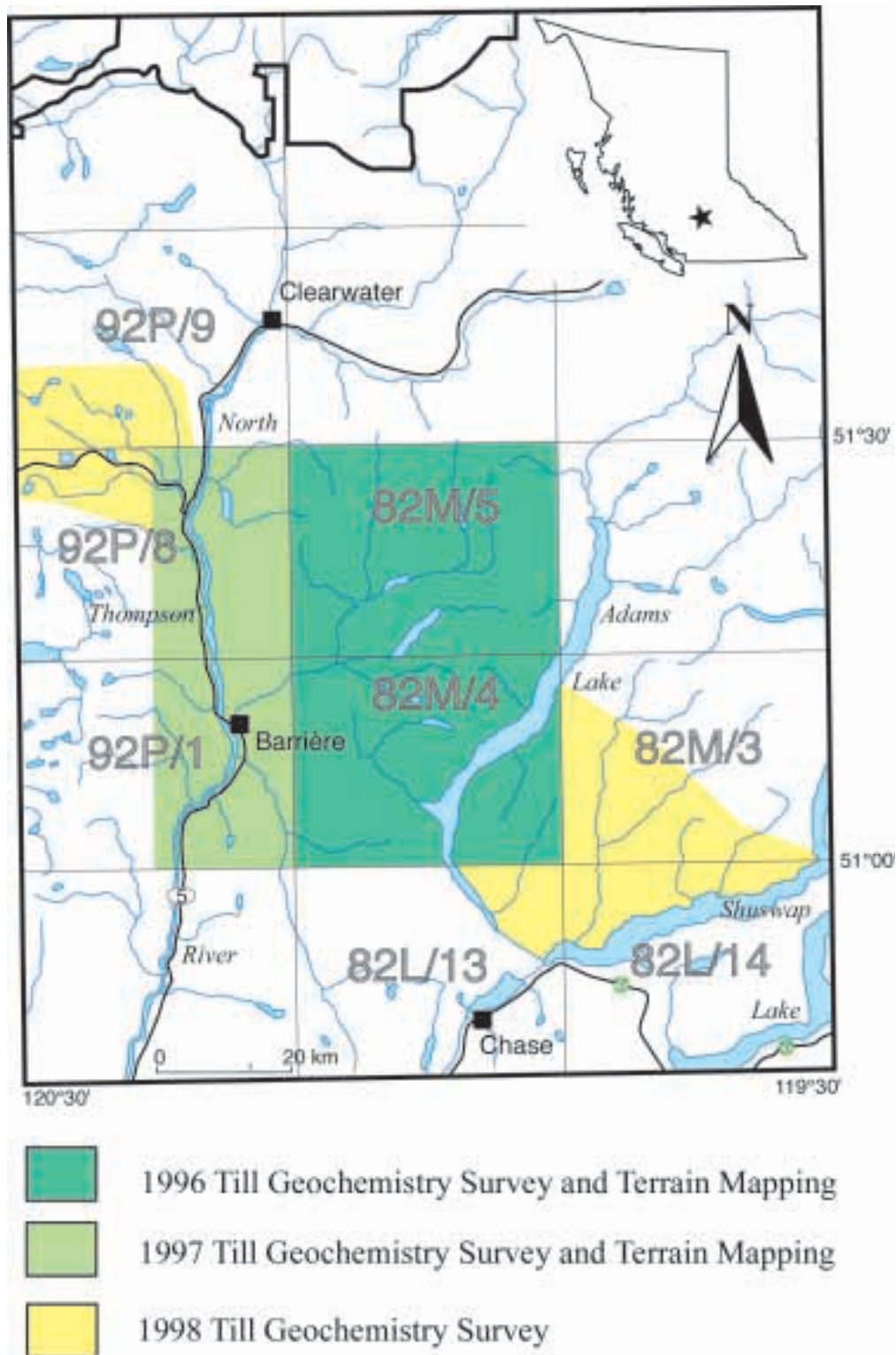


Figure 1. Location of the Eagle Bay drift exploration project (1996-1998) study area in south central British Columbia.



Photo 1. Typical topography of the study area, looking north up Scotch Creek towards the Adams Plateau.

BACKGROUND AND SETTING

The sampling survey focused on two separate regions in south-central British Columbia. The initial sampling took place in the southeastern part of the Adams Plateau that lies in the southern part of the Shuswap Highland, within the Interior Plateau (Holland, 1976). The region is characterized by moderate to high relief, glaciated and fluvially dissected topography (Photo 1). Elevations range from 370 metres above sea level along the north shore of Shuswap Lake to 1980 metres above sea level at Crowfoot Mountain, west of Seymour Arm (Shuswap Lake). Ground moraine dominates the landscape, followed in turn by colluvial, glaciofluvial, fluvial and glaciolacustrine sediments; the latter is restricted to the glacial lakes that occupied the Shuswap Basin during the most recent glacial event (Fulton, 1969).

Phase two of the program took place in the northeastern part of the Thompson Plateau, within the Interior Plateau. Topography is dominated by the high elevations of the Bonaparte Hills and the Nehalliston Plateau and is dotted with numerous small lakes and stream systems. Elevations range from 670 metres to 1680 metres above sea level. Ground moraine of various thickness dominates the landscape, followed in turn by collu-

vial, glaciofluvial, fluvial and organic sediments. As such, both regions are extremely favorable for a till geochemistry survey.

Bedrock Geology

The area lies within a belt of structurally complex low-grade metamorphic rocks that occur along the western margin of the Omineca Belt. This belt is flanked by high grade metamorphic rocks of the Shuswap Complex to the east and by rocks of the Intermontane Belt to the west (Figure 2). Lower Paleozoic to Mississippian rocks of the Eagle Bay Assemblage (Kootenay Terrane) underlie a major part of area. These consist of calcareous phyllite, calc-silicate schist and skarn or mafic metavolcanics overlain by felsic and locally intermediate metavolcanics and clastic metasediments. The eastern part of the Adams Plateau and west of Seymour Arm is underlain by the western margin of the Shuswap Metamorphic Complex (Silver Creek Formation, Mount Ida Group). These comprise strongly foliated and lineated assemblages of Cambrian-Ordovician paragneiss and schists intruded by Jurassic-Cretaceous dykes, sills and small irregular bodies of granitic rocks (Okulitch, 1974).

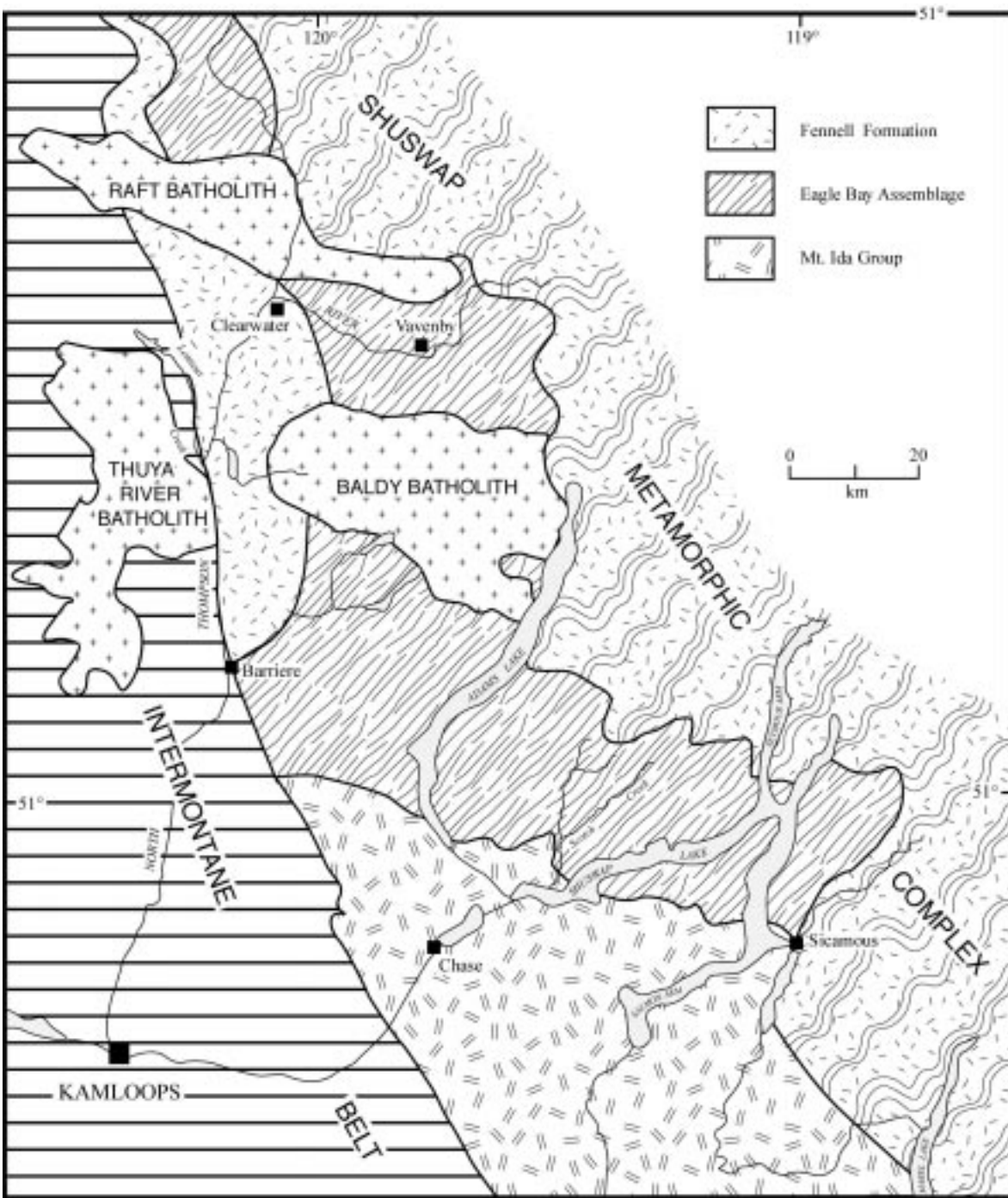


Figure 2. Geologic setting of the Adams Plateau - Clearwater - Vavenby area, modified after Schiarrizza and Preto (1987) and Campbell and Tipper (1971). Not shown are Tertiary volcanics and numerous granitic plutons.

North of Barriere, the Permian to Devonian rocks of the Fennell Formation comprise imbricated oceanic rocks of the Slide Mountain Terrane. The rocks consist of bedded cherts, gabbro, diabase, pillowed basalt and volcanogenic metasediments. The rocks are in fault contact with Permo-Triassic andesites, tuffs, argillites, greywacke and limestone of the Nicola Group (Schiarrizza and Preto, 1987) to

Early Jurassic porphyritic andesite breccia, tuff and flows of the Quesnel Terrane. Mid-Cretaceous granodiorite and quartz monzonite intrusions of the Baldy Batholith and the Late Triassic - Early Jurassic monzo-granite and granodiorite of Thuya Batholith (Campbell and Tipper, 1971) underlie the area.

A major north-south fault paralleling the North Thompson River valley separates the

Kootenay and Slide Mountain terranes from the younger Quesnel Terrane. This fault is a single break to Lemieux Creek, where it separates into several splays. This extensive block faulting signifies a major, unknown structural event (Campbell and Tipper, 1971) in a highly mineralized package of Nicola Group rocks within the northwest trending Quesnel Trough.

Polymetallic precious, sedimentary exhalative and Noranda/Kuroko type VMS base metal occurrences are hosted by Devonian-Mississippian felsic to intermediate metavolcanic rocks of the Eagle Bay Assemblage. Massive sulphides are hosted in oceanic basalts of the Fennell Formation. Skarn mineralization and silver-lead-zinc mineralization occur as numerous vein deposits within the Fennell Formation near the Cretaceous granitic intrusions. Porphyry copper and copper-gold skarns are hosted in the Nicola Group and molybdenite mineralization occurs near the southern margin of the Raft Batholith. The MINFILE database lists a total of 38 occurrences in the study area, 23 occur in the Eagle Bay Assemblage, 11 occur in the Nicola Group, three are associated with the Raft Batholith and one is hosted in the Silver Creek Formation. In total, there are 11 occurrences of gold, of which one is placer. Detailed property studies at various MINFILE occurrences are discussed in Lett *et al.* (1999).

METHODS

Fieldwork was based out of two camps: one in Magna Bay on Shuswap Lake for work in NTS 82M/3, 82L/13 and 82L/14 and a second near Tod Mountain for work in 92P/8 and 92P/9. Access to both areas was excellent. There is an extensive network of logging roads on the slopes and plateaus with minor access on steeper slopes. Fieldwork was conducted with 4-wheel drive vehicles along all major and secondary roads and trails of varying condition. In some cases, traverses were completed on foot where access was blocked or non-existent.

Initial work consisted of compiling and evaluating all existing terrain information available for the area. Regional Quaternary mapping completed by the Geological Survey of Canada (Tipper, 1971; Fulton, 1975) provided information on the types and distribution of the surficial sediments. Detailed local ice-flow directions were obtained

by measuring and determining the directions of striations, grooves and local roche moutonnées. The MINFILE database was examined to gain insight on the local mineral showings with respect to the deposit types and host rock relationships.

At each ground-truthing field station some or all the following observations were made: GPS-verified UTM location, identifying geographic features (i.e. creek, cliff, ridge, plateau, etc.), type of bedrock exposure if present, unconsolidated surface material and expression (terrain polygon unit), general slope, orientation of striations/grooves on bedrock or of bullet-shaped boulders, large scale features of streamlined landforms, elevations of post-glacial deposits (glaciofluvial and glaciolacustrine) and active geological processes.

Bulk sediment samples (1-5 kilograms) were collected for geochemical analysis over much of the study area. Emphasis was placed on collecting basal till deposits (first derivative products according to Shilts, 1993), although ablation till, colluviated till and colluvium were also collected under certain circumstances. Natural exposures and hand excavation were used to obtain samples from undisturbed, unweathered C-horizon (parent material) deposits. At each sample site (Photo 2), the following information was recorded: type of exposure (gully, roadcut, etc.), depth to sample from top of soil, thickness of A and B soil horizons, total exposed thickness of the surficial unit, stratigraphy of the exposure, clast percentage, matrix or clast-supported diamicton, consolidation, matrix texture, presence or absence of structures, bedding, clast angularity (average and range), clast size (average and range), clast



Photo 2. Roadcut exposing basal ground moraine at a sample site.

lithologies, and colour. The samples were evaluated as being derived from one of the three categories; basal till, ablation till, or colluviated/reworked basal till. Sediment samples were sent to Eco Tech Laboratories in Kamloops for processing. This involved air drying, splitting and sieving to <63 µm. The pulps, <63 µm sample and unsieved split were subsequently returned to the BCGS. The <63 µm fraction of each sample was split and one part will be subjected to aqua regia digestion and analysis for 30 elements by ICP (inductively coupled plasma emission spectroscopy) and for major oxides by LiBO₂ fusion - ICP (11 oxides, loss on ignition and 7 minor elements). The other portion will be submitted for INA (thermal neutron activation analysis) for 35 elements.

RESULTS

A total of 408 bulk sediment samples were collected for the till geochemistry study. Sample density averaged one per 2.45 km² for the total survey and provides a very high level of reconnaissance information for the region. Most of the samples taken for geochemical analysis were representative of basal till, most likely lodgement till. Of the 408 samples, 360 or 88% represented this sediment type which is the best media to sample for drift exploration. Ablation till only accounted for 24 samples or 6% of the total. Basal till which has undergone minor downslope movement was classed as colluviated till and this material accounted for 24 samples or 6% of the total. Together, the 12% of the samples that were collected from ablation till and colluviated till are valid, but much more difficult to interpret. Results and interpretation of the till geochemistry survey for this study will be released as a BCGS Open File at a later date.

A total 60 mineralized rock grab samples were taken from the study area, 23 are float and 37 are from reported or new gossanous outcrops. A total of 77 gossanous bedrock showings were recorded and these discoveries prompted further sampling beyond the planned boundaries of the 1998 survey area. Efforts were particularly concentrated in the paragneiss to schistose metasediments of the lower Eagle Bay Assemblage in 82M/3 and in the block faulted, brecciated mafic to andesitic volcanic and volcanogenic rocks of the Nicola Group in 92P/9. The samples will be

split, one half to be assayed and the other retained for petrologic study if necessary. The analytical results and corresponding locations will be released later.

Previous geochemical studies in the area provide an indication as to the style of mineralization, configuration of the anomaly plumes and regional dispersal patterns expected for this area. Examples shown in Bobrowsky *et al.* (1997) and Paulen *et al.* (1998a) show the clastic down-ice dispersal patterns that parallel the regional ice-flow from northwest to southeast in the North Thompson River Valley and the Adams Plateau. An additional example of a property scale geochemical sampling program presented here from Crowfoot Mountain, west of Seymour Arm, is provided as a precursor to the expected ice-flow patterns in the eastern part of the Adams Plateau, which is to the southwest (Fulton *et al.*, 1986).

At the Fluke Claims (MINFILE 082M104), in the flat alpine saddle between Crowfoot Mountain and Mount Moberly (NTS 82M/3), B-horizon soil geochemistry (Figure 3) illustrates a

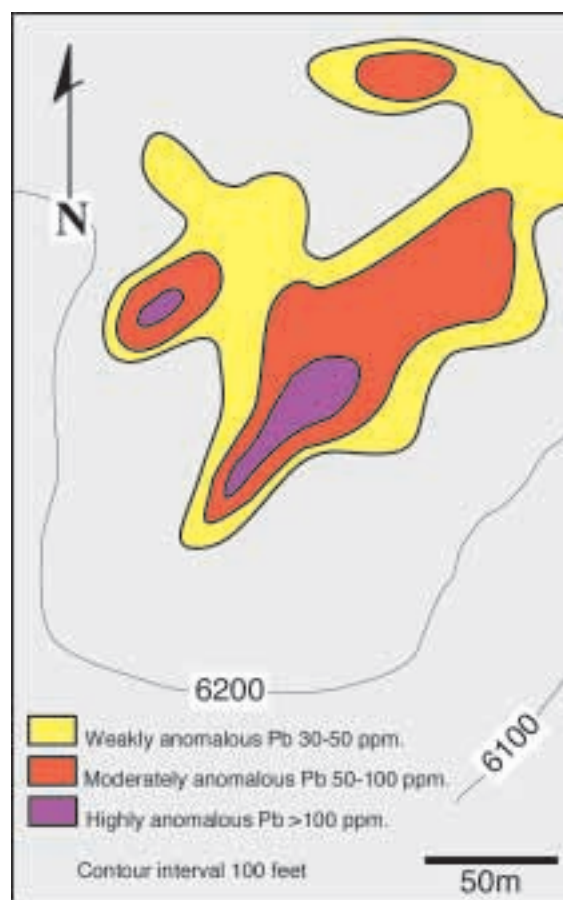


Figure 3. Lead soil anomaly for the Fluke claims (Crowfoot Property). Modified after Allen (1977).

thin ribbon anomaly of lead (Allen, 1977). The lead in B-horizon soils shows a down-ice dispersal pattern with the axis of symmetry paralleling the regional ice flow from north-northeast to south-southwest and thus reflects a typical clastic dispersal train (DiLabio, 1990).

Ice Flow Indicators

The striation record in the map area is poor due to the lack of preserved outcrop exposure. Striations were recorded at a few locations where recent logging has exposed fresh bedrock (Photo 3) There is an abundance of sculpted landforms on the plateau tops that provide regional ice flow information during the peak of glacial activity (Figure 4). Local paleo-ice flows are documented to be coincident with regional south to southeast flows (Fulton *et al.*, 1986). In the northern region (NTS 92P), regional ice flow directions are to the southeast, with deviations to the south in the North Thompson River valley. In the centre of the study area, the ice flowed in a southerly direction across the Adams Plateau, except in areas of variable relief where topography deflected ice flow. Fabric data in the basal tills on the lower Adams Plateau show a strong southerly trend in agreement with the striation and landform directions (Dixon-Warren, 1998). In the easternmost region (NTS 82M/3E), the landforms and striae show a south-southwesterly flow direction as ice was diverted into the Shuswap Basin. Where the southeast and southwest flowing ice converged is unknown due to the poor striation record and an obvious



Photo 3. Striae measured from freshly exposed outcrop of Eagle Bay mafic metavolcanics.



Photo 4. Copper Island in Shuswap Lake. Ice flow direction from right (northeast) to left (southwest).

lack of medial moraines, but it likely occurred near the southeastern edge of the Adams Plateau, west of Scotch Creek. Ice flow during deglaciation here would have converged southward, into the Shuswap Basin with a local deviation up to 45 degrees (Photo 4).

GLACIAL HISTORY AND STRATIGRAPHY

According to Fulton and others (Clague, 1989; Fulton, 1975; Fulton and Smith, 1978; Ryder *et al.*, 1991), the present day landscape of south-central British Columbia is the result of two glacial cycles, one interglacial and vigorous early-Holocene erosion and sedimentation. Evidence for only the latter glacial deposits and the post-glacial deposits are present in the study area. Although not necessarily present in the study area, the following lithological units and their correlative geological climate units have been identified in south-central British Columbia.

Stratigraphically oldest and identified only at two locations to the south of the study area, are the interglacial Westwold Sediments. The deposits consist of cross-stratified gravely sand capped by marl, sand, silt, and clay, all of which are equivalent to the Highbury non-glacial interval in the Fraser Lowland (Sangamonian). Next in age are Okanagan Centre Drift deposits, consisting of coarse, poorly-stratified gravel, till and laminated silt. The sediments were deposited during the Okanagan Centre Glaciation, equivalent to the Semiahmoo Glaciation in the Fraser Lowland (early Wisconsinan). Middle Wisconsinan, Olympic Non-Glacial Bessette Sediments overlie the Okanagan Centre Drift.

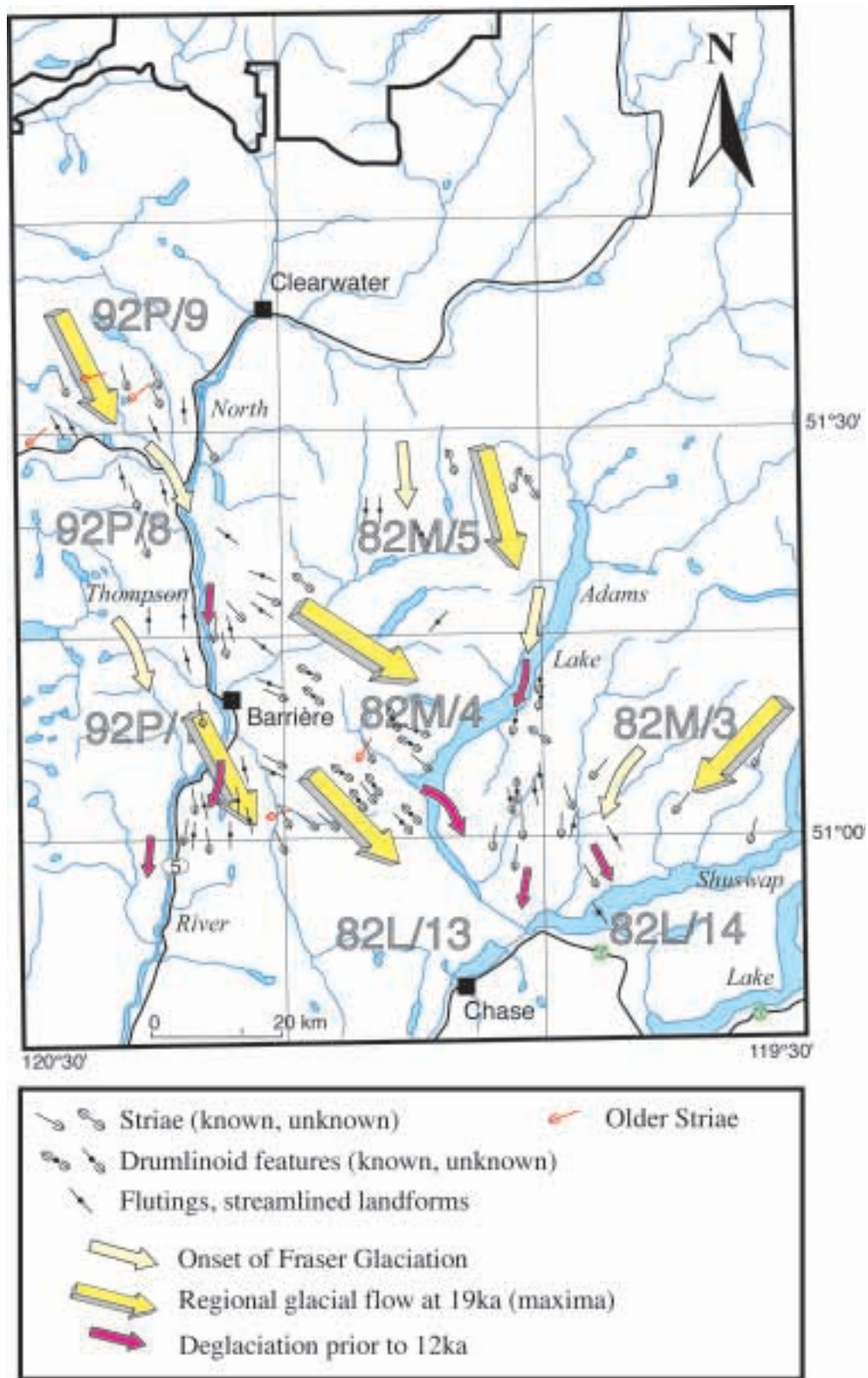


Figure 4. Summary of ice flow indicators for the Eagle Bay Project (1996-1998). Data compiled from the Eagle Bay project terrain geology maps (Dixon-Warren *et al.*, 1997b; Leboe *et al.*, 1997; Paulen *et al.*, 1998b; Paulen *et al.* 1998c) and 1998 field observations

They consist of nonglacial silt, sand and gravel with some organic material and up to two tephra. The Kamloops Lake Drift (20.2 ka; Dyck *et al.*, 1965) overlies the Bessette sediments, and underlies the present-day surface cover of postglacial deposits. This unit consists of silt, sand, gravel and till deposited during the Fraser Glaciation (Late Wisconsinan).

Rare older striae preserved on bedrock surfaces suggest an early glacial advance from the northeast to the southwest, but there is no evidence of this in the sediment record. The surface and near-surface sediments sampled in both the southern and northern regions directly result from the last cycle of glaciation and deglaciation (Fraser Glaciation), as well as ensuing post-glacial activity.

Fraser Glaciation

The onset of Fraser glaciation began in the Coast, Cariboo and Monashee Mountains. Valley glaciers descended to lower elevations to form piedmont lobes in the Interior Plateau, and eventually coalesced to form a mountain ice sheet (Ryder *et al.*, 1991). Ice sheet margins reached a maximum elevation between 2200 and 2400 metres along rimming mountains; the entire Shuswap Highland was completely buried beneath an ice cap by approximately 19 ka. At Fraser Glaciation maximum, regional ice flow was to the south-southeast on the Bonaparte and Adams plateaus (Tipper, 1971) with deviations up to 45° (Fulton *et al.*, 1986). This deviation was particularly noted in the eastern part of the study area, where ice from the north and west coalesced with ice flowing from the Monashee Mountains and was subsequently directed into the Shuswap Basin. Basal till deposits, which range widely in texture with the underlying bedrock, blanketed the land surface.

Deglaciation of the Interior Plateau was rapid; the equilibrium line likely rose considerably, reducing the area of accumulation for the Cordilleran ice sheet, and the ice mass decayed by downwasting. Ablation till was deposited by stagnating ice in several high-elevation portions of the region. As uplands were deglaciated prior to low benches and valleys, meltwater was channeled to valley sides, resulting in kame terraces and ice-contact sediments. Valleys clear of ice above the stagnating glaciers in their lower reaches became the confinement for meltwater

blocked from drainage, thereby resulting in local mantles of glaciolacustrine sediments. The Shuswap basin experienced up to six lake level stages during deglaciation. Most of the basin exhibits fjord-like characteristics and little evidence is retained from the former glacial lakes. Radiocarbon dates of 11.3 ka at McGillivray Creek (Clague, 1980), 10.5 ka at Chase (Lowdon and Blake, 1973) and 10.1 and 9.84 ka on Mount Fademear Plateau (Blake, 1986) indicates that deglaciation began about 12 ka and the modern drainage pattern was established prior to 8.9 ka (Dyke *et al.*, 1965; Fulton, 1969).

Holocene Post-Glacial

Once ice-dammed lakes drained, meltwaters carrying heavy sediment loads deposited thick units of stratified sand and gravel in valleys. As sediment loads decreased, deposition was replaced by erosion, and water courses cut down through valley fills, leaving glaciofluvial terraces abandoned on valley sides. Following the complete deglaciation of the region, unstable and unvegetated slopes were highly susceptible to erosion and sedimentation. Intense mass wasting of surface deposits on oversteepened valley slopes resulted in the deposition of colluvial fans and aprons along valley bottoms. Most post-glacial deposition occurred within the first few hundred years of deglaciation, and certainly before the eruption of Mt. Mazama, circa 7000 radiocarbon-years ago, which deposited tephra near the present-day ground surface. Fluvial fan deposits and active talus slopes typify the modern sedimentation in the area.

SURFICIAL SEDIMENTS

Several types of surficial deposits were observed in the study area including: ground moraine (basal till and ablation till), colluvial, fluvial, glaciofluvial, glaciolacustrine, organic, and anthropogenic. General observations suggest the plateaus and hills are mainly covered by combinations of till, colluvium and minor glaciofluvial deposits, whereas glaciolacustrine, glaciofluvial and fluvial sediments occur mainly in the valleys. Anthropogenic deposits are not widespread and can be found only near developed prospects and the larger communities. Organic deposits occur locally in all types of terrain.



Photo 5. Basal lodgement till exposed in a recent roadcut.

Basal Till

Throughout the region, the bedrock topography is mantled by variable amounts of massive, very poorly-sorted matrix-supported diamicton (Photo 5). Deposits range in thickness from thin (<1 metre) veneers to thick (>8 metre) blankets. Characteristics of this diamicton suggest that it is most likely a lodgement depositional environment (Dreimanis, 1988). Basal till facies tend to be variable with respect to the underlying bedrock.

In general, basal till (lodgement) deposits are primarily massive to poorly-stratified, light to dark olive grey, moderately to highly consolidated sediments derived from greenstone metavolcanics and metasediments of the Eagle Bay Assemblage, Fennell Formation or Nicola Group. The matrix is fissile and has a clayey silt to a silty-sand texture. Deposits are dense, compact, cohesive with irregular jointing patterns. Clast content ranges from 15-35%, usually averaging about 25%, and clasts range in size from granules to boulders (over 2 metres) averaging 1-2 centimetres. The clasts are mainly subrounded to subangular in shape and consist of various lithologies of local and exotic source. A number of clasts have striated and faceted surfaces.



Photo 6. Exposed section of ground moraine over the Thuya River Batholith. A blanket of stoney ablation till is draped over finer basal lodgement till.

Ablation Till

Massive to crudely stratified clast-supported diamicton occurs frequently throughout the study area (Photo 6). Most commonly, deposits of ablation till occur as a thin mantle overlying basal till and/or bedrock on the higher plateaus. Deposits also occur in areas of hummocky terrain where evidence of recessional ice and mass wasting occurred during deglaciation. In contrast to the basal tills, the diamictons are light to medium grey, moderately compact and cohesive. The sandy matrix is poorly consolidated and usually contains less than 5% silt and clay. Clast content ranges from 30-60% and average clast size is 2-5 centimetres. Clast lithology is variable but often deposits are monolithologic, primarily granodiorites and monzonite derived from the Thuya River, Baldy and Raft batholiths. The diamictons are interpreted as supraglacial or ablation till deposits, resulting from deposition by stagnating glacier ice (Dreimanis, 1988).

DRIFT EXPLORATION IMPLICATIONS

The thin drift mantling the upland plateaus and the defined valley systems provide an excellent landscape for drift prospecting. Basal tills in this region directly overlie the bedrock and are representative of the last glaciation to have affected the region. No sediments that predate this event were observed in the area. Thin deposits of basal tills, like those seen on the upland plateaus, usually reflect a more proximal source area for the sediments (Bobrowsky *et al.*, 1995). Basal tills are the dominant sediment type and this media has been recognized as the ideal sampling media for drift prospecting (Shilts, 1993). If there are no complications of multiple ice-flow directions to interpret, then a dispersal plume should reflect the last glacial event. Finally, the ice flow direction is generally east-southeast to south-southeast over the Bonaparte and Adams plateaus and is south-southwest over the hills east of Scotch Creek. Such a pattern is ideal for both reconnaissance and property scale drift prospecting. Caution must be taken when following up regional anomalies where bedrock strike is parallel to ice-flow directions. Such is the case with Eagle Bay stratabound type deposits. Multiple deposits along strike can be geochemically masked or expressed as a single ribbon anomaly.

Reported geochemical anomalies from known mineral occurrences indicate that the dispersal plumes conform to classic down-ice shapes, usually proximal to the source bedrock. It is further expected that clastic dispersal patterns associated with any anomalous values detected from this reconnaissance survey will most likely parallel ice flow and be imprinted with minor fluctuations from hydromorphic downslope dispersal. It is expected that these anomalies will occur less than 100 metres from source rock. However, boulder tracing of the Eakin Creek anomaly (Bobrowsky *et al.*, 1998) has shown that in areas of particularly thick drift, and at the edges of the plateau, the dispersal train can be several kilometres in length.

CONCLUSION

The Eagle Bay project area is underlain by Nicola Group (Quesnel Terrane), Fennell (Slide Mountain), Eagle Bay (Kootenay) and Mount

Ida Group (Kootenay) which is part of the complicated and poorly understood North American continental margin (Dawson *et al.*, 1991). There is potential for alkalic porphyry Cu-Au-Ag deposits (plutonic assemblages), Mo-Cu porphyry deposits (plutonic assemblages), volcanogenic massive sulphide Cu (Fennell Formation) and precious metal enriched Cu-Zn-Pb sedimentary exhalative stratiform and Cu-Pb-Au volcanogenic stratabound deposits (Schiarizza and Preto, 1985).

Results from the 1996 and 1997 till sampling surveys have generated recent staking activity and led to the discovery of a tombstone-style vein or stockwork gold prospect along the margin of the Baldy Batholith (Bobrowsky *et al.*, 1997b). Several other gold anomalies in till near the margins of the Thuya Batholith and associated with elevated values of Bi, As, Sb and Mo suggest that potential bulk-tonnage, intrusion hosted gold deposits may occur near outliers of the Jurassic-Cretaceous monzonites and deserve to be prospected (M. Cathro, pers. comm. 1998). Plutonic-related gold deposits of this nature are similar in nature to the Tombstone-type deposits (Pogo) in Alaska (Woodsworth *et al.*, 1977) and Laforma prospects (Dawson *et al.*, 1991) hosted in the calc-alkalic plutonic suites in the Stikinia Terrane (Intermontane Belt).

Due to the high number of gossanous outcrops in an area with little historical exploration, future work should expand along the mineralized belt of paragneiss in the northwestern part of 82M/3. These showings follow a continuous mineralized trend roughly along strike with the Pet (MINFILE 082M143) and Mosquito King (MINFILE 082M016) occurrences in the southeastern corner of NTS 82M/4. Till sampling should continue into the northeastern part of NTS 82M/3 to follow up the recent results in the poorly understood, drift covered region. There is excellent access due to extensive logging in recent years.

Renewed industry interest in the northwest (NTS 92P) and recent exploration programs should provide impetus for additional work in the highly mineralized, poorly understood Quesnel Trough. Historically, exploration in this region has applied soil geochemistry for reconnaissance exploration with limited success. As such, proven successful methods using C-hori-

zon till sampling should be employed. Detailed till studies should be conducted around the Lakeview occurrence (MINFILE 092P010) as a model for clastic dispersal on the Bonaparte Plateau. Regional till sampling should extend northward and follow the Nicola Group volcanic terrane. Finally, surficial mapping at 1:50,000 scale would complement a bedrock mapping program of the same scale.

The lack of bedrock exposure in some areas implies that the proper genetic interpretation of glacial overburden is essential in delimiting and understanding potential areas of mineralization. Knowledge of ice-flow history is very critical for a drift exploration program and known geochemical anomalies that exhibit classic down-ice dispersal patterns follow the regional ice flow patterns. This indicates that the local terrain is highly suitable for drift exploration studies. Local and regional ice flow patterns are readily determined in the field at the site level. Integration of the surficial geology maps and reconnaissance till survey should now be pursued at the property scale of exploration to locate potential sites of buried mineralized zones.

ACKNOWLEDGMENTS

This work was completed as part of the British Columbia Geological Survey Branch, Eagle Bay Project. We extend our thanks to the Kamloops office of the Ministry of Energy and Mines for providing logistical services. Insight into the bedrock geology and the local mineral deposits were provided by Mike Cathro, regional geologist for the Ministry of Energy and Mines and Ron Wells of Kamloops Geological Services. Our thanks are extended to many of the prospectors who were informative and cooperative. Wayne Jackaman and Ayisha Yeow assisted with the till sampling.

REFERENCES

- Allen, G.B. (1977): Detailed geochemical exploration program on the Fluke Claims of Resourcecx Limited; *B.C. Ministry of Energy, Mines and Petroleum Resources*, Assessment Report 6230.
- Blake, W., Jr. (1986): Geological Survey of Canada Radiocarbon Dates XXV; *Geological Survey of Canada*, Paper 85-7, 32 p.
- Bobrowsky, P.T., Sibbick, S.J., Matysek, P.F. and Newell, J. (1995): Drift Exploration in the Canadian Cordillera; *B.C. Ministry of Energy, Mines and Petroleum Resources*, Paper 1995-2.
- Bobrowsky, P.T., Leboe, E.R., Dixon-Warren, A., and Ledwon, A. (1997a): Eagle Bay Project: Till geochemistry of the Adams Plateau (82 M/4) and North Barriere Lake (82M/5) map areas; in *Geological Fieldwork 1996*, D.V. Lefebure, W. J. McMillan, and G. McArthur, Editors, *B.C. Ministry of Employment and Investment*, Paper 1997-1.
- Bobrowsky, P.T., Leboe, E.R., Dixon-Warren, A., Ledwon, A., MacDougall, D. and Sibbick, S.J. (1997b): Till geochemistry of the Adams Plateau-North Barriere Lake Area (82M/4 and 5); *B.C. Ministry of Employment and Investment*, Open File 1997-9.
- Bobrowsky, P.T., Paulen, R., Little, E., Prebble, A., Ledwon, A., and Lett, R. (1998): Till Geochemistry of the Louis Creek - Chu Chua Creek area (NTS 92P/1E and 92P/8E); *B.C. Ministry of Energy and Mines*, Open File 1998-6.
- Campbell, R.B. and Tipper, H.W. (1971): Geology of Bonaparte Lake map area, British Columbia; *Geological Survey of Canada*, Memoir 363.
- Clague J.J. (1980): Late Quaternary geology and geochronology of British Columbia, Part 1: Radiocarbon Dates; *Geological Survey of Canada*, Paper 80-13, 28 p.
- Clague, J.J. (1989): Quaternary Geology of the Canadian Cordillera; Chapter 1 in *Quaternary Geology of Canada and Greenland*, R.J. Fulton, Editor; *Geological Survey of Canada*, Geology of Canada, no. 1 (also *Geological Society of America*, *The Geology of North America*), v. K-1, pages 15-96.
- Dawson, K.M., Panteleyev, A., Sutherland Brown, A. and Woodsworth, G.J. (1991): Regional metallogeny; Chapter 19 in *Geology of the Cordilleran Orogen in Canada*, H. Gabrielse and C.J. Yorath, Editors; *Geological Survey of Canada*, Geology of Canada, no. 4 (also *Geological Society of America*, *The Geology of North America*), v. G-2, pages 707-768.
- DiLabio, R.N.W. (1990): Glacial Dispersal Trains; in *Glacial Indicator Tracing*, R. Kujansuu, and M. Saarnisto, Editors, *A.A. Balkema*, Rotterdam, pages 109-122.
- Dixon-Warren, A. (1998): Terrain mapping and drift prospecting in south-central British Columbia; MSc. Thesis, *Simon Fraser University*,

- Vancouver, British, Columbia.
- Dixon-Warren, A., Bobrowsky, P.T., Leboe, E.R. and Ledwon, A. (1997a): Eagle Bay Project: Surficial Geology of the Adams Plateau (82 M/4) and North Barriere Lake (82M/5) map areas; *in Geological Fieldwork 1996*, D.V. Lefebure, W. J. McMillan, and G. McArthur, Editors, *B.C. Ministry of Employment and Investment*, Paper 1997-1.
- Dixon-Warren, A., Bobrowsky, P.T., Leboe, E.R. and Ledwon, A. (1997b): Terrain Geology of the Adams Plateau; *B.C. Ministry of Employment and Investment*, Open File 1997-7.
- Dreimanis, A. (1988): Till: Their Genetic Terminology and Classification; *in Genetic Classification of Glaciogenic Deposits*, R.P. Goldthwait and C.L. Matsch, Editors, *Balkema*, p. 17-67.
- Dyck, W., Fyles, J.G. and Blake, W., Jr., (1965): Geological Survey of Canada Radiocarbon Dates IV; *Geological Survey of Canada*, Paper 65-4, 23 p.
- Fulton, R.J. (1969): Glacial Lake History, Southern Interior Plateau, British Columbia; *Geological Survey of Canada*, Paper 69-37.
- Fulton, R.J. (1975): Quaternary geology and geomorphology, Nicola-Vernon area, British Columbia (82L W and 92 E); *Geological Survey of Canada*, Memoir 380.
- Fulton, R.J. and Smith, G.W. (1978): Late Pleistocene stratigraphy of south-central British Columbia; *Canadian Journal of Earth Sciences*, Volume 15, pages 971-980.
- Fulton, R.J., Alley, N.F., and Achard, R.A. (1986): Surficial geology, Seymour Arm, British Columbia; *Geological Survey of Canada*, Map 1609A, 1:250 000.
- Holland, S.S. (1976): Landforms of British Columbia, a physiographic outline; *B.C. Ministry of Energy, Mines and Petroleum Resources*, Bulletin 48.
- Höy, T. (1999): Massive sulphide deposits of the Eagle Bay Assemblage, Adams Plateau, south central British Columbia (82M3, 4); *in Geological Fieldwork 1998*, *B.C. Ministry of Energy and Mines*, Paper 1999-1, this volume.
- Leboe, E.R., Bobrowsky, P.T., Dixon-Warren, A. and Ledwon, A. (1997b): Terrain Geology Map of North Barriere Lake; *B.C. Ministry of Employment and Investment*, Open File 1997-6.
- Lett, R. E., Jackaman, W. and Yeow, A. (1999): Detailed geochemical exploration techniques for base and precious metals in the Kootenay Terrane; *in Geological Fieldwork 1998*, *B.C. Ministry of Energy and Mines*, Paper 1999-1 this volume.
- Lowdon, J.A. and Blake, W., Jr. (1973): Geological Survey of Canada radiocarbon dates XIII; *Geological Survey of Canada*, Paper 73-7, 61 pages.
- Okulitch, A.V. (1974): Stratigraphy and Structure of the Mount Ida Group, Vernon (82L), Seymour Arm (82M), Bonaparte Lake (92P) and Kettle River (82E) map-areas, British Columbia; *Geological Survey of Canada*, Paper 74-1, Part A, pages 25-30.
- Paulen, R.C., Bobrowsky, P.T., Little, E.C., Prebble, A.C. and Ledwon, A. (1998a): Surficial Deposits in the Louis Creek and Chu Chua Creek Area; *in Geological Fieldwork 1997*, D.V. Lefebure, and W. J. McMillan, Editors, *B.C. Ministry of Employment and Investment*, Paper 1998-1.
- Paulen, R.C., Bobrowsky, P.T., Little, E.C., Prebble, A.C. and Ledwon, A. (1998b): Terrain geology of the Louis Creek area, NTS 92P/1E, scale 1:50 000; *B.C. Ministry of Employment and Investment*, Open File 1998-2.
- Paulen, R.C., Bobrowsky, P.T., Little, E.C., Prebble, A.C. and Ledwon, A. (1998c): Terrain geology of the Chu Chua Creek area, NTS 92P/8E, scale 1:50 000; *B.C. Ministry of Employment and Investment*, Open File 1998-3.
- Ryder, J.M., Fulton, R.J. and Clague, J.J. (1991): The Cordilleran ice sheet and the glacial geomorphology of southern and central British Columbia; *Géographie Physique et Quaternaire*, Volume 45, pages 365-377.
- Schiarizza, P. and Preto, V.A. (1987): Geology of the Adams Plateau-Clearwater-Vavenby area; *B.C. Ministry of Energy, Mines and Petroleum Resources*, Paper 1987-2.
- Shilts, W.W. (1993): Geological Survey of Canada's contributions to understanding the composition of glacial sediments; *Canadian Journal of Earth Sciences*, Volume 30, p. 333-353
- Tipper, H. (1971): Surficial Geology, Bonaparte Lake, British Columbia; *Geological Survey of Canada*, Map 1278A, 1:250 000.
- Woodsworth, G.J., Pearson, D.E. and Sinclair, A.J. (1977): Metal distribution patterns across the eastern flank of the Coast Plutonic Complex, south-central British Columbia; *Economic Geology*, v. 72, pages 170-183.